PAGES 189–412

ISSN 0003–2654

The Analyst

A monthly international journal dealing with all branches of analytical chemistry.

SAC 83

SPECIAL ISSUE

Papers Presented at the 6th SAC International Conference on Analytical Chemistry

Edinburgh, UK, 17–23 July 1983

Vol. 109 No. 3
March
1984

ROYAL SOCIETY OF CHEMISTRY

The Analyst

The Analytical Journal of The Royal Society of Chemistry

Editorial Office: The Royal Society of Chemistry, Burlington House, Piccadilly, London, W1V 0BN. Telephone 01-734 9864. Telex No. 268001

Advertisements: Advertisement Department, The Royal Society of Chemistry, Burlington House, Piccadilly, London, W1V 0BN. Telephone 01-734 9864. Telex No. 268001

The Analyst (ISSN 0003–2654) is published monthly by The Royal Society of Chemistry, Burlington House, London W1V 0BN, England. All orders accompanied with payment should be sent directly to The Royal Society of Chemistry, The Distribution Centre, Blackhorse Road, Letchworth, Herts. SG6 1HN, England. 1984 Annual subscription rate UK £112.00, Rest of World £118.00, USA $223.00. Purchased with *Analytical Abstracts* UK £257.50, Rest of World £270.00, USA $514.00. Purchased with *Analytical Abstracts* plus *Analytical Proceedings* UK £287.50, Rest of World £302.00, USA $574.00. Purchased with *Analytical Proceedings* UK £141.00, Rest of World £148.00, USA $281.00. Air freight and mailing in the USA by Publications Expediting Inc., 200 Meacham Avenue, Elmont, NY 11003.
USA Postmaster: Send address changes to: *The Analyst,* Publications Expediting Inc., 200 Meacham Avenue, Elmont, NY 11003. Second class postage paid at Jamaica, NY 11431. All other despatches outside the UK by Bulk Airmail within Europe, Accelerated Surface Post outside Europe. PRINTED IN THE UK.

Information for Authors

Full details of how to submit material for publication in *The Analyst* are given in the Instructions to Authors in the January issue. Separate copies are available on request.

The Analyst publishes papers on all aspects of the theory and practice of analytical chemistry, fundamental and applied, inorganic and organic, including chemical, physical and biological methods. There is no page charge.

The following types of papers will be considered:

Full papers, describing original work.

Short papers, also describing original work, but shorter and of limited breadth of subject matter; there will be no difference in the quality of the work described in full and short papers.

Communications, which must be on an urgent matter and be of obvious scientific importance. Rapidity of publication is enhanced if diagrams are omitted, but tables and formulae can be included. Communications should not be simple claims for priority: this facility for rapid publication is intended for brief descriptions of work that has progressed to a stage at which it is likely to be valuable to workers faced with similar problems. A fuller paper may be offered subsequently, if justified by later work.

Reviews, which must be a critical evaluation of the existing state of knowledge on a particular facet of analytical chemistry.

Every paper (except Communications) will be submitted to at least two referees, by whose advice the Editorial Board of *The Analyst* will be guided as to its acceptance or rejection. Papers that are accepted must not be published elsewhere except by permission. Submission of a manuscript will be regarded as an undertaking that the same material is not being considered for publication by another journal.

Regional Advisory Editors. For the benefit of potential contributors outside the United Kingdom, a Panel of Regional Advisory Editors exists. Requests for help or advice on any matter related to the preparation of papers and their submission for publication in *The Analyst* can be sent to the nearest member of the Panel. Currently serving Regional Advisory Editors are listed in each issue of *The Analyst*.

Manuscripts (three copies typed in double spacing) should be addressed to:
The Editor, *The Analyst,*
Royal Society of Chemistry,
Burlington House,
Piccadilly,
LONDON W1V 0BN, UK

Particular attention should be paid to the use of standard methods of literature citation, including the journal abbreviations defined in Chemical Abstracts Service Source Index. Wherever possible, the nomenclature employed should follow IUPAC recommendations, and units and symbols should be those associated with SI.

All queries relating to the presentation and submission of papers, and any correspondence regarding accepted papers and proofs, should be directed to the Editor, *The Analyst* (address as above). Members of the Analytical Editorial Board (who may be contacted directly or via the Editorial Office) would welcome comments, suggestions and advice on general policy matters concerning *The Analyst.*

Fifty reprints of each published contribution are supplied free of charge, and further copies can be purchased.

Applications of High Speed HPLC in the Hospital Laboratory

The rapid analysis of several commonly abused drugs by high speed liquid chromatography is described. Chromatographic analysis times of one to three minutes are reported for some groups while a comprehensive toxicological screen is complete in six minutes.

Introduction

In routine therapeutic drug monitoring, the major groups analysed include tricyclic antidepressants, antiasthmatics, anticonvulsants, antineoplastic drugs, antiarrythmics and other cardiac drugs.

In addition to routine monitoring, emergency analyses of these drugs are often required in cases of accidental overdose. Many of these drugs can be also classified as abused drugs along with narcotic, sedatives and hallucinogens. In many overdose situations, the nature of the drug is unknown and frequently more than one drug may be involved.

At present, various techniques are currently in use for determining drug levels in body fluids. The advantages of gas and liquid chromatography are that numerous drugs can often be determined during the same analysis with high sensitivity and selectivity. This, coupled with the wide range of sample types that can be handled by L.C., makes it the most attractive method for drug analysis.

Recently, major advances in L.C. have been achieved in the quality and packing of small particle liquid chromatographic supports which now permit highly efficient separations to be achieved in shorter times.

Instrumentation

The L.C. system used was a Perkin-Elmer Series 4 Liquid Chromatograph equipped with a Model 7125 S loop injector. The detector was a Perkin-Elmer LC-85 variable wavelength UV/VIS detector (190 – 600nm) having a 2.4μl flow cell and a fast response time (290ms full scale). A Perkin-Elmer SIGMA 15 Chromatography Data Station was used for data handling. The L.C. columns used in this study were Perkin-Elmer high speed columns packed with 3 or 5μm supports. The 3μm columns were 100mm x 4.6mm i.d., whereas the 5μm were 125mm x 4.6mm i.d.

Figure 1. Tricyclic antidepressants

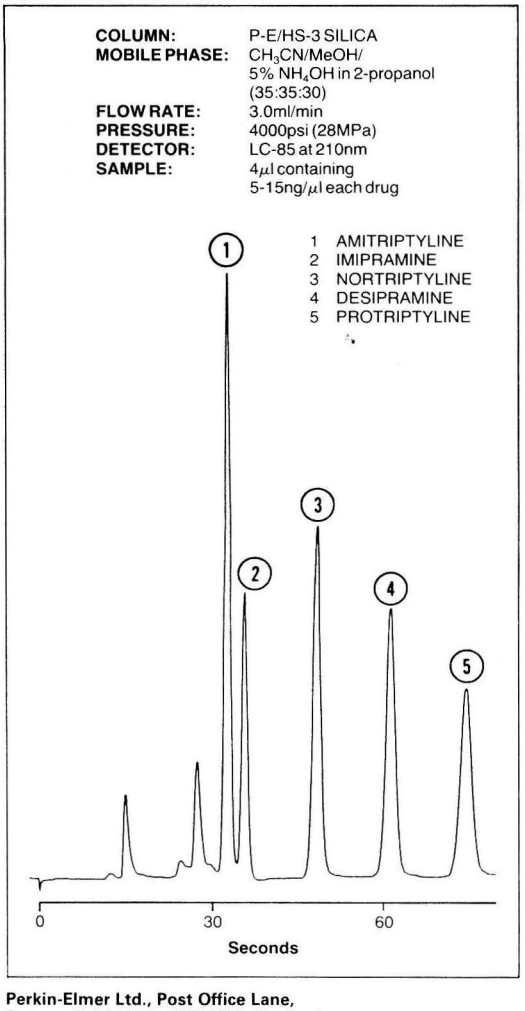

Figure 2. Tricyclic antidepressants

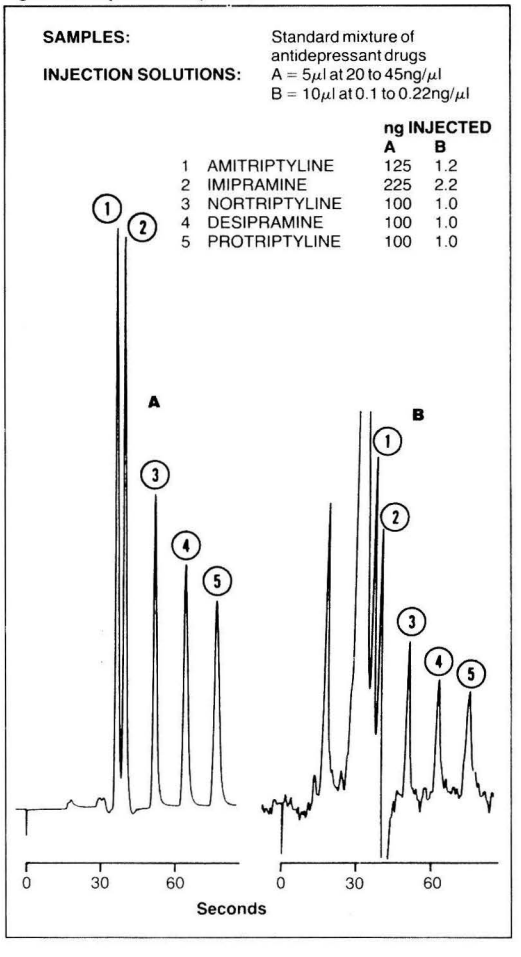

Perkin-Elmer Ltd., Post Office Lane, Beaconsfield, Bucks HP9 1QA, England
Telephone: Beaconsfield (049 46) 6161.

Advertisement Feature

Results and discussion

Several investigations have explored various chromatographic techniques for separating the major tricyclic antidepressant drugs (1, 2, 3).

Additionally, Haefelfinger (4) used a silica column with an acidic mobile phase containing sodium dodecyl sulphate as an ion-pairing reagent, while Schmidt (5) showed the advantage of a high -pH mobile phase and elevated temperatures using both silica and various bonded phases. Similar conditions have been utilised with a high -pH ternary mobile phase consisting of 35% each of acetonitrile and methanol and 30% of a 5% solution of ammonium hydroxide in isopropanol.

Figure 1 shows the separation of five common tricyclic antidepressants on a 3μm silica column using a detection wavelength of 210nm. The analysis is complete in just over one minute with baseline resolution of all components. The need for a highly sensitive analytical technique is necessary when analysing blood plasma samples for therapeutic concentrations. Figure 2 shows chromatograms of tricyclic antidepressants at very low levels with apparent detection limits about ten-fold below this.

Barbiturates represent another important class of drugs where rapid and accurate analysis is frequently crucial. Recently some publications have appeared using liquid chromatography techniques (6, 7) using either normal or reverse phase chromatography. Figure 3 shows the separation of eight common barbiturates on a 3μm C18 bonded phase, where the analysis is complete in just over three minutes using a mobile phase consisting of methanol and di-ammonium hydrogen phosphate. Although the levels of barbiturates generally encountered are quite high relative to the tricyclic antidepressants, some of these compounds have poor chromophores necessitating low U.V. monitoring in order to obtain sufficient sensitivity.

The analysis of anticonvulsants is required mainly for therapeutic drug monitoring. Frequently more than one drug is utilised, thereby making chromatographic methods attractive. Typical analysis times for these compounds have been in the range of 10 to 15 minutes. Figure 4 shows the separation of four of the common anticonvulsants along with an internal standard in approximately two minutes. A chromatogram of a serum sample which contained phenytoin and phenobarbitol at levels of 8.3 and 22mg/L is shown.

A toxicological drug screen can be extremely important in instances where overdose is suspected, but the identity of the drug or drugs is not known. A rapid analytical technique is needed which can detect a wide range of suspected drugs.

Figure 3. Barbiturates

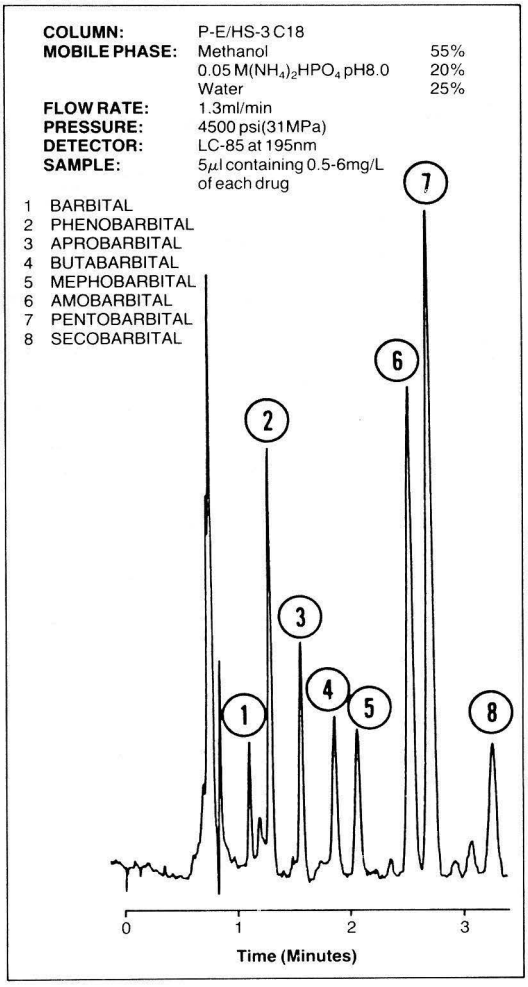

Figure 4. High Speed analysis of anticonvulsants

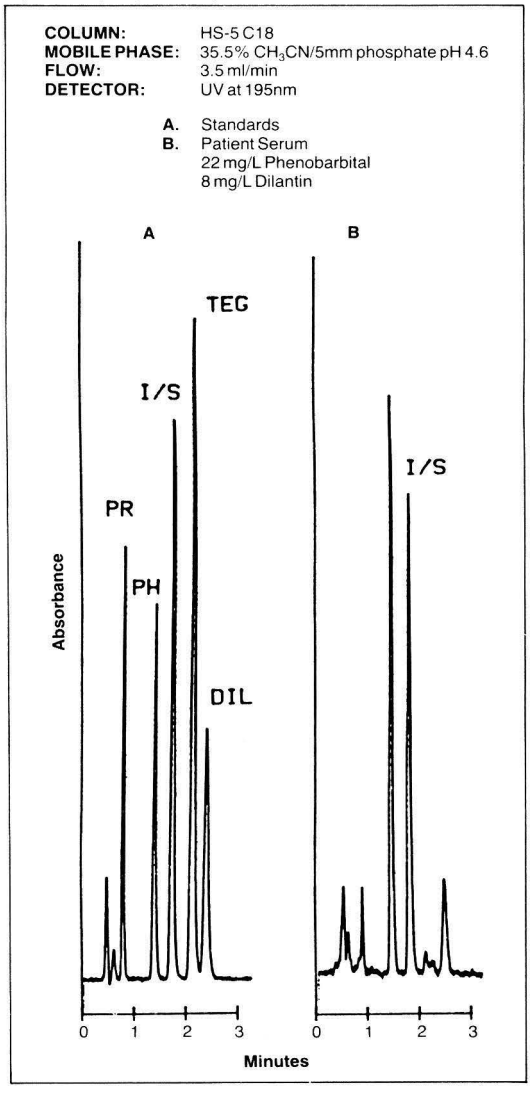

Liquid chromatography has proven very useful in this respect (8) and now with the use of small particle high speed columns comprehensive screens can be completed in less than ten minutes. Figure 5 shows a chromatogram containing 18 drugs of diverse categories. The analysis is complete in six minutes using a 5μm bonded phase eluted with a linear gradient of acetonitrile in a phosphate buffer, low U.V. detection (210nm) permits most of these drugs to be observed with adequate sensitivity.

Conclusion

The availability of high quality small particle silica and silica bonded phases has permitted substantial reduction in analysis time to be achieved without sacrificing resolution.

Columns used in this work			Part No.
P-E/HS-3	Silica	10cm x 4.5mm i.d.	0258-1500
P-E/HS-3	C18	10cm x 4.6mm i.d.	0258-1501
P-E/HS-5	C18	12.5cm x 4.6mm i.d.	0258-1001
P-E/HS-5	C8	12.5cm x 4.6mm i.d.	0258-1002

Other useful columns for high speed drug analysis are the Perkin-Elmer 3 x 3 columns. These are 3.2cm columns packed with 3μm particles. Further information is available in LC applications sheet CA/LC8.

P-E 3 x 3	C18	3.2cm x 4.6mm i.d.	0258-0160
P-E 3 x 3	C18	(10 column pack)	0258-0161

For further information, please contact your local LC sales specialist or Paul Gillyon.

References

1. J.E. Wallace, E.L. Shimek, S.C. Harris, J. Anal. Toxicol 5, 20 (1981)
2. I.D. Watson, M.J. Stewart. J. Chromatogr. 134, 182 (1977).
3. B. Mellstrom. G. Tybring. J. Chromatogr. 163, 310 (1979).
4. Haefelfinger. J. Chromatogr. Sci 17, 345, (1979).
5. G. Schmidt. Humana Press Inc. Liquid Chromatogr. in Clinical Analysis P.187–208.
6. M.J.M. Wells, C.R. Clark. J. Chromatogr. Sci, 19, 573 (1981).
7. G.K. Shiv, E.M. Nemoto. J. Chromatogr. 227, 207 (1982).
8. P. M. Kabra, B. E. Stafford, Humana Press N.J. Liquid Chromatogr. in Clinical Analysis P.243–249.

Figure 5. Toxicology screen

COLUMN: P-E HS-5 C8
MOBILE PHASE: 20% to 60% CH_3CN in 0.05M PHOSPHATE BUFFER (pH4.4) in 5 min.
FLOW RATE: 3.5ml/min
PRESSURE: 4000 psi (28MPa)
DETECTOR: LC-85 at 210nm
SAMPLE: 2μl of drug standards at 50-300mg/l (except Ethosuximide at 2000 mg/l)

1 THEOPHILLINE
2 ACETAMINOPHEN
3 CAFFEINE
4 ETHOSUXIMIDE
5 PRIMIDONE
6 ACETYL SALICYLIC ACID
7 PHENOBARBITAL
8 CHLORDIAZEPOXIDE
9 BUTABARBITAL
10 PENTABARBITAL
11 AMOBARBITAL
12 DILANTIN
13 ETHCHLORVYNOL
14 GLUTETHEMIDE
15 SECOBARBITAL
16 AMITRIPTYLINE
17 METHAQUALONE
18 DIAZEPAM

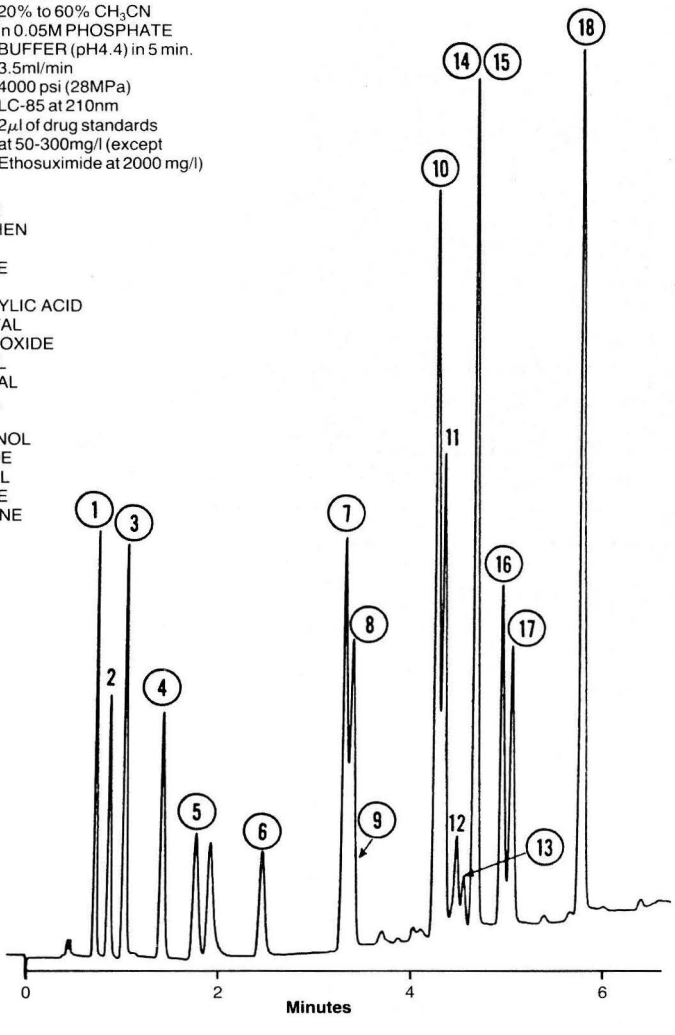

EDITORIAL

SAC 83—Edinburgh, Scotland, July 17–23, 1983

As a consequence of the publication of the SAC 83 Conference Handbook as the June 1983 issue of *Analytical Proceedings* (1983, **20**, 223–340) and the appearance of the abstracts of conference papers in that issue, it was decided that to avoid duplication, publication of the usual extended summaries of conference papers in *Analytical Proceedings* would not be adopted. Instead, authors were invited to submit the full text of their papers presented at the conference for consideration for publication in a Special SAC 83 Issue of *The Analyst*. This current, "bumper," issue of *The Analyst* is the result, and the Analytical Editorial Board hopes you will find it informative and a valuable insight into the wide range of topics and new developments presented at the conference.

Of the 210 papers presented in Edinburgh, 67 were submitted for publication in *The Analyst* and 46 of these appear in this issue. A number have been rejected by the normal refereeing procedure of *The Analyst*, and a few, which were submitted late or have been delayed, will appear in later issues of the journal. Most of the delays are due to the time taken by authors to modify their manuscripts to comply with referees' comments and are quite normal with a proportion of submitted manuscripts in any primary journal.

The papers in this issue include the four Plenary Lectures presented at SAC 83, each of which was very well received by delegates and contributed an excellent and balanced overview of developments in specific fields of analytical research. These papers: "Recent Developments in Fluorescence and Chemiluminescence Analysis," by J. N. Miller (p. 191); Capillary Separation Methods; a Key to High Efficiency and Improved Detection Capabilities," by M. V. Novotny (p. 199); "Design and Application of Neutral Carrier-based Ion-selective Electrodes," by W. Simon *et al.* (p. 207); and "Continuum Source Atomic-absorption Spectrometry: Past, Present and Future Prospects," by T. C. O'Haver (p. 211), offer a mini-review of their respective topics and we believe they make a substantial contribution to the literature, equivalent to the major contribution made by the authors' lectures to the success of the conference. The Board is particularly grateful to the Plenary Lecturers for their willingness and efforts in producing their manuscripts promptly for this issue of the journal. The SAC 83 conference was sponsored both by IUPAC, the International Union of Pure and Applied Chemistry, and FECS, The Federation of European Chemical Societies. IUPAC sponsorship normally carries with it the requirement for publication of the Plenary Lectures in the IUPAC journal, *Pure and Applied Chemistry*. However, on this occasion IUPAC waived their right to publish the Plenary Lectures and the Conference Organisers are very grateful for this helpful decision, and for the general support given by both IUPAC and FECS.

Of the large number of contributed papers presented both orally and as posters at the conference, this issue contains approximately one fifth. In view of the fact that many conference papers are not suitable for publication in the same format, and that a number of workers will always prefer to publish their work elsewhere, this proportion is roughly in line with that anticipated by the Editorial Board when it initiated this venture. The Board would like to thank all authors who have submitted their manuscripts to *The Analyst*, and in most instances would also thank them for their efforts to meet the deadlines essential for the publication of a Special Issue of a journal.

We hope our subscribers find the publication of this Special Issue a valuable contribution to the wider dissemination of knowledge and research presented in Edinburgh last July. Non-subscribers may like to know that copies of this issue are also available for personal purchase from the Royal Society of Chemistry Distribution Centre, Blackhorse Road, Letchworth, Hertfordshire, SG6 1HN (price £15).

Many individuals have contributed to the rapid publication of this issue, but the Board is particularly conscious of the extra effort required from the editorial staff in the production of such a large issue of the journal. This is the second Special Issue of *The Analyst* to be published and follows that in February 1983 which covered papers presented at the First Biennial National Atomic Spectroscopy Symposium. A number of others are already planned by the Analytical Editorial Board, and these will appear in future issues. The Executive Committee of SAC 86, to be held in July 1986 at the University of Bristol, has recently met for the first time. At this stage it seems very likely that they will adopt the same policy with regard to the Conference Handbook and publication of papers as that adopted for SAC 83, and we look forward to the publication of an even larger Special Issue on that occasion.

J. M. Ottaway
Chairman, Analytical Editorial Board

Recent Developments in Fluorescence and Chemiluminescence Analysis

Plenary Lecture

James N. Miller
Department of Chemistry, Loughborough University of Technology, Loughborough, Leicestershire, LE11 3TU, UK

Recent developments in photoluminescence and chemiluminescence spectroscopy are summarised, with particular reference to methods for improving the selectivity of luminescence analyses. The acquisition and manipulation of contour spectra and the problems and benefits of generally available corrected fluorescence spectra are discussed. Fluorescence and chemiluminescence immunoassays are evaluated and some probable future developments in these areas are indicated.

Keywords: *Fluorescence analysis; chemiluminescence analysis*

This paper presents a brief review of the recent advances in fluorescence and chemiluminescence analysis methods. This dynamic area of analytical science is in the midst of a period of considerable expansion: new instrumentation and techniques complement new luminescent reagents and reactions to produce many dividends in terms of enhanced sensitivity, selectivity and convenience. The present survey inevitably represents a personal selection of those advances which seem to be of the greatest theoretical interest or practical promise. Many of the areas which receive scant treatment here have been well reviewed elsewhere and appropriate references to such reviews are given.

Fluorescence Spectra

To an analyst, the outstanding feature of luminescence methods is their sensitivity. With appropriate compounds picogram concentrations can be detected using fluorimetric and phosphorimetric methods, and much lower levels still are detectable using chemiluminescence and bioluminescence methods.[1] The principal applications areas of all these methods are in biochemical and environmental analyses, where such sensitivity is especially important. The basis of this sensitivity is well known (Fig. 1). In the analysis of a very dilute solution, absorptiometry involves detecting a small change in a large light intensity, a very difficult thing to do; in contrast, using the characteristic and still almost universal right-angled optics familiar in fluorimetry, the small fluorescence signal is detected against a background which is (ideally) zero. This difference produces a vast improvement in limits of detection even though the fluorescence spectrometer may in practice collect only a small fraction of the emitted fluorescence.[2] In chemiluminescence spectrometers, which fundamentally consist of a cuvette holder and an adjacent photomultiplier, the light gathering is very efficient and the sensitivity correspondingly greater.

The availability of two monochromators in most fluorescence spectrometers permits the collection of two simple types of spectra. Scanning the excitation monochromator at a constant emission wavelength yields the *excitation spectrum*; scanning the emission monochromator at a fixed excitation wavelength provides the *fluorescence or emission spectrum*, which occurs at longer wavelengths than the excitation spectrum (other types of fluorescence spectrum will be discussed below). Fig. 2 shows the excitation and fluorescence spectra of Lucifer Yellow VS, a new and very promising fluorescent dye molecule developed by Stewart.[3] The most noticeable feature of the spectra, and indeed of the spectra of most organic molecules, is their band width; they cover 100 nm or more. One result of this is that the apparently additional selectivity of fluorimetry is largely illusory. In theory two species with similar emission wavelengths might have different excitation wavelengths (and *vice versa*). In practice, the spectral band widths are so large that even apparently distinct spectra overlap strongly, so discrimination is difficult. This is shown very clearly by comparing Lucifer Yellow VS with

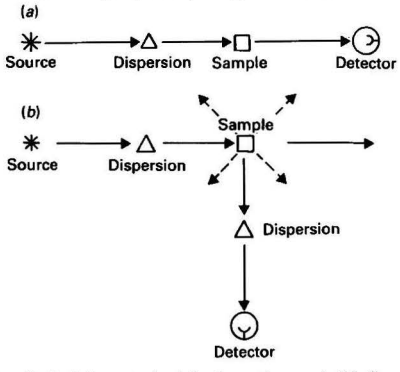

Fig. 1. Optical layouts in (*a*) absorption and (*b*) fluorescence spectroscopy

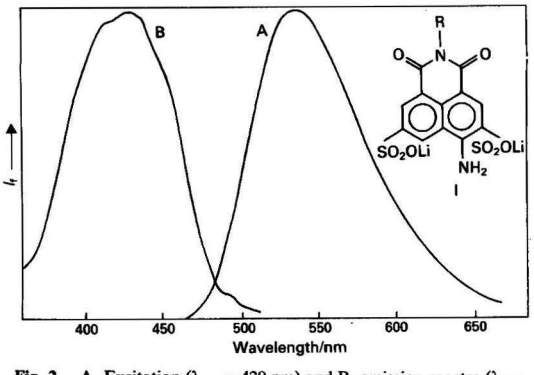

Fig. 2. A, Excitation ($\lambda_{ex.}$ = 429 nm) and B, emission spectra (λ_f = 535 nm) of Lucifer Yellow VS (I) in water. In this compound, R = $C_6H_5SO_2CH{=}CH_2$

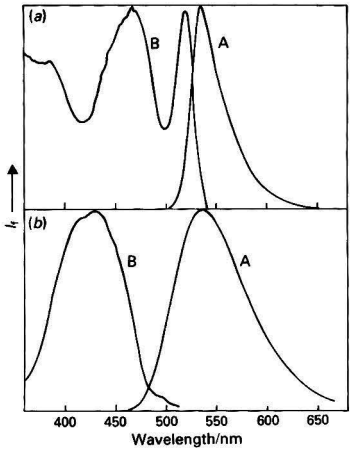

Fig. 3. A, Excitation and B, emission spectra of (*a*) fluorescein and (*b*) Lucifer Yellow VS in water. Fluorescein: $\lambda_{ex.} = 465$ nm; $\lambda_f = 535$ nm. Lucifer Yellow VS: $\lambda_{ex.} = 429$ nm; $\lambda_f = 535$ nm

fluorescein (Fig. 3): the two dyes have similar emission wavelengths, but very different excitation wavelengths. It is nonetheless very hard to choose a pair of excitation and emission wavelengths that would permit the observation of one of them without interference by the other. In practice, these spectral overlaps also have a serious effect on the limits of detection attainable in fluorimetry. In studies of a "real" multi-component sample, the background signal is very appreciable because of overlapping spectra; hence the main theoretical advantage of fluorescence spectrometry is largely lost and limits of detection suffer accordingly. It is very evident that good methods of reducing spectral band widths or otherwise improving spectral selectivity will be of great benefit in fluorimetric analysis.

Corrected Spectra and their Uses

Before considering that point further, however, a practical problem related to fluorescence spectra must be discussed. Because almost all fluorescence spectrometers are single-beam instruments, excitation and emission spectra will reflect both instrumental and sample properties unless appropriate corrections are made.[4] Thus an "uncorrected" emission spectrum will reflect not only the sample properties, but also the wavelength dependence of the emission grating efficiency and of the photomultiplier sensitivity. One of the great benefits of the microelectronics revolution is that the correction factors needed to eliminate such effects can easily and automatically be incorporated into the spectrometer using a microprocessor or microcomputer. In principle, therefore, the time is approaching where all fluorescence spectrometers should give the same spectrum for a particular sample examined under comparable conditions. Complacency about the benefits that this will produce must be tempered by the performance of the correction procedures in practice. Table 1 shows a fragment of the corrected emission spectrum of quinine sulphate (this compound is regaining favour as a primary fluorescence standard) as obtained on two different instruments. One is a standard spectrometer in the NBS laboratory in the USA[5]; the other is a commercially available "corrected" instrument in the author's laboratory. It is seen that, after normalisation, the agreement between the spectra is fairly good, but it is by no means perfect. Such results have to be borne in mind in considering the possible benefits of corrected spectra.

Table 1. Corrected emission spectra. Quinine sulphate in 0.1 M perchloric acid ($\lambda_{ex.} = 350$ nm)

Wavelength/ nm	Spectrum* 1	2
400	0.170	0.177
410	0.359	0.376
420	0.586	0.608
430	0.792	0.814
440	0.940	0.957
450	0.999	0.999
460	0.982	0.982
470	0.897	0.924
480	0.782	0.808
490	0.659	0.675
500	0.541	0.551

* Spectrum 1 was obtained at the National Bureau of Standards (reference 5) and spectrum 2 in the author's laboratory.

Two particular benefits are apparent. Firstly, if all spectrometers yield the same spectra, it is possible in principle to build up a library of spectra (similar to those available in other branches of spectroscopy) and use them for comparison and identification purposes. For example, it is now feasible, with the aid of a diode-array spectrometer or similar device, to determine the fluorescence spectrum of a discrete fraction separated by HPLC "on the fly." Comparison of this spectrum with a computer-stored reference spectrum will allow rapid identification of the solute.[6,7] It is important to remember, however, that the fluorescence properties of a compound, both spectral distribution and intensity, are solvent dependent to a far greater extent than is true in, for example, absorption spectroscopy. To be really useful a library collection of spectra must therefore cover a variety of commonly used solvent systems. In the author's laboratory, such a collection of spectra is being accumulated (previous collections have contained *uncorrected* spectra) and it is hoped that this library will eventually become generally available in hard-copy and floppy-disc forms.

The second application of a collection of universally applicable spectra is more fundamental. In the past, a major deterrent to the systematic use of fluorescence spectroscopy has been the paucity of adequate information on structure - spectra correlations. In other words, which structural factors cause a molecule to have a high fluorescence quantum yield?; which factors affect the wavelength and intensity of this fluorescence?; and what are the exact effects of one or more substituent groups on the fluorescence properties of organic and organometallic compounds? Although some general rules are well known,[8] much detailed information is still lacking and it remains hard to predict the luminescence properties of even the simplest compounds. Once again there is no doubt that progress in this direction has been hampered by the simple fact that, until recently, different spectrometers have given different spectral results. However, the author's laboratory has recently embarked on a programme that will apply pattern recognition methods[9] to the library of corrected spectra, so as to identify structural features responsible for particular spectroscopic properties. While this topic is too complex to consider in detail, it is pertinent to note that a necessary preliminary is the coding of spectroscopic properties into a purely numerical form. The coding method must produce sufficiently distinctive data for different compounds, but must also be simple enough to allow reasonably rapid calculations to be made.[10] (This second requirement arises because the same method of coding spectra will be used in pattern recognition studies and in the comparisons of experimental and library spectra already discussed.) Table 2 lists the photoluminescence properties that we might wish to incorporate in a complete "profile" of a compound; note that it

Table 2. Profile of a photoluminescent compound

Solvent	
Maxima and minima in excitation spectrum*	
Maxima and minima in fluorescence spectrum*	
Maxima and minima in phosphorescence spectrum*	
Quantum yield of fluorescence	
Quantum yield of phosphorescence	
Lifetime of fluorescence	
Lifetime of phosphorescence	

* In these instances several spectral features may be involved: the excitation, fluorescence and phosphorescence maxima will normally be recorded, but the method of moments may be used instead (see Fig. 4).

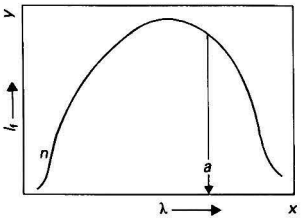

Fig. 4. Calculation of the six moments of a hypothetical spectrum. The moments are a (the mean value of x), U_{2-4}, S and K where $U_{2-4} = \Sigma(x_i - a)^{2-4}\, y_i/\Sigma y_i$; $S = U_3/(U_2)^{3/2}$; and $K_4 = U_4/(U_2)^2 - 3$. Further details are given in reference 11

Table 3. Fluorescence profile of anthracene

Feature	Data	Notes
Solvent	001	Cyclohexane
Excitation maxima . .	357 376 340	Maxima at 357, 376 and 340 nm in order of decreasing intensity
Emission maxima . .	400 379 000	Maxima at 400 and 379 nm in order of decreasing intensity; the code 000 is used where the feature is absent or not measured
Quantum yield . .	360	*i.e.*, 0.36
Lifetime	049	*i.e.*, 4.9 ns

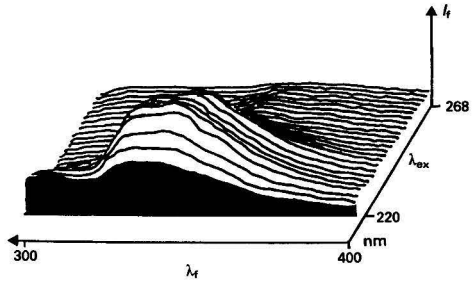

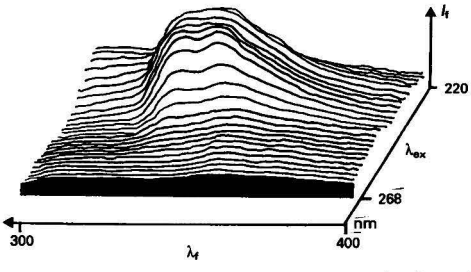

Fig. 5. Projected three-dimensional spectra of a crude oil sample in cyclohexane (concentration, 4 μg ml^{-1}). Computer software allows the spectrum to be examined from the high or low excitation wavelength directions. Individual traces represent 2-nm excitation wavelength increments

includes lifetime and quantum yield data, and both phosphorescence and fluorescence spectra. For many compounds the available data may be incomplete for a number of reasons. The pattern recognition and spectral comparison methods used must take this into account.

Several methods of expressing spectral data numerically can be considered. A simple approach involves expressing each characteristic of the compound as a three-digit code. An example of this approach is given in Table 3; note that the code 000 is used wherever the information is not available or where a spectral feature does not occur. Of course, each piece of information is subject to experimental error, perhaps ±2 nm with characteristic wavelengths, and so on. A satisfactory comparison program must make allowance for this, but must not make so much allowance that the comparison method loses its discriminating power. Another interesting method of describing spectra has recently been suggested.[11] It involves using *moments* to express spectral band shapes. Moments are useful in describing any distribution function, particularly where the mathematical form of that function is not known. They have been used in infrared spectrometry[12] and in other areas of chemistry.[13] As is shown in Fig. 4, the first four moments are readily calculated, and two additional parameters, the skewness (S) and the kurtosis (K), are readily determined from them. Tests on model compounds[11] have shown that the combination of these six parameters gives a high degree of discrimination between fluorescence spectra, whether or not the latter are distinguished by vibrational bands. Moreover, the data are easily collected and the moments determined in real time, and the moments are remarkably insensitive to spectral band width and to smoothing procedures. Possible disadvantages are that the system applies only to the spectra themselves and not to other data such as lifetimes and quantum yields, and that the higher moments are very sensitive to base-line errors and to small changes at the extremes of a spectrum, such as might be caused by scattered light signals or contaminating fluorophores.

It is apparent that much more work needs to be done to compare the efficiencies of different methods of expressing fluorescence spectra digitally. Within a short time, however, extended collections of corrected fluorescence spectra will be available in both digital and analogue form, and they will certainly find many applications.

Synchronous and Contour Spectra

This section considers the further question of selectivity in fluorescence spectroscopy, and in particular the possibility of obtaining characteristic spectra with narrow band widths. It is first necessary to recall that conventional excitation and emission spectra are not complete descriptions of the spectral distribution of a compound. The excitation spectrum is obtained at only a single emission wavelength and the emission spectrum is obtained using only one excitation wavelength. A complete description requires a *three-dimensional spectrum*,[14] in which one axis is the excitation wavelength scale, a second axis represents the emission wavelength and the third axis is the intensity axis. Such spectra are known also as excitation - emission matrix spectra, contour spectra and total luminescence spectra. The simpler way of expressing such results is shown in Fig. 5. This spectrum is a projection containing (in this instance) 30 individual spectra,

superimposed with the aid of a "hidden line removal" routine. The latter simplifies and clarifies the spectra, and does not sacrifice information because, as can be seen, it is also possible (using software only) to reverse the direction of the excitation axis and hence see "behind the hill." These spectra take about 1 h to accumulate (unless a diode-array spectrometer is available), most of this time being taken up by the individual spectral scans. An interfaced microcomputer stores and presents the spectra. The projected spectra give excellent general pictures of the properties of samples but it is more difficult to extract detailed information, *e.g.*, fluorescence intensities at any pair of wavelengths, from them.

The second method of acquiring "total luminescence" spectra is illustrated in Fig. 6. Here the two normal axes represent the emission and excitation wavelengths, while the intensities are expressed as a series of contours. In the figure contours are drawn at 90%, 70%, 50%, etc., of the peak intensity, but clearly contours at other levels should also be available. It is obvious that this method is much more informative than the former, especially where quantitative data are needed, but contour spectra are also more difficult to obtain. The computer-interfaced spectrometer must first accumulate all the necessary data, and then calculate the contours with the aid of an interpolation program that estimates the points of equal fluorescence intensity. Contouring programs are available for some commonly used computers,[15] but the process remains time consuming.

The process of accumulating contour data can sometimes be accelerated with the help of Vavilov's law,[16] which proposes that the closely related processes of excited state vibrational relaxation and internal conversion, which rapidly (*ca.* 10^{-12} s) take an excited molecule to the lowest vibrational level of the first singlet excited state, should occur with a quantum yield of unity. This means that the spectral distribution of the emission spectrum should be independent of the excitation wavelengths (and *vice versa*). Fig. 7 shows this principle in operation for Lucifer Yellow VS. The emission spectra excited at 429 and 388 nm are of equivalent shape; the latter has half the maximum intensity of the former because 388 nm is the half-maximum wavelength of the excitation spectrum. It is evident that an extension of this principle would allow the calculation of a complete contour spectrum of a compound from a knowledge of its excitation and emission spectra. Fig. 8 shows that, for Lucifer Yellow at least, the principle holds good. Remembering the interpolation processes involved in producing contour spectra, it is apparent that the experimental contour spectra, obtained directly by using all possible excitation and emission wavelengths, agree very well with the contours calculated with the aid of the Vavilov's law method. This method has two important limitations. Firstly, it is applicable only to pure compounds, not to mixtures; and secondly, a number of important exceptions to Vavilov's law itself have been identified. These include many benzene derivatives and aromatic amino acids.[17] Nonetheless, it may be useful to be able to calculate the contour spectrum of a single analyte and thus to compare it with the known contour spectrum of a common sample matrix. Further, a comparison between the calculated and experimental contour spectra is a good test of the validity of Vavilov's law. Additionally, recent methods permitting quantitative evaluation of complex contour spectra may assume that Vavilov's law applies,[18,19] so the method discussed is of more than academic interest.

One of the most important merits of contour spectra is that sections through them give very useful information. Thus a vertical section, *i.e.*, at constant emission wavelength, is equivalent to an excitation spectrum and a horizontal section is equivalent to a conventional fluorescence spectrum. A 45° section with both monochromators set to the same wavelength corresponds to first-order Rayleigh scattered light emission. A 45° section with a (fixed) wavelength difference between the two monochromators produces a "synchronous" spectrum

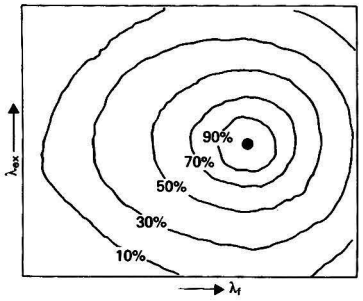

Fig. 6. Contour spectrum of a hypothetical fluorophore. The dark spot represents the wavelengths of maximum excitation and emission, and the contours join points with fluorescence intensities 90%, 70%, etc., of this maximum

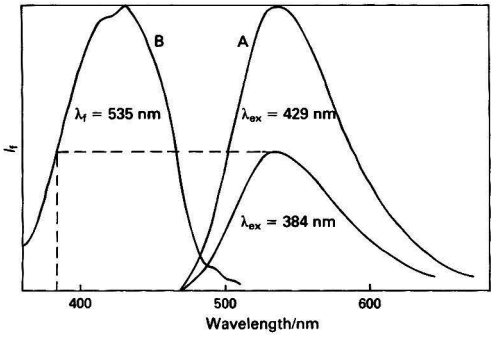

Fig. 7. Application of Vavilov's law in the fluorescence of Lucifer Yellow VS. The emission spectrum obtained at an excitation wavelength of 384 nm (at which the excitation spectrum is at half its maximum intensity) is the same shape as that obtained at the maximum excitation wavelength (429 nm) but has half the intensity

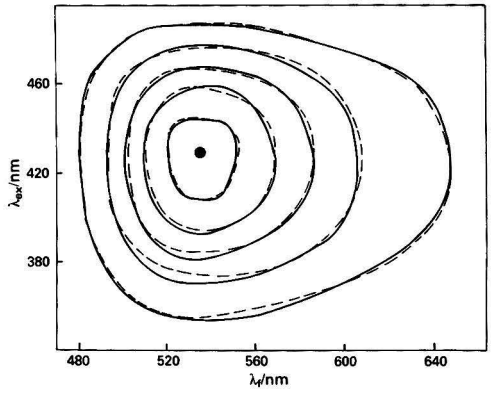

Fig. 8. Contour spectra of Lucifer Yellow VS. Experimental contours are continuous lines; broken lines are contours calculated from conventional excitation and emission spectra using Vavilov's law

(Fig. 9). It was shown over 10 years ago by Lloyd[20] that such spectra are simpler, narrower and hence more characteristic than conventional spectra. This extra selectivity is illustrated in Fig. 10. Three oil samples (a new sample of a light lubricating oil, a used sample of the same oil and a third unrelated oil) have conventional excitation and emission spectra that are remarkably similar. However, the synchronous spectra show clearly which oil is the odd one out;

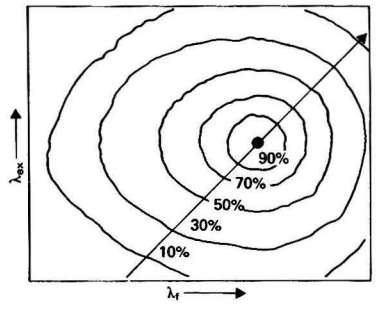

Fig. 9. Representation of a synchronous spectrum as a 45° section of a contour spectrum

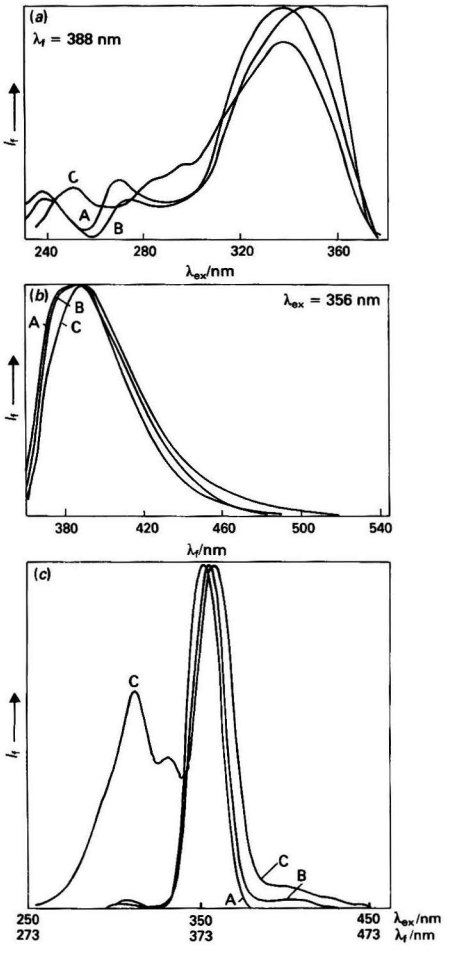

Fig. 10. Use of synchronous scanning spectrometry to characterise oil samples. Three oils (A–C) have similar (*a*) excitation and (*b*) emission spectra, but oil C has (*c*) a characteristic synchronous spectrum. The synchronous spectrum of B is very similar to that of A but has an additional high-wavelength component characteristic of a used oil

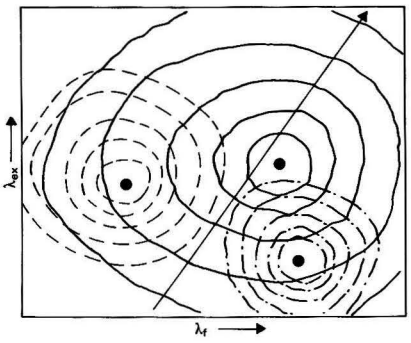

Fig. 11. Use of variable-angle synchronous scanning spectrometry to study a mixture of three fluorophores. The analyte is shown as continuous contours; interferences have broken contours. The scan shown narrowly fails to pass through the fluorescence maximum of the analyte, but achieves a high degree of discrimination against the interferences

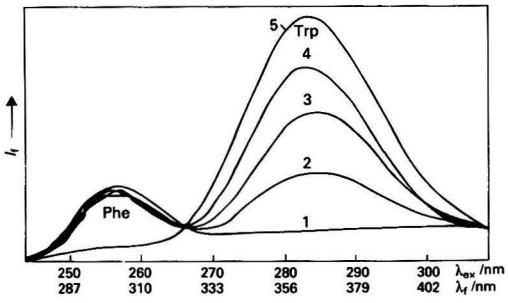

Fig. 12. Simultaneous analysis of phenylalanine (Phe) and tryptophan (Trp) by variable-angle synchronous scanning spectrometry. Excitation and emission monochromators had starting wavelengths of 245 and 275 nm, respectively, and were scanned at rates of 0.40 and 0.93 nm s^{-1}, respectively. Solutions contained 1, 50 μg ml^{-1} Phe; 2, 50 μg ml^{-1} Phe + 0.5 μg ml^{-1} Trp; 3, 50 μg ml^{-1} Phe + 1 μg ml^{-1} Trp; 4, 50 μg ml^{-1} Phe + 1.5 μg ml^{-1} Trp; and 5, 2 μg ml^{-1} Trp

moreover, the used oil shows small but very characteristic differences from its unused counterpart.

There is increasing interest in a further selective variant of fluorescence spectrometry, which we have called variable-wavelength or variable-angle synchronous scanning.[21] Fig. 11 shows the same contours as Fig. 6 but superimposed on them now are hypothetical contours of two further compounds. In this instance conventional spectroscopy will clearly be very non-selective, as one of the contaminants has the same excitation wavelength and the other contaminant the same emission wavelength as the target compound. It is evident, however, that a non-45° section through the matrix might still give a high degree of selectivity. Variable-angle synchronous scans can be obtained either indirectly (by accumulating the whole contour spectrum and using the interfaced computer to cut the desired section) or directly by scanning the two monochromators of the spectrometer at different rates. (In the example given it will evidently be necessary to scan the excitation monochromator faster than the emission monochromator.) Clearly, the latter approach will be the simpler and in the author's laboratory an instrument has been modified to record such spectra.[22] Two different but related types of application of variable-angle scanning are feasible. In addition to the type just mentioned, *i.e.*, optimum resolution of overlapping specta, there is a second application, illustrated in Fig. 12. Examination of the contours of the amino acids

phenylalanine and tryptophan shows that there is very little overlap between their spectra, so little that two entirely separate experiments would normally be necessary to determine both these compounds in a mixture. However, using variable-angle scanning both compounds can be studied in a single spectrum and can be determined in the presence of each other. This approach has a number of potentially interesting applications.

Fluorescence Immunoassays

This section considers some more applied aspects of luminescence spectrometry. An area of application of great current interest is the development of immunoassays. Such methods are largely used in clinical medicine at present, but they have tremendous potential also in veterinary, food and environmental analysis. Apart from the use of fluorescence as a detector in HPLC systems, immunoassays probably represent the most important current use for fluorescence methods, and the same will probably soon be true in chemiluminescence. Even more important, applications in this area present the same problems as are found in many other areas of application of fluorescence. So many of these problems and many of the possible solutions are of general relevance in fluorescence analysis.

Fluorescence immunoassays are of two general types.[23] Most attention recently has been devoted to the homogeneous type of assay.[24] This utilises the principle that the fluorescence properties of a labelled molecule may change when that molecule binds to an appropriate antibody. Antibody-bound and unbound molecules can thus be distinguished without a physical separation step, and the method is simple and easily automated. These homogeneous methods have the intrinsic disadvantage that any native fluorescence from the original samples is still present at the final measurement step of the immunoassay, and adversely affects the limits of detection attainable. In contrast, heterogeneous assays[25] require a separation for the physical separation of antibody-bound and unbound molecules; this is inconvenient, especially if automation is envisaged, but it at least serves to remove much of the background interference, and better limits of detection are consequently available.

Perhaps the best known type of homogeneous assay is that based on fluorescence polarisation studies.[26] Fluorescence polarisation measurements have been made for at least 60 years and have found several applications apart from immunoassays.[27] These include the reduction of scattered light interference, and studies of molecular shape, structure and interactions. In practice, the only instrumental modification required for polarisation studies involves the insertion of two polarising films immediately before and after the sample in the light path. The excitation polariser is generally oriented with a vertical plane of polarisation, and the emission polariser can be rotated to be oriented either vertically or horizontally. Electro-optic polarisers have recently been used with success. Automatic changing of the polariser orientation and rapid calculation of the polarisation value, p, is readily accomplished; p is given by $p = I_{\parallel} - I_{\perp}/I_{\parallel} + I_{\perp}$, where $I_{\parallel}$ and $I_{\perp}$ represent fluorescence intensities measured between parallel and crossed polarisers, respectively.

The significance of p is that it is close to zero for low relative molecular mass fluorophores which can tumble freely and lose all trace of their initial orientation during the 10 ns or so of the excited state lifetime. For macromolecules or macromolecular complexes, however, the tumbling motion is much slower, so their fluorescence emission is partially polarised. In an immunoassay this permits a distinction between the unbound fluorescent labelled molecule, which has p close to 0, and its antibody-bound counterpart. In the presence of a sample containing the unlabelled X molecule, the labelled molecule is displaced from the antibody and its polarisation falls. Fig. 13

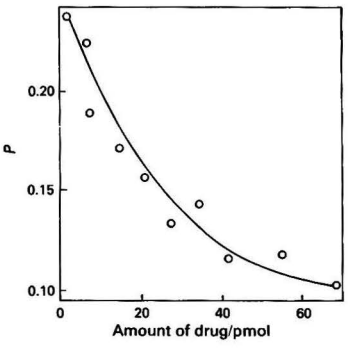

Fig. 13. Fluorescence polarisation immunoassay of lysergic acid diethylamide (LSD) using a fluorescein-labelled LSD derivative. Experimental details are given in reference 28

shows the application of this principle to the determination of a fluorescein derivative of LSD.[28] The measurements were made using a very simple fluorimeter, and the detected changes in the value of p were small, but picomolar levels of the drug could be determined. Such results were obtainable in pure solutions of the drug and in urine samples; much poorer limits of detection were obtained in serum samples, however, because of the fluorescence background effect already referred to.

A closer examination of this background signal is profitable. It is caused in part by scattered light and in part by the fluorescence of endogenous materials. The effects of scattered light are considerable; solutions containing proteins and other macromolecules scatter much more light than solutions of low relative molecular mass species, and many of the labels used in immunoassays have small Stokes shifts—fluorescein is the most obvious example—and so are particularly vulnerable to scattered light interference. A great number of methods for the reduction of background signals have been suggested; here two of them, the use of adsorbents and the use of fluorescence lifetime measurements, are discussed.

Blood serum samples contain about 7% by mass of protein, and many of the individual proteins are capable of binding small molecules, so it is reasonable to suppose that at least part of the background fluorescence of serum will be associated with the protein fraction. This is certainly true of the most intense fluorescence band of serum, with maximum emission at about 350 nm. Although this band is very broad and contributes to the background at wavelengths up to at least 450 nm (*cf.*, the discussion of bandwidth above), it is less important in practice than the much weaker fluorescence bands occurring in the visible region of the spectrum. There are two or three of the latter and it is astonishing that they are not better characterised. Studies are proceeding on the use of adsorbents to minimise these interferences in a rapid pre-assay column chromatographic step. Thus an immobilised form of Cibacron Blue, an active dye well known in preparative biochemistry[29] for its strong affinity for human serum albumin and some enzymes, is effective. If a sample of serum is passed through a small column of this affinity medium, the albumin is almost totally removed; the process takes only a few minutes and does not necessarily involve any serious dilution of the sample. A fluorescence band which occurs at about 440 nm is reduced by about two thirds by the action of the immobilised dye, and is therefore probably due to an albumin- or enzyme-bound fluorophore. In contrast, a further fluorescence band, centred at about 650 nm, is largely unaffected by the affinity column, so is presumably not due to albumin associated fluorescence. (It is worth noting that the existence of this latter band, which seems not to have been studied

before, puts into some doubt the assumption that high-wavelength labels are the most desirable in fluorescence immunoassays.) Suitable adsorbents, either singly or in combination, will be very effective in reducing the background fluorescence of serum, and they are cheap, rapid and simple to use. By removing proteins from the sample, they also contribute to a reduction of the scattered light interference.[30]

The possible use of fluorescence lifetimes in analytical work is based to a great extent on Weider's survey of the fluorescence lifetimes of organic molecules.[31] Most organic molecules have fluorescence lifetimes of less than 30 ns. The use of a fluorescent label with a lifetime of $\geqslant$50 ns in conjunction with a gated detector that only detects light emitted more than, *e.g.*, 50 ns after an exciting light pulse would largely eliminate the background fluorescence and scattering signals. In practice there are two versions of this approach. The first possibility, and the one more often attempted up to the present, has been to use lanthanide ions as labels. In principle this is a promising approach.[32,33] The lanthanides (in practice, terbium or europium) have lifetimes of about 1 ms, and the necessary time discrimination is readily accessible on instruments with pulsed xenon flash-tube sources, the pulse width being a few microseconds. Lanthanide fluorescence is also distinguished by very narrow spectral band widths (this will further help background rejection) and although the free ions are only feebly fluorescent, many of their chelate complexes can be detected at picogram levels.[34] A major difficulty in practice involves the production of complexes that do not dissociate when placed in a biological sample. At present the conclusion must be that this approach is photochemically easy, but chemically difficult. The second approach involves the use of a conventional fluorophore with a long lifetime; the group most often suggested is pyrene, with a lifetime of 100 ns or more.[35] This presents no chemical problems—for example, pyrenesulphonyl chloride is commercially available—but it requires a very sophisticated instrument to measure nanosecond lifetimes. In the future, simpler nanosecond spectrometers may be developed, and this approach will then be the more promising.

There is a further reason encouraging the use of organic labels in fluorescence lifetime immunoassays. The fluorescence transitions in lanthanide ions arise from energy levels that are well protected from the environment and that are therefore not likely to change much when, for example, a lanthanide labelled material is bound to an antibody. The chances of developing a homogeneous assay are thus small. The lifetimes of conventional organic molecules are, in contrast, very susceptible to minor changes in structure and environment,[36] and might well be suitable for the development of homogeneous assays. One reason for caution is that even pure samples of some compounds may show non-exponential decays.[37] Whatever the reason for this phenomenon it could complicate data handling in lifetime assays.

The significance of light scattering interference has already been mentioned; a third possible way of reducing it is to have no incident light source at all, that is, to use a chemiluminescence immunoassay. The development of a variety of chemiluminescence and bioluminescence assays, which combine simple equipment with exquisite sensitivity, has been one of the major developments in analytical science in recent years.[38,39] So far as immunoassays are concerned most attention has been given to methods involving luminol[40] and acridine labels.[41] Despite very low quantum yields (often $\leqslant$1%) and some difficulties in preparing labelled compounds these assays have proved very sensitive, but they seem to suffer from non-specific quenching interferences and have yet to make a serious impact on the real world of immunoassay.

Also worthy of attention is a different form of chemiluminescence assay, based on the reaction of an oxalate ester, such as bis(2,4,6-trichlorophenyl) oxalate, TCPO, with hydrogen peroxide. This reaction generates a highly energetic intermediate which is capable of exciting the luminescence of many conventional fluorophores. This reaction has been known for at least 16 years[42] and its analytical use was first investigated about 8 years ago,[43] but it has not so far been widely applied[44] to the immunoassay area. Its potential advantages are clear. Apart from the elimination of scattered light effects, the TCPO reaction has a high quantum yield (typically 20–25%) and can be used to excite the fluorescence of conventional and easily handled fluorophores such as fluorescein, fluorescamine and dansyl. Such labels can be introduced very readily into a variety of analyte molecules. The TCPO reaction can also be studied using simple luminometers, and the combination of luminometry and flow injection analysis (FIA) is especially suitable, because very reproducible reagent mixing is required in chemiluminescence assays, and FIA provides just that.[45] It has proved possible to detect about 10 fmol of fluorescein with a relative standard deviation of *ca.* 3% using only a modified filter fluorimeter as detector: similarly *ca.* 10 pmol concentrations of fluorescamine derivatives can be detected, whereas it is difficult to detect sub-nanomolar concentrations by conventional fluorimetry. The TCPO reaction has been used to detect trace amounts of fluorescent labelled molecules after HPLC separation,[46] with the TCPO reaction being used in a fairly simple post-column reactor. Limits of detection for intrinsically fluorescent hydrocarbons are apparently not so good, but the discovery of the enhanced detection limits with amino derivatives is very interesting and merits further study.[47]

The use of the TCPO and similar systems in immunoassays reveals two particular difficulties. One is the non-specific quenching problem mentioned above; this seems to be a drawback of chemiluminescent systems and it will be as important to overcome it as it is to reduce background signals in fluorescence assays. Recent work indicates that the extent of quenching by proteins in the TCPO system may be dependent on the relative molecular mass of the proteins.[48] A second major problem is that TCPO is not water soluble. Not only is it rapidly hydrolysed in aqueous systems, it also forms turbid solutions. Neither this possibility, nor the use of mixed organic - aqueous solvent systems, is satisfactory in immunoassays. However, recent work in the author's laboratory shows that it is possible to overcome both these problems and to develop a series of highly sensitive assays that are very easy to perform.

Conclusions

This brief survey has omitted topics such as the use of lasers as light sources in fluorimetry,[49] derivative fluorescence spectrometry,[50] the encouraging developments in room-temperature phosphorimetry,[51,52] the use of matrix isolation methods,[53] the interesting possibilities of fluorimetry in micellar solutions,[54,55] combinations of luminescence methods and thin-layer chromatography[56] and new bioluminescent systems.[57] However, it is apparent that, with the increasing demand for highly sensitive and selective analyses in many areas of organic and biological chemistry, photoluminescence and chemiluminescence techniques will continue to provide important and fascinating fields of research.

I thank the Science and Engineering Research Council, the Medical Research Council, The Home Office, The Department of Health and Social Security, Perkin-Elmer Ltd., Baird Atomic Ltd., Glaxo Operations UK and The Boots Company for financial support of research in the areas described in the paper. I also thank Professor D. Thorburn Burns of The Queen's University, Belfast, and Professor J. W. Bridges of the University of Surrey for their long-standing co-operation and many research colleagues for their essential contributions.

References

1. Serio, M., and Pazzagli, M., *Editors*, "Luminescent Assays," Raven Press, New York, 1982.
2. Parker, C. A., "Photoluminescence of Solutions," Elsevier, Amsterdam, 1968.
3. Stewart, W. W., *Nature (London)*, 1981, **292**, 17.
4. Roberts, G. C. K., *in* Miller, J. N., *Editor*, "Standards in Fluorescence Spectrometry," Chapman and Hall, London, 1981, p. 49.
5. Velapoldi, R. A., and Mielenz, K. D., *Natl. Bur. Stand. (U.S.) Spec. Publ.*, 1980, No. 260–64.
6. Jadamec, J. R., Saner, W. A., and Talmi, Y., *Anal. Chem.*, 1977, **49**, 1316.
7. Pellizzari, E. D., and Sparacino, C. M., *Anal. Chem.*, 1973, **45**, 378.
8. Schulman, S. G., "Fluorescence and Phosphorescence Spectroscopy: Physicochemical Principles and Practice," Pergamon Press, Oxford, 1977.
9. Varmuza, K., "Pattern Recognition in Chemistry," Springer-Verlag, Berlin, 1980.
10. Lyons, J. N., Hardesty, P. T., Baer, C. S., and Faulkner, L. R., *in* Wehry, E. L, *Editor*, "Modern Fluorescence Spectroscopy," Volume 3, Plenum Press, New York, 1981, p. 1.
11. Mulkerrin, M. G., and Wampler, J. E. *Anal. Chem.*, 1982, **54**, 1778.
12. Tamura, T., Tenabe, K., Hirashi, J., and Saeki, S., *Bunseki Kagaku*, 1979, **28**, 591.
13. Wampler, J. E., Mulkerrin, M. G., and Rich, E. S., *Clin. Chem. (Winston-Salem, NC)*, 1979, **25**, 1628.
14. Christian, G. D., Callis, J. B., and Davidson, E. R., *in* Wehry, E. L., *Editor*, "Modern Fluorescence Spectroscopy," Volume 4, Plenum Press, New York, 1981, p. 111.
15. Giering, L. P., *Ind. Res. Dev.*, 1978, **20**, 134.
16. Birks, J. W., "Photophysics of Aromatic Molecules," Wiley-Interscience, London and New York, 1970.
17. Tatischeff, I., and Klein, R., *in* Birks, J. B., *Editor*, "Excited States of Biological Molecules," Wiley, London, 1976, p. 375.
18. Vo Dinh, T., *Anal. Chem.*, 1978, **50**, 396.
19. Williams, W. P., Murtz, N. R., and Rabinovitch, E., *Photochem. Photobiol.*, 1969, **9**, 455.
20. Lloyd, J. B. F., *Nature (London)*, 1971, **231**, 64.
21. Eastwood, D., *in* Wehry, E. L., *Editor*, "Modern Fluorescence Spectroscopy," Volume 4, Plenum Press, New York, 1981, p. 251.
22. Miller, J. N., Ahmad, T. A., Bower, A. F., and Fell, A. F., to be published.
23. Smith, D. S., Hassan, M., and Nargessi, R. D., *in* Wehry, E. L., *Editor*, "Modern Fluorescence Spectroscopy," Volume 3, Plenum Press, New York, 1981, p. 143.
24. Ullman, E. F., Bellet, N. F., Brinkley, J. M., and Zuk, R. F., *in* Nakamura, R. M., Dito, W. R., and Tucker, E. S., *Editors*, "Immunoassays; Clinical Laboratory Techniques for the 1980s," Alan R. Liss, New York, 1980, p. 13.
25. Maggio, E. T., *in* Nakamura, R. M., Dito, W. R., and Tucker, E. S., *Editors*, "Immunoassays; Clinical Laboratory Techniques for the 1980s," Alan R. Liss, New York, 1980, p. 1.
26. Dandliker, W. B., Kelly, R. J., Dandliker, J., Farquhar, J., and Levin, J., *Immunochemistry*, 1973, **10**, 219.
27. Weigert, F., *Z. Phys.*, 1922, **23**, 232.
28. Hubbard, A. R., Miller, J. N., Law, B., Mason, P., and Moffat, A. C., *Anal. Proc.*, 1983, **20**, 606.
29. Travis, J., Bowen, J., Tewksbury, D., Johnson, D., and Pannell, R., *Biochem. J.* 1976, **157**, 301.
30. Miller, J. N., and Gossain, V., to be published.
31. Weider, I., *in* Knapp, W., Holubar, K., and Wick, G., *Editors*, "Proceedings of the 6th International Conference on Immunofluorescence," Elsevier-North Holland, Amsterdam and New York, 1978, p. 67.
32. Soini, E., and Kojola, H., *Clin. Chem. (Winston-Salem, NC)*, 1983, **29**, 65.
33. Meurman, O. H., Hemmila, I. A., Lovgren, T. N., and Halonen, P. E., *J. Clin. Microbiol.*, 1982, **16**, 920.
34. Petterson, K., Sutari, H., Hemmila, I. A., Soini, E., Lovgren, T., Hanninen, V., Tanner, P., and Stenman, U.-H., *Clin. Chem. (Winston-Salem, NC)*, 1983, **29**, 60.
35. Spencer, R. D., Vaughan, W. M., and Weber, G., *in* Lim, E. C., *Editor*, "Molecular Luminescence," W. A. Benjamin, New York, 1969, p. 72.
36. Cline Love, L. J., and Shaver, L. A., *Anal. Chem.*, 1980, **52**, 154.
37. Gauduchon, P., Donzel, B., and Wahl, P., *in* Birks, J. B., *Editor*, "Excited States of Biological Molecules," Wiley, London, 1976, p. 404.
38. Cormier, M. J., Hercules, D. M., and Lee, J., *Editors*, "Chemiluminescence and Bioluminescence," Plenum Press, New York and London, 1973.
39. DeLuca, M. A., *Editor*, "Bioluminescence and Chemiluminescence," (*Methods in Enzymology*, Volume 57), Academic Press, New York, 1978.
40. Hersh, S. L., Vann, W. P., and Wilhelm, S. A., *Anal. Biochem.*, 1979, **93**, 267.
41. Simpson, J. S. A., Campbell, A. K., Woodhead, J. S., Richardson, A., Hart, R., and McCapra, F., *in* DeLuca, M., and McElroy, W. D., *Editors*, "Bioluminescence and Chemiluminescence," Academic Press, New York, 1981, p. 673.
42. Rauhut, M. M., Bollyky, L. J., Roberts, B. G., Loy, M., Whitman, R. H., and Iannotta, A. V., *J. Am. Chem. Soc.*, 1967, **89**, 6515.
43. Williams, D. C., Huff, G. F., and Seitz, W. R., *Anal. Chem.*, 1976, **48**, 1003.
44. Mandle, R. M., and Wong, Y. N., *Int. Pat. Appl.*, No. PCT/US80/01485, 1981.
45. Mahant, V. K., Miller, J. N., and Thar, H., *Anal. Chim. Acta*, 1983, **145**, 203.
46. Kobayashi, S., and Imai, K., *Anal. Chem.*, 1980, **52**, 424.
47. Sigvardson, K. W., and Birks, J. W., *Anal. Chem.*, 1983, **55**, 432.
48. Mahant, V. K., *PhD Dissertation*, Loughborough University of Technology, 1983.
49. Richardson, J. H., *in* Wehry, E. L., *Editor*, "Modern Fluorescence Spectroscopy," Volume 4, Plenum Press, New York, 1981, p. 1.
50. Miller, J. N., Ahmad, T. A., and Fell, A. F., *Anal. Proc.*, 1982, **19**, 37.
51. Miller, J. N., *Trends Anal. Chem.*, 1981, **1**, 31.
52. Parker, R. T., Freedlander, R. S., and Dunlap, R. B., *Anal. Chim. Acta*, 1980, **120**, 1.
53. Stroupe, R. C., Tokousbalides, P., Dickinson, R. B., Wehry, E. L., and Mamantov, G., *Anal. Chem.*, 1977, **49**, 701.
54. Zachariasse, K. A., *Chem. Phys. Lett.*, 1978, **57**, 429.
55. Kalyanasundaram, K., Gneser, F., and Thomas, J. K., *Chem. Phys. Lett.*, 1977, **51**, 501.
56. Hurtubise, R. J., "Solid Surface Luminescence Analysis," Marcel Dekker, New York, 1981.
57. Dunlap, J. C., Hastings, J. W., and Shimomura, O., *Proc. Natl. Acad. Sci. USA*, 1980, **77**, 1394.

Paper A3/307
Received September 6th, 1983

Capillary Separation Methods: a Key to High Efficiency and Improved Detection Capabilities

Plenary Lecture

Milos Novotny
Department of Chemistry, Indiana University, Bloomington, IN 47405, USA

The current status of capillary separation techniques is reviewed. While capillary gas chromatography has reached a degree of maturity with respect to both column technology and instrumental systems, capillary separations with the condensed mobile phases still present many challenges to future developments. At present, micro-column liquid chromatography offers both chromatographic performance and novel detection techniques owing to the very low flow-rates encountered with this method; some unique applications have already appeared. Capillary supercritical fluid chromatography has also attracted much attention during the last 2 years because of its unique position between gas chromatography and high-performance liquid chromatography. High-voltage capillary electrophoresis shares some instrumental aspects with the remaining capillary techniques, but also offers some distinct advantages of its own.

Keywords: *Capillary separation; gas chromatography; capillary supercritical fluid chromatography*

Throughout the entire history of modern chemistry, there has been a continuing (and at certain times intensive) effort to identify and measure various chemical substances in increasingly smaller amounts and doing so in extremely complex sample matrices is hardly unique to the current scientific efforts. Let us be reminded of the outstanding work of the past generations of chemists who established, for the first time, the presence of mammalian hormones, vitamins, insect pheromones, alkaloids, etc., in plant and animal samples that often contained hundreds or thousands of interfering compounds. Likewise, the discovery that benzo[*a*]pyrene is a cancer-causing principle of coal tar (through its isolation, structural elucidation and biological testing) was a non-trivial task in view of the complexity of the sample. All this important work of the past generations is even more admirable if we consider the primitive analytical techniques that those pioneers of modern science had at their disposal.

While many primary objectives of analysing complex samples today are somewhat similar to those of past generations of chemists, *i.e.*, identification and accurate measurement of the substances of interest, the pace at which this task is accomplished has increased dramatically. Reliable analyses of complex organic mixtures are frequently a key to the solution of many problems facing our technological society. During the last two decades, high-resolution chromatography and electrophoresis have started to assume a central role in such endeavours. An extensive application of high-resolution separation techniques is also desirable for the further development of reliable measurement techniques based on modern spectroscopy and electrochemistry.

It has rapidly become established that the concept of the open tubular chromatographic column, developed in the late 1950s by M. J. E. Golay,[1] has been one of the most important developments in modern analytical chemistry. However, only after two decades has capillary gas chromatography reached a high degree of maturity through the necessary instrumental developments and highly sensitive detection and ancillary techniques. Although the method is obviously confined to relatively volatile compounds, it has now been applied widely in analytical practice.

During recent years, the geometrical simplicity of the open tubular column has also invited both theoretical and instrumental developments with condensed mobile phases. Thus, the methods of capillary liquid chromatography, capillary supercritical fluid chromatography and capillary zone electrophoresis have recently emerged as worthwhile areas of analytical research. While the necessary instrumental developments in these directions are technologically demanding, the same has been true of almost any new analytical development in the past. The goal of high resolution with complex non-volatile mixtures is eminently worthwhile in itself. In addition, some unique analytical advantages are offered through this direction.

Both fundamental developments and a wealth of new applications have been particularly characteristic of capillary separation techniques during the last decade. This paper attempts to summarise the most important developments in this field and to point out certain directions that are worth pursuing and may be particularly fruitful in the near future.

Capillary Gas Chromatography

After a relatively slow period during the 1960s, a sudden increase of interest in capillary gas chromatography (GC) has been characteristic for the last decade. The main reasons for this were that certain patent restrictions were eased, opening the area for a wide-scale commercialisation; that technology of highly efficient and inert glass capillary columns was sufficiently developed; and that several relatively simple procedures for direct sample introduction were devised. The development of flexible fused-silica capillary columns by Dandeneau and Zerenner[2] further removed "the psychological barrier" that numerous chemists have had with respect to the relatively fragile glass capillaries. Further instrumental developments and various forms of professional education in this "technique-orientated" analytical approach have also played a significant role in the acceptance of capillary GC as both a research and routine analytical method.

Perhaps the most exciting period in the over-all development of capillary GC is associated with glass capillary columns. Using such column types, Desty's initial success[3] with petrochemical applications was soon followed by the separations of isotopic molecular species[4] and, eventually, some extremely complex mixtures such as tobacco smoke.[5,6] As the earlier applications of capillary GC employed almost exclusively split injection, the biochemical and environmental applications of this method were not feasible (owing to typically limited sample amounts) until new sampling procedures became available during the 1970s. With the arrival of such concentration and splitless injection techniques, the

prevailing view that capillary GC was an unattractive method for trace analysis became no longer justified. There is extensive use of this technique in environmental analysis and biochemical research and there are now numerous examples of trace determinations.[7–9]

The importance of improved sampling methods for quantitation in capillary GC can hardly be overstated. Direct injection procedures have been developed during the last decade that utilise large aliquots of available samples for analysis, while minimising the initial band dispersion at the capillary column inlet. The splitless injection method that employs the so-called "solvent effect",[10] the falling-needle technique[11,12] and various pre-column methods[13–16] are among the most versatile approaches to sample introduction in capillary GC. Some of these sampling techniques have been automated, resulting in improved reproducibility. It is felt that the pre-column sampling methods deserve increasing use in analytical work, as they frequently serve a double function: removal of solvents or derivatisation agents; and protection of the analytical column from non-volatile impurities contained in the injected samples. The chemical nature of pre-column packing can also be varied to suit a particular sample type. The principle of "selective sampling," *i.e.*, various forms of double-column GC procedures, has been increasingly advocated to improve various aspects of capillary GC determination.[16,17]

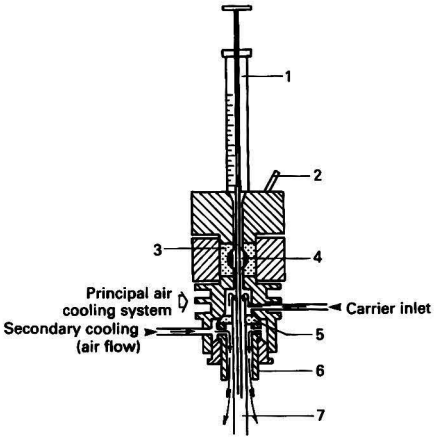

Fig. 1. Capillary on-column injector, including the secondary cooling system. 1 = Microsyringe; 2 = valve lever; 3 = valve seal; 4 = stainless-steel rotating valve; 5 = column seal; 6 = cooling jacket; 7 = capillary column. Reproduced from reference 19 with permission of Elsevier Publishing Company

One of the most important recent advances in capillary GC appears to be the method of direct (on-column) sample deposition developed by Grob and co-workers[18,19]; in this method a thin syringe needle is inserted directly inside a 0.2–0.4 mm i.d. capillary column (see Fig. 1), while depositing a "cold sample" on to the first column segment. While this sampling procedure is obviously technique-orientated, and cannot be readily automated for routine work, a quantitative sample transfer is achieved under the correct operating conditions. Excellent quantitative results have been reported[19] to counter a general scepticism following the introduction of this sampling technique. The major advantages of this on-column sampling procedure are a minimum thermal decomposition of labile compounds (observed occasionally with other injector types), as well as the lack of discrimination towards the later eluting components.

Gradually improving capillary column technology has also been crucial in quantitative determinations. While the problems of deposition of various stationary phases on the column wall in the form of a uniform film have finally been solved to provide efficient columns, increasingly the attention of researchers has now been turned towards column deactivation problems (removal of "residual adsorption" associated with the column wall). There is a general agreement that the fused-silica capillaries are much easier to deactivate than glass capillaries. Numerous examples of chromatography with "difficult samples," such as either strongly basic or acidic compounds at low-nanogram amounts, are now demonstrated throughout the literature.

Preparation of the immobilised films of liquid phases[20–22] has also added to the over-all analytical capability of capillary GC. Immobilised polymeric phases are essential to the correct use of the on-column sampling techniques. With ordinary stationary phases, migration of the film easily occurs following the sample injection, thus causing adsorption problems at the column inlet and a possible loss of column efficiency. Various aspects of capillary column technology have been reviewed recently.[23]

A decrease in the column diameter leads to further increases in the column efficiency, as well as a shortening of analysis time. These effects are a straightforward consequence of the chromatographic theory. Desty has already demonstrated the power of this approach in his pioneering work[3] on capillary GC. Recently, several laboratories have started to pursue this direction further. As calculated by Guiochon,[24] the small-diameter columns (around 50–100 μm) could be utilised if certain sampling and detection-volume problems were adequately solved. Although it is quite clear that significant departures from today's GC instrumental parameters will be necessary to make this approach attractive to analytical laboratories, some preliminary results appear promising. As an example, Fig. 2 shows a chromatographic

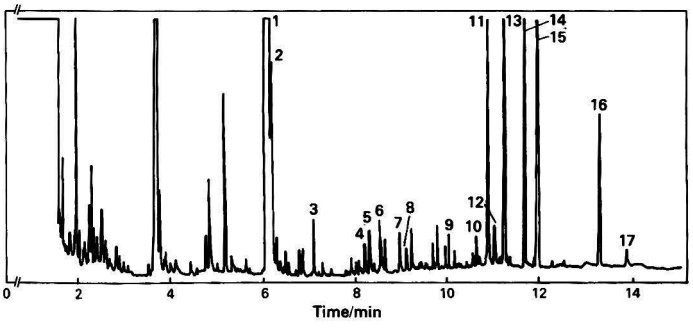

Fig. 2. A capillary GC profile of the silylated components from a uraemic serum, using the splitless injection technique. Reproduced from reference 25 with permission of Hüthig Publishers.

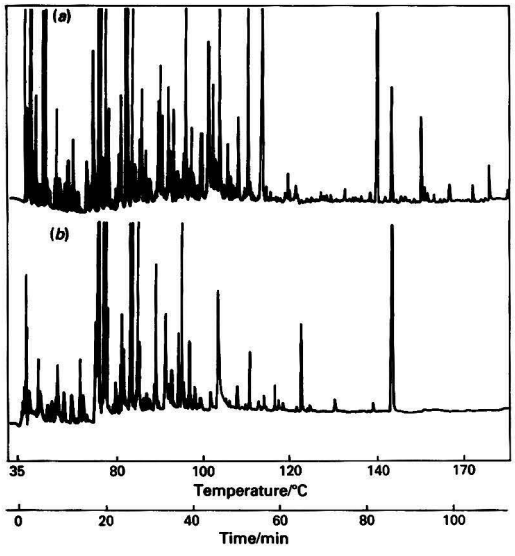

Fig. 3. Capillary chromatograms of volatiles from a 24-h urine of a normal male detected by: (*a*) a flame ionisation detector; and (*b*) a nitrogen-sensitive thermionic detector. Reproduced from reference 26 with permission of Elsevier Publishing Company

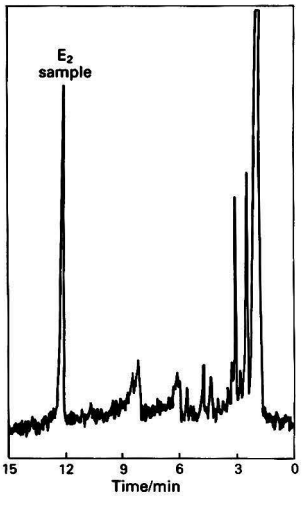

Fig. 4. Mass-fragmentographic analysis of estradiol from a sample of female rat plasma. Reproduced from reference 32 with permission of Elsevier Publishing Company

profile of body fluid constituents[25] that was obtained (with an 8.5 m × 50 μm i.d. capillary column) in an analysis time considerably shorter than is achievable with conventional, 0.25 mm i.d., columns. However, with decreased column diameters and film thicknesses, column capacity and surface deactivation problems become more apparent.

Contemporary GC offers an impressive number of highly sensitive and selective detectors and ancillary tools. Fortunately, capillary GC combines effectively with most of these devices and, in some instances, even strengthens their capabilities. Thus, flame ionisation detectors, as well as the selective flame detectors based on the flame-photometric and thermionic principles, are now commonly employed with capillary columns. While the detection selectivity is often needed to trace the compounds of interest in complex sample matrices, peak by peak comparisons of chromatograms obtained simultaneously with a universal and a selective detector (see, for example, reference 26, Fig. 3) can often have considerable value in peak identification studies (provided that some other information is available). A parallel operation of several detectors combined with a single capillary column is now technically feasible.

Whereas the widely used flame-photometric and thermionic detectors provide the often-needed selectivity towards certain elements (nitrogen, phosphorus, sulphur, etc.) in the separated molecules, there is still a need for additional detection capabilities in capillary GC. Thus, the search in this area is likely to continue for some time. An example of the adaption of a previously used detection principle to capillary GC is shown in a recent work by Estes *et al.*[27] on the microwave plasma detection of lead compounds in gasoline.

Detectors that benefit most from their combination with capillary columns are various concentration-sensitive devices. As the column diameters are small, and the volumetric flow-rates are correspondingly reduced, the mass sensitivity of these concentration-sensitive detectors is significantly enhanced. Numerous efforts have therefore been made to design such detectors with very small volumes, including the electron capture,[28] the ultraviolet spectroscopic[29] and the photoionisation[30] detectors. Significant increases in mass sensitivity appear to make it worthwhile miniaturising the detector cells further.

Mass spectrometry has become the most important ancillary method to GC. Advances in both coupling technology and mass spectrometer design have made it now entirely feasible to monitor the capillary column effluent in both low- and high-resolution spectral modes of operation. More recently, Fourier-transform infrared spectroscopy has also been effectively combined with capillary GC,[31] reducing an earlier gap between sensitivities of mass-spectral and optical methods. Besides their obvious identification power, both ancillary methods can also be employed as highly selective GC detectors. An example of this is seen in widely used mass-fragmentographic techniques that revolutionised pharmacological, biomedical and environmental monitoring procedures. Impressive sensitivites down to less than picogram amounts have now been widely documented using a mass spectrometer as a "selective detector." A typical demonstration[32] of such a progress in high-sensitivity measurements is Fig. 4; here, a perfluorinated derivative of the female hormone, 17β-estradiol, has been measured selectively from a 120-μl aliquot of rat plasma.

Capillary Liquid Chromatography

Liquid chromatography (LC) becomes the obvious choice for a separation method if a sample lacks either volatility or chemical stability, an effective use of GC thus being prevented. The rapid growth of high-performance liquid chromatography (HPLC) during the last decade has made numerous new applications feasible; with this method, sample complexity problems are typically attacked through the detection selectivity approach. There are, however, many instances where this approach falls short in providing adequate results without improved chromatographic efficiency.

Some attempts have recently been made to provide an equivalent to capillary GC in the area of LC, as far as resolving power is concerned. Although theoretical prediction of the separating potential for both GC and LC[33] places the latter in a very competitive position, LC column efficiencies of the order of 10^3 theoretical plates were the state of the art until recently.

Since 1976, our research group at Indiana University has been exploring various ways of increasing the resolving power of LC techniques. Firstly, the potential of (semi-permeable) packed capillaries[34] and open tubular columns[35] was briefly assessed. The small values of the solute diffusion coefficients in the mobile phase dictate that the column dimensions should be reduced drastically compared with the situation encountered in capillary GC. Such column dimensions, in turn, dictate extensive miniaturisation of the sample introduction and detection technology. While microlitre-volume instrumental components are quite acceptable in conventional HPLC, nanolitre volumes are generally required to comply with the small dimensions and extremely low flow-rates associated with LC micro-columns. Approaches toward the miniaturisation of LC equipment have been first described in the pioneering studies of Ishii *et al.*[36] and Scott and Kucera.[37]

It appears that effective utilisation of open tubular columns in LC will not be feasible for at least several years because of the enormous technological difficulties associated with the approach. The optimisation studies by Knox and Gilbert[38] and Jorgenson and Guthrie[39] show that the capillary inner diameters must be reduced to 10 μm or less. Without a major technological breakthrough, it may be difficult to achieve this "ultimate goal." Yet, significant improvements have already been made through the work of Ishii *et al.*[40] and Tsuda *et al.*,[41] who successfully explored open tubular columns with inner diameters below 30 μm. Such efforts are exemplified by Fig. 5,[40] showing separation of synthetic oligomers on an open tubular column operated in a reversed-phase mode.

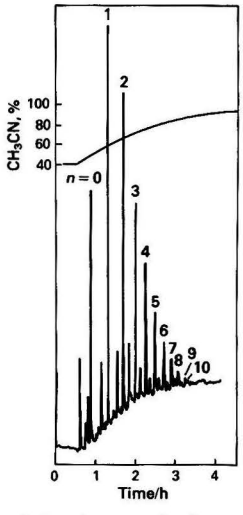

Fig. 5. Gradient elution of epoxy resin oligomers from a 22 m × 31 μm i.d. open tubular column, bonded with an octadecylsilyl stationary phase. Column temperature 44 °C; UV detection at 225 nm. Reproduced from reference 40 with permission of Elsevier Publishing Company

At this stage of development it should be noted that "capillary LC" is not necessarily synonymous with "open tubular LC." Additional types of columns that fall under this loosely defined category include the above mentioned semi-permeable packed capillaries[34,42] as well as slurry-packed columns of capillary dimensions.[43–45] The geometrical characteristics of different micro-columns are illustrated in Fig. 6.

While separating power, *i.e.*, large numbers of theoretical plates, was among the chief incentives to research on micro-column HPLC originally, realisation of some unique additional capabilities of this method quickly followed. These additional advantages are a direct consequence of drastically reduced flow-rates: decreased consumption of expensive or environmentally hazardous mobile phases; and the possibility of using "exotic" mobile phases for the sake of either improved separation or detection techniques.

In order to receive such benefits of micro-column LC, it is essential that the over-all chromatographic system be designed to match the geometrical characteristics of the micro-columns. Specifically, sampling and detection volumes must be drastically reduced in order to minimise extra-column broadening of the chromatographic zones. Much effort has already gone into designing miniaturised LC systems; however, new technological directions are still needed. Fortunately, coherent laser beams and micro-electrodes, among other approaches, are perfectly in tune with the very small (nanolitre) detection volumes that are required in micro-scale HPLC.

While certain conventional detectors have now been miniaturised to volumes below 100 nl,[36,46–48] outstanding opportunities now exist for new directions in HPLC detection. In contrast with a typical flow-rate of 1 ml min^{-1} in conventional HPLC, capillary micro-columns pass only a few μl min^{-1} into a detector. These drastically reduced flow-rates make it now feasible to couple micro-columns directly to the flame detectors[49–51] or a mass spectrometer.[52] The flame and plasma detection devices, in conjunction with micro-columns, may hold a key to the development of a highly desirable (so far, largely undeveloped) element-selective detection in HPLC. An example of such flame detection devices is shown

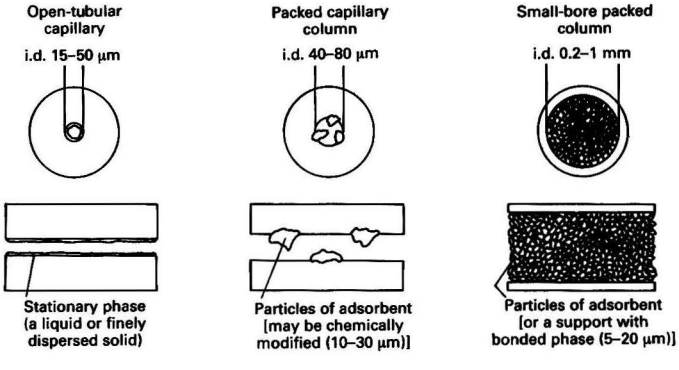

Fig. 6. Types of LC micro-columns

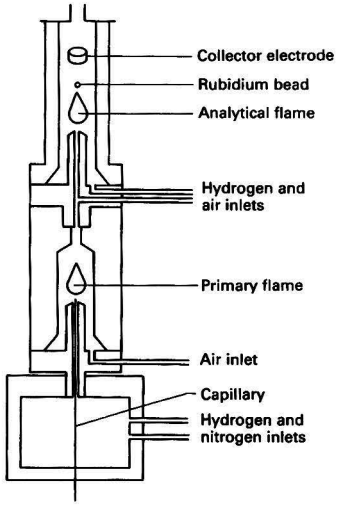

Fig. 7. Dual-flame thermionic detector for micro-column LC

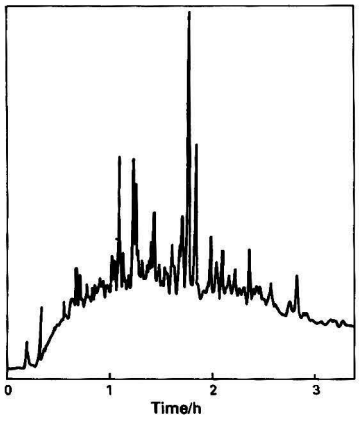

Fig. 8. High-efficiency separation of polycyclic aromatics from the neutral fraction of a coal-derived fluid on a 0.85 m × 240 μm i.d. capillary, packed with 3 μm ODS particles. Reproduced from reference 44 with permission of Pergamon Press

in Fig. 7. This particular detector is used in a thermionic mode[50,51] for the selective detection of solutes containing phosphorus or, alternatively, nitrogen atoms in their structures. Unlike its well known GC counterpart, which utilises a single flame and a rubidium source, the micro-scale LC detector has two flames: the primary flame, which causes combustion, solute volatilisation and breakdown; and the analytical flame, which can be optimised for a maximum response. Performance, analytical attributes, as well as some applications of this detector, have recently been described.[51] In addition, the flame photometric detection principle has also been successfully explored in micro-scale LC.[49] Both types of detectors possess sensitivities down to the low nanogram levels; actually, their typical sensitivities are only 1–2 orders of magnitude worse than those encountered in GC detection.

As certain devices for sampling nanolitre volumes into HPLC micro-columns have gradually been developed[39,46,51] together with satisfactory column technology, the last 2 years have marked the beginning of some unique applications of the miniaturised LC techniques. While development of open tubular HPLC still remains a matter for future studies, packed capillary columns of the types shown in Fig. 6 offer currently the best compromise between column performance and sample capacity.

With the use of slurry-packed capillary columns[44] and miniaturised UV or fluorescence detectors, our laboratory has been able to resolve complex non-volatile mixtures, such as those derived from coal liquids[52] or biological samples.[53–55] An example is shown in Fig. 8; a 0.85 m × 240 μm i.d. column, packed with 3 μm ODS particles (generating over 110 000 theoretical plates), has been used to resolve an aromatic mixture of up to nine-ring polycyclic compounds.[44,52] Compounds that do not possess readily detectable features in their molecules can frequently be "tagged" with appropriate structural moieties prior to chromatography. Whereas the post-column derivative formation has proved popular in overcoming certain detection problems in the past, there is significant rationale to explore increasingly the formation of suitable derivatives prior to micro-column LC. A certain loss of the solute - solvent interaction selectivity can be compensated for by a significant increase in plate numbers and a choice of chemical derivatisation scheme is not restricted to fast reactions only. Recently, our laboratory has successfully applied several useful pre-column derivatisation procedures to enhance detection capabilities for complex mixtures of steroids,[53–55] prostaglandins,[55] bile acids[54] and biological ketones.[56]

With concentration-sensitive detectors, mass sensitivity can be significantly enhanced by the use of micro-columns and small-volume detectors.[57] This advantage has now been demonstrated for UV, spectrofluorimetric and electrochemical detectors. Outstanding examples of this have been demonstrated in a recent paper of Manz and Simon,[58] who employed open tubular LC and a miniaturised ion-selective electrode to achieve femtomole sensitivities, and a communication of Knecht *et al.*[59] on a micro-voltammetric detector.

The use of a laser as an excitation source for fluorescence detection has the predictable effect of signal enhancement because of the high intensity of the incident beam. Several laser-based LC detection systems have been reported in the literature.[60–63] Among them, we find the helium - cadmium laser particularly attractive because of its relatively low cost and simplicity; in our laboratory, certain reagents have been synthesised[54,55] so that their optimum fluorescent properties are compatible with the 325-nm characteristic emission of the helium - cadmium laser. The use of appropriate laser detection systems in micro-column LC should result in sub-picogram detection possibilities for numerous biologically and environmentally important substances.

Capillary Supercritical Fluid Chromatography

The first attempts at supercritical fluid chromatography (SFC) can be traced to a pioneering study of Klesper *et al.*,[64] who achieved the migration of porphyrins using a chromatographic column with a pressurised Freon mobile phase. Interesting, but technologically demanding, investigations of the 1960s into SFC were largely overshadowed by the advent of a new, powerful and simple method of HPLC. However, certain obvious merits of SFC, for both analytical and preparative purposes, have recently been re-evaluated. In particular, the idea of using open tubular columns in SFC[65] has revitalised the general approach.

When used under appropriate conditions, certain supercritical fluids can combine advantages of both gases and liquids. Importantly, the values of solute diffusivity and viscosity, which are of the utmost importance to a chromatographic process, are, in SFC, between those encountered in the gas and liquid phases. However, the fluid densities approach those of liquids; gradually increasing densities are

important to achieve solvation of large, non-volatile molecules during pressure-programmed chromatographic runs. A simple control of retention through pressure-induced equilibrium shifts without a change of solvent composition is of much importance to certain spectroscopic techniques (*e.g.*, IR detection). In comparison with liquids, some supercritical fluids give only minimum background signals in certain detectors. In addition, they are far easier to remove from the measured solute molecules prior to detection in flames or a mass spectrometer.[66]

An optimisation study[67] of capillary SFC indicates that, under reasonable conditions, efficiencies in the range of 10^5–10^6 theoretical plates can be attained. Such high efficiencies are now feasible with capillary inner diameters between 50–100 μm. This is now well within the technological possibilities of low-volume sampling and detection, as previously developed for micro-column LC. A typical capillary SFC system[65] is shown in Fig. 9. A high pressure syringe pump is filled with an appropriate fluid, which is subsequently transformed into a supercritical medium in a heated oven. A pressure controller adjusts this fluid to an appropriate density, while the sample is introduced through a low-volume valve. After the sample has separated into its components during the passage through a fused-silica capillary column, the solutes are detected in a high-pressure cell, followed by decompression at the capillary restrictor end.

While many substances could be converted into supercritical fluids, only certain mobile phases are of immediate interest. The obvious advantage of SFC is its capability to handle thermally labile molecules without decomposition; for instance, supercritical carbon dioxide can be used as the mobile phase slightly above the ambient temperature to separate labile organics, such as peroxides or azo compounds, with efficiences comparable[68] to capillary GC.

The choice of a supercritical-fluid mobile phase can be made approximately according to the "polarity" scale suggested by Giddings *et al.*,[69] based on values of the Hildebrand solubility parameter. Table 1 lists the critical parameters of several useful mobile phases. An adequate polarity range can be covered while using these supercritical media at very reasonable values of pressure and temperature. As capillary columns typically pass a few microlitres of a fluid per minute, it is feasible to employ "exotic" mobile phases. The solute retention in SFC is primarily controlled by the column pressure and, correspondingly, by the density of solvating molecules.[70] Thus, density programming is primarily employed, while some selectivity adjustments can also be made with the application of a polar "modifier".[71,72]

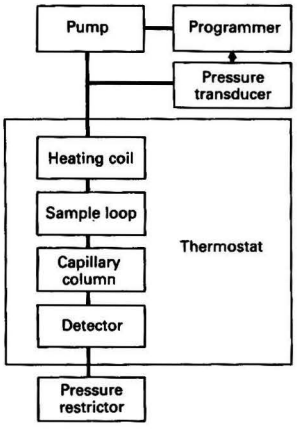

Fig. 9. Capillary supercritical-fluid chromatograph

Owing to the relatively large solute diffusion coefficients in C_2–C_5 hydrocarbons,[73] these media are among the best for capillary SFC separations. A typical application, using supercritical pentane as the mobile phase, is shown in Fig. 10; the aromatic fraction of coal tar has been separated here with a 110 μm i.d. glass capillary column and detected with a spectrofluorimetric detector.[74]

One of the most interesting aspects of capillary SFC is the fact that some LC as well as GC detection techniques can be used. A wide application of flame-based and plasma detection devices in future investigations is anticipated. Some promising results have already been reported with a combination of capillary SFC and mass spectrometry.[66] Recently, the relative transparency of some supercritical fluids in the infrared region has been utilised to couple SFC to a Fourier-transform infrared spectrometer;[75,76] this combination is very likely to make any attempts to achieve LC - infrared spectrometry obsolete.

Capillary Electrophoresis

While electrophoresis is generally considered to be a superior approach to the separation of ionic macromolecules, it is also probably the least understood and most underrated of all separation techniques. Flat-bed techniques are considerably more common in electrophoresis than the column techniques; a recent considerble success of the two-dimensional method of O'Farell[77] attests to the great versatility of the planar approach in high-resolution analysis of biopolymers.

The use of capillary columns in electrophoresis is uncommon. A notable exception is the method of isotachophoresis (displacement electrophoresis). In addition, zone electrophoresis in narrow PTFE tubes was investigated by Mikkers *et al.*[78] in order to reduce the zone dispersion originating from the convection currents.

Table 1. Critical parameters of some mobile phases

Fluid	Critical temperature/ °C	Critical pressure/ atm	Critical density/ g cm^{-3}
Carbon dioxide ..	31.3	72.9	0.448
Dichlorotetra-fluoroethane ..	146.7	33.5	0.582
Propan-2-ol	253.3	47.0	0.273
Propane	96.7	41.9	0.217
Butane	152.0	37.5	0.228
Pentane	196.5	33.2	0.237

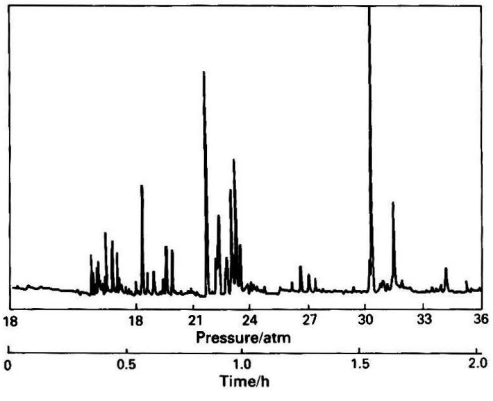

Fig. 10. Chromatogram of fluorescent components from the aromatic fraction of coal tar, as recorded by the capillary supercritical-fluid chromatograph. Reproduced from reference 74 with permission of the American Chemical Society

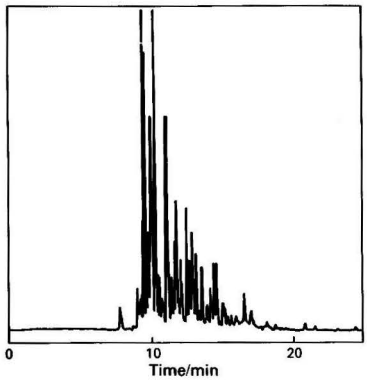

Fig. 11. Capillary electropherogram of a hydrolysed protein sample. Reproduced from reference 80 with permission of Elsevier Publishing Company

More recently, Jorgenson and Lukacs[79,80] have described a very promising version of capillary electrophoresis. Noting a theoretical prediction by Giddings[81] that the zone breadth is inversely proportional to the applied voltage, Jorgenson and Lukacs[79] designed a system in which a relatively short capillary, attached to the respective reservoirs, was subjected to voltages in excess of 30 kV. An application of such high voltages in previous electrophoretic experiments had largely been limited by the heat generated during the process. However, in the experimental arrangement of Jorgenson and Lukacs,[79] using a narrow capillary tube (75 μm or less), heat was easily dissipated through the wall.

Whereas the experimental set-up of capillary electrophoresis[79] is somewhat reminiscent of capillary LC, the results with the former are considerably better, as long as the substances are ionic in nature. Specifically, large "plate numbers" can be generated in relatively short analysis times because, unlike chromatography, any diffusion-controlled processes are to be minimised. Efficiencies in excess of 400 000 theoretical plates have been demonstrated. Fig. 11 shows an example of a very efficient separation; here, fluorescamine-labelled peptides from a tryptic digest of chicken ovoalbumin present a very complex pattern.[80]

Except for employing unusually high voltages, the method of capillary electrophoresis is relatively simple. Glass or fused silica capillaries (typically 1-m long) are used, while the separated solutes are detected spectroscopically using the "on-column approach." Other instrumental aspects have been described.[79,80]

Further developments in capillary electrophoresis are highly desirable from the theoretical as well as practical point of view. Eventually, this technique could entirely replace analytical ion-exchange chromatography.

Conclusions

In spite of the early powerful demonstrations of capillary GC techniques, applications of this method during the 1960s were infrequent and confined to a few research laboratories. Technological innovations of the following decade have brought capillary GC close to the full realisation of its theoretical potential. Developments in micro-column (capillary) LC, initiated in the late 1970s, have been stimulated both by an improved understanding of the column processes and by miniaturisation technology. While column efficiency improvements achieved by micro-scale LC remain important, this approach is even more essential to the development of optimum detection devices. Some of these directions are further reinforced by the advent of capillary supercritical fluid chromatography. Finally, high-voltage capillary electrophoresis further complements the other existing capillary techniques with respect to highly efficient separations of ionic species. Although there are numerous challenges and experimental difficulties associated with modern capillary separation techniques, the potential benefits are eminently worthwhile attaining.

During the past 5 years, research on capillary and micro-column chromatography in the author's laboratory has been aided by the following grants: GM 24349 (National Institute of General Medical Sciences, US Public Health Service); DOE DE-AC02-81 ER 60007 (US Department of Energy); N14-82-K-0561 (Office of Naval Research); and NSF CHE 82-00034 (National Science Foundation).

References

1. Golay, M. J. E., *in* Desty, D. H., *Editor*, "Gas Chromatography 1958," Academic Press, New York, 1958, p. 36.
2. Dandeneau, R., and Zerenner, E. H., *J. High Resolut. Chromatogr.*, 1979, **2**, 351.
3. Desty, D. H., and Goldup, A., *in* Scott, R. P. W., *Editor*, "Gas Chromatography 1960," Butterworths, London, 1960, p. 162.
4. Bruner, F. A., and Cartoni, G. P., *Anal. Chem.*, 1964, **36**, 1522.
5. Grob, K., *Helv. Chim. Acta*, 1968, **51**, 718.
6. Bartle, K. D., Bergstedt, L., Novotny, M., and Widmark, G., *J. Chromatogr.*, 1969, **45**, 256.
7. Novotny, M., *Anal. Chem.*, 1981, **53**, 1294A.
8. Jennings, W. G., "Applications of Glass Capillary Gas Chromatography," Marcel Dekker, New York, 1981.
9. Novotny, M., *in* Natusch, D. F. S., and Hopke, P. K., *Editors*, "Analytical Aspects of Environmental Chemistry," Wiley and Sons, New York, 1983, p. 61.
10. Grob, K., and Grob, K., Jr., *J. Chromatogr.*, 1974, **94**, 53.
11. Van den Berg, M. J., and Cox, T. P. H., *Chromatographia*, 1972, **5**, 301.
12. Verzele, M., Redant, G., Qureshi, S., and Sandra, P., *J. Chromatogr.*, 1980, **199**, 105.
13. Novotny, M., Lee, M. L., and Bartle, K. D., *Chromatographia*, 1974, **7**, 333.
14. Novotny, M., and Farlow, R., *J. Chromatogr.*, 1975, **103**, 1.
15. Vogt, W., Jacob, K., Ohnesorge, A.-B., and Obwexer, H. W., *J. Chromatogr.*, 1979, **186**, 197.
16. Schomburg, G., Husmann, H., and Weeke, F., *J. Chromatogr.*, 1974, **99**, 63.
17. Schomburg, G., *in* Kaiser, R. E., *Editor*, "Proceedings of the 4th International Symposium on Capillary Chromatography," Hüthig, Heidelberg, 1981, p. 371.
18. Grob, K., and Grob, K., Jr., *J. Chromatogr.*, 1978, **151**, 311.
19. Galli, M., and Trestianu, S., *J. Chromatogr.*, 1981, **203**, 193.
20. Grob, K., Grob, G., and Grob, K., Jr., *J. Chromatogr.*, 1981, **211**, 243.
21. Stark, T., Wright, B. W., Peaden, P. A., and Lee, M. L., *J. Chromatogr.*, 1982, **248**, 17.
22. Springston, S. R., Melda, K., and Novotny, M., *J. Chromatogr.*, 1983, **267**, 395.
23. Lee, M. L., and Wright, B. W., *J. Chromatogr.*, 1980, **184**, 235.
24. Guiochon, G., *Anal. Chem.*, 1978, **50**, 1812.
25. Schutjes, C. P. M., Vermeer, E. A., Rijks, J. A., and Cramers, C. A., *in* Kaiser, R. E., *Editor*, "Proceedings of the 4th International Symposium on Capillary Chromatography," Hüthig, Heidelberg, 1981, p. 687.
26. Hartigan, M. J., Purcell, J. E., Novotny, M., McConnell, M. L., and Lee, M. L., *J. Chromatogr.*, 1974, **99**, 339.
27. Estes, S. A., Uden, P. C., and Barnes, R. M., *J. Chromatogr.*, 1982, **239**, 181.
28. Grob, K., *Chromatographia*, 1975, **8**, 423.
29. Novotny, M., Schwende, F. J., Hartigan, M. J., and Purcell, J. E., *Anal. Chem.*, 1980, **52**, 736.
30. Jaramillo, J. F., and Driscoll, J. N., *J. High Resolut. Chromatogr.*, 1979, **2**, 536.
31. Smith, S. L., and Adams, G. E., *J. Chromatogr.*, 1983, **279**, 623.

32. Tetsuo, M., Eriksson, H., and Sjövall, J., *J. Chromatogr.*, 1982, **239**, 287.
33. Giddings, J. C., *Anal. Chem.*, 1964, **36**, 1890.
34. Tsuda, T., and Novotny, M., *Anal. Chem.*, 1978, **50**, 271.
35. Tsuda, T., and Novotny, M., *Anal. Chem.*, 1978, **50**, 632.
36. Ishii, D., Asai, K., Hibi, K., Jonokuchi, T., and Nagaya, M., *J. Chromatogr.*, 1977, **144**, 157.
37. Scott, R. P. W., and Kucera, P., *J. Chromatogr.*, 1977, **144**, 157.
38. Knox, J. H., and Gilbert, M. T., *J. Chromatogr.*, 1979, **186**, 405.
39. Jorgenson, J. W., and Guthrie, E. J., *J. Chromatogr.*, 1983, **255**, 335.
40. Takeuchi, T., and Ishii, D., *J. Chromatogr.*, 1983, **279**, 439.
41. Tsuda, T., Tsuboi, K., and Nakagawa, G., *J. Chromatogr.*, 1981, **214**, 283.
42. McGuffin, V. L., and Novotny, M., *J. Chromatogr.*, 1983, **255**, 381.
43. Yang, F. J., *J. Chromatogr.*, 1982, **236**, 265.
44. Gluckman, J. C., Hirose, A., McGuffin, V. L., and Novotny, M., *Chromatographia*, 1983, **17**, 303.
45. Hirata, Y., and Jinno, K., *J. High Resolut. Chromatogr.*, 1983, **6**, 196.
46. Hirata, Y., and Novotny, M., *J. Chromatogr.*, 1979, **186**, 521.
47. Hirata, Y., Lin, P. T., Novotny, M., and Wightman, R. M., *J. Chromatogr.*, 1980, **181**, 287.
48. Slais, S., and Krejci, M., *J. Chromatogr.*, 1982, **235**, 21.
49. McGuffin, V. L., and Novotny, M., *Anal. Chem.*, 1981, **53**, 946.
50. McGuffin, V. L., and Novotny, M., *J. Chromatogr.*, 1981, **218**, 179.
51. McGuffin, V. L., and Novotny, M., *Anal. Chem.*, 1983, **55**, 2296.
52. Novotny, M., Hirose, A., and Wiesler, D., submitted for publication.
53. Novotny, M., Alasandro, M., and Konishi, M., *Anal. Chem.*, 1983, **55**, 2375.
54. Novotny, M., Karlsson, K.-E., Konishi, M., and Alasandro, M., *J. Chromatogr.*, in the press.
55. Karlsson, K.-E., Alasandro, M., Wiesler, D., and Novotny, M., submitted for publication.
56. Raymer, J., Holland, M. L., Wiesler, D., and Novotny, M., submitted for publication.
57. Scott, R. P. W., and Kucera, P., *J. Chromatogr.*, 1979, **185**, 27.
58. Manz, A., and Simon, W., *J. Chromatogr. Sci.*, 1983, **21**, 326.
59. Knecht, L., Guthrie, E. J., and Jorgenson, J. W., *Anal. Chem.*, in the press.
60. Folestad, S., Johnson, L., Josefsson, B., and Galle, B., *Anal. Chem.*, 1982, **54**, 925.
61. Diebold, G. J., and Zare, R. N., *Science*, 1977, **196**, 1439.
62. Hershberger, L. W., Callis, J. B., and Christian, G. D., *Anal. Chem.*, 1979, **51**, 1444.
63. Sepaniak, M. J., and Yeung, E. S., *J. Chromatogr.*, 1981, **211**, 95.
64. Klesper, E., Corwin, A. H., and Turner, D. A., *J. Org. Chem.*, 1962, **27**, 700.
65. Novotny, M., Springston, S. R., Peaden, P. A., Fjeldsted, J. C., and Lee, M. L., *Anal. Chem.*, 1981, **53**, 407A.
66. Smith, R. D., Felix, W. D., Fjeldsted, J. C., and Lee, M. L., *Anal. Chem.*, 1982, **54**, 1883.
67. Springston, S. R., and Novotny, M., *Chromatographia*, 1981, **14**, 679.
68. Lee, M. L., Fjeldsted, J. C., Campbell, R. M., and Kong, R. C., *J. Chromatogr.*, in the press.
69. Giddings, J. C., Myers, M. N., McLaren, L., and Keller, R. A., *Science*, 1968, **162**, 67.
70. Fjeldsted, J. C., Jackson, W. P., Peaden, P. A., and Lee, M. L., *J. Chromatogr. Sci.*, 1983, **21**, 222.
71. Novotny, M., Bertsch, W., and Zlatkis, A., *J. Chromatogr.*, 1971, **61**, 17.
72. Gere, D. R., Board, R., and McManigill, D., *Anal. Chem.*, 1982, **54**, 736.
73. Springston, S. R., and Novotny, M., *J. Chromatogr.*, 1983, **279**, 417.
74. Peaden, P. A., Fjeldsted, J. C., Lee, M. L., Springston, S. R., and Novotny, M., *Anal. Chem.*, 1982, **54**, 1090.
75. Shafer, K. H., and Griffiths, P. R., *Anal. Chem.*, 1983, **55**, 1939.
76. Olesik, S. V., French, S., Smith, S. L., and Novotny, M., submitted for publication.
77. O'Farell, P. H., *J. Biol. Chem.*, 1975, **250**, 4007.
78. Mikkers, F. E. P., Everaerts, F. M., and Verheggen, P. E. M., *J. Chromatogr.*, 1979, **169**, 11.
79. Jorgenson, J. W., and Lukacs, K. D., *Anal. Chem.*, 1981, **53**, 1298.
80. Jorgenson, J. W., and Lukacs, K. D., *J. Chromatogr.*, 1981, **218**, 209.
81. Giddings, J. C., *Sep. Sci.*, 1969, **4**, 181.

Paper A3/385
Received November 7th, 1983

Design and Application of Neutral Carrier-based Ion-selective Electrodes

Plenary Lecture

W. Simon,* E. Pretsch, W. E. Morf, D. Ammann, U. Oesch and O. Dinten
Department of Organic Chemistry, Swiss Federal Institute of Technology (ETH), CH-8092 Zürich, Switzerland

The requirements for neutral complexing agents behaving as ion carriers (ionophores) in membranes of ion-selective electrodes are discussed. Emphasis is placed on the lipophilicity of such compounds, on the kinetics (free energy of activation) of the ligand exchange reaction, and on the parameters inducing selectivity, *e.g.*, molecular structures and aspects of membrane technology.

Keywords: *Ion-selective electrodes; neutral carrier-based*

Ion carriers (a class of ionophores) are lipophilic complexing agents having the capability to bind ions reversibly and to transport them across organic membranes by carrier translocation.[1] Ideally, selective ion carriers render a membrane permeable for one given sort of ion I only. If such ionophore-based membranes are used in cell assemblies of the type

External reference electrode	Sample solution (solution 1)	Membrane	Internal reference system (solution 2)

and if an electric potential gradient is applied between solutions 1 and 2, an exclusive transport of the ions I across the membrane should result, the transport number being then $t_I = 1$. For the same membrane electrode cell the electric potential difference at zero current (e.m.f.) between the external and the internal reference system would depend on the ratio of the activities of the ion I in solutions 1 and 2. If a constant composition of solution 2 is used, the activities of the selected ion in solution 1 may therefore be measured potentiometrically according to the Nernst equation.[2] Neutral carriers in particular, defined as ionophores that carry no charge when

* To whom correspondence should be addressed.

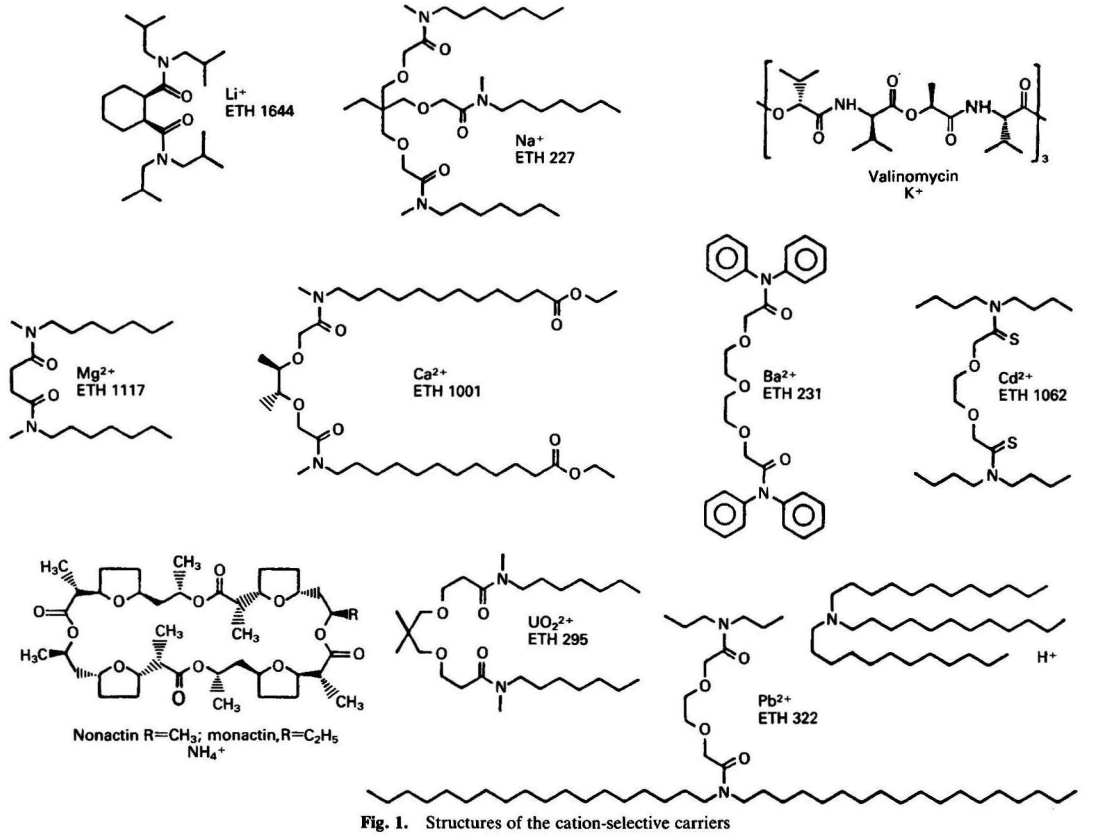

Fig. 1. Structures of the cation-selective carriers

not complexed by the transported ion, have led to such ion-selective electrodes with a wide range of available selectivities.[1]

Analytically relevant ionophores have to meet at least the following three requirements:

1. For a continuous-use lifetime of solvent polymeric membranes[3] [*ca.* 32% *m/m* poly(vinyl chloride), *ca.* 65% *m/m* plasticiser, 1–3% *m/m* ionophore] of at least 1 year, the ionophore has to be very lipophilic. A partition coefficient, K, of the carrier between the aqueous sample solution and the membrane phase larger than $10^{5.5}$ is necessary.[4] Incorporating adequate structural elements (*e.g.*, alkyl groups) into ionophores, the required lipophilicity may easily be obtained. A reliable estimate for P (partition coefficient of a carrier between water and octan-1-ol) and therefore of K may be obtained by thin-layer chromatography (TLC)[5] (Figs. 1 and 2). From Fig. 2, it becomes obvious that, *e.g.*, the ligand ETH 231 does not exhibit a sufficient lipophilicity for the required membrane lifetime.

2. The free energy of activation of the ligand exchange reaction

$$IS + S' \rightleftharpoons IS' + S$$

where S and S′ are ionophores, has to be relatively low.

For Zn^{2+} or Cd^{2+} complexes of ligand ETH 1062 (Fig. 1), free energies of activation of the ligand-exchange reaction of $\lesssim 45$ kJ mol^{-1} (in acetonitrile) have been measured.[6] Cation permselectivity is indeed observed with $CdCl_2$ in the sample solution (see Fig. 3). As $CdCl^+$ is probably the permeating species, a slope of the electrode response of approximately 60 mV (25 °C) is obtained.[7,8] In systems with a free energy of activation of the ligand exchange reaction of $\gtrsim 65$ kJ mol^{-1} (in acetonitrile), however, the cationic complexes of the ionophore act as anion exchangers (*e.g.*, complexes with Pt^{2+} or Pd^{2+}). An electrode containing the $PdCl_2$ complex of ETH 1062 in the membrane phase therefore responds to the chloride anions in a sample solution of $CdCl_2$ (see Fig. 4).

In order to keep the free energy of activation of the ligand exchange reaction sufficiently small, the design of ionophores has been focused on non-macrocyclic structures (see Fig. 1).

3. The ionophore has to induce ion-permeability selectivity in membranes. As the ion selectivity of a membrane is related to the free energies of transfer of the ions from the aqueous phase (sample) to the membrane phase, the selectivity of neutral carrier-based ion sensors obviously depends on various factors. Such factors are mainly[1] (a) the selectivity behaviour of the carrier ligand used, which can be completely characterised by complex stability constants, (b) the extraction properties of the membrane solvent (plasticiser), (c) the concentration of the free ligand in the membrane phase and (d) the concentration of ionic sites in the membrane. The effects of (b), (c) and (d) can be described to a large extent by model calculations and may be controlled by adequate membrane technology.[1,9,10] The design of ionophores with a given selectivity is more problematic (a). Although an overwhelming activity in designing host molecules (ionophores) for selected guest species (ions) is in evidence,[11–18] only modest use has been made of model calculations describing the host - guest interaction.[12,19–22]

Classical electrostatic models are useful for calculating the ion - molecule interactions near the energy minima for Group IA/IIA cations.[21] However, they require a knowledge of molecular parameters normally not available. It has been shown[21] that semi-empirical quantum chemical treatments of ion - ligand interactions often lead to unrealistic results. In contrast, *ab initio* computations give reliable results even if small but well balanced basis sets are chosen.[23–26] The application to realistic ionophores is usually prohibited by the extent of the computation even if small basis sets are used. Through *ab initio* calculations on model complexes and a representation of the interaction energies by pair potentials,[27–31] such large systems are easily made amenable to analysis (see also reference 26). For a discussion of the stability of the complexes the sum of the interaction energies and the conformational energy relative to the most stable conformation of the free ligand is relevant. Unfortunately, the computation of such conformational energy changes is still too uncertain.[32,33]

Using such model calculations, CPK model building and adequate membrane technology, it has nevertheless been possible to design neutral carrier-based membranes that show analytically relevant ion selectivities for Li^+, Na^+, K^+, Mg^{2+}, Ca^{2+}, Ba^{2+}, Cd^{2+}, NH_4^+, UO_2^{2+} and H_3O^+. Pungor *et al.* revealed a useful lead selectivity for ligands of the type ETH 322[34] (Fig. 1). Although the synthetic ionophores shown in Fig. 1 are non-macrocyclic (see section 2), there are several reports on the successful application of macrocyclic ionophores (*e.g.*, crown compounds) in ion-selective electrodes[35,36] (for a review, see reference 1). Recently, neutral carriers for anions have been unravelled[37].

Some of the neutral carriers shown in Fig. 1 have found wide application, especially in clinical chemistry and physiology. About 200 references for such applications are given in a

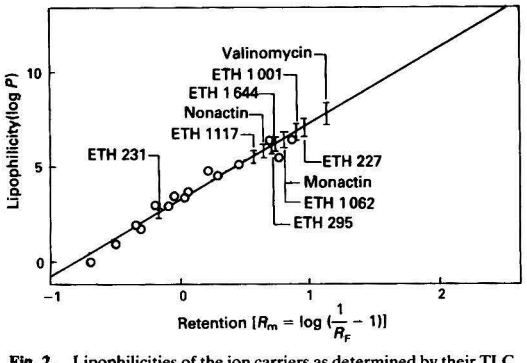

Fig. 2. Lipophilicities of the ion carriers as determined by their TLC retention, R_F. The TLC system is calibrated with a set of reference compounds (open circles) of known lipophilicities. TLC plate, RP KC 18F; ethanol - water (70 + 30); 23 °C. (See Fig. 1 for the chemical structures of the ion carriers depicted)

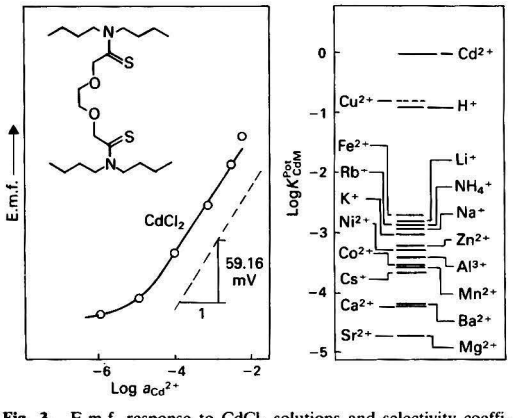

Fig. 3. E.m.f. response to $CdCl_2$ solutions and selectivity coefficients (K_{CdM} for different cations M^{z+}) of membrane electrodes based on the carrier ETH 1062. Membrane composition: carrier, 1% *m/m*; (10-hydroxydecyl)butyrate, 65% *m/m*; PVC, 34% *m/m*

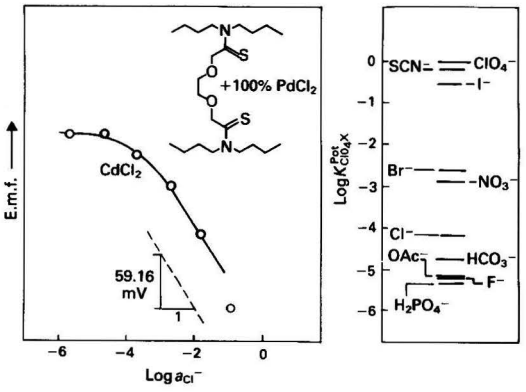

Fig. 4. E.m.f. response to $CdCl_2$ solutions and selectivity coefficients (K_{ClO_4X} for different anions X^-) of membrane electrodes containing the carrier ETH 1062 and an equimolar amount of $PdCl_2$. Membrane composition: carrier + additive, 1.8% *m/m*; *o*-nitrophenyl octyl ether, 66% *m/m*; PVC, 32.2% *m/m*

recent review.[1] Most recent reports on the use of some selected ionophores can be found in references 38 and 39 (Mg^{2+} - ionophore, ETH 1117), 40–42 (H^+ - ionophore, tridodecylamine) and 43 (UO_2^{2+} - ionophore, ETH 295).

This work was partly supported by the Schweizerischer Nationalfonds zur Förderung der wissenschaftlichen Forschung.

References

1. Ammann, D., Morf, W. E., Anker, P., Meier, P. C., Pretsch, E., and Simon, W., *Ion Select. Electrode Rev.*, 1983, **5**, 3.
2. Nernst, W., *Z. Phys. Chem.*, 1889, **2**, 613; 1889, **4**, 129.
3. Moody, G. J., Oke, R. B., and Thomas, J. D. R., *Analyst*, 1970, **95**, 910.
4. Oesch, U., and Simon, W., *Anal. Chem.*, 1980, **52**, 692.
5. Oesch, U., Dinten, O., Ammann, D., and Simon, W., *in* Kessler, M., *Editor*, "Proceedings of the International Symposium on the Theory and Application of Ion-selective Electrodes in Physiology and Medicine, Burg Rabenstein, FRG, 12–15th September, 1983," Springer-Verlag, Berlin, 1984, in the press.
6. Hofstetter, P., Pretsch, E., and Simon, W., *Helv. Chim. Acta*, 1983, **66**, 2103.
7. Hofstetter, P., *Dissertation*, ETH No. 7128, ADAG Administration und Druck AG, Zürich, 1982.
8. Schneider, J. K., Hofstetter, P., Pretsch, E., Ammann, D., and Simon, W., *Helv. Chim. Acta*, 1980, **63**, 217.
9. Meier, P. C., Morf, W. E., Läubli, M., and Simon, W., *Anal. Chim. Acta*, in the press.
10. Morf, W. E., and Simon, W., *in* Freiser, H., *Editor*, "Ion Selective Electrodes in Analytical Chemistry," Plenum Press, New York, London, Washington, Boston, 1978, p. 211.
11. Cram, D. J., and Cram, J. M., *Science*, 1974, **83**, 803.
12. Lehn, J.-M., *Struct. Bonding (Berlin)*, 1973, **16**, 1.
13. Weber, E., and Vögtle, F., *Chem. Ber.*, 1976, **109**, 1803.
14. Pedersen, C. J., *J. Am. Chem. Soc.*, 1967, **89**, 2495; 1967, **89**, 7017; 1970, **92**, 386; 1970, **92**, 391.
15. Prelog, V., *Pure Appl. Chem.*, 1978, **50**, 893.
16. Stoddard, J. F., *Chem. Soc. Rev.*, 1979, **8**, 85.
17. Poonia, N. S., and Bajaj, A. V., *Chem. Rev.*, 1979, **79**, 389.
18. Morf, W. E., Ammann, D., Bissig, R., Pretsch, E., and Simon, W., *in* Izatt, R. M., and Christensen, J. J., *Editors*, "Progress in Macrocyclic Chemistry," Volume 1, Wiley-Interscience, New York, 1979, p. 1.
19. Morf, W. E., and Simon, W., *Helv. Chim. Acta*, 1971, **54**, 2683.
20. Simon, W., Morf, W. E., and Meier, P. C., *Struct. Bonding (Berlin)*, 1973, **16**, 113.
21. Schuster, P., Jakubetz, W., and Marius, W., *Top. Curr. Chem.*, 1975, **60**, 1.
22. Timko, J. M., Moore, S. S., Walba, D. M., Hiberty, P. C., and Cram, D. J., *J. Am. Chem. Soc.*, 1977, **99**, 4207.
23. Pullman, A., Berthod, H., and Gresh, N., *Int. J. Quantum Chem. Symp.*, 1976, **10**, 59.
24. Kolos, W., *Theor. Chim. Acta*, 1980, **54**, 187.
25. Gianolio, L., and Clementi, E., *Gazz. Chim. Ital.*, 1980, **110**, 179.
26. Gresh, N., and Pullman, A., *Int. J. Quantum Chem.*, 1982, **22**, 709.
27. Clementi, E., "Lecture Notes in Chemistry," Volume 2, Springer-Verlag, Berlin, 1976; Vol. 19, Springer-Verlag, Berlin, 1980.
28. Corongiu, G., Clementi, E., Pretsch, E., and Simon, W., *J. Chem. Phys.*, 1979, **70**, 1266.
29. Corongiu, G., Clementi, E., Pretsch, E., and Simon, W., *J. Chem. Phys.*, 1980, **72**, 3096.
30. Pretsch, E., Bendl, J., Portmann, P., and Welti, M., *in* Naray-Szabo, G., *Editor*, "Proceedings of the Symposium on Steric Effects in Biomolecules, Eger, Hungary, 1981," Akadémiai Kiadó, Budapest, 1982, p. 85.
31. Pretsch, E., Gratzl, M., Pungor, E., and Simon, W., *in* Pungor, E., and Buzás, I., *Editors*, "Proceedings of the 3rd Symposium on Ion-Selective Electrodes, Matráfüred, Hungary, October 13–15, 1980," Akadémiai Kiadó, Budapest, 1981, p. 315.
32. Bendl, J., and Pretsch, E., *J. Comput. Chem.*, 1982, **3**, 580.
33. Uiterwijk, J. W. H. M., Harkema, S., van de Waal, B. W., Göbel, F., and Nibelling, H. T. M., *J. Chem. Soc., Perkin Trans. 2*, in the press.
34. Lindner, E., Tóth, K., Pungor, E., Behm, F., Welti, D., Ammann, D., Oggenfuss, P., Morf, W. E., Pretsch, E., and Simon, W., *Anal. Chem.*, submitted for publication.
35. Kimura, K., Tamura, H., and Shono, T., *J. Chem. Soc., Chem. Commun.*, 1983, 492.
36. Bussmann, W., Lehn, J.-M., Oesch, U., Plumeré, P., and Simon, W., *Helv. Chim. Acta*, 1981, **64**, 657.
37. Wuthier, U., Pham, H. V., Zünd, R., Welti, D., Funck, R. J. J., Bezegh, A., Ammann, D., Pretsch, E., and Simon, W., *Anal. Chem.*, accepted for publication.
38. Hess, P., Metzger, P., and Weingart, R., *J. Physiol.*, 1982, **333**, 173.
39. Alvarez-Leefmans, F. J., Gamino, S. M., and Rink, T. J., *J. Physiol.*, in the press.
40. Kurkdjian, A. C., and Barbier-Brygoo, H., *Anal. Biochem.*, 1983, **132**, 96.
41. Kraig, R. P., Ferreira-Filho, C. R., and Nicholson, C., *J. Neurophysiol.*, 1983, **49**, 831.
42. Coray, A., and McGuigan, J. A. S., *J. Physiol.*, 1982, **336**, 66P.
43. Bertrand, P. A., Choppin, G. R., Rao, L. F., and Bunzli, J.-C. G., *Anal. Chem.*, 1983, **55**, 364.

Paper A3/302
Received September 5th, 1983

Continuum-source Atomic-absorption Spectrometry: Past, Present and Future Prospects

Plenary Lecture

Thomas C. O'Haver
Department of Chemistry, University of Maryland, College Park, MD 20742, USA

The possibility of using a continuum primary source in atomic-absorption spectrometry, rather than separate line sources for each element as is the conventional practice, has been a recurring theme in the literature of atomic absorption for many years. Past efforts have not been particularly successful. Recent advances in optical technology and data processing techniques have made this approach much more promising. Simultaneous multi-element atomic absorption, with flame and electrothermal atomisation, is now being carried out routinely with prototype instrumentation built by researchers. This approach may offer a future path for the continued development of atomic absorption.

Keywords: *Atomic-absorption spectrometry; continuum source*

The Past

When Sir Alan Walsh first proposed atomic-absorption spectrometry as a method for chemical analysis in 1955,[1] it was concluded that the most practical approach would be to use narrow spectral line sources rather than the continuum light sources that had been commonly used in molecular absorption spectrometry. This turned out to be an important factor in the ultimate success of atomic absorption, for it meant that an instrument of very high effective resolution could be constructed using a small, low-cost, medium-resolution monochromator. Prior to Walsh's work, analytical atomic spectrometry was performed most commonly by arc or spark emission spectrography, utilising very large high-resolution spectrometers, or by flame emission photometry, ordinarily utilising more modest optical equipment. Walsh's atomic absorption system was not much more complex or expensive than a simple flame photometer, yet it offered useful sensitivity for a wider range of elements and it was far less susceptible to spectral interferences. Thus, the "image" of atomic absorption was established early on as an effective yet low-cost and easy-to-use method.

In spite of the valid reasons for the use of narrow spectral line sources in atomic absorption, researchers have for many years sought ways to utilise continuum sources effectively. In the early days of atomic absorption, continuum sources were occasionally utilised to survey the absorption lines of elements for which hollow-cathode lamps were not yet available.[2] In 1962, Gibson *et al.*[3] suggested the use of a continuum source for analytical purposes, primarily because of the convenience of using a single light source for many elements. Early experience with the continuum source used with conventional atomic-absorption instrumentation, however, showed that the expected disadvantages of poor sensitivity and restricted calibration graph linearity were indeed serious limitations.[4,5] Some investigators attempted to improve the sensitivity of measurement by utilising organic solvents,[6] multi-pass optics[6] or long-path absorption tubes.[7] The difficulty with these studies is that the same measures could just as easily have been applied to line-source measurements, with the same expectation of sensitivity improvement. Moreover, these techniques may lead to more serious chemical and spectral background interferences and thus cannot be recommended for general analytical work.

Since about 1970, work on continuum-source atomic absorption has centred on improving the sensitivity by increasing the effective spectral resolution and on reducing noise by utilising high-intensity light sources and various modulation schemes. Wavelength modulation, first applied to continuum-source atomic absorption by Snelleman[8] in 1968, is effective in compensating for broad-band atomiser background emission and background absorption, and for reducing the effects of low-frequency source flicker noise. Elser and Winefordner[9] tried a double modulation scheme utilising both source chopping and wavelength modulation, which corrected also for analyte atomic emission.

Attempts to improve the effective resolution have been based on the use of interferometers, resonance monochromators, selective line modulation and échelle spectrometers. Nitis *et al.*[10] and Veillon and Merchant[11] used Fabry - Perot interferometers in conjunction with medium-resolution monochromators. They were able to achieve characteristic concentrations comparable to line source measurement, but the complex optical systems did not prove suitable for routine work. Cochran and Hieftje[12] used an interesting selective-line modulation technique that utilises two identical burner systems, one for the analytical solution and one for a reference solution containing a high concentration of the sought-for species. A mirrored chopper directs the primary continuum radiation alternately through and around the reference flame. In this way the intensity of the primary beam is intensity-modulated only in the very narrow spectral region of the absorption profile to the analyte. Very high effective resolution is thereby achieved with only a small conventional monochromator. A related approach is the use of a resonance monochromator, which has been described by Bower *et al.*[13] and Blackburn and Winefordner.[14]

A comparatively straightforward way to achieve high spectral resolution is simply to use a high-resolution spectrometer. In the past, these have been large and costly, but newer designs based on the échelle grating are much more practical, although still larger and more expensive than small, medium-resolution monochromators. Keliher and Wohlers[15,16] were the first to apply an échelle spectrometer to continuum-source atomic absorption. They showed that it was indeed possible to obtain characteristic concentrations and calibration graphs comparable to line-source atomic absorption. One of the most significant aspects of this approach is that it is optically and operationally simple, at least externally. Although the optics of an échelle spectrometer are sophisticated, this is an internal complexity. As far as the user is concerned, an échelle spectrometer is a commercially available "black box," much like any other monochromator. The operation of an échelle spectrometer is fairly simple and familiar, in comparison with interferometers, resonance monochromators and selective line modulation devices.

The most extensive recent work in continuum-source atomic absorption has been based on the system first described in 1976 by Zander *et al.*[17] This system, which combines the use of a high-resolution échelle spectrometer with Snelleman's wavelength modulation technique, exists in two different

configurations: a single-element version referred to as a CEWM-AA system, and a 16-channel simultaneous multi-element version called SIMAAC. The CEWM-AA and SIMAAC system have now been applied to over 30 elements and to the analysis of large numbers of practical samples and reference materials using both flame and electrothermal atomisation.[18–40]

The Present

A schematic diagram of a single-channel continuum-source atomic-absorption spectrometer employing wavelength modulation is shown in Fig. 1. A SIMAAC system is illustrated in Fig. 2. There are five main parts: the continuum primary source, the atomiser, the spectrometer, the wavelength modulator and the signal processing electronics or computer.

As a primary source we have used xenon short-arc lamps with integral parabolic reflectors. These lamps were initially manufactured by the Eimac division of Varian and are now available from ILC Technology under the name of Cermax. This type of lamp has been extensively applied in various areas of analytical spectrometry, where it has been found to offer significant intensity advantages over conventional designs. In its application to continuum-source atomic absorption, it is of interest to compare the intensity of the Cermax lamp with that of the hollow-cathode lamps normally used in line-source atomic absorption.[22] In Fig. 3, the circles represent the photoanodic currents measured at the resonance lines of various elements when a 300-W Cermax lamp is used in a typical continuum-source atomic-absorption set-up with an

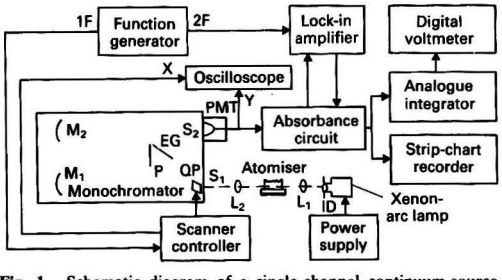

Fig. 1. Schematic diagram of a single-channel continuum-source wavelength-modulated atomic-absorption spectrometer with analogue signal processing electronics. Reprinted by permission from reference 35

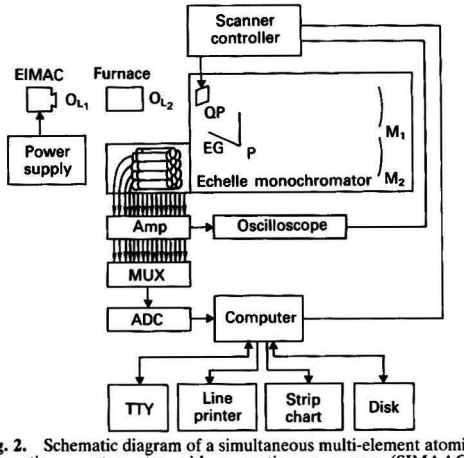

Fig. 2. Schematic diagram of a simultaneous multi-element atomic-absorption spectrometer with a continuum source (SIMAAC). Reprinted by permission from reference 27

échelle spectrometer (slit width 25 μm; resolution 0.003 nm at 300 nm). The vertical lines represent the corresponding measurements of commercial hollow-cathode lamps operated at the recommended currents and measured with the same optical system. One can see that the total system response decreases rapidly at short wavelengths, but that in spite of that, the continuum source is at least as bright as the hollow-cathode lamps, even at 193.7 nm, and is considerably brighter in the visible region.

The atomisers we have used have been conventional, commercially available designs. We have experience with both air - acetylene and dinitrogen oxide - acetylene flames and with various models of tubular carbon furnace atomisers (mostly Perkin-Elmer models), as well as the Instrumentation Laboratory Fastac system. The use of a L'vov platform or other atomisation substrate has often been found valuable.

The spectrometer is a Spectraspan III (Spectrametrics Inc., Andover, MA, USA) échelle spectrometer. Wavelength modulation is accomplished by a 3-mm quartz refractor plate mounted on an optical scanner torque motor. The refractor plate is positioned immediately behind the entrance slit. The selection of the slit widths and heights of the échelle spectrometer is a compromise between signal to noise ratio and calibration graph linearity. The most linear calibration graphs are obtained at small slit widths, which improve resolution, and small slit heights, which minimise order-overlap stray light. However, the resulting lower light transmission reduces signal to noise ratio and degrades detection limits. Harnly[32] has shown experimentally that the best detection limits are obtained with larger slit heights and widths. In general, the choice depends on the type of instrument system. In single-channel systems with analogue electronics, in which the analytical calibration is ordinarily performed manually, small heights and widths have been used in order to improve linearity and thereby simplify the calibration and curve-fitting procedure. On the other hand, when a computer is used for data acquisition and reduction, as in the multi-element SIMAAC system, the choice has been to optimise detection limits.

The multi-element SIMAAC system utilises a multi-channel cassette with 20 exit slits and photomultipliers positioned for 20 pre-selected wavelengths. The selection of the optimum line for each element is comparatively straightforward; in most instances, the usual resonance line is used. Because of the spectral simplicity of atomic absorption, alternative lines do not have to be used to avoid spectral interferences, as is often the case in plasma emission spectrometry. The exit slit heights and widths can be chosen individually. Inasmuch as the dispersion of the order-sorting prism is greater in the ultraviolet than in the visible region, it is advantageous to use larger exit slit heights at low wavelengths to increase intensity and smaller slit heights at longer wavelengths to reduce order-overlap strong light. At wavelengths below 250 nm, solar-blind photomultiplier tubes are used to reduce stray light originating from the much more intense visible region of the xenon lamp spectrum.

The single-channel CEWM-AA system utilises analogue signal-processing electronics consisting of a sine-wave oscillator to drive the refractor plate torque motor (usually at 100 Hz), a lock-in amplifier to measure the a.c. component of the photosignal and an operational amplifier circuit to convert the lock-in output to absorbance for measurement on a strip-chart recorder.

In the multi-element (SIMAAC) system a minicomputer (PDP 11/34) is used to generate the wavelength modulation waveform, measure and store intensity data on 16 active channels, average intensities, compute intensity ratios and absorbances, determine peak heights and areas, maintain files of analytical signals and experimental conditions, perform analytical calibration with linear and non-linear least-squares curve-fitting techniques and print out results.

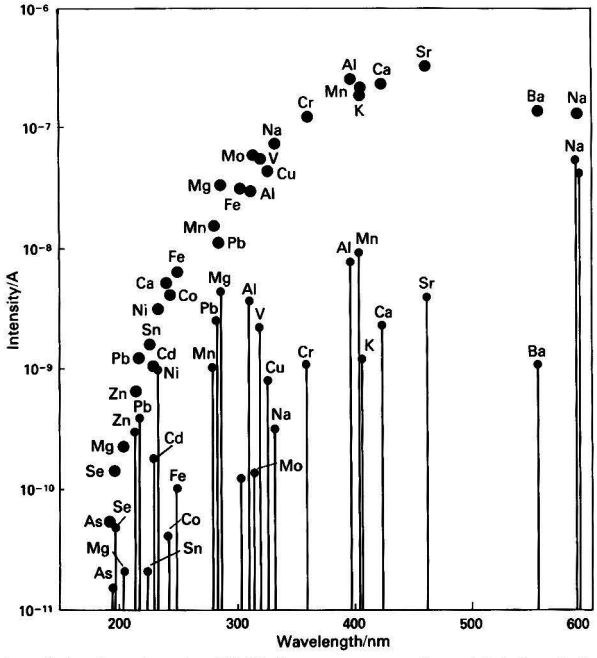

Fig. 3. Comparison of the relative intensity of a 300-W Cermax xenon-arc lamp (circles) to hollow-cathode lamps (vertical lines) measured on a high-resolution échelle spectrometer

In both systems a real-time display of the absorption spectrum within the modulation interval can be displayed on an x - y oscilloscope by connecting the phototube output to the y-axis and the modulation waveform to the x-axis. This display is very useful for checking for wavelength drift, excessive background absorption or unsuspected spectral interferences.

Naturally, the computerised system provides much greater versatility and convenience than the simpler analogue system. For example, the modulation waveform need not be a simple sine or square wave, but can be customised to enhance the signal to noise ratio and analytical range.[28] It is also possible to average many passes through the modulation interval in order to enhance the signal to noise of spectral profile measurements.[30]

Detection Limits

Compared with all previously reported continuum-source atomic-absorption systems, the CEWM-AA and SIMAAC systems provide significantly lower detection limits, on average by about an order of magnitude. This is due, we feel, to the combined effect of the high spectral dispersion of the échelle spectrometer, the wavelength modulation and the ratiometric data processing, which gives the effect of a double-beam measurement. Compared with conventional line-source instrumentation, our detection limits are slightly poorer overall, but tend to be comparable at wavelengths above 280 nm and poorer below, owing to the intensity distribution of the xenon lamp. Tables 1 and 2 show this comparison for flame and electrothermal atomisation, respectively.

Background Correction

The background correction capabilities of wavelength modulation in atomic absorption have been dealt with at length in previous studies.[19,20] The modulation technique offers many of the advantages of the Zeeman and Smith - Hieftje methods, *i.e.*, only a single light source is used and correction is made very close to the analytical line. Moreover, it is well suited to multi-element applications, because a single refractor plate behind the entrance slit modulates all the output channels simultaneously.

The wavelength modulation background correction system has been shown to be able to correct for up to 3.0 absorbance units of static background absorption.[20] Its performance with transient background in electrothermal atomisation is illustrated in Fig. 4, which shows absorbance - time plots for copper in various matrices. Similar experiments have been reported for Pb and Cd.[20]

Analytical Range

One of the problems that must be overcome in any proposed simultaneous multi-element atomic-absorption system is the limited concentration range that is ordinarily considered to be characteristic of atomic-absorption measurement. In our continuum-source atomic-absorption work, we have achieved a greatly extended working concentration range by measuring the absorbance at several wavelengths across the profile of a single analytical absorption line. The absorbance at the line centre is utilised at low to medium concentrations. At higher concentrations, where the absorbance at the line centre is too high to be useful, absorbances measured on the sides of the absorption profile are used. The feasibility of this idea is illustrated by the calibration graphs for sodium by continuum-source atomic absorption shown in Fig. 5. Note that the calibration graphs measured at wavelengths off the line centre extend the useful concentration range all the way to 20 000 μg ml^{-1} in this instance. The detection limit for sodium is less than 0.01 μg ml^{-1}, so the total analytical range is over six orders of magnitude.

In a simultaneous multi-element system, it is not practical to control the wavelength modulation interval individually for each element in response to its concentration in each sample. The SIMAAC system has been designed to acquire and store a

Table 1. Comparison of detection limits of continuum- and line-source flame atomic absorption

Element (flame)	Wavelength/ nm	Detection limit†/μg ml⁻¹ Continuum‡	Line§
Ag	328.068	0.007	0.009
Al (NA)	396.1/309.3‖	0.1	0.1
Au	242.795	0.17	0.04
Ba (NA)	553.548	0.07	0.09
Be (NA)	234.861	0.01	0.003
Bi	223.061	0.3	0.09
Ca (NA)	422.673	0.003	0.003
Cd	228.802	0.03	0.003
Co	240.745	0.07	0.02
Cr (NA)	357.869	0.1	0.1
(AA)		0.02	0.009
Cu	324.754	0.01	0.007
Fe	248.327	0.07	0.02
K	766.49	0.007	0.005
Li	670.784	0.003	0.005
Mg	285.213	0.001	0.0009
Mn	279.482	0.01	0.004
Mo (NA)	313.259	0.3	0.06
Na	588.995	0.003	0.001
Ni	352.454/232.0‖	0.07	0.1
Pb	283.3/217‖	0.1	0.06
Pd	244.8/247.6‖	0.1	0.03
Pt	265.945	1	0.3
Rh	343.489	0.07	0.03
Sb	217.58	1	0.08
Si (NA)	251.6	0.7	0.5
Sn (AA)	286.333	1	1
(NA)		1	3
Sr (NA)	460.733	0.02	0.06
Te	214.281	0.7	0.1
Ti (NA)	365.35	0.3	0.2
Tl	276.789	0.1	0.07
V (NA)	318.54	0.3	0.2
Zn	213.856	0.07	0.003

* NA = dinitrogen oxide - acetylene; AA = air - acetylene.
† Defined as a signal to noise ratio of 3 for a 5-s integration time.
‡ Background corrected. Calculated for 300-μm slit height and square-wave modulation, from data measured with 100-μm slit height and sine-wave modulation.[35]
§ Not background corrected. Measured on a Perkin-Elmer 5000.
‖ First wavelength given is optimum for continuum source, second is optimum for line source.

Table 2. Graphite furnace instrumental detection limits. Based on 20-μl sample size, peak-height measurement, signal to noise ratio of 3, atomisation from the tube wall

Element	Detection limit/ng ml⁻¹ SIMAAC	Perkin-Elmer
Co	0.9	0.2
Cr	0.3	0.08
Cu	0.1	0.2
Fe	0.7	0.2
Mn	0.1	0.08
Mo	0.7	0.2
Ni	2	2
V	0.9	2
Zn	0.4	0.008

fixed pattern of points across the entire absorption profile of each element, as shown in Fig. 6. Sufficient data are taken to allow the calculation of six double-beam, background-corrected absorbances of different sensitivities. Thus, when the system is calibrated, the six absorbances measured for each calibration solution are used to prepare a set of six calibration graphs such as shown in Fig. 7. When an unknown sample is measured, it also produces six absorbance readings, each of which is read off the corresponding calibration graph

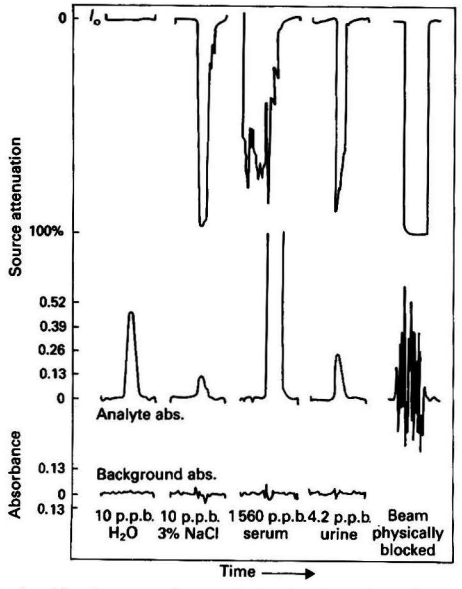

Fig. 4. Absorbance *vs.* time graphs for the electrothermal atomisation of Cu in various matrices, illustrating the background-correction ability of the wavelength modulation method. Reprinted by permission from reference 20

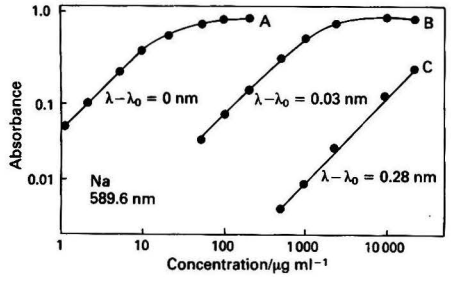

Fig. 5. Calibration graphs for sodium by continuum-source atomic-absorption spectrometry with flame atomisation. A, Measured at the centre of the sodium absorption line; B and C, measured on the edges of the line as the indicated distance from the line centre

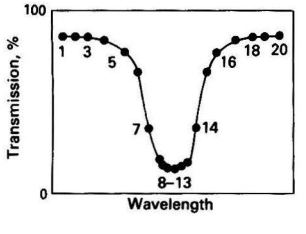

Fig. 6. Intensity measurement points across the absorption profile with a digitally sampled data acquisition system. Six types of absorbances calculated [absorbance = log (I_0/I)]: type 1, I_0 = 1–5 and 16–20, I = 6–15; type 2, I_0 = 1 and 20, I = 6 and 15; type 3, I_0 = 1 and 20, I = 5 and 16; type 4, I_0 = 1 and 20, I = 4 and 17; type 5, I_0 = 1 and 20, I = 3 and 18; type 6, I_0 = 1 and 20, I = 2 and 19

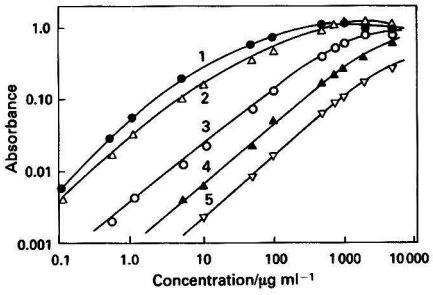

Fig. 7. A family of calibration graphs obtained using absorbance data acquired by sampling the absorption profile as in Fig. 6 (λ = 285 nm)

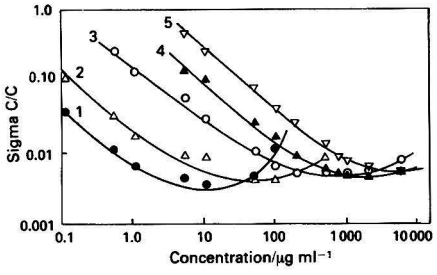

Fig. 8. Relative concentration error for the calibration graph shown in Fig. 7

to give a set of six estimates of the sample concentration. Ideally, the six estimates of the concentration should be identical but, because of noise and curve-fitting errors, they will never be exactly the same. Moreover, they will not be equally useful; at low sample concentrations, the measurements taken far from the line centre will be unusable because of poor signal to noise ratio, whereas at high sample concentrations, measurements taken near the line centre will be unusable because of curve-fitting errors. The selection of the optimum concentration estimate, or the optimum combination of concentration estimates, can be done in a number of ways. We have based our selection on the observation of relative concentration errors (RCE), which are calculated in the following way. For each sample measured by flame atomisation, the integration period (usually 5 s) is divided into 28 equal segments over which each of the six absorbances is calculated. This yields an estimate of the mean and standard deviation of each of the six absorbances. Each of these is converted into an equivalent mean and standard deviation of concentration by utilising the corresponding calibration graph in conjunction with some method of curve fitting or interpolation. The relative concentration error (RCE) is the ratio of the standard deviation of concentration to the mean concentration. In our work we have computed the reported concentration for each sample solution on the weighted average of the six concentration estimates, where the weighting factor is taken as the reciprocal of the square of the RCE. Thus, each of the concentration estimates is utilised to the extent that it can contribute useful information.

The use of six calibration graphs seems reasonable when one inspects plots of the calibration graphs themselves; the linear ranges of the graphs overlap over a total concentration range of four to six decades. However, the manipulation of six absorbances and six analytical calibrations considerably complicates the computer software. Moreover, a critical inspection of plots of RCE *versus* concentration shows that not all graphs are really necessary. A typical example is shown in Fig. 8. It can be seen here that the regions of lowest RCE on each graph overlap extensively. This is due to the fact that, by utilising appropriate curve-fitting procedures, the useful region of each calibration graph can be extended considerably above the upper limit of calibration graph linearity. As a result, it is possible to achieve acceptably low values of RCE over a five-decade concentration range by using only two graphs, Nos. 1 and 4.

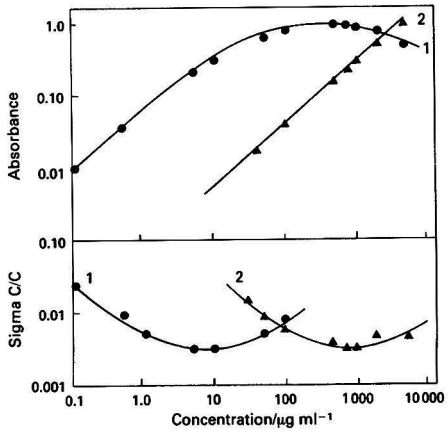

Fig. 9. Simplified calibration graphs obtained using a stairstep modulation waveform

In our system the data acquisition rate during the wavelength modulation cycle is constant; therefore, the distribution of the measured points with respect to wavelength is determined by the shape of the modulation waveform. For line profile measurements we use a triangular waveform, which gives a uniform point distribution. On the other hand, for quantitative analytical applications, a bigaussian waveform[17] has been used. This waveform results in a concentration of points near the centre of the line profile which allows the most sensitive (graph 1) absorbance to be calculated from a total of 20 intensity readings, resulting in a reduction of random noise (including quantisation noise). The less sensitive absorbances, however, are calculated from only four intensity readings and therefore tend to be noisier. It is for this reason that the RCE for the less sensitive graphs never achieves as low a value as that of the most sensitive graph. In recent work we have solved this problem, and also have simplified the calibration algorithms considerably, by using a stairstep modulation waveform[39] which in essence redistributes the measured points across the modulation interval in such a way as to allow the calculation of only two absorbances, similar to Nos. 1 and 4, but with better signal to noise ratio. The results for magnesium are shown in Fig. 9. Even for this very sensitive element, measurement of good precision can be made up to 5 000 μg ml^{-1} using only the 285.213-nm resonance line.

It should be pointed out that the technique just described is completely compatible with simultaneous multi-element operation and does not compromise the background correction capabilities or the detection limits of the system. Perhaps the greatest practical benefit of this approach is that it is not necessary to estimate beforehand the approximate concentration of each sample (except, of course, that the samples must fall within the range of the standards in order to avoid extrapolation errors).

Spectral Profiles

Conventional line-source atomic-absorption spectrometry is in the unique position of being the only kind of modern absorption spectrometry that is ordinarily performed with non-tunable monochromatic light sources. It is therefore impossible to measure the absorption spectrum of a sample. Certainly, in other areas of spectroscopy the measurement of the spectrum is considered to be essential. In practical terms, this means that one has no assurance that an absorption signal measured for a given sample is indeed due to the pure atomic absorption of the analyte, rather than to some unsuspected problem from excessive or structured background absorption or from some unsuspected spectral interference. Of course, atomic-absorption spectra are fairly simple, so the occurrence of spectral interference is rare. Certainly, conventional deuterium arc background correctors do work satisfactorily in many instances. However, the point is that there is no way to be sure that there are no spectral complications, because the spectrum cannot be observed. The potential for such problems can be expected to become greater as more sensitive methods, such as electrothermal atomisation, are applied to more complex and unfamiliar materials.

With the SIMAAC system, the measurement of spectral profiles is facilitated by the ability to perform ensemble averaging over selected time intervals during the atomisation and to plot the resulting profiles on the line printer. The system has been used to measure both flame[30] and time-resolved furnace[37] profiles, to study several spectral interferences and to characterise some previously unmeasured absorption lines.[30]

Applications

Table 3 lists some of the samples to which the continuum source method has been applied, the elements which have been measured and the mode of atomisation. Many of these are reference materials. In general, we find that the accuracy of single-element CEWM-AA measurement, in which the analytical conditions are individually optimised for each element, is equal to that of line-source atomic-absorption measurements of the same samples. The accuracy of simultaneous multi-element measurement under compromise analytical conditions is generally slightly poorer than the accuracy that can be obtained by optimised single-element measurement. This is not unexpected, of course. Based on a large number of measurements of many different reference materials over a period of about 5 years, it has been found that accuracies of the order of 5–15% can generally be obtained for those elements whose concentrations are well above the detection limit. When electrothermal atomisation is used, the best results are generally obtained by using a platform and by basing quantitation on peak-area measurement.[40]

The prototype of the SIMAAC system is now installed at the Nutrient Composition Laboratory, US Department of Agriculture, Beltsville, MD, USA, where it is under the supervision of Dr. J. M. Harnly. The system is in daily use both for routine sample analysis and for research purposes.

Atomic Emission

A significant advantage of the wavelength modulation technique compared to other methods of background correction is that it also provides background-corrected *emission* measurements, which is something commercial atomic-absorption systems do not provide. The technique is equally applicable to flame, plasma and electrothermal atomisation. Moreover, the extended range and profile measurement capabilities also apply to emission measurement. Simultaneous multi-element analysis by carbon furnace atomic emission has been shown to be feasible using the SIMAAC instrumentation.[41]

Table 3. Applications of continuum-source method

Material*	Elements determined	Atomisation
Bronze (IPT Standard 10A)	Fe, Ni, Sb, Sn, Zn, Pb	Flame
Brass (IPT Standard 40)	Pb, Sn, Zn	Flame
Sub-bituminous coal (SRM 1635)	Cu	Electrothermal
Limestone (SRM 1c)	Ca	Flame
Water (SRM 1643a)	Ag, Cr, Cu, Fe Ni, Ba, Mo, Al, V, Co, Pb, Zn, Mn	Electrothermal
Bovine liver (SRM 1577)	Mn, Fe, Cu, Mg, Na, K, Ca, Zn	Flame
	Cu, Mn, Fe, Zn, Ca, K	Electrothermal
Orchard leaves (SRM 1571)	Mn, Zn, Cu, Fe, Mg, Ca, Na, K	Flame
Fly ash (SRM 1633, 1633a)	Mn, Zn, Cu, Fe, Cr, Co, Mg, Ca, Na, K	Flame
USGS rocks AGV-1 (GSP-1, BCR-1)	Mn, Zn, Cu, Fe, Cr, Mg, Ca, Na, K	Flame
Wheat flour (SRM 1567)	Mn, Zn, Fe, Cu, Mg, K	Flame
Rice flour (SRM 1563)	Mn, Zn, Fe, Cu, K	Flame
	Mn, Cu, Fe, Zn, Ca, K	Electrothermal
Spinach leaves (SRM 1570)	Mn, Zn, Fe, Cu, Mg, K	Flame
Manganese nodules, USGS A1 and P1	Mn, Zn, Co, Ni, Na, K, Mg, Fe, Cu	Flame
Orange, tomato, pineapple, apple, prune juice	Mn, Zn, Fe, Cu, Mg, Na, Cr, Ni, Co	Flame
Urine (pool sample)	Cr	Electrothermal
Blood serum	Na, K, Mg, Ca, Zn, Cu, Fe	Flame

* IPT, Instituto de Pesquisas Techológicas; SRM, National Bureau of Standards Standard Reference Materials; USGS, US Geological Survey.

The Future

The use of a continuum primary source in atomic-absorption measurement is a rational alternative to the conventional line source method. The advantages are clear: the convenience of a single source, excellent background correction, the ability to measure spectral profiles, greatly extended analytical range and the proved ability to make useful simultaneous multi-element measurements with either flame or electrothermal atomisation. However, the disadvantages are equally clear: the detection limits for several elements in the low-UV region are significantly poorer and the present multi-element system is expensive and complex. Indeed, the commercial production of such a system would present many challenging engineering problems. We believe, however, that this is not an unreasonable future prospect. Atomic-absorption spectrometry may be a mature technique, but it is not a static one. The range of commercial equipment now encompasses not only simple low-cost models, but also elaborate, automated, top-of-the-line systems whose cost now approaches that of many plasma atomic-emission systems. The newest sequential multi-element systems are exceedingly complex optically and electromechanically, with multiple lamp turrets, programmable power supplies, beam splitters and choppers, separate

background corrector lamps (possibly two, deuterium and tungsten), automatically controlled monochromators, etc. The continuum-source approach, on the other hand, is optically simple, even elegant. Its complexity lies more in the data acquisition and processing, and indeed the computer system and the software required to run SIMAAC is elaborate. However, this is one area of modern technology where the performance/cost ratio is increasing dramatically and rapidly. There are now comparatively low-cost computer systems available whose memory and computing power far exceed those of our prototype system. It is not likely that that will long remain a limiting factor.

In the future development of the continuum-source method, perhaps the most pressing need is to improve the detection limits. In this connection the most serious limitation is the comparatively small slit area of presently available high-resolution spectrometers, primarily due to slit-height restrictions. Harnly[42] has predicted, on the basis of signal to noise calculations, that presently available 0.5-m monochromators based on large holographic gratings could offer a 5-fold signal to noise advantage over the present échelle spectrometer for the photon-noise limited case. This would mean that a single-channel continuum-source atomic-absorption system could be constructed now that would provide detection limits better than those at line-source instruments for many elements.

Even considering its present limitations, however, the continuum-source method has proved to be a very useful method, capable of solving many analytical problems with convenience and speed. With continued development, there is every reason to believe that this approach will also play a role in the future of analytical atomic spectrometry.

References

1. Walsh, A., *Spectrochim. Acta,* 1955, **7**, 108.
2. Allan, J. E., *Spectrochim. Acta,* 1962, **18**, 259.
3. Gibson, J. H., Grossman, W. E., and Cooke, W. D., *Appl. Spectrosc.,* 1962, **16**, 47.
4. Manning, D. C., and Kahn, H. L., *At. Absorpt. Newsl.,* 1965, **4**, 224.
5. Frank, C. W., Schrenk, W. G., and Meloan, C. E., *Anal. Chem.,* 1967, **39**, 534
6. Fassel, V. A., Mossotti, V. G., Grossman, W. E. L., and Kniseley, R. N., *Spectrochim. Acta,* 1966, **22**, 347.
7. McGee, W. W., and Winefordner, J. D., *Anal. Chim. Acta,* 1967, **37**, 429.
8. Snelleman, W., *Spectrochim. Acta, Part B,* 1968, **23**, 403.
9. Elser, R. C., and Winefordner, J. D., *Anal. Chem.,* 1972, **44**, 698.
10. Nitis, G. J., Svoboda, V., and Winefordner, J. D., *Spectrochim. Acta, Part B,* 1972, **27**, 345.
11. Veillon, C., and Merchant, P., Jr., *Appl. Spectrosc.,* 1973, **27**, 361.
12. Cochran, R. L., and Hieftje, G. M., *Anal. Chem.,* 1978, **50**, 791.
13. Bower, J., Bradshaw, J., and Winefordner, J., *Talanta,* 1979, **26**, 249.
14. Blackburn, M. B., and Winefordner, J. D., *Can. J. Spectrosc.,* 1982, **27**, 137
15. Keliher, P. N., and Wohlers, C. C., *Anal. Chem.,* 1974, **46**, 682.
16. Keliher, P. N., and Wohlers, C. C., *Anal. Chem.,* 1976, **48**, 140.
17. Zander, A. T., O'Haver, T. C., and Keliher, P. M., *Anal. Chem.,* 1976, **48**, 1166.
18. O'Haver, T. C., Harnly, J. M., and Zander, A. T., *Anal. Chem.,* 1977, **49**, 665.
19. Zander, A. T., O'Haver, T. C., and Keliher, P. N., *Anal. Chem.,* 1977, **49**, 838.
20. Harnly, J. M., and O'Haver, T. C., *Anal. Chem.,* 1977, **49**, 2187.
21. Guthrie, B. E., Wolf, W. R., and Veillon, C., *Anal. Chem.,* 1978, **50**, 1900.
22. O'Haver, T. C., Harnly, J. M., and Zander, A. T., *Anal. Chem.,* 1978, **50**, 1918.
23. O'Haver, T. C., "Wavelength Modulation Spectroscopy," *in* Hercules, D. M., *Editor,* "Contemporary Topics in Analytical and Clinical Chemistry," Plenum, New York, 1978, p. 1.
24. Epstein, M. S., and Zander, A. T., *Anal. Chem.,* 1979, **51**, 915.
25. O'Haver, T. C., *Anal. Chem.,* 1979, **51**, 91A.
26. Veillon, C., Wolf, W. R., and Guthrie, B. E., *Anal. Chem.,* 1979, **51**, 1022.
27. Harnly, J. M., O'Haver, T. C., Golden, B., and Wolf, W. R., *Anal. Chem.,* 1979, **51**, 2007.
28. Harnly, J. M., and O'Haver, T. C., *Anal. Chem.,* 1981, **53**, 1291.
29. Harnly, J. M., Miller-Ihli, N. J., and O'Haver, T. C., *J. Autom. Chem.,* 1982, **4**, 54.
30. Miller-Ihli, N. J., O'Haver, T. C., and Harnly, J. M., *Anal. Chem.,* 1982, **54**, 799.
31. Harnly, J. M., *Anal. Chem.,* 1982, **54**, 876.
32. Harnly, J. M., *Anal. Chem.,* 1982, **54**, 1043.
33. Kane, J. S., and Harnly, J. M., *Anal. Chim. Acta,* 1982, **139**, 297.
34. Harnly, J. M., Kane, J. S., and Miller-Ihli, N. J., *Appl. Spectrosc.,* 1982, **36**, 637.
35. Messman, J. D., Epstein, M. S., Rais, T. C., and O'Haver, T. C., *Anal. Chem.,* 1983, **55**, 1055.
36. Harnly, J. M., Patterson, K. Y., Veillon, C., Wolf, W. R., Marshall, J., Littlejohn, D., Ottaway, J. M., Miller-Ihli, N. J., and O'Haver, T. C., *Anal. Chem.,* 1983, **55**, 1417.
37. Miller-Ihli, N. J., O'Haver, T. C., and Harnly, J. M., *Appl. Spectrosc.,* 1983, **37**, 429.
38. Miller-Ihli, N. J., O'Haver, T. C., and Harnly, J. M., *Anal. Chem.,* in the press.
39. Harnly, J. M., Wolf, W. R., and Miller-Ihli, N. J., "Quality Assurance of Analysis of Inorganic Nutrients in Foods," *in* Stewart, K., *Editor,* "Modern Methods of Food Analysis," Proceedings of 7th IFT-IUFOST Basic Symposium, 43rd Annual Meeting of International Food Technology, New Orleans, LA, June, 1983.
40. Harnly, J. M., Miller-Ihli, N. J., and O'Haver, T. C., *Spectrochim. Acta,* in the press.
41. Marshall, J., Littlejohn, D., Ottaway, J. M., Harnly, J. M., Miller-Ihli, N. J., and O'Haver, T. C., *Analyst,* 1983, **108**, 178.
42. Harnly, J. M., *Anal. Chem.,* in the press.

Paper A3/270
Received August 19th, 1983

Combined Use of Photoacoustic Spectroscopy and Differential Thermal Analysis in Mineralogical Analysis

Malcolm S. Cresser and Neil T. Livesey
Department of Soil Science, University of Aberdeen, Old Aberdeen, AB9 2UE, UK

The ultraviolet - visible and near-infrared absorption spectra of minerals can be conveniently studied by photoacoustic spectroscopy. The spectra show considerable overlap, which limits their value for qualitative mineralogical analysis. However, the changes in mineral PA spectra on heating, which correspond mainly to dehydration or dehydroxylation reactions, changes in bonding of iron or oxidation of Fe(II), show considerable potential for the identification of the minerals themselves and of the processes that take place during their alteration. The changes are discussed briefly for a wide range of common minerals, and the analytical potential of this approach is critically appraised.

Keywords: *Minerals; photoacoustic spectroscopy; thermal analysis*

Although some interest has been shown in the photoacoustic spectra of minerals over the UV - visible and near-IR regions,[1-3] and reflectance spectra have been published for many minerals over the same regions,[4-6] virtually no use is made of photoacoustic spectroscopy (PAS) or reflectance spectroscopy in routine mineralogical analysis. The reasons for this restricted interest are readily apparent. Most near-IR bands are attributable to overtone or combination bands involving bonding to hydrogen, which for most common minerals means to OH bonds; visible spectra are dominated by the oxidation state of iron present and its bonding. Thus, although the PA spectra of different single minerals may exhibit distinct differences, there is a high probability of substantial overlap of spectra of the diverse minerals present in samples such as soils or ground rocks. However, changes in spectra attributable to specific dehydration, dehydroxylation or iron oxidation reactions, which occur only after heating at certain specific temperatures and which may be readily identified, lend themselves to examination by PAS. The purpose of this investigation was to assess the potential value of changes in mineral PA spectra in the qualitative analysis of minerals and to elucidate the changes that they undergo during heating.

Experimental

Apparatus

The PA spectrometer used was an OAS 400 (EDT Research Ltd.) controlled by a Commodore 32K minicomputer using the manufacturer's software. The computer was used to produce ratios of all spectra to carbon black reference spectra (Darko G60, dried at 105 °C), to compensate for differences in the responses of the PA detector and reference detector to radiation of different wavelengths and in non-uniformity in the absorption of radiation between leaving the spectrometer beam splitter and reaching the sample or reference cells, *e.g.*, from water on silica surfaces.

Differential thermal analysis (DTA) and thermogravimetric (TG) traces were run at 10 or 20 K min^{-1} on Stanton Redcroft Model DTA 673-4 and TG 750 instruments, respectively, to allow selection of suitable heating temperatures. All mineral samples were run in air, apart from a series of ochre samples containing up to 30% of organic matter, which were run in oxygen-free nitrogen.

Materials

Samples of minerals and related materials were obtained from the authors' Departmental collection or from Gregory, Bottley & Lloyd, London. All were identified by thermal analysis and/or X-ray diffraction and it was established that they were composed almost exclusively of one mineral, except for those reported otherwise.

Samples were air dried and ground, if necessary, to pass a 240-mesh (64-μm) sieve, either by hand with an agate pestle and mortar or, for hard materials, with a Grindex ball-mill using tungsten carbide balls. Except where otherwise stated, the powdered samples were oven-dried overnight at 105 °C, cooled and stored in desiccators over calcium chloride prior to running PA spectra. The sample cell was filled with unpacked powder (*ca.* 50 mg) and the sample surfaces were levelled with the edge of a microspatula.

Results and Discussion

Iron Oxides and Oxyhydroxides

Common oxides, oxyhydroxides and hydroxides, particularly those of iron, are of great interest because of their importance in distinguishing soil types and because of their role in soil physico-chemical processes. Moreover, the capability of PAS for investigation of changes in absorption spectra with depth below particle surfaces via changes in detector phase or in the modulation frequency used is potentially valuable for the study of oxide coatings. For these reasons, and because of the frequent difficulty in chemical characterisation of oxides and hydroxides by alternative techniques, this group was the first selected for study.

Goethite

Goethite (α-FeOOH) is the most frequently occurring iron oxide in soils, because of its high stability under a wide range of soil conditions.[7] Heating goethite at about 380 °C causes a mass loss corresponding to dehydroxylation to haematite

$$\underset{\text{goethite}\\(\text{yellow - brown})}{2\alpha\text{-FeOOH}} \xrightarrow{\text{heat}} \underset{\text{haematite}\\(\text{bright red})}{\alpha\text{-}Fe_2O_3 + H_2O}$$

The mass loss started at 312 °C on the sample used and was complete at 393 °C. The change in the UV - visible PA spectrum is clearly visible, the spectrum after heating (in air) at 394 °C resembling closely that of haematite [Fig. 1 (*a*) and (*b*)] and, like that of haematite, remaining unchanged on further heating to 1 000 °C. The near-IR spectrum of goethite, like the reported reflectance spectrum,[6] is devoid of diagnostically useful features.

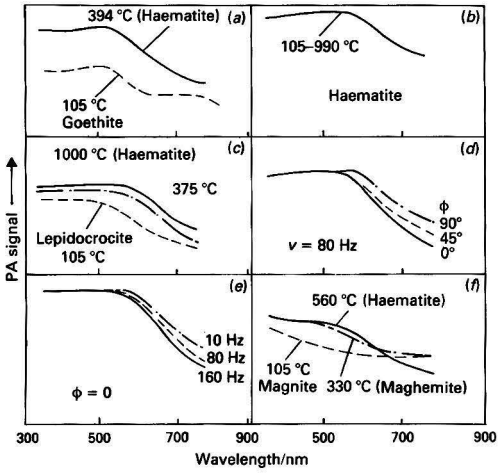

Fig. 1. UV - visible PA spectra of iron minerals, heated in air to the temperatures indicated. Names of products are given in parentheses

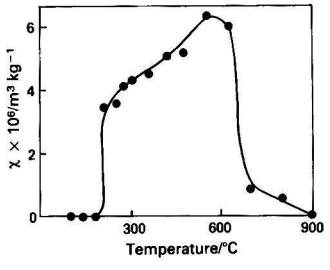

Fig. 2. Variation in the mass magnetic susceptibility, χ, of lepidocrocite, from "ochre," on heating in air

Haematite

In soil, haematite (α-Fe_2O_3) often occurs in association with goethite, where it has a strong red pigmenting effect.[7] The mineral is stable over a wide temperature range, the small reversible peak observed at around 680 °C[8] being of no consequence in this study. As already mentioned, the UV - visible PA spectrum [Fig. 1(*b*)] is unchanged as a result of heating up to 1 000 °C. The near-IR spectrum is broad and featureless over the range 1.2–2.5 μm, like the reported reflectance spectrum,[6] and is also not significantly influenced by heating.

Lepidocrocite

Lepidocrocite (γ-FeOOH) is found, often associated with goethite, only in hydromorphic soils where Fe(II) is produced at very low oxygen concentrations.[7] An ochre sample from a waterlogged site at Peatfold Burn, Glenbuchat, Grampian Region, Scotland, was identified as impure lepidocrocite from its DTA trace and from the variation in its mass magnetic susceptibility with heating (see Fig. 2). Lepidocrocite dehydrates to maghemite when heated at 275–410 °C.[9,10] The sample heated in air at 210 °C exhibited a substantial increase in susceptibility, indicative of maghemite formation. The maghaemite is stable to *ca.* 625 °C because of impurities,[9,11] but then undergoes exothermic conversion to haematite, with a corresponding decrease in susceptibility. The UV - visible PA spectra after heating at 105, 375 and 1 000 °C are shown in Fig. 1(*c*). The spectrum of the impure lepidocrocite differs slightly from those of goethite and haematite, but the difference would be more readily discernible from comparison of the derivative PA spectra, as suggested for goethite and haematite.[12] For pure lepidocrocite, it might be expected that a PA spectrum corresponding to maghemite would be obtained on heating at 375 °C, and at 1 000 °C a spectrum corresponding to haematite should be observed. On the authors' sample, however, the PA spectrum after heating the impure lepidocrocite at 375 °C was closer to that of haematite than to that of maghemite, which may be more reliably obtained by low-temperature oxidation of magnetite.[9] This probably reflects the conversion of maghemite to haematite, at or near particle surfaces, to an extent that depends on the nature and distribution of impurities.[9] It was therefore decided to investigate the homogeneity of the particles of lepidocrocite after heating in air at 375 °C.

Generally, the higher the modulation frequency or the smaller the phase lag between the irradiation period and the detector response, the more the characteristics of the PA spectrum obtained are dominated by the sample surface. Lower frequencies or a higher phase favour a greater contribution from sub-surface zones of the sample particles. For the sample in question, lower phase and/or higher frequency yielded a spectrum increasingly similar to that of haematite [Fig. 1(*d*) and (*e*)], confirming the presence of haematite rather than maghemite, at least at the particle surfaces. The spectra in Fig. 1(*c*) were plotted at a modulation frequency of 80 Hz and a phase of 105°, conditions found by the authors to give optimum signal to noise ratios for numerous mineral samples: the higher frequency reduces the effective sampling depth. The results must, however, be interpreted with great caution because, for particles in the silt-size range, the particle size becomes limiting in this approach.

Provided spectra are normalised at one wavelength, to allow comparisons of PA spectra to be made easily, the authors have found scanning PA spectra at different frequencies and/or phase angles to be useful for investigation of particle homogeneity, in spite of the change in PA signal with frequency of modulation. Some ochre samples studied, for example, appear to be completely uniform, whereas others show a marked lack of homogeneity.

Maghemite

Samples of "pure" maghemite (γ-Fe_2O_3) of natural origin are not readily available. However, it may be assumed that the PA spectrum from magnetite after heating in air to 330 °C corresponds to maghemite [Fig. 1(*f*)]. At higher temperatures maghemite is converted into haematite. The near-IR spectrum was featureless over the range 1.2–2.5 μm.

Magnetite

The UV - visible PA spectrum of magnetite (Fe_3O_4) is clearly very different from the spectra of other iron oxides and hydroxides [Fig. 1(*f*)], but the near-IR PA spectrum, like the reflectance spectrum,[6] is completely featureless. According to Mullins,[9] magnetite oxidises to maghemite at 150–250 °C, but this is a low temperature range for natural samples.[8] The authors' sample gave the first DTA peak at 328 °C, a more typical value, and the features of the UV - visible spectrum after heating at this temperature may be attributed to maghemite, which is increasingly oxidised to haematite at higher temperatures, depending on purity.

"Limonite"

"Limonite" is now obsolete as a mineral name, but in the past was extensively used to describe brown, rusty iron oxide accumulations, generally containing appreciable amounts of goethite.[7] PA spectra of a "limonite" sample have been published elsewhere by the authors.[12] That particular sample, which was shown by X-ray diffraction to be predominantly

quartz, gave, when oven dried, a UV - visible PA spectrum closer to those of haematite or lepidocrocite than that of goethite. "Cryptocrystalline lepidocrocite along with haematite and additional water in some form," one suggestion for the nature of limonite,[6] would certainly fit the PAS data, as would the slight dehydration at *ca.* 335 °C. Unlike goethite, the limonite sample showed an absorption band at 2.46 μm, which disappeared after heating to 335 °C.

Carbonates

Hunt and Salisbury[5] commented that most of the broad bands in the 1-μm region of the reflectance spectra of carbonates are attributable to the presence of iron substituted for the appropriate metal ion in the carbonate. This is true even when the iron is present at relatively low concentrations. The near-IR reflectance spectra also show a series of bands between 1.6 and 2.5 μm, attributable to overtone and combination tones of the internal vibrations of the CO_3^{2-} radical or of the CO_3^{2-} radical with vibrations of the entire structure.

Calcite

The DTA trace for calcite gave a very strong endothermic peak at 962 °C, well within the usual range of 860–1 010 °C quoted for this mineral.[13] The TG showed negligible loss up to *ca.* 720 °C, followed by rapid mass loss of 37.5 and 43% for two different samples studied, attributable to evolution of CO_2. The near-IR PA spectra of oven-dried samples were similar to the reflectance spectrum reported by Hunt and Salisbury,[5] with absorption bands at 1.9–2.0, 2.2–2.4 and 2.5 μm [Fig. 3(*a*)]. Heating samples at 800 or 960 °C gave two similar spectra, the main features being a broad band at 1.2–1.6 μm and a sharper band at around 2.25 μm. The magnitude of the former in the carbonate samples studied was related to their iron concentration, as determined by dissolution and flame atomic-absorption spectroscopy. The dominant feature in the UV - visible spectra of both calcite samples and, indeed, of all the carbonates studied, was the appearance of a broad absorption band at around 300 nm. This band becomes even stronger on heating to high temperatures [Fig. 3(*b*)], but for calcite the spectrum obtained on heating was different to that obtained on heating chalk, marble or dolomite samples [Fig. 3(*e*)].

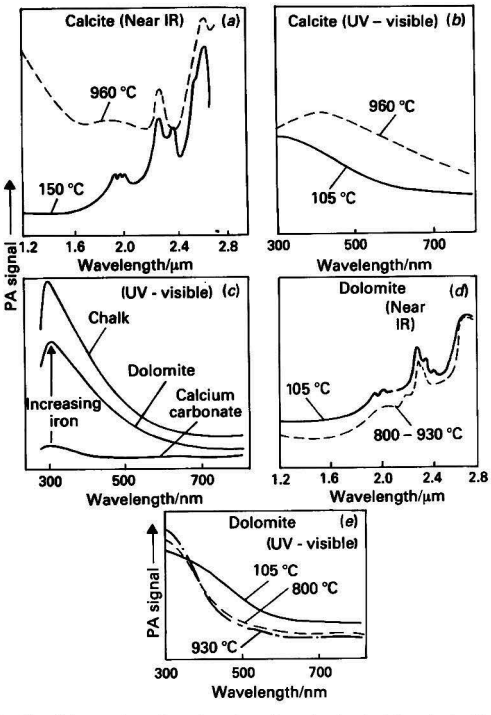

Fig. 3. PA spectra of carbonate minerals, heated in air to the temperatures indicated. Calcium carbonate, analytical-reagent grade

Chalk and marble

The near-IR PA spectra of chalk and marble dried at 105 °C were similar to that of calcite, although there were slight changes in the relative peak heights. The particular marble sample selected had a low iron content and did not give a strong absorption band at around 1.2 μm on heating to 960 °C. The dominant features of the UV - visible spectra have already been summarised. Fig. 3(*c*) shows the spectra of chalk, dolomite and analytical-reagent grade calcium carbonate, which contained low, very low and negligible amounts of iron, respectively.

Dolomite

Fig. 3(*d*) shows typical near-IR spectra for a dolomite sample low in iron. The spectrum of the oven-dried sample is similar in most respects to that of calcium carbonate. Although the DTA trace for dolomite showed two distinct strong endothermic peaks, as is invariably the case,[13] heating a small finely ground sample for 1 h in a furnace at 800 °C may have been sufficient to remove CO_2 from both magnesium and calcium carbonates. It is difficult to state with certainty whether any residual carbonate was contributing to the near-IR PA spectrum after heating to this temperature. It seems improbable, bearing in mind that identical spectra were obtained after heating at 800 and 930 °C. Further heating above 800 °C also had only a very minor influence on the UV - visible spectrum of dolomite.

After heating to high temperatures, the spectra obtained from all carbonates except calcite were very similar to those obtained from heating appropriate oxide samples at the same temperature, although the features attributable to iron still varied with the iron concentration.

Silicates

Most useful diagnostic information for silicate identification comes from spectral features corresponding to dehydration and/or dehydroxylation reactions in the near-IR region. The UV - visible PA spectra are generally of less value, again being dominated by the effects of iron, especially after heating at elevated temperatures.

Talc

DTA curves for talc [$Mg_3Si_4O_{10}(OH)_2$] are reported to be very consistent, with a solitary endothermic peak at 950–1 000 °C.[14] The TG trace showed that mass loss commenced at *ca.* 950 °C, corresponding to dehydroxylation, and was complete at >1 000 °C. Two different talc samples gave virtually identical sets of near-IR PA spectra and only one example is, therefore, included [Fig. 4(*a*)]. Bands were observed for the oven-dried sample at 1.45, 2.14, 2.18, 2.27, 2.36, 2.43 and 2.50 μm, but only a band at 2.26 μm was conspicuous after heating at 1 040 °C. The spectrum is similar to the reflectance spectrum published by Hunt and Salisbury,[4] although the strong OH band they reported at *ca.* 1.4 μm is much reduced here, presumably as a result of oven drying. The UV - visible PA spectrum of the oven-dried sample was featureless, but the heated sample exhibited strong absorption attributable to iron substituted for small amounts of magnesium [Fig. 4(*b*)]. This spectrum is typical of those obtained on

heating most iron-containing silicates, and bears some similarity to that obtained from strongly heated dolomite [Fig. 3(*e*)].

Montmorillonite

The composition of montmorillonite $[(M_y^+.nH_2O)(Al_{2-y}Mg_y)Si_4O_{10}(OH)_2]$ is very variable, and considerable differences between the near-IR absorption spectra of different samples might be expected and have, indeed, been reported.[4] The PA spectrum shown, for an air-dried sample from Japan, is similar to that reported for an air-dried sample from the USA,[4] having strong bands at 1.48, 1.97 and 2.27 μm. The band at 1.97 μm is relatively much enhanced if an air-dried rather than an oven-dried sample is used. This PA spectrum shows small, but significant, shifts in the band positions relative to those for a different sample (Wyoming bentonite) reported by the authors elsewhere.[12] In both of the authors' samples, the band at around 1.5 μm was negligible for the oven-dried material, because of the low temperature of the first stage of dehydration.

Micas

There is a considerable difference between the near-IR and UV - visible absorption spectra of muscovite $[KAl_2(Si_3Al)O_{10}(OH)_2]$ and biotite $[K(Mg,Fe)_3(Si_3Al)O_{10}(OH)_2]$. The near-IR PA spectrum of muscovite [Fig. 4(*d*)] is strikingly similar to the reflectance spectrum,[4] with strong absorption bands at 1.47, 2.26, 2.40, 2.44 and 2.48 μm. It also closely resembles a PA absorption spectrum reported elsewhere.[1] The TG trace showed mass loss from 670 °C, becoming more rapid at around 850 °C. The strong OH bands are not present in the PA spectrum at these elevated temperatures because of the dehydroxylation. Muscovite absorbs very little light over the range 350–800 nm, until strongly heated. At 860 and 1015 °C, the PA spectra are similar to that of talc heated to 1040 °C. The near-IR PA spectrum of biotite is very different from that of muscovite in that it is dominated by the broad absorption band in the 0.8–2.0 μm region, caused by Fe(II) and Fe(III) ions,[4] and exhibits negligible fine structure, in this respect closely resembling the reflectance spectrum. The near-IR and UV - visible PA spectra indicate oxidation of Fe(II) to Fe(III) at elevated temperature [see Fig. 4(*e*) and (*f*)].

The near-IR spectrum of oven-dried hydrous mica ("illite") shows relatively little fine structure because dehydration invariably commences for this type of mica at a temperature below 100 °C, with further dehydroxylation taking place at around 550 °C.[14] This second DTA peak occurred at 585 °C for the sample studied. The unresolved series of peaks at around 2.4–2.5 μm were still present after the sample was heated at 420 °C, but disappeared after heating at 590 °C [Fig. 5(*a*)]. An unexpected feature of the DTA trace was a small endothermic peak at 420 °C. Heating at this temperature caused the major change in the UV - visible PA spectrum, which was similar to that obtained after heating at 590 °C, as shown in Fig. 5(*b*), presumably owing to a change in oxidation state of iron present as an impurity.

Kaolinite

The DTA curves of kaolinites $[Al_2Si_2O_5(OH)_4]$ are dominated by a strong endothermic dehydroxylation peak at 500–700 °C, and a sharp exothermic peak at around 1000 °C.[14] On the samples studied, slight mass loss commenced at around 450 °C. The near-IR PA spectrum [Fig. 5(*c*)] showed strong bands at 1.47, 2.23 and 2.26 μm and weaker bands at 1.88, 1.96 and 2.43 μm, after drying at 105 °C. The bands at 1.47 and 1.96 μm were, in fact, much more intense on air-dried samples. After dehydroxylation at 600 °C, only weak bands at around 1.9 μm and a stronger band at 2.26 μm remained. This spectrum is very similar to the reflectance spectra reported by Hunt and Salisbury.[4] Another sample of kaolinite from Japan gave a very similar PA spectrum and behaved in the same way on heating. However, for this sample the 2.23-μm band was stronger than that at 2.26 μm.

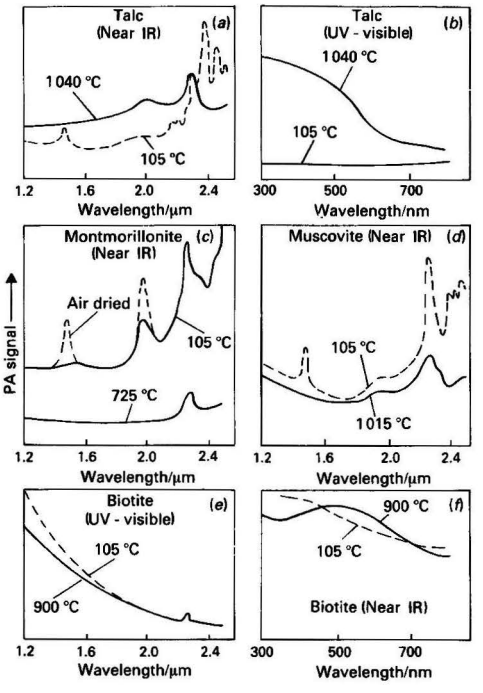

Fig. 4. PA spectra of sheet silicate minerals, heated in air to the temperatures indicated

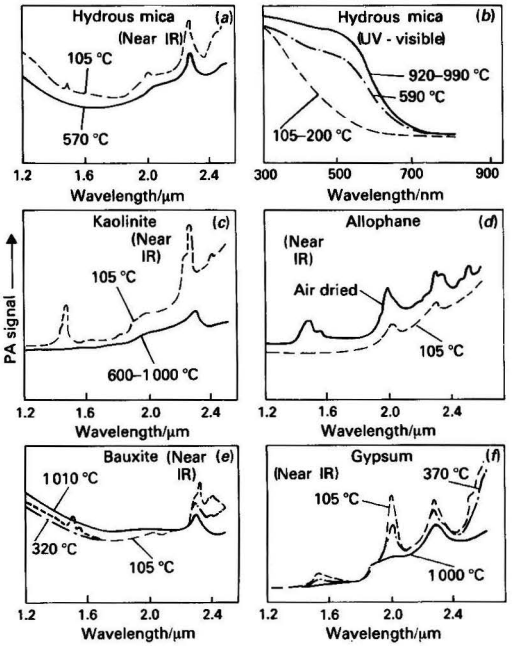

Fig. 5. PA spectra of various minerals, heated in air to the temperatures indicated

Allophane

There are several minerals included under the general name allophane[15] [$mAl_2O_3.nSiO_2.pH_2O$]. The authors' sample came from Japan and its behaviour is probably typical of a wide range of these materials. The changes in the near-IR PA spectrum on heating this sample occur below normal oven-drying temperature. Thus, although there is a considerable change on oven drying an air-dried sample, subsequent changes on heating at 600 °C were negligible. On heating at 105 °C, peaks at 1.48, 2.44 and 2.52 μm were lost and that at 1.99 μm was greatly reduced [Fig. 5(*d*)].

Feldspars

The feldspars are generally thermally inert, the examples studied giving mass losses of <1% over the range 20–1 000 °C. A small endotherm was obtained for oligoclase at 908 °C. The PA spectra in the near-IR region were generally of limited diagnostic value, showing only peaks corresponding to liquid-filled vacuoles, very similar to those observed for reflectance spectra.[4] This was true for microcline, orthoclase, anorthoclase, albite and oligoclase, the five samples studied. Changes occurred in the UV - visible PA spectra on heating to around 1 000 °C, owing to the presence of small amounts of iron.

Quartz

As might be expected, quartz shows little of interest in TG or in its near-IR PA spectrum, although weak included-water bands were observed at *ca.* 1.9, 2.5 and 2.6 μm for milky quartz. Heating one of the samples studied at 1 000 °C produced weak spectral features in the UV - visible region attributable to iron. This is surprising unless the sample was slightly contaminated with iron during milling, although a tungsten carbide ball-mill was used and this seems unlikely.

Other Minerals

Bauxite

A sample of bauxite gave a sharp endothermic peak only at 320 °C, and was, therefore, predominantly gibbsite [γ-$Al(OH)_3$]. The near-IR PA spectrum [Fig. 5(*e*)] was also similar to the reflectance spectrum reported for a sample of gibbsite from Brazil.[6] Dehydration proceeded rapidly from 245 °C, with a distinct change of slope in the TG trace at 315 °C. Mass loss was complete only at *ca.* 600 °C. The effect of heating on the near-IR PA spectra also indicates clearly that dehydroxylation proceeds in at least two stages, the formation of γ-AlOOH occurring as the first stage.[8]

Gypsum

The DTA trace for gypsum showed the expected double endotherm, the first corresponding to loss of water to give the hemihydrate, $CaSO_4.½H_2O$, and the higher temperature endotherm corresponding to dehydration to anhydrite. At ambient temperature, gypsum shows very strong absorption bands at 2.02 and 2.30 μm, and at 2.50 and 2.57 μm (unresolved), with weaker bands at around 1.5 μm. The PA signal intensity is reduced significantly on oven drying at 105 °C through partial dehydration [Fig. 5(*f*)]. Dehydration was still incomplete after heating at 370 °C, but complete at 1 000 °C.

Conclusion

As might have been expected, the near-IR region of the PA spectra of minerals is dominated by OH with a lesser contribution coming from CO_3^{2-} and SO_4^{2-} radicals vibrating as entities in the mineral structure. Therefore, minerals where O^{2-} is the predominant anionic species, the feldspars for example, show no fine structure of diagnostic value and little change on heating. In some respects this contributes to improved selectivity for the qualitative analysis of mixtures. However, these minerals are also often difficult to identify conclusively by other thermal methods of analysis.

The UV - visible PA spectra for the minerals studied are dominated by the presence of iron, and its position(s) and oxidation state within the mineral structure. The results for the characterisation of iron oxides, oxyhydroxides and hydroxides are encouraging, especially bearing in mind that differentiation between some of these substances may be difficult by alternative techniques. One of the strengths of PAS is that it may be used to characterise both surface coatings and the material immediately underlying these coatings to a certain extent. PAS may, therefore, be a useful tool for investigating surface reactions that occur during DTA or TG. However, PA results must sometimes be interpreted with caution. The lepidocrocite sample in this study was shown conclusively from magnetic susceptibility measurements to have been converted to a maghemite on moderate heating, whereas the PA spectrum of the particle surfaces was closer to that of haematite, indicating a surface phase change. Thus, it should always be remembered that PA spectra identify surface minerals in non-uniform materials.

Some hydrated minerals of interest gave particularly strong absorption bands in the near-IR region. It seems probable that near-IR PAS may be useful for the quantitative determination of minerals such as gypsum.

It is worth considering briefly the potential usefulness of the technique for qualitative and/or semi-quantitative analysis of relatively simple mixtures of X-ray amorphous minerals. If two or more minerals contain OH groups, but undergo dehydroxylation at considerably different temperatures, then a careful choice of heating conditions may allow positive identification. The presence of minerals that do not contain OH should not complicate such procedures. Where carbonate is present, the possibility exists for improving selectivity by simple acid dissolution. The latter approach may, in fact, be particularly suitable for confirming the presence of carbonate suspected from a near-IR PA spectrum.

The authors are indebted to The Royal Society, London, for the award of a grant for the purchase of the PA spectrometer and to Anthony Edwards, Prof. T. Fujisawa, David Grierson, Fiona Mitchell and Hazel Moir for the contributions they have made to this study.

References

1. Schmidt, R. L., *in* Stucki, J. W., and Banwart, W. L., *Editors*, "Advanced Chemical Methods for Soil and Clay Minerals Research," Reidel, Dordrecht, 1980, p. 451.
2. Adams, M. J., Beadle, B. C., King, A. A., and Kirkbright, G. F., *Analyst*, 1976, **101**, 553.
3. Adams, M. J., Beadle, B. C., and Kirkbright, G. F., *Analyst*, 1977, **102**, 569.
4. Hunt, G. R., and Salisbury, J. W., *Mod. Geol.*, 1970, **1**, 283.
5. Hunt, G. R., and Salisbury, J. W., *Mod. Geol.*, 1970, **2**, 23.
6. Hunt, G. R., Salisbury, J. W., and Lenhoff, C. J., *Mod. Geol.*, 1971, **2**, 195.
7. Schwertmann, U., and Taylor, R. M., *in* Dixon, J. B., and Weed, S. B., *Editors*, "Minerals in Soil Environments," Soil Science Society of America, Madison, WI, 1977, Chapter 5, p. 145.
8. Mackenzie, R. C., and Berggren, G., *in* Mackenzie, R. C., *Editor*, "Differential Thermal Analysis", Academic Press, London, 1970, Chapter 9, p. 271.
9. Mullins, C. E., *J. Soil Sci.*, 1977, **28**, 223.
10. Scheffer, F., Meyer, B., and Babel, U., *Beitr. Miner. Petrogr.*, 1959, **6**, 371.
11. Stacey, F. D., and Banerjee, S. K., "The Physical Principles of Rock Magnetism," Elsevier, Amsterdam, 1974.
12. Livesey, N. T., and Cresser, M. S., *in* Miller, B., *Editor*, "Thermal Analysis," Volume 1, Wiley, Chichester, 1982, p. 325.

13. Webb, T. L., and Krüger, J. E., *in* Mackenzie, R. C., *Editor*, "Differential Thermal Analysis," Academic Press, London, 1970, Chapter 10. p. 303.

14. Mackenzie, R. C., *in* Mackenzie, R. C., *Editor*, "Differential Thermal Analysis," Academic Press, London, 1970, Chapter 18, p. 497.

15. Wada, K., *in* Dixon, J. B., and Weed, S. B., *Editors*, "Minerals in Soil Environments," Soil Science Society of America, Madison, WI, 1977, Chapter 16, p. 603.

Paper A3/224
Received July 25th, 1983
Accepted August 25th, 1983

Determination of the Stoicheiometry of Uranium Dioxide by Differential-pulse Polarography*

Pier Luigi Buldini and Donatella Ferri
CNR-Lamel, Laboratorio Analisi Chimica dei Materiali, Via dell'Idraulico 17/2, I-40127 Bologna, Italy
and Ego Pauluzzi and Mario Zambianchi
Agip Nucleare, Direzione Laboratori, Via Sabbionara 611, I-40059 Medicina, Italy

Uranium dioxide is widely used as a nuclear fuel and usually it exists as a non-stoicheiometric hyperstate UO_{2+x} because of the oxygen interstitial arrangement. The proposed method for determining the oxygen to uranium ratio in uranium oxides is based on the dissolution of the nuclear fuel in concentrated phosphoric acid under an inert atmosphere, to preserve the uranium oxidation states. After complete dissolution, sulphuric acid is added in order to obtain a 1.47 M H_3PO_4 - 1.5 M H_2SO_4 supporting electrolyte. Differential-pulse polarographic determination of uranium(VI) directly follows at −0.09 V *versus* S.C.E. An aliquot of this solution is then oxidised with an almost equivalent amount of cerium(IV) sulphate solution, converting all uranium(IV) into uranium (VI); the total uranium content is then determined in the same way. The proposed method permits determinations of uranium(VI) levels as low as 0.2 μg ml^{-1} with a relative standard deviation of about 2%.

The oxygen to uranium ratio is calculated by the equation O/U = 2.000 0 + U(VI)/total U and a result of 0.001 unit is obtainable with a coefficient of variation of about ±0.1%.

Keywords: *Uranium dioxide; stoicheiometry; differential-pulse polarography; nuclear fuels*

Uranium dioxide is well known as a nuclear fuel; its composition approaches the theoretical ratio of uranium to oxygen of 1 : 2, but the exact stoicheiometry is seldom attained and usually uranium dioxide exists as a hyperstate UO_{2+x} because of the oxygen interstitial arrangement. Knowledge of the oxygen to uranium ratio is required in nuclear fuel specification and it is important for fuel behaviour in the reactor cycle.

The oxygen to uranium ratio in uranium oxides has been determined by several methods: fusion, ignition, titrimetry and the determination of uranium(VI) in the oxide. The determination of uranium(VI) is the most precise of these methods and perhaps the least susceptible to interference. Oxygen is chemisorbed interstitially in the crystal lattice of uranium dioxide and oxidises uranium(IV) to a higher oxidation state. Thus, the determination of the uranium(VI) serves as a measure of the excess oxygen and, coupled with total uranium determination, as a way to determine the exact composition of the oxide.

Several techniques, such as potentiometry,[1,2] spectrometry[3] and coulometry,[4,5] have been applied to the determination of uranium(VI) in the oxide. Polarography has also been applied to the determination of the oxygen to uranium ratio,[6-8] but no advantage was taken either of the use of modern pulsed techniques or of the uranium(VI) and total uranium determination. Modern pulsed techniques permit a highly accurate determination of the stoicheiometry values close to the theoretical one and the determination of U(VI) and total uranium with the same technique under the same conditions makes the calibration step unnecessary because the oxygen to uranium ratio is calculated as a ratio of U(VI) and U(IV + VI) without needing to know the absolute values.

The method described here is based on the dissolution of the nuclear fuel in non-oxidising conditions with concentrated phosphoric acid under an argon stream. After complete dissolution, sulphuric acid is added in order to obtain a 1.47 M H_3PO_4 - 1.5 M H_2SO_4 supporting electrolyte. A differential-pulse polarographic determination of uranium(VI) follows. An aliquot of this solution is then oxidised with an almost equivalent amount of cerium(IV) sulphate solution, so converting all uranium(IV) into uranium(VI) and determining total uranium in the same way.

* Research performed within the framework of the AGIP NUCLEARE - ENEA agreement for thermal reactor fuel development.

Experimental

Apparatus

A Metrohm (Herisau, Switzerland) E 506 Polarecord, equipped with an E 505 stand, was used. A forced-drop time of 2 s was imposed on the EA 1019/1 dropping-mercury electrode (DME). A Metrohm Model EA 285 platinum-wire counter electrode and a Metrohm Model EA 427 silver - silver chloride reference electrode were used. The differential-pulse polarographic conditions used were: DP, damping zero, mm/t_{drop} 0.5 and U_{pulse} −100 mV.

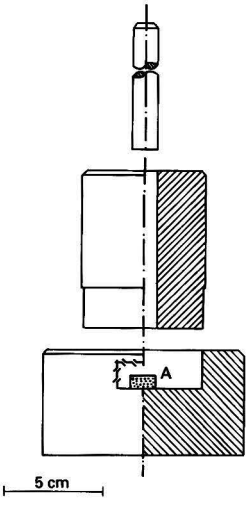

Fig. 1. Steel (AISI 316) mortar. A, Nuclear fuel pellet

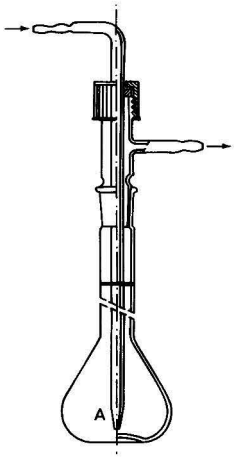

Fig. 2. Pyrex dissolution flask. A, Ar bubbler; capacity 50 ml

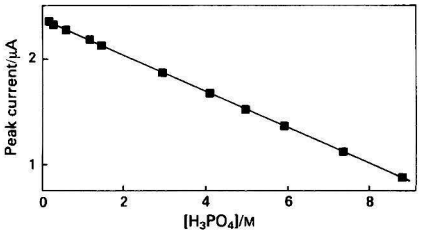

Fig. 3. Effect of H_3PO_4 concentration. U(VI) concentration, 2 μg ml^{-1}; polarographic conditions as reported under Experimental

The solutions were de-aerated with pure nitrogen for 5 min before polarographic analysis. All measurements were carried out at 25.0 ± 0.1 °C.

Nuclear-fuel pellets were crushed to a coarse powder in a steel mortar (see Fig. 1) and then the sample was directly weighed into the Pyrex dissolution flask shown in Fig. 2.

The calibrated flasks were filled with concentrated phosphoric acid, heated, left overnight and rinsed with doubly distilled water before use. If a set of equipment is kept for uranium determination only, it is sufficient to wash it after use with distilled water until it is required again.

Reagents

Erbatron electronic-grade reagents were used. The cerium(IV) sulphate was supplied by Merck (Darmstadt, FRG) and its saturated solution was obtained by dissolving 3.4 g of $Ce(SO_4)_2$ in 2 M H_2SO_4 in a 50-ml calibrated flask. Normal precautions for trace analysis were taken throughout.

Working standards were prepared by diluting a uranium(VI) stock solution (1 000 μg ml^{-1}) obtained by dissolving 0.1179 g of U_3O_8 (JMC Specpure 765) in 4 ml of hot 1 + 1 nitric acid. The solution was twice evaporated to dryness. After the nitric acid had been completely removed, the residue was dissolved by adding 20 ml of hot 85% H_3PO_4 and the solution was diluted to 100 ml with doubly distilled water.

Study of Polarographic Working Conditions

The polarographic behaviour of uranium is well known.[9,10] In order to couple the highest sensitivity with the best sample dissolution requirements, it was necessary to define the best working conditions with respect to the supporting electrolyte composition, the formation and oxidation kinetics and the influence of the oxidising agent.

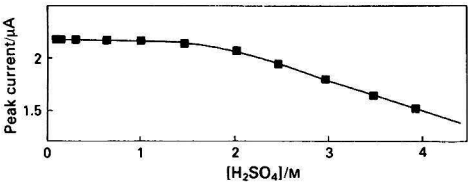

Fig. 4. Effect of H_2SO_4 concentration. U(VI) concentration, 2 μg ml^{-1}; polarographic conditions as reported under Experimental; supporting electrolyte, 1.47 M H_3PO_4

Table 1. Interferences due to foreign species

Ion	Mass excess over U(VI) (1 μg)	Error, %
Al(III)	5	−7.5
Cr(VI)	0.25	−8.0
Cu(II)	1	−4.0
Fe(III)	0.25	−4.0
Mn(II)	5	−5.0
Mo(VI)	0.5	−10.0
Pb(II)	5	−10.0
Si(IV)	5	−7.0
Ti(IV)	0.12	+5.0
Zn(II)	5	−7.0

Because hot concentrated phosphoric acid is used to dissolve the nuclear fuel under an inert environment in order not to influence the uranium valency, the same acid was considered as the supporting electrolyte. As shown in Fig. 3, the sensitivity of the peak response in dilute phosphoric acid is better than that in concentrated acid, but it must be pointed out that uranium phosphate gels may be formed when the acid concentration is less than 0.5–1 M. The optimum acid concentration seems to be 3 M.

Sulphuric acid was added in order to avoid gel formation without using more concentrated phosphoric acid, because it was found that the addition of sulphuric acid does not influence the uranium peak when present in concentrations up to 1.5 M (Fig. 4); the best sensitivity was reached when a 1.47 M H_3PO_4 - 1.5 M H_2SO_4 supporting electrolyte was used. When using this supporting electrolyte it was shown that the uranium(VI) response is constant for about 3 h and after this period it decreases.

The amount of phosphoric acid required for the supporting electrolyte was found to dissolve up to 200 mg of sample; the dissolution time may vary from 10–15 min to 2 h, depending on the coarse powder size.

An aliquot of the sample solution was oxidised with a saturated solution of cerium(IV) sulphate in 2 M sulphuric acid. The presence of a drop of methyl red indicator, changing its colour from red to yellow, indicates an excess of cerium(IV) and the completion of the uranium(IV) oxidation to uranium(VI). It was shown that this oxidation step is completed within 5 min at room temperature, and that it is also stable when a small excess of oxidising agent is present. The excess is not critical; the peak response does not change even if a 40 : 1 cerium excess over uranium is present.

Effect of Foreign Species

More than 20 elements including aluminium, bismuth, cadmium, cerium, chromium(III) and -(VI), cobalt, copper, lead, manganese, molybdenum, nickel, rare earths, silicon, titanium, vanadium, zinc and zirconium were tested. Table 1 shows the effect of the ions that interfere. No interferences were observed in the presence of greater than a 40-fold mass excess of the other elements mentioned above.

Table 2. Oxygen to uranium ratio of nuclear-fuel pellets

Type	Reference value	Gravimetric analysis: O/U ± s.d. (95%)	Polarographic analysis: O/U ± s.d. (95%)	No. of determinations	Polarographic analysis[8]: O/U ± s.d. (95%)	No. of determinations
Po/1/82	2.10	2.100 ± 0.002	2.097 5 ± 0.002 0	10	2.096 5 ± 0.003 5	4
Po/2/82	2.10	2.105 ± 0.002	2.104 0 ± 0.001 2	8	2.108 5 ± 0.005 4	4
Po/2/82/UG			2.103 4 ± 0.002 2	8	2.106 2 ± 0.003 2	4
Po/2/82/UG-C			2.104 0 ± 0.001 5	8	2.103 0 ± 0.002 0	4
Po/2/82/UG-B			2.104 2 ± 0.002 0	8	2.106 4 ± 0.002 8	4
P/58G	2.02–2.03		2.021 5 ± 0.001 2	10	2.021 2 ± 0.001 8	4
P/58G/B5			2.022 2 ± 0.001 6	8	2.023 0 ± 0.002 2	4
P/58G/B1			2.019 5 ± 0.001 0	8	2.020 5 ± 0.002 4	4
P/58G/C5			2.023 4 ± 0.001 4	8	2.023 0 ± 0.002 0	4
P/58G/C1			2.020 2 ± 0.001 9	8	2.020 4 ± 0.002 4	4
P/BL	2.00–2.01		2.008 5 ± 0.001 0	10	2.009 0 ± 0.001 5	4
U_3O_8 JMC 765 Specpure	2.667		2.672 ± 0.008	20	2.669 ± 0.008	4

Procedure

Crush the pellet sample to a coarse powder in a steel mortar (Fig. 1) and weigh 50–150 mg of the coarse powder into a Pyrex dissolution flask (Fig. 2). Cover the sample with 5 ml of 85% H_3PO_4 and de-aerate the flask by bubbling argon through it. After 10 min, heat the flask to 210 ± 10 °C in order to complete the dissolution of the sample. Keep argon bubbling at a rate that ensures an inert atmosphere is maintained over the solution during both the dissolution step and the cooling stage. Add 12.5 ml of 6 M H_2SO_4, washing the bubbler and the neck of the flask. Dilute to the mark with doubly distilled water with constant shaking in order to avoid gel formation at the interface.

Transfer 1 ml of this solution into a 25-ml calibrated flask. Add one drop of 0.1% methyl red indicator and add, dropwise, the saturated solution of cerium(IV) sulphate in 2 M H_2SO_4, until the colour of the solution changes from red to yellow. Wait for 5 min and add 2.4 ml of 85% H_3PO_4 and 5.75 ml of 6 M H_2SO_4. Dilute to the mark with doubly distilled water.

De-aerate both solutions for 5 min and record the polarograms from +0.4 to −0.5 V *versus* S.C.E.

The absolute value of the uranium content can be calculated by means of a calibration graph or standard additions method.

The uranium(VI) content of the sample may be calculated from the first polarogram and, after uranium(IV) oxidation, total uranium is found from the second polarogram.

Results

The described method was tested on certified U_3O_8 and compared with reference values, results from gravimetric analysis, when possible, and polarography.[8] Some results are shown in Table 2.

The polarographic data are substantially coincident. The method described by Papež *et al.*[8] is more time consuming and less precise, probably owing to the errors occurring when pipetting the $Ce(SO_4)_2$ - $K_2Cr_2O_7$ titrant and the determination of the equivalence point of amperometric titration of total uranium.

Several pellets were analysed and then spiked with uranium(VI) standard solution, to provide an amount of several milligrams of uranium(VI), and re-analysed. The added amount of uranium was recovered without noting any uranium(IV) oxidation. The proposed method allows good accuracy for samples covering a wide range of oxygen to uranium ratios. When the prescribed conditions are used, the method permits the determination of uranium at concentrations as low as 0.2 μg ml^{-1} of U(VI), with a relative standard deviation of about 2%.

The calibration graph is linear and reproducible up to uranium concentrations of at least 0.35 mg ml^{-1} of U(VI).

The oxygen to uranium ratio can be calculated by the following equation:

$$\frac{O}{U} = 2.000\,0 + \frac{U(VI)}{U(IV + VI)} = 2.000\,0 + \frac{C_1V_1}{M} \cdot \frac{M}{C_2V_2}$$
$$= 2.000\,0 + \frac{h_1}{25h_2}$$

where C_1 and C_2 are the U(VI) and U(IV + VI) contents (mg ml^{-1}), M the mass of the sample, h_1 is the height of the uranium(VI) polarographic peak and h_2 is the height of the total uranium peak.

The proposed method is very simple and rapid. It needs only one dissolution to determine both uranium(VI) and total uranium. Excluding the dissolution step, a few minutes are necessary for both determinations.

The presence of other oxides and/or sintering additives in the nuclear-fuel pellets did not influence the uranium determination.

In order to evaluate the influence of atmospheric oxygen on the uranium(IV) oxidation, crushing and weighing steps were performed under an inert atmosphere in a glove-box and then both deoxygenated sulphuric acid solution and doubly distilled water were added to the sample solution. No difference was noted, even when analysing nuclear fuels having an oxygen to uranium ratio close to 2, in comparison with performing normal manipulations as previously described.

References

1. Herczynska, E., *Nukleonica*, 1976, **21**, 285.
2. Kuvik, V., Krtil, J., and Moravec, A., *Radiochem. Radioanal. Lett.*, 1982, **54**, 209.
3. Khun, E., Baumgaertel, G., Schmieder, H., and Goergenyi, T., *Fresenius Z. Anal. Chem.*, 1973, **267**, 103.
4. Schaefer, E. A., and Hibbits, J. O., *Anal. Chem.*, 1969, **41**, 254.
5. Bartscher, W., *Fresenius Z. Anal. Chem.*, 1982, **310**, 413.
6. Sipos, L., and Branica, M., *J. Polarogr. Soc.*, 1968, **14**, 3.
7. Cheng-I Wu, Fu-Chung Chang and Yu-Chai Yeh, *Nucl. Sci. J.*, 1981, **18**, 108.
8. Papež, V., Večernik, J., and Krtil, J., *Radiochem. Radioanal. Lett.*, 1982, **55**, 141.
9. Szefer, P., *Mikrochim. Acta*, 1979, **I**, 463.
10. Sinyakova, S. I., *in* Ryabchikov, D. I., and Senyavin, M. M., *Editors*, "Analytical Chemistry of Uranium," IPST, Jerusalem, 1963, pp. 134–176.

Paper A3/187
Received June 27th, 1983
Accepted September 12th, 1983

Electroanalytical Studies of Phenothiazine Neuroleptics at Gold and Platinum Electrodes

E. Bishop and W. Hussein*
University of Exeter, Chemistry Department, Stocker Road, Exeter, EX4 4QD, UK

Coulometry and voltammetry at platinum and gold rotating disc electrodes (RDE) in aqueous media have been applied to *N*-substituted phenothiazines (chlorpromazine, fluphenazine, perphenazine, promazine, promethazine and trimeprazine). All display three anodic waves of one, one and two electrons, while piperazine derivatives consume a further two electrons in the side chain. All steps involve EC mechanisms, but all the primary products either disproportionate or react with the solvent and the sole and stable product is the sulphoxide, or the in-chain 1,4-dihydropyrazine for piperazine derivatives. Although any step may be used in voltammetric determinations, the first step gives the best results, as it also does for potentiostatic coulometry. Mechanisms have been elucidated, and the electrode kinetic parameters have been determined for the first two steps of each compound.

Keywords: *Rotating disc electrode voltammetry; coulometry; mass- and charge-transfer kinetic parameters; N-substituted phenothiazines; tranquilliser drugs*

The *N*-substituted phenothiazine tranquillisers metabolise rapidly to give numerous products[1] of varying antipsychotic effectiveness.[2] Chlorpromazine, a dopamine inhibitor, is the most commonly prescribed, others additionally possess antiemetic, antihistaminic, anti-Parkinson and other properties. Direct oxidation at platinum in 2–6 mol l^{-1} sulphuric acid has been reported[3–5] to give two waves and one wave in 0.5 mol l^{-1} sulphuric acid. Chemical oxidation and electron spin resonance (ESR)[6] or isolation of the species[7] indicate the radical nature of the intermediate, which is stabilised in strong sulphuric acid.[3] No third wave has previously been reported and the presence of chloride obscures the interpretation of the electrode process. Secondary processes with coulometrically generated bromine, cerium(IV) and manganese(III) have been investigated.[8–10] Determinations in non-aqueous media,[11] and by polarography after derivatisation,[12] have also been made.

The present investigation is directed at primary reactions by using high-precision rotating disc electrode voltammetry with the determination of kinetic parameters, in the natural clinical environment of aqueous media in the over-all biological direction of oxidation, with careful removal of chloride or other unwanted oxidisable species. The compounds examined are given in Table 1.

Experimental

Apparatus

Glassware. Calibrated NPL "A" grade glassware was used, in conjunction with a Stanton CL3 balance with a standard deviation of 3 μg. All glassware was cleaned with Aristar nitric acid and rinsed thoroughly with high-purity distilled water.[13] Contact with chromic acid, detergents or de-ionised water was avoided.

Rotating electrode assembly. The electrodes, disc, split disc, ring disc and split-ring-disc, of platinum, gold, silver or glassy carbon are self centering to within a run-out of 5 μm, and can be interchanged within 15 s. The disc area is 0.503 cm^2. The rotator shaft is driven by a powerful, reversible, d.c. tacho-servo motor on a massive, rigid, vibration-free mount, and shaft speed is photoelectrically monitored via a frequency standard counter, the SM 200. The relaxation time to a speed constancy of ±0.01 Hz is 15 s from rest to maximum speed, or from 5 to 50 Hz, and the drift is <0.03 Hz h^{-1} at 50 Hz and <0.006 Hz h^{-1} at 5 Hz. A full description is given elsewhere.[14] The electronics[15] incorporate a ±2 V ± 100 mA potentiostat and amperostat, a bidirectional ramp generator of 0.001 mV to 2 000 V min^{-1}, cyclic voltammetry from 0.001 to 1 200 Hz, voltage and current follower outputs, and output offset and attenuation/expansion. Measurements of current (through a calibrated standard resistance) and potential were made on a 7-digit SEL transfer standard digital voltmeter (DVM) Model SM215 and of elapsed time on a 10-MHz frequency standard counter. The readout was displayed on a Bryans A3 *X* - *Y*/*T* recorder 20170/S or a calibrated dual-beam measuring oscilloscope HP 1200 A. Assembly and instruments were driven from a 1.5-kW saturable reactor, additionally loaded by heating elements to 96–98% of full output. Dummy loads with fast TTL switching were used on thermostats and electrolytic cells. Brush noise was smoothed and filtered. The thermostated, jacketed cell was provided with a ceramic plug

Table 1. Compounds investigated

Compound	C.A. No.	Generic name	R_1	R_2	Batch No.	Supplier	Proprietary name
A	50-53-3	Chlorpromazine hydrochloride	$-CH_2(CH_2)_2N(CH_3)_2$	Cl	J48	May and Baker Ltd.	Largactil
B	—	Chlorpromazine sulphoxide	$-CH_2(CH_2)_2N(CH_3)_2$	Cl	AJ1598	Smith, Kline and French	—
C	69-23-8	Fluphenazine	$-CH_2(CH_2)_2$-*N*,*N*'-piperazinyl-CH_2CH_2OH	CF_3	39076	E. R. Squibb and Sons Ltd.	Modecate
D	58-39-9	Perphenazine	$-CH_2(CH_2)_2$-*N*,*N*'-piperazinyl-CH_2CH_2OH	Cl	L/8	Allen and Hanbury	Fentazine
E	58-40-2	Promazine hydrochloride	$-CH_2(CH_2)_2N(CH_3)_2$	H	181	Wyeth Laboratories	Sparine
F	60-87-7	Promethazine hydrochloride	$-CH_2CH(CH_3)N(CH_3)_2$	H	K598	May and Baker Ltd.	Sonergan
G	84-96-8	Trimeprazine tartrate	$-CH_2CH(CH_3)CH_2N(CH_3)_2$	H	893	May and Baker Ltd.	Vallergan

* Present address: Department of Pharmaceutics, Faculty of Pharmacy, University of Karachi, Karachi-32, Pakistan.

separated side-arm filled with the same supporting electrolyte as the cell for connection of the platinum spiral counter electrode, and an entry for the Luggin capillary bridge, similarly filled (and replaced every hour), into which the ceramic-terminated, saturated potassium chloride bridge, from the large capacity saturated calomel electrode, was fitted. A machined and drilled PTFE cap on the cell permitted reproducible presentation by elevator to the rotating electrode, and carried gas entry and exit ports.

Electrode activation. Of overriding importance in mechanistic and kinetic work and for defined coulometric current efficiencies is the nature and condition of the electrode surface. Unless a fouled or deactivated surface was deliberately required, the following pre-treatment was applied before each scan or other individual operation. (1) Inspect the electrode surface for imperfections or staining, and, if necessary, polish metallographically to an optical flat. (2) Remove adsorbate by immersion in warm aqua regia (platinum) or nitric acid (gold) for 1 min, and rinse with pure water. (3) For a working anode, anodise then cathodise for 30 s at 30 mA cm^{-2} for three cycles in 0.5 mol l^{-1} Aristar sulphuric acid and finally anodise for 60 s at 60 mA cm^{-2}. For a working cathode, cathodise then anodise for 30 s at 30 mA cm^{-2} each operation for three cycles, and finally cathodise for 60 s at 30 mA cm^{-2}. For a clean electrode, treat as for a cathode and then short circuit to a working saturated calomel electrode for 6 min. Rinse with pure water and transfer it to the working electrolyte without allowing it to dry. In this study the primary deactivating species is the adsorbed cation diradical of the sulphoxide.

Reagents

Aristar reagents were employed throughout, being further purified by pre-electrolysis where necessary, together with high-purity water,[13] previously out-gassed. The phenothiazine derivatives were of drug standard grades, and kindly provided by the manufacturers listed in Table 1. Solids and solutions were protected from light by wrapping the containers in aluminium foil.

Chloride-free drug standard stock solutions, 0.01 mol l^{-1}. A 5-ml column was charged with Amberlite IRA 400(Cl) anion-exchange resin, analytical grade (2 g dry mass), which was converted into sulphate by washing with 0.4 mol l^{-1} Aristar sodium sulphate until it was free from chloride and washed with water. Approximately 2.5 mmol of the drug, accurately weighed, were dissolved in water, transferred into the column, fully eluted with water into a 250-ml calibrated flask containing 25 ml of 1.0 mol l^{-1} sulphuric acid and diluted to volume. Conversion to perchlorate was analogously effected.

Working solutions. An appropriate aliquot of the stock solution was transferred into a calibrated flask, any necessary reagents were added and the solution was diluted to volume with water. All working solutions were prepared freshly.

General Procedure

Voltammetry

Before each set of measurements is performed on a sample, a set is run on a supporting electrolyte of the same composition and volume, to serve as a blank and as a check on electrode performance giving a "worst case" current efficiency.[16] Although the sample electrode process commonly shifts the background process to more extreme potentials, the merging of background and final sample waves makes extraction of accurate background kinetic parameters difficult. At intervals also, series of voltammograms are run under variation of rotation speed and concentration on mixtures of hexacyanoferrates(II) and -(III) to check electrode condition and instrumental performance and calibration.[14]

The specimen solution is placed in the cell and brought to thermostated temperature while being de-oxygenated (30 min for anodic processes and 6 h for cathodic processes) with nitrogen passed through two scrubbers containing chromium(II) sulphate and one containing water, and the electrode is then activated. The instrumentation operational amplifiers are checked for offset; X and Y zeros, calibrations and scale lengths are checked; start and terminate potentials and ramp speed are set. With the starting potential on hold, the electrode is allowed to stabilise at the pre-set rotation speed, and after 30–60 s the voltammogram is recorded, using hold to observe the precise limiting current values for each wave. After termination the potential returns to the start value in stand by, and the electrode is activated before the next scan. Once a definitive voltammogram for a given set of conditions is established the $E_{\frac{1}{4}}$ value is noted, and further scans are performed during which hold is used at selected intervals to allow precise current and potential values for kinetic calculations to be obtained from the DVM, conveniently by printer. At least 20 points are evaluated for each scan.

Coulometric determination of n *values*

The same equipment is used, except that if the permissible maximum current attainable at the disc electrode involves too long an electrolysis time, a platinum gauze electrode of 70 cm^2 area is inserted into the cell and control transferred to it for the coulometric operation; the solution is stirred magnetically.

For potentiostatic determination, the cell is charged with supporting electrolyte, the control potential set to a proper value on the limiting current plateau of the selected wave for the sample and the residual current recorded. The sample solution is added, a voltammogram recorded and the appropriate limiting current determined. The control potential is reset and electrolysis conducted until the current falls to the residual value. The total charge passed (number of coulombs) is determined by precise RC integration,[17] or by planimetry or cut-and-weigh of the recorded current *versus* time curve. A voltammogram is again recorded.

For amperostatic determination, the sample and electrolyte are placed in the cell and a voltammogram recorded to define the limiting current density. A constant current is selected such that the resultant current density is less than half of the limiting current density expected at the termination of the electrolysis. Electrolysis is conducted for the required time, and a second voltammogram is recorded and the new limiting current is measured. For example, if the number of coulombs (the charge) passed corresponds to oxidation of half of the sample, assuming a one-electron reaction, and the new limiting current is 75% of the original, one quarter of the sample has been electrolysed by a two-electron reaction. Further determinate charges are passed and the decrease in limiting current measured for each step. Voltammograms are recorded at intervals thereafter to discover any sequential chemical reactions of the product.

Results and Discussion

Voltammetry in 0.1 mol l^{-1} Acid

All the compounds (apart from B) listed in Table 1 gave three regular, reproducible and well defined anodic waves in 0.1 mol l^{-1} sulphuric or perchloric acid at gold and platinum electrodes, with the exception of platinum in perchloric acid when the third wave was not resolved from the background. Potentials were about 100 mV more positive in perchloric acid than in sulphuric acid. Continued scanning without pre-treatment of the electrode resulted in a positive shift in half-wave potentials and a decrease in limiting current for all waves. As the mass transfer rate increased with increase in rotation speed and/or concentration, the third wave, first at gold then at platinum, changed to a peak with the peak current obeying the Levich relationship and then further increase in mass-transfer rate caused the peak to collapse with departure

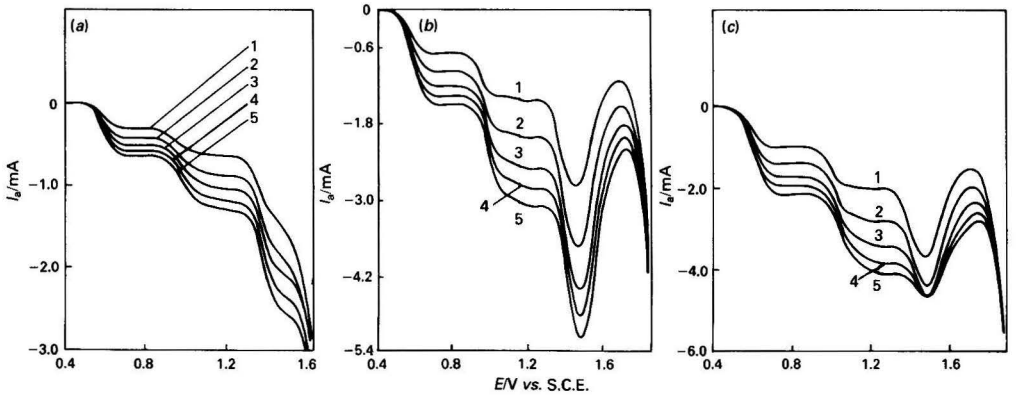

Fig. 1. Anodic voltammetry of chlorpromazine in 0.1 mol l^{-1} sulphuric acid, electrode area 0.503 cm^2, rotation speeds 10, 20, 30, 40 and 50 Hz, scan speed 5 mV s^{-1}. (*a*) 0.002 mol l^{-1} chlorpromazine, platinum electrode; (*b*) 0.005 mol l^{-1} chlorpromazine, gold electrode; and (*c*) 0.008 mol l^{-1} chlorpromazine, gold electrode

Table 2. Example calibration results for voltammetry at RDE. Electrode area, 0.503 cm^2; medium, 0.1 mol l^{-1} sulphuric acid; temperature, 25 °C; and $n = 4$

Phenothiazine	Nominal frequency/ Hz	Slope/mA l mmol^{-1}	Intercept/ mA	Correlation coefficient	SD of residuals/ mA	SD of slope/mA l mmol^{-1}	RSD of slope, %
Promethazine	10	0.1582	0.019 90	0.997 23	0.003 57	0.000 59	3.73
(0–10^{-3} mol l^{-1}, 1st wave gold)	20	0.229 9	0.016 29	0.998 93	0.003 22	0.000 53	2.31
	30	0.279 2	0.019 22	0.999 63	0.002 30	0.000 38	1.36
	40	0.318 3	0.021 02	0.999 97	0.000 71	0.000 12	0.37
	50	0.343 2	0.024 96	0.999 77	0.002 25	0.000 37	1.08
Perphenazine	10	0.116 32	0.037 93	0.999 99	0.001 42	0.000 23	0.20
(0–10^{-2} mol l^{-1}, 1st wave platinum)	20	0.167 34	0.024 04	0.999 98	0.002 87	0.000 47	0.28
	30	0.195 09	0.060 57	0.999 63	0.016 06	0.002 65	1.36
	40	0.230 19	0.040 17	0.999 86	0.011 66	0.001 92	0.83
	50	0.247 67	0.069 40	0.999 87	0.012 26	0.002 02	0.82
Promethazine	10	0.144 2	0.029 85	0.999 16	0.001 79	0.000 30	2.05
(0–10^{-3} mol l^{-1}, 2nd wave platinum)	20	0.205 1	0.033 06	0.999 41	0.002 14	0.000 35	1.72
	30	0.253 4	0.035 37	0.999 12	0.003 22	0.000 53	2.10
	40	0.292 5	0.037 18	0.999 86	0.001 49	0.000 25	0.84
	50	0.331 5	0.032 27	0.999 71	0.002 43	0.000 40	1.21

from the Levich relationship. The normal behaviour at platinum is illustrated in Fig. 1(*a*), the peak pattern at gold in (*b*) and the collapse at gold in (*c*). All three waves, including the peaks developed up to the stage in Fig 1(*b*), gave linear plots of limiting current against square root of frequency and against concentration in obedience to the Levich relationship. The limiting current of the third wave approximated to the sum of the limiting currents of the first two waves, except for the piperazine derivatives C and D when it became twice that magnitude. The sulphoxide B gave a single wave corresponding to the third wave of A.

Kinetic parameters are not wholly meaningful for the third wave, as will be shown, but have been evaluated for the first two waves by pattern theory[18,19] for all compounds, except B, and for the background. The variation from platinum to gold and from compound to compound is small, preventing their separate determination in mixtures, although C and D could be resolved from others by differential-pulse voltammetry. A tabulation of the results of 120 definitive sets of measurements is obtainable from the authors. The half-wave potentials either remain constant or increase marginally with increasing rotation speed and concentration, and, in extreme, span the ranges 0.565–0.660 V *vs.* S.C.E. for the first wave, and 0.860 to 1.090 V *vs.* S.C.E. for the second wave, C and D being some 50 mV more positive for the first and 50 mV more negative for the second wave. The charge-transfer rate constants show a slightly greater range, from 2.11×10^{-6} to 9.95×10^{-6} l cm^{-2} s^{-1} with extreme values of 1.93×10^{-6} and 19.2×10^{-6} l cm^{-2} s^{-1} and 1.16×10^{-6} to 14.7×10^{-6} l cm^{-2} s^{-1} for the first and second waves, respectively. These values are related to the half-wave potentials because conditional potentials are not accessible. The charge-transfer coefficient, β, shows considerable variation, from 0.57 to 0.99 with one extreme value of 0.26 for the first wave, and from 0.42 to 0.81 with one extreme value of 1.00 for the second wave; this generates a considerable range of wave slopes, but is not diagnostically useful.

For analytical purposes, the first wave is generally better, as judged by correlation coefficients and standard deviations (SD), although the second wave is marginally better for promethazine. There is little to choose between gold and platinum as the electrode material. Examples of calibration results for first and second waves at platinum and first waves at platinum and gold are given in Table 2. Excipients in dosage forms do not interfere with the determinations. To test the reliability of the method in rapid analysis, a series of four solutions of each of the drug standards in the range 2×10^{-4}–2×10^{-2} mol l^{-1} was prepared. A single measurement of the limiting current was made at each of five rotation speeds and the concentration calculated from the slope and intercept of the calibration lines. The percentage relative standard deviations (RSD) of each group of five determinations are presented in Table 3. This involves the propagation of error in using five calibration graphs, and also the error in setting the

Table 3. Precision of determinations by RDE voltammetry. Each result arises from the measurement of the limiting current at 0.75–0.80 V *vs.* S.C.E. of the first wave at each of 5 rotation speeds. Electrode area, 0.503 cm²; and medium, 0.1 mol l⁻¹ sulphuric acid

	Chlorpromazine		Fluphenazine		Perphenazine		Promazine		Promethazine		Trimeprazine	
Electrode	Concentration/ mmol l⁻¹	RSD, %	Concentration/ mmol l⁻¹	RSD, %	Concentration/ mmol l⁻¹	RSD, %	Concentration/ mmol l⁻¹	RSD, %	Concentration/ mmol l⁻¹	RSD, %	Concentration/ mmol l⁻¹	RSD, %
Platinum	1.999 86	6.3	0.215 383	8.7	2.000 17	2.0	2.000 12	3.7	0.200 012	4.4	3.994 76	5.6
	4.999 65	1.3	0.538 458	3.6	5.000 93	1.4	5.000 30	2.5	0.500 030	4.6	9.986 90	1.8
	7.999 45	2.4	0.861 533	2.7	8.000 69	2.5	8.000 48	1.8	0.800 048	5.5	15.979 04	2.6
	9.999 31	2.0	1.076 916	4.9	10.000 86	3.0	10.000 60	4.4	1.000 06	0.5	19.973 80	3.2
Gold	1.999 86	2.3	0.215 383	3.6	2.000 17	3.1	2.000 12	7.0	0.200 012	2.3	3.994 76	1.3
	4.999 65	1.8	0.538 458	8.9	5.000 93	1.4	5.000 30	2.9	0.500 030	8.8	9.986 90	4.3
	7.999 45	2.1	0.861 533	9.1	8.000 69	3.1	8.000 48	1.3	0.800 048	2.3	15.979 04	1.8
	9.999 31	1.1	1.076 916	3.4	10.000 86	0.5	10.000 60	1.8	1.000 06	2.6	19.973 80	1.8

Table 4. Effect of pH on the anodic waves of chlorpromazine. Electrode area, 0.503 cm²; rotation speed, 50 Hz; chlorpromazine, 10^{-3} mol l⁻¹; medium, sulphuric acid (pH = 0, 1) or citrate - phosphate buffer adjusted to exact pH; temperature, 25 °C; potentials, *vs.* S.C.E.

	Platinum electrode						Gold electrode			
	Half-wave potential/V			Limiting current/mA			Half-wave potential/V		Limiting current/mA	
pH	1st wave	2nd wave	3rd wave	1st wave	2nd wave	3rd wave	1st wave	2nd wave	1st wave	2nd wave
0	0.54	0.91	1.29	0.26	0.25	0.48	0.55	0.90	0.30	0.28
1	0.48	0.90	1.39	0.48	0.48	1.00	0.58	0.94	0.35	0.35
2	0.63	1.06	P.d.*	0.28	0.22	P.d.	0.63	0.94	0.28	0.23
3	0.615	1.00	P.d.	0.27	0.20	P.d.	0.60	0.87	0.36	0.10
4	0.59	0.945	1.355	0.28	0.15	0.27	0.59	0.83	0.24	0.18
5	0.59	0.935	1.315	0.32	0.10	0.39	0.58	0.805	0.30	0.12
6	0.58	P.d.	1.28	0.40	P.d.	0.47	0.58	P.d.	0.36	P.d.
7	0.58	P.d.	1.30	0.46	P.d.	0.48	0.58	P.d.	0.44	P.d.

* Poorly defined.

rotation speed by Helipot (RSD 0.15–0.72%), as opposed to adjusting the frequency to an exact value. The RSD averages about 2.5% for concentrations greater than 10^{-3} mol l⁻¹ and about 3.3% overall. The duration of each group of five determinations is less than 10 min: 7 min for electrode activation and solution handling, 30 s for speed stabilisation, current measurement and calculation.

Voltammetry in Buffer Media

The citrate - phosphate buffers[20] exerted no specific influence on the electrodes and the electrode processes. The charge-transfer rate constant for the background reaction decreased with increasing pH, but the charge-transfer coefficient was little affected. At platinum, three anodic waves appear throughout the pH range 0–7, but only a single wave at an unactivated electrode in the pH range 2–7; all waves reach a maximum height at pH 1. The first wave is well developed throughout, but the second wave is less pronounced at pH 6 and 7. The third wave is well developed at pH 0, 1 and 2, is poorly defined at pH 3 and reappears at pH 4–7. At gold, all three waves are well developed up to pH 5, the second step is less marked at pH 6, and disappears at pH 7; the second wave is poorly defined at an unactivated electrode. The third wave is in the form of a peak generated by deactivation of the electrode by adsorption of the product. The half-wave potentials and limiting currents are shown in Table 4 for chlorpromazine; the potentials are little affected by change of pH.

Potentiostatic Coulometry

To determine the number of electrons involved in each step and to gain information on the mechanisms as well as to evaluate the coulometric determinations, the drugs were examined by both potentiostatic and amperostatic coulometry. Compounds A, E, F and G (Table 1) displayed similar behaviour, and will be described through the example of chlorpromazine. Compounds C and D also behaved similarly for the first and second waves, but differed in respect of the third wave, and will be discussed through the example of perphenazine.

On potentiostatic oxidation of 10^{-3} mol l⁻¹ chlorpromazine in 0.1 mol l⁻¹ sulphuric acid at 0.8 V *vs.* S.C.E., the plateau voltage of the first wave, to a negligible residual current, the solution first turned red and on approaching completion of the reaction the colour faded to light red. A scan showed that the first two waves had entirely disappeared and that the third wave was enhanced in height by 35%. The current *versus* time integral showed the transfer of two electrons. The UV - visible spectrum of the solution was identical with that of authentic sulphoxide, B, and scans at gold and platinum electrodes were reproducible and identical with those of an equimolar solution of the sulphoxide. The potentiostatic oxidation at 0.8 V *vs.* S.C.E. was stopped when the current - time integral showed the transfer of one electron equivalent and the solution was blood red. Scanning revealed the continued existence of both first and second waves at half of their original height and an unchanged third wave; the spectrum did not match that of a mixture of chlorpromazine and sulphoxide and also contained a peak at 520 nm. After standing for 24 h, the colour had disappeared, the voltammogram remained the same, but the spectrum then matched that of an equimolar mixture of chlorpromazine and sulphoxide. On passage of a further charge corresponding to half of an electron equivalent, still at 0.8 V, the same behaviour was observed, the first two waves now being 25% of their original height, and the spectrum differing initially, but matching that of the appropriate mixture after disappearance of the colour.

Potentiostatic electrolysis at 1.2 V *vs.* S.C.E., the plateau potential of the second wave, to a negligible residual current, produced first a blood-red colour, which faded to faint pink at the end of the reaction. An immediate scan at an activated platinum electrode showed that the first and second waves had entirely disappeared, while the third wave was enhanced in

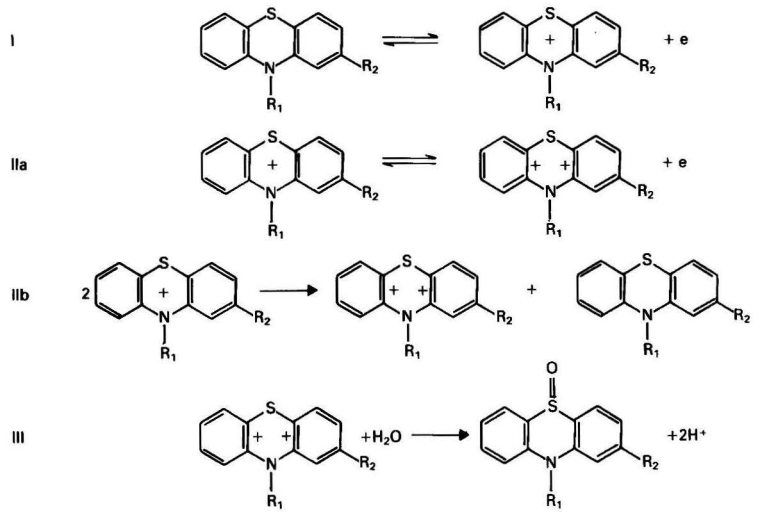

Fig. 2. Reaction scheme for phenothiazine undergoing potentiostatic coulometry

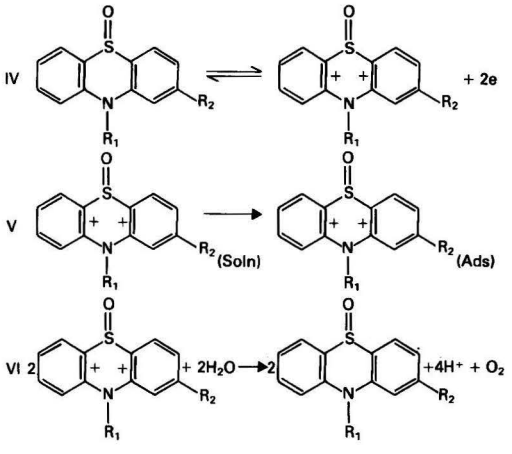

Fig. 3. Reaction scheme for phenothiazine undergoing amperostatic coulometry

height by 36%. Scans of this solution at gold and platinum were reproducible and identical with those of an equimolar solution of authentic sulphoxide, and the spectra of the two solutions were identical. The faint pink colour vanished quickly and no other colour appeared. No further electrolysis occurred in this solution.

These observations can be explained by the reaction scheme in Fig. 2. The first wave involves the reversible one-electron oxidation to the monocation radical in step **I.** Continuation of electrolysis to the second wave results in direct oxidation to the dication diradical, **IIa**, but if the potential is restrained to the first wave, the monocation radical disproportionates, **IIb**, giving the dication radical and regenerating the original phenothiazine, which continues to be oxidised by step I until all of the material is converted into the dication radical. If electrolysis is interrupted, then any monocation present disproportionates. By whichever pathway the dication radical is formed, it then reacts with the solvent to form the colourless sulphoxide in step **III**. Oxidation at 0.8 V *vs.* S.C.E. is therefore an ECC reaction: oxidation to the monocation, disproportionation and reaction with the solvent. Oxidation at 1.2 V *vs.* S.C.E. is an EEC reaction: oxidation to the monocation, direct oxidation of this to dication and chemical reaction thereof with the solvent. The charges are probably distributed, but the radical site must finally be the sulphur atom for step **III**. At 1.2 V there will be a contribution from step **II(b)**.

Amperostatic Coulometry

To examine the third wave in isolation, 10^{-3} mol l^{-1} chlorpromazine in 0.1 mol l^{-1} sulphuric acid was first oxidised potentiostatically at 1.2 V *vs.* S.C.E. to completion. The solution was then scanned at 50 Hz to obtain the limiting current and oxidised amperostatically at less than one third of the limiting current until a charge of half of an electron equivalent had passed. The solution turned yellow, and a scan showed that the third wave had been almost totally suppressed. On standing, the colour vanished and a further scan showed that the third wave regained its original height. The operation was repeated, and the resultant solution scanned repeatedly at an electrode freshly activated before each scan. Each successive scan showed an increase in wave height, until after 7 scans and 60 min the original wave height was regained and further scans precisely superimposed. Authentic chloropromazine sulphoxide was examined, omitting the potentiostatic electrolysis, and displayed exactly similar behaviour. Deactivation of the electrode and regeneration of the starting material prevent precise measurement of the number of electrons involved, but comparison with known waves of similar molecules[21] is an accepted alternative, and this, together with comparison with the first and second waves, strongly supports a two-electron step.

The mechanisms in Fig. 3 serve to explain the situation. The two-electron third wave and the colour arise from step **IV** with the formation of the sulphoxide diradical cation, with the sulphur and nitrogen atoms each bearing one charge. This radical is strongly adsorbed on the electrode surface in step **V**, and the greater its concentration the more severely is the electrode deactivated [Fig. 1(*b*) and (*c*)], so that immersion of a freshly activated electrode in a solution of the radical results in its deactivation. Regeneration of the sulphoxide is quantitative, and so step **VI** proceeds to completion by reaction with the solvent. This mechanism renders undesirable the use of the third wave in voltammetric determination.

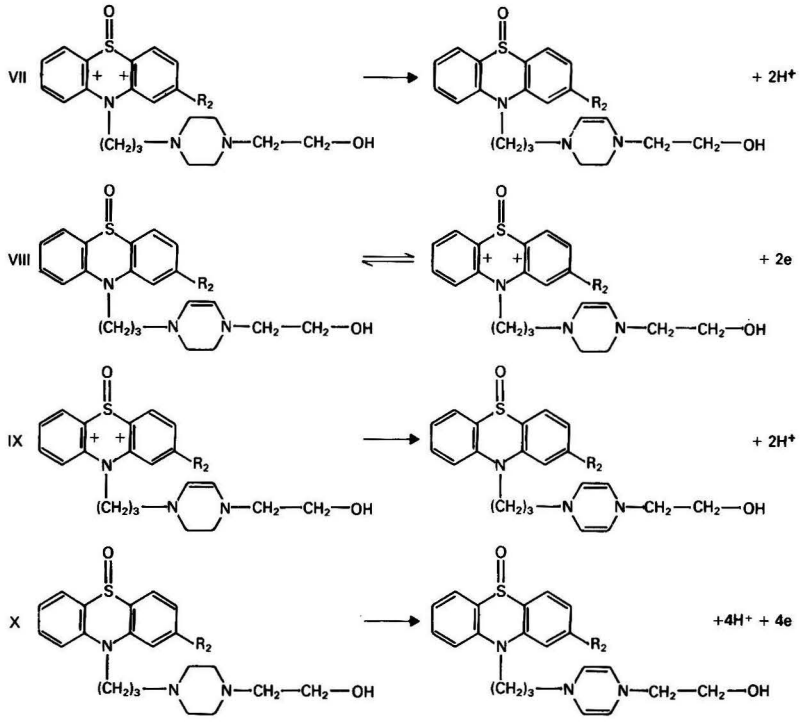

Fig. 4. Reaction scheme for piperazineethanol derivatives undergoing amperostatic coulometry

Piperazineethanol Derivatives

Fluphenazine and perphenazine give first and second waves similar to those of the other compounds, and although the colour of the radical intermediate appears orange - brown it has the same $\lambda_{max.}$ at 520 nm, but the third wave is different, being twice the height. Potentiostatic electrolysis at 1.2 V *vs.* S.C.E. produced two electrons as before, and amperostatic electrolysis of this solution did yield a decrease in wave height of 12.8% after passage of a charge corresponding to half an electron equivalent, which became 25.5% after passage of a further similar charge, confirming a four-electron wave. Electrode inhibition and regeneration were also observed. Direct oxidation of the piperazine ring to the 1,4-dihydropyrazine derivative in step **X** of Fig. 4 may be possible, but it is more likely that this is a two-stage process. Although there is no voltammetric evidence of separated waves, the potential separation may be too small to be observed. The reaction is the same as in Fig. 3 to the production of the sulphoxide dication, which then undergoes internal electron transfer as in step **VII** to give the half oxidised form, which is re-oxidised to the sulphoxide radical in step **VIII** and further internal electron transfer as in step **IX.** The pyrazine derivative may suffer further oxidation to the sulphoxide radical, which then regenerates by reaction with the solvent, as in step **VI** of Fig. 3.

The very rapid, but not highly precise, determinations by voltammetry can be supplemented in more critical assays by potentiostatic coulometry at potentials between 0.8 and 1.2 V *vs.* S.C.E.

We thank Allen and Hanbury, May and Baker Ltd., Smith, Kline and French, E. R. Squibb and Sons Ltd. and Wyeth Laboratories for the gift of materials listed in Table 1 and the Royal Society for the SEL Transfer Standard DVM. W.H. thanks the Government of Pakistan for the award of a Scholarship and the University of Karachi for granting leave of absence.

References

1. Usdin, E., *CRC Crit. Rev. Clin. Lab. Sci.*, 1971, **2**, 347.
2. Pevel, J. M., and Manian, A. A., *in* Shiraki, L. R., and Greevic, N., *Editors*, "Neurotoxicology," Raven Press, New York, 1977, p. 9.
3. Merkle, F. H., and Discher, C. A., *J. Pharm. Sci.*, 1964, **53**, 620.
4. Merkle, F. H., and Discher, C. A., *Anal. Chem.*, 1964, **36**, 1639.
5. Kabasakalian, P., and McGlotten, J., *Anal. Chem.*, 1959, **31**, 431.
6. Schieser, D. W., and Tuck, L. D., *J. Pharm. Sci.*, 1962, **51**, 694.
7. Merkle, F. H., Discher, C. A., and Felmeister, A., *J. Pharm. Sci.*, 1964, **53**, 965.
8. Kross, W., and Roth, H., *Pharm. Ztg.*, 1976, **121**, 1831.
9. Patriarche, G. J., and Lingane, J. J., *J. Pharm. Belg.*, 1970, **25**, 57.
10. Patriarche, G. J., *Mikrochim. Acta*, 1970, **5**, 950.
11. Livertoux, M., and Bessiere, J., *Talanta*, 1981, **28**, 81.
12. Dumortier, A. G., and Patriarche, G. J., *Fresenius Z. Anal. Chem.*, 1973, **264**, 153.
13. Bishop, E., and Sutton, J. R. B., *Anal. Chim. Acta*, 1960, **22**, 590.
14. Wright, D. T., *PhD Thesis*, University of Exeter, 1974.
15. Cofré, P., *PhD Thesis*, University of Exeter, 1976.
16. Bishop, E., *Chem. Anal. Warsaw*, 1972, **17**, 511.
17. Bishop, E., and Hitchcock, P. H., *Analyst*, 1973, **98**, 572.
18. Bishop, E., *Analyst*, 1972, **97**, 761.
19. Bishop, E., *Analyst*, 1972, **97**, 772.
20. Dien, K., and Lentner, C., *Editors*, "Scientific Tables," Seventh Edition, Geigy Pharmaceuticals, Macclesfield, 1975.
21. Butkiewics, K., *J. Electroanal. Chem.*, 1972, **39**, 407.

Paper A3/174
Received June 13th, 1983
Accepted June 28th, 1983

Bipotentiometric Titrations with Standard Solutions of Manganese(III) and Manganese(IV)

Tibor J. Pastor* and M. M. Antonijević
Department of Chemistry, Faculty of Sciences, University of Belgrade, P.O. Box 550, 11001 Belgrade, Yugoslavia

The stability of standard solutions of manganese(III) and manganese(IV) was studied and conditions for bipotentiometric determinations of iron(II), potassium hexacyanoferrate(II), arsenic(III), oxalate and hydroquinone with these oxidants were investigated. Arsenic(III) can be determined only in the presence of suitable catalysts. The reversibility of redox pairs formed in the course of titration depends on the composition of the solution and the current used for the polarisation of the electrodes. The results obtained were good and reproducible.

Keywords: *Bipotentiometric titration; standard solutions; manganese(III) and (IV); redox pair; reversibility*

Tervalent manganese compounds are strong oxidising agents. In the presence of complexing agents, the redox potential of the Mn(III) - Mn(II) system is decreased, whereas the stability of standard solutions of these oxidants is increased. The possibility of using manganese(III) as a titrant has been widely investigated in the past 30 years, presumably because of its selectivity in the oxidation of organic compounds.[1-3] Only since 1976, however, have conditions for determining reducing substances with manganese(IV) been investigated in any detail,[4-8] after Mandal and Sant[4] described a simple procedure for the preparation of a standard solution of this oxidant in sulphuric acid.

In previous research involving titrations with Mn(III) and Mn(IV), the end-point was detected either visually or by using photometric,[1,2,4-6,8,9] potentiometric[1-4,7,8] or amperometric methods.[2,9]

The object of this work was to verify the stability of standard solutions of manganese(III) and manganese(IV) prepared in the presence of sulphuric acid, to establish conditions for the bipotentiometric titration (controlled-current potentiometric titration with two indicator electrodes) of reducing substances with solutions of these oxidants and to study the effect of the composition of the sample solution and the current used for the polarisation of the electrodes on the reversibility of redox pairs present in the solutions.

Experimental

Apparatus

The apparatus used for bipotentiometric titrations is shown in Fig. 1. The current source was a dry 1.5-V battery. An Elektrozverze MA 2110 decade resistance box, from 1 kΩ to 11 MΩ, was used to adjust the current for the polarisation of the electrodes (from 1.0×10^{-4} to 1.0×10^{-6} A). The potential difference between the electrodes was measured with a Radiometer PHM 26 instrument. The electrodes used were made of platinum wire, 15 mm long × 0.5 mm diameter, sealed in glass rods to ensure that their distance apart (10–15 mm) would remain constant during titration. Potentiometric titrations were carried out with the tube voltmeter by means of a platinum indicator electrode of surface area 20 cm² and a saturated calomel reference electrode.

Absorption spectra of manganese(III) and manganese(IV) solutions were recorded on a Varian Superscan 3 spectrophotometer and a Spekol spectral colorimeter was used to observe changes in solution absorbance.

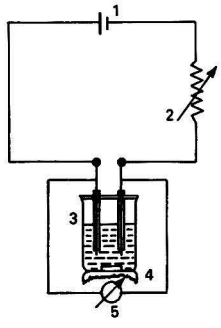

Fig. 1. Apparatus for bipotentiometric titration: 1, dry battery; 2, decade resistance box; 3, vessel with electrodes; 4, voltmeter; and 5, magnetic stirrer

Chemicals and Solutions

All chemicals used were of analytical-reagent grade.

Standard solutions of potassium permanganate (0.1 and 0.02 M), iron(II) sulphate (0.1 M), sodium oxalate (0.05 M), potassium hexacyanoferrate(II) (0.1 M), arsenic(III) (0.025 and 0.05 M) and hydroquinone (0.01 and 0.03 M) were prepared according to standard procedures.[10,11] The exact concentration of the manganese(II) sulphate solution (0.4 M) was determined by potentiometric titration with standard potassium permanganate solution in a pyrophosphate medium (pH 6.0–6.5)[12] and by the gravimetric method in the form of pyrophosphate.[11]

Standard manganese(III) sulphate solution (0.05 M) was prepared by the oxidation of manganese(II) with potassium permanganate solution of known concentration in 10 M sulphuric acid. Following titration, the solution was quantitatively transferred into a calibrated flask and diluted to a suitable volume. The concentration of sulphuric acid in the solution thus obtained was 6 M, whereas the concentration of manganese(II) was approximately equal to that of manganese(III). A solution of manganese(III) pyrophosphate of known concentration was prepared using a similar procedure, but in the presence of sodium pyrophosphate (0.2 mol l^{-1}) and at pH 6.0–6.5. The amount of manganese(II) in this solution was small.

The concentration of manganese(III) in the solutions obtained was calculated from the amount of permanganate consumed and was verified by titrations with standard solutions of suitable reducting agents, *e.g.*, iron(II) sulphate.

* To whom correspondence should be addressed.

Manganese(IV) sulphate solutions were prepared as follows. The amounts of potassium permanganate required were accurately weighed and dissolved in 150 ml of 7, 9 or 12 M sulphuric acid by stirring for 6–8 h.[4] The solutions obtained were then transferred into 250-ml calibrated flasks and diluted to the mark with sulphuric acid of a corresponding concentration. The exact concentrations of these solutions were determined by titration with standard iron(II) sulphate solution.

Procedure

A known volume of the solution to be analysed and 50 ml of the supporting electrolyte (0.3–3.0 M HCl or 0.3–10.0 M H_2SO_4) were poured into a 150-ml beaker. During titration the solution was stirred vigorously. Readings of potential differences were recorded with a millivoltmeter after the potential had stabilised at the electrodes.

In order to establish optimum conditions for the bipotentiometric titration of reducing substances with manganese(III) and manganese(IV), and for the reverse titrations, changes were made to the current for the polarisation of the electrodes with the same concentration of supporting electrolyte, and to the concentration of supporting electrolyte with the same current.

Results and Discussion

Stability of Solutions of Manganese(III) and Manganese(IV)

It was observed that a 0.05 M solution of manganese(III) prepared by titrating manganese(II) sulphate with potassium permanganate in 2–8 M sulphuric acid is unstable, giving rise to a precipitate after standing for 24 h. Therefore, this procedure[13] was modified by carrying out the oxidation of manganese(II) in 10 M sulphuric acid, the concentration of which was subsequently adjusted to 6 M. The solution thus obtained is stable at room temperature for 30 d; after 60 d its concentration is decreased by only 2%. However, in hydrochloric acid solutions, which have a concentration higher than 1 M, manganese(III) is reduced (Fig. 2).

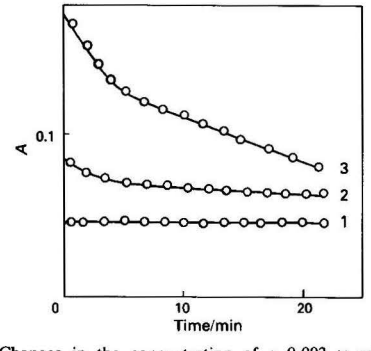

Fig. 2. Changes in the concentration of a 0.003 M solution of manganese(III) sulphate in (1) 1 M, (2) 3 M and (3) 6 M hydrochloric acid, followed by spectrophotometric method

Table 1. Stability of tetravalent manganese ions in solutions of sulphuric acid

	Mn(IV) found, %					
	0.05 M Mn(IV) solution			0.005 M Mn(IV) solution		
H_2SO_4/M	Fresh solution	After 15 d	After 30 d	Fresh solution	After 15 d	After 30 d
7	97.6	93.4	91.9	96.9	63.2	56.3
9	98.9	98.7	98.2	96.8	72.2	66.4
12	97.3	92.4	87.3	96.6	57.7	53.4

The data in Table 1 show that a 0.05 M solution of manganese(IV) prepared in 9 M sulphuric acid is stable for longer than 1 month at 20–30 °C. After heating at 50 °C for 60 min, however, its concentration is decreased by 5%, and at 80 °C its concentration is further decreased by as much as 40% and a precipitate forms. These values, and those given in Table 1, were calculated with respect to the amount of permanganate taken, assuming the following reaction in the solution:

$$4\,KMnO_4 + 10\,H_2SO_4 = 2\,K_2SO_4 + 4\,Mn(SO_4)_2 + 3\,O_2 + 10\,H_2O$$

The validity of this reaction is confirmed by the evolution of oxygen in the course of permanganate dissolution. More dilute solutions of manganese(IV) are less stable. Changes in the composition of manganese(IV) sulphate solution after standing were confirmed by recording their absorption spectra in the 200–400-nm region. Manganese(IV) solutions appear to be less stable in sulphuric acid solutions that have concentrations either lower or higher than 9 M. In the presence of hydrochloric acid, manganese(IV) is reduced; reverse titrations were therefore not performed in hydrochloric acid solutions.

Bipotentiometric Titrations

Bipotentiometric titrations of iron(II) sulphate with manganese(III) and manganese(IV) can be carried out in solutions of sulphuric and hydrochloric acids. The redox pair thus formed is reversible, and the titration curves display a sharp maximum at the end-point (Fig. 3). The total change in potential difference decreases during titration with decrease in the current used for polarising the electrodes. Thus, for example, in titrations with manganese(III) in 2 M sulphuric acid, changes in potential difference of 800 and 450 mV occur when electrodes are polarised with currents of 6×10^{-5} and 2.5×10^{-6} A, respectively. In sulphuric acid solutions, at the start of titration and after the end-point, the potential at the electrodes is established within 1 min; only near the end-point is a wait of about 5 min needed after adding the titrant. The presence of pyrophosphate has no significant effect on either the behaviour of the redox systems present in the solution or the titration conditions. The potential at the electrodes is more rapidly established in hydrochloric acid solutions than in the presence of sulphuric acid; even near the end-point a wait of no more than 1 min is needed. The reversibility of redox pairs present in the solution is also higher in hydrochloric than sulphuric acid.

Titration curves of manganese(IV) with iron(II) sulphate in sulphuric acid display two maxima (Fig. 3): the first peak is not sharp and corresponds to the reduction of manganese(IV) to manganese(III); the other is sharp, making end-point detection possible, and appears at the end of the reduction of manganese(III) to manganese(II). Corresponding changes in the colour of the solution were also observed during titration.

Determination of conditions suitable for the titration of potassium hexacyanoferrate(II) is more complex because of the formation, either before the start or in the course of titration, of precipitates in supporting electrolytes of either low or high concentrations. Under optimum conditions manganese(III) reacts with hexacyanoferrate(II) similarly to the way its behaves with iron(II), except that the total changes in potential differences are smaller (750–400 mV). In the titration of hexacyanoferrate(II) with manganese(IV) in the presence of sulphuric acid, the sharpness of the peak at the end-point is less than in the presence of hydrochloric acid. This is due to the slight slope of the titration curve after the end-point, *i.e.*, to a slight reversibility of the manganese(IV) and the corresponding reduced form in the solution. It should also be noted that in titrations of manganese(IV) with potassium hexacyanoferrate(II) in sulphuric acid, more pro-

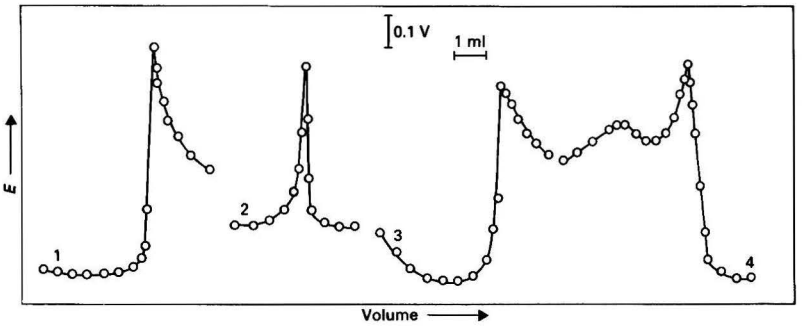

Fig. 3. Bipotentiometric titration curves of iron(II) with manganese(III) sulphate in (1) 3 M sulphuric acid at $I = 7.5 \times 10^{-6}$ A and in (2) 1 M hydrochloric acid at $I = 5 \times 10^{-6}$ A, (3) of iron(II) with manganese(IV) sulphate in 4.5 M sulphuric acid at $I = 7.5 \times 10^{-6}$ A and (4) of manganese(IV) with iron(II) sulphate in 4.5 M sulphuric acid at $I = 7.5 \times 10^{-5}$ A

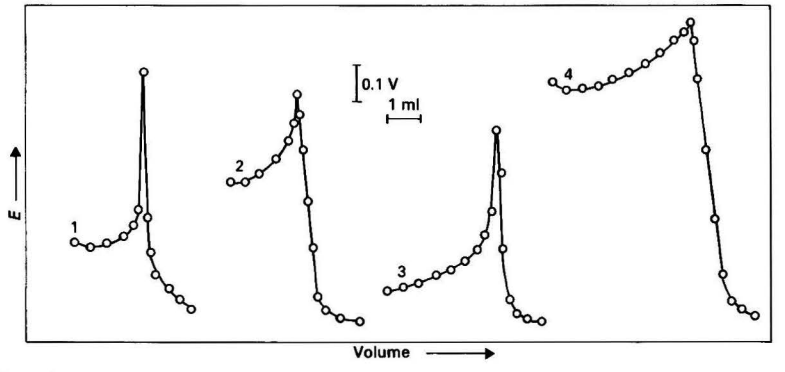

Fig. 4. Bipotentiometric titration curves of arsenic(III) with manganese(III) in (1) 1 M sulphuric acid at $I = 3 \times 10^{-6}$ A and in (2) 1 M hydrochloric acid at $I = 5 \times 10^{-6}$ A and of arsenic(III) with manganese(IV) in (3) 2 M sulphuric acid at $I = 7.5 \times 10^{-5}$ A and (4) in 1 M hydrochloric acid at $I = 7.5 \times 10^{-5}$ A

Table 2. Results of bipotentiometric titrations of reducing substances with manganese(III) and manganese(IV)

	Titration with manganese(III)					Titration with manganese(IV)				
Substance titrated	Taken/ mg	No. of determinations	*I*/A	Supporting electrolyte	Found,* %	Taken/ mg	No. of determinations	*I*/A	Supporting electrolyte	Found,* %
Iron(II) sulphate ..	39.4	6	7.5×10^{-6}	3.0 M H_2SO_4	100.0 ± 0.1	55.6	6	7.5×10^{-5}	4.5 M H_2SO_4	100.4 ± 0.2
	39.4	6	8.8×10^{-6}	3.0 M HCl	100.1 ± 0.1					
Potassium hexacyanoferrate(II) ..	91.9	6	2.5×10^{-6}	1.0 M H_2SO_4	99.2 ± 0.2	70.2	4	6.0×10^{-5}	2.0 M H_2SO_4	100.2 ± 0.3
	91.9	6	3.0×10^{-6}	0.5 M HCl	98.9 ± 0.1	70.2	4	7.5×10^{-5}	1.0 M HCl	100.4 ± 0.2
Arsenic(III) chloride ..	15.5	6	3.0×10^{-6}	1.0 M H_2SO_4	100.2 ± 0.3	19.8	6	7.5×10^{-5}	2.0 M H_2SO_4	99.4 ± 0.2
	15.5	6	5.0×10^{-6}	1.0 M HCl	100.1 ± 0.2	19.8	6	7.5×10^{-5}	0.6 M HCl	99.4 ± 0.2
Sodium oxalate	15.3	12	5.0×10^{-6}	0.5 M H_2SO_4	99.7 ± 0.2	26.8	6	7.5×10^{-5}	4.5 M H_2SO_4	100.0 ± 0.1
	15.3	8	1.5×10^{-5}	1.0 M HCl	99.7 ± 0.2	26.8	4	6.0×10^{-5}	1.0 M HCl	100.0 ± 0.2
Hydroquinone	7.5	6	2.1×10^{-6}	1.0 M H_2SO_4	100.0 ± 0.2	16.5	9	7.5×10^{-5}	1.0 M H_2SO_4	99.6 ± 0.3
	7.5	6	1.6×10^{-6}	1.0 M HCl	99.9 ± 0.2	16.5	6	5.0×10^{-5}	1.0 M HCl	99.9 ± 0.2

* Mean ± standard deviation.

nounced potential differences occur during the reduction of manganese(IV) to manganese(III). Conditions suitable for these determinations have not been established, however, owing to the separation of precipitates in a wide range of acid concentrations.

The oxidation of arsenic(III) with manganese(III) and manganese(IV) is slow. A solution of osmium(VIII) oxide[14,15] can be used as a catalyst in both supporting electrolytes, whereas potassium iodide may be used only in hydrochloric acid. The As(V) - As(III) redox pair is more reversible in sulphuric acid solutions than in the presence of hydrochloric acid (Fig. 4). This can be attributed to the formation of complex compounds of arsenic with chloride ions, similar to antimony.[16] The total changes in potential difference in titrations of arsenic vary with the composition of the solution and with the current used for the polarisation of the electrodes. Under optimum working conditions (Table 2), the total changes in potential difference in the titration of

arsenic(III) with a solution of manganese(III) in sulphuric acid were 800–900 mV, whereas in hydrochloric acid they were about 800 mV. However, in the titration of arsenic(III) with a solution of manganese(IV) in the presence of sulphuric acid, the changes were about 600 mV, and in the presence of hydrochloric acid, they ranged from 800 to 900 mV. In the presence of a catalyst, the potential at the electrodes is established within 1–2 min throughout the whole titration.

It has been shown elsewhere that manganese(III) oxidises oxalate to carbon dioxide,[17,18] but oxalate had to be determined by back-titration because of the slow rate of reaction at room temperature. With the bipotentiometric method, however, we were able to determine oxalate directly with manganese(III) and manganese(IV). For example, in titrating with manganese(III) in 0.5–1.0 M sulphuric acid solutions at room temperature, the electrode potentials stabilise within 1 min of adding the reagent, except in the vicinity of the end-point, where stabilisation takes 2–5 min. As in titrations of arsenic(III), the redox components of this substance are more reversible in sulphuric acid solutions than in the presence of hydrochloric acid.

It was also of interest to establish conditions suitable for the potentiometric titration of hydroquinone, which is often used as a primary standard and which, together with quinone, represents a characteristic reversible redox pair. As expected, titration curves obtained in the determination of this substance with manganese(III) in both supporting electrolytes were found to be characteristic of a reversible system, whereas the potential at the electrodes is established rapidly, except in the vicinity of the end-point, where a wait of 5–10 min after adding the titrant is needed. The irreversible behaviour of manganese(IV) and the corresponding reduced form may be attributed to their interaction with the titrand.

Optimum conditions for bipotentiometric titration of those substances investigated are given in Table 2. The accuracy and reproducibility of the results are good, even when determining small amounts of substances.

The titrations of iron(II) and arsenic(III) in the presence of the catalyst and the titration of hydroquinone require 30–40 min. The determination of potassium hexacyanoferrate(II) takes 40–50 min, and that of oxalate 60–80 min. However, some titrations, for instance the determination of manganese(IV) with iron(II) in 4.5 M sulphuric acid, can be carried out within 20 min. Hence the method described in this paper can be used for routine analyses of several types of substances under suitable experimental conditions.

In addition, in contrast with other methods, the bipotentiometric method gives some information on the reversibility of the redox pairs present in the solution, on the basis of the shape of the titration curves obtained.

The authors acknowledge financial support from the Research Fund of SR Serbia.

References

1. Berka, A., Vulterin, J., and Zýka, J., "Newer Redox Titrants," Pergamon Press, Oxford, 1965.
2. Barek, J., and Berka, A., *CRC Crit. Rev. Anal. Chem.*, 1980, **9**, 55.
3. Barek, J., Berka, A., and Procházková, I., *Talanta*, 1974, **21**, 157.
4. Mandal, S. K., and Sant, B. R., *Talanta*, 1976, **23**, 485.
5. Murthy, N. K., Prasad, G. U., and Rao, K. R., *Talanta*, 1979, **26**, 1049.
6. Rukmini, N., Kavitha, V. S. N. P., and Rao, K. R., *Analyst*, 1979, **104**, 1201.
7. Berka, A., Barek, J., and Cafourková, M., *Microchem. J.*, 1980, **25**, 111.
8. Pastor, T. J., Dobričić, M., and Žižić, B., *Microchem. J.*, in the press.
9. Selim, R. G., and Lingane, J. J., *Anal, Chim. Acta*, 1959, **21**, 536.
10. Kolthoff, I. M., Sandell, E. B., Meehan, E. J., and Bruckenstein, S., "Quantitative Chemical Analysis," Fourth Edition, Macmillan, New York, 1971.
11. Vogel, A. I., "Quantitative Inorganic Analysis Including Elementary Instrumental Analysis," Third Edition, Longmans, London, 1961.
12. Lingane, J. J., and Karplus, R., *Ind. Eng. Chem., Anal. Ed.*, 1946, **18**, 191.
13. Barek, J., Berka, A., and Korečková, J., *Chem. Anal. (Warsaw)*, 1975, **20**, 749.
14. Belcher, R., and West, T. S., *Anal. Chim. Acta*, 1952, **6**, 322.
15. Mallela, S. P., and Khandelwal, B. L., *Fresenius Z. Anal. Chem.*, 1977, **285**, 257.
16. Brown, R. A., and Swift, E. H., *J. Am. Chem. Soc.*, 1949, **71**, 2719.
17. Berka, A., Barek, J., and Hladikova, A., *Microchem. J.*, 1979, **24**, 431.
18. Barek, J., Berka, A., and Jakubec, K., *Microchem. J.*, 1979, **24**, 454.

Paper A3/319
Received September 14th, 1983
Accepted October 25th, 1983

Coulometric Cerimetric Determinations in Acetic Acid in the Presence of Sodium Perchlorate

Tibor J. Pastor* and Ivan Ćirić
Department of Chemistry, Faculty of Sciences, University of Belgrade, P.O. Box 550, 11001 Belgrade, Yugoslavia

Studies were made to determine conditions for electrochemically generating cerium(IV) with high current efficiency in solutions of sodium perchlorate in acetic acid, and procedures were developed for coulometrically determining reducing substances with the oxidant obtained. Titration end-points were detected using biamperometric and potentiometric methods. The effects of water and acetic anhydride on the current efficiency and end-point detection were studied. The formal redox potential of the cerium(IV) - cerium(III) system changes to more positive values as the concentration of sodium perchlorate in the solution is increased. The effect of perchloric acid is similar but more pronounced. Perchloric acid, when present in the anolyte, also increases the rate of oxidation of test substances with cerium(IV) in acetic acid.

Keywords: *Coulometric titration; anodic generation; cerium(IV); acetic acid; cerium(IV) - cerium(III) system*

Non-aqueous solvents have been widely used as media for acid - base titrimetry.[1] Determinations based on redox reactions, however, have not often been performed in organic solvents, although they might be useful in titrations of substances that are slightly soluble in water, or react with it. This is due to the low solubility of most inorganic oxidants and reducing agents in solvents. Of the non-aqueous solvents used, glacial acetic acid and acetonitrile have been used most often because of the suitability of their physical and chemical properties. Cerimetric determinations of reducing substances with ammonium hexanitratocerate(IV) have also been performed in the solvents mentioned.[2–18] Difficulties caused by the instability of cerium(IV) in acetic acid, requiring frequent standardisation of the titrant,[2] can be overcome by anodic generation of the oxidant with 100% current efficiency in the presence of 0.3–1.8 M potassium acetate.[19] Coulometric titrations of a few compounds that are rapidly and quantitatively oxidised in potassium acetate supporting electrolyte have also been carried out with electrochemically generated cerium(IV).

This paper describes studies carried out to determine conditions for generating cerium(IV) with high current efficiency in solutions of sodium perchlorate in acetic acid. In the presence of perchloric acid in solutions containing sodium perchlorate, the redox potential of the cerium(IV) - cerium(III) system and the rate of oxidation reactions are increased. Hence the presence of perchloric acid in the anolyte offers possibilities for further development of coulometric cerimetric determinations in acetic acid.

Experimental

Apparatus and Chemicals

The equipment used for coulometric titrations with biamperometric and potentiometric end-point detection, for measuring the redox potential of the cerium(IV) - cerium(III) couple and for recording the current - potential graph at the anode has been described elsewhere.[19,20]

A platinum working electrode with a 2 cm^2 active surface area and a similar auxiliary electrode separated by a sintered-glass disc were used. Bright platinum electrodes, area 0.2 cm^2, were used for biamperometric indication. The redox potential of the cerium(IV) - cerium(III) system was measured with a platinum indicator electrode and a mercury - mercury(I) acetate reference electrode.

All reagents were of analytical-reagent grade and were dried by procedures described earlier.[19–21]

The catholytes used were 0.1–0.6 M solutions of sodium perchlorate in acetic acid and 0.2 M solutions of sodium perchlorate in the presence of 0.05–0.5 M perchloric acid.

The anolyte was prepared by dissolving 0.5 g of cerium(III) nitrate, which had been previously dried over phosphorus(V) oxide, in 100 cm^3 of the respective catholyte solution. The exact concentration of cerium(III) in the solution used for determining the formal potential of the cerium(IV) - cerium(III) system was determined by titrations with EDTA,[19,22] and was 0.011–0.013 M.

Standard solutions of reducing substances (0.01–0.001 M) were prepared by precise weighing. The purity of 2-chlorohydroquinone was checked by potentiometric titration with potassium dichromate solution in the presence of sulphuric acid, and the purity of citric acid was established by titration with sodium hydroxide solution.

Procedures

Determinations of the reducing substances with anodically generated cerium(IV) were performed in the following two ways: (*i*) a suitable volume of sample solution was measured into the anode compartment prior to titration, and cerium(IV) was continuously generated until the end-point was reached; and (*ii*) a solution of the test substance was added to the anolyte after 95–97% of the theoretically required amount of the reagent had been generated, and the reagent was then generated in small amounts (3–5 s at a current of 0.50–3.00 mA) until the end-point was reached. A more detailed description of these procedures was given earlier.[20,23]

The formal redox potential of the cerium(IV) - cerium(III) system in solutions of sodium perchlorate in acetic acid in the absence or presence of perchloric acid was determined using procedures described earlier.[19,21]

Results and Discussion

Data on the reactions of acetic acid with cerium(IV), in both aqueous solution and glacial acetic acid, were taken from the literature.[2] As soon as the solubility of cerium(III) nitrate in the solutions of sodium perchlorate in acetic acid had been found and the possibilities for generating cerium(IV) investigated, the stability of the reagent solution obtained was investigated using the biamperometric method. The results obtained (Fig. 1) show that in the presence of potassium

* To whom correspondence should be addressed.

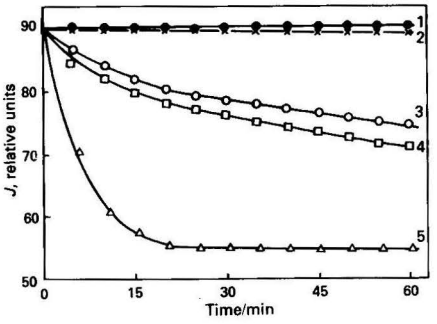

Fig. 1. Changes with time of the concentration of cerium(IV) in acetic acid solutions. Concentration changes were measured by the biamperometric method in the following supporting electrolytes: 1, 0.9 M potassium acetate; 2, 0.2 M sodium perchlorate; 3, 0.2 M sodium perchlorate + 0.05 M perchloric acid; 4, 0.2 M sodium perchlorate + 0.2 M perchloric acid; and 5, 0.2 M sodium perchlorate + 0.5 M perchloric acid

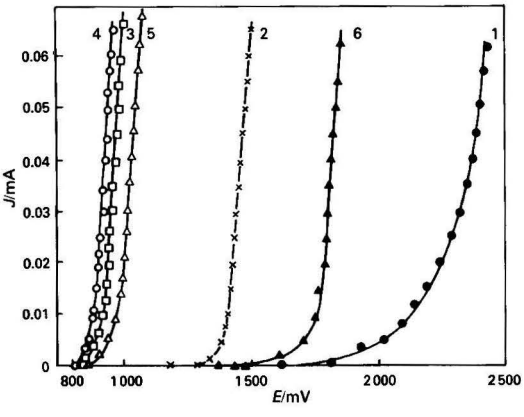

Fig. 2. Current *versus* potential graphs at the anode in 1, 0.2 M sodium perchlorate; and in the same electrolyte after the addition of 2, cerium(III) nitrate; 3, hydroquinone; 4, 2-methylhydroquinone; 5, 2-chlorohydroquinone; and 6, a mixture of perchloric acid (0.05 mol dm^{-3}) and cerium(III) nitrate

acetate or sodium perchlorate the concentration of the reagent remains constant or changes slowly with time. The presence of perchloric acid, even in small amounts, accelerates the reaction of the obtained oxidant with the solvent. The rate at which the oxidant concentration decreases is proportional to the concentration of acid in the solution.

The current - potential graphs at the anode recorded in a 0.2 M solution of sodium perchlorate in acetic acid, and graphs for the solution in which cerium(III) nitrate had been dissolved, show that cerium(III) is oxidised at a more negative potential than the supporting electrolyte (Fig. 2). The presence of perchloric acid in the solution changes the oxidation potential of cerium(III) to more positive values. All of the test substances used were oxidised at even more negative potentials, so that these substances could be titrated coulometrically with anodically generated cerium(IV) in both of the supporting electrolytes studied in this work. When the oxidation potentials of certain compounds in 0.9 M potassium acetate are compared with those of the same compounds in 0.2 M sodium perchlorate, a shift to more positive values is found in the perchlorate supporting electrolyte.

By titrating six consecutive samples of each standard substance, it was found that by passing 1 C through 20 cm^3 of

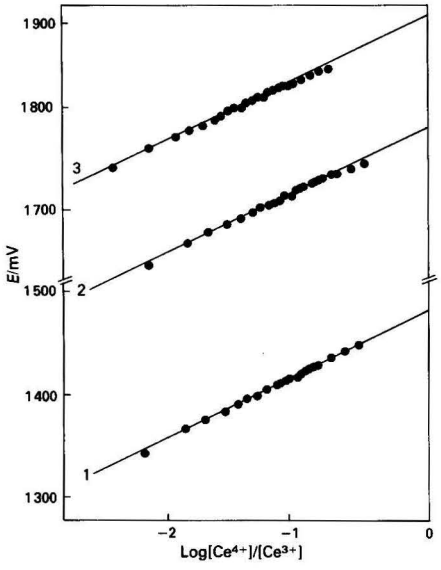

Fig. 3. Dependence of the redox potential of the cerium(IV) - cerium(III) system on log[Ce(IV)]/[Ce(III)] in acetic acid solutions in the presence of the following electrolytes: 1, 0.2 M sodium perchlorate; 2, 0.2 M sodium perchlorate + 0.05 M perchloric acid; and 3, 0.2 M sodium perchlorate + 0.2 M perchloric acid

anolyte prepared in 0.2 M sodium perchlorate solution, the current efficiencies of oxidant generation were 99.7 ± 0.2, 98.1 ± 0.1 and 95.3 ± 0.3% with generation currents of 1.00, 2.00 and 3.00 mA, respectively. When 2.00, 3.00 and 4.00 C were passed through to the same amount of anolyte with a current of 1.00 mA in the generation circuit, the current efficiencies of generation of cerium(IV) were found to be 99.2 ± 0.3, 98.6 ± 0.3 and 97.9 ± 0.2%, respectively. An increase in the concentration of cerium(III) nitrate in the anolyte, from 0.012 to 0.02 M, did not affect the current efficiency appreciably.

The presence up to 0.8% of water in the anolyte (this being the maximum concentration studied) did not affect the accuracy of the hydroquinone determination, *i.e.*, the amount of the reagent generated. Because of acetylation of hydroquinone with acetic anhydride it was difficult to study the influence of the anhydride on current efficiency in generations of cerium(IV), but it was observed that the presence of the anhydride does not affect the shape of biamperometric titration curves.

In order to determine the formal redox potential of the cerium(IV) - cerium(III) system, different but known amounts of cerium(IV) were generated in a measured volume of anolyte containing a known concentration of cerium(III), and the appropriate redox potentials were measured. Graphs of the values obtained against log[Ce(IV)]/[Ce(III)] were straight lines. The intersections of the lines with the ordinate, at log[Ce(IV)]/[Ce(III)] = 0, gave the formal potentials of the system. It can be seen from Fig. 3 that in the presence of a small amount of perchloric acid in the anolyte the potentials obtained by prolonged generation of cerium(IV) are beneath the corresponding straight line, *i.e.*, are lower than expected. This is due to the instability of cerium(IV) under these conditions. Because of this, the formal potential in solutions that were more than 0.2 M in perchloric acid was not determined.

From the data in Table 1 it can be seen that an increase in the concentration of sodium perchlorate in the solutions shifts

Table 1. Formal redox potentials (mV) of the Ce(IV) - Ce(III) system in the presence of sodium perchlorate and perchloric acid in acetic acid

0.2 M $NaClO_4$		0.4 M $NaClO_4$		0.5 M $NaClO_4$		0.2 M $NaClO_4$ + 0.05 M $HClO_4$		0.2 M $NaClO_4$ + 0.2 M $HClO_4$	
E'_0	Tan α	E'_0	Tan α	E'_0	Tan α	E'_0	Tan α	E'_0	Tan α
1480	60.0	1497	59.5	1506	58.0	1780	58.0	1890	59.0
1482	61.5	1498	60.0	1507	58.5	1782	58.5	1892	60.0
1482	61.0	1500	60.5	1509	60.0	1782	58.5	1890	59.0

Table 2. Coulometric titration of reducing substances with electrochemically generated cerium(IV) in perchlorate supporting electrolyte in acetic acid (end-points detected by the biamperometric method with platinum electrodes)

Substance titrated	Taken/ mg	No. of determinations	Found, %	Procedure	Current/ mA	Supporting electrolyte
Hydroquinone	0.550	11	98.9 ± 0.6	(*i*)	1.00	0.2 M $NaClO_4$
	0.550	6	99.2 ± 0.3	(*ii*)	1.00	0.2 M $NaClO_4$
	0.275	6	99.3 ± 0.3	(*i*)	0.50	0.2 M $NaClO_4$
	0.275	6	99.2 ± 0.4	(*ii*)	0.50	0.2 M $NaClO_4$
2-Methylhydroquinone	0.620	6	99.9 ± 0.2	(*ii*)	1.00	0.2 M $NaClO_4$
	0.310	4	100.3 ± 0.4	(*ii*)	0.50	0.2 M $NaClO_4$
2-Chlorohydroquinone	0.724	6	99.0 ± 0.3	(*ii*)	1.00	0.2 M $NaClO_4$
Oxalic acid	0.630	6	99.4 ± 0.3	(*i*)	1.00	0.2 M $NaClO_4$ + 0.1 M $HClO_4$
Mandelic acid	0.760	6	99.4 ± 0.3	(*i*)	1.00	0.2 M $NaClO_4$ + 0.2 M $HClO_4$
Ascorbic acid	0.880	6	99.5 ± 0.3	(*i*)	1.00	0.2 M $NaClO_4$ + 0.1 M $HClO_4$
Citric acid	0.528	6	99.6 ± 0.3	(*i*)	1.00	0.2 M $NaClO_4$ + 0.2 M $HClO_4$
Thiourea	0.760	6	99.7 ± 0.3	(*i*)	1.00	0.2 M $NaClO_4$ + 0.1 M $HClO_4$

* Mean ± standard deviation.

the formal potential of the cerium(IV) - cerium(III) system to more positive values. Perchloric acid exerts a similar but more pronounced effect, in the same way as it does in aqueous media.[24] The slope of the graphs (tan α) corresponds to a one-electron change at the electrode, as expected for oxidation of cerium(III) to cerium(IV).

Coulometric Titrations with Electrogenerated Cerium(IV)

The anodically generated cerium(IV) in a 0.2 M solution of sodium perchlorate in acetic acid reacts rapidly with hydroquinone, but not with the other substances tested (Table 2). Because of this, hydroquinone was used as a reference substance in all the studies described above and in an investigation into the accuracy and reproducibility of the procedures used for coulometric determinations. Under the conditions used in this work, 2-methyl- and 2-chlorohydroquinone can be determined only by using procedure (*ii*)—generating the cerium(IV) in small amounts and allowing enough time (3–5 min) between each two generations to ensure completion of the reaction with the oxidant.

The perchlorate supporting electrolyte used in this work has advantages over the potassium acetate electrolyte in determinations of the remaining substances given in Table 2. Thus, for instance, ascorbic acid is slowly oxidised by cerium(IV) in the presence of potassium acetate, and can only be determined by discontinuous generation of the oxidant in the vicinity of the end-point [procedure (*ii*)], or by the back-titration method.[19] In the perchlorate supporting electrolyte in the presence of perchloric acid, however, the redox potential of the Ce(IV) - Ce(III) system and the rate of the oxidation reaction are increased, so that reasonable results are also obtained by method (*i*) in which the titrated substance is added to the anolyte prior to the titration and the oxidant is generated continuously. In this way, the duration of the titration is considerably shortened and the procedure can be automated. Oxalic, mandelic and citric acids and thiourea can be determined only in the perchlorate supporting electrolyte in the presence of perchloric acid by procedure (*i*). The optimum composition of the supporting electrolyte for the analysis of each particular substance is given in Table 2.

Most of the compounds investigated react with 2 mol of cerium(IV) each. The only exception is thiourea, which is oxidised with 1 mol of the oxidant to the corresponding disulphide (formamidine disulphide).[10,12] Citric acid in perchlorate supporting electrolyte that is 0.2 M in perchloric acid consumes 4 mol of the oxidant. The reaction mechanism, which is complex, and the products of the oxidation were not studied.

The titration end-point was determined using the biamperometric method, with platinum electrodes polarised with a 400–800 mV potential difference. In titrations of all substances a current minimum was observed at the end-point. It was observed that an increase in current in the presence of the excess of oxidant, *i.e.*, after the end-point had been reached, was less marked when the concentration of perchloric acid in the anolyte was higher than 0.1 M. This is due to the faster rate of reaction of cerium(IV) with the solvent. The potentiometric method was also used successfully for end-point detection. From the titration graphs obtained in this way it can be seen that a potential jump in the vicinity of the end-point is more pronounced in the presence of perchloric acid owing to the effect of the acid on the oxidation potential of the cerium(IV) - cerium(III) system.

The accuracy and reproducibility of the developed coulometric methods can be seen from the results in Table 2.

The authors acknowledge financial support from the Research Fund of the Socialist Republic of Serbia.

References

1. Gyenes, I., "Titrationen in Nichtwässrigen Medien," Akadémiai Kiadó, Budapest, 1970.
2. Hinsvark, O. N., and Stone, K. G., *Anal. Chem.*, 1956, **28**, 334.
3. Prabhakar Rao, G., and Vasudeva Murthy, A. R., *Fresenius Z. Anal. Chem.*, 1960, **177**, 86.

4. Prabhakar Rao, G., and Vasudeva Murthy, A. R., *Fresenius Z. Anal. Chem.*, 1961, **180**, 169.
5. Prabhakar Rao, G., and Vasudeva Murthy, A. R., *Fresenius Z. Anal. Chem.*, 1961, **182**, 358.
6. Prabhakar Rao, G., and Vasudeva Murthy, A. R., *Fresenius Z. Anal. Chem.*, 1962, **187**, 96.
7. Prabhakar Rao, G., and Vasudeva Murthy, A. R., *Fresenius Z. Anal. Chem.*, 1963, **195**, 406.
8. Prabhakar Rao, G., and Vasudeva Murthy, A. R., *Indian J. Chem.*, 1966, **4**, 49; *Chem. Abstr.*, 1966, **65**, 12 g.
9. Gatto, J. T., and Stone, K. G., *Talanta*, 1966, **13**, 597.
10. Mruthyunjaya, H. C., *Curr. Sci.*, 1967, **36**, 537.
11. Mruthyunjaya, H. C., and Vasudeva Murthy, A. R., *Indian J. Chem.*, 1967, **5**, 430; *Chem. Abstr.*, 1968, **68**, 74813t.
12. Verma, B. C., and Kumar, S., *Talanta*, 1973, **20**, 916.
13. Verma, B. C., and Kumar, S., *Talanta*, 1976, **23**, 241.
14. Verma, B. C., and Kumar, S., *J. Indian Chem. Soc.*, 1973, **53**, 1015.
15. Ventura, M., Rauret, G., and Rubio, R., *An. Quim.*, 1978, **74**, 1321; *Anal. Abstr.*, 1979, **37**, 1A17.
16. Bruno, P., Caselli, M., Difano, A., and Traini, A., *Anal. Chim. Acta*, 1979, **104**, 379.
17. Verma, B. C., Kumar, S., and Atval, B. S., *Zh. Anal. Khim.*, 1980, **35**, 386.
18. Verma, B. C., and Sood, R. K., *Talanta*, 1981, **28**, 960.
19. Pastor, T. J., Vajgand, V. J., and Ćirić, I., *Anal. Chim. Acta*, 1982, **138**, 87.
20. Pastor, T. J., Vajgand, V. J., and Kićović, Z., *Mikrochim. Acta*, 1976, **II**, 525.
21. Pastor, T. J., Vajgand, V. J., Antonijević, V. V., and Veličković, Z., *Anal. Chim. Acta*, 1979, **106**, 347.
22. Lyle, S. J., and Rahman, M. M., *Talanta*, 1963, **10**, 1177.
23. Pastor, T. J., Vajgand, V. J., and Antonijević, V. V., *Mikrochim. Acta*, 1978, **II**, 131.
24. Skoog, D. A., and West, D. M., "Fundamentals of Analytical Chemistry," Holt, Rinehart and Winston, London, 1973, p. 433.

Paper A3/129
Received May 10th, 1983
Accepted June 15th, 1983

Analytical Investigation of Some Fluorogenic Reactions of Indol-3-yl Acids with *o*-Phthalaldehyde Part I. Solution Fluorimetric Studies

Tereza C. M. Pastore, Ezer M. de M. Nicola* and Clausius G. de Lima†
Departamento de Química, Universidade de Brasília, Brasília, D.F.-70 910, Brazil

An investigation of the parameters that may affect the fluorogenic reaction of some indol-3-yl acids with *o*-phthalaldehyde in sulphuric acid medium has been carried out. Indol-3-ylacetic acid, a compound of biological interest, which was used as a model compound, was carefully examined together with seven other similar compounds. The influence of the concentration of sulphuric acid, oxygen, temperature, interferences and ultraviolet radiation was investigated. In the last instance, a beneficial effect on the fluorescence signal was observed with most compounds and this led to the proposal of a photochemical - fluorimetric method of analysis.

Keywords: *Indol-3-ylacetic acid; phytohormones; photochemical - fluorimetric method; o-phthalaldehyde reagent*

Interest in the determination of indol-3-yl acids and related compounds comes from two distinct areas: from the field of plant biology, as some of these compounds are or behave as phytohormones,[1,2] and in the medical field, as some derivatives of these acids occur in the cerebral tissue or appear in the excreta, mainly as a consequence of metabolic disturbances.[3–5] The fluorimetric determination of one of these phytohormones, indol-3-ylacetic acid (IAA), is usually carried out by condensation with acetic anhydride (catalysed by an acid), which produces a fluorescent product (2-methylindole-α-pyrone).[6] The spectrofluorimetric method of determination of IAA via the formation of α-pyrone has been reviewed by Mousdale *et al.*[7] Also, the quantitative analytical methods employed in the determination of plant hormones have recently been examined and described by Reeve and Crozier.[8]

o-Phthalaldehyde (OPA), particularly in the presence of 2-mercaptoethanol, is a well known reagent (Roth's reagent)[9,10] employed for the determination of several types of compound of biological interest such as amino acids, peptides and proteins.[10–12] The utilisation of OPA as a fluorimetric reagent for the determination of amino acids has been reviewed by Lee and Drescher.[13] Also, OPA has been found to react with other compounds such as iodinated amino acids,[14] amino sugars,[15] histamine,[16] spermidine,[17] glutathione,[18] sulphanilamides,[19] hydrazine, ammonia[20] and cyclohexanedione.[21]

In contrast to ninhydrin, OPA does not seem to react with secondary amines; proline and hydroxyproline react only after being oxidised.[13] The reaction of OPA with compounds that have an indole nucleus was reported by Maickel and Miller[22,23] when, after examining several indole compounds, it was found that, among others, 5-hydroxyindol-3-ylacetic acid (5-HIAA) and 5-methoxyindol-3-ylacetic acid (5-MIAA) reacted with OPA in acidic medium (*ca.* 6 N HCl, 100 °C). 5-HIAA and 5-hydroxyindole were also found to react with OPA (in the presence of cysteine) in sulphuric acid medium (*ca.* 9.3 N, 95 °C) by Garnier *et al.*[24] However, under the conditions examined by Maickel and Miller, no reaction was observed with IAA.[22]

Other compounds with an indole nucleus have also been found to react with OPA, including some ergolenes and corresponding ergolines, using OPA in concentrated sulphuric acid as a TLC spray reagent,[25] and an α-blocking drug, 4-(2-hydroxy-3-isopropylaminoproproxy)indole, which reacted with OPA in dilute hydrochloric acid.[26] In the latter instance no reaction was observed when the indole nucleus was substituted by a naphthalene nucleus [giving (1-isopropylamino)-3-(1-naphthyloxy)propan-2-ol].[26]

By examining further the possibility of a reaction of IAA with OPA in acidic medium we found that at H_2SO_4 concentrations higher than 9 N a fluorogenic reaction occurs. Later, we found that the reaction also occurs with other indol-3-yl acids examined, such as 3-(indol-3-yl)propionic acid (IPA), 4-(indol-3-yl)butyric acid (IBA), 3-(indol-3-yl)lactic acid (ILA) and indol-3-ylpyruvic acid (IPyA). Also, 5-HIAA and 5-MIAA, which are known to react with OPA in acidic medium,[22–24] and the ethyl ester of IAA (IAAEE) were examined. An investigation of the parameters that may affect the reaction (sulphuric acid concentration, effect of oxygen, temperature, interferences and, mainly, ultraviolet irradiation around 365 nm) was carried out and analytical figures of merit are reported. Qualitative tests were made with the methyl ester of IAA, 5-hydroxytryptamine (serotonin) and tryptophan.

Experimental

Apparatus

A Zeiss RPQ 20A spectrophotometer (Carl Zeiss, Oberkochen/Wurt, FRG), modified according to the manufacturer's instructions by coupling a fluorescence attachment (ZFM 20), was employed in most of the experiments. A mercury-vapour discharge lamp (Zeiss St 40 or St 41) and a filter that isolated the 365-nm region was used.

Later, a laboratory-assembled spectrofluorimeter was used to determine both the emission and excitation spectra. This instrument consisted basically of a 150-W xenon lamp (Engelhard Hanovia, Newark, NJ, USA) driven by an appropriate power supply (Bausch and Lomb, Rochester, NY, USA), an excitation monochromator, 0.45 m, *f*/8, linear reciprocal dispersion 1.75 nm mm^{-1} (Pacific Precision Instruments, Concord, CA, USA), a sample holder (a quartz test-tube, 100 × 14 mm o.d., could be used) and an emission monochromator, 0.45 m, *f*/8, linear reciprocal dispersion 3.5 nm mm^{-1} (Model 1018; MacKee-Pedersen Instruments, Danville, CA, USA). The signal from an RCA 1P28 photomultiplier (S-5 spectral response; RCA Electronic Components, Harrison, NY, USA), which was operated at 800 V by using a high-voltage supply (Keithley Instruments, Cleveland, OH, USA), was amplified using an electrometric/operational amplifier (Model 1032; Pacific Precision Instruments) and fed to a recorder (Model L201; Zeiss - Jena, GDR). The fluorescence spectra are reported without correction. All signal intensity readings were corrected when needed using standard quinine sulphate solution (in 0.1 N H_2SO_4).

* Present address: Conselho Nacional de Petróleo, SGAN-603, Brasília, D.F.-70 830, Brazil.
† To whom correspondence should be addressed.

The solutions were irradiated using either the fluorescence attachment of the Zeiss assembly (using the fluorimeter cell) or a Rayonet photochemical reactor (Model RPR-100; Southern N.E. Ultraviolet Co., Hamden, CT, USA), operating with 12 lamps (24 W each, $\lambda_{max.}$ at 350 nm), using quartz test-tubes (150 × 15 mm o.d.).

Photometric titrations were carried out in a laboratory-modified photocolorimeter (Model J; Dr. B. Lange, Berlin, FRG).

Materials and Reagents

Most of the indol-3-yl acids used were purchased from Sigma (St Louis, MO, USA). The methyl ester of IAA was synthesised by methylation of IAA according to Knapp[27] (m.p. 48–50 °C; lit.[28] 49–53). Standard solutions of the indolic compounds were prepared in ethanol - water (1 + 9) at a concentration of 200 μg ml^{-1} and diluted as required. The OPA reagent (Sigma) was used as received, as after purification by sublimation identical results were obtained.

Analytical-reagent grade absolute ethanol and H_2SO_4 (Merck Industria Brasileira, Rio de Janeiro, Brazil) were used without previous purification. The other acids tested and the salts used in the interference study were of analytical-reagent grade and of different origin. The content of the metal was determined by complexometry using EDTA and appropriate metal indicators.[29] The end-point was determined either visually or by photometric titration.

Procedure

A 1-ml volume of a standard solution of the indole compound was added to a 10-ml calibrated flask, followed by the addition of 1 ml of OPA reagent (0.15% *m/V* absolute ethanol) and 8 ml of H_2SO_4 (with a known concentration corresponding, after dilution, to an optimum concentration, according to Table 2). Whenever necessary the solution was irradiated before the readings in the Zeiss assembly or in the photochemical reactor. Before irradiation, gentle stirring to increase the contact of the solution with air seems to produce better results (see Effect of Oxygen).

Results and Discussion

Some parameters that could affect the reaction were examined, using IAA as a model compound in most instances.

Stability of the OPA Reagent

Attempts to replace ethanol with sulphuric acid (17.5 N) as a solvent in the preparation of the OPA reagent showed that the stability of the reagent decreased (from 2 weeks to approximately 2 d) even when the solutions were maintained at *ca.* 7 °C in the dark.

Effect of the Order of Addition

The order of addition does not affect the fluorescence signal of the product obtained with IAA if the readings are made immediately. However, it does affect it if the IAA solution is added to the H_2SO_4 solution and after a certain time the addition of the OPA solution is made, followed by the reading. Under such circumstances a decrease in the fluorescence signal is observed that is proportional to the time of contact between the IAA solution and the H_2SO_4 solution. Consequently, the order of addition: analyte, OPA, H_2SO_4, is suggested.

Effect of Other Acids

Preliminary attempts confirmed the finding of Maickel and Miller[22] that in HCl, the reaction between IAA and OPA does not occur. Examination of perchloric, phosphoric and trichloroacetic acids showed that only in perchloric acid did the reaction succeed, the optimum concentration range being *ca.* 5.7–6.7 N. No further studies were made with this medium as H_2SO_4 is cheaper and more readily available.

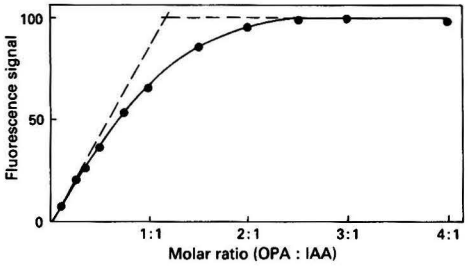

Fig. 1. Effect of variation of molar ratio on the signal intensity

Table 1. Effect of interferences on the IAA - OPA fluorophore; values given as percentages of the original signal

Ion	Interferent to IAA molar ratio 1:1	10:1	100:1
Hg^{2+}	105	101	79
Fe^{3+}	101	98	77
I^-	102	78	23

Effect of Temperature and Light

Only two initial temperatures were examined (0 and 26 °C, which increase to *ca.* 25 and 37 °C, respectively, after the addition of H_2SO_4), but no differences were observed in the fluorescence signal of the fluorophore yielded by the reaction of IAA with OPA. Also, no effect was observed under room (fluorescent) lighting, with the exception of the instability of the IPyA solution, which required surroundings with a low level of illumination.

Molar Ratio of IAA to OPA

Fig. 1 shows the results obtained after the molar ratio of OPA to IAA was changed from 0.25 : 1 to 10 : 1. An intersection at 1 : 1.15 suggests a molar ratio of 1 : 1. At low OPA concentrations it was necessary to take the signal readings 60 min after the mixing owing to the slow reaction rate observed.

Some attempts to identify the major product of the reaction of IAA with OPA were made, which resulted in the isolation (by extraction with ethyl acetate followed by silica gel column chromatography) of reddish brown crystals with a melting-point in the range 110–125 °C (with decomposition). This material, although it fluoresces after being dissolved in H_2SO_4, showed a weaker signal and different spectral characteristics, compared with the IAA - OPA fluorophore before isolation, suggesting either a modification of the structure during the process of isolation or an incomplete separation, being in reality a mixture.

Effect of Interferences

Using IAA as a model compound, possible interferences from various cations (Ni^{2+}, Co^{2+}, Cu^{2+}, Fe^{3+}, Mn^{2+}, Cd^{2+}, Cr^{3+}, Hg^{2+} and Zn^{2+}) and anions (F^-, Cl^-, Br^- and I^-) with molar ratios (interferent to IAA) of 1 : 1, 10 : 1 and 100 : 1 were examined. Table 1 gives the results observed with the only ions (Hg^{2+}, Fe^{3+} and I^-) found to interfere, showing typical examples of the heavy-atom effect or the influence of paramagnetic species such as Fe^{3+}.

An examination of the $\lambda_{max.}$ of emission of the fluorophores obtained after the reaction of the indole compounds with OPA (Table 3) revealed that partial or direct spectral interferences are possible if the indole compounds are not previously separated.

Table 2. Analytical characteristics of the compounds examined (using the Zeiss assembly)

Compound	Optimum H_2SO_4 concentration/N	Irradiation time/min	S_i/S_0*	Limit of detection/ ng ml^{-1} (ng)†	Linear range/ng ml^{-1}
IAA	14–16	30‡	0.44	2.3 ± 0.28 (6.9)	2.3–1.0 × 10^3
IPA	13.8–14.3	10‡	10.0	5.2 ± 0.85 (15.6)	5.2–2.5 × 10^3
IPyA	13–14	4§	1.4	110 ± 9.5 (330)	1.1 × 10^2–1.0 × 10^3
ILA	15	10‡	7.0	6.0 ± 0.67 (18)	6.0–2.5 × 10^3
IBA	16	30‡	5.0	8.0 ± 0.1 (24)	8.0–2.5 × 10^3
5-HIAA	12.7–*ca.* 14	30‡	1.0	2.3 ± 0.62 (6.9)	2.3–1.0 × 10^3
5-MIAA	11.4	10§	2.3	2.0 ± 0.1 (6.0)	2.0–1.0 × 10^3
IAAEE	12.8–13.3	60§	2.0	60 ± 12.46 (180)	60–2.5 × 10^3

* Ratio between the signal after irradiation (S_i) and the signal before irradiation (S_0), reading the signal at the $\lambda_{max.}$ and with an analyte concentration of 1 μg ml^{-1}.

† Absolute limit of detection, with a fluorimeter cell using a volume of 3 ml.

‡ Irradiated in the reactor.

§ Irradiated in the Zeiss assembly.

Table 3. Spectral characteristics of the compounds examined

Compound	Before irradiation		After irradiation	
	$\lambda_{ex.}$/nm*,†	$\lambda_{em.}$/nm*	$\lambda_{ex.}$/nm*,†	$\lambda_{em.}$/nm*
IAA	293, 353 *372, 390*	*410* *429*	‡	‡
IPA	293, *342*	*410*	295, *357*	*463*
IPyA	250, 295 *343*	*402*	250, 295 *343*	*402*
ILA	293, *343*	*407*	256, 297 *357*	*463*
IBA	*347*	*404*	275, 295 *359*	*465*
5-HIAA	*357*	*471*	*357*	*471*
5-MIAA	295, *360*	*460*	295, *360*	*460*
IAAEE	295, *340* 363	*403*	—	*467*

* The uncertainty in the wavelength is estimated to be ±2 nm; $\lambda_{ex.}$, excitation peak; $\lambda_{em.}$, emission peak; $\lambda_{max.}$ values are the italicised wavelengths.

† These values were collected using the spectrofluorimeter assembled in the laboratory.

‡ A decrease in signal intensity is observed [see Fig. 2(*a*)].

Effect of Irradiation

Although the ultraviolet (UV) irradiation (365-nm region) treatment, after the reaction, had no effect on the 5-HIAA - OPA fluorophore and had a detrimental effect on the IAA - OPA fluorophore, for most of the compounds the UV irradiation was beneficial, suggesting the possibility of a photochemical - fluorimetric method of analysis for such compounds. At first, UV irradiation experiments were made in the Zeiss fluorimeter attachment. However, as some compounds. At first, UV irradiation experiments were carried out in the Zeiss fluorimeter attachment. However, as some compounds (IBA, ILA and IPA) took a long time to attain a plateau, irradiation was carried out in the photochemical reactor. The fluorophore produced after the reaction of IAAEE with OPA also increased the signal with UV irradiation, but at a slow rate, taking over 60 min to attain a maximum signal even in the reactor. In this instance it was more practical to read the signal without irradiation.

analyte. The best results were obtained with IPA, ILA and IBA. The fluorophores obtained with IPyA, 5-HIAA and 5-MIAA did not change their spectral characteristics when irradiated. After irradiation, the corresponding fluorophores of IPA, ILA and IBA show similar spectral characteristics [excitation at 357 ± 2 and emission at 463 ± 2 nm; see Fig. 7(*b*)]. The irradiation of the fluorescent reaction product of IAA with OPA [Fig. 2(*a*)] showed not only a decrease in the intensity but also a change in the relative intensity of the emission maxima (at 410 and 429 nm).

A high concentration (20 μg ml^{-1}) of IPyA showed, before irradiation, a $\lambda_{max.}$ at 451 nm and a shoulder at 402 nm, the latter increasing during irradiation. However, only the 402-nm peak was observed when the concentration was decreased to 1 μg ml^{-1}.

Effect of Sulphuric Acid Concentration

At first, on increasing the H_2SO_4 concentration from 9.0 to 17.0 N, the fluorescence signal increases until a maximum or a plateau is reached. Table 2 shows the concentrations or concentration ranges where the best signal is attained. Fig. 4 shows some of the curves obtained. For the fluorophores obtained from IAA, IPA, IPyA, 5-HIAA and IAAEE, where a plateau or almost a plateau is observed, the choice of the H_2SO_4 concentration is much more easily made.

Effect of Oxygen

From the abnormal behaviour observed with IBA, where less reproducible results were found after UV irradiation, it was concluded that previous aeration was necessary to produce reproducible results, which also resulted in an increase in the fluorescence intensity (Fig. 4E and E′). Similar results were observed when IPA and ILA were tested, the most striking effect being observed with IPA, Fig. 4, which shows the curves obtained with IPA, ILA and IBA in the presence of oxygen (curves B, D and E) and after deaeration with nitrogen, suggest that the photochemical reaction envolved is probably a photo-oxidation. Similar experiments with IAA (where UV irradiation is not needed) showed that deaeration also decreased the fluorescence signal. From these observations it is recommended that the mixture is stirred in the presence of air during the reaction.

Stability of the Fluorophore

The fluorophore resulting from the reaction of IAA with OPA proved to be stable at 0 °C for at least 24 h. At room temperature, however, the stability decreases to *ca.* 1 h. The products of photoreaction of IPA, IBA, and ILA are stable

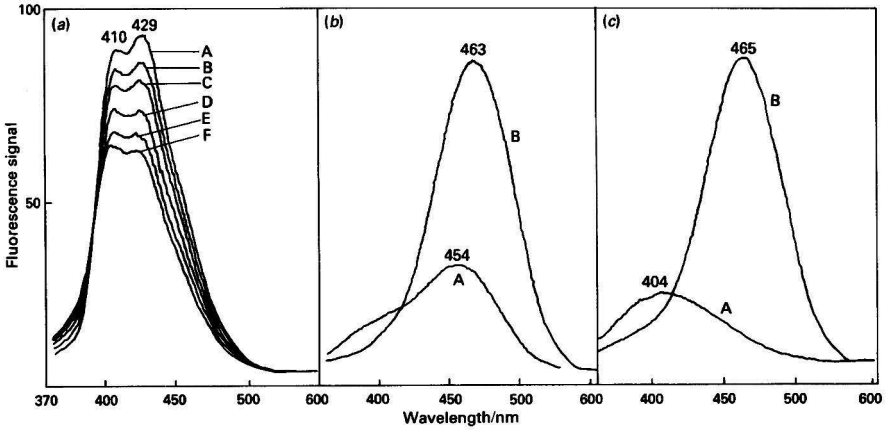

Fig. 2. Effect of irradiation on the fluorescence spectra of the fluorophores obtained after reaction with OPA. (*a*) IAA for A, 4; B, 13; C, 25; D, 30; E, 40; and F, 50 min of irradiation. (*b*) ILA. (*c*) IBA for A, immediate reading; and B, after 10 min of irradiation

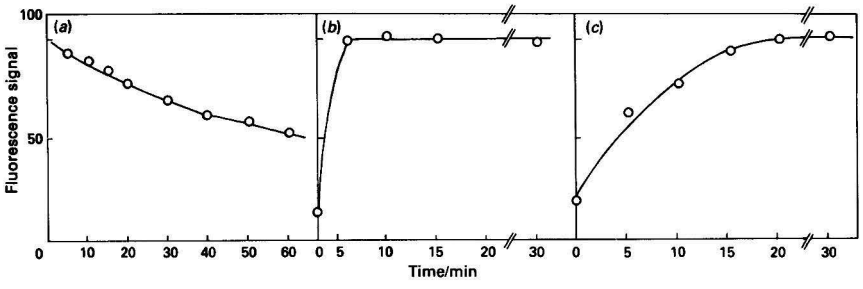

Fig. 3. Effect of irradiation time on the fluorescence signal intensity of the fluorophores. (*a*) IAA; (*b*) ILA; and (*c*) IBA. The readings at time zero were taken at 407 nm (ILA) or 404 nm (IBA) and the others at 463 nm (ILA) or 465 nm (IBA)

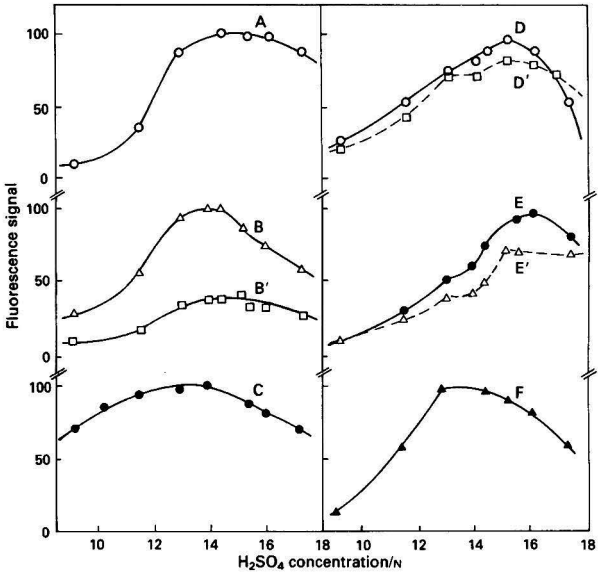

Fig. 4. Effect of H_2SO_4 concentration and oxygen on the fluorescence signal. A, IAA; B, IPA (in the presence of oxygen); B', as B but deaerated; C, IPyA; D, ILA; (D', deaerated); E, IBA; (E' deaerated); and F, 5-HIAA. All experiments used a final concentration of 1 μg ml^{-1}

for 24 h at 0 °C. Fig. 5 shows some of the results obtained with the compounds studied at 0 °C. The fluorophore from 5-HIAA is stable during the first hour, the signal decreasing by 10% after 24 h; 5-MIAA is relatively stable for *ca.* 30 min, with a decrease of 5% in 1 h and 10% in 24 h.

Analytical Figures of Merit

Tables 2 and 3 and Figs. 6–8 show the results obtained using the Zeiss assembly and the laboratory-assembled spectrofluorimeter.

The excitation and emission spectra of the fluorescent reaction product of IAA with OPA differ from the other spectra (Fig. 6). The excitation spectrum is characterised by one shoulder at 353 nm and three peaks (at 293, 372 and 390 nm). In the emission spectrum two distinct peaks (at 410 and 429 nm) can be observed. The excitation spectral characteristics of this fluorophore also show that there is a reasonable coincidence with the excitation lines utilised (365–366 nm) in the Zeiss fluorimeter. The fluorescent products obtained from IPA [Fig. 7(*b*)] ILA, IBA, 5-MIAA and 5-HIAA exhibit an $\lambda_{max.}$ of excitation partially coincident with the 365-nm excitation wavelength. However, the IAAEE - OPA fluorophore shows an excitation maximum distant from 365 nm, although it has a shoulder at 363 nm. In general, the excitation using the system employing a mercury-vapour discharge lamp and a 365-nm filter, which are frequently found in filter fluorimeters and viewing boxes, can be utilised.

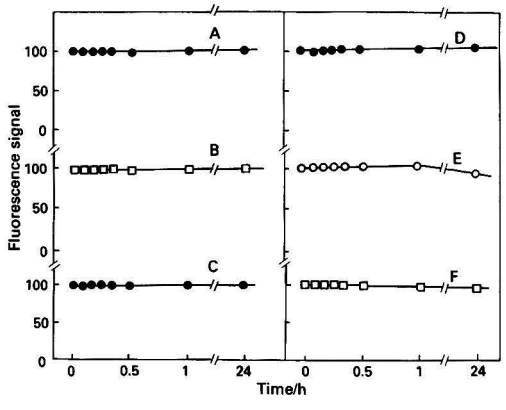

Fig. 5. Stability of the fluorophores at 0 °C. A, IAA; B, IPA, C, IBA; D, ILA; E, 5-HIAA; and F, 5-MIAA

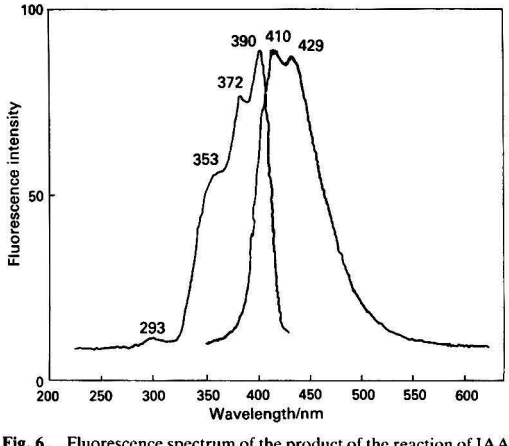

Fig. 6. Fluorescence spectrum of the product of the reaction of IAA with OPA

During the determination of the limits of detection (analyte signal equals twice the blank signal, following the equation proposed by Komesu and Thompson[30] during a study of OPA as a fluorimetric reagent for the determination of serotonin), we observed that, mostly when UV irradiation improved the signal, by reducing the OPA concentration to 0.05 from 0.15%, the blank signal suffers a reduction of 75% (after irradiation for 30 min). With the compounds for which the UV treatment is not of interest, changes in the OPA concentration do not affect the blank signal. This blank signal is still small compared with the blanks found after UV irradiation. As a consequence, to improve the limit of detection, a concentration of 0.05% *m/V* of OPA was used. This reduction also produced a slight increase in the linear range (on the high concentration side) of IBA, IPA and ILA. Table 2 shows that the best limits of detection found are with IAA, 5-HIAA and 5-MIAA. The high limits of detection observed with IPA, ILA and IBA are considered to be due to the increase in the background signal, as explained before.

The detection limit found with IAA (2.3 ng ml^{-1}) is smaller than those found by Yamamato *et al.*[31] when the α-pyrone method (20 ng ml^{-1}), or the method that employs formaldehyde as a fluorimetric reagent (90 ng ml^{-1}), were independently examined. However, when the α-pyrone method was first suggested by Stoessl and Venis,[6] an absolute limit of detection of 1 ng was found. Lower limits of detection of 5-HIAA have been reported in the literature (0.1 ng ml^{-1}) after reaction with OPA - cysteine in the presence of 18 N H_2SO_4. In our work, better limits of detection can be expected if further studies in this direction were to be made, decreasing

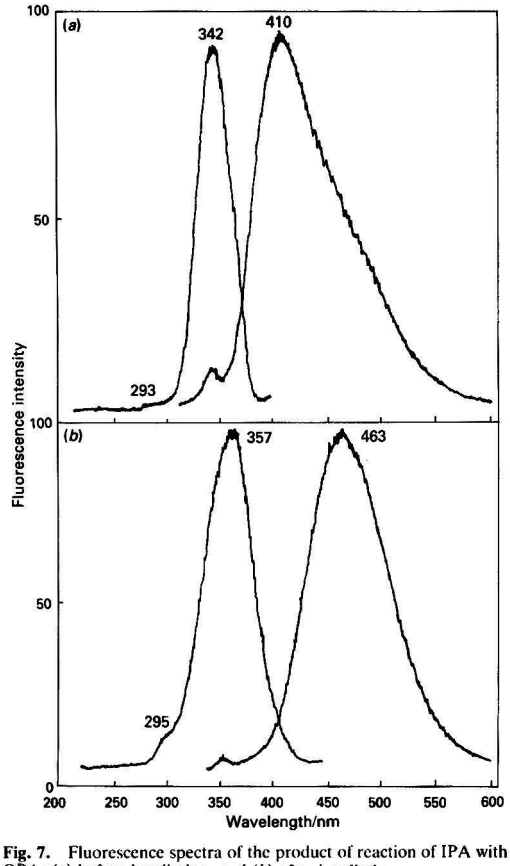

Fig. 7. Fluorescence spectra of the product of reaction of IPA with OPA: (*a*) before irradiation; and (*b*) after irradiation

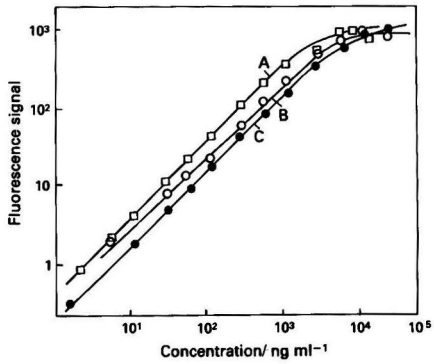

Fig. 8. Fluorescence analytical calibration graphs of some of the compounds examined. A, 5-HIAA; B, IBA; and C, IAA. Concentrations refer to final reaction mixture concentrations. The relative intensities of the graphs were arbitrarily adjusted

the background or with the use of microcells. The linear ranges are usually approximately three decades, with the exception of IPyA and IAAEE. The relative standard deviation is *ca.* 30% at low concentrations and *ca.* 3% at high concentrations.

Reaction with Other Compounds

Further qualitative experiments were made in order to examine whether the OPA - sulphuric acid reagent reacts with other compounds. A reaction was observed with the methyl ester of IAA (using an H_2SO_4 concentration of 14 N), resulting in a fluorophore with a $\lambda_{max.}$ of excitation at 333 nm and a $\lambda_{max.}$ of emission at 401 nm. 5-Hydroxytryptamine and tryptophan also reacted, giving a $\lambda_{max.}$ of emission at 478 and 463 nm, respectively. Although the tryptophan - OPA fluorophore was affected by UV irradiation, with a shift in the $\lambda_{max.}$ to 470 nm and an increase in the signal intensity, the 5-hydroxytryptamine fluorophore was not affected. Indole, neither alone nor in the presence of acetic acid, reacted with OPA - sulphuric acid in the preliminary experiments attempted. Ammonia seemed not to react also.

Some attempts were also made to examine the effect of 2-mercaptoethanol (2-ME) in the reaction of the compounds examined with OPA in H_2SO_4. Using the optimum H_2SO_4 concentration and other parameters previously established, all eight compounds were tested in the presence of 0.0075% *V/V* 2-ME. Using IAA, IBA and IAAEE as analytes, quenching was observed; no variation was detected with IPyA or ILA. Although with 5-HIAA and 5-MIAA an increase in the signal was detected, the limit of detection showed no statistically significant difference in comparison with the limits found in the absence of 2-ME. Further studies to investigate the effect of 2-ME more deeply would be of interest.

Application of the Method

Based on the previous findings, it can be seen that the present method is non-specific, a preliminary separation being necessary if a mixture of indol-3-yl acids or other interfering compounds is present. Compared with the α-pyrone method, where no reaction was observed with ILA, IPA or IPyA, the present method shows a positive signal for these compounds. The OPA - H_2SO_4 reagent seems to be appropriate as a TLC spray reagent and has been tested as such.[32] Possibly it could be used as an HPLC post-reaction reagent, using a photochemical reactor, to enhance the signal.

Despite this problem of non-specificity, we examined the utilisation of the OPA - H_2SO_4 reagent in the determination of IBA in two commercial phytohormones (Seradix and Stim-Root). We found, by direct comparison with a calibration graph, contents of 0.070 ± 0.003% and 0.022 ± 0.002% (*m/m*, dry basis), respectively. By the standard additions method, however, values of 0.090 ± 0.004% and 0.026 ± 0.002%, respectively, were found, suggesting that a quencher was present, principally in the first sample. As no other method for the determination of IBA was found in the literature examined, it was not possible to determine the accuracy of the present method.

The authors thank O. O. S. Campos, C. C. Fortes and H. J. Monteiro for useful discussions and cooperation and F. B. Barreto and E. F. Lima for technical assistance throughout the work. They also thank S. G. de Lima for linguistic advice.

References

1. Mandava, N. B., *Editor*, "Plant Growth Substances," ACS Series III, American Chemical Society, Washington, DC, 1979.
2. Kefeli, V. I., "Natural Plant Growth Inhibitors and Phytohormones," Dr. W. Tank Publ., Boston, MA, 1978.
3. Armstrong, M. D., Shaw, K. N. F., Gontatowski, M. J., and Singer, H., *J. Biol. Chem.*, 1958, **232**, 17.
4. Byrd, D. J., Kachen, W., Idzko, D., and Knorr, E., *J. Chromatogr.*, 1974, **94**, 85.
5. Hoskins, J. A., and Pollit, R. J., *J. Chromatogr.*, 1975, **109**, 436.
6. Stoessl, A., and Venis, M. A., *Anal. Biochem.*, 1970, **34**, 344.
7. Mousdale, D. M. A., Butcher, D. N., and Powell, R. G., "Isolation of Plant Growth Substances," Cambridge University Press, Cambridge, 1978.
8. Reeve, D. R., and Crozier, A., *in* MacMillan, J., *Editor*, "Encyclopedia of Plant Physiology," New Series, Vol. 9, Springer-Verlag, Berlin, 1980, p. 203.
9. Roth, M., *Anal. Chem.*, 1971, **43**, 880.
10. Roth, M., and Hampai, A., *J. Chromatogr.*, 1973, **83**, 533.
11. Edvinsson, L., Håkanson, R., Rönnberg, A. L., and Sundler, F., *J. Chromatogr.*, 1972, **67**, 81.
12. Viets, J. W., Deen, W. M., Troy, J. L., and Brenner, B. M., *Anal. Biochem.*, 1978, **88**, 513.
13. Lee, K. S., and Drescher, D. G., *Int. J. Biochem.*, 1978, **9**, 457.
14. Miller, J. N., and Thakrar, H., *Anal. Chim. Acta*, 1981, **124**, 221.
15. Carroll, S. F., and Nelson, D. R., *Anal. Biochem.*, 1979, **98**, 190.
16. Håkanson, R., and Rönnberg, A. L., *Anal. Biochem.*, 1974, **60**, 560.
17. Kremzer, L. T., *Anal. Biochem.*, 1966, **15**, 270.
18. Cohn, V. H., and Lyle, J., *Anal. Biochem.*, 1966, **14**, 434.
19. Amano, T., and Mizukami, S., *Yakugaku Zasshi*, 1965, **85**, 1035.
20. Danielson, N., and Conroy, C. M., *Talanta*, 1982, **29**, 401.
21. Sawicki, E., and Johnson, H., *Anal. Chim. Acta*, 1966, **34**, 381.
22. Maickel, R. P., and Miller, F. P., *Anal. Chem.*, 1966, **38**, 1937.
23. Miller, F. P., and Maickell, R. P., *Life Sci.*, 1970, **9**, 747.
24. Garnier, J. P., Bosquet, B., and Dreux, C., *Analusis*, 1979, **7**, 355.
25. Szabó, A., and Karácsony, E. M., *J. Chromatogr.*, 1980, **193**, 500.
26. Pacha, W. L., *Experientia*, 1969, **25**, 802.
27. Knapp, D. R., "Handbook of Analytical Derivatization Reactions," Wiley-Interscience, New York, 1979. p. 21.
28. Pourchet, C. J., "The Aldrich Library of Infrared Spectra," Aldrich, Milwaukee, WI, 1970.
29. West, T. S., "Complexometry with EDTA and Related Reagents," Third Edition, BDH Chemicals, Poole, 1969.
30. Komesu, N., and Thompson, J. H., *Eur. J. Pharmacol.*, 1971, **16**, 248.
31. Yamamoto, D., Tsukada, M., and Segawa, T., *Bunseki Kagaku*, 1975, **24**, 663.
32. de Lima, C. G., and Pastore, T. C. M., to be published.

Paper A3/231
Received July 21st, 1983
Accepted October 4th, 1983

Fluorimetric Semiautomatic Catalytic Titrations

A. Moreno, M. Silva, D. Perez-Bendito and M. Valcárcel*
Department of Analytical Chemistry, Faculty of Sciences, University of Córdoba, Córdoba, Spain

The fluorimetric control of semiautomatic catalytic titrations is described. The influence of several variables on the instrumental titration is established. A set of tests is proposed for evaluating the reliability of the device. This technique has been applied to the direct determination of EDTA ($1.25–3.75 \times 10^{-5}$ M, relative error 1.4%), which acts as an inhibitor of the oxidation of 2-hydroxybenzaldehyde thiosemicarbazone by hydrogen peroxide catalysed by iron(III). Methods are also described for the indirect catalytic titrations of iron(III) and alkaline-earth metal ions at parts per million levels (accuracy *ca.* 1%).

Keywords: *EDTA direct catalytic titration; iron and alkaline-earth metal ions indirect catalytic titration; 2-hydroxybenzaldehyde thiosemicarbazone; fluorimetric semiautomatic catalytic titration*

Catalytic titrations have been used for the determination of metallic ions, ligands and organic acids. The first paper on the possibility of using catalytic reactions for end-point indication was published by Yatsimirskii and Fedorova[1] and the use of inhibition reactions in catalytic titrations was reviewed by Mottola[2] and Hadjiioannou.[3] Weisz and Pantel[4] discussed the theoretical aspects of this application of catalytic titrations. These reactions have been followed by various methods: by visual means, spectrometry, amperometry, potentiometry, constant-current potentiometry and thermometry. In this work, fluorimetric control has proved to be very suitable for semiautomatic catalytic titrations.

Continuing our previous investigations [5–7] on the possibilities of using thiosemicarbazones in catalytic titrations, in this paper the direct catalytic titration of EDTA and the indirect determination of iron(III) and alkaline-earth metal ions are described. The oxidation of 2-hydroxybenzaldehyde thiosemicarbazone (HBTS) by hydrogen peroxide in the presence of ammonia is the indicator reaction, which is catalysed by the initial excess of the titrant (Fe^{3+}). Although iron(III) is a common catalyst in kinetic analysis, this is the first time that it has been used as a titrant in catalytic titrations.

Experimental

Reagents

All solvents and reagents used were of analytical-reagent grade.

2-Hydroxybenzaldehyde thiosemicarbazone solution, 0.03% *m/V in ethanol*. This product was synthesised according to the Sah and Daniels procedure.[8]

EDTA solution 0.1 M. This solution was prepared from the dihydrated disodium salt dissolved in distilled water, and standardised potentiometrically. More dilute solutions (5×10^{-4} M) were prepared immediately before use.

Standard iron solution, 1.000 mg ml^{-1}. This solution was prepared from 1.000 g of pure iron dissolved in 50 ml of nitric acid (1 + 1 *V/V*) and diluted to exactly 1 l with distilled water. Solutions of lower concentrations were prepared by appropriate dilution.

Standard calcium(II), magnesium(II), strontium(II) and barium(II) solutions, 1.000 mg ml^{-1}. These solutions were prepared from the carbonate salts and standardised by titration with EDTA,[9] except calcium carbonate, which is a primary standard.

Apparatus

A diagram of the complete instrumentation for carrying out the fluorimetric semiautomatic catalytic titrations is presented in Fig. 1. A fluorescence spectrophotometer (Perkin-Elmer 650-10S) equipped with a thermostat was used for kinetic measurements. All measurements were performed in the spectrofluorimeter with sensitivity ×0.3 and excitation and emission slits of 6 nm. Rectangular or cylindrical quartz titration vessels with the following characteristics were used: rectangular cell, made of Herasil quartz with dimensions 100 × 40 × 40 mm and a volume of *ca.* 100 ml; cylindrical vessel, made of Heralux quartz with a height of 100 mm, an external diameter of 40 mm and a volume of *ca.* 80 ml; both cells had their sides optically polished. The thermostated sample compartment is made of stainless steel. These accessories were designed by us in order to couple them with the spectrofluorimeter. A Mettler DL40 MemoTitrator, which is an independently operating, microprocessor-controlled compact instrument equipped with high-capacity storage facilities, stored the titration methods. As shown in Fig. 1, this instrument is the controller of the instrumental variables in the catalytic titrations. Other instrumentation consisted of a fan stirrer, the speed of which is measured by an electrical revolution sensor (IKA-TRON DZM1) in the range 5–500 rev min^{-1}, a Mettler GA14 compact recorder with a measuring range of 50–5 000 mV and a chart drive between 1.6 and 20 mm ml^{-1} when a 10-ml burette is used and a Mettler GA40 thermal printer with a capacity of 20 characters per line.

Performance Check Procedure

In order to test the reliability of the system, a semiautomatic acid - base titration with fluorimetric end-point indication was carried out, in which hydrochloric acid was titrated with sodium hydroxide using the 2-hydroxybenzaldehyde thiosemicarbazone itself as a fluorimetric indicator. Ordinary titrations by fluorimetric control can be carried out by this approach. Both titration vessels (rectangular and cylindrical) produce similar results (titration curves with a 90° slope change at the end-point and an accuracy of 0.6%), but the rectangular cell can be recommended because of its higher volume and easier handling.

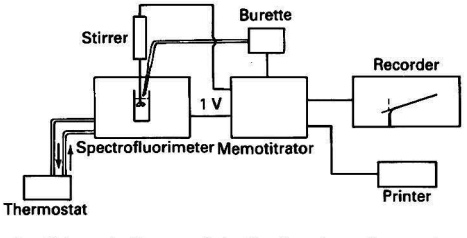

Fig. 1. Schematic diagram of the fluorimetric semiautomatic catalytic titration instrumentation

* To whom correspondence should be addressed.

Procedures

Direct semiautomatic catalytic titration of EDTA

In a 100-ml titration vessel place a mixture containing 370–1100 μg of EDTA, 2 ml of 0.03% *m/V* HBTS solution in ethanol, 2 ml of 1% *V/V* hydrogen peroxide solution, 1 ml of 4.32 M ammonia solution, 14 ml of ethanol and 1.6 ml of 2.5 M potassium chloride solution and dilute to *ca.* 80 ml with distilled water. All reagents must be pre-heated at 45 °C before mixing. Transfer the titration vessel into the thermostated sample compartment and wait 2 min before the titration in order for the required temperature (45 °C) to be reached. Stir this solution for 5 s and start the titration with 20 μg ml^{-1} Fe titrant solution (the titrant is at room temperature) at a rate of addition of 2 ml min^{-1}. The stirring speed is fixed at 115 rev min^{-1} and the autocontrol system at position 3. The chart width is adjusted to 10 mm ml^{-1} and the initial fluorescence is fixed at 15%. From the titration curve (fluorescence intensity as a function of titrant volume), the end-point of the semiautomatic catalytic titration is determined graphically from the intersection of straight-line extrapolations before and after the equivalence point.

Indirect semiautomatic titration of metal ions

To a solution containing 20–70 μg of iron or 20–100 μg of calcium(II), 20–100 μg of magnesium(II), 20–140 μg of strontium(II) and 20–100 μg of barium(II) ions in a 100-ml titration vessel, add a suitable volume of 5×10^{-4} M EDTA solution and process as described under *Direct semiautomatic catalytic titration of EDTA*. By mean of these back-titrations the metal ion content in the sample can be calculated from the excess of the aminopolycarboxylic acid.

Results and Discussion

Fluorimetric Semiautomatic Catalytic Titrations

Ammoniacal solutions of 2-hydroxybenzaldehyde thiosemicarbazone show a green fluorescence (λ_{ex} = 380 nm, λ_{em} = 480 nm) and can be easily oxidised to a product with an intense blue fluorescence (λ_{ex} = 365 nm, λ_{em} = 440 nm) by the action of hydrogen peroxide in the presence of manganese(II) or iron(III), which act as catalysts in this indicator reaction. These catalysed reactions have been used to determine submicrogram amounts of manganese[10] and iron.[11]

In the study of interferences in the kinetic determination of iron, aminopolycarboxylic acids such as EDTA and 1,2-diaminocyclohexanetetraacetic acid (DCTA) had an inhibitory effect on this reaction owing to the formation of stable complexes with iron(III). These effects can be advantageously applied to the direct determination of these aminopolycarboxylic acids by means of fluorimetric semiautomatic catalytic titrations. In this work, two reasons were taken into account in selecting the direct catalytic determination of EDTA: its higher inhibitory effect and the frequency with which this complexone is used in catalytic titrations.

As the volume of catalytic titrant added that is required to start the indicator reaction is proportional to the amount of inhibitor present, this titration can be performed. A sharp change in the fluorescence intensity due to the reaction

$$HBTS_{red} + H_2O_2 \xrightarrow[NH_3]{Fe^{3+}} HBTS_{ox}$$

permits the titration of microgram amounts of EDTA with iron(III) and catalytic end-point indication. The agreement between equivalence-point and end-point depends on several factors, such as instrumental and chemical variables, which must be fixed and studied in order to obtain more accurate and reproducible titration curves.

Influence of chemical variables

Instrumental variables were adjusted during the course of this study so that the chemical variables affect only the development of the titration curves. Further, in all experiments 3 ml of 5×10^{-4} M EDTA solution were added to the titration vessel, which corresponds to 3.72 ml of 30 μg ml^{-1} Fe at the end-point.

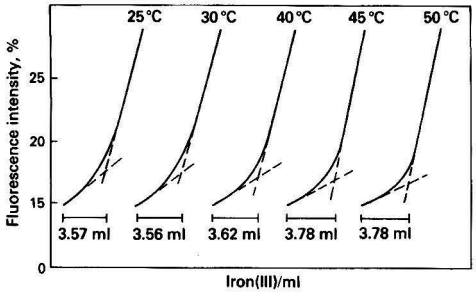

Fig. 2. Catalytic titration curves for 744.48 μg of EDTA titrated with 30 μg ml^{-1} of Fe at different temperatures. Conditions: 2 ml of 0.03% HBTS solution, 2 ml of 1% *V/V* hydrogen peroxide solution and 1 ml of 4.32 M ammonia solution. Theoretical end-point, 3.72 ml

The influence of temperature on the titration curves was studied in the range 25–50 °C. As can be observed in Fig. 2, temperatures lower than 40 °C give negative errors, and this behaviour could be assigned to the substoicheiometric formation of the Fe - EDTA complex. A temperature of 45 °C was chosen for the experimental measurements. However, in this study another consideration must be taken into account: the method of adjusting the temperature. Although a thermostated sample compartment was used, owing to the greater volume of the titration vessel (100 ml) 15 min are necessary in order to reach the required temperature. Therefore, in the experimental procedure all reagents are brought to the working temperature first and then mixed, the waiting time then being only 2 min.

The effects of the most important chemical variables are summarised in Figs. 3 and 4. A maximum or an inflection point corresponds to a suitable value of the variable being studied. The chosen concentrations agree with those given in the procedure. Two other points should be explained. The influence of pH was studied by addition of an appropriate volume of sodium hydroxide solution or hydrochloric acid and the ammonia concentration was kept constant (1 ml of 4.32 M ammonia solution) in all experiments. On the other hand, the titrated solutions exhibit a slightly reddish brown colour, which can be ascribed to the formation of an Fe - EDTA - peroxo complex according to the studies carried out by Cheng and Lott.[12]

Other variables were also studied. A final volume between 70 and 90 ml does not appreciably affect the performance of the method. The lowest concentration of iron(III) catalyst giving accurate and reproducible results was investigated as shown in Table 1; several volumes of 5×10^{-4} M EDTA solution (2–6 ml) were titrated with standard iron(III) solutions. The optimum concentration range for the titrant was between 20 and 30 μg ml^{-1} of iron (error less than ± 2%). A catalyst titrant of concentration 20 μg ml^{-1} Fe was chosen.

Influence of instrumental variables

The rate of addition of the titrant and the autocontrol system are the variables that have the greatest effects on the titration curves. The rate of addition of the titrant was studied in the range 1–5 ml min^{-1}, as shown in Fig. 5(*a*). Satisfactory results were obtained with a rate of addition of iron(III) solution of 2 ml min^{-1} (average error ±1%); at higher flow-rates the error was increased. According to the Fig. 5(*b*), the use of the autocontrol system is recommended. The most accurate results are obtained when this system is fixed at a position in the range 3–4. Position 3 was chosen because the titration is carried out more quickly.

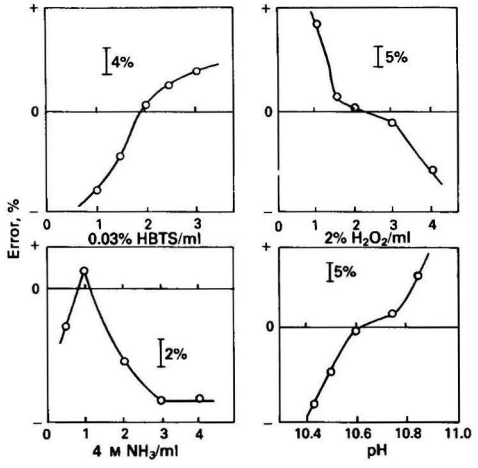

Fig. 3. Choice of the most important chemical variables in the direct catalytic titration of EDTA. In all instances the EDTA concentration is 2.5×10^{-5} M and the samples were titrated with a standard 30 p.p.m. Fe(III) solution

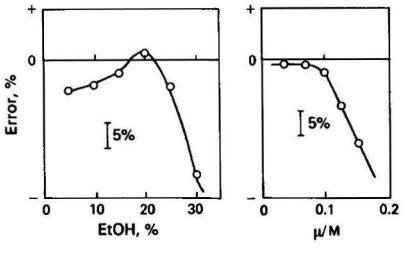

Fig. 4. Influence of the percentage of ethanol and ionic strength on the accuracy on the titration curves. The EDTA and titrant concentrations are as given in Fig. 3

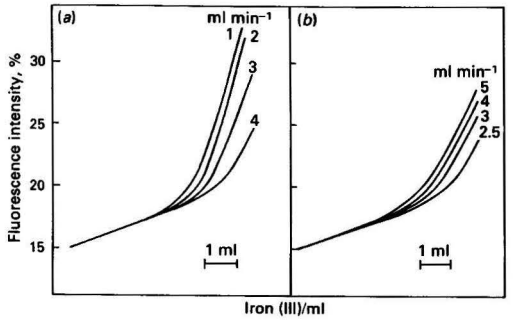

Fig. 5. Titration curves for EDTA according to the procedure. (*a*) Effect of titrant addition rate and (*b*) influence of autocontrol. 3 ml of 5×10^{-4} M EDTA solution equivalent to 4.19 ml of 20 μg ml^{-1} Fe solution

Table 1. Influence of catalytic titrant concentration on titration curves

Iron(III) titrant/ μg ml^{-1}	5×10^{-4} M EDTA added/ml	Theoretical end-point/ ml	Experimental end-point/ ml	Error, %	Average error, %
15	2.0	3.72	3.50	−5.98	−5.98
			3.50	−5.98	
20	3.0	4.19	4.20	0.48	−1.02
			4.20	0.48	
			4.10	−2.12	
30	4.0	3.72	3.72	0.00	−1.87
			3.77	1.25	
			3.63	−2.50	
40	6.0	4.19	4.40	5.01	4.42
			4.35	3.84	

Table 2. Microgram titration of EDTA by catalytic end-point indication. Titrant: 20 μg ml^{-1} Fe solution

EDTA taken/ μg	EDTA found/μg		Accuracy, %	
	Method A*	Method B*	Method A*	Method B*
372	380	369	2.1	−0.8
465	460	465	−1.2	0.0
558	566	573	1.5 (0.51)†	2.6 (0.47)†
651	633	688	−2.8	3.6
744	740	746	−0.6	0.2
838	847	861	1.1	2.7
931	940	936	1.0	0.6
1 024	1 040	1 031	1.6	0.7
1 117	1 126	1 133	0.9	1.5
		Average:	1.4	1.4

* Method A, proportional method; method B, calibration graph method.

† Relative standard deviation in parentheses ($n = 11$).

Table 3. Tolerance limits in the determination of 1.87×10^{-5} M of EDTA

Molar ratio, [ion]: [EDTA]	Ions tolerated
1	IO_4^-, DCTA, DTPA
2	$P_2O_7^{4-}$, citrate, EGTA, SCN^-, $S_2O_8^{2-}$
5	Br^-, ClO_4^-
10	F^-, tartrate, CO_3^{2-}, SO_4^{2-}, $B_4O_7^{2-}$
25	$S_2O_3^{2-}$, $C_2O_4^{2-}$, acetate, I^-, NO_3^-

Table 4. Determination of iron(III) by reversed catalytic titration against EDTA: 5 ml of 5×10^{-4} M solution, equivalent to 0.139 mg of Fe, applied

Fe(III) taken/ μg	Fe(III) found/μg		Accuracy, %	
	Method A*	Method B*	Method A*	Method B*
20.0	20.6	20.3	3.1	1.7
30.0	29.6	29.4	−1.3	−2.2
40.0	39.6	39.3	−1.0	−1.8
50.0	48.6	48.3	−2.8 (0.82)†	−3.4 (0.85)†
60.0	59.6	59.5	−0.6	−0.8
70.0	71.2	72.0	−2.0	−2.9
		Average:	1.8	2.1

* Method A, proportional method; Method B, calibration graph method.

† Relative standard deviation in parentheses ($n = 11$).

Other instrumental variables were tested. The stirring speed (65–145 rev min^{-1}), the optimum volume of titrant that can be added without causing dilution error (3–9 ml) and the initial relative fluorescence intensity (10–20%) did not noticeably affect the titration curves. Further, the chart width was studied on two scales, 10 and 20 mm ml^{-1}, for different concentrations of EDTA. Both scales gave similar errors when the volume of titrant (20 μg ml^{-1} Fe) was higher than 3 ml, but for smaller values a chart width of 20 mm ml^{-1} gave rise to a better performance (average error *ca.* ± 2.5%).

Direct Catalytic Determination of EDTA

Under the optimum conditions used, two methods are proposed for the fluorimetric semiautomatic catalytic titration of EDTA. In the first, the proportional method, the experimental data for the samples are compared with those obtained when a standard EDTA solution is used, and in the second, the calibration graph method, the EDTA content in the sample is obtained from a calibration graph in which the molar concentrations or micrograms of EDTA are plotted against the final volumes of titrant. The results obtained for EDTA solutions of known concentration by both methods are shown in Table 2. In both instances amounts of EDTA in the range 370–1 100 μg ($1.25–3.75 \times 10^{-5}$ M) can be determined with a relative error of 1.4%. The mean values of results from 11 samples each containing 558.36 μg (1.87×10^{-5} M) gave a relative standard deviation of the method of 0.5%.

EDTA (1.87×10^{-5} M) was determined in the presence of various amounts of foreign anions. The tolerance limits up to a 25-fold molar excess are shown in Table 3. Other polyaminocarboxylic acids such as DCTA, ethylene glycol bis(β-aminoethyl ether)-*N,N,N'N'*-tetraacetic acid (EGTA) and diethylenetriaminepentaacetic acid (DTPA) do not cause interferences in the direct catalytic determination of EDTA. Metallic ions that react with EDTA must be absent.

Indirect Titration of Metal Ions

The indirect titration most closely related with this determination is the reverse catalytic titration of the catalyst. Thus, iron(III) can be determined by titrating the excess of a known amount of EDTA added to the titration vessel. The results of this study are shown in Table 4.

Other ions can be determined by this back-titration. For this purpose two conditions are necessary: these ions must not show catalytic activity towards the indicator reaction and they must complex with EDTA in the reaction medium with a conditional formation constant higher than that for iron(III) in order to avoid displacement reactions. In these instances, a known amount of the ligand is added and the excess is back-titrated with standard iron(III) solution. The proportional and the calibration graph methods can be used. The results obtained for the analysis of alkaline-earth metal ions for this method are shown in Table 5 and it can be seen that

Table 5. Fluorimetric semiautomatic indirect catalytic titration results for aqueous alkaline-earth metal ion solutions. Titrant, 20 μg ml^{-1} iron(III) solution

5×10^{-4} M EDTA taken/ml	Metal ion	Metal ion taken/μg	Metal ion found/μg		Accuracy, %	
			Method A*	Method B*	Method A*	Method B*
6	Ca(II)	20.0	19.7	20.0	−1.4	0.2
		30.0	29.5	29.1	−1.8	−1.7
		40.0	41.3	41.6	3.2	4.1
		50.0	49.9	50.1	−0.3	0.1
		60.0	59.9	60.7	−0.1	1.2
		70.0	70.0	71.1	0.0 (0.70)†	1.6 (0.80)†
		80.0	79.6	81.0	−0.5	1.2
		90.0	89.4	90.8	−0.7	0.9
		100.0	95.1	96.5	−4.9	−3.5
				Average:	1.4	1.6
6	Mg(II)	20.0	20.3	20.1	1.3	0.3
		30.0	30.3	29.9	0.9 (1.19)†	−0.5 (1.23)†
		40.0	39.8	40.3	−0.4	0.6
		50.0	49.4	49.5	−1.2	−1.0
		60.0	59.0	59.3	−1.7	−1.2
10		70.0	69.8	69.5	−0.4	−0.7
		80.0	78.9	79.1	−1.4	−1.1
		90.0	90.2	89.8	0.2	0.3
		100.0	100.2	99.3	0.2	0.8
				Average:	0.9	0.7
3	Sr(II)	20.0	20.0	20.5	−0.2	2.5
		40.0	38.9	39.3	−2.7 (1.19)†	−1.9 (1.42)†
		60.0	60.9	59.6	1.5	−0.7
4		80.0	81.2	79.1	1.5	−1.1
		100.0	98.9	99.3	−1.6	−0.8
6		120.0	118.6	119.0	−1.2	−0.8
		140.0	139.0	139.3	−0.7	−0.7
				Average:	1.3	1.2
3	Ba(II)	20.0	20.2	19.8	0.9	−1.3
		40.0	38.9	39.0	−2.8 (1.76)†	−2.5 (0.92)†
		60.0	58.5	58.5	−2.5	−2.5
		80.0	80.7	81.3	−0.8	1.6
		100.0	97.9	99.0	−2.1	−1.0
				Average:	1.8	1.8

* Method A, proportional method; method B, calibration graph method.
† Relative standard deviation in parentheses ($n = 11$).

these ions can be determined with high sensitivity (below the 1 p.p.m. level) with a relative standard deviation of *ca.* 0.5%.

This work was financed with the support of a grant given by CAICYT to project No. 0248.

References

1. Yatsimirskii, K. B., and Fedorova, T. I., *Proc. Acad. Sci. USSR*, 1962, **143**, 143.
2. Mottola, H. A., *Talanta*, 1969, **16**, 1267.
3. Hadjiioannou, T. P., *Rev. Anal. Chem.*, 1976, **3**, 82.
4. Weisz, H., and Pantel, S., *Anal. Chim. Acta*, 1972, **62**, 361.
5. Ternero, M., Pino, F., Perez-Bendito, D., and Valcarcel, M., *Anal. Chim. Acta*, 1979, **109**, 401.
6. Ternero, M., Perez-Bendito, D., and Valcarcel, M., *Microchem. J.*, 1981, **26**, 61.
7. Raya-Saro, T., and Perez-Bendito, D., *Analyst*, 1983, **108**, 857.
8. Sah, P. P. T., and Daniels, T. C., *Recl. Trav. Chim. Pays-Bas*, 1950, **49**, 1545.
9. Schwarzenbach, B., and Flaschka, H., "Complexometric Titrations," Methuen, London, 1969.
10. Moreno, A., Silva, M., Perez-Bendito, D., and Valcarcel, M., *Talanta*, 1983, **30**, 107.
11. Moreno, A., Silva, M., Perez-Bendito, D., and Valcarcel, M., *Anal. Chim. Acta.*, in the press.
12. Cheng, K. L., and Lott, P., *Anal. Chem.*, 1956, **28**, 462.

Paper A3/367
Received October 19th, 1983
Accepted November 28th, 1983

Improved Derivatisation Method for the Gas - Liquid Chromatographic Determination of the Herbicide Oryzalin*

Promode C. Bardalaye and Willis B. Wheeler
Pesticide Research Laboratory, Department of Food Science and Human Nutrition, University of Florida, Gainesville, FL 32611, USA

A rapid derivatisation method is described for the determination of the herbicide oryzalin. It involves the use of dimethylsulphinyl anion and methyl iodide or ethyl iodide. Gas - liquid chromatography is used with either an N - P or an electron-capture detector. The method was applied to the residue analysis of fortified sweet potatoes, soils and water. With an electron capture detector, residues as low as 0.01 μg g^{-1} in sweet potatoes and soils and 0.001 μg g^{-1} in water may be detected. For an N - P detector the limits of detection are 0.05 μg g^{-1} in sweet potatoes or soils and 0.005 μg g^{-1} in water. Recoveries ranged from 80–90% from these matrices at fortification levels of 0.08–0.5 μg g^{-1}. The choice of using either the methyl or the ethyl derivative is an added advantage.

Keywords: *Oryzalin; dimethylsulphinyl anion; alkyl iodide; gas - liquid chromatography; residues*

Oryzalin (trademark Surflan) (3,5-dinitro-N^4,N^4-dipropylsulphanilamide) (**I**) is a selective pre-emergent surface-applied herbicide for control of annual grasses and broadleaf weeds in soybeans, cotton, bearing and non-bearing fruit trees, nut trees, vineyards and established ornamentals.[1]

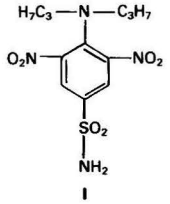

I

It has a solubility of *ca.* 2.5 μg g^{-1} and a low vapour pressure (*ca.* 1 × 10^{-7} mmHg at 30 °C).[2] Dinitroanilines are also strongly adsorbed[3] on to soil. Additionally, field losses of these types of chemicals can occur by sediment-water run off. It was claimed at one time that oryzalin caused birth defects[4] in children of male workers exposed to the chemical, although the implication could not be substantiated. All these factors necessitate information concerning its residue data in various plant and animal matrices and its pollution potential, *i.e.*, its fate in agricultural run off and other aquatic environments. A convenient method of residue analysis is, therefore, needed for oryzalin in different matrices. A high-performance liquid chromatographic method for its residue analysis in soil without derivatisation was described[5] with a limit of detection of 0.02 μg g^{-1}. A gas - liquid chromatographic method with a detection limit of 0.001 μg g^{-1} in water and limits ranging from 0.01 to 0.1 μg g^{-1} in various other substrates has also been reported.[6-8]

The currently used gas - liquid chromatographic determination of oryzalin involves alkylation of the herbicide, in the presence of sodium carbonate, followed by overnight incubation.[6-8] This derivatisation technique is long and time consuming, and hence the need for an alternative and faster derivatisation procedure is desirable.

In this work, the use of the strongly basic dimethylsulphinyl anion and methyl or ethyl iodide to prepare the *N*-alkylated derivative of oryzalin, for the gas - liquid chromatographic determination of the herbicide, is reported. The method was tested for residue determinations in water, soils and sweet potatoes.

* Florida Agricultural Experiment Station Journal Series No. 5192.

Experimental

Reagents

Solvents. Pesticide grade.

Dimethyl sulphoxide (DMSO). Analytical-reagent grade, purchased from Mallinckrodt, Inc., St. Louis, MO, USA.

Methyl iodide and ethyl iodide. Obtained from Eastman Chemical Products, Hauppauge, NY, USA.

Sodium hydride. Dry or 50% dispersion in mineral oil, purchased from Alfa Division, Ventron Corp., Danvers, MA, USA.

Oryzalin, 99.5%. Standard grade, obtained from EPA, USA.

Apparatus

A Hewlett-Packard Model 5840A gas chromatograph equipped with a ^{63}Ni electron-capture detector operating at 300 °C was used under the following conditions: glass column, 183 cm × 4 mm, packed with 1.95% QF-1 + 1.5% OV-17 on 80–100-mesh Gas-Chrom Q (Applied Science, PA, USA); oven and injector temperatures, 225 °C (or 3% OV-17 on the same kind of support at an oven temperature of 175 °C and injector temperature of 215 °C); carrier gas, argon - methane (95 + 5), flow-rate 60 ml min^{-1}; and attenuation 10^7– 10^{10}.

A Hewlett-Packard Model 5880A gas chromatograph equipped with an N - P detector operating at 300 °C was used under the following conditions: glass column, 183 cm × 2 mm, packed with 1.95% QF-1 + 1.5% OV-17 on 80–100-mesh Gas-Chrom Q; oven temperature, 225 °C; injector temperature, 225 °C; carrier gas, nitrogen, flow-rate 30 ml min^{-1}; hydrogen flow-rate, 5 ml min^{-1}; and air flow-rate, 50 ml min^{-1}. The voltage to the detector was adjusted for a current of 1.8 × 10^{-11} A or 10% of full-scale deflection at an attenuation of 2.[2]

Procedures

Preparation of dimethylsulphinyl anion[9-11]

Sodium hydride (2 g if it is dry and 4 g if it is a 50% dispersion in mineral oil) was taken in a 50-ml serum bottle, 20 ml of dry DMSO were added and the bottle was capped with a rubber-sleeve serum stopper with needle septum. An 18-gauge hypodermic needle was inserted into the cap to allow the escape of hydrogen gas evolved during the reaction. A rubber tube was used to connect the needle to a disposable glass pipette immersed in dry DMSO in a test-tube; the DMSO had been dried previously by storing over molecular sieves. The bottle was heated in a water-bath at 50 °C for *ca.*

6 h. This arrangement allows the escape of hydrogen by bubbling through DMSO and also prevents any moisture or air entering the bottle after the reaction is complete. After 6 h, the bottle was cooled to room temperature and allowed to stand for 4 h, but preferably overnight. The needle was withdrawn, and the dimethylsulphinyl anion was thus sealed in an atmosphere of hydrogen. Under such conditions, the solution may be stored frozen at 5 °C for many months and be brought to room temperature just before use. (**Caution**—Great care must be taken in handling the hydride and DMSO. Gloves and safety glasses should be worn to avoid contact with the skin or eyes when preparing this solution. A well ventilated hood should be used and the hydride should be kept away from heat and water to avoid explosion. There have been reports of violent explosions when some laboratories used very large amounts of hydride and DMSO. A severe accident was recently reported.[12])

Fortification procedure

Representative samples (25 g) of tap water, sweet potatoes (previously chopped) and soil samples were fortified with known volumes of stock or working standard solutions of oryzalin in benzene to give a 0.08–0.5 μg g^{-1} concentration of herbicide. Sweet potatoes and soil samples were not dried but were weighed as they were. The fortified samples were mechanically shaken and allowed to stand for 1 h before extraction. The entire contents were extracted without any sub-sampling. All fortification levels were replicated three times with each substrate. (**Caution**—Benzene is highly toxic and appropriate precautions should be taken.)

Preparation of samples

Soils. A representative 25-g soil sample taken in a Mason jar was blended with 200 ml of methanol using an Omni-mixer. The supernatant was filtered by suction or decanted. The crude extract was transferred into a separating funnel containing 100 ml of dichloromethane and 50 ml of 5% sodium chloride and the mixture shaken. After separation the dichloromethane layer was retained, and the aqueous layer was re-extracted with two 50-ml portions of dichloromethane. The combined dichloromethane extracts were dried by using anhydrous sodium sulphate. The solution was concentrated to *ca.* 50 ml with the aid of a rotary evaporator at 30 °C. The solution was transferred, in small portions, into a 20-ml serum bottle containing 0.5–1 ml of DMSO as keeper and dichloromethane was completely removed by rotary evaporation at 30 °C, using a reducing adapter at the rotary evaporator and a short polyethylene tube, one end of which was sleeved over the ground-glass joint of the adapter and the other end sleeved over the neck of the serum bottle. Final trace amounts of moisture, if any, were removed by vacuum desiccation over phosphorus(V) oxide and the serum bottle was tightly capped with a rubber-sleeve serum stopper.

Sweet potatoes. A representative 25-g chopped sample was extracted with 100 ml of methanol using a Polytron homogeniser for 1 min at medium speed. The crude extract was filtered by suction and concentrated to *ca.* 20 ml. The concentrated crude extract was shaken with 80 ml of 5% sodium chloride in a separating funnel. The extract container was washed with 20 ml of methanol and the washings were added to the separating funnel. The aqueous methanol mixture was washed twice with 30-ml portions of hexane, and the hexane washes were discarded. The pH of the aqueous methanol was brought to 12 by adding 1.0 M sodium hydroxide solution. The aqueous methanol layer was again washed with 30 ml of dichloromethane and the wash was discarded. Saturated boric acid solution (*ca.* 40 ml) was added to the aqueous methanol portion to give a pH of 8–9. The mixture was extracted twice with 40 ml of dichloromethane and the resulting extract was dried by using anhydrous sodium sulphate. Dichloromethane was finally evaporated off in the presence of 0.5–1 ml of dry DMSO using the technique described for the soil samples.

Water. Representative 25-ml samples of tap water were extracted with 80 ml of benzene - methanol (3 + 1 *V/V*) using a Polytron homogeniser for 2 min at medium speed. A larger sample size and correspondingly larger volumes of solvents could be used depending on the limits of detection desired. The mixture was transferred into a separating funnel. The water layer was discarded and the benzene layer was dried by slowly dripping through anhydrous sodium sulphate. Benzene was then evaporated off in the presence of 0.5–1 ml of dry DMSO, as keeper, using the technique described for soil samples.

Derivatisation

The serum bottle containing the sample was flushed with nitrogen by inserting two hypodermic needles, one for introducing nitrogen and the other for venting, and the needles were then withdrawn. A multifit syringe, fitted with an 18-gauge needle was flushed with nitrogen and was filled with a few millilitres of dimethylsulphinyl anion solution. An aliquot of 0.5–1 ml of the dimethylsulphinyl anion solution was added to the sample by injection through the septum of the bottle. It was placed in an ultrasonic bath for *ca.* 1 min to gradually liquefy the gel produced on addition of the anion and until an homogeneous, viscous solution was formed. The reaction, giving an amine base solution, is completed within 10–15 min.

For the alkylation reaction, the amine base solution was cooled in an ice - water bath and 3 ml of methyl iodide (or ethyl iodide) were added at such a rate that the temperature of the reaction mixture did not rise above 25 °C. This was done by inserting the needle of the syringe filled with alkyl iodide through the septum and another needle to act as a vent. The following arrangements proved very convenient for routine analysis: alkyl iodide was drawn into a 10-ml multifit B–D syringe fitted with a 23-gauge × 2.5 cm long needle bent into a right or obtuse angle. The syringe was clamped horizontally and the needle was inserted into the cap of the serum bottle so that the bottle could rest hinged to the needle in a vertical or tilted position, while being dipped up to its neck into a beaker of ice - water. The plunger of the syringe was pushed slowly, by means of a threaded metal nut, on to a screw clamped and positioned right against the plunger. During addition of the reagent, the bottle was lightly shaken, by tapping, to facilitate mixing. The needles were then withdrawn and the contents were allowed to stand for *ca.* 20 min at room temperature.

At this stage 10 ml of hexane were added, the contents were well shaken by hand for 1 min and allowed to stand. After 10–15 min, 5–10 ml of water were slowly added to destroy any residual hydride and the contents were well shaken. The layers were allowed to separate, and the organic layer was filtered through Whatman No. 1 phase-separating paper. Alkyl iodide was removed by gently flushing with nitrogen and residual DMSO was removed by washing the resulting organic phase with water. Finally, the hexane or benzene volume was adjusted to the desired volume. For analysis 1 or 5 μl were injected into the gas chromatograph.

Results and Discussion

Oryzalin cannot be quantitatively determined directly by gas chromatography even under a wide range of operating conditions. The problem is probably due to the high polarity and hydrogen-bonding potential of the sulphonamide group. When oryzalin is derivatised to its dimethylated product excellent chromatographic properties are exhibited. Alkylation of compounds having an NH_2– or NH= function using a base and methyl iodide has been reported[13,14] by a number of workers using different procedures. The reaction depends on the initial removal of proton(s) from the nitrogen atom to

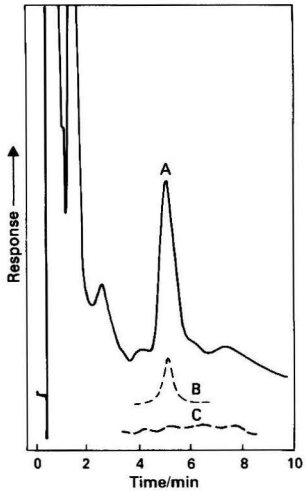

Fig. 1. Chromatogram of (A) derivatised extract from water (25 ml) fortified with 0.08 μg g^{-1} of oryzalin; (B) standard, corresponding to 0.05 ng of oryzalin determined as the dimethyl derivative; and (C) control. Conditions: electron-capture detector; glass column, 183 cm × 4 mm, packed with 3% OV-17 on Gas-Chrom Q, 80–100 mesh; oven temperature, 175 °C; injection, 1 μl per 10 ml

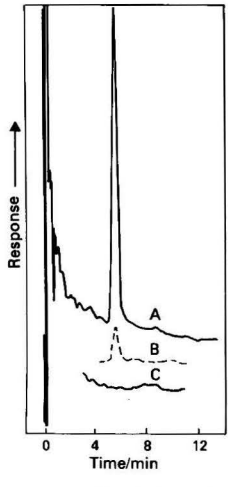

Fig. 2. Chromatogram of (A) derivatised extract from sweet potatoes (25 g) fortified with 0.16 μg g^{-1} of oryzalin; (B) standard corresponding to 0.20 ng of oryzalin determined as the dimethyl derivative; and (C) control. Conditions: N - P detector; glass column, 183 cm × 2 mm, packed with 1.95% QF-1 + 1.5% OV-17; oven temperature, 225 °C; injection, 5 μl per 10 ml

form the corresponding anion. The added alkylating reagent then reacts with the anion to yield the *N*-alkylated derivative. Any free base in the reaction mixture competes with the anion of the compound in question for the alkylating reagent. In the initial reaction, an equilibrium is established at a point dependent on the strength and concentration of the base. Rapid and complete conversion to the anion $-N^{2-}$ requires a base stronger than OH^-. In aqueous media no base stronger than OH^- can exist, as stronger bases react with water to form the OH^- ion. A non-aqueous medium, DMSO, and the very strongly basic dimethylsulphinyl carbanion are, therefore, used in this method and the reaction is carried out under moisture-free conditions.

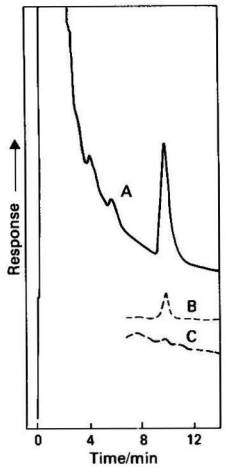

Fig. 3. Chromatogram of (A) derivatised extract from soil (25 g) fortified with 0.2 μg g^{-1} of oryzalin; (B) standard corresponding to 0.45 ng of oryzalin determined as the dimethyl derivative; and (C) control. Conditions: electron-capture detector; glass column, 183 cm × 4 mm, packed with 1.95% QF-1 + 1.5% OV-17; oven temperature, 225 °C; injection 5 μl per 10 ml

The equilibrium in this reaction lies almost completely in the direction of $-N^{2-}$ formation. The competing reaction between the excess of dimethylsulphinyl anion and alkyl iodide does not interfere as long as the alkyl iodide is added in excess of the total base. The time required to carry out the derivatisation reaction in this method is about 15 min, compared with the overnight incubation time in the currently used method, employing sodium carbonate. The dimethylsulphinyl anion requires overnight preparation, and enough caution and a certain amount of laboratory bench expertise are required to handle the explosive NaH and DMSO. But once prepared, the anion can be stored in a sealed vial at 5 °C for many months without affecting its stability. Once the anion is available, the over-all advantage in terms of efficiency and rapidity of analysis time more than offsets the initial efforts involved. The choice of derivatising to dimethyl oryzalin by using methyl iodide or to diethyl oryzalin by using ethyl iodide is also an added advantage because the two derivatives have different retention times. This property can be used to circumvent possible interference in certain environmental matrices, and/or to obtain simple confirmation of identity.

The method was applied to oryzalin residue analysis in soils, water and sweet potatoes. With an electron-capture detector, the limit of detection was found to be 0.01 μg g^{-1} in sweet potatoes and soils and 0.001 μg g^{-1} in water. Using an N - P detector the limits of detection were 0.05 μg g^{-1} in sweet potatoes or soils and 0.005 μg g^{-1} in water. Although in terms of sensitivity electron-capture detection is the better, unless DMSO is removed almost to dryness, a huge interfering signal is obtained along with the solvent front. However, no real interference from DMSO is observed when an N - P detector is used for analysis.

Fig. 1 shows the chromatogram of water fortified with oryzalin at a level of 0.08 μg g^{-1}; Fig. 2 is the chromatogram of sweet potatoes at a fortification of 0.16 μg g^{-1}; and Fig. 3 is that of soils at a fortification of 0.2 μg g^{-1}. These chromatograms are the results of extraction, clean-up and GLC analysis of the herbicide derivatised to the dimethylated product. The recoveries ranged from 80 to 90% at fortification levels of from 0.08 to 0.5 μg g^{-1}.

Conclusion

An efficient and rapid method is presented for residue analysis of oryzalin in soils, water and sweet potatoes using the dimethylsulphinyl anion and alkyl iodide.

References

1. Berg, G. L., *Editor,* "Farm Chemicals Handbook," Meister Publishing Co., Wiloughby, OH, 1983, p. 225.
2. Probst, G. W., Golab, T., and Wright, W. L. *in* Kearney, P. C., Kaufman, D. D., *Editors,* "Herbicides," Volume 1, Marcel Dekker, New York, 1975, p. 453.
3. Helling, C. S., *J. Environ. Qual.,* 1976, **5**, 1.
4. Dickson, D., *Nature* (*London*), 1979, **282**, 220.
5. Macy, T. D., and Loh, A., *Anal. Chem.,* 1980, **52**, 1381.
6. Sieck, R. F., Johnson, W. S., Cockerill, A. F., Mallen, D. N. B., Osborne, D. J., and Barton, S. J., *J. Agric. Food Chem.*, 1976, **24**, 617.
7. Smith, S., and Willis, G. H., *J. Agric. Food Chem.,* 1978, **26**, 1473.
8. "Pesticide Analytical Manual," Volume II, Food and Drug Administration, Washington, DC, 1977, Section 180.304.
9. Bardalaye, P. C., Thompson, N. P., and Carlson, D. A., *J. Assoc. Off. Anal. Chem.,* 1980, **63**, 511.
10. Conrad, H. E., *Methods Carbohydr. Chem.*, 1972, **6**, 361, and references cited therein.
11. Lindberg, B., *Methods Enzymol.*, 1972, **28**, 178.
12. Le Noble, W. J., *Chem. Eng. News,* 1983, **61**, 2.
13. Lawrence, J. F., and Laver, G. W., *J. Agric. Food Chem.,* 1975, **23**, 1106.
14. Glad, G., Popoff, T., and Theander, O., *J. Chromatogr. Sci.,* 1978, **16**, 118.

Paper A3/210
Received July 7th, 1983
Accepted October 25th, 1983

Comparison of Detectors for the Determination of Curcumin in Turmeric by High-performance Liquid Chromatography

Roger M. Smith and Barbara A. Witowska
Department of Chemistry, Loughborough University of Technology, Loughborough, Leicestershire, LE11 3TU, UK

The use of ultraviolet spectrophotometric and electrochemical detectors for the determination of curcumin from turmeric powder is compared. The retention indices of the major constituents in different eluents are reported; a solvent extraction procedure has been developed to reduce separation times.

Keywords: Curcuma longa; *turmeric; curcumin determination; liquid chromatography; electrochemical detection*

Turmeric (*Curcuma domestica* Val. Syn. *C. longa* Koenig *non* L.) is a widely used spice from the Zingiberaceae family indigeneous to Southern Asia. The mature rhizomes are ground to give an aromatic yellow powder, employed as a colouring ingredient of curry powder, in folk medicine and as an insect repellant. Its production and chemistry have recently been reviewed by Govindarajan.[1] The main yellow pigment (0.5–6.0%) is curcumin [1,7-bis-(4′-hydroxy-3′-methoxyphenyl)hepta-1,6-diene-3,5-dione, **I**], which is accompanied by two related minor curcuminoids, demethoxycurcumin (**II**) and bisdemethoxycurcumin (**III**), and a number of sesquiterpenes including turmerone (**IV**) and *ar*-turmerone (**V**).

The principal criterion of the commercial value of the spice is its colour and a number of methods of assay have been described.[1,2] Most of these are based on colorimetry, sometimes involving pre-separation by thin-layer chromatography or extraction. Recently, a high-performance liquid chromatographic (HPLC) method using ultraviolet spectrophotometric detection has been reported, but the chromatogram was complex and each sample required over 40 min for complete elution.[3]

This paper describes studies carried out to improve the separation conditions for curcumin and to avoid interferences from other constituents by using an electrochemical detector to give increased selectivity. The analysis times were reduced by changing the sample preparation procedure. While this work was being prepared for publication, an alternative HPLC analysis using fluorimetric detection and an amino-bonded silica column was reported.[4]

Experimental

Apparatus

Liquid chromatography was carried out using a Pye Unicam XPS pump and a PU4020 variable wavelength detector and a Kipp Analytical Model 9205 electrochemical detector. The samples were injected using a Rheodyne 7125 valve on to a 25 cm × 5 mm i.d. column packed with 5-μm ODS-Hypersil (Shandon Southern Ltd., Runcorn) and the signals were analysed using a Hewlett-Packard 3390 integrator. GC - MS was carried out using a 0.5-mm CP-SIL5 column at 150 °C in an Erba Science 4200 chromatograph coupled to a Kratos MS-80 mass spectrometer.

Reagents and Standards

Turmeric. Commercial samples from Schwartz.

Curcumin. Sigma London Chemical Co., Poole, Dorset.

Methanol, acetonitrile and tetrahydrofuran. HPLC grade from Fisons Scientific Apparatus, Loughborough.

Buffers. Analytical-reagent grade chemicals.

Procedure

Powdered turmeric (0.1 g) was mixed with light petroleum (boiling range 40–60 °C) (10 ml) and allowed to stand overnight. The solvent was discarded and the powder was extracted overnight with methanol (10 ml) at room temperature. Samples (10 μl) of the methanolic extract were injected on to the HPLC column. The curcumin was determined using coupled ultraviolet (254 nm) and electrochemical (+0.8 V *vs.* Ag - AgCl) detectors by comparison with standard samples of curcumin.

Results and Discussion

Although electrochemical detectors have been widely used in liquid chromatography for the detection of catecholamines, few applications have been reported in which relatively non-polar compounds have been examined. Following an earlier study of the determination of the gingerols in ginger,[5] it appeared that electrochemical detection could also be a suitable method for curcuminoids. Its high selectivity could be an important advantage as it would reduce the necessity for the pre-separation of closely eluting interfering substances before analysis.

Commercial samples of ground dried turmeric were extracted overnight with methanol at room temperature, which had been found to give complete extraction of the curcuminoids.[3] The pale yellow extracts were then examined directly by HPLC. Elution with acetonitrile - water (60 + 40) was unsatisfactory because the peaks tailed badly. In the earlier study of turmeric, acetic acid had been added to suppress ionisation,[3] but it was decided to use a phosphate buffer (pH 4.4) in this study as it would also act as the supporting electrolyte for the electrochemical detector.

The chromatogram obtained using an ultraviolet detector at 254 nm and acetonitrile - buffer (pH 4.4) (60 + 40) as eluent was very similar to that reported earlier.[3] In addition to a major peak ($k' = 2.25$), which could be identified as curcumin by comparison with an authentic sample, there were two minor peaks with similar retention times ($k' = 1.93$ and 2.09), which were also present in the standard. On examination using an electrochemical detector at 0.8 V *vs.* Ag - AgCl, curcumin and the two closely related minor peaks responded in both the extract and curcumin standard, suggesting that they were probably the minor curcuminoids (**II** and **III**). In the turmeric extract they were more prominent than in the standard and the ratio was similar to the composition reported by other workers.[1] The turmeric extract also contained three major peaks with much longer retention times ($k' = 11.09$, 17.33 and 17.86). However, these were electrochemically inactive.

Although these later peaks did not interfere with the determination, their presence prolonged the over-all analysis time. It was found that they could be selectively removed by washing the powder with light petroleum (boiling range 40–60

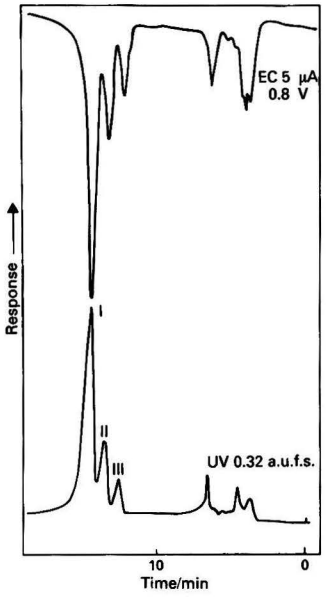

Fig. 1. HPLC separation of curcumin and minor curcuminoids using acetonitrile - buffer (pH 4.4) (50 + 50) as eluent

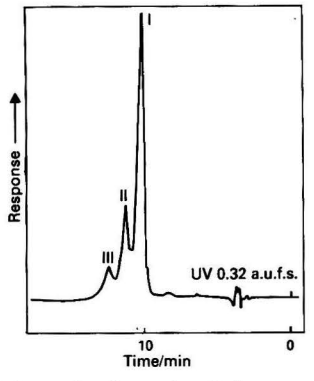

Fig. 2. HPLC separation of curcumin and minor curcuminoids using tetrahydrofuran - buffer (pH 4.4) (45 + 55) as eluent

°C) before the extraction of the curcuminoids. No curcumin was lost and significantly shorter analysis run times were required. Examination of the light petroleum extract by GC - MS showed the presence of three major components (retention times 14.0, 14.1 and 16.25 min). The mass spectra of the first and largest peak corresponded to *ar*-turmerone (**V**, M^+, m/z 216).[6] The other two compounds were isomeric (M^+, m/z 218) and the last peak is probably turmerone (**VI**).[6] The other isomer could be the recently reported curlone (**VII**).[7] However, authentic samples of these ketones were not available so it was not possible to compare them on HPLC with the extract.

Eluent Selection

In the absence of the ketones the separation of the curcuminoids could be improved by using acetonitrile - buffer (50 + 50) as the eluent (Fig. 1). Because there was still a small overlap between the curcuminoid peaks, it was decided to examine alternative eluents with similar over-all polarity. With methanol - buffer (70 + 30), all three curcuminoids were eluted as a single unresolved peak. This system could have the advantage of giving a single peak when total curcuminoid content was required in quality control. In contrast, elution of the extracts with tetrahydrofuran - buffer (45 + 55) caused the curcuminoids to be eluted in the reverse order to acetonitrile - buffer. This separation was very suitable for spectrophotometric determination as the tailing of the peaks did not interfere as significantly with quantification (Fig. 2). However, the tetrahydrofuran was incompatible with the electrochemical detector as it attacked the cell spacers and gave a high background current at greater than +0.7 V.

Table 1. Capacity factors of curcuminoids on liquid chromatography

Compound	Capacity factors in different solvents* MeCN - buffer (60 + 40)	MeOH - buffer (70 + 30)	THF - buffer (45 + 55)
I	2.25	5.0	3.38
II	2.09	5.0	3.75
III	1.93	5.0	4.14

* Buffer: 0.05 M phosphate (pH 4.4).

Table 2. Retention indices* of curcuminoids and retention standards in different eluents

Compound	Eluent† MeCN - buffer (60 + 40)	MeOH - buffer (70 + 30)	THF - buffer (45 + 55)
I	941	1098	969
II	920	1098	996
III	898	1098	1022
Retention standards—			
Toluene	1018	1042	1085
Nitrobenzene	866	856	911
2-Phenylethanol	674	782	713
p-Cresol	755	804	867

* Defined in references 9, 11 and 12.
† Buffer: 0.05 M phosphate (pH 4.4).

The capacity factors (k') of the curcuminoids in the three eluents were compared (Table 1). It has been suggested that because of the difficulty in measuring accurate values for the column void volume, t_0, capacity factors may not be a suitable parameter for reporting retentions that are intended as standard methods.[8] Alternative systems using retention indices that are virtually independent of small errors in t_0 or in eluent composition have been proposed, based on either the alkylaryl ketones[9] or alkan-2-ones.[10] It has also been proposed that by using a set of standard compounds the over-all separation system can be defined in a similar manner to the use of Rohrschneider constants in GLC. The indices of the standards can also be used to compare different columns or eluent systems.[11,12]

This method was applied to the present study and, by using four alkyl aryl ketones (acetophenone–valerophenone) as index standards, the retention indices of curcumin, the minor curcuminoids and the reference standards (nitrobenzene, toluene, 2-phenylethanol and *p*-cresol) were determined (Table 2). The identification of the curcuminoids could only be tentative but was based on the progression of structural features and the reported composition of turmeric. The differences between the retention indices of the standards in the three eluents reflects the markedly different interactions that are present. Although all three curcuminoids are phenolic, the different methoxy substitution presumably alters the intermolecular hydrogen bonding and causes the reversal of the elution order in different eluents.

Table 3. Calibration graphs for curcumin using ultraviolet and electrochemical detectors. Eluent: MeCN - buffer (pH 4) (60 + 40)

	Detector response: peak height/mm	
Standard curcumin/ mg l^{-1}	Ultraviolet: 254 nm, 0.04 a.u.f.s.	Electrochemical: 0.8 V, 5 μA
41.92	168	203
31.44	127	155
20.96	81	101
15.72	64	77
10.48	46	56
5.24	25	32
Correlation coefficient	0.999	0.999
Slope	3.90	4.70
Intercept	3.40	5.52

Table 4. Determination of curcumin in turmeric powder using different detectors. Eluent: MeCN - buffer (pH 4.4) (60 + 40)

	Curcumin concentration, %	
	Ultraviolet detection	Electrochemical detection
	4.64	4.22
	4.58	4.58
	4.54	4.58
Mean:	4.59	4.46

Comparison of Detectors

Although it had been hoped to compare the ultraviolet and electrochemical detectors in all three eluent systems, the electrochemical detector cell was incompatible with tetrahydrofuran and no separation of the curcuminoids occurred with the methanol eluent. The comparison was therefore restricted to the acetonitrile - buffer (60 + 40) system. The response of both detectors was linear over the range 0–40 mg l^{-1} (Table 3). However, if higher concentrations were examined the surface of the electrode in the electrochemical detector was apparently inactivated by the reaction products and the response became irreproducible. Similar problems were also observed in the earlier study of the gingerols.[5]

At the concentration level at which the electrochemical detector was giving a linear response, the ultraviolet detector was near to the limit of its sensitivity (0.02 a.u.f.s.). However, the electrochemical detector could have been operated at a much higher sensitivity and would therefore be the method of choice if sample sizes were restricted or if the test was being carried out on food samples in which curcumin was a minor flavouring component.

The calibration graphs were used to determine the curcumin content of triplicate extracts of turmeric powder (Table 4). The results of the different detection methods were comparable. The calculations were based on the assumption that the standard curcumin was pure. As a result, because the proportions of the minor components of the standard curcumin were unknown, the reported concentrations of curcumin will be slightly over-estimated. For accurate studies a pure standard would be required. It was noted that the minor constituents gave a similar relative response in both detectors. However, in a recent study using an amino-silica column the responses were markedly different.[4]

As curcumin fluoresces in acetonitrile solution, an attempt was made to detect it in the aqueous acetonitrile - buffer eluent using a fluorescence detector ($\lambda_{exc.}$ 420 nm, $\lambda_{em.}$ 508 nm) but it was unsuccessful. The solvent used is clearly important as ethanol has been reported to give satisfactory results.[4]

Conclusion

The two methods of detection gave comparable results for the quantitative analysis of turmeric. The increased selectivity of the electrochemical detector was not needed as little interference occurred with the ultraviolet detector, although it might be advantageous if more complex food samples were being studied at low curcumin concentrations.

References

1. Govindarajan, V. S., *CRC Crit. Rev. Food Sci. Nutr.*, 1980, **12**, 199.
2. Salzer, U.-J., *Int. Flavours Food Addit.*, 1975, **6**, 206.
3. Asakawa, N., Tsuno, M., Hattori, T., Ueyama, M., Shinoda, A., Miyake, Y., and Kagei, K., *Yakugaku Zasshi*, 1981, **101**, 374.
4. Tonnesen, H. H., and Karlsen, J., *J. Chromatogr.*, 1983, **259**, 367.
5. Smith, R. M., *Chromatographia*, 1982, **16**, 155.
6. Su, H. C. F., Horvat, R., Jilani, G., *J. Agric. Food Chem.*, 1980, **30**, 290.
7. Kiso, Y., Susuki, Y., Oshima, Y., and Hikino, H., *Phytochemistry*, 1983, **22**, 596.
8. Krstulovic, A. M., Colin, H., and Guiochon, G., *Anal. Chem.*, 1982, **54**, 2438.
9. Smith, R. M., *J. Chromatogr.*, 1982, **236**, 313.
10. Baker, J. K., and Ma, C.-Y., *J. Chromatogr.*, 1979, **169**, 107.
11. Smith, R. M., *J. Chromatogr.*, 1982, **236**, 321.
12. Smith, R. M., *Anal. Chem.*, in the press.

Paper A3/267
Received August 12th, 1983
Accepted October 3rd, 1983

Chlorogenic Acid Composition of Instant Coffees

Luiz C. Trugo and Robert Macrae
Department of Food Science, University of Reading, London Road, Reading, RG1 5AQ, UK

A method, based on high-performance liquid chromatography, is described for the determination of chlorogenic acid isomers in instant coffee. Identification of the individual components was assisted by the preparation of isomeric mixtures by the isomerisation of available compounds and quantification based on published ultraviolet molar absorptivities. A number of extraction and clearing techniques were studied to determine the optimum conditions for the recovery of all the isomers present. The developed method was applied to a wide range of commercially available instant coffees.

Keywords: *Chlorogenic acids; high-performance liquid chromatography; coffee*

The chlorogenic acid composition of coffee products is extremely complex with at least five major groups of compounds present: caffeoylquinic acids (CQA), dicaffeoylquinic acids (diCQA), feruloylquinic acids (FQA), *p*-coumaroylquinic acids (CoQA) and caffeoylferuloylquinic acids (CFQA).[1] The general structure of chlorogenic acids is shown in Fig. 1.

There are also a wide range of more minor chlorogenic acid components that have received little attention. Several attempts have been made to correlate (inversely) the levels of chlorogenic acids with beverage quality and to correlate specific sensory attributes, such as astringency, to the presence of specific chlorogenic isomers. There is little evidence in the literature to support these ideas but it is generally accepted that Arabica coffee, with a lower chlorogenic acid content, is superior to Robusta coffee.[1]

A significant loss of chlorogenic acids, in some instances up to 90%,[2] takes place on roasting. Additionally, the levels found in instant coffees will depend on the extraction conditions. These factors, coupled with a large difference between varieties, means that commercial instant coffees would be expected to vary widely in terms of chlorogenic acid composition. A number of methods have been described in the literature for the determination of chlorogenic acids in green, roasted and instant coffees. The simplest methods for analysis are based on ultraviolet absorption of alcoholic extracts[3] or colorimetry.[4] The former lacks specificity and the latter, even using differential colorimetric techniques, is subject to interferences and individual isomers cannot be determined.[1] Chromatographic techniques have greatly improved the precision of analytical data and, even though gas chromatography provides excellent resolution,[5] high-performance liquid chromatography (HPLC) is preferred, as it avoids the derivation step in the analysis.[6,7]

This paper presents an HPLC method for the determination of the nine main chlorogenic acids in a range of commercial instant coffees. Particular attention has been paid to extraction efficiency and the optimisation of chromatographic resolution, factors that have received only brief consideration in some published methods.

Experimental

Reagents

All reagents and solvents were of analytical-reagent grade unless otherwise specified.

Carrez solutions (clearing agent). Solution (I) was prepared by dissolving 21.9 g of crystallised zinc acetate, $Zn(C_2H_3O_2)_2.2H_2O$, and 3 ml of glacial acetic acid in distilled water and diluting to 100 ml. Solution (II) consisted of 10.6 g of potassium hexacyanoferrate(II) in 100 ml of distilled water.

Ammonia solution, approximately 4 M.

Hydrochloric acid, approximately 4 M.

Extraction solvents, aqueous methanol (40 and 70% V/V), aqueous propan-2-ol (70% V/V) and aqueous ethanol (70% V/V).

Chromatography solvents, tripotassium citrate ($K_3C_6H_5O_7.H_2O$), 0.01 M. Adjusted to pH 2.5 with dilute hydrochloric acid and HPLC-grade methanol.

Chlorogenic acid solutions. The IUPAC nomenclature[8] is used to name chlorogenic acid isomers. 5-Caffeoylquinic acid (commerically termed chlorogenic acid) was obtained from Sigma, UK.

5-Feruloylquinic acid solution, 1 mg ml^{-1}. Obtained from Dr. M. Clifford (University of Surrey).

Dicaffeoylquinic acid mixture (commercially termed isochlorogenic acid). Obtained from Roth, F.R.G.

Apparatus and Chromatographic Conditions

An Applied Chromatography Systems liquid chromatograph (two pumps, Model 750/03, and a programmer, Model 750/36) was used. Injection was achieved by means of a fixed-loop Rheodyne injection valve, Model 7120 (20 µl). A pre-column (50 × 5 mm i.d.) dry packed with coarse silica (70–150 µm) was placed in-line before the injection valve in order to saturate the mobile phase. A Spherisorb 5-ODS column (Phase Separations Ltd., UK, 250 × 5 mm i.d.) was used for the chromatographic separations. The final conditions used were a gradient of methanol (see Fig. 3) in 0.01 M tripotassium citrate solution (pH 2.5), increasing from 20 to 70% with 5-min linear segments of 0, 1, 1, 2, 1, 1, 2, 2 and 0% min^{-1} and a flow-rate of 1 ml min^{-1}. Peak integration was achieved by means of a Hewlett-Packard 3390-A integrator.

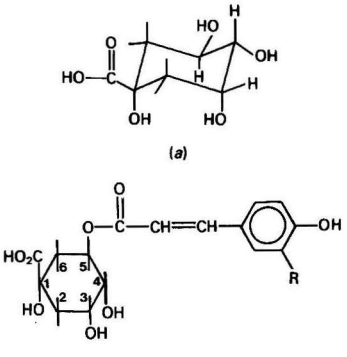

Fig. 1. Structure of chlorogenic acids. (*a*) D-(−)-Quinic acid. (*b*) R = H, 5-*p*-coumaroylquinic acid; R = OH, 5-caffeoylquinic acid; and R = OCH_3, 5-feruloylquinic acid. Esterification is also possible at carbon atoms 3 and 4 of the quinic acid

Procedure

Extraction

Finely ground instant coffee (0.5 g) was dissolved in 80 ml of an aqueous methanol solution (40%) and transferred into a 100-ml calibrated flask. Carrez solution (2 ml of each component) was added and the mixture was allowed to stand for 10 min after making up to volume. The precipitate was removed by filtration under gravity (using Whatman No. 1 filter-paper) and the filtrate was used directly for chromatography. For testing extraction efficiencies 70% *V/V* aqueous solutions of propan-2-ol, ethanol and methanol were also used.

Isomerisation of chlorogenic acids

5-Caffeoylquinic acid (200 mg) was dissolved in distilled water (20 ml) and the pH was adjusted to 8 with dilute ammonia solution. This solution was heated for 30 min in a boiling water-bath. The pH was then adjusted to 2.5–3.0 with dilute hydrochloric acid, after cooling to room temperature. For the preparation of feruloylquinic acid isomers, 20 μl of the standard solution of 5-feruloylquinic acid were added to 5 ml of water, adjusted to pH 8 with dilute ammonia solution and heated for 15 min in a boiling water-bath before being evaporated to dryness under reduced pressure and the residue dissolved in 0.1 ml of dilute hydrochloric acid. These solutions were then used directly for chromatography.

Quantification

Quantification was achieved by peak-area measurement and by comparison with a 5-caffeoylquinic acid standard. It was possible to quantify the individual isomers using their molar absorptivities, according to the equation

$$C = \frac{RF \times \varepsilon_1 \times M_{r_2} \times A}{\varepsilon_2 \times M_{r_1}}$$

where C is the concentration of the isomer in milligrams per millitre; RF is the response factor of 5-caffeoylquinic acid standard (concentration in milligrams per millilitre per unit area); ε_1 is the molar absorptivity of 5-caffeoylquinic acid; ε_2 is the molar absorptivity of the isomer in question; M_{r_1} is the relative molecular mass of 5-caffeoylquinic acid; M_{r_2} is the relative molecular mass of the isomer in question; and A is the area of the peak corresponding to the isomer in question.

Molar absorptivities ($\times 10^4$) are as follows: at $\lambda_{max.}$ 330 nm, 5-CQA = 1.95, 4-CQA = 1.80, 3-CQA = 1.84, 3,4-diCQA = 3.18, 3,5-diCQA = 3.16 and 4,5-diCQA = 3.32; and at $\lambda_{max.}$ 325 nm, 5-FQA = 1.93, 4-FQA = 1.95 and 3-FQA = 1.90 l mol^{-1} cm^{-1}.[9]

Calibration graphs were plotted using the CQA and diCQA isomer mixtures diluted at five different concentrations. These concentrations varied from 10 to 100 μg ml^{-1} in the CQA group and from 1 to 15 μg ml^{-1} in the diCQA group. Recoveries were checked by the method of standard additions. The levels of addition to the samples (in grams of isomer per 100 g of sample) were 3-CQA, 0.3–1.6; 4-CQA, 0.3–1.5; 5-CQA, 0.3–1.7; 3,4-diCQA, 0.1–0.8; 3,5-diCQA, 0.2–1.9; and 4,5-diCQA, 0.2–1.7. The samples (0.2 g) were dissolved in aqueous methanol (40%), spiked with the isomer solutions, cleared with Carrez reagent, made up to volume (100 ml) and filtered. The filtrates were used directly for chromatography.

Calibration and recovery data were not obtained for 5-feruloylquinic acid as only trace amounts of the material were available.

Results and Discussion

When only a total chlorogenic acid value is required the AOAC method,[10] based on differential ultraviolet absorption before and after precipitation of the chlorogenic acids, is adequate for quality control purposes. However, where the determination of individual components is required, HPLC provides the simplest method. With reference to the published HPLC methods[6,7] there appear to be three areas where improvements could be made (unambiguous peak assignment, greater chromatographic resolution and substantiation of the methods in terms of recovery and precision) and these aspects are addressed in this paper.

The problem of peak assignment is mainly due to the non-availability of chromatographic standards. 5-Caffeoylquinic acid and a mixture containing the three dicaffeoylquinic acids are available. This range of standards can be extended by isomerising the 5-caffeoylquinic acid to yield an equilibrium mixture of the 3-, 4- and 5-isomers. The normal isomerisation conditions consist of heating the chlorogenic acid, either in a phosphate buffer of pH 7–7.2[11] or in saturated sodium hydrogen carbonate solution.[12] However, a much cleaner reaction can be realised simply by heating the acid in dilute ammonia solution at pH 8. The rate of isomerisation can be readily followed by HPLC, the reaction being stopped by acidification after various intervals (Fig. 2). The graphs show clearly that one isomer is initially formed at a greater rate than the other and that the final concentrations are approximately equal. This is consistent with the isomerisation taking place via an intramolecular mechanism with the 4-isomer being formed first and subsequently isomerising to yield the 3-isomer. On this basis the isomer initially formed at the greater rate was assumed to be 4-CQA. This assignment is also supported by a consideration of the polarity of the structures (see Fig. 1). The 3-isomer contains two equatorial and one axial hydroxyl groups and the 4-isomer contains one equatorial and two axial hydroxyl groups, conferring greater polarity to the former.[13]

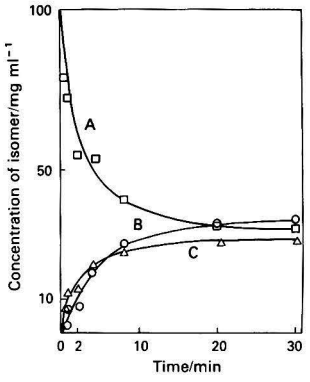

Fig. 2. Isomerisation of (A) chlorogenic acid (5-CQA) yielding (B) 3-CQA and (C) 4-CQA. Conditions as described in the text

Table 1. Recovery of chlorogenic acid isomers using HPLC. Average of five levels of addition for each isomer (values are in grams of isomer per 100 g of sample for wet matter)

Isomer	Range of addition, g per 100 g	Average recovery, %	Standard deviation, %
3-CQA	0.3–1.6	101.7	4.9
4-CQA	0.3–1.5	99.3	4.4
5-CQA	0.3–1.7	104.2	4.9
3,4-diCQA . .	0.1–0.8	99.9	3.6
3,5-diCQA . .	0.2–1.9	97.3	4.4
4,5-diCQA . .	0.2–1.7	97.8	5.6

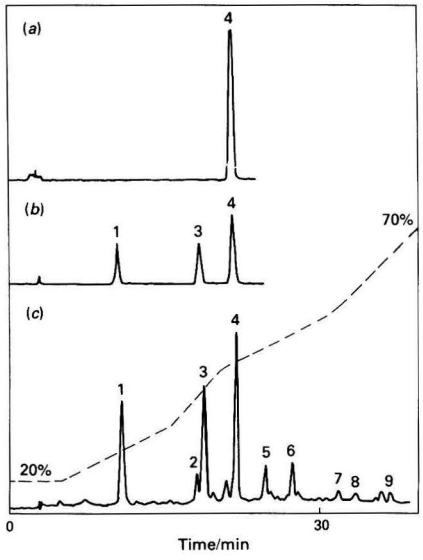

Fig. 3. Chromatograms of (*a*) chlorogenic acid standard, (*b*) CQA isomers mixture and (*c*) instant coffee using Spherisorb 5-ODS and gradient elution. (1) 3-CQA; (2) 3-FQA; (3) 4-CQA; (4) 5-CQA; (5) 4-FQA; (6) 5-FQA; (7) 3,4-diCQA; (8) 3,5-diCQA; and (9) 4,5-diCQA. Detection at 325 nm; flow-rate, 1 ml min^{-1}; and solvent and gradient conditions as described in the text

The same procedure was adopted with a sample of 5-feruloylquinic acid to allow the assignment of the peaks due to the 4- and 5-isomers. In each instance the coffee extracts were spiked with standards, or isomerised mixtures, to aid peak assignment.

Quantification of the isomers in the coffee samples was achieved by comparison of peak areas with a standard of 5-caffeoylquinic acid, allowing for differences in molar absorptivities between the isomer in question and the standard. Pure reference compounds were not available and thus the molar absorptivities could not be determined experimentally. Consequently literature values were used,[9] which were recorded at the $\lambda_{max.}$ values for each component. However, the $\lambda_{max.}$ values only varied from 325 to 330 nm and so by using a common detection wavelength (325 nm) only a very small error was introduced. From a study of the absorption spectrum of one isomer (5-CQA) this error was calculated to be about 1–1.5%, which is acceptable in terms of the over-all experimental accuracy.

The major source of error in HPLC methods such as these is not in the chromatographic stages but in the preceding extraction and clean-up procedures. A number of extraction systems were evaluated and of these, the following three produced good recoveries: (a) 70% propan-2-ol; (b) hot water (80 °C) followed by clearing with Carrez solution; and (c) 40% methanol followed by clearing with Carrez solution. System (a) produced a clean extract but the presence of propan-2-ol in the sample produced severe distortion of the chromatogram. With this system it is essential to evaporate the solvent and redissolve the residue in water or buffer solution prior to injection, a process that complicates the analytical scheme and may cause losses by oxidation. System (b) produced chromatograms with interfering peaks and showed losses of dicaffeoylquinic isomers, compared with systems (a) and (c). Consequently, system (c) was chosen for this study. The efficiency of this solvent system based on the recoveries of added amounts of CQA and diCQA isomers from one coffee sample is shown in Table 1.

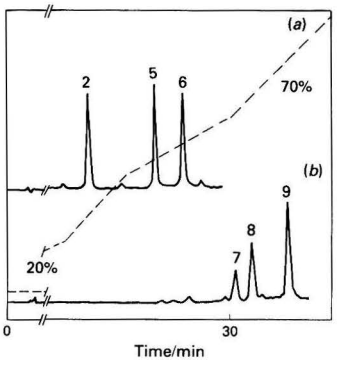

Fig. 4. Chromatograms of (*a*) FQA isomers mixture and (*b*) diCQA isomers mixture. Peaks as described in Fig. 3 and conditions as described in the text

Table 2. Coefficient of variation of chlorogenic acid isomers in an instant coffee by HPLC. Results obtained from six different extractions from the same sample (values are in grams of isomer per 100 g of sample for wet matter)

Isomer	Mean, g per 100 g	Coefficient of variation, %
3-CQA	1.49	0.8
4-CQA	1.67	1.2
5-CQA	2.12	1.0
3-FQA	0.27	2.5
4-FQA	0.37	3.0
5-FQA	0.52	3.0
3,4-diCQA ..	0.17	5.4
3,5-diCQA ..	0.12	4.0
4,5-diCQA ..	0.24	2.2

Linearity of the detection system was established over the concentration range expected from the samples, showing good correlation for all isomers studied (correlation coefficients: 5-CQA, 0.999 92; 4-CQA, 0.999 94; 3-CQA, 0.999 8; 3,4-diCQA, 0.999 5; 3,5-diCQA, 0.999 995; and 4,5-diCQA, 0.999 90). The major problem encountered with the chromatographic resolution was between the peaks due to 4-caffeoylquinic acid and 3-feruloylquinic acid, although with careful selection of the gradient and solvent conditions adequate resolution can be achieved. Chromatograms of standards, isomer mixtures and of instant coffee samples are shown in Figs. 3 and 4.

All determinations were carried out in duplicate and one sample was analysed six times to obtain an idea of the precision for each isomer and the results are shown in Table 2. The established method was then applied to the determination of chlorogenic acid isomers in 13 commercial instant coffees, with the results shown in Table 3. The major isomer in all the samples was 5-caffeoylquinic acid, accounting for about 30% of the total, whereas the sum of the caffeoylquinic isomers accounts for approximately 70%. Similarly, the feruloylquinic acid group and the dicaffeoylquinic acid group represent about 20 and 10%, respectively. However, it has been suggested that these low levels of dicaffeoylquinic acids are nonetheless very important for sensory qualities of coffee.[14] The highest total level found was 10.7% from a "mild" coffee and the lowest (3.6%) was from a decaffeinated coffee, suggesting that there are considerable losses of chlorogenic acid during processing.

Table 3. Chlorogenic acid isomer contents in instant coffees. Average of duplicate determinations for dry matter

Isomer	Samples, grams of isomer per 100 g of sample												
	C-1	C-2	C-3	C-4	C-5	C-6	C-7	C-8	C-9	C-10	C-11	C-12	C-13
3-CQA	1.38	1.35	0.90	0.92	1.89	1.44	0.75	1.40	1.00	1.43	1.08	0.72	0.70
4-CQA	1.65	1.55	1.04	1.03	2.25	1.62	0.87	1.70	1.16	1.56	1.25	0.84	0.81
5-CQA	2.25	2.15	1.38	1.36	3.50	1.89	1.02	2.28	1.69	1.93	1.74	1.07	1.04
Total CQA	5.28	5.05	3.32	3.31	7.64	4.95	2.64	5.38	3.85	4.92	4.07	2.63	2.55
3-FQA	0.25	0.25	0.17	0.18	0.35	0.25	0.15	0.23	0.21	0.22	0.20	0.17	0.15
4-FQA	0.59	0.34	0.44	0.37	0.76	0.29	0.32	0.54	0.49	0.26	0.37	0.43	0.40
5-FQA	0.58	0.45	0.32	0.32	0.82	0.36	0.27	0.52	0.41	0.28	0.41	0.29	0.30
Total FQA	1.42	1.04	0.93	0.87	1.93	0.90	0.74	1.29	1.11	0.76	0.98	0.89	0.85
3,4-diCQA	0.21	0.20	0.10	0.10	0.39	0.16	0.09	0.22	0.12	0.14	0.13	0.08	0.07
3,5-diCQA	0.16	0.16	0.07	0.07	0.29	0.11	0.07	0.17	0.08	0.10	0.08	0.06	0.06
4,5-diCQA	0.03	0.02	0.14	0.14	0.48	0.17	0.07	0.19	0.10	0.14	0.14	0.10	0.09
Total diCQA	0.40	0.38	0.31	0.31	0.16	0.44	0.23	0.58	0.30	0.38	0.35	0.24	0.22
Total chlorogenic acids	7.10	6.47	4.56	4.49	10.73	6.29	3.61	7.25	5.26	6.06	5.45	3.76	3.62

The authors thank Conselho Nacional de Desenvolvimento Cientifico Tecnologico, Universidade Federal do Rio de Janeiro, Brazil, the Committee of Vice-Chancellors and Principals of the Universities of the UK for sponsorship and Dr. M. Clifford (University of Surrey) for providing the FQA fraction.

References

1. Clifford, M. N., and Wight, J., *J. Sci. Food Agric.*, 1976, **27**, 73.
2. Clifford, M. N., *Process Biochem.*, 1975, May, 13.
3. Weiss, L. C., *J. Assoc. Off. Agric. Chem.*, 1953, **36**, 663.
4. Hansermann, M., and Bradenbergen, H., *Z. Lebensm. Unters. Forsch.*, 1961, **115**, 516.
5. Konig, W. A. and Sturm, R., "Tenth International Scientific Colloquium on Coffee," Association Scientifique Internationale du Café, (ASIC), Paris, in the press.
6. Rees, D. I., and Theaker, P. D., "Eighth International Scientific Colloquium on Coffee," ASIC, Paris, 1979, p. 79.
7. van der Stegen, G. H. D., and van Duijn, J., "Ninth International Scientific Colloquium on Coffee," ASIC, Paris, 1980, p. 107.
8. IUPAC Commission on the Nomenclature of Organic Chemistry and IUPAC - IUB Commission on Biochemical Nomenclature, *Biochem. J.*, 1976, **153**, 23.
9. Rubach, K., *Dissertation*, Technical University of Berlin, 1969.
10. "Official Methods of Analysis of the Association of Official Analytical Chemists," Thirteenth Edition, Association of Official Analytical Chemists, Washington, DC, 1980, p. 233.
11. Scarpati, M. L., and Guiso, M., *Tetrahedron Lett.*, 1964, **34**, 285.
12. Nagels, L., van Dongen, W., Brucker, J., and Pooter, H., *J. Chromatogr.*, 1980, **187**, 181.
13. Corse, J., Lundin, R. E., Sondheimer, E., and Waiss, A. C., Jr., *Phytochemistry*, 1966, **5**, 767.
14. Ohiokpehai, O., Brumen, G., and Clifford, M. N., "Tenth International Scientific Colloquium on Coffee," ASIC, Paris, in the press.

Paper A3/115
Received April 25th, 1983
Accepted June 21st, 1983

Comparative Assessment of High-performance Liquid Chromatographic Methods for the Determination of Ascorbic Acid and Thiamin in Foods

Ishbel A. Nicolson and Robert Macrae
Department of Food Science, University of Reading, Reading, RG1 5AQ, UK
and David P. Richardson
Cadbury Schweppes PLC, The Lord Zuckerman Research Centre, University of Reading, Reading, RG6 2LA, UK

A comparative assessment of HPLC methods for vitamin analysis was designed in which a number of institutions were asked to carry out the determination of ascorbic acid and thiamin in three samples (1, a mixture of thiamin and ascorbic acid in glucose; and 2 and 3, fortified breakfast cereals). Coefficients of variation between laboratories for sample 1 (ascorbic acid 5.6 and thiamin 6.9%) were much lower than for samples 2 and 3 (ascorbic acid 23 and 19% and thiamin 47 and 34%, respectively), the latter being considerably greater than is desirable. It is concluded that HPLC will not become a widely accepted technique for the determination of vitamins in foods until all the stages of the analysis, including extraction, clean-up and HPLC, are thoroughly validated.

Keywords: *Ascorbic acid determination; thiamin determination; collaborative studies; high-performance liquid chromatography; food*

The last two decades have seen an increasing awareness of the nutritional quality of food by the public, industry and regulatory agencies. This trend is exemplified by the recent introduction of nutritional labelling, both in the USA and elsewhere,[1] and has led to the increased demand for rapid and accurate methods of analysis for all nutrients, but particularly for vitamins.

At present, vitamins are determined separately using widely different techniques—chemical, physicochemical, microbiological and biological. These methods are frequently time consuming and are often limited by the number of interfering compounds found in the food matrix. HPLC techniques could offer advantages of speed and increased specificity, using equipment that is versatile in its application. In recent years many papers have been published on the application of HPLC to the analysis of ascorbic acid[2–20] and thiamin,[2,21–31] the two most labile water-soluble vitamins in food processing. However, little mention has been made of the difficulties in extracting vitamins from specific food matrices and the subsequent deterioration of analytical columns.

The work described in this paper was prompted by the many problems encountered in this laboratory when using HPLC for the analysis of ascorbic acid and thiamin in more complex food systems, such as fortified breakfast cereals and food beverages. A survey was conducted to examine and quantify the variability of analytical results obtained from several laboratories, using HPLC methodologies, when each investigator was supplied with identical food samples. The three samples for the trial (one sugar based and two cereal based) were chosen to provide both a relatively straightforward analysis with no extraction problems and also samples requiring more complex extraction procedures.

Experimental

Materials

Three samples were prepared by the organising laboratory (Department of Food Science, University of Reading). Sample 1 was a mixture of 20 g of L-ascorbic acid (BDH Chemicals, Poole, Dorset), 10 g of thiamin hydrochloride (also BDH Chemicals) and 970 g of anhydrous D-glucose (Fisons Scientific Apparatus, Loughborough, Leics.). The powder was mixed for 1 h (Kenwood Chef, Model A70 1A). Samples 2 and 3 were proprietary oat-based breakfast cereals fortified with ascorbic acid, nicotinic acid, riboflavin, thiamin, vitamin A, vitamin D, calcium and iron, the levels of ascorbic acid being approximately 10–50 and 20–50 mg per 100 g, respectively, and the levels of thiamin 0.5–2.0 and 1.0–4.0 mg per 100 g, respectively. Both were ground to pass a 20-mesh sieve and mixed using a planetary mixer for 15 min (Morton Machine Co. Ltd., Wishaw, Scotland). All samples were sealed immediately in aluminium foil - polyester - polyolefin laminated pouches (Metal Box Ltd., Wantage). Homogeneity was checked by systematic sampling and found to be satisfactory.

General Instructions

Each participating laboratory was chosen on the basis of their use of HPLC methodologies and willingness to co-operate. They were asked to make duplicate extracts of each sample and then duplicate determinations for each vitamin, on each extract, using their own methods, equipment and standards. The moisture content of the samples was determined by each laboratory using an oven at 105 °C for 4 h.

Results, Statistical Analysis and Discussion

Ascorbic Acid

Six participants (including this laboratory) reported results. Extraction procedures, chromatographic conditions and the results obtained are summarised in Tables 1, 2 and 3. To determine more specifically the sources of error in the method, an analysis of variance was carried out (Table 4). Three sources of variation were investigated: (*a*) between the laboratories; (*b*) between the extracts within the laboratories; and (*c*) between the analyses on each extract. Analysis of variance indicated that there were significant differences in the results obtained by the laboratories for all three samples (highly significant for samples 2 and 3). There were also differences between the extracts in samples 1 and 2.

The coefficient of variation (CV) measures the precision of the experimental readings and is calculated by taking the square root of the estimated variance component and dividing

it by the mean. For sample 1 the coefficient of variation is much smaller than for samples 2 and 3 (Table 4). As the levels in sample 1 are much higher and the sample matrix is less complex, one might expect less variation in the results.

Horwitz *et al.* have suggested[32,33] that precision (coefficient of variation, CV) can be represented by the following equation:

$$CV(\%) = 2^{(1-0.5\log C)} \quad . \quad . \quad . \quad . \quad (1)$$

where C is the concentration expressed as powers of 10 (*e.g.*, 1 p.p.m. = 10^{-6}). When the concentrations of vitamins used in the samples are substituted into this equation, the values obtained in this trial are well above the predicted CVs obtained using the above equation, and are therefore greater than the guidelines for precision that have been suggested. Table 4 shows a summary of the statistical data and Table 5 a comparison between the CVs obtained in this trial compared with those predicted using the above equation.

Table 1. Summary of extraction procedures used by investigators for the determination of ascorbic acid

Investigator	Extraction procedure
1	Sample dissolved in 3% *m/V* metaphosphoric acid containing 8% *V/V* acetic acid, diluted to volume. Samples 2 and 3 were centrifuged and filtered
2	Sample extracted with 1.5% *m/V* metaphosphoric acid containing 4% *V/V* acetic acid, diluted to volume. Samples 2 and 3 were filtered
3	Sample shaken with 50 + 50 H_2O - MeOH containing 300 μg ml^{-1} EDTA and filtered in the dark
4	Sample homogenised with 6% *m/V* metaphosphoric acid for 30 min and filtered
5	Sample suspended in 6% *m/V* metaphosphoric acid + 1 ml of butylated hydroxyanisole and mixed for 2 min. Samples 2 and 3 were centrifuged and filtered
6	Sample extracted twice with 0.1% thiodiglycol containing *p*-aminobenzoic acid as internal standard. Supernatants after centrifuging were diluted to volume and then dialysed (using dialyser from Technicon AutoAnalyzer)

Thiamin

Seven participants (including this laboratory) reported results. Extraction procedures, chromatographic conditions and the results obtained are summarised in Tables 6, 7 and 8. Again, analysis of variance was carried out (see Table 9). Apart from sample 1, there were highly significant differences between the laboratories. In samples 1 and 2 there were also highly significant differences between the extracts. On looking at the data in Table 8, it can be seen that for sample 1 (no significant difference between laboratories) the large difference in the extracts may be due to data contributed by investigators 3, 5 and 7. The coefficients of variation show a similar trend to those of the ascorbic acid results, *i.e.*, a small CV for sample 1, but very high CVs for samples 2 and 3 (Table 5). When compared with the predicted CVs (using Horwitz's equation, Table 5), they exceeded the guidelines suggested.

Comments and Conclusions

There are various factors that could have contributed to the inter-laboratory variation. Extraction and stability of the aqueous extract are both important in the determination of ascorbic acid. A wide range of extractants were used, with a mixture of metaphosphoric acid and acetic acid being the most popular. There was also a wide range of chromatographic conditions, two laboratories (3 and 5) used amino columns and

Table 2. Summary of chromatographic conditions used by investigators for the determination of ascorbic acid

Investigator	Column dimensions, length × i.d./cm	Stationary phase	Particle size/μm	Mobile phase	Pressure/bar	Flow-rate/ml min^{-1}	Injection volume/μl	Measurement method*	Detection	Retention time/min	Capacity factor
1	30 × 0.39	μBondapak C_{18}†	10	H_2O - MeOH - acetic acid (93 + 5 + 2)	112	1.5	20‡	E, PA	UV 254 nm: (1) 2 a.u.f.s.; (2) (3) 0.2 a.u.f.s.	2.42	0.9
2	30 × 0.4	Micropak MCH	10	H_2O containing 0.06% acetic acid + 0.5 g of TAHS,§ pH 5	110	2	11	E, PA	UV 264 nm: (1) 0.128 a.u.f.s.; (2) (3) 0.016 a.u.f.s.	5.8	2.6
3	20 × 0.46	Partisil amino-propyl†	5	H_2O - MeOH (75 + 25) containing 0.1% citric acid	135	1	10	E, PA	UV 255 nm: 0.01 a.u.f.s.	4.35	1.56
4	30 × 0.39	μBondapak C_{18}	10	1% H_3PO_4	50	1	20	M, PA	UV 254 nm: (1) 2.0 a.u.f.s.; (2) (3) 0.05 a.u.f.s.	3.68	—
5	25 × 0.46	LiChrosorb NH_2†	10	MeOH - 0.1% citric acid (55 + 45)	100	2	20	E, PA	UV 254 nm: 0.16 a.u.f.s.	2.70	2.0
6	15 × 0.46	Spherisorb ODS-2†	5	0.001 M citrate - MeOH (95 + 5) containing 0.005 M TBAP,¶ pH 5.3	100	(1) 2 (2) (3) 1	20	(1) M, PH (2) (3)‖ E, PA	UV 254 nm: 0.05 a.u.f.s.	9.4	8.4

* E, electronic integration; M, manual; PA, peak area; and PH, peak height.
† Pre-column used.
‡ WISP Autoinjector used.
§ TAHS, tetrahexylammonium hydrogen sulphate.
¶ TBAP, tetrabutylammonium phosphate.
‖ Calculations based on recovery of internal standard.

Table 3. Collaborative trial results for the determination of ascorbic acid by HPLC (all in mg per 100 g of sample and corrected to 100% dry matter)

	Sample 1		Sample 2		Sample 3	
Investigator	Extract 1	Extract 2	Extract 1	Extract 2	Extract 1	Extract 2
1	2188	2189	27.1	27.1	46.3	43.5
	2140	2222	27.0	24.7	46.7	42.7
2	1737	1879	14.9	13.5	35.0	34.5
	1819	1933	15.2	14.7	34.5	36.2
3	2029	2110	18.8	20.1	42.2	44.5
	2041	2094	18.6	19.8	42.3	44.4
4	2121	2094	16.0	16.5	27.2	27.4
	2175	2109	15.4	16.1	32.3	27.0
5	2173	2103	18.7	19.7	46.8	53.5
	2255	2167	19.6	19.7	50.4	50.8
6	2088	2079	25.2	24.7	44.2	44.5
	2087	2087	25.7	25.1	44.6	43.0
Mean	2080		20.2		41.0	
S.d.	125.04		4.51		7.52	

Table 4. Summary of statistical data for ascorbic acid determinations

Sample	Source of variation	Mean square (d.f.*)	*F* ratio	Component of variance	CV, %
1	Between laboratories	60237.4 (5)	10.28	13594.81	5.61
	Between extracts in laboratories	5858.17 (6)	5.48	2394.92	2.36
	Between analyses in extracts	1068.33 (12)	—	1068.33	1.57
2	Between laboraories	88.359 (5)	80.55	21.816	23.2
	Between extracts in laboratories	1.097 (6)	5.97	0.456	3.36
	Between analyses in extracts	0.184 (12)	—	0.184	2.13
3	Between laboratories	247.663 (5)	40.95	60.404	18.96
	Between extracts in laboratories	6.048 (6)	2.75	1.924	3.38
	Between analyses in extracts	2.20 (12)	—	2.20	3.62

* Degrees of freedom.

Table 5. Comparison of coefficients of variation (CV) obtained from trial with those predicted by equation (1)

		Coefficient of variation, %	
Vitamin	Sample	Trial results	Equations
Ascorbic acid	Sample 1	5.6	3.6
	Sample 2	23.2	7.2
	Sample 3	19.0	6.5
Thiamin	Sample 4	6.9	4.1
	Sample 5	47.2	11.0
	Sample 6	34.1	9.9

only one laboratory (6) used an internal standard. Additionally, only one group (6) used a clean-up procedure.

Thiamin analysis involves the additional problems of extraction and detection. All but one of the investigators carried out the full hydrolysis procedure, *i.e.*, both acid and enzymic hydrolyses. Laboratory 1 used acid hydrolysis only, but the results that were obtained are not significantly different from the others. The levels of thiamin in samples 2 and 3 are very low, although not as low as the levels naturally present in most foods. To overcome the problem of sensitivity, two of the investigators prepared a fluorescent derivative by oxidising thiamin to thiochrome with alkaline potassium hexacyanoferrate(III), and used a fluorescence detector.

Inadequate resolution of the vitamin from other compounds in the extract will also produce variability, especially if manual methods of quantification are used. The results from this survey show that there are considerable problems when HPLC is applied to the determination of ascorbic acid and thiamin in foods, many of which may be attributed to the non-standardised methods employed. A number of participating laboratories did not manage to complete the analysis (their

Table 6. Summary of extraction procedures used by investigators for the determination of thiamin

Investigator	Extraction procedure
1	Sample 1 was determined simultaneously with ascorbic acid (investigator 3, Tables 1 and 2). Samples 2 and 3 were refluxed with 50 + 50 MeOH - 0.2 N HCl for 15 min, shaken for 15 min and filtered
2	Sample hydrolysed at 120 °C for 30 min with 0.25 N H_2SO_4, cooled, incubated with takadiastase for 45 min (after pH adjustment); protein precipitated with 45% trichloroacetic acid, heated at 50–60 °C for 5 min, centrifuged and filtered
3	Sample 1 dissolved in H_2O and diluted to volume. Samples 2 and 3 were hydrolysed at 95 °C for 60 min with 0.25 N H_2SO_4, cooled, incubated with a mixture of pancreatin, lipase and takadiastase at 60 °C for 45 min, cooled and filtered
4	Sample 1 was analysed simultaneously with ascorbic acid (investigator 5, Tables 1 and 2). Samples 2 and 3 were hydrolysed at 120 °C for 15 min with 0.2 N H_2SO_4, cooled, incubated with claradiastase at 45 °C for 2 h. Thiamin oxidised to thiochrome with alkaline potassium hexacyanoferrate(III) solution
5	Sample hydrolysed in autoclave at 15 lb in^{-2} for 1 h with 0.05 N H_2SO_4, cooled, incubated with takadiastase at 45 °C for 3 h and filtered. Thiamin oxidised to thiochrome with alkaline potassium hexacyanoferrate(III) solution
6	Sample hydrolysed at 100 °C for 30 min with 0.1 N HCl, cooled, incubated with α-amylase at 45 °C for 2 h and filtered
7	Sample 1 dissolved in water and diluted to volume. Samples 2 and 3 hydrolysed at 90 °C for 45 min with 0.1 N HCl, cooled, incubated with α-amylase at 65 °C for 45 min, centrifuged and filtered

Table 7. Summary of chromatographic conditions used by investigators for the determination of thiamin

Investigator	Column dimensions, length × i.d./cm	Stationary phase	Particle size/ μm	Mobile phase	Pressure/ bar	Flow-rate/ ml min^{-1}	Injection volume/ μl	Measurement method*	Detection	Retention time/min	Capacity factor
1	15 × 0.46	Spherisorb ODS†	5	MeOH - H_2O (50 + 50) containing 1% Na acetate, 50 °C	79	1	10	E, PA	UV 265 nm: 0.01 a.u.f.s.	6.35	2.97
2	30 × 0.39	μBondapak C_{18}	10	Phosphate buffer, pH 6.5	67	1	20	M, PA	UV 254 nm: (1) 0.05 a.u.f.s.; (2) (3) 0.005 a.u.f.s.	8.78	—
3	25 × 0.4	μBondapak C_{18}	10	0.1% *m/V* HSA,‡ 1% *V/V* TEA§ and (1) 2.2% MeOH, (2) (3) 0.75% MeOH	100	(1) 2 (2) (3) 3	(1) 12 (2) 30 (2) 40	M, PH	UV 244 nm: (1) 0.16 a.u.f.s.; (2) (3) 0.04 a.u.f.s.	(1) 4 (2) (3) 5	(1) 1.5 (2) (3) 4.0
4	25 × 0.46	LiChrosorb RP-8†	10	MeOH - CH_3CN - 2-methylpropan-1-ol (80 + 10 + 10), 20 °C	55	2	50	E, PA	Fluorescence: ex. 370 nm, em. 425 nm	2.25	—
5	25 × 0.4	LiChrosorb Si60	5	$CHCl_3$ - MeOH - H_2O (90 + 9 + 1)	164	2	10	E, PA	Fluorescence: ex. 360 nm, em. 440 nm	7.7	4.1
6	15 × 0.46	Spherisorb ODS-2†	5	MeOH - 0.005 M KH_2PO_4 (50 + 50) containing 0.005 M OSA¶	100	1	20	E, PA	UV 255 nm: 0.02 a.u.f.s.	1.17	1.4
7	25 × 0.46	Spherisorb ODS†	5	MeOH - 0.05 M KH_2PO_4 (50 + 50) containing 0.005 M OSA	68	1	20	E, PA	UV 266 nm: 0.02 a.u.f.s.	8.8	2.11

* See footnote to Table 2.
† See footnote to Table 2.
‡ HSA, heptanesulphonic acid.
§ TEA, triethylamine.
¶ OSA, sodium octanesulphonate.

Table 8. Collaborative trial results for the determination of thiamin by HPLC (all in mg per 100 g of sample and corrected to 100% dry matter)

	Sample 1		Sample 2		Sample 3	
Investigator	Extract 1	Extract 2	Extract 1	Extract 2	Extract 1	Extract 2
1	924	950	1.47	1.39	2.64	2.75
	924	949	1.50	1.37	2.69	2.72
2	916	918	1.76	1.92	3.87	4.01
	903	927	1.79	1.76	3.89	3.71
3	969	852	0.74	0.85	2.26	1.93
	962	848	0.64	0.85	2.15	1.93
4	896	909	1.50	1.83	3.04	2.82
	910	939	1.50	1.83	3.04	2.82
5	799	746	1.52	1.43	2.66	2.61
	791	737	1.54	1.44	2.73	2.49
6	757	745	0.79	0.75	2.11	2.19
	759	746	0.84	0.84	2.10	2.04
7	790	1026	0.29	0.28	1.35	0.94
	850	1118	0.27	0.30	1.17	1.05
Mean	877.1		1.18		2.49	
S.d.	95.55		0.54		0.81	

results have not been included) and others expressed dissatisfaction with their results (these data have been included to give a proper idea of the range in results encountered.) Ideally it would have been more satisfactory if a greater number of laboratories had been involved. However, at the beginning of the trial, when trying to find analysts who had experience in using HPLC for the determination of ascorbic acid and thiamin in foods, it was found that the technique is not as widely used as one might expect from a scan of the literature.

Some semi-specific colorimetric methods are still in use and in some instances microbiological assays are relied on. This survey has demonstrated conclusively that there are serious problems with clean-up and HPLC methodologies that must be overcome. Until methods appear in the literature in which attention is paid to these problems, HPLC will not develop into a widely accepted technique for the analysis of these vitamins in foods and HPLC results quoted for these two vitamins should be viewed with caution.

Table 9. Summary of statistical data for thiamin determinations

Sample	Source of variation	Mean square (d.f.*)	*F* ratio	Component of variance	CV, %
1	Between laboratories	26 429.17 (6)	2.28	3 710.04	6.94
	Between extracts in laboratories	11 589.00 (7)	23.81	5 551.18	8.50
	Between analyses in extracts	486.64 (14)	—	486.64	2.52
2	Between laboratories	1.263 (6)	55.59	0.310 1	47.19
	Between extracts in laboratories	0.022 7 (7)	12.71	0.010 5	8.68
	Between analyses in extracts	0.001 79 (14)	—	0.001 79	3.59
3	Between laboratories	2.920 (6)	100.69	0.722 8	34.14
	Between extracts in laboratories	0.029 (7)	3.72	0.010 6	4.14
	Between analyses in extracts	0.007 79 (14)	—	0.007 79	3.55

* Degrees of freedom.

The authors thank the following research workers for participating in this survey: Dr. P. R. Belgaars, Food Inspection Service, Maastricht, The Netherlands; G. Findlay and Dr. A. A. Wagland, Roche Products Ltd., Welwyn Garden City, Herts., UK; Dr. D. Hammond, Cadbury Schweppes Group Research, Reading, UK; W. S. Hawer and Kee Bong Suh, Food Research Institute, Dangsoo, Banwol, Kyongki-do, Republic of Korea; N. Joyce and Dr. A. G. Croft, Dalgety Spillers Ltd., Cambridge, UK; Dr. G. Van de Haar, Food Inspection Service, Groningen, The Netherlands; Dr. P. J. Van Niekerk, National Food Research Institute, Pretoria, South Africa; and Mr. K. D. Marriage, Beecham Products, Brentford, Middlesex, UK.

The authors are grateful to Dr. D. Collett, Department of Applied Statistics, University of Reading, for statistical advice and to Mr. A. Turner, Cadbury Schweppes PLC, Bournville, Birmingham, UK, for advice on the preparation of this paper.

References

1. Richardson, D. P., *Proc. Inst. Food Sci. Technol.*, 1981, **14**, 87.
2. Wills, R. B. H., Shaw, C.-G., and Day, W. R., *J. Chromatogr. Sci.*, 1977, **15**, 262.
3. Floridi, A., Fini, C., Palmerini, C. A., and Rossi, A., *Riv. Sci. Technol. Aliment. Nutr. Um.*, 1976, **6**, 197.
4. Williams, R. C., Baker, D. R., and Schmit, J. A., *J. Chromatogr. Sci.*, 1978, **11**, 618.
5. Sood, S. P., Sartori, L. E., Wittmer, D. P., and Haney, W. G., *Anal. Chem.*, 1976, **48**, 796.
6. Pachla, L. A., and Kissinger, P. T., *Anal. Chem.*, 1976, **48**, 364.
7. Rousseff, R., *in* Charalambous, G., *Editor*, "Liquid Chromatographic Analysis of Food and Beverages," Volume I, Academic Press, New York and London, 1979, p. 161.
8. Schuster, R., *Anal. Chem.*, 1980, **52**, 617.
9. Archer, A. W., Higgins, V. R., and Perryman, D. L., *J. Assoc. Public Anal.*, 1980, **18**, 99.
10. Ruckemann, H., *Z. Lebensm. Unters. Forsch.*, 1980, **171**, 357.
11. Bui-Nguyên, M. H., *J. Chromatogr.*, 1980, **196**, 163.
12. Shaw, P. E., and Wilson, C. W., *J. Agric. Food Chem.*, 1982, **30**, 396.
13. Dennison, D. B., Brawley, T. G., and Hunter, G. L. K., *J. Agric. Food Chem.*, 1981, **29**, 927.
14. Finley, J. W., and Duang, E., *J. Chromatogr.*, 1981, **207**, 449.
15. Geigert, J., Hirano, D. S., and Neidleman, S. L., *J. Chromatogr.*, 1981, **206**, 396.
16. Lookhart, G. L., Hall, S. B., and Finney, K. F., *Cereal Chem.*, 1982, **59**, 69.
17. Rose, R. C., and Nahrwold, D. L., *Anal. Biochem.*, 1981, **114**, 140.
18. Augustin, J., Beck, C., and Marousek, G. I., *J. Food Sci.*, 1981, **46**, 312.
19. Van Niekerk, P. J., Smit, S. C. C., and Strydom, E. S. P., personal communication.
20. Hedlund, C. B., 1981, personal communication.
21. Callmer, K., and Davies, L., *Chromatographia*, 1974, **7**, 644.
22. Van de Weerdhof, T., Wiersum, M. L., and Reissenweber, H., *J. Chromatogr.*, 1973, **83**, 455.
23. Henshall, A., *in* Charalambous, G., *Editor*, "Liquid Chromatographic Analysis of Food and Beverages," Volume V, Academic Press, New York and London, 1979, p. 31.
24. Toma, R. B., and Tabekhia, M. M., *J. Food Sci.*, 1979, **44**, 263.
25. Kamman, J. F., Labuza, T. P., and Warthesen, J. J., *J. Food Sci.*, 1980, **45**, 1497.
26. Mauro, D. J., *Diss. Abstr. Int. B*, 1980, **40**, 3502.
27. Bognar, V. A., *Dtsch. Lebensm.-Rundsch.*, 1981, **77**, 431.
28. Ang, C. Y. W., and Moseley, F. A., *J. Agric. Food Chem.*, 1980, **28**, 483.
29. Skurray, G. R., *Food Chem.*, 1981, **7**, 77.
30. Gulber, C. J., and Hemming, B. C., *Methods Enzymol.*, 1979, **62**, 63.
31. Kimura, M., Fujita, T., Nishada, S., and Itokawa, Y., *J. Chromatogr.*, 1980, **188**, 417.
32. Horwitz, W., Kamps, L. R., and Boyer, K. W., *J. Assoc. Off. Anal. Chem.*, 1980, **63**, 1344.
33. Horwitz, W., *Anal. Chem.*, 1982, **54**, 67A.

Paper A3/260
Received August 8th, 1983
Accepted September 30th, 1983

Improved Capillary Gas-chromatographic - Mass Spectrometric Method for the Determination of Anabolic Steroid and Corticosteroid Metabolites in Horse Urine Using On-column Injection with High-boiling Solvents

Edward Houghton, Philip Teale and Minoo C. Dumasia
Racecourse Security Services Laboratories, P.O. Box 15, Snailwell Road, Newmarket, Suffolk, CB8 7DT, UK

When analysing large numbers of samples containing high-boiling components by capillary column gas chromatography, the analysis time using hexane as solvent in the splitless mode is prohibitive. In order to reduce the analysis time for the steroid TMS and MO-TMS derivatives but yet maintain a solvent effect, the use of solvents with high boiling-points has been investigated. The use of solvents with high boiling-points has now been extended to on-column injection without any loss in resolution or adverse effects on column lifetime.

Keywords: *On-column injection; gas chromatography - mass spectrometry; steroid analysis; corticosteroid analysis; horse urine*

The technique of cold on-column injection allows liquid samples to be introduced directly into a capillary column and offers some advantages over conventional injection techniques. As prior heating of the sample for vaporisation is avoided, discrimination of sample components is minimal even when they have a wide range of volatilities. Decomposition of thermolabile compounds is also reduced to a minimum and, as the injector is septumless, the technique eliminates the problems associated with septum bleed. The different types of on-column injection techniques and the factors affecting accuracy, precision and discrimination have been discussed in detail.[1-8]

In a previous paper[9] we discussed the use of capillary column gas chromatography - mass spectrometry (GC - MS) in the analysis of anabolic steroid residues in horse body fluids. To reduce the analysis time but yet maintain a solvent effect in the splitless injection mode, injections were made at elevated temperatures using solvents of high boiling-point (undecane and dodecane). This technique has also been applied to confirm the administration of synthetic corticosteroids to horses using capillary column GC and negative ion chemical ionisation mass spectrometry.[10] The use of solvents of high boiling-point allowed for rapid analysis of the high relative molecular mass methoxime trimethylsilyl (MO-TMS) derivatives of the corticosteroids whilst still maintaining chromatographic integrity. In order to take advantage of the superiority of on-column injection and also maintain short analysis times we have now investigated the analysis of anabolic and corticosteroid derivatives using high-boiling solvents in the on-column injection mode.

Experimental

Materials

Dichloromethane, hexane and chloroform were redistilled before use. 5α-Estrane-3β,17α-diol was synthesised by Organon, Oss, The Netherlands. All other steroids, reagents and solvents were obtained from Sigma London Chemical Co. Ltd., Poole, Dorset, UK.

Extraction of Corticosteroids from Urine

The urine (10 cm^3) was extracted by rolling it gently with dichloromethane (1 × 50 cm^3) for 10 min. The extract was dried over anhydrous Na_2SO_4, filtered and then evaporated to dryness *in vacuo*. The residual material was derivatised (MO-TMS) for analysis by GC - MS.

Derivatisation of Steroids

A mixture of C_{18} - C_{19} steroids (5α-estrane-3β,17α-diol, 5α-androstane-3β,17β-diol, 19-nortestosterone and testosterone) was treated with methoxylammonium chloride in dry pyridine (5% *m/V*; 50 μl) and heated at 80 °C for 30 min. The solvent was removed under nitrogen at 40 °C and *N,O*-bis-(trimethylsilyl)acetamide (BSA) (50 μl) and trimethylchlorosilane (TMCS) (25 μl) were added; silylation was carried out at 80 °C for a further 2 h. Excess of silylating reagents was removed under nitrogen at 40 °C and the residue passed down a short column of Sephadex LH-20 slurry-packed in a Pasteur pipette using chloroform - hexane (1 + 1) as eluent. The steroid MO-TMS derivatives were eluted in the first 2 ml of eluate and the solvent was removed under nitrogen. The residue was dissolved in the appropriate solvent for analysis by capillary column GC - MS.

The methoxime derivative of a mixture of corticosteroids (prednisone, cortisol, betamethasone and dexamethasone) was prepared as described above. Silylation was carried out using trimethylsilylimidazole (50 μl) at 80 °C for 2 h and the sample was then prepared for GC - MS analysis by filtration through Sephadex LH-20.[10]

Gas Chromatography - Mass Spectrometry

Capillary column GC - MS was carried out using a Finnigan 4000 gas chromatograph - mass spectrometer interfaced to a Model 6110 data system. The on-column injector, constructed in this laboratory, was placed in an unheated region on top of the oven of the Finnigan 9610 gas chromatograph. The injector utilised the syringe technique (fused silica needles, 0.17 mm o.d.), injections being made via a PTFE stop valve. A constricted glass capillary tube guided the fused silica needle into the capillary column (30 m × 0.25 mm i.d., SE-54). Secondary cooling was controlled via a solenoid valve operated through the microprocessor on the Model 9610 gas chromatograph. Details of the construction of the injector and its installation on to the Model 9610 gas chromatograph will be described elsewhere.

Electron-impact (EI) mass spectra were recorded at 70 eV. Negative ion chemical ionisation mass spectra of the corticosteroids were obtained using the pulsed positive ion - negative ion chemical ionisation (PPINICI) accessory on the Finnigan 4000 instrument. Scans were recorded every 1 s over the range 100–450 a.m.u. for the derivatised C_{18} - C_{19} steroid mixture in the EI mode and 300–700 a.m.u. for the derivatised corticosteroid mixture in the negative ion CI mode (ammonia was used as reagent gas).

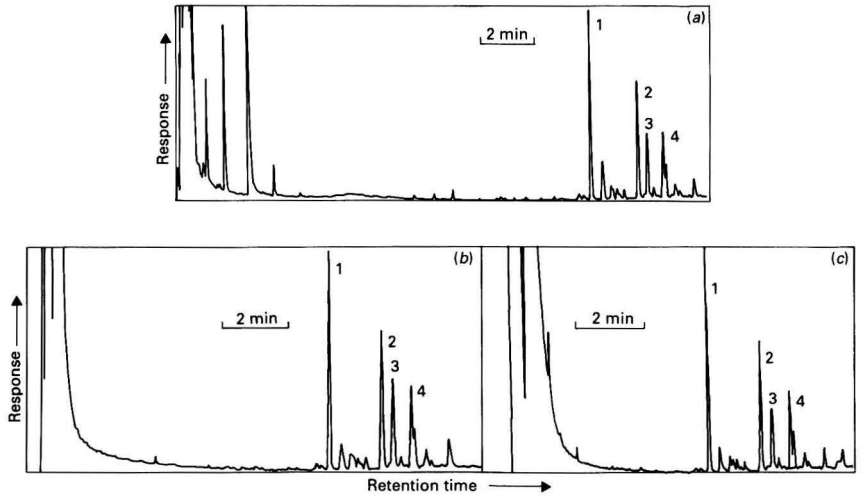

Fig. 1. Reconstructed gas chromatograms of a mixture of 1, 5α-estrane-3β,17α-diol bis-TMS; 2, 5α-androstane-3β,17β-diol bis-TMS; 3, 19-nortestosterone MO-TMS; and 4, testosterone MO-TMS using on-column injection and different solvents. (*a*) Hexane; initial temperature 80 °C; retention times for peaks 1–4, 14.91, 16.51, 16.83 and 17.4 min, respectively. (*b*) Nonane; initial temperature 160 °C; retention times for peaks 1–4, 9.24, 10.85, 11.16 and 11.73, respectively. (*c*) Undecane; initial temperature 205 °C; retention times for peaks 1–4, 6.83, 8.36, 8.67 and 9.23 min, respectively. Column conditions: initial temperature held for 2 min, programmed at 15 °C min^{-1} to 220 °C and then at 5 °C min^{-1} to 270 °C in all instances; helium was used as carrier gas

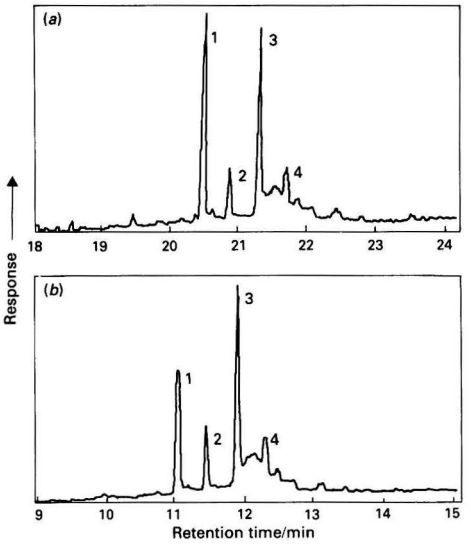

Fig. 2. Reconstructed gas chromatograms of a mixture of 1, prednisone MO-TMS; 2, cortisol MO-TMS; 3, betamethasone MO-TMS; and 4, dexamethasone MO-TMS using splitless injection and different solvents. (*a*) Hexane; initial temperature 50 °C; retention times for peaks 1–4, 20.56, 20.92, 21.34 and 21.75 min, respectively. (*b*) Dodecane; initial temperature 190 °C; retention times for peaks 1–4, 11.02, 11.43, 11.87 and 12.27 min, respectively. Column conditions: initial temperature held for 2 min, programmed to 280 °C at 15 °C min^{-1} and then at 5 °C min^{-1} to 325 °C

Results

Fig. 1(*a*)–(*c*) show the reconstructed gas chromatograms obtained for the derivatised C_{18} - C_{19} steroid mixture using different solvents in the on-column injection mode. The initial column temperature was adjusted in each instance for the particular solvent.

Fig. 2(*a*) and (*b*) show the reconstructed gas chromatograms obtained for the derivatised corticosteroid mixture using hexane and dodecane as solvents in the splitless injection mode. The corresponding reconstructed gas chromatograms obtained using on-column injection are shown in Fig. 3(*a*) and (*b*). The on-column analysis for endogenous cortisol and cortisone in a horse urine extract is shown in Fig. 4. The mass chromatograms at *m/z* −472 and −459 demonstrate the presence of derivatised cortisone and cortisol, respectively.

Discussion

When analysing large numbers of samples containing high-boiling components by capillary column GC - MS in the splitless mode, the analysis time using hexane as solvent is prohibitive as injections have to be made at 50–60 °C. To overcome this problem injections can be made at higher column temperatures using solvents of high boiling-point.[9] The extension of the use of solvents of high boiling-point to on-column injection is demonstrated in Fig. 1. Using nonane and undecane as solvents, significantly reduced retention times for derivatised components of the C_{18} - C_{19} steroid mixture were obtained in comparison with the use of hexane as solvent. The separation of the *syn*- and *anti*-isomers of testosterone MO-TMS derivative (peak 4, Fig. 1) indicated that there was no apparent loss in resolution.

The choice of a suitable solvent is obviously limited by solute volatility. The broad solvent peak obtained using on-column injection with solvents of high boiling-point (Fig. 1) requires a marked difference in volatility between solvent and solute in order to maintain chromatographic integrity. The technique is therefore applicable only to components of low volatility. This requirement is met in the field of steroid analysis in biological fluids.

The parameters affecting solute band shortening of injection are less stringent for the on-column technique than for the splitless technique and injections can be made at column temperatures 5–10 °C above the boiling-point of the solvents[4,8] (nonane, boiling-point 151 °C; undecane, boiling-point 196 °C). The use of secondary cooling eliminates any discriminatory effects that may arise owing to volatilisation from the tip of the syringe needle in the heated zone of the column oven.[4]

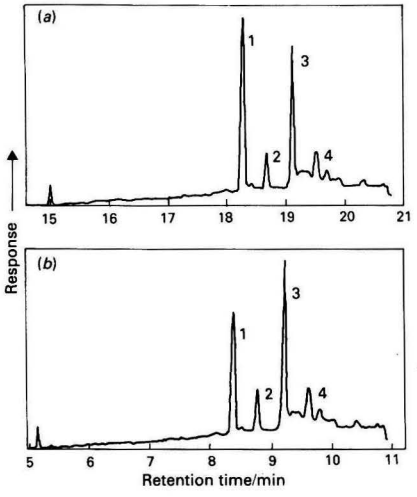

Fig. 3. Reconstructed gas chromatogram of the derivatised corticosteroid mixture using on-column injection and different solvents. (*a*) Hexane; initial temperature 80 °C; retention times for peaks 1–4, 18.27, 18.65, 19.07 and 19.47 min, respectively. (*b*) Dodecane; initial temperature 225 °C; retention times for peaks 1–4, 8.33, 8.73, 9.17 and 9.58 min, respectively. Temperature programme conditions as in Fig. 2

A comparison of the splitless and on-column modes of injection for the derivatised mixture of corticosteroids is shown in Figs. 2 and 3 using hexane and dodecane as solvents. For both injection techniques the advantage of short analysis times when using dodecane as solvent is clearly demonstrated. On-column injection offers a further reduction in analysis time as injection can be made at a column oven temperature of 225 °C as opposed to 190 °C in the splitless mode.

The reduction in the height of the peak corresponding to prednisone MO-TMS (peak 1, Figs. 2 and 3) when using dodecane as solvent in both the splitless and on-column injection modes is difficult to explain as discrimination against the most volatile component in the mixture is not expected. A possible explanation is that with dodecane as solvent, there is a slight increase in resolution resulting in the partial separation of the *syn*- and *anti*-isomers of the MO-TMS derivative of this component, thus accounting for the peak broadening and corresponding reduction in peak height. The *syn*- and *anti*-isomers of cortisone MO-TMS derivative are clearly separated by capillary GC.

The analysis of a biological extract using on-column injection with dodecane as solvent is shown in Fig. 4, which demonstrates the presence of endogenous cortisone and cortisol in horse urine.

The analysis of trace components in biological extracts by capillary GC or GC - MS requires injections to be made in the splitless or on-column mode. When these trace components are of low volatility, as in the steroid field, the choice of a suitable solvent of high boiling-point offers the advantage of reduced analysis times without apparently affecting the resolution in both these modes of injection. The on-column injector, being non-volatilising and septumless, offers the additional advantages of better sample transfer and the complete elimination of septum bleed peaks from chromatograms in comparison with the splitless injector. On-column injection is now used routinely in this laboratory for the analysis of both anabolic and corticosteroid residues in horse body fluids by GC - MS.

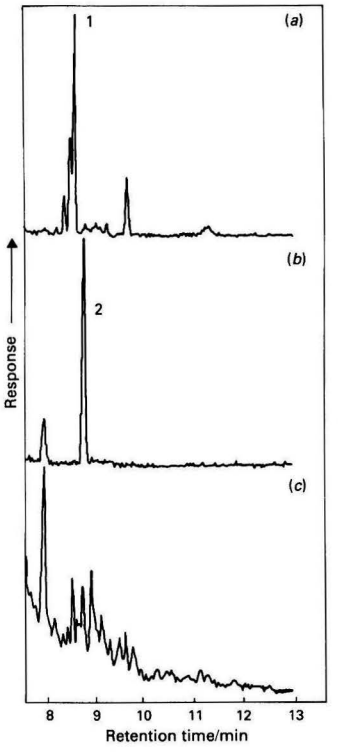

Fig. 4. Analysis of a derivatised horse urine extract showing the presence of (*a*) cortisone (mass chromatogram $m/z = -472$), (*b*) cortisol (mass chromatogram $m/z = -459$) and (*c*) reconstructed gas chromatogram using on-column injection and negative ion GC - MS. Retention times for peaks 1 and 2, 8.49 and 8.7 min, respectively. Column conditions as in Fig. 3; dodecane as solvent

The authors extend their thanks to the Director of the Laboratories, Dr. Michael Moss, for his continuous interest and encouragement.

References

1. Schomburg, G., Behlau, H., Dielmann, R., Weeke, F., and Husmann, H., *J. Chromatogr.*, 1977, **142**, 87.
2. Grob, K., and Grob, K., Jr., *J. Chromatogr.*, 1978, **151**, 311.
3. Grob, K., *J. High Resolut. Chromatogr. Chromatogr. Commun.*, 1978, **1**, 263.
4. Galli, M., Trestianu, S., and Grob, K., Jr., *J. High Resolut. Chromatogr. Chromatogr. Commun.*, 1979, **2**, 366.
5. Grob, K., *J. Chromatogr.*, 1979, **178**, 387.
6. Grob, K., and Neukom, H. P., *J. Chromatogr.*, 1980, **189**, 109.
7. Schomburg, G., Husmann, H., and Rittmann, R., *J. Chromatogr.*, 1981, **204**, 85.
8. Jenkins, R., and Jennings, W., *J. High Resolut. Chromatogr. Chromatogr. Commun.*, 1983, **6**, 228.
9. Houghton, E., and Teale, P., *Biomed. Mass Spectrom.*, 1981, **8**, 358.
10. Houghton, E., Teale, P., Dumasia, M. C., and Wellby, J. K., *Biomed. Mass Spectrom.*, 1982, **9**, 459.

Paper A3/284
Received August 23rd, 1983
Accepted October 3rd, 1983

Gas-chromatographic Determination of Aromatic Molecules by Supersonic Jet Spectrometry with Resonance Multi-photon Ionisation

Totaro Imasaka, Tsukasa Shigezumi and Nobuhiko Ishibashi*
Faculty of Engineering, Kyushu University, Hakozaki, Fukuoka 812, Japan

The sample separated by a chromatographic column was expanded through a supersonic nozzle. The ultra-cold molecules thus produced were successively multi-photon ionised by a tightly focused dye laser beam and detected by an electron multiplier. When the wavelength was adjusted to 492.75 nm, which corresponds to one of the transitions ($14_0^1 1_0^1$, $^1A_{1g} \rightarrow {}^1B_{2u}$) of benzene, a large peak was observed. Aniline could be excited through a weakly resonanced, two-photon excitation process at around this wavelength, and provided a relatively weak peak. The solvent molecule of ethanol gave no appreciable peak. The detection limit of benzene was about 1 μg.

Keywords: *Aromatics determination; gas chromatography; supersonic jet spectrometry; resonance multi-photon ionisation; laser fluorimetry*

Laser fluorimetry is attractive because of the large radiant flux and good monochromaticity of the laser. However, conventional room-temperature spectrometry gives a broad band, as electrons are populated in various vibrational and rotational levels of the ground state. A supersonic jet technique, which is based on the idea of expanding the sample vapour from a small pinhole into a vacuum, provides a molecular flow with a narrow velocity distribution, and the molecules can be cooled to a few degrees absolute.[1,2] The electrons are then populated in the lowest ground state, and therefore the congestion of rotational lines in the spectrum can be removed. It gives a very sharp vibrational line structure, and the sample species can be selectively determined. Warren *et al.*[3] have demonstrated the identification of naphthalene and its derivatives with laser fluorimetry based on resonance-line excitation. Amirav *et al.*[4] have demonstrated the selective determination of isotopic species of 9,10-dichloroanthracene. Hayes and Small[5] have pointed out the advantage of this supersonic jet spectrometry when combined with laser fluorimetry and gas chromatography, and have reported the selective determination of aromatic molecules in crude oil.

The fluorescence detection method requires a monochromator or filters for fluorescence isolation, so that the collection efficiency of fluorescence photons is less than 1%. This is an inevitable disadvantage of fluorimetry. Laser multi-photon ionisation is very sensitive, and it could potentially detect single ions produced by strong irradiation by a laser beam.[6] Lubman and co-workers[7-9] have used multi-photon ionisation for the isotope analysis of iodine and the mass analysis of hydrocarbon molecules.

In this study we show the advantage of the use of a resonance multi-photon ionisation detector in gas chromatography for the selective determination of aromatic molecules, and discuss the sensitivity of this method in comparison with laser-induced fluorimetry.

Experimental

The apparatus illustrated in Fig. 1 was used. A sample solution is injected from the inlet port of a gas chromatograph equipment (Shimadzu, GC-8A) and, after being separated by a column, the vaporised sample is expanded into a vacuum through a pinhole of diameter 0.5 mm. The first chamber is evacuated by a 4-in diffusion pump (Ulvac, ULK-04) followed by mechanical booster (Shimadzu, MV-100V) and rotary (Shimadzu, KD300G) pumps. The jet molecule passes through a skimmer (i.d. 0.5 mm) and is introduced into the second chamber. The molecule is excited by an excimer-laser-pumped dye laser (Lambda Physik, EMG102E, FL2002). The laser beam is tightly focused by a quartz lens (focal length 3 cm) installed in the chamber. The second chamber is evacuated by a 6-in diffusion pump (Ulvac, ULK-06) followed by the same mechanical booster and rotary pump system. The sample molecule is multi-photon ionised and is detected by an electron multiplier (Murata, Ceratron EMS-6081B), the applied voltage of which is adjusted to 3.4 kV. The signal is amplified by a home-made operational amplifier and recorded on a strip-chart recorder. Argon is used as the carrier gas, and the stagnation pressure is measured by a Bourdon tube pressure gauge (Nagano, compound gauge).

The separation column of the chromatograph is 25 cm long (stainless steel, i.d. 3 mm), and is packed with silicone SE-30 (Gas Chromatograph Co.), which was developed for the separation of polycyclic aromatic hydrocarbons. The stainless-steel connecting tube was wrapped with heating tape. Typical temperatures of the column and the nozzle were 150 and 100 °C, respectively. The typical stagnation pressure was 200

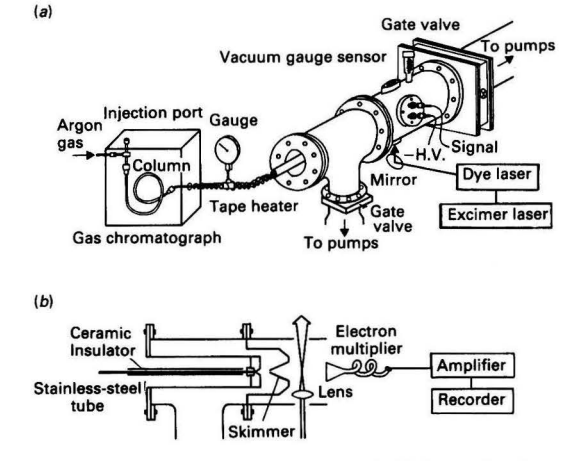

Fig. 1. Gas chromatograph system equipped with detector based on supersonic jet and multi-photon ionisation: (*a*) projection; (*b*) cross-section of nozzle and chamber

* To whom correspondence should be addressed.

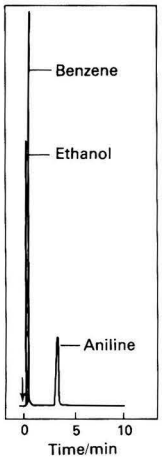

Fig. 2. Chromatogram of a mixture of ethanol (1 μl) and aniline (1 μl) measured with a flame-ionisation detector. The arrow indicates the time of sample injection

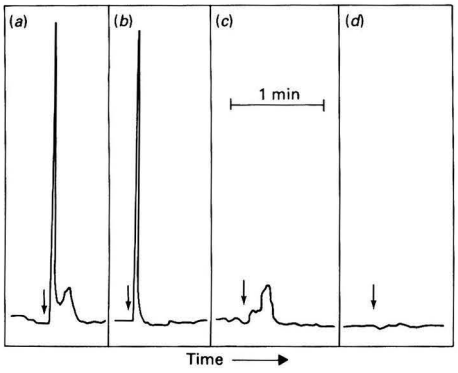

Fig. 3. Chromatograms of standard compounds measured with the multi-photon ionisation detector. (*a*) Ethanol (4 μl) + benzene (2 μl) + aniline (4 μl); (*b*) benzene (2 μl); (*c*) aniline (4 μl); and (*d*) ethanol (4 μl). The arrows indicate the time of sample injection

Torr, the pressure of the second chamber being 10^{-4} Torr during the measurement. The samples were of extra-pure grade and were used without further purification.

Results and Discussion

By bubbling the carrier gas through liquid benzene continuously, the multi-photon ionisation spectrum of benzene was measured. The observed band structure was identical with the previous result reported by Murakami *et al.*[10] A sharp band was observed at 492.75 nm, which corresponds to $14_0^1 1_0^1$ transition from $^1A_{1g}$ to $^1B_{2u}$ states of benzene. Fig. 2 shows a typical chromatogram of a mixture of benzene, aniline and ethanol measured by using a conventional flame-ionisation detector (FID). All the injected components are observed in the chromatogram and there is no drastic difference in their integrated intensities. Fig. 3 shows a gas chromatogram obtained using the multi-photon ionisation method. Benzene gives the largest peak, as the molecule is excited through a strongly resonanced, two-photon process. On the other hand, aniline gives a relatively weak peak. The two-photon energy of the exciting source exceeds the vibronic origin at 293.84 nm of the first allowed singlet - singlet transition ($^1A_1 \rightarrow {}^1B_2$).[11] Then, the exciting wavelength corresponds to the transition into the highly congested levels. Therefore, this small peak is considered to appear as a result of a weakly resonanced two-photon excitation process. Ethanol does not give a peak, as a much larger photon energy is required for two-photon resonance excitation. It is emphasised that a laser chromatographic detector based on supersonic jet and multi-photon ionisation is very useful for the selective determination of sample species and gives no solvent peak.

The retention times and the resolutions are not identical for the chromatograms shown in Figs. 2 and 3, because the stagnation pressure decreased to 200 Torr owing to the high flow-rate of the supersonic jet. A pulsed nozzle may be useful for maintaining the pressure of the carrier gas at the optimum value for sample separation. Further, it increases the density of the molecular beam without increasing the capacity of the pumping system, so that it improves the sensitivity of analysis.

When the applied voltage of the Ceratron was increased to 3.5 kV, three chromatographic peaks corresponding to the three injected components were observed without irradiation of the laser beam. These peaks are useful for clarifying the retention time of all the components. However, there is no selectivity by resonance excitation in this instance. This phenomenon seems to arise from ionisation occurring by friction of sample molecules with the surface of the high-temperature nozzle. These non-specific chromatographic peaks were sensitive to the applied voltage. The latter was carefully adjusted to a value slightly lower than 3.5 kV, thus eliminating these non-specific peaks and allowing a sensitive and selective determination.

A linear calibration graph was obtained from 0 to at least 10 μl of neat benzene. The detection limit achieved by multi-photon ionisation was about 1 μg, where the sample was prepared by stepwise dilution of benzene with methanol. The detection limit was determined by the available laser power. Fluorescence of benzene could not be detected even when saturated benzene vapour was introduced from the nozzle into the chamber. This result shows that the multi-photon method is more sensitive than the fluorimetric method. Alternatively, Hayes and Small[5] have reported obtaining detection limits of 60 ng for naphthalene, 40 ng for α-methylnaphthalene and 14 ng for β-methylnaphthalene by gas chromatography combined with laser fluorimetry. In their study the samples were excited through a one-photon resonance process. The poor detection limit obtained for the multi-photon ionisation method in this study may be due mainly to the small cross-section of the two-photon resonance transition and partly to the low beam density of the supersonic jet. Under the present experimental conditions ($\sigma = 10^{-51}$ cm^4 s photon^{-1} for benzene,[10] laser 500 kW, 20 ns), one molecule is excited to the singlet excited state per laser shot among 2 000 molecules. This is far from optical saturation. An even lower detection limit could be achieved if a strong UV laser source were available for one-photon resonance excitation.

Fig. 4(*a*) shows the chromatogram of a sample of solvent-refined coal measured with a flame-ionisation detector. The chromatogram is composed of many unresolved components, as many aromatic hydrocarbon compounds were present in the sample. Fig. 4(*b*) shows the chromatogram of a mixture of benzene and solvent-refined coal. The peak at the retention time indicated by A might possibly be assigned to benzene from these data. The concentration of benzene in solvent-refined coal could be calculated to be 2.5%, but this was found to be wrong as shown below from the results measured with the multi-photon ionisation technique. Fig. 5(*a*) shows the chromatogram of solvent-refined coal measured with the multi-photon ionisation detector. It can be seen that no peak appears just after sample injection. As shown in Fig. 5(*b*), benzene provides a sharp peak just after injection. From these results, the concentration of benzene in solvent-refined coal

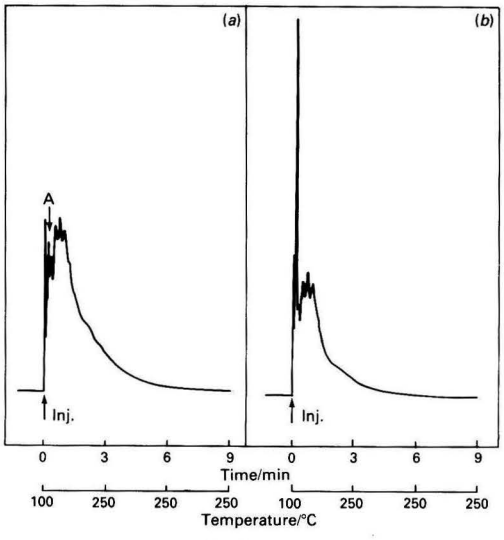

Fig. 4. Chromatograms of real samples measured with a flame-ionisation detector. (*a*) Solvent-refined coal (7 μl); and (*b*) solvent-refined coal (7 μl) + benzene (0.5 μl)

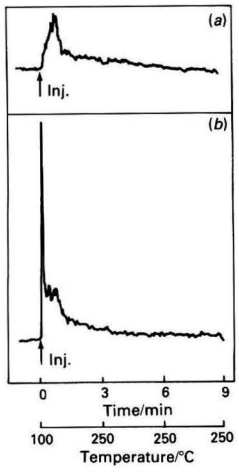

Fig. 5. Chromatograms of real samples measured with the multi-photon ionisation detector. (*a*) Solvent-refined coal (20 μl); and (*b*) solvent-refined coal (20 μl) + 2% benzene in methanol (10 μl)

was calculated to be less than 0.05%. This accurate determination arises from the good selectivity of the supersonic jet technique. It should be noted that the relative sensitivity of benzene to the solvent-refined coal sample is 20 times greater for the multi-photon ionisation detector than the flame-ionisation detector. The components eluting at around the retention time of benzene may have low relative molecular masses and compact structures, and therefore they could not absorb visible emission from the exciting laser. Benzene can exceptionally absorb visible emission owing to a resonanced two-photon absorption process, as the wavelength of the dye laser is exactly adjusted to the two-photon exciting wavelength of the $14_0^1 1_0^1$ transition from $^1A_{1g}$ to $^1B_{2u}$. On the other hand, the flame-ionisation detector is non-specific and is sensitive to other small organic compounds. The present results indicate that the use of a supersonic jet technique and a multi-photon ionisation detector is advantageous for the reliable and selective determination of specific molecules in real samples.

In the multi-photon ionisation method no problem occurs from the background due to light scattering and no loss of sensitivity in ion detection. It is emphasised that multi-photon ionisation provides a very versatile chromatographic detection technique because of its potentially high sensitivity and good selectivity. A fluorescence detector is essentially more selective than the present multi-photon ionisation method, as it has the capability of resolving components in the fluorescence spectrum as well as in the excitation spectrum. However, time-of-flight mass spectrometric analysis[9,12] allows more accurate determinations, and therefore it provides a powerful tool for the trace analysis of real samples containing a large number of unknown compounds.

We thank Yōsuke Maekawa of the Government Industry Development Laboratory, Hokkaido, for a gift of solvent-refined coal. This research was supported by a Grant-in-Aid for Scientific Research (Grant No. 57430016) from the Ministry of Education of Japan.

References

1. Levy, D. H., Wharton, L., and Smalley, R. E., *in* Moore, C. B., *Editor*, "Chemical and Biochemical Applications of Lasers," Volume 2, Academic Press, New York, 1977, Chapter 1.
2. Hayes, J. M., and Small, G. J., *Anal. Chem.*, 1983, **55**, 565A.
3. Warren, J. A., Hayes, J. M., and Small, G. J., *Anal. Chem.*, 1982, **54**, 140.
4. Amirav, A., Even, U., and Jortner, J., *Anal. Chem.*, 1982, **54**, 1666.
5. Hayes, J. M., and Small, G. J., *Anal. Chem.*, 1982, **54**, 1204.
6. Smalley, R. E., *J. Chem. Educ.*, 1982, **59**, 934.
7. Lubman, D. M., and Kronick, M. N., *Anal. Chem.*, 1982, **54**, 1546.
8. Lubman, D. M., and Zare, R. N., *Anal. Chem.*, 1982, **54**, 2117.
9. Lubman, D. M., and Kronick, M. N., *Anal. Chem.*, 1982, **54**, 660.
10. Murakami, J., Kaya, K., and Ito, M., *J. Chem. Phys.*, 1980, **72**, 3263.
11. Leutwyler, S., and Even, U., *Chem. Phys. Lett.*, 1981, **81**, 578.
12. Rhodes, G., Opsal, R. B., Meek, J. T., and Reilly, J. P., *Anal. Chem.*, 1983, **55**, 280.

Paper A3/264
Received August 16th, 1983
Accepted October 10th, 1983

Complementary Analytical Methods for Cyanide, Sulphide, Certain Transition Metals and Lanthanides in Ion Chromatography

Wang-nang Wang, Yeong-jgi Chen and Mou-tai Wu
Chung Shan Institute of Science and Technology, P.O. Box No. 1–4, Lung-Tan, Taiwan, Republic of China

Conventional ion chromatography excludes the analyses of anionic species with pK > 7, and transition metals that can form hydroxide precipitates at neutral pH. These limitations come from the combined characteristics of the suppressor column and the electrical conductivity detector. By suitable selection of the detection system, an extension of analytical limits can be achieved. For fast and accurate analyses of cyanide and sulphide ions, with an electrochemical method involving a silver sulphide based ion-selective electrode and a high pH buffered eluent, the detection limit can reach the p.p.b. level. For determinations of transition and rare earth metal ions, a spectrophotometric detection system is proposed. By post-column mixing with the colour-forming reagents PAR and Arsenazo I, respectively, transition metal and rare earth metal ions can be monitored by measuring the absorbance at 498 and 600 nm. The detection limit can reach the 0.1 p.p.m. level with good precision. The working principle and reaction mechanism of the proposed methods are also discussed in detail.

Keywords: *Ion chromatography; cyanide ion-selective electrode; spectrophotometry; transition metals; lanthanides*

Ion chromatography,[1] with its special separating resin, suppressor column and conductimetric detector, has become a uniquely powerful tool for solving problems involving ions with multi-element detection and matrix problems.

The evolution of ion chromatography in recent years has been somewhat different from that of gas and high-performance liquid chromatography. Performance capabilities have been improved mainly in the field of packing materials, whereas very little has been done in the development of new detectors. The basic limitations in the detection of weak acids and transition metals are not yet totally solved.

The problems involving the detection of weak organic acids are partially solved by the introduction of ion chromatography exclusion mode/ion chromatography (ICE/IC),[2] a single chromatographic system combining ion exclusion and ion chromatography. For cyanide and sulphide determinations, resistivity detection with use of a high conductivity eluent[3] provides one solution; the indirect determination of cyanide by converting HCN with I_2 into I^- and ICN[4] also proves to be a good method. However, the detection limits of either method cannot fulfil the requirements of most environmental protection agencies.

Recently, when the amperometric method[5,6] was developed, the detection limit of cyanide and sulphide finally reached the p.p.b. level. Separations of cyanide and sulphide with other anions also reduced the interferences, but the interference of sulphide in the determination of cyanide was still serious. In practical applications, the hypochlorite and hydrogen peroxide in the cyanide oxidation systems also interfered.

This paper describes an attempt to apply an ion-selective electrode method to the detection system of ion chromatography. Evaluation of this method[7] under flow-stream conditions has shown that it is well suited to the measurement of cyanide in the concentration range 10^{-2}–5×10^{-5} M. The electrode indicator technique[8] extends the detection limit to the 10 p.p.b. level.

Two main types of cyanide electrode are at present commercially available: one of these is manufactured by Orion and consists of a solid membrane of mixed silver sulphide and silver iodide; the other electrode, developed by Pungor and co-workers, consists of a silver iodide impregnated silicone-rubber membrane. However, the work carried out by Veselý and co-workers[9] has shown that a simple silver sulphide electrode also gives a good response to cyanide considering the over-all sensitivity and interferences.

The major drawback in ion chromatography with an ion-selective electrode is the slow response time. In the work described in this paper we tried to obtain in some solutions by considering the flow-rate, effect of pH, influence of temperature, ionic strength, liquid junction of the reference electrode and a modification to the membrane of the working electrode. The normal two-column and single separators, with or without post-column mixing systems, were studied to obtain an optimum condition for the determination of cyanide.

For the separation and detection of transition metals and lanthanides, ion chromatography is limited because the hydroxide-form suppressor column would precipitate most polyvalent cations. A single-column chromatographic system has therefore been developed and different column technologies and a detection system have been studied.

A coulometric detector was developed by Takata and Fujita[10] to study the rapid separation of heavy metal ions by cation-exchange chromatography using sodium tartrate solution as the eluent. Some home-made small particle (8–11 μm) polystyrene - divinylbenzene resins were used as packing materials and the separation of a six-component mixture of metal ions (copper, zinc, nickel, lead, cobalt and cadmium) was completed within 2 min under optimum conditions. Girard[11] modified the detection system by using primary and secondary controlled-potential coulometry, which extended the capabilities of the ion chromatography technique to the analyses of rare earths and heavy metals. Elchuk and Cassidy[12] interfaced a post-column reactor to the high-performance chromatograph; 4-(2-pyridylazo)resorcinol monosodium salt (PAR) was used as the colour-forming reagent, and with spectrophotometric detection at 540 nm most metal ions could be determined in the ng ml^{-1} and pg ml^{-1} ranges. Later Elchuk and Cassidy[13] compared the small particle polystyrene - divinylbenzene resins with bonded-phase packing material; they found that it was difficult to pack stable column beds with small particle resins. Bonded-phase packings, on the other hand, are fairly rigid and exhibit good mass transfer. The narrow pH range over which bonded-phase packings were stable, considered to be 2–8, was a limitation because of the hydrolysis of many metal ions in this pH range; however, this problem can be overcome for most metal ions if complexing agents are used to help effect the separation and keep the metal ions in solution. Sevenich and Fritz[14] developed a single-column method that used a conductivity detector and 1,2-diaminoethane tartrate eluent; this technique not only provided a rapid and highly selective

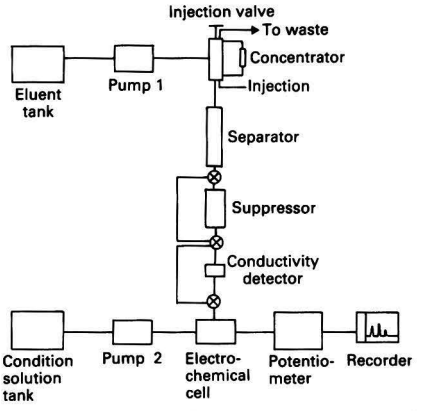

Fig. 1. Schematic diagram of the flow system for the determination of cyanide

method for separating and determining magnesium, calcium and strontium but also extended the application of conductivity detection to some heavy metals.

In the work described in this paper, a single bonded-phase ion-exchange column and post-column mixing system was adopted and two types of mixing chambers were compared. Gradient elution was applied to the separation of transition metals. Various kinds of eluents were tested in order to obtain the optimum conditions.

Experimental

The flow system for cyanide detection is shown in Fig. 1. A Dionex Model-10 Ion Chromatograph was used, the secondary condition solution pump was a Sage Model 375A tubing pump and the detection cell was a modified Metrohm Model 656 electrochemical cell. The fabrication of the silver sulphide and silver sulphide - silver iodide (1 mol + 1 mol) working electrodes has been described elsewhere.[15] Direct connection with nickel wire was used in the solid membrane. The reference electrode was a Metrohm Model EA444 silver - silver chloride electrode. A Beckman Model 3500 digital pH meter was used for potentiometric measurements, and the output from the potentiometer was displayed on a Metrohm Model E586 labograph.

The separator used was a 3 × 250 mm column, slurry packed with 250–325 mesh XAD-1 anion-exchange resin prepared by chloromethylation and amination,[16] the capacity being 0.04 mequiv. g^{-1}. The eluents for this column were a series of 1×10^{-5} potassium hydrogen phthalate solutions, which were adjusted to pH 4.1, 6.25 and 7.1 by the use of sodium tetraborate(III) solution. A Dionex HPIC-AS1 column was also used. For the latter column, 0.003 N sodium hydrogen carbonate plus 0.002 4 N sodium carbonate and 0.01 N sodium hydroxide solutions were used as eluents. The temperature of the system was controlled by a Brookfield Model EX-200 thermostat. Modifications to the working electrodes were carried out by coating the membrane surfaces with Nafion 427 cationic membrane, MA 3475 anionic membrane and Celguard 3501 polypropylene film. To study the basic characteristics of electrodes, the flow system was used without the separator. Interferences before and after the separator was positioned were compared.

Chemicals of analytical-reagent grade (from Aldrich, Fluka and Merk) were used without further purification. Stock solutions of 0.01 N sulphide and cyanide in 0.01 N sodium hydroxide solution were freshly prepared every week and protected in an inert atmosphere. Cyanide and sulphide samples of various concentrations were prepared by dilution of the stock solution just before analysis.

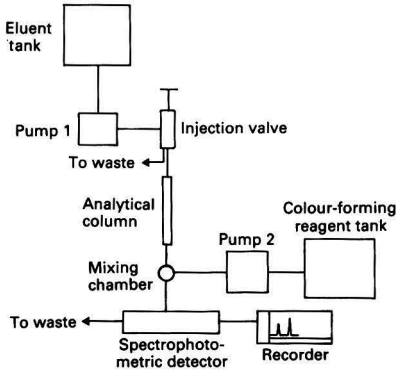

Fig. 2. Schematic diagram of the flow system for the determination of transition metals and lanthanides

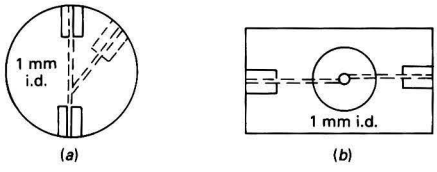

Fig. 3. Configuration of the mixing chamber; (*a*) Y-type; (*b*) tangent-type

The flow system for the detection of transition metals and lanthanides is shown in Fig. 2. Gradient elutions were performed with two M6000A Waters Associates pumps equipped with a Waters M660 gradient programmer. Samples were injected via a Rheodyne M7125 valve. The post-column reactant was added with a constant flow SAGE Model 375A tubing pump at the same flow-rate as was used for elution of the metal ions from the column. The eluate was monitored with a Spectra Physics Model 770 ultraviolet - visible spectrophotometer.

All samples were injected directly or after simple dilution and the 20-µl sample loop was used for both cation and anion analyses. For on-column pre-concentration, the sample was injected by a syringe into the concentrator column in the reverse direction to normal eluent flow. The concentrator column for cyanide was composed of 4 × 10 mm polypropylene tubing packed with 250–325 mesh XAD-1 anion-exchange resin was 0.04 mequiv. g^{-1} capacity; that for transition metals was the same type of column packed with surface sulphonated XAD-1 resin of 0.5 mequiv. g^{-1} capacity. The output from the detector was fed directly into a Shimadzu CR-1A Chromatopac for the calculation of peak areas and retention times.

All wetted components and tubing were either coated with or made of PTFE except the column and injection valve. The eluate and post column colour-forming reagent were mixed via two types of mixer, the tangent-type and the Y-type (Fig. 3). Vydac 401 TP 4.6 20 µm, Nucleosil SA 10 µm and Partisil SCX 10 µm 4 × 300 mm columns were used as separators. Different types of chelating eluents, such as citric acid, tartaric acid, 2-methyllactic acid and lactic acid were studied. The pH effect of eluents were also tested.

All metals were reagent grade nitrate or perchlorate salts. The colour-forming reagents for the detection of the metal ions were PAR [4-(2-pyridylazo)resorcinol monosodium salt] (Aldrich Chemical Co., Milwaukee, WI, USA) and Arsenazo I [3-(2-arsenophenylazo]-4,5-dihydroxy-2,7-naphthalene-disulphonic acid trisodium salt] (Eastman Organic Chemicals, Rochester, NY, USA).

PAR 1 reagent was prepared by adding 121.1 g of tris(hydroxymethyl)aminomethane (THAM) and 0.125 g of PAR to about 500 ml of de-ionised water, following which the pH was adjusted to 9.0 with concentrated hydrochloric acid. The solution was then diluted to 1 l with de-ionised water. PAR 2 was prepared by dissolving 0.005% PAR in 2 M ammonia solution and 1 M ammonium acetate, the pH being about 11. PAR - ZnEDTA reagent was prepared by first mixing equivalent amounts of standardised 0.01 M zinc perchlorate and 0.01 M EDTA solutions, then adding an equimolar amount of 0.05 M PAR solution at pH 11. The Arsenazo I (1×10^{-3} mol l^{-1}) solution was dissolved in 3 ml l^{-1} ammonia solution.

Results and Discussion

Determination of Cyanide

Measurements for calibration of the electrode under flow conditions were carried out with a cyanide concentration of from 10^{-1} to 10^{-7} M with 0.01 M sodium hydroxide solution as the background electrolyte. The calibration graph for the silver sulphide - silver iodide electrode is shown in Fig. 4. The calibration graph for the silver sulphide electrode is similar. The potential response over background electrolyte for the mixed electrode was about −232 mV, and the daily drift was below 5 mV. A silver sulphide electrode gave a faster and more negative response (−349 mV).

The purpose of this study was to apply the ion-selective electrode to the detection system for ion chromatography. Therefore, the slow response time of the ion-selective electrode became the major problem. (The measured response time is defined as the time required for the electrode to reach 90% of its steady-state potential after a rapid change in ion activity.) In the course of the study various factors were tested to obtain the optimum conditions. The effect of pH on the electrode response is shown in Fig. 5. Neither the sensitivity nor the response time showed any significant improvement for pH values above 10.

The flow-rate dependence of electrodes was anticipated (Fig. 6), because the electrode response was established via a diffusion layer. The sensitivity decreased with increase in flow-rate, but the response time was reversed. An improvement of about three-fold was observed from 0.76 to 3.04 ml min^{-1} (equivalent response time from 3 to 1 min). Therefore, the 2 ml min^{-1} flow-rate was adopted for future experiments.

From 25 to 50 °C, the silver sulphide electrode showed a response about −46 mV more negative for 10^{-4} M cyanide, the response for background electrolyte being −10 mV more negative. The net increase in sensitivity was about 30%. The temperature gradient for a silver sulphide electrode is therefore about 0.72 mV $°C^{-1}$.

Controlling the ionic strength of the eluent and using concentrated filling solutions in the liquid junction of the reference electrode did not give any significant improvement in sensitivity or response time, but a reproducible potential was obtained from day to day.

The results of modifying the electrode surface with different films are shown in Fig. 7. Both ionic membrane coatings gave non-Nernstian and poor sensitivity. However, Nafion 427 cation-exchange membrane showed a faster response. The Celguard gave almost the same sensitivity as a normal electrode but a slower response time. Consequently, considering all the basic characteristics of electrodes, the silver sulphide electrode was used as the working electrode. The calibration graph of cyanide with a simple XAD-1 separator and 0.01 N sodium hydroxide solution eluent is shown in Fig. 8. In order to examine on-column pre-concentration with home-made XAD-1 anion-exchange resin, 1 ml of each of four samples containing 4, 8, 17 and 26 p.p.b. of cyanide was

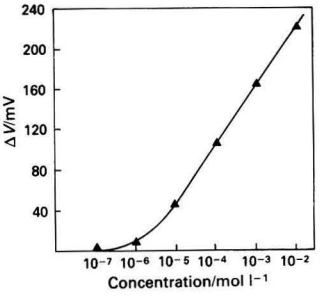

Fig. 4. Calibration graph of cyanide using mixed silver sulphide - silver iodide electrode

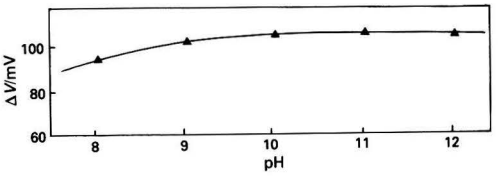

Fig. 5. Effect of pH on the potential response of mixed silver sulphide - silver iodide electrode

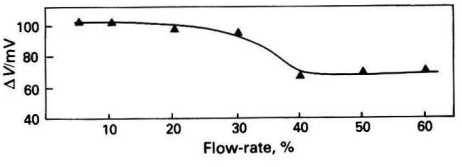

Fig. 6. Dependence of electrode response on flow-rate. A silver sulphide electrode was used; 10^{-4} M cyanide solution; 100% flow-rate = 460 ml h^{-1}

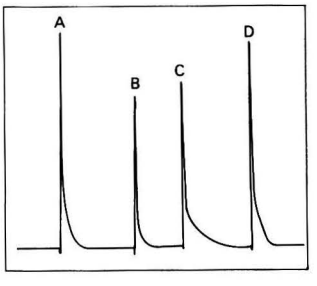

Fig. 7. Response curves of different surface coatings: A, normal electrode; B, cationic membrane; C, anionic membrane; and D polypropylene film

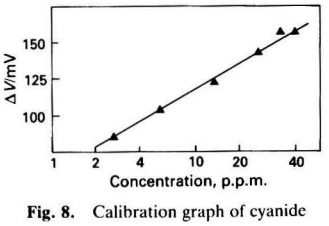

Fig. 8. Calibration graph of cyanide

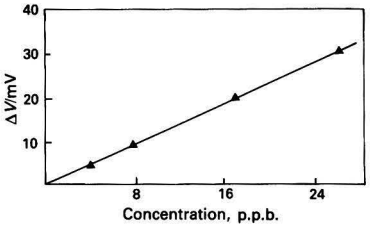

Fig. 9. Calibration graph of 1 ml of pre-concentrated cyanide sample

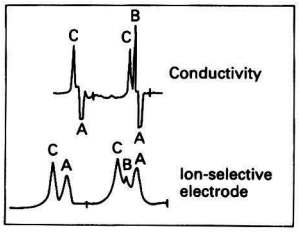

Fig. 10. Separation of cyanide from bromide and iodide: A, H_2O + HCN (CN^-, 2.6 p.p.m.); B, Br^-, 5 p.p.m.; and C, I^-, 5 p.p.m.

tested. Non-Nernstian response was observed and a linear relationship between concentration and potential was obtained (Fig. 9). After the separator was employed, bromide, iodide and thiocyanate ions no longer interfered. A test run using XAD-1 anion-exchange separator, 1×10^{-5} M potassium hydrogen phthalate solution (pH 6.25) eluent and post-column mixing with 0.02 N sodium hydroxide conditioning solution gave very reproducible recoveries (Fig. 10).

As the H_2S and HS^- forms exist under these eluent conditions, sulphide interferences were still present but were being reduced. By using an HPIC-AS1 column and 0.01 N sodium hydroxide solution eluent, sulphide interferences were mostly removed. Under these conditions the sulphide can also be determined without interference from cyanide. On an anion-exchange column of HPIC-AS4, using an eluent consisting of 14.7 mM 1,2-diaminoethane, 10 mM sodium dihydrogen borate and 1.0 mM sodium carbonate solutions, the sulphide can be separated and detected with even greater sensitivity.

Determination of Transition Metals and Lanthanides

For all three reagents, colour formation was instantaneous and the colour was stable for at least 30 min; the relative absorbances of some transition metals with PAR 1, PAR 2 and PAR - ZnEDTA is shown in Table 1. Except with Pb^{2+} and Mn^{2+}, the PAR 1 solution gave good responses.

Lactic acid and 2-methyllactic acid have been shown to be the best complexing reagents available for the ion-exchange separation of both transition metals and lanthanides. Because all of the eluents were complexing reagents, the competition reactions between eluents and post-column colour-forming reagents were studied. The absorbance in the three PAR reagents was hardly influenced by any of the eluents tested. For some lanthanide - Arsenazo I complexes, there was a slight enhancement of absorbance at higher concentrations of 2-methyllactic acid and lactic acid and this was attributed to possible ternary complex formation.

The important factors that influence the sensitivity and resolution of metal ions are dead volume effects, the rate of reaction between reagent and metal ions, background absorbance and noise and the efficiency of the mixing cell. The dead volume of both tangent-type and Y-type mixing chambers is

Table 1. Relative absorbance for some metals with PAR 1, PAR 2 and PAR - ZnEDTA. Detector at 498 nm (0.1 a.u.f.s.); 10 p.p.m. sample; 20-μl injection volume

Metal	Absorbance × 10^2		
	PAR 1	PAR 2	PAR - ZnEDTA
Fe^{3+}	6.2	5.1	1.0
Cu^{2+}	11.5	11.7	11.7
Zn^{2+}	11.1	11.0	9.8
Ni^{2+}	9.6	10.0	9.2
Co^{2+}	6.8	7.0	7.0
Pb^{2+}	0.7	0.6	2.9
Cd^{2+}	2.5	2.6	1.5
Fe^{2+}	3.0	2.2	0.8
Mn^{2+}	0.7	0.6	4.2

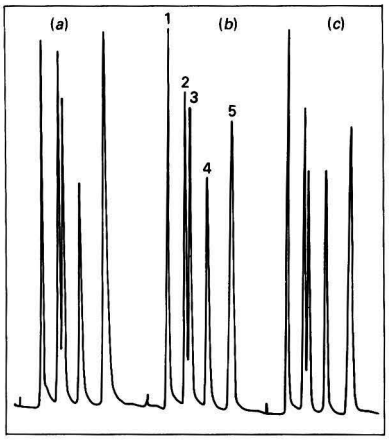

Fig. 11. Separation of transition metals on 10-μm Nucleosil SA with different PAR reagents and mixing chambers. (*a*) Tangent-type, PAR 1; (*b*) tangent-type, PAR - ZnEDTA; (*c*) Y-type, PAR - ZnEDTA. (1) Cu, 16.0 p.p.m.; (2) Zn, 9.5 p.p.m.; (3) Ni, 10.3 p.p.m.; (4) Co, 10.7 p.p.m.; and (5) Cd, 56.8 p.p.m.

about 1 μl. The resolution and mixing efficiency of these mixing devices are shown in Fig. 11. For a total flow-rate of 2 ml min^{-1}, the tangent-type device has shown a better mixing efficiency, but the Y-type device gave the better resolution and was consequently used in the detection of metal ions.

To minimise the short-term fluctuations in flow-rate, a Tracor Model 950 HPLC pump was used in isocratic elution, the switch being set to constant-flow mode. Filling the reference cell with the mixing solution of reagent and eluent, removing the heat exchanger of the ultraviolet - visible spectrophotometer and de-gassing and filtering the eluent and reagent reduced the background absorbance and noise to a minimum; this noise level could be maintained at 2×10^{-4} absorbance unit in routine analysis.

The results shown in Figs. 12 and 13 are representative of the separations that were obtained on the different ion exchangers studied in this work. The column packed with 10-μm Nucleosil SA gave the best results, with a total separation time of 16 min. The resolution of the home-made cation-exchange resin was very poor, the main reason being the large particle size (40 μm) and the column pressure of only 380 lb in^{-2}.

The effect of pH on the separations was examined and it was found that at the start of the separation on bonded phases the eluent was susceptible to significant pH changes as a result of protons liberated on complexation with lactic acid. The isocratic separation of some metals under pH 3.5 is shown in Fig. 14.

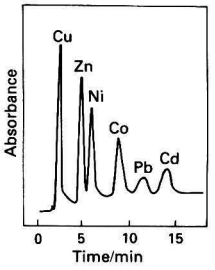

Fig. 12. Separations of the transition metals on Vydac 401 TP 4.6, 300 × 4 mm i.d. column. Experimental conditions: 20-µl sample loop; 0.12 mol l^{-1} sodium lactate, pH 4.5; 0.1 a.u.f.s.; detection at 498 nm after post-column reaction with PAR - THAM

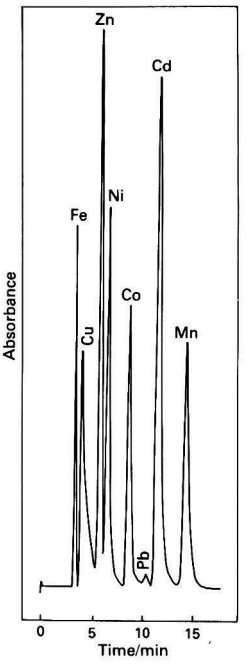

Fig. 13. Separation of transition metals on 10-µm Nucleosil SA. Sample size: Fe(III), 10 p.p.m.; Cu, 10 p.p.m.; Zn, 10 p.p.m.; Ni, 10 p.p.m.; Co, 10 p.p.m.; Pb, 0.5 p.p.m.; Cd, 50 p.p.m.; and Mn, 10 p.p.m. Experimental conditions: 300 × 4 mm i.d. column; 20-µl sample loop; 0.1 M sodium lactate, pH 4.5; detection at 498 nm after post-column reaction with PAR - THAM

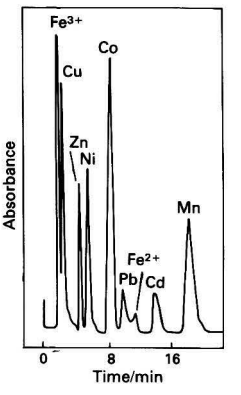

Fig. 15. Separation of transition metals on 10-µm Nucleosil SA. Sample size: Fe(III), 22 p.p.m.; Cu, 10 p.p.m.; Zn, 10 p.p.m.; Ni, 10 p.p.m.; Co, 26 p.p.m.; Pb, 4.4 p.p.m.; Fe(II), 5 p.p.m.; Cd, 10 p.p.m.; and Mn, 50 p.p.m. Experimental conditions: 300 × 4 mm i.d. column; 20-µl sample loop; linear programme from 0.04 to 0.12 mol l^{-1} sodium lactate over a 20-min period at flow-rate 1 ml min^{-1} and pH 4.5; detection at 510 nm after post-column reaction with PAR - ZnEDTA

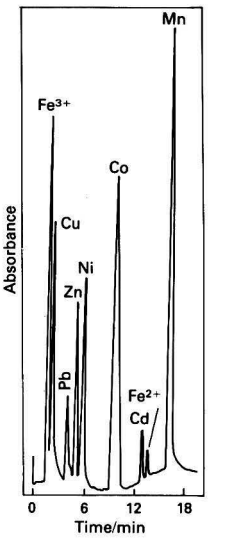

Fig. 16. As Fig. 15, except a linear programme from 0.04 to 0.18 mol l^{-1} sodium tartrate eluent was used

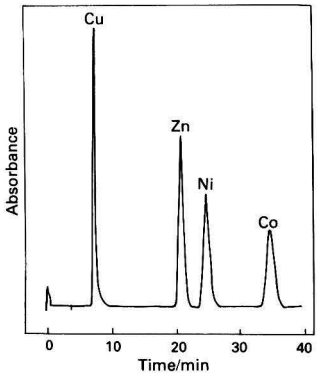

Fig. 14. Separation of transition metals on 10-µm Nucleosil SA. Experimental conditions as in Fig. 13, except the pH of sodium lactate is 3.5

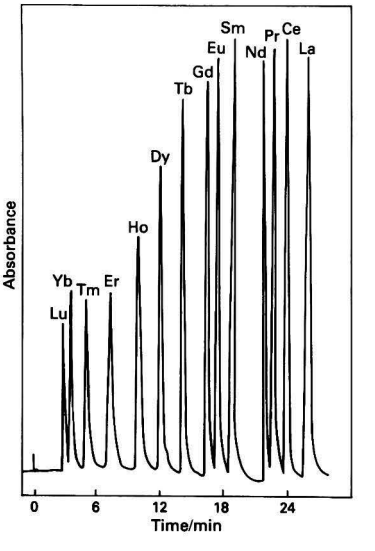

Fig. 17. Separation of lanthanides on 10-µm Nucleosil SA. Experimental condition: 300 × 4 mm i.d. column; 20 µl of a solution containing *ca.* 10 µg ml^{-1} of each lanthanide; linear programme from 0.01 to 0.04 mol l^{-1} 2-methyllactic acid over a 30-min period at flow-rate 1 ml min^{-1} and pH 4.6; detection at 600 nm after post-column reaction with Arsenazo I

Better separation of transition metals and lanthanides with gradient elution is shown in Figs. 15, 16 and 17. Iron(III) and iron(II) could be determined simultaneously without the interferences from other transition metals. The elution time of lead(II) changed owing to its different complex formation constants with tartrate and lactate.

The optimum reagent concentrations were found to be 1×10^{-3} M for PAR and Arsenazo I, and with the flow system used in this work a linear working range from 5 to 2 000 ng for most metal ions was obtained. The reproducibility of eight transition metal separations was very good with an average relative standard deviation below 2.0%.

Fig. 18 shows a chromatogram that was obtained after a 10-ml sample, containing 5 p.p.b. of lead, 5 p.p.b. of manganese and 0.1 p.p.m. of other metals, was preconcentrated on-column on to a 40-µm home-made cation-exchange resin. The peak to peak resolution of the metal ions was similar to those obtained from normal separations.

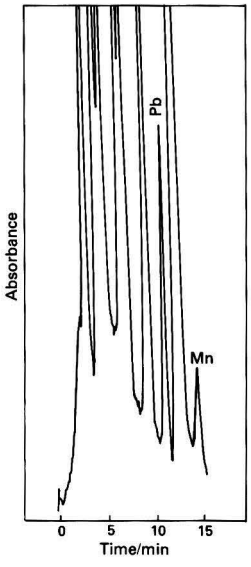

Fig. 18. Separation of transition metals after on-column pre-concentration of 5 p.p.b. of Pb, 5 p.p.b. of Mn and 0.1 p.p.m. of six other metals. Experimental conditions as in Fig. 13

Conclusion

Potentiometric measurement using a silver sulphide based ion-selective electrode proved to be a feasible method for the detection system of ion chromatography, although some further studies on the improvement of response time will be necessary. The silver sulphide and the mixed silver sulphide - silver iodide electrodes both provided sensitive and reproducible responses for cyanide and sulphide. The silver sulphide electrode gave the faster and more sensitive response compared with the mixed electrode. Employment of the separator removed most anionic interferences for the detection of cyanide: pH 10–12 background electrolytes, 2–3 ml min^{-1} flow-rate, double-junction reference electrode with concentrated filling solution (4 M potassium nitrate solution) and a linear-type cell geometry comprised the optimum experimental conditions.

PAR and Arsenazo I proved to be very sensitive reagents in the spectrophotometric detection of transition metals and lanthanides. Post-column mixing with conditioning solution is not only a viable method for the efficient and sensitive detection of small concentrations of metal ions, but also provides a larger space in the selection of eluents for the separation and detection of cyanide.

On-column pre-concentration is an attractive method for the quantitative analysis of ultra-trace concentrations of cyanide and metal ions, the detection limit of cyanide and most transition metals reaching the p.p.b. level.

The preliminary test of the cyanide residue determination in oxidation systems of cyanide waste treatment is very promising, and future applications of the spectrophotometric determination of transition metals in plating industries are now also under investigation.

References

1. Small, H., Sevens, T. S., and Bauman, W. C., *Anal. Chem.*, 1975, **47**, 1801.
2. Rich, W., Smith, F., Jr., McNeil, L., and Sidebottom, T., *in* Mulik, J. D., and Sawicki, E., *Editors*, "Ion Chromatographic Analysis of Environmental Pollutants," Volume 2, Ann Arbor, MI, 1978, p. 17.
3. Pinschmidt, R. K., *in* Mulik, J. D., and Sawicki, E., *Editors*, "Ion Chromatographic Analysis of Environmental Pollutants," Volume 2, Ann Arbor, M1, 1978, p. 41.
4. DuVal, D. L., Fritz, J. S., and Gjerde, D. T., *Anal. Chem.*, 1982, **54**, 830.
5. Pihlar, B., Kosta, L., and Hristovski, B., *Talanta*, 1979, **26**, 805.
6. Rocklin, R. D., and Johnson, E. L., *Anal. Chem.*, 1983, **55**, 4.
7. Fleet, B., and Von Storp, H., *Anal. Chem.*, 1971, **43**, 1575.
8. Frant, M. S., Ross, J. W., Jr., and Riseman, J. H., *Anal. Chem.*, 1972, **44**, 2227.
9. Veselý, J., Jensen, O. J., and Nicolaisen, B., *Anal. Chim. Acta*, 1972, **62**, 1.
10. Takata, Y., and Fujita, K., *J. Chromatogr.*, 1975, **108**, 255.
11. Girard, J. E., *Anal. Chem.*, 1979, **51**, 836.
12. Cassidy, R. M., and Elchuk, S., *J. Chromatogr. Sci.*, 1980, **18**, 217.
13. Elchuk, S., and Cassidy, R. M., *Anal. Chem.*, 1979, **51**, 1435.
14. Sevenich, G. J., and Fritz, J. S., *Anal. Chem.*, 1983, **55**, 12.
15. Cammann, K., *translated by* Schroeder, A. H., "Working with Ion-Selective Electrodes," Springer-Verlag, New York, 1979, p. 61.
16. Gjerde, D. T., *PhD Thesis*, Iowa State University, Ames, IA, 1980.

Paper A3/257
Received August 11th, 1983
Accepted October 10th, 1983

Variable Time-constant Differentiation in Chromatography

John C. Berridge and Keith S. Andrews
Analytical Chemistry Department, Pfizer Central Research, Sandwich, Kent, CT13 9NJ, UK

The mathematical process of differentiation is useful for enhancing the resolution of chromatographic peaks and reducing interferences caused by a slowly changing detector response. Conventional differentiators use fixed time constants and this necessarily means that, when the chromatographic conditions are held constant, later eluting peaks are increasingly attenuated. By using a microcomputer to store chromatograms and calculate derivatives, the time constant of the derivative can be increased through the chromatogram so that the time constant is optimum for the whole of the derivative. Examples from gas and liquid chromatography are given to demonstrate the value of the technique for qualitative and quantitative analysis.

Keywords: *Gas chromatography; high-performance liquid chromatography; differentiation; time constant; resolution enhancement*

The mathematical derivative technique as an aid to qualitative and quantitative analysis has been applied to many areas of spectroscopy[1,2] and, more recently, to gas, liquid and thin-layer chromatography.[3–7] The most usual procedure for chromatography is to differentiate the detector output to generate first, second or higher order derivatives of the output voltage with respect to time. It is principally the even-ordered derivatives that find analytical use as they are characterised by a central peak that is coincident with, but narrower than, the original zero-order peak. This property makes differentiation a useful tool for the enhancement of resolution. Additionally, the derivative process discriminates against broad bands increasingly as the derivative order increases, thereby permitting the suppression of broad overlapping peaks and base-line variations.

The production of derivatives in HPLC and GLC can be readily achieved using analogue resistance - capacitance devices,[3,4] or by a microcomputer using a suitable algorithm.[8] However, the use of analogue devices and of computational methods, such as Savitsky - Golay polynomials,[9] can be limited by the fixed time constants of these methods. In isocratic liquid chromatography and isothermal gas chromatography the peak width increases approximately in proportion to time and the sensitivity of the derivative method will decrease as the chromatogram proceeds. Excoffier and Guiochon[10] have recently reported the use of a pseudo derivative function for enhanced peak sensing. We decided to investigate the possibility of overcoming the problems of decreasing derivative sensitivity by extending their concept to the calculation of derivatives of chromatograms stored in the computer memory by a method that enables the time constant of the derivatives to be increased throughout the chromatogram.

Theoretical

A chromatogram is stored in the computer memory as a set of digitised detector signals (y_i) sampled at equally spaced time intervals Δt. The first derivative may be obtained as the detector signal differences between points α increments apart with the computed values plotted at the mid-point of the differentiating interval[11]:

$$y_i' = y_{i+\frac{\alpha}{2}} - y_{i-\frac{\alpha}{2}} \quad \ldots \quad (1)$$

The differentiating interval α should be as large as possible to maximise the signal to noise ratio, consistent with the degree of resolution enhancement required. Optimum values of α will usually be found in the range 0.1–1W, where W is the band width at half-height.

A fundamental property of the derivative process is the discrimination against broad bands in favour of sharper bands, for a given derivative time constant. Thus the relative nth derivative amplitudes A_{n1} and A_{n2} of two peaks of band widths W_1 and W_2 ($W_1 > W_2$) will be[1]

$$\frac{A_{n1}}{A_{n2}} \propto \frac{W_2^n}{W_1^n} \quad \ldots \quad (2)$$

This discrimination is clearly of great utility in the suppression of chromatographic interferences but also has the consequence of reducing the derivative amplitude of later eluting, broader chromatographic peaks.

A pseudo derivative function, mathematically analogous to that reported by Excoffier and Guiochon,[10] can be defined [equation (3)], in which the differentiation interval is increased with time:

$$y_i' = y_{i+j} - y_{i-j} \quad \ldots \quad (3)$$

$j = 1, 2, 3, \ldots$ Here j is increased as the chromatogram proceeds to give optimum resolution enhancement throughout the derivative and maximum signal to noise ratio, consistent with the resolution enhancement. One application of the pseudo derivative function will, therefore, yield a first derivative in which later peaks have not suffered progressive attenuation. The band widths of the derivative peaks will be reduced compared with the original chromatogram but will, of course, still increase during the derivative. Thus, a similar argument, with similar conclusions, applies to the generation of higher order derivatives that are simply produced by successive applications of the original function. The qualitative improvements in performance are self-evident and the procedure should also be of quantitative value provided that all chromatograms and derivatives are obtained in an identical manner.

Experimental

Gas Chromatography

A Pye 304 gas chromatograph equipped with a flame-ionisation detector was used. The glass column was 2.1 m × 4 mm i.d., packed with 3% OV-17 on acid-washed Chromosorb W. The column temperature was 150 °C.

Liquid Chromatography

A Pye LC3 pump and variable-wavelength detector operating at 219 nm were used. The column was 10 × 0.5 cm i.d., packed with Spherisorb ODS of 5 μm diameter. The injection size was 10 μl and samples were injected with a curtain flow valve

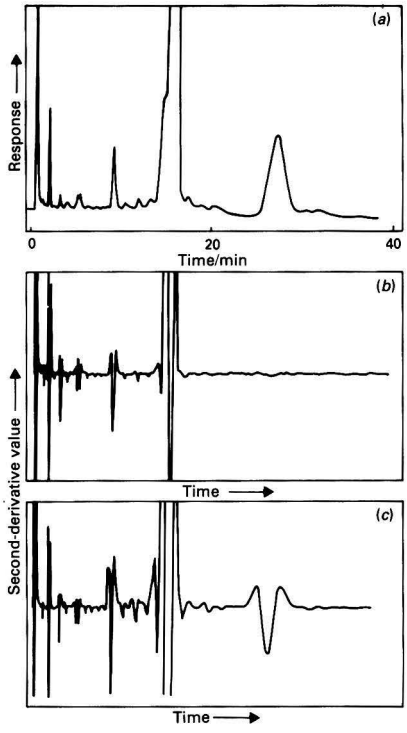

Fig. 1. (*a*) Gas-chromatographic separation of impurities in hexacosane; (*b*) second derivative using fixed time constant; and (*c*) second derivative using an increasing time constant

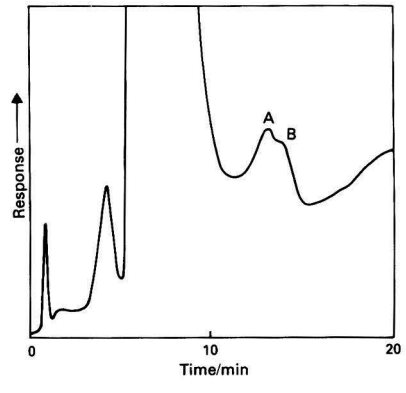

Fig. 2. HPLC separation of impurities in crude tioconazole. For conditions see text

injector.[12] The mobile phase was methanol - acetonitrile - water - ammonia (200 + 220 + 200 + 1) and the flow-rate was 1 ml min^{-1}.

Calculations

Chromatograms were digitised at a sampling rate of 0.5 Hz and stored in memory using a Model 301 computing integrator (Laboratory Data Control). Derivatives were calculated by programs written in BASIC and machine code. Fixed time base

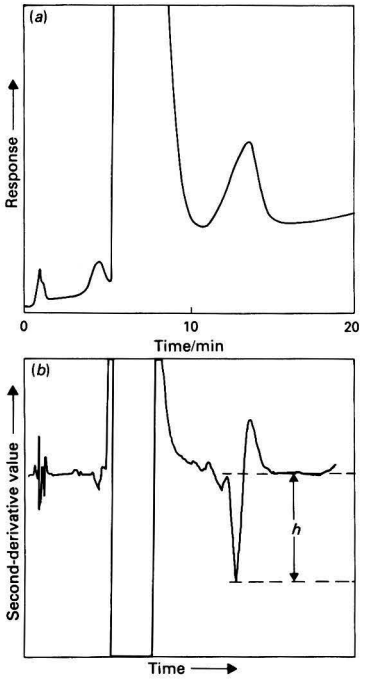

Fig. 3. HPLC separations of impurities in a crude tioconazole sample spiked with 3% impurity B. (*a*) Zero order; and (*b*) second derivative using an increasing time constant

derivatives were calculated by successive differences using a program entitled DIFF.[13] Variable time base derivatives were calculated by successive differences using a program entitled VARDIFF; the differentiation interval was increased every 100 points.

Results and Discussion

Gas Chromatography: Qualitative Application

Fig. 1(*a*) shows the gas-chromatographic analysis of trace impurities in a sample of hexacosane. The zero-order chromatogram shows partially resolved peaks at the start of the chromatogram and a partially resolved component on the leading edge of the main peak. Fig. 1(*b*) shows the second derivative calculated with a fixed time constant. Resolution enhancement of early peaks is clearly seen but the peak amplitude deteriorates rapidly as the chromatogram proceeds: indeed, the last peak, clearly seen in the original chromatogram, has been lost in the noise of the second derivative.

In Fig. 1(*c*), the second derivative was calculated with an increasing differentiation interval for both the first- and second-derivative calculations. The resolution enhancement is as before but the signal to noise ratio is improved throughout the whole derivative. Moreover, the amplitudes of the derivative peaks closely follow the peak heights seen in the original chromatogram.

Liquid Chromatography: Quantitative Application

Tioconazole is a recent broad-spectrum antifungal agent.[14] During the development of synthetic routes to this compound, it was necessary to monitor the levels of reaction by-products in the crude material; HPLC was the method of choice.

Even with a highly optimised chromatographic system, the separation of impurities A and B is incomplete and very dependent on column performance. A below-standard column will produce the separation shown in Fig. 2. However, the levels of the impurities A and B can be readily determined using the standard additions method. To overcome the inadequate resolution, the peak heights are measured from the second derivative, as calculated by the variable time-constant program, VARDIFF. Fig. 3(*a*) shows a sample of crude tioconazole spiked with 3% *m/m* of impurity B; note the drift in the base line and the lack of resolution between components A and B. Fig. 3(*b*) is the second derivative of the chromatogram. Here the base-line fluctuations have been eliminated and adequate resolution between peaks due to A and B has been achieved. Despite a modest increase in noise, the peak height (h) due to B can be measured without difficulty.

A linear calibration graph was fitted to the plots of the amplitudes of the second derivatives (y'') against percentage added for duplicate injections of an unspiked test solution and standard additions of 1.0, 2.0 and 3.0% *m/m* of the impurities A and B. The equations of the curves were determined as

$$y_A = 2.74[A] + 2.04 \text{ correlation coefficient } r = 0.998$$

and

$$y_B = 1.27[B] + 1.67 \text{ correlation coefficient } r = 0.999$$

respectively, enabling the concentration of A and B to be determined as 0.7 and 1.3% *m/m*, respectively, in the sample of crude tioconazole under test whose chromatogram is shown in Fig. 2.

Conclusions

Variable time constant derivative techniques can be used successfully for both qualitative and quantitative chromatographic applications. Such methods confer the advantages of optimised resolution enhancement throughout the chromatogram and maximum signal to noise ratios without extra smoothing.

References

1. Fell, A. F., *UV Spectrom. Bull.*, 1980, **5**, 5.
2. Talsky, G., Mayring, L., and Kreuzer, H., *Angew. Chem., Int. Ed. Engl.*, 1978, **17**, 785.
3. Linnett, L. M., and Atkinson, D. J., *J. Chromatogr.*, 1980, **197**, 1.
4. Zelt, D. T., Owen, J. A., and Marks, G. S., *J. Chromatogr.*, 1980, **189**, 209.
5. Fell, A. F., *Anal. Proc.*, 1980, **17**, 512.
6. Berridge, J. C., *Chromatographia*, 1982, **16**, 172.
7. Travaset, J., Such, V., Gonzalo, R., and Gelpi, E., *J. Chromatogr.*, 1981, **204**, 51.
8. Gans, P., *Anal. Proc.*, 1982, **19**, 33.
9. Savitsky, A., and Golay, M. J. E., *Anal. Chem.*, 1964, **36**, 1627.
10. Excoffier, J. L., and Guiochon, G., *Chromatographia*, 1982, **15**, 543.
11. Butler, W. L., and Hopkins, D. W., *Photochem. Photobiol.*, 1970, **12**, 451.
12. Andrews, K. S., and Turner, D., *Chromatographia*, 1982, **16**, 175.
13. "Application Note No. 8202A," Laboratory Data Control, Stone, Staffs.
14. Jevons, S., Gymer, G. E., Brammer, K. W., Cox, D. A., and Leeming, M. R. G., *Antimicrob. Agents Chemother.*, 1979, **15**, 597.

Paper A3/259
Received August 11th, 1983
Accepted October 5th, 1983

Automated Multiparameter Optimisation of High-performance Liquid Chromatographic Separations Using the Sequential Simplex Procedure

John C. Berridge
Analytical Chemistry Department, Pfizer Central Research, Sandwich, Kent, CT13 9NJ, UK

The use of the sequential simplex procedure for the automated optimisation of mobile phase composition, temperature and flow-rate is described. The simplex procedure has been incorporated into a BASIC program for a microcomputer-controlled chormatograph and has been used in the development of reversed-phase ion-pair separations where pH, ion-pair concentration, ternary mobile phase composition, eluent flow-rate and temperature have all been simultaneously and automatically optimised.

Keywords: *High-performance liquid chromatography; sequential simplex procedure; automated optimisation*

There is increasing interest in the automation of separation development in high-performance liquid chromatography (HPLC) and there are several schemes[1-4] that have been applied to the automated optimisation of separations. The major emphasis of these schemes has been on the optimisation of selectivity of reversed-phase separations using two, three or even four solvents. Little attention has been given to the automated optimisation of pH, ion-pair concentration, flow-rate or temperature, even though their effects on the separation may be at least as important as those of the main mobile phase constituents.

It has been demonstrated recently[4,5] that both reversed-phase and normal-phase separations can be optimised automatically using the sequential simplex procedure[6] and a microcomputer-controlled chromatograph. The simplex procedure is a general optimisation procedure and is ideally suited to the optimisation of many interdependent variables such as are found in HPLC. The aim of this work was to demonstrate the applicability of the sequential simplex procedure to the automated optimisation of temperature, flow-rate and mobile phase composition, the mobile phase to be selected from three constituents to give control over solvent strength, pH and/or ion-pair concentration.

Experimental

The system used was an Analyst 7800 chromatograph (Laboratory Data Control, Stone, Staffs., UK), consisting of a Spectromonitor III variable-wavelength ultraviolet spectrophotometric detector, two Constametric III pumps and a 60-position autosampler. For three-component mobile phases a third Constametric III pump was added. The separations were carried out using stainless-steel columns packed with Ultrasphere I.P. (Beckman), 15 cm × 0.46 cm i.d. or 4 cm × 0.46 cm i.d. The columns were contained in a water-jacket (Alltech Associates, Carnforth, Lancs., UK), the water being heated by a recirculating heater (Haake, Karlsruhe, FRG). The whole system was controlled by a Chromatography Control Module (CCM; Laboratory Data Control).

Column temperature monitoring was achieved by using an integrated circuit temperature transducer (Part No. 590KH, R.S. Components, London, UK) and resistance circuit to produce a voltage directly proportional to temperature; this voltage was fed to the second integration channel of the CCM for analogue to digital conversion. The heater of the water-bath was controlled by using a relay contained within the CCM HPLC interface. Over-all temperature control could be maintained within ±0.5 °C with an accuracy of ±1 °C.

All solutes were of analytical-reagent grade and were used as received. Commercially available buffer salts and ion-pair reagents were used without further purification. Water was freshly distilled in glass and methanol was of HPLC grade (Rathburn Chemicals, Peebles, UK).

Software

The optimisation of three solvent mobile phases, flow-rate and column temperature was carried out under the control of a BASIC program entitled MULTOPT. The program is essentially an extension of a program TERNOPT, which has been described previously.[4] The program uses the modified sequential simplex procedure[6] to direct the adjustment of experimental parameters towards the conditions that give the best chromatographic separation. The quality of each separation is assessed at the end of the chromatogram by calculating the value of a chromatography response function (*CRF*),[4,5] which describes the separation quality in terms of resolutions, the number of peaks detected and the analysis time. The form of the *CRF* used in this work was

$$CRF = \Sigma R + N^a - b|T_L - T_A| + c(T_1 - T_o)$$

where

R	=	resolution between adjacent peaks;
N	=	number of peaks detected;
T_A	=	specified analysis time (minutes);
T_L	=	retention time of last peak;
T_1	=	retention time of first peak;
T_o	=	specified minimum retention time;
a,b,c	=	operator-selectable weightings.

Although at first sight the optimisation of three solvents, flow-rate and temperature appears to be a five-variable optimisation, it is easily reduced to four variables as the proportion of the third solvent is directly dependent on the proportions of the other two. To define the first simplex for a four-variable optimisation it is necessary to choose five initial experiments. Although it may often be that the chromatographer's experience will aid the location of the starting simplex, for the optimisation of unknown mixtures the use of the largest possible simplex is usually the most successful. The MULTOPT program assumes that a large starting simplex will be used, although provision is made for alternative starting conditions to be set.

Results

The use of MULTOPT to optimise reversed-phase ion-pair separations is demonstrated by the optimisation of the separation of five aromatic bases using 0.05 M aqueous potassium dihydrogen phospate adjusted to pH 3 with

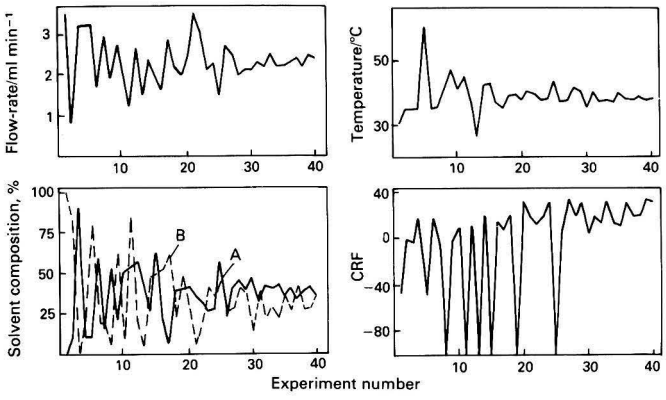

Fig. 1. Values of experimental variables and *CRE* as a function of experiment number

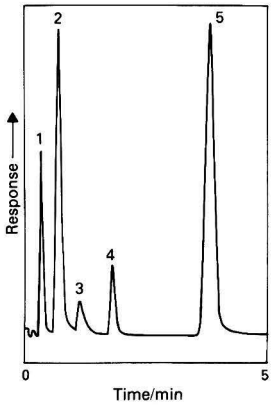

Fig. 2. Optimised separation of organic bases (for conditions see text). Elution order: 1, α-aminoacetophenone; 2, 2,4-dimethoxybenzylamine; 3, 2,4-xylidine; 4, indole; and 5, 2-methylindole

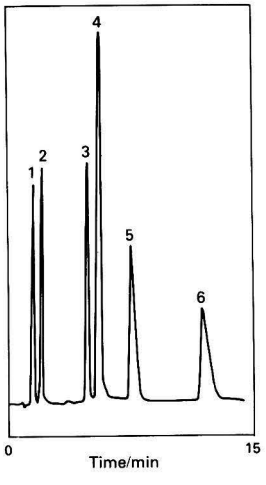

Fig. 3. Optimised separation of aromatic and heterocyclic acids and bases (for conditions see text). Elution order: 1, noradrenaline; 2, DOPA; 3, 3,4-dihydroxyphenylpropionic acid; 4, 5-hydroxyindole-2-carboxylic acid; 5, tryptophanamide; and 6, tryptophan

Table 1. Location of starting experiments

Variable	Range	Experiment No. 1	2	3	4	5
Solvent A, %	0–100	0	10	90	10	10
Solvent B, %	0–99.9	99	81	1	19	81
Flow-rate/ml min^{-1} . .	0.5–3.5	3.5	0.8	3.2	3.2	3.2
Temperature/°C . .	30–65	30	35	35	35	60

orthophosphoric acid (solvent A), methanol (solvent B) and pH 3 phosphate buffer containing 300 mg l^{-1} of sodium heptanesulphonate (solvent C). The mobile phase flow-rate range was 0.5–3.5 ml min^{-1} and the temperature range was 30–65 °C. The requested separation time for the 4-cm column was 4 min and each chromatogram was allowed to run for a maximum of 6 min. The values for the weightings *a*, *b* and *c* for the *CRF* were set to 2; no other values were investigated on this occasion.

The five initial experiments are listed in Table 1. The values of the experimental variables as a function of experiment number and the value of the resulting *CRF* are shown in Fig. 1. Values of −50 for the *CRF* result from chromatograms for which no peaks were detected. A value of −100 for the *CRF* means that at least one variable was set at an impossible value, lying outside the normal range, and thus an experiment was not conducted.

The amount of memory available in the controlling computer precludes the storage of results from more than 40 experiments and so the procedure is halted at experiment 40. Experiment 20 was the first chromatogram to give an adequate resolution between all components but further improvement is possible; inspection of Fig. 1 reveals that an optimum composition, flow-rate and temperature have all been approximately located by experiment 32 and subsequent experiments are just a function of the simplex contracting on to the optimum conditions. The final optimum conditions of solvent A : solvent B : solvent C = 43 : 31 : 26, flow-rate = 2.35 ml min^{-1} and temperature = 38 °C were calculated by averaging the variable values for the last eight experiments. The separation obtained using these conditions is shown in Fig. 2.

A particular feature of the simplex procedure is its powerful capability for optimising many interdependent variables. The selectivity of ion-pair separations is controlled not only by the concentration of the ion-pair agent but also by the pH of the mobile phase and the proportion of organic modifier. As trichloroacetic acid can act both as a pH-controlling agent and

as an ion-pair agent in its own right, developing separations with its use can be extremely difficult by trial and error methods. Fig. 3 shows the optimised separation of a mixture of aromatic and heterocyclic acids and bases. The solvents used were 0.01 M sodium trichloroacetate (solvent A), methanol (solvent B) and 0.01 M trichloroacetic acid (solvent C). A 15-cm column was used with a desired maximum retention time of 15 min. The flow-rate range was 0.5–2.5 ml min^{-1} and the temperature range 30–70 °C. The MULTOPT program had no difficulty in locating an optimum separation, despite the interdependence of solvents A and C. The optimum conditions giving the separation shown as Fig. 3 were solvent A: solvent B: solvent C = 40 : 23 : 37, flow-rate = 1.2 ml min^{-1} and temperature = 38 °C.

Conclusions

Using the sequential simplex procedure with a microcomputer-controlled chromatograph provides a powerful and versatile system for the automated optimisation of HPLC separations. The multidimensional optimisation capabilities of the simplex procedure can be applied to the control of any of the continuous parameters that affect the selectivity of HPLC separations. The MULTOPT program has been shown to be useful in the simultaneous optimisation of solvent strength, pH, ion-pair concentration, temperature and flow-rate. Future applications are likely to be limited only by the ingenuity of the chromatographer and programmer and by the interface and control capabilities of the microcomputer.

References

1. Glajch, J. L., Kirkland, J. J., Squire, K. M., and Minor, J. M., *J. Chromatogr.*, 1980, **199**, 57.
2. Glajch, J. L., Kirkland, J. J., and Snyder, L. R., *J. Chromatogr.*, 1982, **238**, 269.
3. Drouen, A. C. J. H., Billet, H. A. H., Schoenmakers, P. J., and de Galan, L., *Chromatographia*, 1982, **16**, 48.
4. Berridge, J. C., *J. Chromatogr.*, 1982, **244**, 1.
5. Berridge, J. C., *Chromatographia*, 1982, **16**, 172.
6. Deming, S. N., and Morgan S. L., *Anal. Chem.*, 1973, **45**, 278A.

Paper A3/258
Received August 11th, 1983
Accepted September 29th, 1983

Multi-phase Solids and the Intensity - Concentration Relationship in X-ray Fluorescence Analysis: a Monte Carlo Simulation

Jef A. Helsen and Bruno A. R. Vrebos
Department Metaalkunde, Katholieke Universiteit Leuven, De Croylaan 2, B-3030 Heverlee, Belgium

A correction algorithm for quantitative X-ray analysis is suggested for samples with a non-homogeneous distribution of elements over the matrix. The treated data were obtained by Monte Carlo simulation of the X-ray fluorescence processes in a binary composite. As an example, a mixture of iron and chromium was studied.

Keywords: *X-ray fluorescence analysis; correction algorithm; Monte Carlo simulation; non-homogeneous samples; iron - chromium alloy*

In recent papers we demonstrated by computer simulation of X-ray fluorescence (XRF) processes the extent to which the intensity of X-ray fluorescence is modified by a non-homogeneous distribution of elements in the matrix.[1,2] The samples studied may be either a pile of thin foils or a dispersion of particles. For layered samples, each layer contained one of the considered elements, or a solid solution of the elements considered but in a concentration different from the neighbouring layer. The same composition configuration was maintained when the second phase was presented as a set of spherical particles dispersed in a matrix. It was striking that, *e.g.*, for an iron - chromium mixture the influence on the fluorescence intensity of iron is important down to very small particle radii. When expressed as the influence coefficient of chromium on iron in the correction equation of Lachance and Traill,[3] the difference between the coefficient for a solid solution and for the second element, *i.e.*, in this example iron, segregated from the matrix as spherical particles with a radius of 1 μm is up to 20%.

The example given is a hypothetical one, as an iron - chromium alloy will never be segregated to that extent. However, segregation along the equilibrium lines of the phase diagram occurs and is the rule rather than the exception. Of course, this is not limited to binary alloys but is true for all complex solids containing molecular partners that are not completely soluble in each other at the temperature at which their fluorescence is measured. The effect of non-homogeneity has been recognised for a long time for particulate materials. For these materials, different correction methods have been worked out, taking into account average particle diameter, packing fraction and back-scattering.

In a valuable paper, Berry *et al.*[4] reviewed the important papers up to 1969 on the dependence of X-ray intensity on particle size, and added their own theory. When applied to the results they presented, the theory was a definite improvement. Nevertheless, some criticism of the choice of the most appropriate correction is possible for the results presented in their Fig. 3 (a or d), 4 (a,d or f), 8 (a,b or c), 9 (a or c) and 10 (a or c and b or d) while in the correction for the packing fraction (Fig. 7) apparently none of the theories seems to be satisfactory. The uncertainty is generally increased by the distribution in particle diameter, not accounted for in the equations used.

In a more recent paper, Hunter and Rhodes[5] introduced equations for continuous distributions. An experimental test was carried out by Holynska and Markowicz,[6] who concluded that the theory was valid only for thin layers. For practical reasons, the verification was also difficult in the small diameter range. Berry *et al.* accepted for spherical particles a radiometric diameter d equal to two thirds of the geometric diameter. This concept was discussed by Markowicz *et al.*,[7] who evaluated the difference in the resulting X-ray intensity for a π or $\pi/2$ geometry and the intensity obtained from the classical equation [equation (1) in reference 7] with the radiometric diameter equal to the average volume-to-area ratio of the particle (Figs. 2 and 5 in reference 7). Further, we do not know how reliable the equation proposed by Berry *et al.* will be when applied to samples where secondary and tertiary fluorescence are involved. Equation (9) in reference 4 is theoretically describing only the primary contribution to the fluorescent intensity.

Non-homogeneity and its impact on the measured X-ray intensity were also recognised for alloys such as tin - lead solders[8] and it was accepted that they could not be analysed by XRF. However, to the best of our knowledge, no attempt has been made to integrate this complicating factor in a correction algorithm. We started the present study because inconsistent results were obtained for a number of alloys which, with respect to X-ray fluorescence, were described as homogeneous, *e.g.*, Al - Zn, Al - Si or even some stainless steels.

In this paper we attempt to formulate a correction algorithm for a binary alloy as a demonstration that correction is feasible on condition that in addition to the XRF intensities two more parameters are known or can be determined in some convenient way: the composition of the two phases (as obtained from the phase diagram) and the (equivalent) radius r of the dispersed particles. The *ab initio* calculations presented, *i.e.*, by following each photon through the sample, are compared with the homogeneous case as classically calculated by the existing correction algorithms. This approach is different from that followed by the above-mentioned workers and a number of difficulties that they encountered are circumvented by the presented simulation method. Although for the results presented in this paper a distribution of particle sizes is not yet introduced, it can easily be done, and will be done when the experimental verification with commercially existing alloys and composites are described. Mainly small particle diameters will be considered. The main purpose is to demonstrate the internal consistency of the approach when compared with the commonly used algorithms and the potential of an eventual application in analytical practice.

Experimental

The simulation of the two-phase alloy and the computer program used for the Monte Carlo simulation were fully described elsewhere.[2] In brief, the generation of the dispersion of spherical particles is substituted by creating on the photon track a random distribution of line segments with lengths between 0 and $2r$, the diameter of the spherical particles, representing the second phase. The line segments represent parts of photon tracks through the spherical particles imbedded in the matrix. No overlap of spheres is allowed. The sum of these line segments is proportional to the volume concentration of the particles, according to the usual

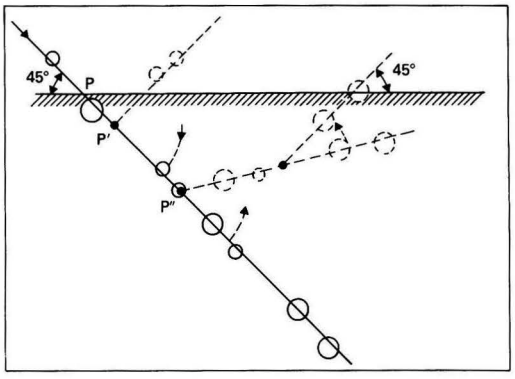

Fig. 1. Simulation of the dispersion (distribution of spheres along the solid line) and of the XRF events (primary photon track, solid line until P′ or P″; fluoresced photon track, broken lines after P′ or P″)

practice in quantitative metallography.[9] Such a photon track is generated at the beginning of a simulation experiment and is used throughout the run. When an interaction takes place, the track is rotated around the point of interaction until coincidence with the new randomly chosen direction of the emerging photon occurs. This technique is clearly demonstrated by Fig. 1. P is the spot where the photon is entering the sample. The interaction points P′ and P″ are selected according to the equation

$$x = (-1/\mu)\ln(Rnd)$$

x being the distance PP′ or PP″, μ the linear absorption coefficient (considered for each phase) and *Rnd* a random number uniformly distributed between 0 and 1.

As a consequence of variance reduction, in each interaction point all fluorescence events are generated with a weight according to the composition of the sample in that position and the physics of the X-ray fluorescence process (fundamental parameters). As a final result, the escape probabilities of all generated photons (primary, secondary and tertiary) can be calculated as they are detected by an ideal detector.

Simulation

For the binary mixture a combination of elements was chosen such that both absorption and enhancement occur and only K-lines are excited. As values the parameters connected with iron and chromium were selected but any other similar combination would suffice. The simulation discussed here is focused on calculating the magnitude of the effect that de-mixing of a binary solution has on the XRF intensities, rather than on case studies.

Results for the binary "alloy" Fe - Cr over the whole (analytical) concentration range are given for a set of particle sizes of the dispersed phase in Fig. 2. The points on the broken line are calculated for the homogeneous case. This can be done either by the simulation program for a two-phase system with both phases having the same composition, or by any current correction program. We used for comparison the NRLXRF program[10]; both methods gave the same result within the statistical error of the simulation. It is clear that for a constant analytical concentration the influence coefficient is a function of the size of the dispersed particles. The inter-relation between intensity and radius of the dispersed particles is well demonstrated in Fig. 3, where the relative intensity is plotted against radius at a constant total concentration. We also used the equation of Berry *et al.* [equation (9) in reference 4] to predict the relative intensities of iron in the Fe - Cr alloy (5% Fe) as function of particle radius. These

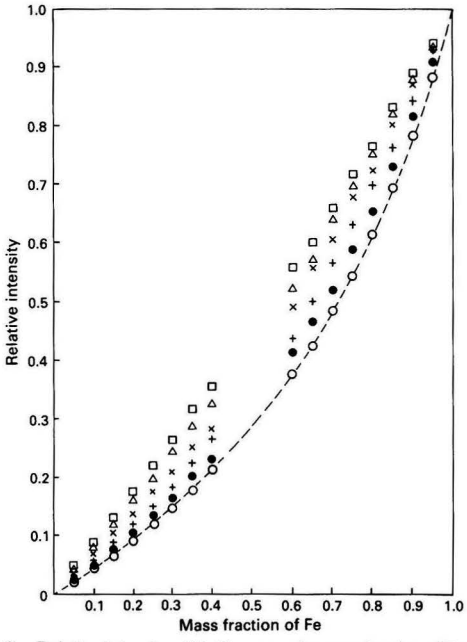

Fig. 2. Relative intensity of Fe Kα *versus* the mass fraction of Fe for different particle radii: □, 20.0; △, 10.0; ×, 5.0; +, 2.5; and ●, 1.0 μm. The broken line (○) is the homogeneous case (simulated or calculated)

intensities deviate by about 10% from our values calculated by simulation. Although not yet verified on real samples, this difference is of a similar order to that given by Markowicz *et. al.*[7] when the $\pi/2$ geometry is used as discussed earlier. This geometry corresponds to the one we used in the simulations. Let us now consider how this effect can be integrated in a usable correction algorithm.

The data for a given particle radius can be fitted to the Lachance - Traill equation:

$$C_{Fe} = R_{Fe}(1 + \alpha C_{Cr}) \quad \ldots \quad (1)$$

where R_{Fe} is the intensity, C the concentration expressed as a mass fraction and α the influence coefficient. It is obvious that this coefficient is not the usual one encountered in the literature. It is sensitive to the combined effect of segregation, absorption and enhancement and will therefore be denoted as α'. When the calculated α' values or the slopes of the rearranged equation (1)

$$C_{Fe}/R_{Fe} = 1 + \alpha' C_{Cr} \quad \ldots \quad (2)$$

are plotted against radius (r), Fig. 4 is obtained. These data fit the equation

$$\alpha' = \frac{1}{a + br} \quad \ldots \quad (3)$$

where a and b are 0.67 and 0.22, respectively, and the linear relationship with radius is also plotted in Fig. 4. When a binary "alloy" is considered

$$C_{Cr} = 1 - C_{Fe} \quad \ldots \quad (4)$$

substituting equation (4) in equation (1) gives:

$$C_{Fe} = R_{Fe}\left(\frac{1 + \alpha'}{1 + \alpha' R_{Fe}}\right) \quad \ldots \quad (5)$$

The coefficient α' is a function of the particle radius r as given by equation (3). Substitution of equation (3) in equation (5) would result in the equation

$$C_{Fe} = f(R_{Fe}, a, b, r) \quad \ldots \quad (6)$$

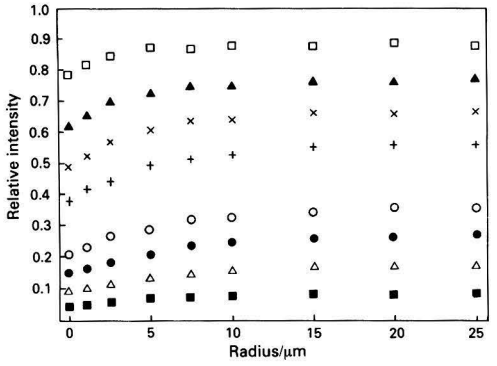

Fig. 3. Relative intensity of Fe Kα *versus* radius of dispersed particles for different concentrations; □, 90; ▲, 80; ×, 70; +, 60; ○, 40; ●, 30; △, 20; and ■, 10%

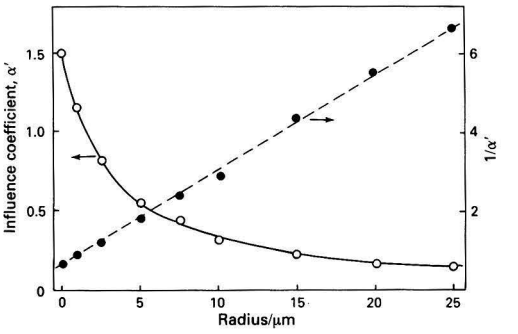

Fig. 4. Influence coefficient, α', and its reciprocal as a function of radius [according to equation (3)]

Discussion

The above treatment of data obtained for non-homogeneous matrices results in a very simple analytical relationship between concentration and intensity with particle radius as a parameter. Obviously only if this parameter is known can the concentration be calculated with reasonable accuracy. This simple relationship is possible only when monochromatic excitation is used and absorption is the only inter-element effect involved. It is, however, applicable in a number of areas, *e.g.*, dispersion hardened alloys or composites. Nevertheless, in general the application will become more complicated if not impossible when the phases are all charged with the same elements but in different proportions. In this event the coefficients will differ less from those calculated for the homogeneous case but nevertheless continue to exist. We consider this to be one of the possible reasons why the determination of influence coefficents by multiple regression methods from experimental data often yields erroneous results. In a series of samples with different compositions the "degree" of segregation is not necessarily the same and it is questionable, from what has been discussed here, if normal (constant) correction coefficients in multi-element samples will be able to account for the effect. However, even when the effect of segregation on influence coefficients can be accounted for by the use of more than one coefficient, it would imply the need to increase the number of standards (for two coefficients by a factor of two). Further complications arise when it is introduced in algorithms already using more than one parameter, such as the Lachance - Claisse equation.[11]

To conclude, it may be stated that for fully segregated binary composites a reliable XRF analysis can be made provided that the particle radius or, for a distribution of radii, the equivalent radius is known. The influence coefficient will be a function of the radius. The same holds for multi-element samples if the element to be determined is present only in the second phase and not in the matrix. For multi-element - multi-phase samples the effect is considered to be attenuated but may not be negligible for a number of cases, as is seen in the analysis of solders, zinc - aluminium alloys and stainless steels. A solution cannot be proposed here for these complex cases. The errors introduced by not accounting for segregation will be much greater in many analyses than the normal counting or instrumental errors in XRF analysis.

References

1. Vrebos, B., and Helsen, J. A., *Spectrochim. Acta, Part B*, 1983, **38**, 835.
2. Helsen, J. A., and Vrebos, B. A. R., *Spectrochim. Acta*, in the press.
3. Lachance, G. R., and Traill, R. J., *Can. Spectrosc.*, 1966, **11**, 43.
4. Berry, P. F., Furuta, T., and Rhodes, J. R., *Adv. X-Ray Anal.*, 1968, **12**, 612.
5. Hunter, C. B., and Rhodes, J. R., *X-Ray Spectrom.*, 1972, **1**, 107.
6. Holynska, B., and Markowicz, A., *X-Ray Spectrom.*, 1981, **10**, 61.
7. Markowicz, A., Van Dyck, P., and Van Grieken, R., *X-Ray Spectrom.*, 1980, **9**, 52.
8. Glade, G. H., and Post, H. R., *Appl. Spectrosc.*, 1970, **24**, 193.
9. Dehoff, R. T., and Rhines, F. N., *Editors*, "Quantitative Microscopy," McGraw-Hill, New York, 1968.
10. Criss, J. W., "NRLXRF: a Fortran Program for X-Ray Fluorescence Analysis," University of Athens, GA, 1977.
11. Lachance, G. R., and Claisse, F., *Adv. X-ray Anal.*, 1980, **23**, 87.

Paper A3/304
Received September 5th, 1983
Accepted October 17th, 1983

Failures and Successes with Pattern Recognition for Solving Problems in Analytical Chemistry

Frans W. Pijpers
Department of Analytical Chemistry, University of Nijmegen, Faculty of Sciences, Toernooiveld, 6525 ED Nijmegen, The Netherlands

In our laboratory, pattern recognition has been used for solving a variety of problems. The purpose of this paper is to demonstrate the potential of this technique in analytical chemical laboratories. Two very different examples are given, one resulting in a temporary failure, another ending succesfully. References to other problems that have been solved in our laboratory are also given.

Keywords: *Pattern recognition; environmental control; alloying*

In our laboratory, pattern recognition has been used in solving a variety of problems: the classification of dithiocarbamate complexes based on ^{13}C NMR and infrared spectroscopic data, aimed at an improved understanding of the chemical complexation and exceptionally high oxidation states[1,2]; the rating of various clinical chemical methods with respect to accuracy, precision and sensitivity both in giving erroneous results and in giving systematically different results in different laboratories, aimed at an objective assessment of a preferred procedure[3,4]; the investigation of a common base of the secondary structure of procaryotic 5S-RNA molecules; and the investigation of the predictability of the superconducting behaviour of elements based on their physical and chemical properties.[5]

This paper describes two problems that we have tried to solve by pattern-recognition techniques, the first (see below) less successfully than the second.

Because of the success of pattern recognition it was decided to investigate the possiblity of describing air pollution in highly industrialised regions. At present the Central Environmental Control Agency "Rijnmond" (DCMR), a government organisation in The Netherlands, collects data on various constituents in polluted air from a number of locations situated near and at a highly industrialised area at the estuary of the river Rhine, near Rotterdam. Occasionally, when weather conditions demand it, in order to prevent an emergency level of air pollution being reached a warning is dispatched to industries in the area, which dictates the limit to which sulphur dioxide (resulting from the burning of sulphur-containing fuel) may be emitted into the atmosphere.

In spite of these well organised actions, complaints from inhabitants of the area, who are encouraged to communicate their observations by telephone to the same office that despatches the warnings, cannot be precluded. Because of the complex situation, which has to be described by a set of parameters pertaining to the constitution of the atmosphere at various locations and to the weather conditions, the application of pattern recognition seemed viable.[6–10] Therefore, the aim of this first investigation was two-fold: to find the relevant features that describe emergency situations; and to predict the evolution of these features in time, in order to forecast a potential emergency situation, which would allow the necessary measures to be taken and alleviate the burden on the inhabitants of the area.

In this paper the details of the numerous pattern-recognition techniques have been omitted,[11] but in applying the technique to the problem of air pollution, the method of problem handling is clearly illustrated.

The second investigation was a critical comparison of various relationships that describe the formation of binary alloys.[12] Amongst the different empirical relationships for this subject the equations given by Miedema and co-workers[13–15] are the most superior with respect to their capability to predict binary alloy formation. In this model the two most important parameters are the electronic work function and the electronic density at the boundary of the Wigner - Seitz cell, each of which was slightly modified in order to give an optimum description. In order to model these parameters, the following must be assessed: the features that are relevant for a successful description of binary alloys; and the reason as to why these features and no others are important.

By means of pattern-recognition techniques, learning machines were constructed from various physical and chemical parameters which were expected to contain information on alloying behaviour.

Experimental

For the period April – June 1979, the hourly collected data on air pollutants at the Rhine estuary near Rotterdam were obtained from the DCMR. These data were collected in three automatic measuring stations at Hoogvliet, Maassluis and Schiedam and, under computer control, sampled on magnetic disks for further evaluation. The meteorological conditions were obtained from a daily report from Zestienhoven airport, near Rotterdam. From these data a selection of 116 hourly reports between 10.00 and 18.00 h was made in which no missing measurements were encountered and weather conditions were reported to be stable.

Simultaneously, sulphur dioxide concentrations were measured at another three locations, and were employed to construct the learning machines discussed.

The thermodynamic properties of binary alloy formation were obtained from Hultgren *et al.*[16] In this investigation 257 binary alloys, resulting from 28 different transition metals, have been incorporated. These alloys have been selected from a set of 378 of which the sign of the heat of formation was known. Alloys with a heat of formation of less than 600 cal mol^{-1} (absolute) were omitted.

Results and Discussion

The area south of the river Rhine is highly industrialised (Fig. 1). Because of the burden to the population caused by air pollution, the governmental organisation DCMR measures concentrations of air pollutants at various locations and also collects telephone complaints from inhabitants of the area. In combination with daily meteorological reports this collection of measurements results in a complex data matrix, which is not easily interpretable. In order to facilitate interpretation, pattern recognition techniques have been employed. Various stages in pattern recognition may be summarised as follows:

(1) definition of problem space and data vectors;
(2) selection of patterns for a training set;
(3) search for clusters by various techniques;
(4) selection, ordering and weighing of relevant features;
(5) predictions for a test set.

(Iteration between steps 3 and 4.)

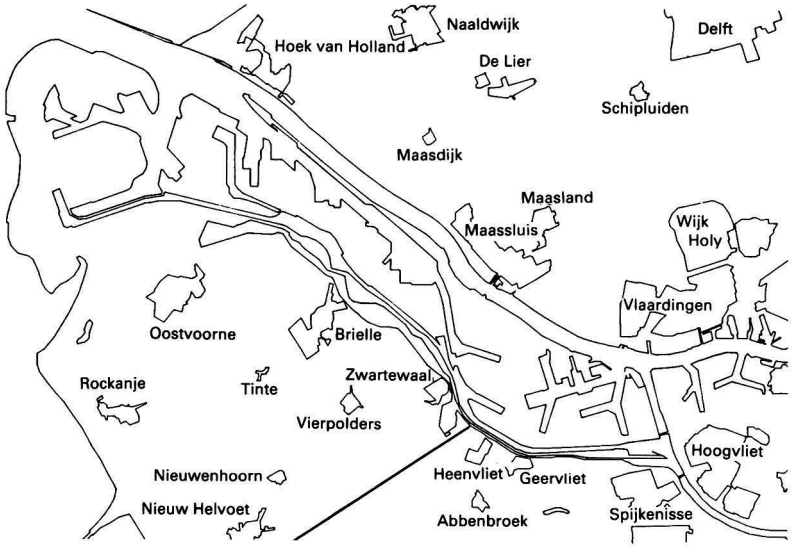

Fig. 1. Map of the estuary of the river Rhine, near Rotterdam

Table 1. List of observed features

Chemical compound	Meteorological condition	Type of complaint
Dinitrogen oxide	Direction of the wind	Soot, dust
Nitrogen oxide	Speed of the wind	Noxious smell
Sulphur dioxide	Relative moisture	Acidic, chemical smell
Standardised smoke	Temperature	Oily smell
Saturated and olefinic hydrocarbons	Sunlight radiation	Smog
Ozone	Amount of downfall	Others
	Duration of downfall	
	Air pressure	
	Cloudiness	
	Stability	

Table 2. Karhuhnen - Loève transformation

Feature	Eigenvector, % First	Second
Sulphur dioxide (loc. 11)	35	12
Saturated hydrocarbons	21	31
Stability	13	21
Sulphur dioxide (loc. 17)	12	12
Sulphur dioxide (loc. 10)	16	15
Olefinic hydrocarbons	2	8
Ozone	1	1
Eigenvalue (= information)	64 +	14 = 78%

The pattern of an atmospheric composition and situation *i.e.*, a data vector comprising all available physical and/or chemical data pertaining to that situation, is positioned in a multi-dimensional feature space that is spanned by all physical (such as meteorological) and chemical (here compositional data) named features.

The definition of the problem space here is the selection of those chemical compositions and meteorological conditions that allow optimum discrimination between hours with and without registered complaints. Here correlation between features is used to diminish the number of dimensions of the multi-dimensional space. In the next step the hours with and without complaints are selected. In this discussion we select a number of consecutive days where a period with many complaints is preceded and followed by an about equal period of "good" days to see whether at least two different clusters of patterns in the feature space may be found that correspond with the property polluted air, *viz.*, fresh air.

In order to obtain balanced results the population of the class of hours with complaints should be about equal to that of the hours without complaints; outliers and incidental complaint hours should be removed in order to construct a reliable learning machine.

When a number of patterns positioned in this feature space group together or cluster, it is obvious that their physical and chemical behaviour is similar, and this will be perceived by the population of the area in the same way. In pattern recognition it is assumed that such a behaviour not only holds for the known physical and chemical data, but also reflects similar behaviour of properties such as fresh air or noxious air. When, according to this scheme, a training set has been obtained, the search for clusters in the multi-dimensional feature space may proceed according to various mathematical techniques.[10,11] Here one aims for two clusters: one cluster representing the hours with complaints and the other representing the hours without. When these two clusters are found, one proceeds by appointing those features that are most relevant for the discrimination. The relevant features are weighed and ranked, with iteration for step 3. Finally the learning machine thus obtained is used to predict hours with complaints based upon the relevant measurements and to test the results employing measurements that were not used for the construction of the algorithms.

In Table 1 the possible relevant features are listed, together with the types of complaints encountered during the investigation. The chemical compounds listed were measured at different locations—the meteorological conditions result from measurements at Zestienhoven airport, near Rotterdam. Finally the limited set of seven features defined as stability, ozone, saturated hydrocarbons, olefinic hydrocarbons and sulphur dioxide at three different locations were sufficient to describe the required learning machine, provided that the weather conditions were stable according to meteorological standards.

In order to visualise the results, a Karhuhnen - Loève transformation was applied and the seven-dimensional feature space defined above was projected on a plane spanned by the two most important eigenvectors. Here the variance of the feature values is interpreted as information to be maximised according to standard procedures.[11] The contribution of each feature to the first two eigenvectors is described in Table 2, which also contains the total information encompassed by these two eigenvectors (78%).

The final result of this exercise is depicted in Fig. 2, in which hours with complaints are clearly separable from hours without complaints. It must be noted, however, that when no stable weather conditions are encountered, the learning machine method cannot be employed.

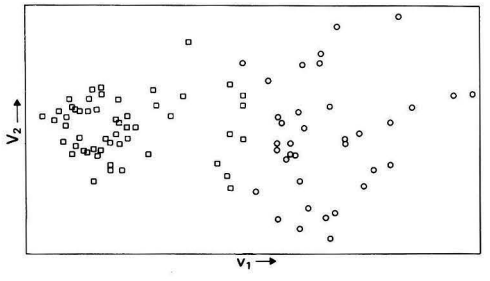

Fig. 2. Projection of hours ○, with complaints and □, without complaints on air pollution on the two most significant eigenvectors of the Karhunen - Loève transformed, seven-dimensional feature space

Another way of employing pattern recognition is encountered when studying alloying of binary metal compositions. Here a well known empirical relation was already available and the aim of this investigation was to see whether other physical quantities could be found, which would enable the prediction of alloying and provide a base for a physical understanding of the results.

Fig. 3 lists the 51 elements of the periodic system investigated. Equation (1) represents the empirical relationship given by Miedema and co-workers.[13–15]

$$\Delta H = f(c)\,[-Pe(\Delta\phi^*)^2 + Q_0(\Delta n^{\frac{1}{3}}_{WS})^2] \quad .. \quad (1)$$

where ΔH is the heat of formation (kJ mol^{-1}); $f(c)$ a function of concentration; ϕ^* the Miedema work function (V); n_{WS} the electron density in the Wigner - Seitz cell; Δ the difference between quantities; and e, P and Q_0 are constants.

According to this equation alloys are formed when ΔH has a negative value. It is seen that a difference between the electronic work function always contributes to alloy formation. This contribution is counteracted by the difference in number of electrons at the boundary of the Wigner - Seitz cell. The latter quantity follows from compressibility data according to

$$n_{WS} = (KV_M)^{-\frac{1}{3}} \quad .. \quad .. \quad .. \quad (2)$$

where K is the compressibility and V_M the volume for one mole of metal M. The predictive power of this algorithm equals 98% for the 257 alloys studied (Fig. 4).

The elements Al, Ga, In, Tl, Sn, Pb and Bi were excluded. The prediction of the numerical value of ΔH is less accurate; deviations between prediction and measurement of 25% were encountered. In order to cope with the above set of excluded elements, another term was added to the empirical relation of

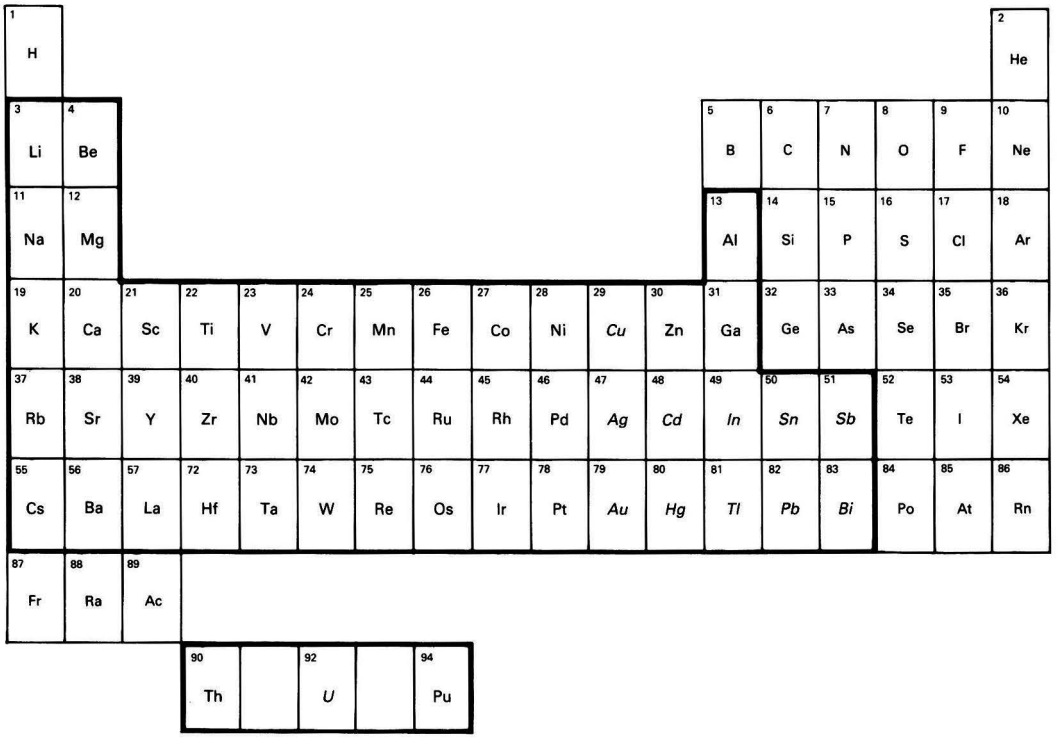

Fig. 3. Elements of the Periodic System; the boxed elements were studied here. The ϕ^* values of the italicised elements do not correlate well with their χ-values (see also Fig. 6)

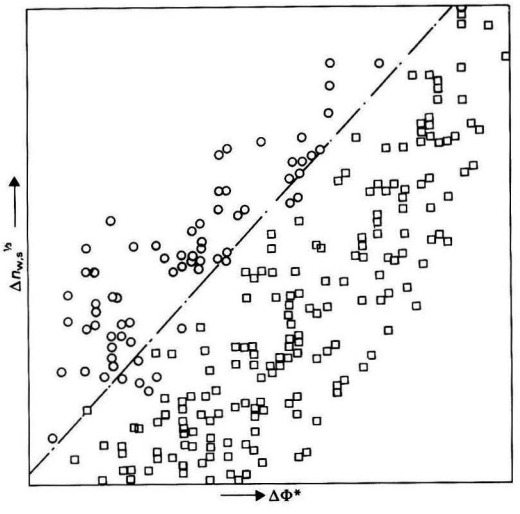

Fig 4. Projection of □, stable alloys and ○, non-stable alloys on a plane spanned by $\Delta n^{\frac{1}{3}}_{WS}$ and $\Delta\phi^*$. The separation between the two categories is well described by the line $\Delta n^{\frac{1}{3}}_{WS} = (Pe/Q_0)^{\frac{1}{3}}\Delta\phi^*$ where the heat of formation equals zero

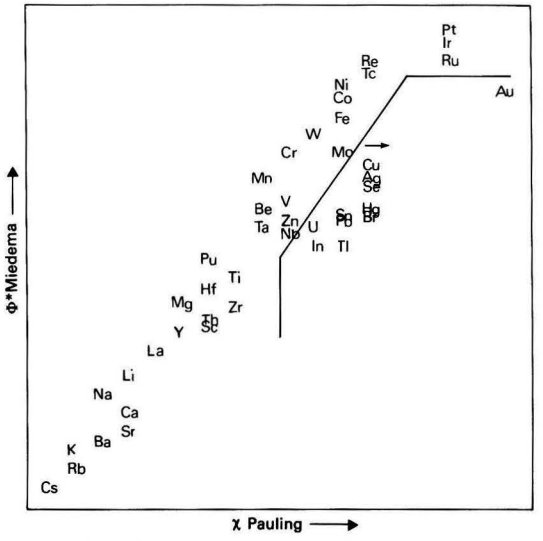

Fig. 6. ϕ^* (Miedema and co-workers) as a function of χ (Pauling) for the metals investigated. Be represents Be and Al; Ru represents Ru, Rh, Pd and Os; Zn represents Zn and Ga; and U represents U and Cd

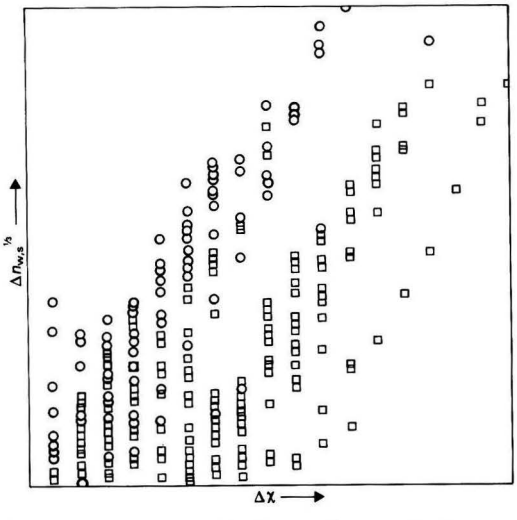

Fig. 5. Projection of □, stable alloys and ○, non-stable alloys on a plane spanned by $\Delta n^{\frac{1}{3}}_{WS}$ and $\Delta\chi$. No sharp division between the two categories is seen

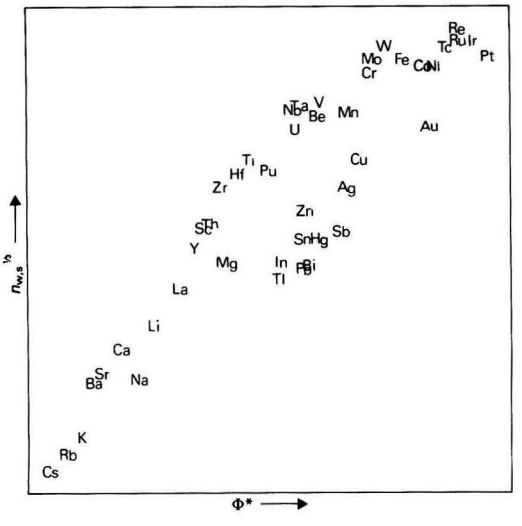

Fig. 7. $\Delta n^{\frac{1}{3}}_{WS}$ as a function of ϕ^* for the metals investigated

Miedema and co-workers. In order to find other physical features that might facilitate interpretations of equation (1), correlation between ϕ^* and $n^{\frac{1}{3}}_{WS}$ and the various features were calculated. The features investigated were as follows: (1) period number of the periodic system of elements; (2) density at 25 °C; (3) specific heat at 25 °C; (4) melting-point; (5) boiling-point; (6) ionic radius in the most common oxidation state; (7) bond length in the solid state at 25 °C; (8) number of relevant valence electrons as given by Miedema and co-workers (calculated from compressibility data); (9) Young's modulus; (10) electronic work function as given by Miedema and co-workers; (11) compressibility; (12) heat of melting; (13) magnetic susceptibility; (14) Debye temperature as obtained from electrical resistivity measurements; (15) linear term in the specific heat; and (16) electrical resistivity at 20 °C. All correlations were disappointingly low. The only relevant feature to be investigated was the Pauling defined electronegativity:

$$\Delta\chi_{AB} = \left[\frac{D_{AB} - \frac{1}{2}(D_{AA} + D_{BB})}{23}\right]^{\frac{1}{2}} \quad \ldots \quad (3)$$

where D_{XY} represents the dissociation energy of the chemical bond between atoms X and Y (in electronvolts per bond) and $\Delta\chi_{AB}$ is given in kcal mol^{-1}.

The correlation between χ and ϕ^* equals 0.963. From Fig. 5 it is seen that the prediction of alloying based upon $\Delta n^{\frac{1}{3}}_{WS}$ and $\Delta\chi$ is much less successful (85% instead of the 98% obtained with $\Delta n^{\frac{1}{3}}_{WS}$ and $\Delta\phi^*$). This means that even when highly correlated electronegativity scales are used the Miedema equation is still superior. In order to interpret this result the correlation between ϕ^* and χ is shown in Fig. 6. Here, one may notice that for some elements the ϕ^* values have been diminished with respect to the corresponding χ values. These elements are in italics in Fig. 3. According to the significantly better alloy prediction with ϕ^* than with χ, this should be explicable. The correlation between ϕ^* and $n^{\frac{1}{3}}_{WS}$ (0.91) has been depicted in Fig. 7 in which a surprisingly high correlation is encountered, which suggests that either ϕ^* or $n^{\frac{1}{3}}_{WS}$ would be exclusively sufficient in order to describe alloying behaviour. However, the extra information present in $n^{\frac{1}{3}}_{WS}$ allows the high predictive ability of the Miedema equation in comparison with other equations. Apparently ϕ^* and $n^{\frac{1}{3}}_{WS}$ constitute an optimised parameter set.

Conclusions

In this paper the applicability of pattern recognition techniques to two different problems has been demonstrated. It was shown that complaints on air pollution can be predicted, provided the weather conditions are stable according to meteorological standards. For unstable weather no predictions on air pollution complaints can be made.

The prediction of alloying behaviour of binary metal mixtures is optimal for the set of two parameters as given by Miedema and co-workers. Significant deviations between the Miedema defined electronegativity values ϕ^* and the Pauling χ-scale have been noticed and the extra information content on $n^{\frac{1}{3}}_{WS}$ has been demonstrated.

Finally it should be remarked that pattern recognition does not provide theories but merely indicates the relevance of certain parameters and can be useful as such for developing theories.

We thank P. J. W. M. Müskens and J. E. Evendijk for making the measured data on air constituents in 1979 by DCMR available, B. R. Kowalski for making the computer program "Arthur" available to us and A. R. Miedema and A. K. Niessen for their stimulating and helpful discussions and for generously supplying us with the necessary data. We also thank P. F. A. van der Wiel for his valuable assistance with computer programming.

References

1. Van Gaal, H. L. M., Diesveld, J. W., Pijpers, F. W., and Van der Linden, J. G. M., *Inorg. Chem.*, 1979, **11**, 3251.
2. Pijpers, F. W., Van Gaal, H. L. M., and Van der Linden, J. G. M., *Anal. Chim. Acta*, 1979, **112**, 199.
3. Jansen, R. T. P., Pijpers, F. W., and De Valk, G. A. J. M., *Ann. Clin. Biochem.*, 1981, **18**, 218.
4. Jansen, R. T. P., Pijpers, F. W., and De Valk, G. A. J. M., *Anal. Chim. Acta*, 1981, **133**, 1.
5. Pijpers, F. W., and Vertogen, G., *J. Phys.*, 1982, **43**, 97.
6. Tan, J. T., and Gonzales, R. C., "Pattern Recognition Principles," Addison - Wesley, Reading, MA, 1979.
7. Jurs, R. C., and Isenhour, T. L., "Chemical Applications of Pattern Recognition," Wiley, New York, 1975.
8. Isenhour, T. L., Kowalski, B. R., and Jurs, R. C., *CRC Crit. Rev. Anal. Chem.*, 1974, **4**, July, 1.
9. Kateman, G., and Pijpers, F. W., "Quality Control in Analytical Chemistry," Wiley, New York, 1981.
10. Masart, D. L., and Kaufman, L., "The Interpretation of Analytical Chemical Data by the Use of Cluster Analysis," Wiley, New York, 1983.
11. Duewer, D. L., Koskinen, J. R., and Kowalski, B. R., "Arthur," Laboratory for Chemometrics, Department of Chemistry BG10, University of Washington, Seattle, WA.
12. Kentgens, A. P. M., Pijpers, F. W., and Vertogen, G., *Anal. Chim. Acta*, 1983, **151**, 167.
13. Miedema, A. R., De Boer, F. R., and De Châtel, P. F., *J. Phys.*, 1973, **3**, 1558.
14. Miedema, A. R., *J. Less Common Metals*, 1973, **32**, 117; and 1975, **41**, 283.
15. Miedema, A. R., De Boer, F. R., and Boom, R., *Calphad*, 1977, **1**, 341.
16. Hultgren, R., Desai, P. D., Hawkins, D. T., Gleiser, M., and Kelley, K. K., "Selected Values of the Thermodynamic Properties of Binary Alloys," American Society for Metals, Metals Park, Ohio, 1973.

Paper A3/208
Received July 7th, 1983
Accepted July 26th, 1983

Random Errors in Analytical Methods

Evgeniy D. Prudnikov and Yunona S. Shapkina
Earth's Crust Institute, State University, Leningrad, 199164, *USSR*

The classification of random errors in analytical chemistry is developed in this paper. It is shown that in the most general case the analyst can meet five random errors: additive, transitive, multiplicative, transitive - non-linear and non-linear. Their values are proportional to element concentration to the powers 0, $\frac{1}{2}$, 1, $\frac{3}{2}$ and 2, respectively. At the same time the dependence of the standard deviation on the concentration in each instance is raised to a power from 0 to 2. This theory is in close agreement with experimental data.

The standard deviation in instrumental analytical measurements is calculated. The theoretical and practical meaning of these results is discussed.

Keywords: *Classification of random errors; standard deviation; metrology*

Random errors and standard deviation (s) play a most important role in analytical chemistry and in the interpretation of experimental results. That is why scientists pay attention to experimental studies of errors in methods under development and their dependence on the concentration of an element (c). A linear function representing the dependence of the random errors on the concentration has been used for a long time[1]:

$$s = a + bc \quad .. \quad .. \quad .. \quad (1)$$

where a and b are constants for the element and method discussed. According to equation (1), the additive (s_{addit}) and multiplicative (s_{mult}) errors are distinguished in the theory of measurements.[2] The additive error is not related to the value of the measured signal, while the multiplicative error is proportional to the signal. Taking into account the law of addition for random error dispersions the standard deviation can also be described by Zil'berstein's equation[3]:

$$s = (s_{addit}^2 + s_{mult}^2)^{1/2} \quad .. \quad .. \quad (2)$$

The dependence of the random errors on the concentration is shown in reference 4:

$$s = (s_f^2 + s_{meas}^2 c^2)^{1/2} \quad .. \quad .. \quad (3)$$

where s_{meas} is the measured and s_f the fluctuation component of error. Boumans[5] tried to find a relationship between the standard deviation and the characteristics of an analytical method and the following expression was proposed:

$$s = \left(\frac{c_m^2}{k_1^2} + A^2c^2\right) \quad .. \quad .. \quad (4)$$

where c_m is the detection limit, k_1 is the coefficient for the confidence level calculated by Kaiser and A is the instability factor of the measurement.

However, in the literature many experimental data are present which are not in agreement with accepted theoretical concepts and equations 1–4 for the dependence $s = f(c)$. According to Schwarz-Bergkampf,[6] the following expression is valid for manganese within a wide range of concentrations:

$$s = 0.007 + 0.13\,c^{0.6} \quad .. \quad .. \quad (5)$$

It is noted that analogous expressions are valid for many components within a range of concentrations. Universal parabolic dependence for different methods of quantitative analysis was proposed by Puschel[7]:

$$s = a_1\,c^{0.73} \quad .. \quad .. \quad .. \quad (6)$$

Fainberg and Ginzburg[8] obtained the following expression for different components in metallurgical analysis:

$$s = 0.045\,c^{0.5} \quad .. \quad .. \quad .. \quad (7)$$

According to Pliner,[9] this general expression is true for many component analyses in metallurgical processes:

$$s = 0.015\,c^{0.5} \quad .. \quad .. \quad .. \quad (8)$$

There is no satisfactory explanation for equations 5–8 in the literature. Yufa[10] has demonstrated that in some instances an increase in relative error with increase in concentration is observed and that the upper limit of detection is reached:

$$s = a + bc + dc^2 \quad .. \quad .. \quad .. \quad (9)$$

where d is a constant. The same phenomenon is known for methods of atomic spectrometry, for example, due to self-absorption.[11] All of these experimental data indicate that there are still some problems to be solved in the field of random errors in analytical methods.

Because of the existence of these problems, further development of the theory of random errors in analytical chemistry is highly desirable. In references 12–14 theoretical calculations of the standard deviation in atomic spectroscopy are given, taking into account all possible fluctuations of the analytical signal. According to reference 12, the standard deviation in atomic-emission spectrometry can be described by the following expression:

$$s = (k_i + k_d S^{-1} q + \Delta^2 S^{-2} q^2)^{1/2} \quad .. \quad .. \quad (10)$$

where k_i is the coefficient of total instrumental noise independent of the concentration of the element; k_d and Δ are the coefficients of shot and flicker noise; S is the reciprocal sensitivity of analysis (characteristic amount of element for the signal $v = 1$); and q is the absolute amount of element. Comparing equation 10 with equations 1–4 one can demonstrate that the first term in 10 can be defined as an additive component of random error and the third term as the multiplicative error. There is no analogue for the second term in the theory of measurements, but at the same time its presence explains the dependence in equations 5–8. These results demonstrate the possibility of theoretical error description in analytical chemistry, which is the aim of this paper.

Sources of Analytical Signal Fluctuations

Any analytical measurement is related to the process of unknown real value transformation into signal (v) and to the process of measurement itself. Observed errors are caused by fluctuations in those processes. It is possible to estimate the fluctuations theoretically by using fundamental laws of physics and chemistry. We have to take into account laws of quantum mechanics, classical mechanics and non-linear physics.

In quantum mechanics the theoretically expected deviation in a process is proportional to its energy to the power $\frac{1}{2}$. These fluctuations are well known in nuclear physics and associated analytical methods.[13–15] They are also observed during photoelectric detection of a weak light flux.[16] Different quantum-mechanical noises are known in electronics,[17] but more often we deal with shot noise (s_d):

$$s_d = (k_d\,v)^{1/2} \quad .. \quad .. \quad .. \quad (11)$$

Quantum-mechanical noises are typical of weak quantised interaction processes.

In classical mechanics process fluctuations are proportional to process energy. Similar fluctuations are well known in electronics[17] and in the theory of measurements (equations 1–4). We often know them as instability noises and flicker noises (s_{fl}):

$$s_{fl} = \Delta v \quad .. \quad .. \quad .. \quad .. \quad (12)$$

Flicker noises are prevalent in processes of normal classical interactions.

The fluctuation problem is not completely solved in non-linear physics. We normally deal with non-linear processes in non-linear media, intensive signals and strong interactions leading to a noise increase in comparison with classical laws of mechanics. In reference 18 amplitude and phase distortions for optical pulses in non-linear optics are determined theoretically. It is demonstrated that in non-linear media distortions are increased proportionally to the square root of wave field intensity. In this instance non-linear noises of a quantum-mechanical type (s_{nd}) occur and fluctuations are proportional to the process energy to the power $\frac{3}{2}$:

$$s_{nd} = (k_k v^3)^{1/2} \quad .. \quad .. \quad .. \quad (13)$$

where k_k is a constant. Such noises are noted in atomic-emission spectrometry when, for high concentrations, the slope of the calibration graph changes from 1 to 0.5 and, accordingly, the measurement error increases.[11]

Theoretical calculations have also demonstrated[2] that non-linearity increases the error dispersion linearly with the square of summary process dispersion at the input. These fluctuations correspond to non-linear noises of classical character (s_n), which are proportional to the square of the process energy

$$s_n = k_n^{1/2} v^2 \quad .. \quad .. \quad .. \quad (14)$$

where k_n is a constant. These calculations are confirmed experimentally in non-linear optics, where the intensities of initial and output signal in non-linear transformations are related by a square-law dependence.[19] Experimental data in reference 10 are in agreement with equation 14 as well.

On the basis of general theoretical positions in quantum and classical mechanics, as well as in non-linear physics, it is necessary to take into consideration four principal sources of analytical signal fluctuation. Each of these sources is a controlling one for a corresponding signal value and can be described by equations 11–14. They create the possibility of theoretical error determination in analytical measurements.

Errors and the Standard Deviation

First of all in analytical measurements it is necessary to take into account instrumental fluctuations when no useful signal exists. These fluctuations characterise the additive standard deviation component, of which the dispersive effect can be written as:

$$s^2_{addit} = k_i \quad .. \quad .. \quad .. \quad (15)$$

Instrumental fluctuations in the no-signal condition can be theoretically predicted by the method that is normally used for the calculation of the limits of detection in instrumental methods.[16]

Fluctuations of the analytical signal itself depend on its intensity. For weak signals the main role is played by quantum-mechanical noises. These noises represent the error in the transitional range between the additive and multiplicative errors.[3] Therefore, the error due to quantum-mechanical noises can be named transitional (transitive, s_{trans}). For the transitive error dispersion we have

$$s^2_{trans} = k_d v \quad .. \quad .. \quad .. \quad (16)$$

With an increase of useful signal value flicker noises and instability noises become prevalent and define the multiplicative error. Its dispersion is

$$s^2_{mult} = \Delta^2 v^2 \quad .. \quad .. \quad .. \quad (17)$$

Non-linear noises of two types can appear for stronger signals. The corresponding errors can be named transitive-non-linear and non-linear:

$$s^2_{tr.non\text{-}lin} = k_k v^3 \quad .. \quad .. \quad .. \quad (18)$$
$$s^2_{non\text{-}lin} = k_n v^4$$

By using equations 11–18, one can obtain the standard deviation for analytical signal measurement. Let the real signal value at the output be equal to $\bar{v}$ where v is the signal created by the correct measured value. In this instance we have:

$$\bar{v} = v + \bar{s} \quad .. \quad .. \quad .. \quad (19)$$

where $\bar{s}$ is the error of measurement. According to equations 11–14, the measured signal, $\bar{v}$, contains different errors and can be rewritten as

$$\bar{v} = v + a + f v^{1/2} + b v + g v^{3/2} + d v^2 \quad .. \quad (20)$$

From equations 19 and 20 one can obtain the measurement error value:

$$\bar{s} = a + f v^{1/2} + b v + g v^{3/2} + d v^2 \quad .. \quad (21)$$

where a, b, d, f and g are constants.

In the general case it can be considered that the previously discussed sources of fluctuation are independent because they are controlled by different processes. By adding error dispersions according to equations 15–18 we obtain a theoretical expression for the standard deviation in analytical measurements:

$$s = (s^2_{addit} + s^2_{trans} + s^2_{mult} + s^2_{tr.non\text{-}lin} + s^2_{non\text{-}lin})^{1/2} \quad (22)$$

$$s = (k_i + k_d v + \Delta^2 v^2 + k_k v^3 + k_n v^4)^{1/2} \quad (23)$$

For a more complete theoretical description of standard deviation it is necessary to relate the analytical signal value to instrumental parameters. The sensitivity of equipment (S_v) can be used for this purpose. The sensitivity characterises the signal value for a unit amount of the element. For a linear calibration function we have:

$$v = S_v c \quad .. \quad .. \quad .. \quad .. \quad (24)$$

Expression 10 shows the reciprocal sensitivity. By using equation 24, equation 23 can be rewritten as follows:

$$s = (k_i + k_d S_v c + \Delta^2 S_v^2 c^2 + k_k S_v^3 c^3 + k_n S_v^4 c^4)^{1/2} \quad (25)$$

Equation 25 represents the dependence of the standard deviation in analytical measurements on instrumental parameters and the concentration of an element. This relationship may be considered to be the most general expression for the metrological and theoretical characterisation of instrumental analytical methods.

Results and Discussion

Theoretical expressions 22, 23 and 25 show that in the most general case the analyst can encounter five random errors: additive, transitive, multiplicative, transitive - non-linear and non-linear. Their values are proportional to the element concentration to the powers 0, $\frac{1}{2}$, 1, $\frac{3}{2}$ and 2, respectively. At the same time the dependence of the standard deviation on the concentration in every instance can be raised to a power from 0 to 2.

Let us compare the theoretical expression 25 with experimental dependences $s = f(c)$. The experimental equations 1–9 are the particular case of the general theoretical equation 25, while equation 10 represents results of the theoretical calculation of standard deviation in atomic-emission spectrometry,

which coincides with three first terms in 25.[12,20] Experimental data are in close agreement with the theory in reference 20 for strontium flame emission spectrometry when the blank sample value is small. In reference 21 the experimental verification, for calculated results, is given for the standard deviation in the atomic-absorption determination of cadmium with flame and with graphite furnace atomisation. In references 12, 20 and 21 the problem of high concentration measurements in a non-linear range is not considered and possible non-linear errors are not characterised.

In reference 21 it is shown that the expression for the relative standard deviation is more universal. It is valid for any calibration function:

$$s_r = \left(\frac{k_i S_v^{-2}}{c^2} + \frac{k_d S_v^{-1}}{c} + \Delta^2 + k_k S_v c + k_n S_v^2 c^2 \right)^{1/2} \quad (26)$$

From equation 26 it follows that the graph of the relative standard deviation *versus* concentration should rise for low and high concentrations. According to reference 22 it actually occurs in the atomic-absorption determination of zinc, copper, nickel and iron. Our results for the atomic absorption of platinum metals are further evidence of this (see Fig. 1).[23] The dependence of the relative standard deviation for a platinum measurement on the amount of metal on the graphite rod atomiser is shown. Experimental data demonstrate the validity of the selection of five random errors in this instance. From Fig. 1, as well from equation 26, it is easy to obtain the upper and the lower detection limits.[12,20,21] They are in agreement with the conclusion concerning the general metrological and theoretical meaning of equations 25 and 26.

Consideration of experimental data indicates the necessity of discussing three new errors in analytical measurements: transitive, transitive - non-linear and non-linear. The existence of transitive error follows from a great number of theoretical and experimental data.[5-9,12-17,20-22] It is known that this error is observed not only for instrumental but also for non-instrumental methods of analysis. This fact can be explained theoretically because the laws of quantum mechanics are valid in quantum chemistry for both chemical and methodical factors. There is not so much theoretical and experimental information available for non-linear errors,[2,10,18,19,22,23] but it is sufficient and convincing. Although in the most general case one can encounter all five random errors, in practice the analyst more often deals with transitive and multiplicative errors. The appearance of other errors indicates that a more suitable analytical method should be used.

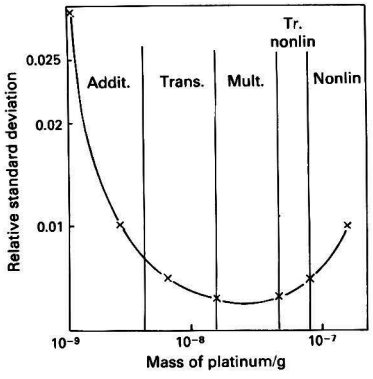

Fig. 1. Relative standard deviation for platinum determination by atomic-absorption spectrometry with graphite rod flame adapter atomiser *versus* mass of platinum on the rod. Intervals corresponding to different random errors are shown by vertical lines

Insofar as laws controlling the appearance of any error are valid for both instrumental and non-instrumental analytical factors the proposed random error discrimination should be valid for instrumental and non-instrumental analytical methods. The general theoretical approach proposed in this paper can be useful for analytical method characterisation, experimental data interpretation and the metrological supply of analytical measurements.

References

1. Nalimov, V. V., "Application of Mathematical Statistics in Analysis of Substances," Fizmatgiz, Moscow, 1960.
2. Kavalerov, G. I., and Mandel'shtam, S. M. "Introduction to Informative Theory of Measurements," Energie, Moscow, 1974.
3. Silberstein, Kh. I., *Editor*, "Spectral Analysis of Pure Substances," Adam Hilger, Bristol, 1977; Khimiya, Leningrad, 1971.
4. Prudnikov, E. D., and Shapkina, Y. S., *Vestn. Leningr. Univ.*, 1978, No. 24, 46.
5. Boumans, P. W. J. M., *Spectrochim Acta, Part B*, 1976, **31**, 147.
6. Schwarz-Bergkampf, E., *Z. Anal. Chem.*, 1966, **221**, 143.
7. Puschel, R., *Mikrochim. Acta*, 1968, No. 6, 782,
8. Fainberg, S. Y., and Ginzburg, L. B., *Zavod. Lab.*, 1956, **22**, 1157.
9. Pliner, Y. L., Svechnikova, E. A., and Ogurzov, V. M., "Control of Quality of Chemical Analysis in Metallurgy," Metallurgy, Moscow, 1979, p. 59.
10. Yufa, B. Ya., *Zavod. Lab.*, 1962, **28**, 329.
11. Poluektov, N. S., "Methods of Analysis by Flame Photometry," Khimiya, Moscow, 1967.
12. Prudnikov, E. D., *Spectrochim. Acta, Part B*, 1981, **36**, 385.
13. Lapp, R. E., and Andrews, H. L., "Nuclear Radiation Physics," Prentice-Hall, New York, 1948; Voenizdat, Moscow, 1956.
14. Fünfer, E., and Neuert, H., "Zahlrohre und Szintillationszähler," Verlag G. Braun, Karlsruhe, 1959; Atomizdat, Moscow, 1961.
15. Price, W. J., "Nuclear Radiation Detection," McGraw-Hill, New York, 1958; IL, Moscow, 1960.
16. Winefordner, J. D., and Vickers, T. J., *Anal. Chem.*, 1964, **36**, 1939.
17. Landee, R. W., Davis, D. C., and Albrecht, A. P., "Electronic Designers' Handbook," McGraw Hill, New York, 1957; Energoizdat, Moscow, 1961.
18. Ostrovskiy, L. A., *in* "Nonlinear Processes in Optics," Nauka, Novosibirsk, 1970, p. 26.
19. Ahmanov, S. A., and Hohlov, R. V., "Problems of Nonlinear Optics," Academia Nauk SSSR, Moscow, 1964, p. 264.
20. Prudnikov, E. D., *Z. Anal. Chem.*, 1981, **308**, 339.
21. Prudnikov, E. D., Bradaczek, H., and Labischinski, H., *Z. Anal. Chem.*, 1981, **308**, 342.
22. Price, W. J., "Analytical Atomic Absorption Spectrometry," Heyden, London, 1972; Mir, Moscow, 1976.
23. Prudnikov, E. D., Kolosova, L. P., Kalachev, V. K., Shapkina, Y. S., Novatskaya, N. V., and Bychkov, Y. A., *Zh. Anal. Khim.*, 1978, **33**, 468.

Paper A3/205
Received July 6th, 1983
Accepted August 1st, 1983

Interferences from Nickel, Lead, Copper and Silver and Their Elimination in the Determination of Mercury by Cold Vapour Atomic-absorption Spectrometry Exemplified by Fly Ash Assays

Nils Bernth and Kirsten Vendelbo
Department of Chemistry, Technological Institute, Gregersensvej, DK-2630 Tåstrup, Denmark

The determination of mercury in the presence of metal ions (nickel, lead, copper and silver) was studied by cold vapour atomic-absorption spectrometry. The results unambiguously showed serious depressing interferences. However, by using EDTA as a complexing agent these interferences could be completely eliminated over a wide concentration range for nickel, lead and copper. For silver the interference could be only partly eliminated. Some fly ash samples were examined with and without EDTA addition.

Keywords: *Mercury determination; cold vapour atomic-absorption spectrometry; sodium borohydride reduction; interferences; fly ash*

Determination of mercury by cold-vapour generation with detection by flameless atomic-absorption spectrometry is a well established and sensitive technique. Since its early development,[1] the method has been improved, increasing the reliability and ease of operation. Solutions of tin(II) salts were first used to generate the mercury vapour. More recently, reduction with sodium tetrahydroborate(III) instead of tin(II) chloride has been widely used. Sodium tetrahydroborate(III) is a strong reducing agent and is able to reduce mercury in most of its compounds, in contrast to tin(II) chloride. Simultaneously many concomitant metal ions are reduced to the metallic state and some of these metals may interfere, probably by amalgation with the released mercury.[2-6]

In the tin(II) chloride reduction method severe interferences from metals more easily reduced from the ionic state than mercury (*e.g.*, gold, platinum and palladium) have been reported by Lindstedt[7] and Ure and Shand.[8] On the other hand, metals less easily reduced than mercury (*e.g.*, copper and silver) had only a slight influence on the analysis.[4,7,8]

Toffaletti and Savory[3] observed, using sodium tetrahydroborate(III) as a reductant, that copper(II) ions at high concentrations in aqueous solution suppressed the response of mercury. Further, Yamamoto *et al.*,[4] applying the same reductant, reported that the silver(I) and copper(II) ions in excess of more than 25 and 2 500 times the concentration of mercury, respectively, caused interference. The presence of nickel(II) and lead(II) in a 10 000-fold excess, however, was tolerable.

Critical concentrations of the noble metals seldom occur in practice, whereas the more electropositive metals are often present in substantial amounts. In the determination of mercury in various fly ash matrices with high concentrations of nickel, lead and copper, we found that the signal was suppressed to a serious extent using sodium tetrahydroborate(III). In view of this, interferences from nickel(II), lead(II), copper(II) and silver(I) at the concentrations often present in fly ash matrices and their elimination have been investigated.

Experimental

Instrumentation

A Perkin-Elmer Model 5000 atomic-absorption spectrometer equipped with a Perkin-Elmer MHS-20 mercury/hydride system and a Perkin-Elmer mercury electrodeless discharge lamp was used. Argon was used as the purge gas. Peak-height readings were taken with a Hitachi Model 056 chart recorder (see Table 1).

Reagents and Standards

De-mineralised water and chemicals of analytical-reagent grade were used throughout this work.

Reductant solution. A solution containing 3% *m/m* sodium tetrahydroborate(III) (Fluka) in 1% *m/m* sodium hydroxide solution was prepared and filtered just before use.

Diluent solution. Concentrated nitric acid (14 M) (Merck) was diluted with water to the required concentration of 0.5 M.

Complexing solution. Disodium ethylenediaminetetraacetate dihydrate was dissolved in water to give a 0.3 M solution of EDTA.

Stock solutions. Aqueous solutions of $Hg(NO_3)_2$, $Ni(NO_3)_2$, $Pb(NO_3)_2$, $Cu(NO_3)_2$ and $AgNO_3$ containing 1 000 μg ml^{-1} of the metals (all BDH Spectrasol standards for atomic-absorption spectrometry) were used.

Mercury(II) working standard solution, 1.0 μg ml^{-1}. The standard solution was freshly prepared from the stock solution by dilution with 0.25 M nitric acid and stabilised by adding 1 ml of 0.012 M potassium iodide per 100 ml of standard solution.

Procedure

In a 100-ml beaker covered with a watch-glass, 2 g of sample were boiled with 50 ml of 14 M nitric acid with slow evaporation until less than 20 ml were left. The procedure was repeated twice and the solution was transferred into a 50-ml calibrated flask and diluted to volume with water. Residues were removed by filtration.

An appropriate volume of standard or sample was pipetted into the reaction vessel containing 10 ml of 0.5 M nitric acid. Pure mercury standards were spiked with various amounts of aqueous standard solutions of nickel(II), lead(II), copper(II) and silver(I), either singly or in mixtures. The effects of the spiked ions or the ions present in the sample matrices were studied with and without the addition of 1.0 ml of 0.3 M EDTA. Duplicate measurements were performed throughout the experiments.

Table 1. Instrumental parameters

Spectrometer parameters—	
Light source	EDL
Wavelength	253.7 nm
Spectral slit width	0.7 nm
Mode	Concentration
Expansion	3
Recorder response (time constant)	0.3 s
Recorder parameters—	
Chart speed	5 mm min^{-1}
Range	20 mV
MHS-20 parameters—	
Mode	$NaBH_4$
Purge I (Ar)	5 s
Reaction (Ar)	10 s
Purge II (Ar)	40 s
Temperature of quartz cell	200 °C

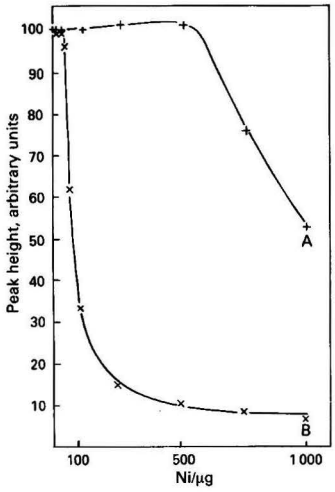

Fig. 1. Effect of nickel concentration on the signal produced by 100 ng of Hg in 0.5 M HNO_3, (A) with and (B) without addition of EDTA

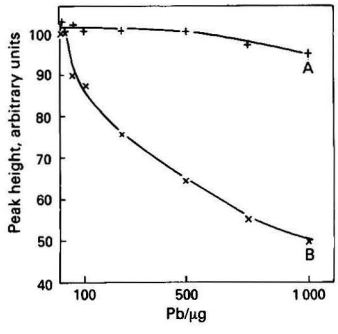

Fig. 2. Effect of lead concentration on the signal produced by 100 ng of Hg in 0.5 M HNO_3, (A) with and (B) without addition of EDTA

The polypropylene flasks used as reaction vessels and the immersion tubes were soaked for at least 1 d in 6 M nitric acid and rinsed with demineralised water before use.

Results and Discussion

The results in Figs. 1–4 (curves B) indicate that lead(II), copper(II) and particularly nickel(II) and silver(I) suppress the response of mercury severely. Further, Figs. 1–3 (curves A) suggest that the interferences observed from nickel, lead and copper can be eliminated over a wide range by adding EDTA to the reaction solution. Interferences from mixtures of nickel(II), lead(II) and copper(II) in 1:1:1 molar ratios could also be overcome, but not to the same extent as observed for the individual ions. Especially nickel(II) exerts an extremely depressive effect in the presence of lead and copper. On the other hand, mixtures of lead and copper resulted in a less pronounced depression. Curve A in Fig. 4 shows the effect of addition of EDTA on the response of mercury in the presence of silver. Clearly only minor effects are observed. The deviations are probably due to the weak complex formation under the acidic conditions, the position of silver in the electromotive series of elements and the easy amalgamation with mercury. Table 2 gives the permissible

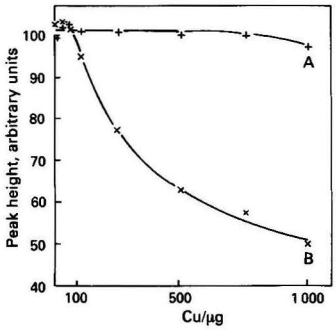

Fig. 3. Effect of copper concentration on the signal produced by 100 ng of Hg in 0.5 M HNO_3, (A) with and (B) without addition of EDTA

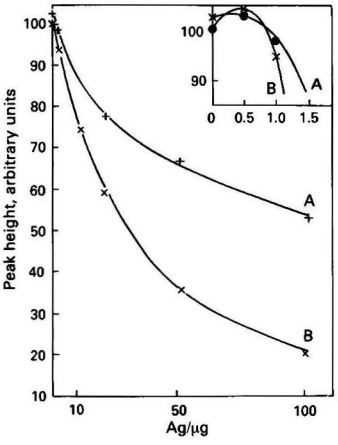

Fig. 4. Effect of silver concentration on the signal produced by 100 ng of Hg in 0.5 M HNO_3, (A) with and (B) without addition of EDTA

upper limits of foreign ions, defined here as the amount giving a signal differing by −5% of the signal for the standard with and without EDTA. The interference effects observed from nickel and lead differ from previous observations, especially those reported by Yamamoto *et al.*[4] Further, the metal ions affect each other, resulting in more or less pronounced interference in comparison with the individual ions. To explain these facts we believe further studies are required in order to gain an insight into the nature of the interferences and the importance of the reduction conditions.

Analysis of Fly Ash Samples

Fly ash samples were collected from a hazardous waste incinerator plant, where the flue gas had been treated with calcium hydroxide slurry in order to minimise pollution of the environment. The results obtained by applying our technique to these samples are given in Table 3. They suggest that using a slightly modified procedure, which does not affect the rapidity of the method, the employment of EDTA makes it possible to determine mercury in the presence of interfering ions. The analysis of the fly ash samples was performed by direct calibration using aqueous mercury standards. Regression analysis resulted in the calibration equation Amount (ng) = 1.8858 × response − 0.75 (r = 1.0000). When EDTA was added to samples spiked with 100 ng of mercury recoveries of

Table 2. Acceptable limits for Ni(II), Pb(II), Cu(II) and Ag(I) with and without EDTA added (within a negative error of 5%)

Ion	[Ion]/[Hg^{2+}] limit	
	Without EDTA	With EDTA
Ni(II)	300	6000
Pb(II)	400	9500
Cu(II)	1000	>10000
Ag(I)	9	12

Table 3. Determination of mercury in fly ash samples from a hazardous waste incinerator plant

Sample	Hg/5μg g^{-1}	
	Without EDTA	With EDTA
I	0.9	3.5
II	0.6	3.1
III	2.0	5.9
RSD,* %	23	7.6

	Ni/μg g^{-1}†	Pb/μg g^{-1}†,‡	Cu/μg g^{-1}†
I	350	31000	1920
II	310	47000	1890
III	460	36000	2060
RSD,* %	2.9	5.8	1.1

* Pooled relative standard deviation derived from duplicate samples.

† Determined by flame atomic-absorption spectrometry.

‡ Determined by inductively coupled plasma atomic-emission spectrometry.

105 ± 6% were obtained. In contrast, spiked samples without added EDTA led to recoveries ranging from 21 to 35%. Obviously, in sample II the content of lead exceeds the excess ratio determined in the interference study (see Table 2). However, as mentioned previously, lead and copper in mixtures affect each other, resulting in more favourable excess ratios. The amount of nickel is well within the tolerance limit. Finally, it should be mentioned that the high acidity of the reaction solution is important, because of a high content of calcium. Otherwise, at higher pH, most of the added EDTA would have been used to complex calcium.

The authors acknowledge the assistance of Dr. H. Olsen and Dr. M. Langkjaer in the preparation of the manuscript and thank Dr. K. K. Nielsen for donating the fly ash samples.

References

1. Hatch, W. R., and Ott, W. L., *Anal. Chem.*, 1968, **40**, 2085.
2. Ure, A. M., *Anal. Chim. Acta*, 1975, **76**, 1.
3. Toffaletti, J., and Savory, J., *Anal. Chem.*, 1975, **47**, 2091.
4. Yamamoto, Y., Kumamaru, T., and Shiraki, A., *Fresenius Z. Anal. Chem.*, 1978, **292**, 273.
5. Suddendorf, R. F., Watts, J. O., and Boyer, K., *J. Assoc. Off. Anal. Chem.*, 1981, **64**, 1105.
6. Suddendorf, R. F., *Anal. Chem.*, 1981, **53**, 2234.
7. Lindstedt, G., *Analyst*, 1970, **95**, 264.
8. Ure, A. M., and Shand, C. A., *Anal. Chim. Acta*, 1974, **72**, 63.

Paper A3/289
Received August 25th, 1983
Accepted October 17th, 1983

A Critical Look at Calibration Procedures for Flame Atomic-absorption Spectrometry

Julian F. Tyson
Department of Chemistry, University of Technology, Loughborough, Leicestershire, LE11 3TU, UK

The present treatment of calibration procedures in the analytical literature is described and the reasons for the poor coverage are discussed. The computational bases of a number of currently available atomic-absorption instrument calibration computer programs are described and discussed. Two computer-based methods are compared using the same calibration data. Additional features of these programs are also discussed. Some desirable features of such programs are proposed. The use of the standard additions method is examined in terms of the shape of the plot of absorbance *versus* concentration of interferent. The success of the method depends on using only the plateau region of this plot.

Keywords: *Calibration; atomic-absorption spectrometry; standard additions*

The relationship between the concentration of analyte and the response of an analytical instrument is usually a complex function of a variety of instrument parameters and interference effects from other components of the sample. Thus all instrumental methods must include a calibration step as an integral part of the over-all procedure. The calibration may simply be to establish the instrument response *versus* concentration relationship or the procedure may be designed to compensate for interference effects arising from other sample components, as in the matching of standards to samples or in the standard additions method. All of these procedures are regularly used in flame atomic-absorption spectrometry as each instrument has its own highly individual response characteristics, heavily dependent on the operating conditions selected by the user and, in many instances, on other components in the sample. The response is individualised to such an extent that manufacturers tend to quote the slope of the calibration function near the origin as, literally, a "figure of merit" for a particular model. Analogous claims for molecular absorbances are never made by manufacturers of solution spectrometers as there are good reasons for expecting the absorbance value measured to be independent of the instrument used. It is unlikely, though, that this situation will ever be achieved with atomic-absorption spectrometers because the complex sequence of physical and chemical steps of atom production is very much a function of an individual instrument's design. In practice, other effects such as the age of the light source and choice of operating parameters will also have a marked influence on the absorbance - concentration relationship.

As calibration procedures are vital for achieving accuracy in any analytical procedure that uses an instrumental finish, it is disappointing that the topic is given such poor coverage in general text books on analytical chemistry, although some of the more recent texts[1,2] do give a small amount of space to the topic. Even in specialist texts on analytical atomic spectrometry,[3,4] the topic is only given minimal treatment. The topic does not appear to be covered adequately in the original literature either, with one or two notable exceptions.[5,6] There is therefore a danger that, with the advent of computer-based calibration procedures, the importance of an accurate calibration procedure will be increasingly overlooked. In addition to fitting a curve to the calibration points, calibration software packages normally include other features such as identification of the linear portion and extrapolation for the standard additions method, resloping of a stored calibration graph based on one standard and indication of when the "curvature" has exceeded a certain value, etc. Currently there appears to be a reluctance on the part of manufacturers to reveal the details of what their various programs actually do.[7] This is exemplified by a recent paper in which the validity of using stored working curves was discussed but no information was provided on how the program "resloped" the calibration.[8] This can only further the blind acceptance of the accuracy of the calibration program.

In this paper, the bases of the computerised calibration procedure of a number of different atomic-absorption instruments are described and the performances of two different instruments evaluated. A problem with the standard additions method that has not been discussed previously in analytical atomic-absorption text books is outlined and discussed in terms of the shape of the plot of percentage interference against interferent to analyte concentration ratio.

Curve Fitting Procedures

Until the recent arrival of inexpensive, readily available calculating devices, either as separate units or built into instruments, calibration has consisted of obtaining the instrument response for a series of analyte concentrations covering the range to be encountered in the analysis in question, plotting the points on graph paper and drawing the calibration graph following visual inspection of the pattern produced by the points using a pencil and ruler or "Flexicurve." Such a procedure is time consuming and naturally there has been a move towards using the readily available computing power to fit equations to the set of points, and then calculate analyte concentrations by substitution of measured absorbance values into the equation.

Manufacturers' literature indicates that a variety of ways are actually used to fit the curve to the calibration points.

Experimental

Information was requested from five manufacturers of atomic-absorption spectrometers currently available in the UK on the method used to fit the curve to the calibration points. To compare different methods, calibration data generated by one instrument (a Shandon Southern A3300) was used for the calibration of two instruments with different curve fitting programs (a Pye Unicam SP9 computer and a Baird Atomic Datacomp Model A5195 connected to a Baird Atomic A3400 spectrometer). In addition, data for chromium taken from Thompson's paper[9] for a situation in which a region of negative slope was observed were also used for calibrating the two instruments.

Procedure

Any convenient hollow-cathode lamp was used. The usual resonance line was selected. The flame was not lit. The integration period was set at 4 s and three replicate readings

were taken. The appropriate calibration points were obtained by slightly changing the monochromator wavelength (neither instrument has a continuously variable slit width) so as to measure absorbance on the wings of the instrument-broadened emission profile from the lamp, thus changing the absorbance reading while leaving the gain setting unchanged. With the Pye Unicam SP9 instrument a chart recorder was used to monitor the absorbance reading as this is not displayed during a calibration run.

Results

The way in which the various programs deal with the calibration data are set out below.

Baird Atomic

The Datacomp accessory[10] used in the experiments reported here uses the equation

$$C = rA^2 + pA + q \quad \ldots\ldots\ldots \quad (1)$$

where C is concentration, A is absorbance and p, q and r are coefficients calculated for a least-squares fit of the curve to the points. Any number of standards up to eight can be accommodated. The Alphastar system[11] (used with the current range of Baird Alpha instruments) uses an equation similar to that of Varian, namely

$$A/C = rA^2 + pA + q \quad \ldots\ldots\ldots \quad (2)$$

The coefficients are calculated by an iterative least-squares procedure and up to 20 standards can be handled. The program includes a "reslope" facility based on correcting subsequent measurements by a sensitivity correction factor calculated from a single new standard result.

Instrumentation Laboratory

A different procedure is used, depending on the number of standards.[8,12] With two standards a quadratic equation is solved so that the curve is forced through the calibration points. If three standards are used, a similar procedure is used for a cubic equation. For four or five standards (the maximum number that can be handled) a cubic equation is used but the best fit curve is computed by a least-squares procedure. The program includes a reslope facility based on a single standard that corrects the absorbances of other standards by a factor calculated from a comparison between the single standard's new absorbance and its original absorbance.[13] If stored calibration data are lost from memory, they may be re-entered via the instrument key-board.

Perkin-Elmer

The program uses the equation

$$C = \frac{pA^2 - rA}{qA - 1} \quad \ldots\ldots\ldots\ldots \quad (3)$$

For three standards, the values of p, q and r are evaluated by solving the simultaneous equations so that the curve passes through the calibration points.[14] For more than three standards (up to eight), the equation is calculated by a least-squares fit procedure.[15]

Pye Unicam

The program does not use a single equation but calculates a different equation between each calibration point.[16] A straight line is drawn between the blank and the lowest standard. The mean of the slope of this line and the slope of the line between the first and second points is used to define a parabola between these points, which is used as the calibration relationship for establishing sample results. The process is repeated for up to five standards, so that a different parabola is calculated for the region between each pair of adjacent calibration points. Single point recalibration is possible and the program will detect the onset of curvature for use in the standard additions mode.[17] This is done by comparing the slope of the straight line between adjacent calibration points with the slope between the two previous points. Curvature is detected when a 5% difference in slopes is observed.

Varian

The program uses the following equation[18]:

$$A/C = rA^2 + pA + q \quad \ldots\ldots\ldots \quad (4)$$

When three standards are used the simultaneous equations are solved so that the curve passes through the calibration points. If one or two standards are used then r and p or r are set equal to zero, respectively. If four or five standards are used then the values of r, p and q are obtained by solving the simultaneous equations corresponding to the two standards below and the one standard above the unknown concentration. This, in effect, generates a family of overlapping parabolas. A reslope facility based on a single standard and a standard additions mode calibration are also available.

Comparison of Curve Fitting Methods

The calibration values generated from the Baird Atomic A3300 for the elements magnesium and nickel are given in Table 1, which also contains data calculated from Fig. 3 of reference 9. The table shows the values calculated by each program when the absorbances of the data points were input as unknowns. The calibration data and calculated concentrations are illustrated in Fig. 1 for nickel and in Fig. 2 for chromium.

Discussion

Although the method of linear regression analysis using the least-squares method is the only "curve" fitting method that is dealt with to any extent in analytical text books, it is obvious that this procedure is of little use in dealing with atomic-

Table 1. Comparison of Pye Unicam (PU) SP9 and Baird Atomic (BA) Datacomp curve fitting programs

Calibration data						Concentrations found, p.p.m.					
Mg		Ni		Cr		Mg		Ni		Cr	
C	*A*	*C*	*A*	*C*	*A*	PU	BA	PU	BA	PU	BA
0.00	0.00	0.00	0.00	0.00	0.00	0.00	0.011	0.00	1.66	0.00	0.12
0.25	0.18	10.0	0.32	5.0	0.36	0.25	0.23	10	6.12	5.0	5.30
0.50	0.34	25.0	0.58	7.5	0.52	0.50	0.47	25	24.3	7.5	7.73
1.00	0.61	50.0	0.82	10.0	0.74	1.00	1.02	50	54.0	11.5	11.11
1.50	0.81	75.0	0.96	12.5	0.72	1.50	1.53	76	76.4	9.9	10.81
2.00	0.96	100	1.07	15.0	1.00	2.00	1.97	100	96.9	14.9	15.2

absorption calibrations that are well known to be, in general, initially straight lines becoming progressively more curved at higher concentrations. Effects such as ionisation and flame reaction kinetics may cause the curve to have a more complex shape with points of inflection and even regions of negative slope. The computational methods of the linear least-squares method are probably used in the programs that fit the "best curve" to the points by calculating coefficients by a least-squares method so that the computation is carried out with a linearised function. Such procedures probably account for the persistence of the term "curve correction," whereas "curve fitting" would be much more appropriate. As is sometimes mentioned in text books,[2] the slope and intercept by the least-squares method have uncertainties associated with them that can be expressed as an interval at the appropriate level of confidence. This means that with a known uncertainty in a measured value, a confidence interval can be calculated for a predicted value. Although this is well known in statistical circles (see, for example, reference 19), the use of such confidence intervals has not been practised in analytical chemistry circles, probably because the equations involved are cumbersome and thus the computations were tedious and time consuming. However, with the computing power that is now readily available in the present generation of instruments, such calculations could be readily performed. The inclusion of a confidence interval on the computer printout would go a considerable way to removing the blind acceptance of the accuracy of results on computer printout that was mentioned earlier.

It is also known that the uncertainty in the measured values of absorbance increases as the concentration increases and, although the absolute standard deviation increases, the relative standard deviation passes through a minimum. As pointed out by van Dalen and de Galan,[6] it is relatively simple to choose a calibration concentration range within which the results have less than a desired relative standard deviation from the Ringbom plot. From the point of view of curve fitting procedures, the increase in uncertainty of the measured points means that a weighted regression analysis should be used, *i.e.*, the curve should be forced to pass closer to some points than others. An exactly similar argument applies to why the use of such weighted procedures has not become common practice as was discussed for the use of confidence intervals on predicted results and exactly the same counter argument applies; with the present generation of instruments the calculations can be readily performed.

Confidence intervals and weighting factors will be discussed at greater length in another paper.[20]

The present position with regard to curve fitting procedures is unsatisfactory in that the current instrumentation uses at least four different equations and one "composite" method. In some instances the curve is a best fit to the points calculated by some "minimising of the squares of the absorbance residuals" procedure and in some instances the curve is forced to pass through the calibration points. The problems associated with trying to fit all calibration graphs to a single type of mathematical function can be readily seen from the poor fit between the calculated curve and the actual curve in the case of nickel (see Fig. 1). Neither method of calibration could cope with the region of negative slope of the chromium calibration (see Fig. 2). Both methods though coped adequately with the much "straighter" and smooth curve of the magnesium calibration.

Conclusions

Attractive as computerised curve fitting procedures are in principle, there are a number of drawbacks with the present generation of atomic-absorption spectrometers. Unless a top of the range instrument with a video display unit is used, it is not possible visually to inspect the data points and various unusual or unexpected features may be overlooked. There could be the presence of outliers due to errors in preparing calibration solutions or the occurrence of inflection points or regions of negative slope.

Although it is important to ensure appropriate selection of optimum spectral band pass and lamp current to minimise the curvature due to stray light while maintaining an adequate signal to noise ratio, it is important that curve fitting procedures can deal with situations exemplified by Fig. 1. The concentration range for which the relative standard deviation is less than a desired value (selected from the Ringbom plot[6]) may permit the use of upper absorbance values well into the curved region of the calibration plot.

Until such time as such display units are available on all instruments and appropriate weighting procedures are used with printout of confidence intervals for predicted results, the accuracy of a given calibration procedure can only be assessed by visual inspection of a manually plotted graph.

Standard Additions Method

Statements such as "the method of standard additions is a well known and useful technique that often makes it possible to obtain accurate determinations in the presence of matrix interferences"[15] are fairly common in manufacturers' literature. The method is usually mentioned briefly in analytical

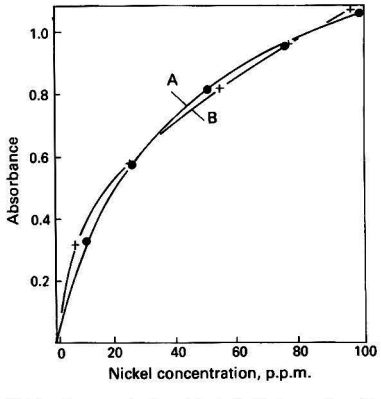

Fig. 1. Calibration graphs for nickel. A, Data produced by a Baird Atomic A3300 instrument; B, best-fit relation from a Baird Atomic Model A5195 Datacomp accessory

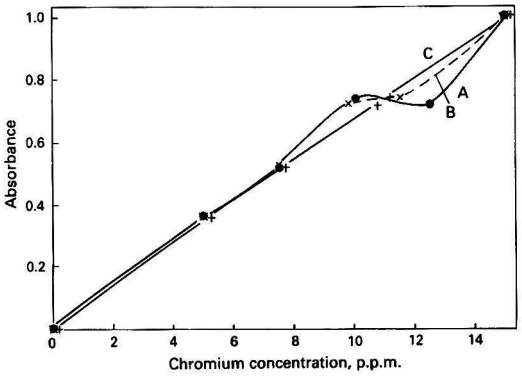

Fig. 2. Calibration graphs for chromium. A, Data from reference 9; B, best-fit relation from a Pye Unicam SP9 computer; C, best-fit from a Baird Atomic A5195 Datacomp accessory

atomic spectrometry texts and the limitations that (1) it is necessary to work with the linear portion of the calibration graph and (2) the method will not correct for errors arising from non-specific background absorption are usually explained.[21] The principle of the method is illustrated in Fig. 3, from which it is clear that for the method to be successful, the interference effect encountered must affect the slope of the calibration (the sensitivity), *i.e.*, each point must be subjected to the same percentage depression.

There are many situations in which this constant percentage depression is not obtained.

Experimental

A Pye Unicam SP 90 Series 2 atomic-absorption spectrometer was used with an air - acetylene flame throughout. Stock 1 000 p.p.m. solutions of calcium and aluminium were obtained from BDH Chemicals and a 1 000 p.p.m. phosphate solution was prepared by diluting AnalaR-grade orthophosphoric acid.

Procedure

The instrumental conditions were selected to give maximum sensitivity for calcium in the absence of interferences.

The effects of increasing the concentration of phosphate and the concentration of aluminium on a fixed concentration of calcium were investigated and a number of solutions containing various amounts of calcium and phosphate or aluminium were analysed by the standard additions procedure.

Results

The results of the study of the phosphate and aluminium interferences are shown in Fig. 4 and the results of the analysis of the various solutions are given in Table 2. It was found that with solutions containing the same concentration of calcium and phosphate ranging from 1 to 50 p.p.m. errors of up to −30% were observed. When the phosphate to calcium ratio was greater than 2, satisfactory results were obtained but no aluminium to calcium ratio could be found for which accurate results were obtained.

Discussion

The shapes of the interference plots (Fig. 4) are similar to those reported by other workers,[22,23] and are typical of the effects of a range of interferences due to stable compound formation of incomplete volatilisation.

The effects observed here may be more severe than observed with other instruments or would be observed for different initial operating conditions. The initial conditions were selected on the basis of maximising sensitivity for calcium in the absence of any interference effects, as it is felt that this is the most commonly used instrument optimising strategy.

It is thus obvious that the standard additions method will be inaccurate in situations that are typified by the calcium - aluminium effect as there is no constant percentage depression plateau, and will only give satisfactory results when situations typified by the calcium - phosphate effect are encountered. In theory, the "calcium - aluminium" type of effect should be detected from an upwards curvature of the calibration, but in practice the magnitude of this effect may be small and it may easily be overlooked. In the work reported here, very good correlation coefficients were achieved for a linear regression analysis of the measured region of the calibration under conditions in which curvature would have been theoretically expected. The use of releasing agents, such as lanthanum, does not provide a simple solution to the problem as the released signal never falls on the horizontal zero interference line and may, in some instances, actually be greater than the signal obtained in the absence of interferent. This is probably due to additional ionisation-suppression effects. The same argument has then to be applied to the enhanced signal, all the measurements for the analysis must be made under conditions at which a constant percentage enhancement is obtained. The extent to which interference effects are observed is often highly dependent on instrumental operating conditions such as fuel to oxidant ratio and observation height. Hence it may be that the operating conditions necessary for successful application of the standard additions method (achieving a linear calibration over the required range with constant percentage depression or enhancement) are different from those selected for maximum sensitivity of the analyte element alone. Problems in the determination of calcium in cement associated with the effects discussed above have been reported by Hosking *et al.*[24]

Table 2. Standard additions method of analysis for calcium

Concentration in test solutions, p.p.m.			
Ca^{2+}	PO_4^{3-}	Al^{3+}	Calcium found, p.p.m.
5	200	—	5.0
20	200	—	20.2
50	200	—	50.0
7	—	2	6.3
10	—	5	7.9

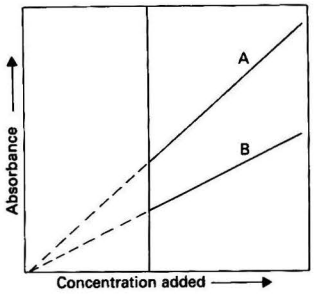

Fig. 3. Principle of the standard additions method. Extrapolation of curve A (no interferences) gives the analyte concentration from the intercept on the concentration axis; extrapolation of B (interferences present) is only accurate if all points on A suffer the same percentage depression

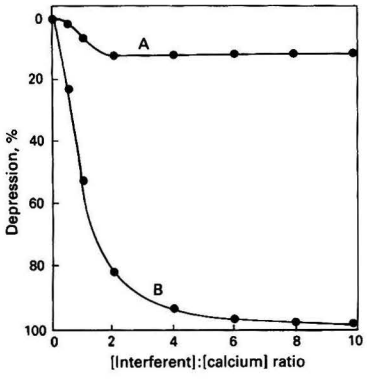

Fig. 4. Graph of percentage depression in calcium absorbance against ratio of interferent concentration to calcium concentration. A, Phosphate interference; B, aluminium interference

Conclusions

The various constraints that apply to the standard additions method mean that great care is needed if accurate results are to be obtained. Method development should, if possible, include investigation of the linearity of the calibration and the shape of the plot of percentage depression or enhancement *versus* ratio of interferent concentration to analyte concentration. In order to be certain of achieving such a constant level of interference it may be necessary, as part of the sample preparation procedure, to add a certain amount of the interferent.

References

1. Braun, R. D., "Introduction to Chemical Analysis," McGraw-Hill, New York, 1982, pp. 159–170.
2. Harris, D. C., "Quantitative Chemical Analysis," Freeman, San Francisco, 1982, pp. 52–58.
3. Price, W. J., "Spectrochemical Analysis by Atomic Absorption," Heyden, London, 1979, pp. 120–127.
4. Ebdon, L., "An Introduction to Atomic Absorption Spectroscopy," Heyden, London, 1982, pp. 71–72.
5. Agterdenbos, J., *Anal. Chim. Acta*, 1979, **108**, 315.
6. van Dalen, H. P. J., and de Galan, L., *Analyst*, 1981, **106**, 695.
7. Morrison, G. H., *Anal. Chem.*, 1983, **55**, 1.
8. Sotera, J. J., Smith, S. B., and Kahn, H. L., *Analyst*, 1982, **107**, 1484.
9. Thompson, K. C., *Analyst*, 1978, **103**, 1258.
10. "Handbook for the Model A5195 Datacomp," Baird Atomic, Braintree, Essex.
11. Hall, J. R., "Notes on Alphastar 2 Atomic Absorption Curve Correction," Baird Atomic, Braintree, Essex, 1982.
12. "Some Applications of the IL 751 Atomic Absorption Spectrometer," Reprint 84, Instrumentation Laboratory, Wilmington, MA, 1977.
13. Batho, A., personal communication.
14. Perkin-Elmer Corporation, Norwalk, CT, *US Pat.*, 4 238 830, 1980.
15. "Software for the Model 3030 Atomic Absorption Spectrophotometer," Perkin-Elmer, Norwalk, CT, 1982.
16. Whiteside, P. J., Stockdate, T. J., and Price, W. J., *Spectrochim. Acta, Part B*, 1980, **35**, 795.
17. "Pye Unicam PU 9000 Atomic Absorption Systems," Pye Unicam, Cambridge.
18. Limbek, B. E., and Rowe, C. J., "Curve Correction in Atomic Absorption," Varian Techtron Lecture Transcript, 1977.
19. Miller, R. G., Jr., "Simultaneous Statistical Interference," McGraw-Hill, New York, 1966.
20. Killoran, G. N., and Tyson, J. F., *Analyst*, to be submitted.
21. Thompson, K. C., and Reynolds, R. J., "Atomic Absorption, Fluorescence, and Flame Emission Spectroscopy," Second Edition, Charles Griffin, London, 1978, p. 28.
22. Greenfield, S., Jones, I. Ll., and Berry, C. T., *Analyst*, 1964, **89**, 713.
23. Magill, W. A., and Svehla, G., *Fresenius Z. Anal. Chem.*, 1974, **268**, 177.
24. Hosking, J. W., Oliver, K. R., and Sturman, B. T., *Anal. Chem.*, 1979, **51**, 307.

Paper A3/271
Received August 19th, 1983
Accepted September 21st, 1983

Extended Calibration of Flame Atomic-absorption Instruments by a Flow Injection Peak Width Method

Julian F. Tyson
Department of Chemistry, University of Technology, Loughborough, Leicestershire, LE11 3TU, UK

The principles of two existing methods of calibration based on flow injection methodology are outlined and the mathematical basis of a method based on peak width is presented. On the basis of the single well stirred tank model, it is shown that peak width at any concentration is proportional to logarithm of a function of concentration. The relationship is verified experimentally over the range 1–1 000 p.p.m. of magnesium. The advantages and limitations of the method are discussed.

Keywords: *Atomic-absorption calibration; flow injection analysis; peak width*

The principles of two flow injection based procedures have already been described.[1] The first of these procedures is based on the use of an exponential concentration gradient (with an accurately known concentration - time relationship) generated by the passage of a step concentration change through a well stirred mixing chamber (volume approximately 8 ml) located just in front of the nebuliser. If the instrument response is recorded as a function of time as the concentration gradient is introduced, then this record is, in fact, a calibration graph for the instrument as the time axis can be replaced by a concentration axis from the known relationship between concentration and time. Samples are introduced in the conventional manner and steady-state values used. Implementation of the method in practice will be discussed in detail elsewhere.[2] The second method provides a means of carrying out the standard additions method of analysis and is based on injection of pure standards into the sample, used as the carrier stream. The method is based on controlling the dispersion of the standard within the sample carrier stream so that the interference effects act on the standards to the same extent as on the analyte. Details of the calculations required to select the required dispersion have already been given,[3] and an example of the application of the method will be given elsewhere.[4]

One of the problems encountered in routine analytical situations is that the analyte concentrations of the sample solutions often do not fall within the rather limited range of concentrations (about one order of magnitude) that a typical flame atomic-absorption instrument can deal with at a given relative standard deviation.[5] Approaches to dealing with samples of concentrations below this range will not be discussed further here. For samples whose concentrations are above this range, a variety of methods have been used. The instrument sensitivity can be reduced by either changing the absorbing path length, usually by rotation of the burner, or selection of a less sensitive line from the light source or reducing the nebulisation efficiency by adjustment of uptake rate or spray production mechanics. Alternatively, the sample may be diluted. This can be done without using pipettes and calibrated flasks by a suitable flow injection manifold. The most elegant method is that of "zone sampling"; after injection of the discrete sample volume, a slice of the dispersed sample zone is injected by a second injection system into the carrier stream flowing to the spectrometer. By controlling the timing of the second injection a variety of dilutions can be achieved.[6]

A new method of dealing with sample solutions that are too concentrated for the normal calibration range is proposed here, based on measurement of the width of peaks produced on flow injection introduction.

Basis of Peak Width Method

Assume the peaks to be composed of exponential rise and fall curves as would be obtained by passage of a volume V_i of concentration C_m through a single well stirred mixing chamber of volume V at flow-rate u. As the leading edge of the sample plug enters the mixing chamber the change in concentration as a function of time is given by

$$\frac{dc}{dt} = \frac{C_m u}{V} - \frac{Cu}{V}$$

Separating the variables and integrating gives

$$\ln(C_m - C) = \frac{-ut}{V} + k$$

where k is a constant of integration. Putting in the initial conditions $t = 0$, $C = 0$ gives $k = \ln C_m$. Therefore,

$$t = \frac{V}{u} \ln \left(\frac{C_m}{C_m - C}\right) \quad (1)$$

{this can be further rearranged to give the more familiar form $C = C_m [1-\exp(-ut/V)]$}.

The peak concentration, C_p, is achieved as the trailing edge of the sample plug just enters the mixing chamber at a time given by

$$t_p = \frac{V_i}{u} \quad (2)$$

Thereafter the rate of change of concentration with time (measured from the peak maximum) is given by

$$\frac{dc}{dt} = -C_p \frac{u}{V}$$

Integrating as above gives

$$t = \frac{V}{u} \ln \left(\frac{C_p}{C}\right) \quad (3)$$

[which can similarly be rearranged to give the more familiar form $C = C_p \exp(-ut/V)$].

Hence the peak width t' at any concentration C' is given by

$$t' = \frac{V_i}{u} - \frac{V}{u} \ln \left(\frac{C_m}{C_m - C'}\right) + \frac{V}{u} \ln \left(\frac{C_p}{C'}\right)$$

This is shown in Fig. 1.

Rearranging and substituting the dispersion, $D = C_m/C_p$, gives

$$t' = \frac{V}{u} \ln \left(\frac{C_m}{C'} - 1\right) - \frac{V}{u} \ln (D - 1) \quad (4)$$

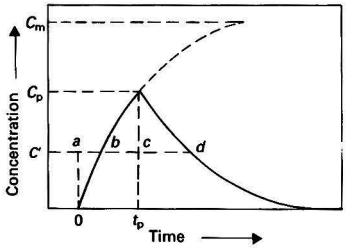

Fig. 1. Exponential rise and fall curves for peak produced by passage of sharp concentration boundaries through a well stirred mixing chamber. Peak width, t', is given by $t' = bd = ac - ab + cd$. C_m is the concentration of the injected solution, C_p is the concentration at the peak maximum and C' is the concentration level chosen for measurement

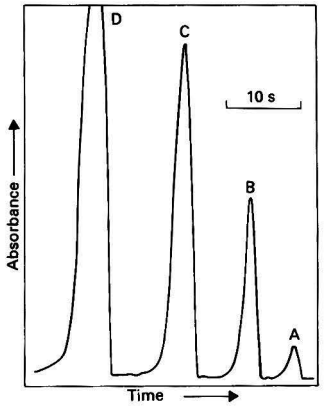

Fig. 2. Chart recordings of typical peaks produced from injection of approximately 100 µl of A, 1; B, 10; C, 100; and D, 1 000 µg ml^{-1} of magnesium

Thus a plot of t' *versus* ln $[(C_m/C') - 1]$ for different values of C_m should be a straight line of slope V/u and intercept (V/u) ln $(D-1)$.

Experimental

Apparatus

A Perkin-Elmer 290B atomic-absorption spectrometer was used with magnesium as the test element. Approximately 100 µl of standard solution were injected via a Rheodyne Model 5020 rotary injection valve into a carrier stream in 0.58 mm i.d. PTFE tubing propelled by an Ismatec Model Mini-S 840 peristaltic pump at a flow-rate of 6.9 ml min^{-1}. The minimum length of tubing possible was used between injection valve and nebuliser.

The dispersion produced is thus dominated by the nebuliser performance characteristics producing a good approximation to the single well stirred tank model. The hypothetical tank volume is approximately 80 µl.

The spectrometer response was monitored with a Philips Model PM8251 chart recorder.

Standard Solutions

Solutions of concentration 1, 10 and 100 p.p.m. were prepared by serial dilution of a stock 1 000 p.p.m. solution (BDH Chemicals). All four were used for the peak-width calibration. Solutions covering the range 0–10 p.p.m. were used for a conventional calibration.

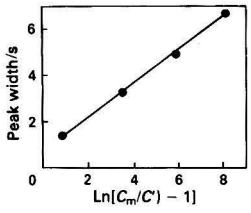

Fig. 3. Graph of peak width, t', against ln$[(C_m/C') - 1]$

Table 1. Data for peak width calibration method

Peak width/mm	Mean peak width/s	C_m, p.p.m.	$\frac{C_m}{C'} - 1$	$\ln\left(\frac{C_m}{C'} - 1\right)$
7.0, 7.0, 7.0	1.4	1.00	2.33	0.85
16.0, 17.0, 16.5	3.30	10.0	32.3	3.48
24.5, 24.5, 24.5	4.90	100	332	5.81
33.5, 34.0, 33.5	6.86	1000	3332	8.11

Procedure

After optimising the instrument response for magnesium and selecting a suitable flow-rate, a conventional calibration was obtained by continuously pumping each standard in turn and noting the steady-state absorbance. The peak-width calibration data were obtained by injecting, in triplicate, approximately 100 µl of each of the standards into a distilled water carrier stream and recording the resulting peak at the recorder's fastest speed of 300 mm min^{-1}. A suitable absorbance value corresponding to C' in equation (4) was selected and the peak widths were measured to the nearest 0.5 mm.

Results

Typical peak shapes for each of four concentrations are shown in Fig. 2. The absorbance scale for the instrument used is arbitrary, but the cut-off at full-scale deflection of the chart recorder for peak d corresponds approximately to 0.5 absorbance unit. The absorbance level selected for peak-width measurements corresponded to a concentration of 0.30 p.p.m. The peak-width calibration data are given in Table 1 and a plot of peak width, t', against ln$(C_m/C' - 1)$ is shown in Fig. 3. A least-squares fit of the best straight line gave a slope of 0.745, intercept 0.716 and correlation coefficient 0.999.

Discussion

The basis of the peak-width method of calibration is that the peaks are exponential in shape. The linear relationship obtained here supports previously reported peak shapes[3] arising from the injection of solutions close to the nebuliser, confirming the validity of the single well stirred tank model already proposed for this experimental arrangement. As the peak width can only be measured to the nearest 0.5 mm from the chart recording, this gives an uncertainty of about ±5% relative over the whole concentration range. This could be improved by increasing the slope of the calibration plot by changing the experimental conditions either to increase V or to decrease u, or both. Processing the spectrometer response with a microcomputer would also lead to an improvement by decreasing the uncertainty associated with measuring the time of the peak width. The method will probably never be as accurate as the conventional calibration procedure owing to the uncertainties in the measured quantities, but would prove useful in providing guidelines for dilution factors for subsequent accurate analysis and of course, is applicable in

situations where the best accuracy is not required. As a strict adherence to a linear relationship is not necessary for a calibration function, some approximations in the method could be tolerated. For example, $\ln C_m$ could be used instead of $\ln(C_m/C' - 1)$ in the calibration function. A plot of t' *versus* $\ln C_m$ for the data listed in Table 1 gives an almost identical correlation coefficient. The peak width should be measured at an absorbance value within the linear part of the absorbance - concentration relationship in order that the absorbance analogue of equation (4) is valid. However, this restriction could probably be relaxed and this, together with the use of $\ln C_m$ in the plot, would avoid the need to determine the concentration corresponding to the absorbances at which the peak width was measured. Finally, strict adherence to exponential peak shapes and the conditions necessary to produce them is probably also not necessary as whatever shapes the peaks are, it is likely that the function relating peak width and the logarithm of the concentration will increase monotonically.

Conclusion

The concentration gradients produced by allowing concentration boundaries to disperse during laminar flow in narrow-bore tubing under precisely controlled conditions have been shown to provide the basis for several different calibration procedures. The combination of flow injection sample introduction techniques with microcomputer data storage and manipulation would appear to offer some interesting possibilities with direct advantages to the practising analyst, not just in the field of atomic-absorption spectrometry but also in other areas of routine instrumental analysis.

References

1. Tyson, J. F., Appleton, J. M. H., and Idris, A. B., *Analyst*, 1983, **108**, 153.
2. Tyson, J. F., and Appleton, J. M. H., *Talanta*, in the press.
3. Tyson, J. F., Appleton, J. M. H., and Idris, A. B., *Anal. Chim. Acta*, 1983, **145**, 159.
4. Tyson, J. F., and Idris, A. B., *Analyst*, 1984, **109**, 23.
5. van Dalen, H. P. J., and de Galan, L., *Analyst*, 1981, **106**, 695.
6. Reis, B. F., Jacintho, A. O., Morlatti, J., Krug, F. J., Zagatto, E. A. G., Bergamin Fº. H., and Pessenda, L. C. R., *Anal. Chim. Acta*, 1981, **123**, 221.

Paper A3/330
Received August 19th, 1983
Accepted September 21st, 1983

Sample Work-up for Graphite Furnace Atomic-absorption Spectrometry Using Continuous Flow Extraction

Kenneth Bäckström, Lars-Göran Danielsson* and Lage Nord
Department of Analytical Chemistry, Royal Institute of Technology, S-100 44 Stockholm, Sweden

Using a flow injection analysis system a two-stage extraction method has been developed to extract metals automatically from aqueous solutions; cadmium, copper, iron, lead, nickel and zinc could be concentrated 25–30-fold without serious losses. However, cobalt gave only a 15-fold enrichment. The metals are concentrated into an aqueous solution totally free from the original matrix. The flow-rate of extract is about 200 μl min^{-1}, making the system compatible with the graphite furnace.

Keywords: *Continuous flow extraction; trace metals; dithiocarbamates; graphite furnace; atomic-absorption spectrometry*

The need for sample work-up prior to chemical analysis has not been diminished by recent instrumental development. In spite of increased sensitivities, extensive automation and data handling facilities now built into analytical instrumentation, the inapplicability to direct analysis of many real samples persists. This was pointed out in a paper by Kraak,[1] where the advantages of liquid - liquid extraction were also emphasised.

In the field of trace metal analysis, extraction has been the preferred technique for sample pre-treatment in connection with atomic-absorption spectrometry (AAS). The extraction step here serves the dual purpose of concentrating the metals of interest and separating them from an interfering matrix. If the determinations are to be performed by graphite furnace atomisation the matrix separation should preferably be as complete as possible. It has been found that at low trace metal concentrations sensitivity changes occur even at moderate matrix concentrations.[2] Fortunately, the volume requirements for this technique are minute. A sample volume of 10–20 μl fed into the tube every 2 min is normally sufficient. This means that for automatic extraction systems to be compatible with the furnace, a flow-rate of extract of 100–200 μl min^{-1} is acceptable.

As the metal concentrations determined by graphite furnace AAS are in the micrograms per litre range, contamination is often a severe problem. A working extraction system at these levels should preferably be as closed as possible and built of components of inert plastics, such as PTFE.

The metal extraction system presented by Nord and Karlberg[3] was developed for use with flame AAS and is not suitable for the graphite furnace. The solubility of water in isobutyl methyl ketone (IBMK) and *vice versa* precludes the use of high phase volume ratios. Further, introduction of metals into the graphite furnace in the form of carbamate complexes is not recommended owing to the volatility of these compounds.

The development of a new system specifically designed for use with the graphite furnace was therefore started. The chemistry of the system is based on the formation of hydrophobic complexes between metals and a mixture of dithiocarbamates. These complexes are then extracted into an organic solvent. After separation the organic phase is segmented with a mercury solution. Mercury, forming stronger complexes with dithiocarbamates, displaces the metals of interest from their complexes. The metals are subsequently transferred into the aqueous solution.

Experimental

Reagents

The extraction reagent was prepared by dissolving 1 g of ammonium tetramethylenedithiocarbamate (ammonium pyrollidinedithiocarbamate, APDC) and 1 g of diethylammonium diethyldithiocarbamate (DDDC) in 1 l of a 0.3 M acetate buffer solution of pH 5.5. Enough ammonia was added in order to neutralise most of the acid in the samples. Samples used for extraction studies were prepared by serial dilutions of 1 000 mg l^{-1} stock standards, prepared from Titrisol ampoules. All samples were made 0.014 M in nitric acid giving an extraction pH of 5. The mercury solution used for back-extraction was also made from Titrisol ampoules, the final solution being 0.20 M in nitric acid. Unless otherwise stated a mercury concentration of 1 000 mg l^{-1} was used. Freon 113 (1,1,2-trichloro-1,2,2-trifluoroethane) was of technical quality and used as purchased. All other chemicals were of analytical-reagent grade.

Manifold Design

The assembly is shown in Fig. 1. In the peristaltic pumps (Gilson Minipuls) Technicon PVC and for Freon 113 Solvaflex pump tubing was used. The other parts of the flow system were made of 0.7 mm i.d. PTFE tubing. The first separator, P1 in Fig. 1, was of the design described by Nord and Karlberg.[4] Here, however, a more efficient recovery was needed as losses of organic phase in the first separator led to a corresponding decrease of the total yield. In order to facilitate nearly quantitative recovery, a supporting polyethylene net, 0.17 mm thick, 150 mesh was placed on the low-pressure side of the membrane. The second separator was a glass T-piece with low dead volume. This type of separator could be used as quantitative recovery is not necessary in this separation. The ratio of the flow-rates of sample (S) and Freon (F) gives the theoretical concentration factor of step 1. Similarly, the ratio

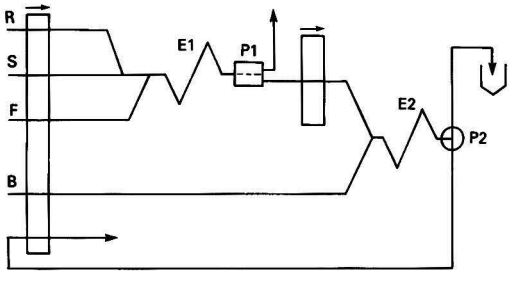

Fig. 1. The extraction assembly. The sample (S) is mixed with reagent (APDC, DDDC) (R) and extracted with Freon 113 (F) in the coil E1. The extract is separated at P1 and segmented by the back-extraction reagent (Hg^{2+}, 0.20 M HNO_3) (B). After extraction in coil E2 the aqueous phase is separated in the T-piece separator P2 and collected in vials. Flow-rates used in the simultaneous extraction of seven elements: sample, 6.0 ml min^{-1}; Freon, 1.5 ml min^{-1}; back-extraction reagent, 0.19 ml min^{-1}; extraction reagent, 1.0 ml min^{-1}

* To whom correspondence should be addressed.

of the flow-rates of Freon (F) and back-extraction reagent (B) gives the theoretical concentration factor of step 2. The obtained concentration factor is the product of the theoretical concentration factors in steps 1 and 2, the separation yield of the first separator and the extraction yield.

In the first experiments the two extractions involved were studied separately. When studies of the first step were undertaken the Freon extracts obtained were shaken with a small volume of 1 000 mg l^{-1} mercury solution transferring the metals back into an aqueous phase. Samples for studies of the back-extraction step were obtained by batch-wise manual extractions.

As a check of the complete system a simultaneous extraction of seven metals from a saline matrix was performed. The solution used was 0.7 M NaCl, acidified with 1 ml l^{-1} HNO_3 (0.014 M). Trace metals were added in the following concentrations: Cu, 0.2 mg l^{-1}; Co, Fe, Ni, Pb, 0.1 mg l^{-1}; Cd, 0.050 mg l^{-1}; and Zn, 0.025 mg l^{-1}. This experiment was performed by running the system continuously during a full working day (8 h). During this time five large samples, 5–10 ml, were collected and analysed for all seven elements. In these extracts sodium was also determined by flame emission. All metal determinations were carried out directly on the final aqueous extract by flame AAS.

Results

The first extraction step used in this work has been carefully studied under batch conditions.[5] Using copper as a test element, rapid extraction behaviour was confirmed for the continuous flow system. A residence time of 13 s in a 0.7 mm i.d. extraction coil was sufficient to give more than 80% yield at a theoretical concentration factor of 3. It was also found that the same length of a larger i.d. tubing would have poorer extraction in spite of longer residence times. In agreement with the experience from batch experiments the extraction yield decreased at higher concentration of metal. In this instance a maximum of 0.3 mg l^{-1} of copper was successfully extracted. At higher copper concentrations precipitation of carbamate complexes in the aqueous phase restricts the efficiency of extraction.

In the second extraction step metals bound to carbamates in the organic phase were displaced by mercury. This type of reaction is often slow and long shaking times were also used when this method of back-extraction was used in batch experiments.[6] As can be seen in Fig. 2 the back-extraction proceeded very rapidly in the continuous flow system. Fig. 2 also shows that increased mercury concentration only slightly shortens the extraction time needed.

Using single-element standards the complete system was tested with the elements cadmium, cobalt, copper, iron, lead, nickel and zinc. Theoretical concentration factors in the range 5–30 were tested with both distilled water and a saline matrix. In all instances except cobalt, total recoveries in the range 80–95% were achieved.

Results of the experiment with simultaneous extraction of seven elements are given in Table 1. The concentrations given have been corrected for the amount of metal found in 0.7 M NaCl by a separate run on the same system. Again good extraction yields were obtained for all elements except cobalt. For six of the elements a concentration factor greater than 25 was obtained. The variations in the final concentrations measured should be regarded as representing the stability of the system over a full day. Further, from repetitive runs on standards it can be seen that at the levels used, considerable variation is generated in the determination step, especially for nickel and cobalt. In the final extracts only trace amounts of sodium, corresponding to the concentration in the mercury solution used, could be found. Thus no sodium passed through the separator and the matrix separation was 100% effective.

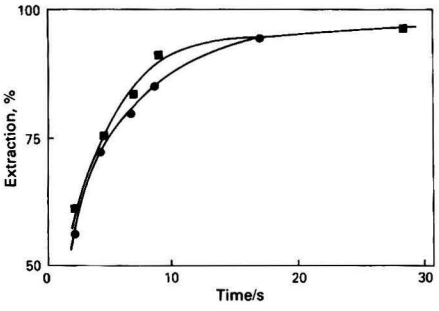

Fig. 2. Efficiency of the back-extraction as a function of residence time in the coil. Back-extraction reagent: ■, 250 p.p.m. Hg^{2+}; and ●, 50 p.p.m. Hg^{2+}. V_{org}/V_{aq} = 3.3. Sample, 1 mg l^{-1} Cu as carbamate complexes in Freon

Table 1. Simultaneous extraction of seven metals from 0.7 M NaCl solution*

Metal	Concentration/mg l^{-1} Sample	Extract	Mean extraction yield, %
Cd	0.050	1.33–1.35	87
Co	0.10	1.3–1.5	46
Cu	0.20	5.1–5.5	86
Fe	0.10	3.0–3.2	97
Ni	0.10	2.5–2.8	87
Pb	0.10	3.2–3.3	104
Zn	0.025	0.81–0.85	108

* Theoretical concentration factor in step 1, 4.0; and in step 2, 7.9; separation yield in the first separator, 97%.

Discussion

One of the main difficulties when designing a two-stage extraction system is the need for efficient phase separation after the first extraction. In order to achieve good separation a certain pressure difference has to be applied over the membrane. Using separators with unsupported membranes this often leads to membrane failure or to leaks in the separator. In both instances part of the sample flow ends up in the extract and the separator has to be dismantled and the membrane changed. With a polyethylene net as a support these problems are greatly reduced and more efficient separations can be performed.

Another important feature of the system is the use of a separate pump for the pumping of the Freon extract. Even if this pump adds dead volume to the system it simplifies handling considerably by separating the two steps pressure-wise. This is of great help when stopping and starting the system.

The extraction yield for all elements tested, except cobalt, seems to be largely unaffected by theoretical concentration factors and matrices within the limits tested. The highest concentration factors achieved for these elements are in the range 40–50. The relatively poor extraction of cobalt is probably due to the slow reaction between the cobalt dithiocarbamate complex and mercury.[7] In this work the sample rate could not be properly evaluated; lacking a graphite furnace we had to collect relatively large samples. However, from our present knowledge of the system it seems to be possible to work up 30–40 samples per hour. Thus the extraction system could be interfaced directly to the graphite furnace.

Conclusions

The FIA method of extraction has been successfully adapted to perform two-stage extraction procedures. Using the Freon - dithiocarbamate system, simultaneous metal extraction with enrichment factors of about 30 could easily be obtained for cadmium, copper, iron, nickel, lead and zinc. Cobalt was also extracted but with lower yield. With this system an aqueous concentrate, devoid of the original matrix, is produced making it very suitable for use with the graphite furnace.

In this procedure the sample consumption is 6 ml min^{-1} and the extract flow-rate is 0.19 ml min^{-1}. More work has to be carried out in order to establish the sampling rate, but 30–40 samples per hour would appear to be possible.

References

1. Kraak, J. C., *Trends Anal. Chem.*, 1983, **2**, 183.
2. Bengtsson, M., Danielsson, L.-G., and Magnusson, B., *Anal. Lett.*, 1979, **12**, 1367.
3. Nord, L., and Karlberg, B., *Anal. Chim. Acta*, 1983, **145**, 151.
4. Nord, L., and Karlberg, B., *Anal. Chim. Acta*, 1980, **118**, 285.
5. Danielsson, L.-G., Magnusson, B., and Westerlund, S., *Anal. Chim. Acta*, 1978, **98**, 47.
6. Lo, J. M., Yu, J. C., Hutchison, F. I., and Wai, C. M., *Anal. Chem.*, 1982, **54**, 2536.
7. Wyttenbach, A., and Bajo, S., *Anal. Chem.*, 1975, **47**, 1813.

Paper A3/338
Received September 30th, 1983
Accepted November 21st, 1983

Simultaneous Multi-element Analysis of Blood Serum by Flow Injection - Inductively Coupled Plasma Atomic-emission Spectrometry

Cameron W. McLeod, Paul J. Worsfold and Allan G. Cox
Department of Chemistry, Sheffield City Polytechnic, Sheffield, UK

A rapid and precise method for the simultaneous determination of Na, K, Ca, Mg, Li, Cu, Fe, and Zn in blood serum by flow injection analysis - inductively coupled plasma atomic-emission spectrometry (FIA - ICP-AES) has been developed using aqueous synthetic multi-element solutions for calibration. Performance characteristics of the FIA - ICP-AES technique are documented in terms of the effects of sample injection volume and carrier stream flow-rate on sensitivity and precision. Matrix interference was detected for injections of undiluted serum and the effect was minimised at low injection volumes and/or by using a relatively high RF power. At dilution factors of 1 + 1 (or greater) interference was not observed and reliable data were obtained for human and bovine serum pools for sample injections of 20 μl.

Keywords: *Blood serum analysis; multi-element analysis; flow injection analysis; inductively coupled plasma atomic-emission spectrometry*

Inductively coupled plasma atomic-emission spectrometry (ICP-AES) and, more recently, flow injection analysis (FIA) based procedures have made great impacts in many areas of chemical analysis and analytical advantages such as high precision, high sampling rates for microlitre sample volumes and freedom from nebuliser or injector tip blockage problems (for samples of high dissolved solids content) have already been demonstrated[1–4] for the combined FIA - ICP-AES technique. These initial studies in the ICP field have concentrated on using FIA as a means for sample introduction, but it is anticipated that on-line FIA systems incorporating ion exchange and/or solvent extraction similar to that reported[5] for atomic-absorption applications will be forthcoming. Alexander *et al.*[4] realised the potential value of the FIA - ICP technique in the clinical field and gave brief results for the determination of Na, K, Ca, Mg and Fe in blood serum using 10-μl sample volumes. Differences in nebuliser efficiency between serum and aqueous standard solutions were reported and to compensate for this it was necessary to use a 5% aqueous albumin matrix for calibration.

In earlier ICP studies on serum analysis using either conventional nebulisation[6] or microlitre injection techniques[7–10] matrix effects, both physical and spectral, were detected, but unfortunately systematic investigation of the interference was not performed. One exception has been the study of Aziz *et al.*[10] who investigated matrix effects due to high Na concentrations.

The aim of this study was to provide basic information on both the origin and the magnitude of serum matrix interference from the viewpoint of developing a rapid and reliable method for the determination of Na, K, Ca, Mg, Li, Cu, Fe and Zn in serum by FIA - ICP-AES. Selection of the elements specified was based primarily on considerations of ICP detection capability and element concentrations in serum[11] but also on the availability of specific analytical channels in the polychromator. Matrix interference was dependent on the volume of serum injected and was demonstrated to be primarily an ICP effect and not physical transport interference. Using normal plasma operating conditions and synthetic multi-element standard solutions for calibration, reliable data were obtained for microlitre injection (20 μl) of serum, diluted 1 + 1 with high-purity water. Use of a relatively high RF power effectively eliminated interference for samples of undiluted serum.

Experimental

Reagents and Materials

Synthetic multi-element solutions containing Na, K, Ca, Mg, Li, Cu, Fe and Zn were prepared from stock solutions of the individual elements (typically 1 000 μg ml^{-1} but 3% *m/V* for Na). High-purity metals and/or salts were used in preparing the stock solutions. All standard solutions were stored in pre-cleaned polypropylene containers (Nalgene). Serum samples were obtained from Northern General Hospital, Sheffield (pooled human serum), the National Institute for Environmental Studies (NIES), Japan (freeze-dried human serum, candidate reference material) and Wellcome Reagents Ltd. (freeze-dried bovine serum for quality control, BCO1 Lot K4527). The last two materials were reconstituted by the addition of exactly 5 and 10 ml of high-purity water to the respective vials. For the NIES material, particulate matter remained even after prolonged agitation (including ultrasonic treatment) so that reconstituted specimens were centrifuged before analysis. An aqueous solution of non-ionic surfactant (0.1% *m/V* Brij, BDH Ltd.) was used instead of high-purity water as the carrier stream for all experiments involving serum.

A Jarrell-Ash (Model ICAP 9000) direct-reading spectrometer (30 channels) equipped with an Apple II microcomputer for data acquisition and analysis was used. Wavelengths utilised in this investigation were: Na 589.0 nm; K 766.5 nm; Ca 317.9 nm; Mg 279.5 nm; Li 670.8 nm; Cu 324.8 nm; Fe 259.9 nm; and Zn 213.9 nm. The flow injection manifold illustrated in Fig. 1 was based on a peristaltic pump (Gilson Minipuls), a rotary injection valve (Rheodyne 7125 with sample-loop volumes of 20, 100, 200, 500 μl and 2 ml) and a high-solids nebuliser (Jarrell-Ash). Operating parameters for the FIA - ICP system, as given in the legend to Fig. 1, were used throughout unless stated otherwise.

Measurement Procedure and Calibration

For operating conditions as described in the legend to Fig. 1, and immediately coincident with sample injection, standard software routines were activated by keyboard command either to record and subsequently display emission *versus* time profiles for the eight elements under investigation or record and output emission intensities or concentration data based on

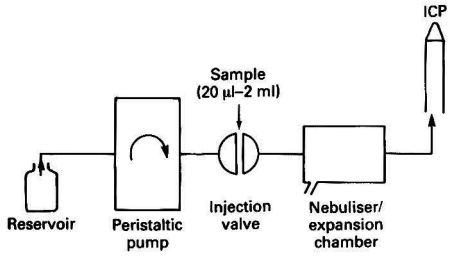

Fig. 1. Sample introduction system for FIA - ICP-AES. Operating parameters: forward power, 1.1 kW; observation height, 15 mm; coolant Ar, 20 l min^{-1}; nebuliser Ar, 1 l min^{-1}; carrier stream flow-rate, 2.2 ml min^{-1}; injection volume, 20–2 000 µl; pump tubing (Tygon) internal diameter, 1.42 mm; and post-injection valve tubing (PTFE), length 22 cm and internal diameter 0.7 mm

peak-area measurement. The former mode was used in preliminary studies with synthetic multi-element solutions and serum samples as important information on peak shape and selection of operating parameters was gained from inspection and analysis of the respective emission *versus* time profiles. The latter mode was used exclusively in quantitative work. For serum analysis, standardisation of the instrument was based on a two-point calibration procedure, using a synthetic multi-element solution (freshly prepared from stock) containing Na (3 000 µg ml^{-1}), K (200 µg ml^{-1}), Ca (100 µg ml^{-1}), Mg (20 µg ml^{-1}), Li (1 µg ml^{-1}), Cu (1 µg ml^{-1}), Fe (1 µg ml^{-1}) and Zn (1 µg ml^{-1}) as the high standard and high-purity water (zero metal concentration) as the low standard.

Results and Discussion

Performance Characteristics

The FIA manifold used in this study (see Fig. 1) corresponded to a limited dispersion situation whereby the sample injection valve was located as close as was physically possible to the nebuliser. This arrangement ensured high sensitivity, subject to the influence of critical FIA parameters such as sample injection volume, carrier stream flow-rate and tube dimensions. Much information on how analytical performance is governed by system parameters was gained from the literature and for initial experiments on aqueous solutions the influence of sample injection volume and carrier stream flow-rate on analytical performance was considered.

Injection volume

The emission - time response graphs of the elements were recorded simultaneously for various injection volumes (20, 100, 200, 500 µl and 2 ml) of a synthetic multi-element solution (Na 100 µg ml^{-1}, K 100 µg ml^{-1}, Ca 10 µg ml^{-1}, Mg 10 µg ml^{-1}, Li 10 µg ml^{-1}, Cu 10 µg ml^{-1}, Fe 10 µg ml^{-1} and Zn 10 µg ml^{-1}) at normal plasma operating conditions. As shown in Fig. 2 the emission profiles for the elements are typical of an FIA-based system, *i.e.*, with increasing injection volume, the peak height response approaches the steady-state signal, which is equivalent to that for conventional nebulisation. It can also be seen in Fig. 2 that the emission - response graphs for all elements occupy the same time domain and thus a single integration time, dependent upon injection volume, was appropriate for simultaneous measurement based on peak area. As a representative element the dispersion and sensitivity data for magnesium are summarised in Table 1 and indicate that a substantial reduction in sensitivity occurred at low injection volumes as a direct result of increased sample dispersion. Increased sensitivity was realised for peak height relative to peak area measurement but precision was found to be better by a factor of about 2 for all elements using the latter measurement mode.

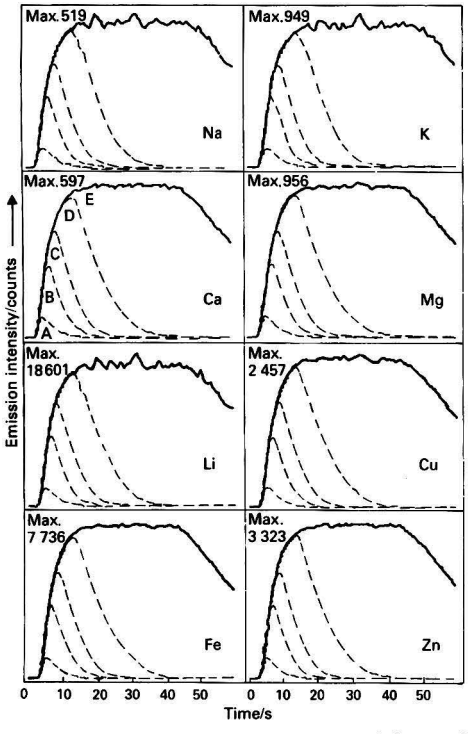

Fig. 2. Effect of sample injection volume on emission *vs.* time response for the elements. Injection volumes: A, 20 µl; B, 100 µl; C, 200 µl; D, 500 µl; and E, 2 ml. Operating conditions, as given in Fig. 1. Solution composition: Na, 100 µg ml^{-1}; K, 100 µg ml^{-1}; Ca, 10 µg ml^{-1}; Mg, 10 µg ml^{-1}; Li, 10 µg ml^{-1}; Cu, 10 µg ml^{-1}; Fe, 10 µg ml^{-1}; and Zn, 10 µg ml^{-1}. Observation time, 60 s

Table 1. Effect of injection volume on dispersion and signal to background ratio for Mg (279.5 nm). Experimental conditions as in Fig. 2. Mg concentration, 10 µg ml^{-1}; integration time, 20 µl, 15 s; 100 µl, 15 s; 200 µl, 20 s; 500 µl, 30 s; and 2 ml, 15 s (at steady state)

Injection volume/µl	Dispersion*	Signal to background ratio†
20	6.9	2.2
100	2.1	5.0
200	1.4	8.5
500	1.1	10.0
2 000	—	23.9

* Based on ratio of peak height to steady-state signal.
† Based on peak area measurement.

Flow-rate

The emission - response graphs for the synthetic multi-element solution (composition as given in the legend to Fig. 2) at various carrier stream flow-rates are presented in Fig. 3. In agreement with the findings of Alexander *et al.*[4] peak height data decreased and peak width data increased with decreasing flow-rate. Further, it can be seen, particularly for Ca and Mg, that the plasma background level increased with decreasing flow-rate and, as would be expected, a gradual deterioration in signal to background ratio resulted. Sensitivity and precision data are summarised in Table 2 and for most elements a flow-rate of 2.2 ml min^{-1} yielded the best performance.

Table 2. Effect of carrier stream flow-rate on signal to background ratio and precision. Values in parentheses are % RSD; total number of measurements, 6; injection volume, 20 µl; integration time, 15 s; and other experimental conditions as in Fig. 2

Element	Signal to background ratio for various carrier stream flow-rates				
	0.6 ml min^{-1}	1.0 ml min^{-1}	1.6 ml min^{-1}	2.2 ml min^{-1}	3.0 ml min^{-1}
Na (589.0 nm)	2.3 (2.5)	6.7 (2.3)	8.7 (0.82)	8.8 (0.92)	9.0 (1.8)
K (766.5 nm)	1.3 (1.4)	2.4 (1.8)	3.0 (0.49)	3.1 (0.47)	3.1 (1.1)
Ca (317.9 nm)	1.1 (0.82)	1.5 (4.9)	1.8 (0.18)	1.8 (0.47)	1.7 (0.47)
Mg (279.5 nm)	1.2 (0.82)	1.8 (1.1)	2.1 (0.40)	2.1 (0.49)	2.1 (0.87)
Li (670.8 nm)	1.9 (2.1)	5.2 (2.5)	6.9 (0.73)	7.1 (0.45)	6.9 (1.3)
Cu (324.8 nm)	2.3 (2.5)	7.2 (2.8)	9.8 (0.89)	10.1 (0.47)	9.9 (1.3)
Fe (259.9 nm)	4.4 (3.4)	14.5 (2.6)	17.5 (0.92)	16.9 (0.42)	15.1 (1.5)
Zn (213.9 nm)	2.8 (2.9)	9.6 (2.9)	13.9 (1.1)	14.7 (0.69)	15.0 (1.6)

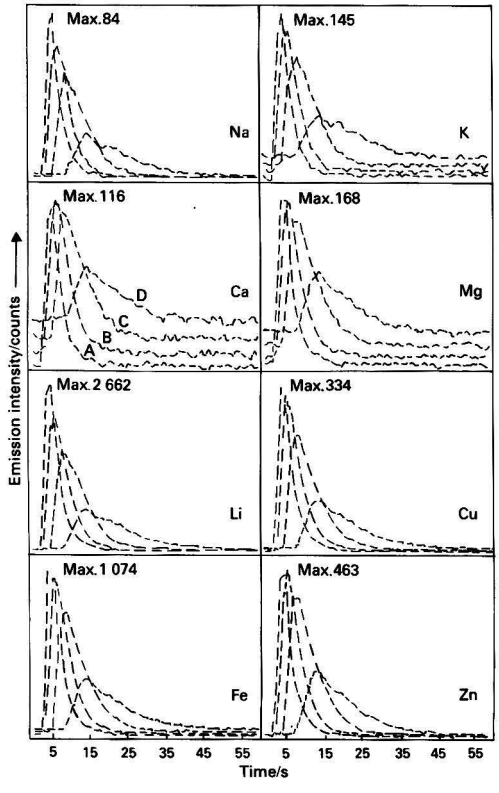

Fig. 3. Effect of carrier stream flow-rate on emission *vs.* time response for the elements. Flow-rates: A, 3.0 ml min^{-1}; B, 2.0 ml min^{-1}; C, 1.0 ml min^{-1}, D, 0.6 ml min^{-1}. Experimental conditions as in Fig. 1. Sample injection volume, 20 µl

Detection limits

The detection limits for the elements were determined for sample (solution composition as given in the legend to Fig. 2) injections of 20 and 200 µl and 2 ml and the results were consistent with the respective signal to background values given in Tables 1 and 2. The data are presented in Table 3 and for comparison purposes the physiological concentration ranges for seven elements in human serum (no data available for Li) are included. For the criterion that the lower limit for quantitative determination is equal to five times the detection limit and, allowing for some degradation of ICP detection

Table 3. Detection limits for elements in synthetic aqueous solution and approximate serum concentrations. Integration time: 20 µl, 15 s; 200 µl, 20 s; and 2 ml, 15 s (at steady state)

Element	Detection limit*/µg ml^{-1}			Concentration* in human serum†/µg ml^{-1}
	20 µl	200 µl	2 ml	
Na (589.0 nm)	0.50	0.15	0.02	3 100–3 560
K (766.5 nm)	0.85	0.13	0.04	140–190
Ca (317.9 nm)	0.23	0.02	0.009	90–110
Mg (279.5 nm)	0.33	0.02	0.007	10–20
Li (670.8 nm)	0.01	0.001	0.000 5	—
Cu (324.8 nm)	0.01	0.002	0.001	0.85–1.5
Fe (259.9 nm)	0.02	0.002	0.002	0.85–1.5
Zn (213.9 nm)	0.01	0.002	0.001	0.8–1.1

* Detection limit is defined as the concentration that corresponds to an emission signal equivalent to twice the standard deviation of the background noise.

† See reference 12.

capability in the serum matrix, it is judged that the FIA - ICP-AES technique offers sufficient sensitivity for simultaneous determination of the seven elements in human serum even at a relatively low injection volume of 20 µl.

Interference Studies

Matrix effects, both physical and spectral, associated with the major components of serum have been reported in a number of studies concerned with the ICP analysis of blood serum. In a study by Dalquist and Knoll[6] for example, sample transport differences between aqueous multi-element standard solutions and four-fold diluted serum occurred and internal standardisation was necessary to compensate for this physical interference effect. In an attempt to reproduce and investigate serum matrix effects the linearity of analyte emission (peak area) as a function of serum (pooled human serum and control serum) dilution was investigated, it being anticipated that interference might become particularly severe for undiluted serum.

To assist in the interpretation of results, identical experiments were performed on a synthetic multi-element solution whose inorganic composition (given in the caption to Fig. 4) matched that of normal human serum. In this way, inter-element effects due specifically to the relatively high concentrations of Na would be similar for both the serum and synthetic solutions. No attempt was made to matrix-match the viscosity or the organic carbon content of serum (approximately 4% *m/V*), which is due principally to serum proteins.

A comparison of the emission *versus* time graphs for undiluted human serum and the synthetic multi-element solution was first performed to check whether integration times, decided upon earlier for aqueous solution, were appropriate for serum. Differences in peak shape between the

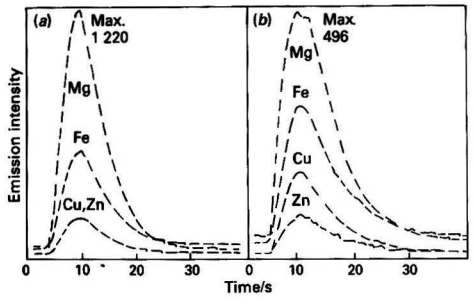

Fig. 4. Emission *vs.* time response for Mg, Fe, Cu, and Zn in (*a*) synthetic multi-element solution and (*b*) serum (human). Operating conditions, as given in Fig. 1. Solution composition: Na, 3 000 μg ml^{-1}; K, 200 μg ml^{-1}; Ca, 100 μg ml^{-1}; Mg, 20 μg ml^{-1}; Li, 1 μg ml^{-1}; Cu, 1 μg ml^{-1}; Fe, 1 μg ml^{-1}; and Zn, 1 μg ml^{-1}. Sample injection volume, 200 μl. Observation time, 40 s

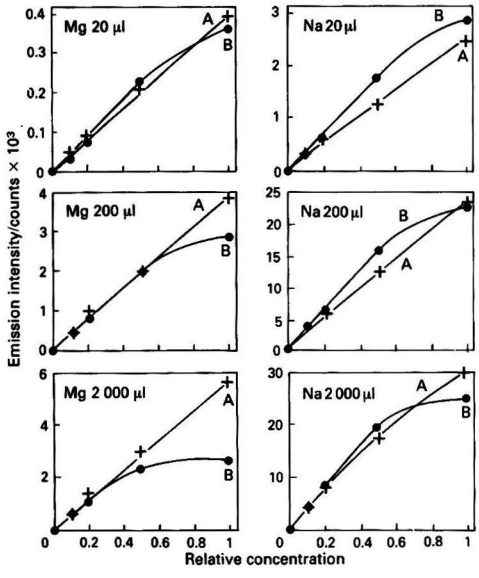

Fig. 5. Emission intensities for Mg and Na as a function of sample dilution at various injection volumes for A, synthetic and B, serum (human) solutions. Experimental conditions as given in Fig. 4. Undiluted sample ≡ relative concentration of 1; 1 + 1 dilution ≡ relative concentration of 0.5; 1 + 5 dilution ≡ relative concentration of 0.2; and 1 + 10 dilution ≡ relative concentration of 0.1

two samples were not detected as shown in Fig. 4 for Mg, Fe, Cu and Zn (similar responses for Na, K, Ca) and thus, no change in measurement conditions was necessary for serum samples.

Effect of serum dilution

The emission intensities for Na and Mg as a function of dilution factor for the two series of samples are presented in Fig. 5 for sample injections of 20 and 200 μl and 2 ml. (Sample injections of 100 and 500 μl are omitted.) First it can be seen that linearity was observed up to a relative concentration of 0.5 (1 + 1 dilution) for the human serum and the synthetic solution whereas beyond this point a serious departure from linearity occurred for serum. Further, for the serum the degree of non-linearity became more pronounced with increasing sample volume. The corresponding graphs for Ca, K, Cu, Fe and Zn are omitted, but similar trends in emission - response were noted; for Na only, non-linearity was detected for the synthetic solution at low dilution (*i.e.*, for the relative concentration range 0.5–1) using both 0.5- and 2-ml sample injections. This departure from non-linearity may be due to the onset of self-absorption at relatively high Na concentrations. Non-linearity was not detected for the corresponding plot at 20 μl where substantial dispersion/dilution of the sample occurred. Similar trends in emission - response were noted for the elements (including Li) for identical experiments performed on the control serum.

A possible explanation for the non-linearity for serum at low dilution was that a physical interference effect was operating (*i.e.*, sample transport or nebulisation efficiency was reduced relative to aqueous solution) owing to the viscous nature of the sample. This interpretation is consistent with the findings of Dalquist and Knoll[6] because for FIA-based sample introduction, sample transport differences might not be detected at the moderate serum dilution used by Dalquist and Knoll (1 + 4 dilution), but instead might only become significant at the low serum dilutions (*e.g.*, 1 + 1 dilution and undiluted) of this study.

Effect of RF power

The effect of serum dilution on linearity of emission was investigated at various RF powers and the results indicated that a physical interference of the type suggested in the preceding paragraph was not operating for this system. The emission - response graphs for a 200-μl injection at RF power levels of 0.9, 1.1, 1.3 and 1.5 kW are presented in Fig. 6 and, again limiting the discussion to Na and Mg, it can be seen that for serum non-linearity was most severe at 0.9 kW, but there was a substantial improvement in linearity with increasing RF power, particularly in the region beyond 1 + 1 dilution. Only at the relatively high power of 1.5 kW, however, was good linearity throughout the range achieved. Again similar behaviour was noted for K, Ca, Li, Cu, Fe and Zn.

In contrast to the results for serum (pooled human serum and control serum), the emission - response graphs for the synthetic solution showed good linearity for the four RF power levels investigated. The above findings indicate that the serum matrix effect detected in this study was not a physical effect as the interference was not only dependent on the RF power, but also was effectively eliminated by adopting a relatively high RF power. It is considered that the suppression of emission intensity, particularly at low RF power, was due to the reduced excitation capability of the plasma source as a result of an increased organic loading by serum. Only at the relatively high power of 1.5 kW was sufficient energy available, for undiluted serum, to break down the organic matrix effectively and achieve efficient analyte excitation. In agreement with the emission - response graphs of Fig. 5 the matrix effect for serum diluted 1 + 1 was barely detected at 1.1 kW, the normal plasma operating power.

The implication of the above findings is that in order to achieve reliable results for blood serum by FIA - ICP-AES using aqueous multi-element standard solutions for calibration, either a relatively high RF power is adopted for injections of undiluted serum or sample injection volumes are kept to a minimum (*e.g.*, 20 μl) and/or serum is diluted at least 1 + 1 with high-purity water before measurement at normal plasma operating conditions. Further experiments on accuracy and precision were limited to the latter approach.

Serum Analysis

Control (Wellcome, Lot K4527) and reference sera (NIES, candidate RM) diluted 1 + 1 with distilled water and in an undiluted form were analysed by the FIA - ICP-AES method using sample injections of 20 μl. The data presented in Tables 4 and 5 reveal a small but significant negative bias for direct

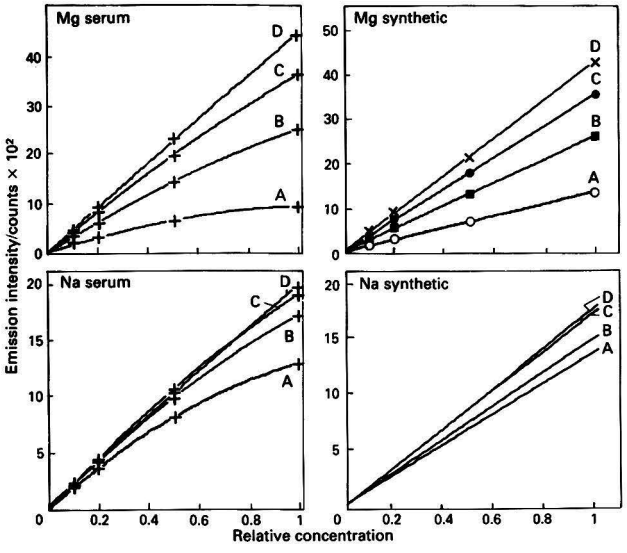

Fig. 6. Emission intensities for Mg and Na as a function of sample dilution at various RF powers. Experimental conditions, as given in Fig. 4

Table 4. Analytical data for control serum (Wellcome BCO1 Lot K4527). Results derived from analyses performed on two separate occasions; total number of measurements, 20; uncertainty limits, ±2σ. Injection volume, 20 µl

Element	Concentration/µg ml⁻¹ 1 + 1 dilution	Direct	Specified range
Na	3215 ± 97	3017 ± 98	3197–3266
K	188 ± 7	175 ± 6	189–193
Ca	94.2 ± 2.7	89.2 ± 3.0	95–102
Mg	12.5 ± 0.3	11.6 ± 0.4	13–15.3
Li	3.81 ± 0.11	3.57 ± 0.10	3.75–4.5
Cu	0.338 ± 0.028	0.316 ± 0.012	—
Fe	2.42 ± 0.10	2.32 ± 0.06	2.05–2.17
Zn	1.62 ± 0.08	1.55 ± 0.05	—

Tables 5. Analytical data for human serum (NIES, candidate RM). Results derived from analyses performed on two separate occasions; total number of measurements, 20; uncertainty limits, ±2σ. Injection volume, 20 µl

Element	Concentration/µg ml⁻¹ 1 + 1 dilution	Direct	Reference*
Na	3175 ± 84	2991 ± 78	3038
K	172 ± 7	161 ± 6	173
Ca	75.8 ± 2.1	72.8 ± 1.4	78.6
Mg	18.0 ± 0.6	16.9 ± 0.3	19.6
Li	<0.02	<0.01	—
Cu	0.994 ± 0.076	0.939 ± 0.066	1.01
Fe	1.01 ± 0.07	0.942 ± 0.038	1.07
Zn	0.882 ± 0.044	0.843 ± 0.030	0.892

* Based on preliminary data for the reconstituted material (5 ml) supplied by Dr. K. Okamoto, NIES.

serum analysis as might be expected, based on the previous development work. The data for analysis at 1 + 1 dilution in general show satisfactory agreement with the reference values. Precision [<2% relative standard deviation (RSD) for all elements except Cu] was significantly better than that reported for alternative microlitre injection studies.[7-10]

Table 6. Recovery data for spike addition to pooled human serum. Values in parentheses, % RSD. Total number of measurements, 10. Injection volume, 20 µl

Element	Original concentration/ µg ml⁻¹	Amount added/ µg ml⁻¹	Amount found/ µg ml⁻¹	Recovery, %
Na	1622	1500	3018 (1.1)	97
K	80.0	100	173 (1.3)	96
Ca	46.1	50	93.9 (1.4)	98
Mg	9.30	10	18.6 (1.1)	96
Li	<0.02	0.5	0.465 (1.5)	93
Cu	0.682	0.5	1.13 (1.1)	96
Fe	0.370	0.5	0.863 (1.9)	99
Zn	0.402	0.5	0.872 (2.8)	97

Table 7. Recovery data for spike addition to control serum (Wellcome BCO1, Lot K4527). Values in parentheses, % RSD. Total number of measurements, 10. Injection volume, 20 µl

Element	Original concentration/ µg ml⁻¹	Amount added/ µg ml⁻¹	Amount found/ µg ml⁻¹	Recovery, %
Na	1619	1500	3072 (1.1)	98
K	94.3	100	190 (1.5)	98
Ca	47.4	50	97.7 (0.90)	100
Mg	6.26	10	15.8 (1.2)	97
Li	1.91	0.5	2.36 (1.4)	98
Cu	0.173	0.5	0.632 (2.2)	94
Fe	1.22	0.5	1.68 (1.2)	99
Zn	0.798	0.5	1.29 (1.7)	98

Further, the use of a dilute solution of non-ionic surfactant (0.1% *m/V* Brij) as the carrier stream, instead of water, improved long-term calibration stability. Corresponding analyses were performed for sample injections of 100 µl and, although improvements in precision were noted (<1% RSD for all elements), data were generally in error by about 5–10%. Although element concentrations in the control and reference sera were of similar magnitude (except Li) the Cu concentration in the former was relatively low (<0.2 µg ml⁻¹

after 1 + 1 dilution) and it is noteworthy that no significant deterioration in precision resulted for Cu determination, thus confirming the earlier statement made concerning detection capability of the FIA - ICP-AES method (see *Detection limits*).

As a further check on accuracy and precision, recovery experiments were performed using control and pooled serum. The spiked samples were prepared by mixing equal volumes (5 ml) of serum (previously analysed at 1 + 1 dilution by the recommended procedure) and the synthetic multi-element standard solution and immediately analysed as above. The results in Tables 6 and 7 again testify to the reliability of the proposed method.

Conclusion

FIA has been combined with ICP-AES and successfully applied to the simultaneous determination of eight elements in microlitre samples of blood serum. The FIA technique was demonstrated to be an attractive and versatile sample introduction system, particularly so in method development studies where an insight into potential errors in serum analysis was gained. Investigations are in progress on extending the present methodology to additional elements and also to apply the technique to whole blood analysis.

We are extremely grateful to Dr. K. Okamoto, National Institute for Environmental Studies, Japan, and Mr. R. Cooper, Northern General Hospital, Sheffield, for providing serum samples. The authors also thank Dr. S. S. Brown for providing critical comments on the manuscript.

References

1. Jacintho, A. O., Zagatto, E. A. G., Bergamin, H. F., Krug, F. J., Reiss, B. F., Bruns, R. E., and Kowalski, B. R., *Anal. Chim. Acta*, 1981, **130**, 243.
2. Greenfield, S., *Ind. Res. Dev.*, 1981, **23**, 140.
3. Greenfield, S., *Spectrochim. Acta, Part B*, 1983, **38**, 95.
4. Alexander, P. W., Finlayson, R. J., Smythe, L. E., and Thalib, A., *Analyst*, 1982, **107**, 1335.
5. Olsen, S., Pessenda, L. C. R., Růžička, J., and Hansen, E. H., *Analyst*, 1983, **108**, 905.
6. Dalquist, R. L., and Knoll, J. W., "Applied Research Laboratories Publication No. 7015," ARL Ltd., Division of Bausch and Lomb, Sunland, CA, 1978.
7. Greenfield, S., and Smith, P. B., *Anal. Chim. Acta*, 1972, **59**, 341.
8. Kniseley, R. N., Fassel, V. A., and Butler, C. C., *Clin. Chem.*, 1973, **19**, 807.
9. Uchida, H., Nojiri, Y., Haraguchi, H., and Fuwa, K., *Anal. Chim. Acta*, 1981, **123**, 57.
10. Aziz, A., Broekaert, J. A. C., and Leis, F., *Spectrochim. Acta, Part B*, 1981, **36**, 251.
11. Morrison, G. H., *CRC Crit. Rev. Anal. Chem.*, 1979, 287.
12. Berman, E., *Appl. Spectrosc.*, 1975, **29**, 1.

Paper A3/334
Received August 26th, 1983
Accepted November 24th, 1983

Catalytic - Fluorimetric Determination of Copper at the Nanograms per Millilitre Level by Flow Injection Analysis

Fernando Lázaro Boza, María Dolores Luque de Castro and Miguel Valcárcel Cases
Department of Analytical Chemistry, Faculty of Sciences, University of Córdoba, Córdoba, Spain

A catalytic - fluorimetric method for the determination of copper(II) at the nanograms per millilitre level is proposed, based on the catalytic action of the copper(II) cation on the oxidation of 2,2'-dipyridyl ketone hydrazone (DPKH) by dissolved oxygen. In order to obtain the maximum analytical signal, two steps are necessary: oxidation of DPKH (basic medium) and development of fluorescence (strongly acidic medium). Flow injection analysis is very suitable for this determination as it is sensitive and rapid. The calibration graph shows two linear intervals, between 8 and 30 ng ml^{-1} [relative standard deviation (r.s.d.) 2.3%] and 40 and 300 ng ml^{-1} (r.s.d. 2.0%). The sampling frequency is 100 h^{-1} for an injected volume of 60 µl. A study of interferences is reported. The use of "reverse" flow injection analysis makes the method more sensitive.

Keywords: *Catalytic - fluorimetric analysis; flow injection analysis; copper determination; 2,2'-dipyridyl ketone hydrazone*

This paper constitutes an important stage in our kinetic - fluorimetric studies based on the oxidation of azomethine compounds that we have been developing.[1] The subject is the system formed by 2,2'-dipyridyl ketone hydrazone (DPKH) and Cu(II). DPKH solutions are very slowly oxidised in air at room temperature with the help of atmospheric oxygen, forming a product that shows a blue fluorescence ($\lambda_{ex.}$ = 350 nm; $\lambda_{em.}$ = 429 nm) in a strongly acidic medium. The presence of cations such as Cu(II), Hg(II), Co(II), Au(III)[2] and Pt(IV)[3] accelerates the appearance of this fluorescence, Cu(II) being the cation that exerts the most intense effect.

Optical detectors have been much more widely used than electrochemical detector in flow injection analysis,[5] so that the scant attention paid to the fluorimetric detector (about 6% of the whole) appears unreasonable.

Experimental

A Tecator 5020 flow injection system was used; it has two peristaltic pumps with a timer mechanism that makes it possible for them to stop and start individually. The Tecator L

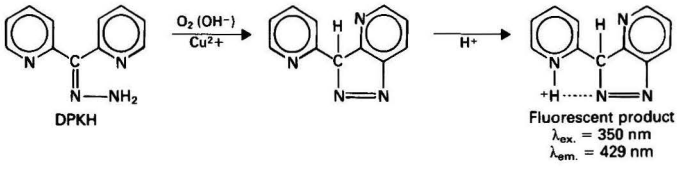

The oxidation reaction does not take place in acidic media, increasing its rate exponentially with increasing basicity of the medium. The fluorescence of this oxidation product is at a maximum at pH 0.7, decreasing with increasing pH until it becomes nil at pH 7.

Taking this system as a basis, we have previously described two methods for the determination of trace amounts of Cu(II): a total method[2] and a kinetic method.[4] In the former, two steps for developing maximum fluorescence are necessary: the generation of the oxidation product, in a neutral medium, which is a slow step (a 90-min development period) and a subsequent step that is instantaneous and is caused by the acidification of the medium. The kinetic method requires one step only, so that it is necessary to use an intermediate pH value (6.3) that does not produce rapid formation of the oxidation product or the maximum development of its fluorescence. A comparison of the two methods showed the high sensitivity of the total method (0.4–1.0 ng ml^{-1}) with a high relative standard deviation (RSD) (4.5% for P=0.05) and a long analysis time (90 min per sample). The kinetic method is less sensitive (0.1–1.0 µg ml^{-1}) with a smaller RSD (2.0% for P=0.05) and an analysis time of 4 min per sample.

Our objective in studying this system by the flow injection analysis technique is to combine the advantages of the two conventional techniques (high sensitivity and small RSD) and also to attain a sampling rate that is greater than in either.

100–1 injection valve has a variable volume. All the reactor coils were made of PTFE tubing (i.d. 0.5 mm). The sample loops were also made of PTFE and were calibrated photometrically using a dye. The two streams met at a Tecator type I manifold. The flow cell was a Hellma 176.52 QS with an inner volume of 25 µl. A Perkin-Elmer MPF-43 A spectrofluorimeter was used as a detector, connected to a Radiometer REC 80 recorder with an REA 112 high-sensitivity unit. The accessory instruments were a Beckman 3500 pH meter, a Perkin-Elmer 402 spectrophotometer and a Selecta S-382 thermostat.

Stock solutions included an aqueous solution (1 g l^{-1}) of DPKH, a copper(II) nitrate solution containing 1.030 7 g l^{-1} of Cu(II), standardised iodimetrically, and 1 M sodium hydroxide, 3 M hydrochloric acid, 1 M ammonia and 30% hydrogen peroxide solutions. They all contained Merck pro analysi materials and were prepared and handled with usual care; there are no special features that merit comment.

The proposed manifold is shown in Fig. 1. A 60-µl volume of copper(II) solution is injected into an alkaline DPKH flow (1.8 ml min^{-1}). Reactor 1 is straight and is 80 cm long; reactor 2 is 160 cm long and is coiled on a 6-mm cylinder diameter; both reactors are made of 0.5 mm i.d. PTFE tubing. The parameters of the fluorimeter are $\lambda_{ex.}$ = 350 nm, $\lambda_{em.}$ = 429 nm, $s_{ex.}$ = 6 nm and $s_{em.}$ = 7 nm. A chart speed for the recorder of 5 mm min^{-1} is sufficient.

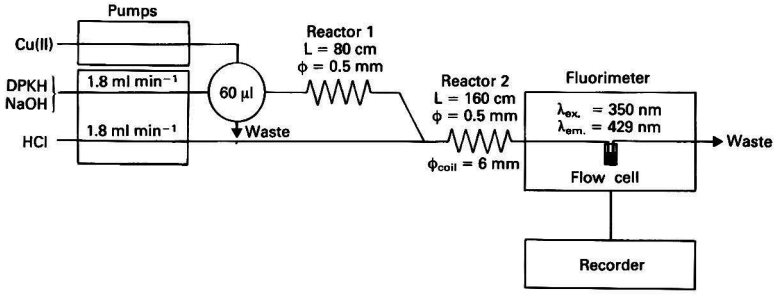

Fig. 1. Scheme of the manifold

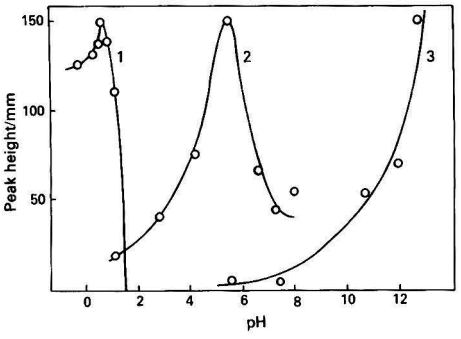

Fig. 2. Influence of the pH on the peak height. 1, pH of the hydrochloric acid solution is varied, maintaining constant the pH of the sample (5.5) and the DPKH solution (12.8). 2, pH of the injected sample is varied, maintaining constant the pH of the hydrochloric acid solution (0.6) and the DPKH solution (12.8). 3, pH of the DPKH solution is varied, maintaining constant the pH of the sample (5.5) and hydrochloric acid solution (0.6)

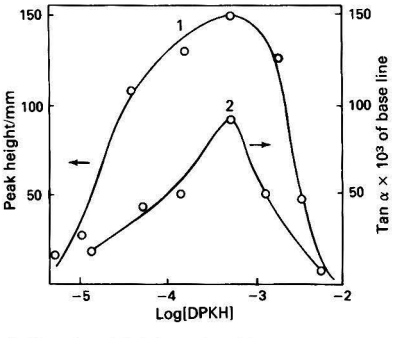

Fig. 3. 1, Plot of peak height *vs.* logarithm of the concentration of DPKH. 2, Influence of the concentration of DPKH on the slope of the base line (tan α)

Results and Discussion

The Chemical System

Influence of pH

The nature of the system, which makes the manifold described above necessary, required a study of three aspects: the concentration of base in carrier 1, the concentration of acid in carrier 2 and the pH of the injected sample.

The alkali concentration in carrier 1 was studied with sodium hydroxide and ammonia solutions with concentrations between 10^{-3} and 10^{-1} M. The fluorescence intensity, I_f, increases with increasing basicity of the reaction medium, as shown in Fig. 2, in which the change of I_f with the pH of the DPKH solution (carrier 1) is plotted. For subsequent experiments a concentration of sodium hydroxide in carrier 1 of 10^{-1} M was chosen as a compromise between the attainment of a higher analytical signal and corrosion of the system under extremely basic conditions.

The use of ammonia gives an analytical signal 35% of that obtained in sodium hydroxide solution of the same concentration, owing to the lower basicity of the ammonia solution together with its complexing action with respect to Cu(II).

The optimum acidity of the reaction product during its passage through the detector to attain the maximum fluorescence intensity was studied with hydrochloric solutions with concentrations between 4×10^{-2} and 3.0 M. As shown in Fig. 2, when the hydrochloric acid concentration in carrier 2 changes between 0.6 and 0.2 M, the fluorescence intensity undergoes only a slight change, increasing slowly for a 0.4 M hydrochloric acid medium.

The optimum pH of the sample of Cu(II) injected is 5.5. The decrease in I_f at higher or lower pH (Fig. 2) can be explained by a decrease in the oxidation rate of DPKH (acidic pH) and by the lower stability of the Cu(II) (neutral or basic pH).

Influence of oxidants

The action of atmospheric oxygen on the oxidation of DPKH has been reported in previous papers[2,4] and this was confirmed by deaerating one, two or all three reagent and sample containers. The peak height becomes minimal, constant and non-zero when the three solutions (carriers 1 and 2 and sample) are free of oxygen. A small I_f is obtained under these conditions because the reactor and sample tubing are made of PTFE, which has a high permeability to atmospheric oxygen.[7] When the solutions of the containers are saturated with oxygen (bubbling air for 30 min), the analytical signal does not increase in relation to that obtained if bubbling of oxygen is omitted, which fact indicates that the oxygen level generally existing in the flow injection analysis system is sufficient for the development of the reaction.

The presence of the other oxidising agents, such as potassium bromate, potassium iodate or hydrogen peroxide, in neutral solutions of DPKH favours the reagent oxidation catalysed by Cu(II), increasing the analytical signal at this pH. When 0.1 M sodium hydroxide solution is utilised as a carrier system for DPKH, the presence of these oxidising agents does not alter the rate of the reaction catalysed by the Cu(II) ion, as the reaction medium itself accelerates this oxidation to a maximum extent.

Influence of reagent concentration

This variable was studied at DPKH concentrations in the range 6.1×10^{-3}–5.1×10^{-6} M, with and without the injection

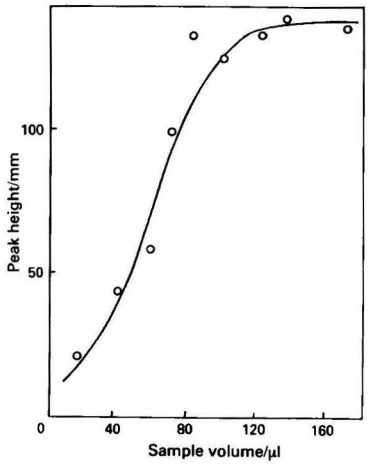

Fig. 4. Influence of the injected sample volume on the peak height

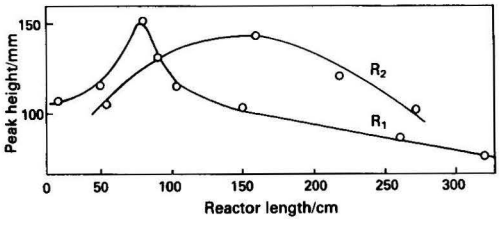

Fig. 5. Effect of reactor 1 (R_1) and reactor 2 (R_2) length on the peak height

of Cu(II) (catalysed and non-catalysed reactions, respectively). These reactions acquire their maximum development of I_f at a DPKH concentration of 5×10^{-4} M (Fig. 3). A concentration of 5×10^{-5} M was chosen as a compromise.

Temperature in the range 10 – 60 °C has little influence on the development of the fluorescent intensity, decreasing almost linearly with a slope of -20 µV °C^{-1}. As there is no horizontal region in the graph of I_f against temperature, a value of 30 °C was chosen for subsequent experiments.

Influence of Flow Injection Analysis Variables

Manifold configuration

As indicated above, the fluorescent species formed by the oxidation of DPKH shows an increasing appearance rate as the basicity of the medium increases; in this medium the I_f of the oxidised product is zero. In contrast, in a strongly acidic medium the analytical signal is at a maximum, but the oxidation of DPKH is extremely slow. Therefore, for the design of the manifold to be used we can consider two types: two-channel and three-channel systems; both types make the development of the two steps possible under optimum conditions for each.

(a) In the two-channel systems, the sample is injected in a basic solution of the reagent. In the three-channel systems (b) and (c) two positions of the injection valve were considered. (b) Injection in the DPKH channel and further basification of the medium gives a smaller analytical signal than (c) when insertion is carried out in a stream of DPKH in basic medium. The sensitivity given by (c) is similar to that of (a), which has as the advantage of greater simplicity.

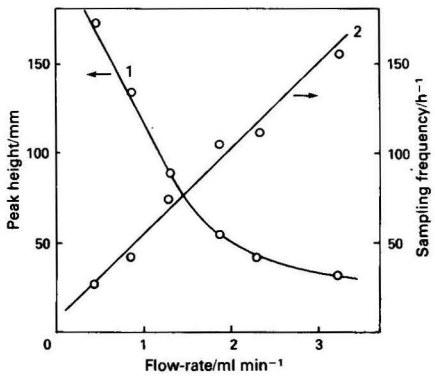

Fig. 6. Influence of flow-rate on (1) the peak height and (2) the sampling frequency

Volume of the sample

Fig. 4 shows that the intensity of the analytical signal as a function of the volume of the sample inserted is almost linear, until it attains a steady value for large sample volumes.

As the use of large volumes of sample provides high sensitivity, whereas with small volumes versatility of the method and economy of reagents are favoured and at the same time the presence of double peaks is avoided, but the analytical signal is smaller, a sample volume of 60 µl was chosen for subsequent experiments as a compromise.

Influence of the length and diameter of the reactors

The influence of the length of reactor 1, R_1, was studied for two R_2 lengths, 80.5 and 140.5 cm, and a catalyst concentration of 51.5 ng ml^{-1}. As shown in Fig. 5, in all instances the analytical signal is at a maximum for $R_1 = 80$ cm, as an optimum result of the influence of two opposing factors: reaction time and dilution of the product formed. The former effect predominates in the interval of the curve before the maximum and the latter in the subsequent interval. Studies carried out at a concentration of Cu(II) of 103 ng ml^{-1} show similar behaviour: a maximum signal for $R_1 = 80$ cm, which implies better contact of the reagent stream with the catalyst under these conditions, although the slope after the maximum is smaller. The diameters of the coils examined were 6 and 23 mm, and a straight tube was also used. The diameter of coil 1 has an anomalous effect on I_f: for a large diameter or a straight reactor the analytical signal remains constant, decreasing with the diameter of the coil when this is small. This behaviour, as opposed to that shown when a dye is injected, was confirmed by injecting into the stream of the carrier the oxidation product previously formed. The diameter of coil 2 has a negligible effect on peak height.

Keeping R_1 straight, R_2 was altered between 60 and 300 cm. The graph of peak height against R_2 (Fig. 5) shows a maximum for $R_2 = 160$ cm, a compromise between the establishment of acidic pH in the oxidation product and dilution at intervals before and after the maximum, respectively. The diameter of coil 2 does not exert any influence on the peak height.

Influence of flow-rate

This study was carried out by changing the flow-rates of both streams, but keeping them both equal. Fig. 6 shows the variation of the peak height and the sampling rate with flow-rate.

On increasing the flow-rate, the analytical signal decreases almost exponentially ($r^2 = 0.969$). This result is to be expected, as when the Reynolds' number increases, the

Table 1. Statistical analysis of the calibration graphs

Parameter	Concentration range/ng ml^{-1} 8–30*	40–300†
n	7	11
$\bar{x}$	76.5 mm	84.5 mm
S	4.66	5.65
$S_m = S/\sqrt{n}$	1.76	1.70
$S_r = S_m \times 100/\bar{x}$	2.30%	2.02%
$E(\%) = S_r \times t_{Student}$	4.48	3.66

* The injected samples contained 20.6 ng ml^{-1} of copper(II).
† The injected samples contained 204.7 ng ml^{-1} of copper(II).

Table 2. Effect of foreign ions on the determination of 20.6 ng ml^{-1} of Cu(II) by the recommended method. Ratio of foreign ion to Cu(II) tolerated = 100. Foreign ions tested: AsO_4^{3-}, Sb(III), Sr(II), Ba(II), Ca(II), Br^-, NO_3^-, Bi(III), SO_4^{2-}, Cl^-, $H_2PO_4^-$, trichloroacetate

Tolerated ratio of foreign ion to Cu(II)	Positive interference	Negative interference
50	I^-	$P_2O_7^{4-}$
20		Ga(III)
15		Zn(II)
10	Fe(III), Au(III), Co(II)	
5		Pb(II)
4		F^-, Mg(II), Cd(II), Mn(II)
3	Hg(II)	
2	Ag(I)	
1.5		Oxalate
1		Ni(II)
Interfere at the same level	Sn(II)	Al(III), Cr(III), S^{2-}, Be(II), EDTA

reaction time decreases and the dilution by convection increases. On increasing the flow-rate the sampling frequency increases almost linearly ($r^2 = 0.988$). We adopted a flow-rate of 1.8 ml min^{-1} as the most suitable, providing a sampling frequency of 100 h^{-1}.

Determination of Trace Amounts of Copper(II)

Calibration graphs

Under optimised operating conditions the following linear intervals of concentration of catalyst were obtained: at 8–30 ng ml^{-1}, $I_f = 1.9 + 1.9[Cu^{2+}]$ ($r^2 = 0.996$); and at 40–300 ng ml^{-1}, $I_f = -0.6 + 0.4[Cu^{2+}]$ ($r^2 = 0.994$). Statistical studies of the system for both of these lines were carried out and 7 and 11 injections, respectively, were made under identical conditions. The statistical parameters for $P=0.05$ are summarised in Table 1.

Interferences

The influence of 34 foreign species on the determination of 20.6 ng ml^{-1} of Cu(II) was tested systematically using the proposed procedure. Table 2 shows the tolerance levels of these species.

Many of the cations and anions do not interfere at a ratio of foreign ion to Cu(II) of 100:1. When a disturbing effect is detected at lower ratios, it can be distinguished as either positive (increase in the signal) or negative (decrease in the signal). Several ions interfere in the range 50:1 to 1:1 with respect to Cu(II). The method has a good selectivity level. Nevertheless, interferences due to Al(III), Cr(III), EDTA, S^{2-} and Sn(II) are noticeable at the same concentration level as the Cu(II) ion.

Use of reverse flow injection analysis (rFIA)

In order to increase the sensitivity of the determination, reverse flow injection analysis was compared with the normal method (nFIA) utilising the following conditions: for nFIA, carrier 1 5.044×10^{-5} M DPKH in 0.1 M sodium hydroxide solution, carrier 2 0.4 M hydrochloric acid and sample 20.6 ng ml^{-1} Cu(II); and for rFIA, carrier 1 20.6 ng ml^{-1} Cu(II), carrier 2 0.4 M hydrochloric acid and sample 5.044×10^{-5} M DPKH in 0.1 M sodium hydroxide solution. The ratio of the analytical signals obtained with the two techniques was rFIA:nFIA = 146:35. The sensitivity was four times higher using rFIA.

With rFIA the following linearity ranges of the calibration graph were determined: at 1.0–6.0 ng ml^{-1}, $I_f = 0.8 + 1.5[Cu^{2+}]$ ($r^2=0.996$); at 6.1–40.6 ng ml^{-1}, $I_f=-32.5 + 3.8[Cu^{2+}]$ ($r^2=0.993$); and at 20.5–124.9 ng ml^{-1}, $I_f=-6.3 + 0.7[Cu^{2+}]$ ($r^2=0.995$). This illustrates the higher sensitivity of rFIA.

Conclusion

The optimisation of the chemical variables of the system shows that more drastic conditions (higher reagent concentration, large pH changes) are necessary in order to obtain a sensitivity similar to that of the conventional method.[4] This behaviour was to be expected owing to the smaller volume of sample used and the dilution that it undergoes in the flow injection analysis system, which makes possible the analysis of copper at a higher speed.

The study of flow injection analysis variables permits the coordination of sensitivity, reproducibility and sample volume necessary to perform the analysis. The optimisation of the reactor lengths and the diameters of the coils provides greater sensitivity and reproducibility of the method; the last feature conflicts with sampling speed and economy of sample (the studies of flow-rate and sample volume) so that among the variables a compromise is adopted for the determination of copper.

The concentration ranges of catalyst in which the method is applicable (8–30 and 40–300 ng ml^{-1}) show similar relative standard deviations (2.3% and 2.0%, respectively), the sampling frequency being 100 h^{-1}. These results can be compared with the classical total[4] and kinetic[2] methods and lead to the conclusion that the use of the flow injection analysis technique with the DPKH - Cu(II) system provides good sensitivity, low error and a high sampling rate.

In the interference study, inhibition of the catalysis produced by Mg(II) was noticeable; this phenonmenon can provide a method for the determination of this cation.

The use of rFIA increases the sensitivity of the determination in two respects: it widens the concentration range of the normal method (from 8.0–30.0 to 6.1–40.9 ng ml^{-1}) and it provides another range of lower concentrations (1.0–6.0 ng ml^{-1}); this feature can be decisive in microtrace analysis, compensating for the handicap of the high consumption of sample required in rFIA.

Several flow injection analysis methods for the determination of copper have been proposed (Table 3).[7–18] In only one of the methods cited does the Cu(II) ion act as a catalyst[9,15]; the principle of the methods in the others is a complex formation reaction, except when there is no chemical reaction.

With regard to detection, photometry is the technique most often used,[7,9,11–15] followed by atomic-absorption spectrometry, in which the classical method is improved by injection in butyl acetate[8] or by extraction after complex formation,[18] and inductively coupled plasma spectrometry.[16,17] The design of a copper ion-selective electrode adapted to flow injection analysis[10] also allowed the potentiometric detection of this cation. It is strange that a fluorimetric detector has not been used for the analysis of copper ions.

Table 3. Flow injection analysis methods for copper determination

Reaction type	Detection technique*	Sample volume/ µl	Sampling frequency/ h^{-1}	Linear range of calibration graph	Relative standard deviation, %	Applications	Observations†	Reference
—	Photometry	—	—	—	—	Industrial (alloys)	—	7
Non-chemical reaction	AAS	100	300	0.1–3 µg ml^{-1}	2.2	—	Improvement of sensitivity	8
Redox catalytic	Photometry	5	250	100–250 µg ml^{-1} 5–‡ µg ml^{-1}	1.8	—	Closed-loop	9
Non-chemical reaction	Potentiometry	130	—	60–600 µg ml^{-1}	—	—	Construction of ISE (Cu)	10
Complex formation	Photometry	5	30	0–4 µg ml^{-1}	—	Environmental (residual water)	Simultaneous determination	11
Complex formation	Photometry	200	150	2–6.5 µg ml^{-1}	—	—	—	12
Non-chemical reaction	Photometry	318	280	0.8–2.4 g l^{-1}	0.2–0.7	Industrial (alloys)	—	13
Complex formation	Photometry	200	300	3–10 ng ml^{-1}	3	—	Utilisation of LED	14
Redox catalytic	Photometry	20	325	0.25–20 µg ml^{-1}	2	Clinical (sera)	Closed-loop	15
Non-chemical reaction	ICP	100	100	µg ml^{-1} level	1.7	Agricultural (plants)	Merging zones	16
Non-chemical reaction	ICP	500	6	0–100 µg ml^{-1}	0.9	—	Merging zones; computer	17
Complex formation, extraction	AAS	110	40	0–50 ng ml^{-1}	1.0	—	Extraction	18
Redox catalytic	Fluorimetry	60	100	8–30 ng ml^{-1}	2.3	—	—	
				40–300 ng ml^{-1}	2.0			This work

* AAS = atomic-absorption spectrometry; ICP = inductively coupled plasma.
† ISE = ion-selective electrode; LED = light-emitting diode.
‡ Upper value not given in reference 9.

The sampling rate is high in all instances, as is usual in flow injection analysis (about 100 samples h^{-1}).

The concentration range of Cu(II) that can be determined is variable, although it is usually in the micrograms per millitre range. Only two other methods exist[14,18] in which the calibration line lies in the nanograms per millilitre range.

Sample volumes reported vary between 5 µl[11] and 500 µl,[17] although the average value is between 100 and 200 µl. In two of the proposed methods[9,15] the "closed loop" technique is used.

References

1. Grases, F., and Valcárcel, M., *Talanta*, 1983, **30**, 139.
2. Grases, F., García-Sánchez, F., and Valcárcel, M., *Anal. Chim. Acta*, 1980, **119**, 359.
3. Grases, F., Estela, J. M., García-Sánchez, F., and Valcárcel, M., *Anal. Lett.*, 1980, **13**, (A3), 181.
4. Grases, F., García-Sánchez, F., and Valcárcel, M., *Anal. Chim. Acta*, 1981, **125**, 21.
5. Valcárcel, M., and Luque de Castro, M. D., *Quim. Anal.*, 1983, **I(4)**, 201.
6. Zief, M., and Mitchell, J. M., "Contamination Control in Trace Element Analysis," Wiley, New York, 1976, pp. 79–80.
7. Kuroda, R., Mochizuki, T., and Oguna, K., *Bunseki Kagaku*, 1980, **29**, 73.
8. Fukamachi, K., and Shibashi, N., *Anal. Chim. Acta*, 1980, **119**, 383.
9. Ramasamy, M., Job, A., and Mottola, H. A., *Anal. Chem.*, 1979, **51**, 1637.
10. Van Der Linden, W. E., and Doste Ruink, R., *Anal. Chim. Acta*, 1978, **101**, 419.
11. Betteridge, D., and Fields, B., *Anal. Chim. Acta*, 1981, **132**, 139.
12. Baban, S., *Anal. Proc.*, 1980, **17**, 535.
13. Kuroda, R., and Mochizuki, T., *Talanta*, 1981, **28**, 389.
14. Betteridge, D., Dagless, E. L., Fields, B., and Graves, N. F., *Analyst*, 1978, **103**, 897.
15. Ramasamy, S. M., and Mottola, H. A., *Anal. Chim. Acta*, 1981, **127**, 39.
16. Jacintho, A. O., Zagatto, E. A. G., Bergamin, H., Krug, F. J., Reis, B. F., Bruns, R. E., and Kowalski, B. R., *Anal. Chim. Acta*, 1981 **130**, 243.
17. Zagatto, A. E. G., Jacintho, A. O., Krug, F. J., Reis, B. F., Bruns, R. E., and Araujo, M. C. U., *Anal. Chim. Acta*, 1983, **145**, 169.
18. Nord, L., and Karlberg, B., *Anal. Chim. Acta*, 1983, **145**, 151.

Paper A3/92
Received March 25th, 1983
Accepted May 23rd, 1983

A Model Immunoassay Using Automated Flow Injection Analysis

Paul J. Worsfold* and Arwel Hughes
Department of Chemistry, Sheffield City Polytechnic, Pond Street, Sheffield, S1 1WB, UK

A model immunoassay between concanavalin A (antibody) and yeast mannan (antigen) was investigated using a microcomputer-controlled flow injection analysis (FIA) manifold with turbidimetric detection at 400 nm. The automated injection procedure gave good precision for a turbidimetric method and the stop-flow merging zones technique gave an acceptable sample throughput (50 samples per hour) with minimum consumption of sample (30 μl). The system described could therefore be used routinely for immunoprecipitin analysis in clinical laboratories, *e.g.*, IgG in human serum, and also to study kinetic aspects of such reactions.

Keywords: *Model immunoassay; concanavalin A; automation; merging zones; stop-flow flow injection analysis*

The first quantitative determination of proteins based on an immunoprecipitin reaction was reported by Heidelberger and Kendall[1] in 1935. This was followed in 1959 by the first such analysis of direct clinical relevance, the determination of human plasma proteins, reported by Schultze and Schwick.[2] The current importance of the immunoprecipitin technique for the analysis of proteins has been emphasised by the development of an automated immunoprecipitin analyser by Ritchie *et al.*[3] and the subsequent use of laser nephelometry to increase the sensitivity of the method.[4] One attraction of the immunoprecipitin technique over other immunochemical methods is the ease with which the procedure can be automated, which contributes to low relative standard deviations (RSDs) and good inter-laboratory correlation.[5] The limitations imposed by the high background scattering of the samples and the time taken for the reaction to reach equilibrium can be overcome by measuring the rate of reaction, typically over a timespan of 30–60 s.[6]

Flow injection analysis (FIA), a technique based on unsegmented continuous flow,[7] provides an attractive high-speed, low-cost alternative to existing instrumentation for the study of immunoprecipitin reactions.[8] The FIA manifold is very flexible (and therefore appropriate for laboratories dealing with small sample batches and a wide range of reaction chemistries), it can be easily automated and used for rate measurements[9] and in the merging zones mode the consumption of sample and reagent is minimised.[10]

This paper describes the results of a study of a model immunoprecipitin reaction between concanavalin A (the model antibody) and yeast mannan (the model antigen) using a stop-flow merging zones FIA manifold, and is a continuation of previously reported preliminary studies.[8] Details of the complete automation of the system using a microcomputer are also presented.

Experimental

Reagents

An aqueous buffer solution containing sodium acetate (10 mM), sodium chloride (0.1 M) and Brij-35 (0.3% *m/V*) was adjusted to pH 6.2 with acetic acid (1 M).

Concanavalin A was obtained as a lyophilised powder from *Canavalia ensiformis* (jack beans; Fluka) and reconstituted in the above buffer solution (2 mg ml^{-1}).

Yeast mannan was obtained after extraction from yeast by the Cetavlon method (Sigma) and standards were prepared in the above buffer solution over the range 0.1–20.0 mg ml^{-1}.

All solutions were filtered through a fine sintered-glass funnel before use and were stored at 4 °C when not in use. Fresh solutions were prepared weekly.

* Present address; Department of Chemistry, University of Hull, Cottingham Road, Hull, HU6 7RX, North Humberside, UK.

Instrumentation and Procedures

Static experiments

These were performed using a microprocessor-controlled UV - visible spectrophotometer (Perkin-Elmer 550S) and micro glass cells (Hellma 6082-Green). Equal volumes (0.2 ml) of concanavalin A and a range of yeast mannan standards were manually mixed in a micro glass cell and the resultant turbidity of the solution was monitored in order to establish the optimum wavelength for analysis and a suitable reaction time for the flow-through method described below. The zone of equivalence for the interaction was also determined using this static system.

Stop-flow merging zones FIA

The manifold used for the merging zones flow injection experiments is shown in Fig. 1. The two buffer streams were pumped at 0.5 ml min^{-1}, using a peristaltic pump (Ismatec Mini S-840), through polypropylene tubing (0.5 mm i.d.). Concanavalin A (30 μl) and yeast mannan (30 μl) were simultaneously injected into separate buffer streams using an automated PTFE rotary valve. Further downstream the concanavalin A and yeast mannan zones were synchronously merged at a T-connector and then passed through a mixing coil (25 cm) into a flow-through cell (7.9 μl volume; 10 mm path length) housed in a spectrophotometer (Varian VUV-50). The turbidity was constantly monitored at 400 nm and the output fed to a recorder and an analogue to digital converter (Hewlett-Packard 3438A; 3.5 digits).

The rate of reaction was determined by stopping a segment of the merged concanavalin A and yeast mannan zones in the flow cell and performing a two-point kinetic analysis. This was achieved by switching off the peristaltic pump 14 s after sample injection (delay time), measuring the turbidity 30 and 60 s later and then reactivating the pump to flush out the reaction mixture.

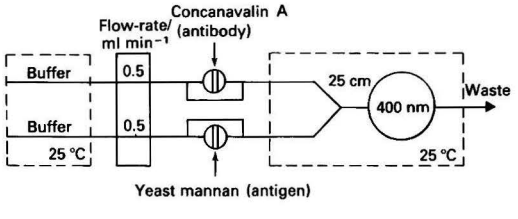

Fig. 1. Merging zones manifold for the immunoprecipitin reaction between concanavalin A (30 μl) and yeast mannan (30 μl) introduced into separate buffer streams (pH 6.2). Mixing coil, 25 cm × 0.5 mm i.d.; dispersion, 15

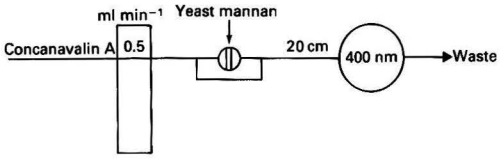

Fig. 2. Single-channel manifold for the immunoprecipitin reaction between concanavalin A (carrier stream) and yeast mannan (30 µl). Mixing coil, 20 cm × 0.5 mm i.d.; dispersion, 6

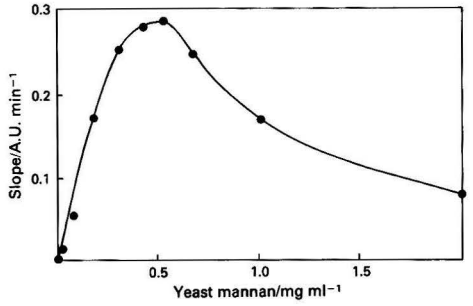

Fig. 3. Turbidity *versus* yeast mannan concentration using a merging zones FIA manifold

A microcomputer (Apple II) was used to control the operation of the injection valve, the switching on and off of the peristaltic pump, the reproducible timing of events and the collection and treatment of data. The necessary accessories included a real-time clock (Mountain Hardware) and an interface board (Stack Computers 6522 VIA) connected to three solid-state relays (Radio Spares 346671). Automated operation of the injection valve was achieved by connecting two of the solid-state relays to two solenoid valves (50 V), which in turn controlled the position of a double-acting pneumatic arm (Economatics, Sheffield) attached to the injection valve. The third solid-state relay was used to control the peristaltic pump. The real-time clock allowed for reproducible timing of events (to within 0.005 s) and raw data were stored on floppy disc and processed on completion of a batch analysis.

Single-channel FIA

For these experiments the FIA manifold was modified to a single stream containing concanavalin A pumped at 0.5 ml min^{-1} as shown in Fig. 2. Yeast mannan standards were injected into the stream and passed through a mixing coil (20 cm) before reaching the detector. In all other aspects the instrumentation was as described above.

Results and Discussion

Static Experiments

A wavelength scan over the range 280–520 nm for concanavalin A, yeast mannan and the resultant precipitin complex showed that turbidimetric detection at 400 nm gave the most sensitive response for the complex with no background absorbance from the reactants. Kinetic experiments showed that measurement after 60 s provided the optimum balance between analysis time and sensitivity. Table 1 shows the results obtained when equal volumes of concanavalin A and a range of yeast mannan standards were mixed and the resultant turbidity was measured at 400 nm after 60 s. The results clearly show the zone of equivalence, in the region of 0.5 mg ml^{-1} yeast mannan, which is characteristic of immunoprecipitin reactions. The region of analytical interest is that part of the graph where the antibody is in excess because there is a quantitative relationship between analyte (antigen) concentration and turbidity. However, it is also important to be able to distinguish between conditions of antibody excess and antigen excess, and this is not possible when carrying out static experiments, but is clearly seen when using FIA.

Table 1. Turbidity *versus* yeast mannan concentration using a static spectrophotometer. All results are means of five experiments

Yeast mannan/ mg ml^{-1}	Turbidity, absorbance units
0.0	0.000
0.1	0.912
0.2	1.208
0.3	1.400
0.4	1.568
0.5	1.680
0.7	1.216
1.0	0.512
1.5	0.280
2.0	0.216

Table 2. Turbidity *versus* yeast mannan concentration using a merging zones FIA manifold. All results are means of five experiments

Yeast mannan/ mg ml^{-1}	Slope/ absorbance units min^{-1}	Standard deviation/ absorbance units min^{-1}	RSD, %
0.0	0.000 1	0.000 6	—
0.05	0.006 1	0.001 0	16.4
0.1	0.044 9	0.005 9	13.1
0.2	0.175 8	0.006 9	3.9
0.3	0.265 8	0.014 8	5.6
0.4	0.294 3	0.008 7	3.0
0.5	0.296 6	0.014 3	4.8
0.7	0.250 5	0.012 7	5.1
1.0	0.169 4	0.012 4	10.3
2.0	0.055 6	0.008 1	14.6

Stop-flow Merging Zones FIA Manifold

The static method described above was adapted to FIA using a merging zones manifold (Fig. 1) to minimise consumption of sample and reagent and to ensure complete mixing between the two. Preliminary studies using a manual injection procedure gave rise to an unsatisfactory precision and so all subsequent experiments were carried out using the automated injection procedure described above. The only manual operation during the entire analysis is, therefore, the loading of sample and reagent into the injection valve, and for routine applications this could easily be automated by interfacing an autosampler to the microcomputer.

A typical set of results for the stop-flow procedure is shown in Table 2. The rate of reaction is expressed as change in absorbance per minute on the basis of a two-point kinetic measurement, as described above. The zone of equivalence (in the region of 0.5 mg ml^{-1} yeast mannan) is clearly seen from a graphical presentation of the data (Fig. 3) and the sensitivity is as expected given the experimental conditions and a dispersion of 15 for the sample in the FIA manifold. The RSDs (each from five results) are acceptable for a turbidimetric analysis, although both precision and sensitivity could be improved by a longer analysis time and a multi-point kinetic measurement (assuming that the slope of the rate curve is linear). The correlation coefficient between yeast mannan concentration and rate of reaction for the analytically important antibody excess region (*i.e.*, yeast mannan concentrations in the range 0.0–0.4 mg ml^{-1}) was 0.980 8 for the relevant data presented in Table 2.

Table 3. Turbidity *versus* yeast mannan concentration using a single-channel FIA manifold. All results are means of five experiments

Yeast mannan/ mg ml^{-1}	Slope/ absorbance units min^{-1}	Standard deviation/ absorbance units min^{-1}	RSD, %
0.00	−0.003 8	0.002 0	—
0.02	0.018 9	0.001 1	5.8
0.05	0.207 1	0.006 1	2.9
0.07	0.357 3	0.021 6	6.0
0.10	0.540 1	0.009 1	1.7
0.15	0.794 1	0.009 1	1.1
0.20	0.931 8	0.029 5	3.2
0.40	1.056 0	0.080 6	7.6
0.50	1.157 6	0.163 3	14.1
0.70	1.094 1	0.204 8	18.7
1.00	0.556 2	0.103 0	18.5
2.00	0.252 7	0.020 8	8.2
4.00	0.104 5	0.010 5	10.0

Temperature control is essential if reproducible results are to be obtained, and for this work the temperature was controlled at 25 °C. A limited number of experiments carried out at 30 °C, however, suggested that there was an improved sensitivity at the higher temperature due to an increased rate of reaction. One practical problem arising from stop-flow work involving turbidimetric detection is occlusion of the cell windows, which leads to base-line drift. This can be overcome by the incorporation of an extra channel, pumping dilute nitric acid through the flow cell, which can be activated via the microcomputer when required.

An alternative to the stop-flow approach is to increase the residence time of the merged zones in the manifold by increasing the length of the mixing coil and reducing the flow-rates. This continuous flow approach does not require microcomputer control but, in the concanavalin A - yeast mannan reaction, an acceptable sensitivity is possible only with excessively long analysis times.

Single-channel FIA Manifold

The major disadvantage of this manifold design is the continuous consumption of a potentially expensive reagent; the attraction is that the results clearly distinguish between the conditions of antibody excess and antigen excess. As the injected sample zone (yeast mannan) travels through the mixing coil physical dispersion in the carrier stream (concanavalin A) occurs, and this results in a continuous sample concentration gradient from zero to some maximum value within the mixing coil. In the region of antibody excess the detector response will therefore be in the form of a single peak with a maximum at the point of maximum sample concentration. In the region of antigen excess, however, the output will be in the form of a double peak with a trough at the point of maximum sample concentration. The same effect occurs in the unsegmented region of segmented continuous flow analysers.[11]

In order to enhance the sensitivity of the single-channel approach a stop-flow technique was used, with a delay time of 10 s and a two-point kinetic measurement 20 and 50 s later. This delay time was chosen so as to stop the zone of maximum sample concentration in the flow cell. The results are given in Table 3 and, as expected, show an increased sensitivity compared with those obtained using a merging zones manifold. In this instance the condition of antigen excess is indicated by a "spike" on the output when the pump is reactivated and more favourable concentration ratios for complex formation are swept through the flow cell.

Conclusions

Flow injection analysis provides a rapid, economical means of fully automating immunoprecipitin reactions. Owing to the simplicity of the manifold design it can also be easily modified to accommodate a wide range of chemical reactions, on-line processes and detection systems. Using the stop-flow merging zones approach sample and reagent consumption are kept to a minimum (30 µl) and quantitative results are obtained within 1–2 min of injection. For the concanavalin A - yeast mannan reaction the sampling rate was 50 samples per hour and a typical correlation coefficient for the analytically important antibody excess region of the calibration graph was 0.980 8. The use of a single-channel manifold offers enhanced sensitivity and clearly distinguishes between antibody excess and antigen excess.

There are differences between the model system discussed above and immunoprecipitin assays; for example, immunoprecipitin interactions are normally carried out at a pH of 7.0–8.5, concanavalin A is a metalloprotein and requires a complement of calcium and manganese ions and antibodies are conventionally obtained in a heterogeneous matrix. It is not unreasonable to assume, however, that the technique described above will also be applicable to routine immunoprecipitin analysis, *e.g.*, the determination of human IgG in serum, and work is at present being carried out in this area.

The authors thank the Science and Engineering Research Council for their financial support for one of them (A.H.) and the Royal Society of Chemistry for the provision of funds for the purchase of biochemicals.

References

1. Heidelberger, M., and Kendall, F. E., *J. Exp. Med.*, 1935, **62**, 467.
2. Schultze, H. E., and Schwick, G., *Clin. Chim. Acta*, 1959, **4**, 15.
3. Ritchie, R. F., Alper, C. A., and Graves, J. A., *Arthritis Rheum.*, 1969, **12**, 693.
4. Deaton, C. D., Maxwell, K. W., and Smith, R. S., *in* Ritchie, R. F., *Editor*, "Automated Immunoanalysis, Part 2," Marcel Dekker, New York, 1978, pp. 375–408.
5. Whicher, J. T., *in* Milford Ward, A., and Whicher, J. T., *Editors*, "Immunochemistry in Clinical Laboratory Medicine," MTP Press, Lancaster, 1979, pp. 51–62.
6. Anderson, R. J., and Sternberg, J. C., *in* Ritchie, R. F., *Editor*, "Automated Immunoanalysis, Part 2," Marcel Dekker, New York, 1978, pp. 409–469.
7. Růžička, J., and Hansen, E. H., "Flow Injection Analysis," Wiley–Interscience, New York, 1981.
8. Worsfold, P. J., *Anal. Chim. Acta*, 1983, **145**, 117.
9. Worsfold, P. J., Růžička, J., and Hansen, E. H., *Analyst*, 1981, **106**, 1309.
10. Růžička, J., and Hansen, E. H., *Anal. Chim. Acta*, 1979, **106**, 207.
11. White, P. A. E., and Strong, R., *in* Milford Ward, A., and Whicher, J. T., *Editors*, "Immunochemistry in Clinical Laboratory Medicine," MTP Press, Lancaster, 1979, pp. 23–34.

Paper A3/282
Received August 22nd, 1983
Accepted October 4th, 1983

Potential Use of a Terbium - Transferrin Complex as a Label in an Immunoassay for Gentamicin

Nichola J. Wilmott, James N. Miller and Julian F. Tyson
Chemistry Department, Loughborough University of Technology, Loughborough, Leicestershire, LE11 3TU, UK

A study has been made of the potential use of a terbium - transferrin complex as a non-isotopic label in the immunoassay determination of the antibiotic gentamicin. The fluorescence properties of the complex have been characterised. The labelled gentamicin was formed using a controlled carbodiimide reaction, conditions being chosen to produce a gentamicin-bound complex containing the correct amount of gentamicin for use in a competitive binding assay. Recognition of the gentamicin-bound complex by antisera to gentamicin was verified using a standard radioimmunoassay for gentamicin.

Keywords: *Fluorescence immunoassay; gentamicin assay; terbium - transferrin label*

The last decade has seen several attempts to develop non-isotopic immunoassays with a view to replacing radioimmunoassay methods which have many well documented disadvantages.

Several approaches have been made to the use of metal ions as labels in immunoassay: Cais[1,2] used derivatives of sandwich compounds such as ferrocene to label steroids and other molecules, detection of the labelled species being carried out by atomic-absorption spectrometry. These labels were relatively insensitive in immunoassays, no doubt partly because the metals used (Fe, Mn, etc.) occur at high concentrations in biological samples. Cais subsequently synthesised metallohaptens by the mercuration of steroid estrogens,[3] where the metal atoms were introduced directly into the molecule of the antigen, and by the formation of cymatrene complexes containing manganese.[4] Leuvering *et al.*[5] have studied the use of colloidal coating with atomic-absorption spectrometric determination.

In this paper we report the potential use of lanthanide ions as labels in immunoassay. In principle, lanthanide ion complexes should form useful labels in immunoassay as they are highly fluorescent and the concentration of lanthanide ions in biological samples is extremely low. In particular, a study has been made of the potential of the complex between terbium and transferrin as a label in the immunoassay of gentamicin.

Human serum transferrin has the function in the body of binding and transporting iron in the plasma in the form of Fe^{3+}. Transferrin binds two iron(III) ions per molecule in specific sites on the polypeptide chain, but in the absence of iron these sites may be occupied by lanthanide ions to form highly fluorescent complexes.

Gentamicin is an aminoglycosidic antibiotic used in the treatment of severe Gram-negative bacteria. Its optimum therapeutic concentration in human serum is 4–12 mg l^{-1} (9–20 μmol l^{-1}), maintained by intramuscular injection: 0.8 mg per kilogram body mass every 8 h. It is extremely effective but has a low therapeutic ratio and therefore its level must be monitored by a simple, rapid and reliable method.

Experimental

Apparatus

All fluorescence spectra were measured on a Perkin-Elmer Model LS-5 luminescence spectrometer fitted with an R928 photomultiplier. Data were recorded using a Perkin-Elmer Model 3600 data station using PECLS II applications software, which permitted the calculation of corrected spectra and phosphorescence lifetimes.

Reagents

Terbium chloride and glycine were obtained from Aldrich Chemical Co. and iron-free transferrin, gentamicin sulphate and 1-ethyl-3-(3-dimethylaminopropyl)carbodiimide hydrochloride from Sigma London Chemical Co.

All radioimmunoassays were carried out using a radioimmunoassay kit supplied by RIA (UK) Ltd.

Antibodies used in the antibody binding experiments were supplied by Sigma Chemical Co. Ltd.

Fluorescence of Terbium and the Terbium - Transferrin Complex

Fluorescence spectra of terbium chloride in aqueous solution and a terbium - transferrin complex in Tris - hydrochloric acid - hydrogen carbonate buffer[6] were recorded.

The limits of detection of the complex and its fluorescence lifetime (the time for the fluorescence of a sample to decay to the background level) were also determined.

The complex for the above experiments was prepared by the addition of aqueous terbium chloride to iron-free transferrin in Tris - hydrochloric acid - hydrogen carbonate buffer in the molar ratio 2:1.

Linkage of Gentamicin to Transferrin

The linkage of gentamicin to transferrin was achieved using a carbodiimide reagent. In this procedure a free acid group on the transferrin molecule is linked to a free amino group on the gentamicin. Experiments were carried out using 1-ethyl-3-(3-dimethylaminopropyl)carbodiimide hydrochloride in aqueous solution.

Iron-free transferrin (30 mg), gentamicin (60 mg) and the carbodiimide (400 mg) were incubated at room temperature in distilled water (2.5 ml) for varying lengths of time before separation of the protein fraction on a Sephadex G-25 column by elution with Tris - hydrochloric acid - hydrogen carbonate buffer (pH 8.5). Verification of gentamicin binding was carried out using ^{125}I-labelled gentamicin.

The carbodiimide procedure was repeated using various glycine to gentamicin ratios for the gentamicin in the original experiment, the reaction time being 5 min in each instance. The reaction products were subsequently analysed for their gentamicin content by radioimmunoassay and their fluorescence was measured after terbium binding.

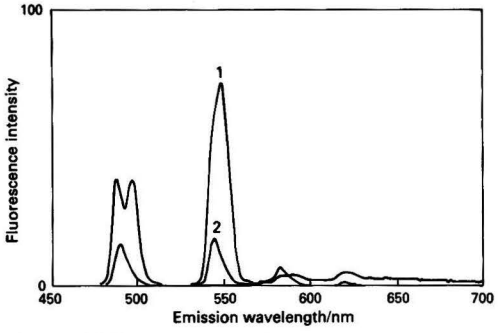

Fig. 1. Emission spectra of terbium chloride and a terbium - transferrin complex. 1, 10^{-5} M terbium - transferrin complex; and 2, 100 mM terbium chloride

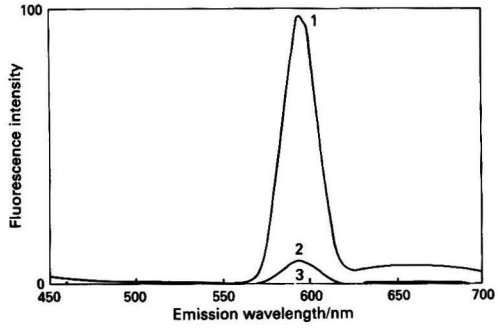

Fig. 2. Emission spectra of 1:100 human serum with various delay times: 1, 0.01; 2, 0.02; and 3, 0.05 ms

Titration of the Gentamicin - Glycine Bound Complex against Anti-gentamicin

The effect on the fluorescence of the complex in various concentrations of antiserum to gentamicin (raised in rabbit) was investigated using the double antibody technique with anti-rabbit IgG. Fluorescence measurements were taken following incubation, precipitation and centrifugation.

Results and Discussion

Fluorescence of Terbium and the Terbium - Transferrin Complex

Fig. 1 shows an enhancement of the fluorescence intensity of terbium of the order of 10^5 when the complex is excited at 295 nm. This fluorescence enhancement is due to an intramolecular energy transfer process within the complex. This is demonstrated by the fact that the complex excitation is in the region of the ligand absorbing region whereas the emission is typical of the "line" emission of the terbium ion.

The limit of detection of the complex was shown to be 10^{-7} M with respect to transferrin, a result which suggests that the complex has a suitable fluorescence intensity for use as a label in the analysis of drugs by immunoassay.

The complex had a lifetime of 1.25 ms. Subsequent delayed fluorescence experiments (Fig. 2) showed that interference due to scattered light from blood serum could be reduced to zero with a delay gate of 0.05 ms. The subsequent decrease in fluorescence intensity of the complex was less than 5%. The following instrumental conditions were thus chosen: excitation slit, 5.0 nm; emission slit, 5.0 nm; excitation wavelength, 295 nm; delay time, 0.05 ms; gate time, 5.0 ms; and fixed-scale mode.

Table 1. Results of analysis of complex for gentamicin by radioimmunoassay

Analyte	C.p.s.	Gentamicin determined/ μg ml^{-1}
0 μg ml^{-1} standard	42039	
1 μg ml^{-1} standard	36557	
2 μg ml^{-1} standard	28737	
4 μg ml^{-1} standard	16771	
8 μg ml^{-1} standard	9860	
16 μg ml^{-1} standard	6481	
Glycine : gentamicin ratio—		
0:20	1023	>16
2:18	540	
5:15	1073	
10:10	1870	
15:5	7497	8–16
18:2	11493	4–8

Table 2. Results of stability tests on the glycine - gentamicin bound complex

Time after formation	Fluorescence intensity in buffer	Fluorescence intensity in 1:100 serum
0 min	104.95	64.19
5 min	109.55	67.48
10 min	103.50	71.19
15 min	104.25	72.84
30 min	107.10	74.07
45 min	106.20	74.80
1 h	107.05	77.45
24 h	109.00	77.46
7 d	110.95	77.46

Linkage of Gentamicin to Transferrin

The experiments carried out using ^{125}I-labelled gentamicin showed that with reaction times from 5 min to 1 h substantial gentamicin binding was occurring.

Analysis of the Gentamicin Content of Complexes with Substituted Glycine

Table 1 shows the amount of gentamicin bound per millilitre of solution for various reaction mixtures as analysed by standard radioimmunoassay for gentamicin.

It can be seen that gentamicin - glycine bound complexes with glycine to gentamicin ratios of less than 15:5 have too high a gentamicin content for use in a competitive binding assay for the therapeutic blood concentration range of gentamicin (4–12 μg ml^{-1}).

Fluorescence measurements on the complexes modified by glycine and gentamicin showed a decrease in fluorescence intensity of less than 5% compared with the original terbium - transferrin complex.

Stability of the Gentamicin - Glycine Bound Complex

It can be seen from Table 2 that a complex containing a glycine to gentamicin ratio of 9:1 is stable in buffer and buffer containing 1:100 human serum over a period of at least 7 d.

Absorbance measurements at 295 nm showed that the decrease in fluorescence intensity in 1:100 serum was due to the increased absorbance of the solution at that wavelength.

Titration of the Glycine - Gentamicin Complex against Anti-gentamicin

Titration of the complex against anti-gentamicin (Fig. 3) shows good antibody recognition of the complex, the curve shape being typical of such a dilution analysis.

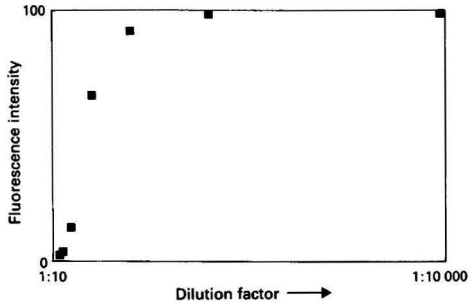

Fig. 3. Antibody dilution analysis of the terbium - transferrin - gentamicin - glycine complex

Conclusion

The results suggest that a glycine - gentamicin bound terbium - transferrin complex has potential as a non-isotopic immunoassay label. However, it is felt that careful consideration should be given to the final format of the immunoassay, owing to possible effects of the macromolecular label. At present the most suitable separation methods are being established.

Although the terbium - transferrin complex shows potential as an alternative label in immunoassay, it has the disadvantage of sensitivity suitable only for the detection of drugs and not hormones. One means of increasing the sensitivity is to increase the fluorescence intensity. Further study of the intramolecular energy transfer process[7,8] such as are involved in the terbium - transferrin complex might prove useful in this respect. The bifunctional reagents that would be suitable are of the type described by Meares and co-workers,[9,10] which have "EDTA" groups and groups suitable for binding to amino acids at opposite extremities of the molecule. Another alternative is the use of bifunctional reagents where the chelating agent is "iminodiacetic acid."[11,12]

The authors thank the Trustees of the Analytical Chemistry Trust Fund of the Royal Society of Chemistry for the award of an SAC Research Studentship.

References

1. Cais, M., *Nature (London)*, 1977, **270**, 534.
2. Cais, M., *US Pat.*, 4 205 952, 1980.
3. Cais, M., *Actual. Chim.*, 1979, No. 7, 14.
4. Cais, M., *Bull. Soc. Chim. Belg.*, 1981, **90**, 27.
5. Leuvering, J. H. W., Thal, P. J. H. M., Van der Waart, M., and Schuurs, A. H. W. M., *J. Immunoassay*, 1980, **1**, 77.
6. Luk, C. K., *Biochemistry*, 1971, **10**, 2838.
7. Weissman, S. I., *J. Chem. Phys.*, 1942, **10**, 214.
8. Crosby, G. A., Whan, R. E., and Aline, R. M., *J. Chem. Phys.*, 1961, **34**, 743.
9. Sundberg, M. W., Meares, C. F., Goodwin, D. A., and Diamanti, C. A., *J. Med. Chem.*, 1974, **17**, 1304.
10. Yeh, S. M., Sherman, D. G., and Meares, C. F., *Anal. Biochem.*, 1979, **100**, 152.
11. De Maulipied, A., *J. Chem. Soc.*, 1905, **87**, 439.
12. Johnson, C., *J. Am. Chem. Soc.*, 1911, **33**, 749.

Paper A3/375
Received October 28th, 1983
Accepted November 29th, 1983

Ultracentrifugal Subfractionation of High-density Lipoprotein

James Shepherd,* Eleanor A. Caine, Dorothy K. Bedford and Christopher J. Packard
Department of Pathological Biochemistry, University of Glasgow, Royal Infirmary, Glasgow, G4 0SF, UK

Knowledge of the structure, function and metabolism of the plasma lipoproteins has been greatly facilitated by refinement of the high-performance ultracentrifuge. Techniques based on anglehead rotors are widely used to isolate different fractions by increasing in a stepwise fashion the plasma solvent density. This simple approach may, for various reasons, result in the selection of inappropriate density intervals and so alternative zonal procedures have been developed that yield a continuous lipoprotein spectral distribution. However, the limited analytical capacity of this kind of system has highlighted the need for more rapid microcomputer-controlled ultracentrifugation techniques. The merits of each of these approaches are discussed with reference to the subfractionation of high-density lipoproteins.

Keywords: *Plasma lipoprotein; ultracentrifugal subfractionation; anglehead rotor; zonal centrifugation; microcomputer*

Current interest in high-density lipoprotein (HDL) stems from the negative association observed between its plasma concentration and the incidence of ischaemic heart disease.[1] This implies that HDL in some way confers protection against the condition, possibly by acting as a tissue cholesterol acceptor with the responsibility of transporting the sterol to the liver to be excreted unchanged or in the form of bile acids.[2] The ultracentrifuge has played an important role in delineating the properties of this lipoprotein by facilitating detailed investigation of its metabolic activities both *in vivo* and *in vitro*. As prepared by classical ultracentrifugal flotation in fixed-angle rotors it comprises approximately 50% protein, but examination of the particle spectral distribution reveals that this is unevenly spread in subpopulations[3] differing in size, density and composition (Table 1). Therefore, any consideration of the cardioprotective action of the lipoprotein must take cognisance of such spectral heterogeneity. In this regard, it is now clear that a significant component of the variability in total HDL cholesterol derives from fluctuations in the level of a minor less dense subfraction, which has been designated HDL_2 and lies in the density interval 1.063–1.125 kg l^{-1}. The majority, with density 1.125–1.21 kg l^{-1}, is conventionally termed HDL_3 and is relatively constant in its plasma concentration from subject to subject.[4–6] In the discussion that follows, the advantages and disadvantages of several ultracentrifugal procedures will be presented in relation to their utility in separating these HDL subfractions; the paper concludes with a description of a new microcomputer-controlled analytical system devised to measure plasma lipoprotein concentrations.

HDL Subfractionation in a Fixed-angle Rotor

Havel *et al.*[3] were the first to describe a practical procedure using a fixed-angle 40 Spinco ultracentrifuge rotor for the preparation of HDL and its subfractions. Their stratagem was to increase in a stepwise fashion the solvent density of the plasma by progressive additions of potassium bromide. This resulted in the separation of apparently discrete fractions in the density ranges <1.019 kg l^{-1} (very low-density lipoprotein, VLDL), 1.019–1.063 kg l^{-1} (low-density lipoprotein, LDL) and 1.063–1.21 kg l^{-1} (HDL). Each of these fractions possesses distinctive physico-chemical properties and exhibits characteristic metabolic activities. The high-density species was subdivided into the two components[7,8] described above (see Table 1) in response to original observations[9,10] made in the analytical ultracentrifuge that indicated a minimum in its spectral distribution at a solvent density of approximately 1.125 kg l^{-1}. Current common practice is to measure HDL_2 and HDL_3 levels after first eliminating the less dense lipoproteins VLDL and LDL by ultracentrifugal flotation or polyanionic precipitation.[7] The HDL is then separated into two components by repeat ultracentrifugation[3] at the density of 1.125 kg l^{-1}. Thereafter, the cholesterol content of the separated subfractions is determined directly. This procedure has several advantges: it is simple, robust, relatively rapid and can handle a large number of samples. Typical values for healthy subjects[6,11–13] are given in Table 2. Comparative studies of males and females have shown that the higher level of HDL in women derives specifically from an increase in HDL_2,[4–6] consonant with the view that it is this subfraction which is cardioprotective.

The fixed angle ultracentrifugal separation procedure is not without disadvantage (Fig. 1). It may be criticised for its reliance on discrete lipoprotein separation at fixed densities which fail to take account of possible inter-individual variations in particle composition or of changes which might occur in response to disease. Moreover, consideration must be given to the fact that gradient formation occurs[10] in the background solute during the centrifugation run [Fig. 1(*b*)]. In fact, the common assumption that this is a fixed-density technique is not strictly accurate as different separation conditions in various rotors may, unless care is taken, result in the selection of an incorrect density interval. This, coupled with the problem of wall effects and the gradient destabilisation that accompanies rotor acceleration and deceleration [Fig. 1(*a*)]

Table 1. Physico-chemical properties of HDL subfractions (taken from references 7 and 8)

Subfraction	Relative molecular mass, daltons	Mean flotation rate ($F_{1.21}$)*	Buoyant density/ kg l^{-1}	Chemical composition, g per 100 g			
				Protein	Phospholipid	Cholesterol	Triglyceride
HDL_2	3.6×10^5	5.9	1.096	40.1	29.9	23.3	6.6
HDL_3	1.7×10^5	2.9	1.143	52.5	27.4	16.1	3.9

*$F_{1.21}$ = negative sedimentation coefficient (in Svedbergs) at 1.21 kg l^{-1} density and 26 °C.

*To whom correspondence should be addressed.

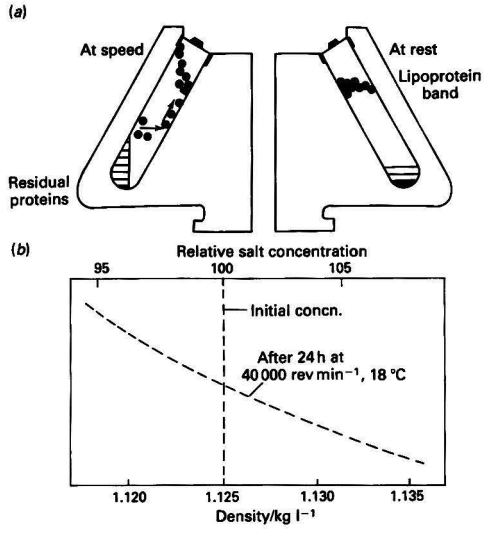

Fig. 1. Anglehead ultracentrifugation of lipoproteins. (*a*) Separation in a fixed-angle tube. (*b*) Salt redistribution during HDL subfractionation

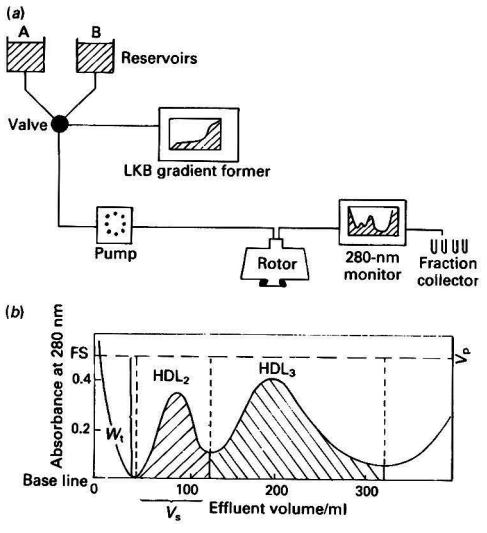

Fig. 2. Zonal ultracentrifugation of lipoproteins.[6,14] (*a*) Flow diagram for the operation of a Ti 14 zonal rotor. A and B contain the starting and limiting salt densities (A, 1.0 kg l^{-1} and B, 1.4 kg l^{-1} NaBr solution, pH 7.0) in the gradient. Typical HDL subfraction profile. Quantitation is achieved by measuring the area under each peak (in absorbance units). The concentration of, for example, HDL_2 is then determined from the equation

$$[\text{Plasma HDL}_2] = \text{FS}.V_s\left(\frac{100\ W_p}{W_t}\right).2E_s.\frac{100}{V_pP}$$

where FS = full scale absorbance; V_s = subfraction volume; W_p/W_t = that fraction of the area FS.V_s corresponding to the lipoprotein absorbance peak; E_s = specific molar absorptivity of subfraction; V_p = volume of plasma applied; and P = percentage of protein in the particle

Table 2. Typical HDL subfraction distributions determined by various ultracentrifugation techniques

Method	HDL_2 cholesterol/ mmol l^{-1}	HDL_3 cholesterol/ mmol l^{-1}	Reference
Anglehead centrifugation at d = 1.125 kg l^{-1}; n = 63, males	0.23	1.0	11
Zonal centrifugation (Ti 14 rotor); n = 25, males and females	0.23	0.91	6
Zonal centrifugation (SW 41 rotor); n = 12, males and females	0.30	0.87	12
Analytical ultracentrifugation; n = 160, males and females	0.33	1.12	13

has led to the development of other procedures that permit monitoring of the separation prior to fractionation of the lipoprotein.

Zonal Centrifugal Separation of HDL

Technological improvements in rotor specification and performance and the introduction of titanium in their construction have permitted the development of techniques for rate zonal ultracentrifugal separation of lipoproteins. Basically, in this procedure a salt gradient is established in the rotor centripetal to the plasma sample whose lipoproteins are then separated by flotation. The fractionation can be achieved either on the basis of equilibrium attainment or on differential flotation rate. The latter is a function of (a) the relative densities of particle and solute and (b) particle size. As lipoproteins are pseudomicellar spheres, variations in shape can largely be ignored.

Two technologies based on different equipment have become popular for the zonal separation of high-density lipoprotein subfractions. Large-capacity, single-chamber zonal rotors (*e.g.*, Beckman Ti 14, Beckman Instrument Co., Palo Alto, CA, USA; MSE B XIV, Measuring and Scientific Equipment, Crawley, UK) permit dynamic separations to be made without subjecting the gradient to reorientation (Fig. 2). In the method of Patsch *et al.*,[14] a discontinuous gradient of sodium bromide between d = 1.0 and 1.4 kg l^{-1} is formed in the slowly spinning rotor prior to introducing the sample to its periphery. Acceleration to an operating speed of 41 000 rev min^{-1} then separates the HDL subfractions in 21 h, free from contaminating lipoproteins and plasma proteins. Thereafter, the rotor is decelerated to loading speed and its contents are expelled through a continuous monitoring system and collected into fractions as required.

This procedure is ideal for preparative separations using large sample volumes and caters for density variations in HDL_2 and HDL_3 from sample to sample, as the spectral distribution obtained is continuous. Wall effects are eliminated and, in a relatively short time, the HDL subfractions can be prepared in amounts suitable for subsequent chemical or metabolic studies. However, only one sample can be analysed per centrifugation run and the procedure is not suited to the examination of small volumes. Moreover, considerable sample dilution occurs and the lipoproteins become exposed, if only for a short time, to substantially higher ionic strengths than employed in fixed-angle centrifugation. This may lead to artifactual changes in particle structure or composition.[15] Fig. 2(*b*) describes a procedure that we have used[6] to quantify HDL_2 and HDL_3 on the basis of the zonal rotor profile. The area under each absorbance peak is measured and plasma concentrations of the subfractions are calculated using specific molar absorptivities determined at 280 nm.

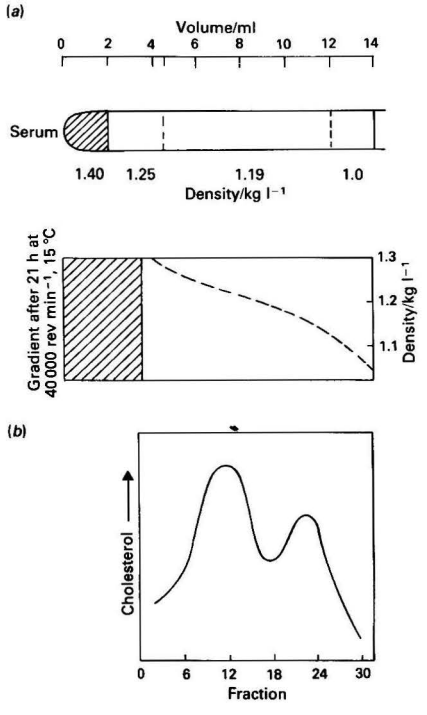

Fig. 3. Zonal ultracentrifugation of lipoproteins.[16] (*a*) Rate zonal separation of HDL subfractions using an SW 40 rotor. (*b*) HDL subfraction profile

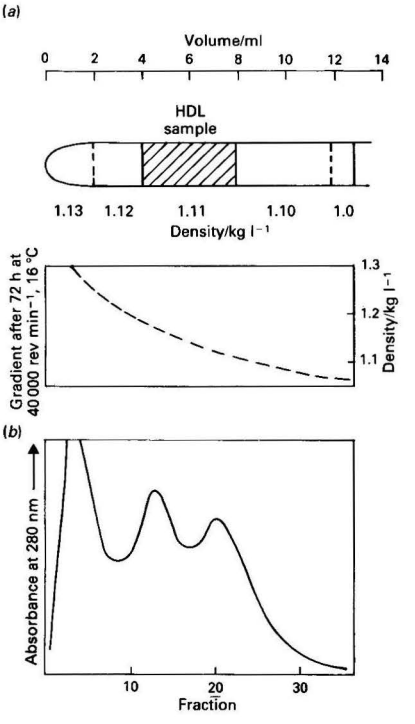

Fig. 4. Isopyknic ultracentrifugation of lipoproteins. (*a*) Isopyknic separation of HDL subfractions. (*b*) HDL subfraction distribution

The second approach to rate zonal separation of HDL subfractions depends on the use of rotors with hinged sample buckets that rotate radially during acceleration and deceleration to eliminate any sample re-mixing that may occur at these times as a result of gradient reorientation. The rotor geometry permits simultaneous separations of up to six samples and the principle is essentially as described above. An example of this procedure[16] is shown in Fig. 3(*a*). The sample is placed at the bottom of the separating tube and above it is constructed a discontinuous salt gradient. During centrifugation, HDL_2 (fractions 18–30) and HDL_3 (fractions 6–18) float to the middle of the tube. Following centrifugation the separated lipoproteins are collected either from the top or bottom of the gradient. The gradient constructed in the tube becomes continuous as a result of diffusion during the centrifugation and permits maximum separation of the HDL subfractions in the centre of the tube. The less dense lipoproteins are rapidly cleared from this area and form a pellicle at the top of the gradient. In this method, which combines the resolving power of the Ti 14 system with the convenient sample handling of the fixed-angle procedure, the HDL subfractions do not band isopyknically but are maximally separated while still in the rate zonal mode. However, to maintain reproducibility, careful attention must be paid to sample fractionation following the centrifugal separation. Additionally, resolution between the denser HDL_3 fraction and the plasma proteins is incomplete. Consequently, it is preferable to quantify the HDL subfractions on the basis of cholesterol rather than total protein content [Fig. 3(*b*)].

If centrifugation in the swinging bucket rotor is continued,[17] the HDL subfraction can be separated on the basis of their differing buoyant densities (Fig. 4). In this situation, however, whole plasma cannot be used as the lipoproteins will be inadequately resolved from each other and from the residual plasma proteins. It is necessary, therefore, to pre-isolate a total HDL fraction (1.063–1.25 kg l^{-1}) and subject this to isopyknic banding, which involves incorporating the HDL into a CsCl gradient as shown in Fig. 4(*a*). Centrifugation continued to equilibrium separates the subfractions on the basis of their buoyant densities; even then, considerable albumin contamination is apparent at the denser end of the gradient [Fig. 4(*b*)] (HDL is contained between fractions 10 and 16 and HDL_2 in fractions 18–25). A second problem with the method is that it requires centrifugation to be continued for prolonged periods (6 d) during which the lipoprotein is exposed to relatively high salt concentrations. This results in at least partial denaturation of the sample.[15]

Hence, in choosing between isopyknic and rate zonal centrifugation, the investigator is in effect determining whether to expose lipoproteins to relatively low salt concentrations for a prolonged period or to high concentrations for a limited period. Studies of lipoprotein stability under these conditions would favour the latter.[15]

Microcomputer-controlled Analytical Ultracentrifugation of Lipoproteins

Analytical ultracentrifugal analysis of lipoproteins is one of the earliest and most useful procedures employed to quantify these plasma constituents. However, the expense and labour involved in operating such a system have limited its popularity. Recently we have attempted to overcome these problems by interfacing a microcomputer (Apple II Europlus, Apple Inc., Cupertino, CA, USA) with the Beckman L8 ultracentrifuge, which itself is operated by a microprocessor and is

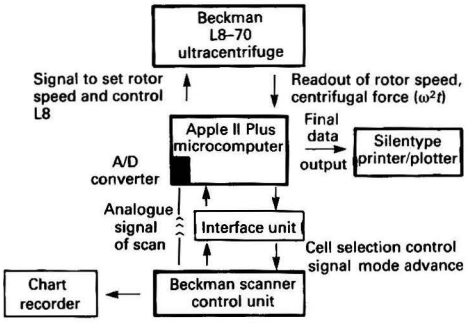

Fig. 5. Schematic diagram of the automated analytical ultracentrifugation system

therefore readily adaptable to external machine control. In the system shown in Fig. 5, the Apple II Plus microcomputer, with a 48K memory, functions to control the ultracentrifuge and the Beckman Prep UV scanner and acquires and processes data from both using a PASCAL program. The custom made input - output cards, computer interface unit, their connections and the PASCAL program are available from Drew Scientific, Barley Mow, Chiswick, London. The microcomputer and ultracentrifuge are linked by a 48-track ribbon cable and ground line. The former is inserted peripherally into the L8 program control unit and into a parallel input - output card in an I/O port of the Apple II. The interface unit between the scanner and microcomputer contains a number of relays responsible for triggering scanner operation at the intervals specified in the program. Scanning information obtained as voltages from the photomultiplier tube is converted into machine-readable form via an analogue-to-digital converter on the interface control card inserted into a second I/O slot in the Apple II. Absorbance changes are stored in memory for analysis at the end of the run. A trace of the absorbance changes is also obtained directly via a chart recorder.

The procedure for sample handling and data analysis is based on earlier work by Lindgren and co-workers.[9,10]

Sample Preparation

The density of a 2.0-ml aliquot of fasting plasma is increased to 1.216 kg l^{-1} by the addition[10] of 4.0 ml of a sodium bromide solution of density 1.31 kg l^{-1}. The preparation is subjected to ultracentrifugation in the Beckman 40.3 rotor for 30 h at 18 °C (40000 rev min^{-1}). One millilitre (containing total plasma lipoproteins) is harvested from the top of the tube into a graduated volumetric cylinder and used for analytical ultracentrifugation. Prior to analysis the sample is diluted with 1.20 kg l^{-1} sodium bromide solution so that during centrifugation the total absorbance at 280 nm does not exceed 1.0. An aliquot of the diluted sample is injected into the sample side of a double sectored cell of the Beckman AN-F rotor.

Ultracentrifugal Analysis

The PASCAL program controlling the L8 ultracentrifuge and the UV scanner was developed in conjunction with a commercial company and is available from Drew Scientific Ltd. The run is initiated following the entry of patient data and separation conditions and is fully automatic. The microcomputer activates the centrifuge and triggers the scanner after a defined centrifugal force has been applied to the sample. This procedure eliminates the approximations inherent in determining $\omega^2 t$ in manual analyses. Following the scan, the run ceases and the data, stored in digital form in the Apple II, are processed to produce the final output.

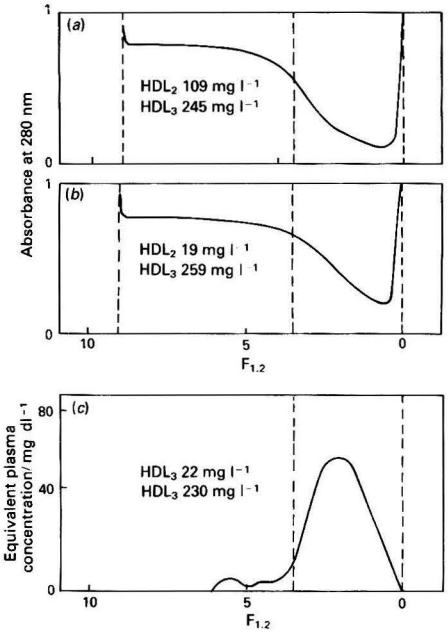

Fig. 6. (*a*) and (*b*) show typical absorbance profiles *vs.* flotation rate for subjects with high and low plasma HDL_2 concentrations. The absorbance change in the interval 0–3.5 represents HDL_3 in the sample while HDL_2 is located between the limits 3.5–9. $F_{1.2}$ represents the negative sedimentation coefficient (in Svedbergs) at a density of 1.20 kg l^{-1} and 26 °C. (*c*) Typical output from the microcomputer in which the corrected HDL subfraction concentrations are presented, together with a profile showing the concentration distribution across the flotation range

Data Handling

Typical HDL profiles obtained by the above procedure are shown in Fig. 6. During the centrifugation, flotation of the lipoprotein is monitored by the change in absorbance recorded in the analytical cell. Under the conditions specified above, HDL is buoyant and so the absorbance at the periphery of the cell decreases progressively and centripetally as the lipoproteins float in the gravitational field. The rate at which they move is a function of their density.

The absorbance profiles [Fig. 6(*a*) and (*b*)], converted into concentration units using specific molar aborptivities, are then corrected for the dependence of flotation on concentration and for the cell sector shape as described by Lindgren *et al.*[10] The sensitivity of the ultraviolet optics of the system allows the sample to be diluted to near standard conditions with $d = 1.20$ kg l^{-1} solution, so that no correction is required for this.

Following the above manipulations, HDL_2 and HDL_3 are quantified as the concentrations of lipoprotein present in flotation ($F_{1.2}$) intervals 3.5–9 and 0–3.5, respectively. $F_{1.2}$ is the negative sedimentation coefficient (in Svedbergs) of the lipoprotein at a solute density of 1.20 kg l^{-1} and 26 °C. The final data are presented as a profile of concentration as shown in Fig. 6(*c*) together with the summed concentrations for HDL_2 and HDL_3 in the original plasma sample.

Machine-controlled data capture and processing are achieved using a PASCAL program, which contains several segments as follows.

Segment 1. This regulates the speed of the ultracentrifuge and monitors the total centrifugal force applied to the sample as recorded on the $\omega^2 t$ indicator on the L8 control panel. Operator input to this segment includes ultracentrifuge speed and the $\omega^2 t$ value at which the scan is initiated.

Segment 2. At the selected ω^2t value, segment 2 sends control signals via the interface unit to the Beckman scanner, causing it to record the absorbance changes occurring in the cells of the analytical rotor. These, initially obtained as voltages, are converted into computer-compatible information that is stored in the memory of the Apple II. ω^2t values are recorded for each cell at the mid-point of its scan.

Segment 3. At the end of the run, the memory contains digitised voltages across the cell and the corresponding ω^2t value. Segment 3 of the program makes the necessary corrections for the cell sector shape and concentration dependence of flotation[10] and converts the raw data into lipoprotein concentrations using pre-determined specific molar absorptivities.

In a series of subjects studied by this system we compared the variation in total HDL cholesterol with changes observed in the HDL subfraction distribution. As we found with the rate zonal technique in the Ti 14 rotor,[6] HDL_2 mass correlated with the variation in HDL cholesterol ($r = 0.82$, $p < 0.0001$, $n = 42$) while the correlation with HDL_3 ($r = 0.36$, $p < 0.025$) was much poorer. By this procedure it is possible to analyse nine HDL samples in 8 h, in contrast to the 21 h required to examine one sample by the Ti 14 zonal system.

Annette Fox prepared the manuscript for publication. The work performed in our laboratory was facilitated by grants from the Scottish Home and Health Department (K/MRS/50/C429) and the Medical Research Council (G 8111558 SA).

References

1. Castelli, W. P., Gordon, T., Hjortland, M. C., Kannell, W. B., and Dawber, T. R., *Am. J. Med.*, 1977, **62**, 707.
2. Tall, A. R., and Small, D. M., *N. Engl. J. Med.*, 1978, **299**, 1232.
3. Havel, R. J., Eder, H. A., and Bragdon, J. H., *J. Clin. Invest.*, 1955, **34**, 1345.
4. Barclay, M., Barclay, R. K., and Skipski, U. P., *Nature (London)*, 1963, **200**, 362.
5. Anderson, D. W. *Lancet*, 1978, **1**, 819.
6. Shepherd, J., Packard, C. J., Stewart, J. M., Vallance, B. D., Lawrie, T. D. V., and Morgan, H. G., *Clin. Chim. Acta*, 1980, **101**, 57.
7. Kostner, G. M., *in* Day, C. E., *Editor*, "High Density Lipoproteins," Plenum Press, New York, 1982, p. 1.
8. Patsch, W., Schonfeld, G., Gotto, A. M., and Patsch, J. R., *J. Biol. Chem.*, 1980, **255**, 3178.
9. Ewing, A. M., Freeman, N. K., and Lindgren, F. T., *Adv. Lipid Res.*, 1965, **3**, 25.
10. Lindgren, F. T., and Jensen, L. C., *in* Nelson, G. J., *Editor*, "Blood Lipids and Lipoproteins: Quantitation, Composition and Metabolism," Wiley-Interscience, New York, 1972, p. 181.
11. Miller, N. E., Hammett, F., Saltissi, S., Rao, S., van Zeller, H., Coltart, J., and Lewis, B., *Br. Med. J.*, 1981, **282**, 1741.
12. Demacker, P. N., van Sommeren-Zondag, D. F., Stalenhoef, A. F., Stuyt, P. M., and van't Laar, A., *Clin. Chem.*, 1983, **29**, 656.
13. Anderson, D. W., Nichols, A. V., Pan, S. S., and Lindgren, F. T., *Atherosclerosis*, 1978, **29**, 161.
14. Patsch, J. R., Sailer, S., Kostner, G., Sandhofer, F., Holasek, A., and Braunsteiner, H., *J. Lipid Res.*, 1974, **15**, 356.
15. Kunitake, S. T., and Kane, J. P., *J. Lipid Res.*, 1982, **23**, 936.
16. Groot, P. H. E., Scheek, L. M., Havekes, L., van Noort, W. L., and van't Hooft, F. M., *J. Lipid Res.*, 1982, **24**, 1342.
17. Cheung, M. C., and Albers, J. J., *J. Lipid Res.*, 1979, **20**, 200.

Paper A3/182
Received June 22nd, 1983
Accepted July 26th, 1983

Mass Spectra of Disodium Pamoate and an Isomer by Electron, Chemical and Fast Atom Bombardment Ionisation

David V. Bowen and Linda A. Broad
Analytical Chemistry Department, Pfizer Central Research, Pfizer Limited, Sandwich, Kent, CT13 9NJ, UK

Timothy Norris
Chemical Process Improvement, Pfizer Limited, Sandwich, Kent, CT13 9NJ, UK

and Michael Barber, Robert S. Bordoli, Gerard J. Elliott, R. Donald Sedgwick and Andrew N. Tyler
University of Manchester Institute of Science and Technology, Manchester, M60 1QD, UK

The EI and CI spectra of these two isomeric salts contained few high mass peaks. The positive and negative FAB spectra showed $[M + H]^+$ and $[M - H]^-$ ions, respectively (where M is the disodium salt). Other strong peaks related to the structure were seen in the relative molecular mass region. The FAB spectra are useful for identifying these salts. For each ionisation technique there were differences between the spectra of the two isomers, but the major differences were observed in the EI and CI spectra. Either EI or CI spectra would be useful for differentiating these isomers.

Keywords: *Disodium pamoate; isomer differentiation; fast atom bombardment ionisation; chemical ionisation; electron ionisation*

In pharmaceutical analysis it is necessary to develop rapid methods for differentiating isomers and for obtaining information on the relative molecular masses and structures of salts. Salts of pamoic acid are used to reduce the solubility of pharmaceuticals such as vitamins or medicines intended for oral administration.[1-3] It is therefore important to be able to observe these salts and to confirm which isomer is present. We have studied the application of mass spectrometry to the analysis of the involatile sodium salts of pamoic acid [4,4'-methylenebis(3-hydroxy-2-naphthoic acid)], A, and of one of its isomers [5,5'-methylenebis(6-hydroxy-2-naphthoic acid)], B.

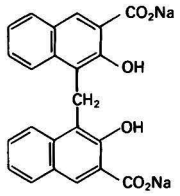

Relative molecular mass = 432

A

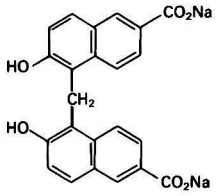

Relative molecular mass = 432

B

Mass spectra were obtained with electron ionisation (EI), chemical ionisation (CI) and fast atom bombardment (FAB) conditions to explore the applications and limitations of these ionisation techniques to the analysis of the isomeric disodium salts A and B. The EI and CI mass spectra of sodium salts are often uninformative. Fast atom bombardment mass spectra of sodium salts generally give strong $(M + Na)^+$ and $(M - Na)^-$ peaks.[4] Indeeed, FAB is applicable to a wide variety of involatile species,[5-7] but its utility for differentiating isomers has not been explored.

Experimental

EI and CI spectra were obtained on a VG 7070F double-focusing mass spectrometer. The electron energy was 75 eV for EI and 100–150 eV for CI experiments. The source temperature was approximately 250 °C and the ion accelerating voltage was 2 kV. For some EI experiments the sample was acidified by dissolving it in 6 N HCl - acetone solution. Samples for CI runs were deposited on to a VG DCI probe from methanol solution and either examined directly or first exposed to the vapours over a bottle of concentrated HCl. Methane was used as the CI reagent gas. EI and CI spectra were collected by a VG 2225 data system calibrated in the EI mode with PFK.

Most of the FAB spectra were obtained on an AEI MS902 mass spectrometer with the FAB source developed at UMIST. The argon atom beam was produced by a modified saddle field ion gun (Ion Tech Ltd., B11N) with a tube current of about 1.0 mA and a beam kinetic energy of 5 keV. The mass spectrometer was operated at an ion accelerating voltage of 8 kV. Samples were dissolved in glycerol and spotted on to the copper stage of the sample probe. Spectra were recorded on to chart paper and were counted and digitised by hand.

To test the reproducibility of the FAB data, a few FAB spectra were obtained with a VG ZAB-HF mass spectrometer at an 8-kV ion accelerating voltage. Xenon was used in the atom beam. Samples were dissolved in methanol and added to glycerol on the stainless-steel probe.

Results and Discussion

The EI and CI spectra of the disodium salts were of low intensity and had no relative molecular mass information. When the sodium salts were treated with hydrochloric acid the EI and CI spectra became stronger and the EI spectra contained a weak peak at *m/z* 388 corresponding to the diacid. Other peaks from the EI and CI spectra can be related to the structure; they are included in the spectra in Tables 1 and 2. The differences between the isomers are highlighted in Fig. 1.

The EI spectra of the two isomers have different base peaks: at *m/z* 170 for A and *m/z* 188 for B. The peak at *m/z* 170 is significantly more abundant for the isomer with the carboxyl and hydroxy groups in the *ortho* position (A). A similar relationship is observed between the peaks at *m/z* 184 and 202. These observations may be explained by a facile loss of water when the hydroxy and carboxyl group are *ortho* (reactions I and II). Loss of water could be more difficult when these groups are at opposite ends of the naphthalene ring.

Only a few fragments occurred above *m/z* 202 in the EI and CI spectra. Peaks were observed at *m/z* 325 and 281 for both isomers. Tentative structures for these ions involve elimination of water and formation of a six-membered ring, shown for the free acid of isomer A (reaction III).

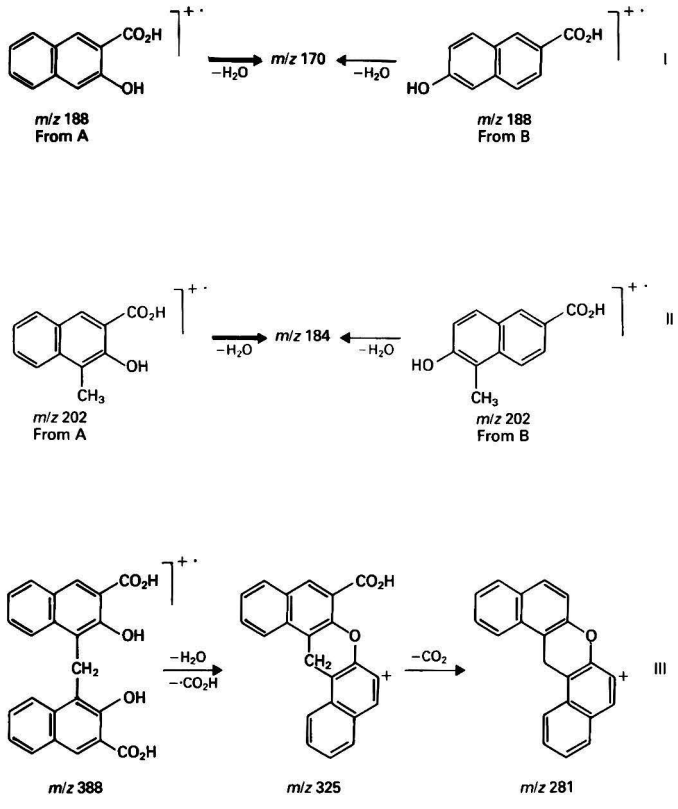

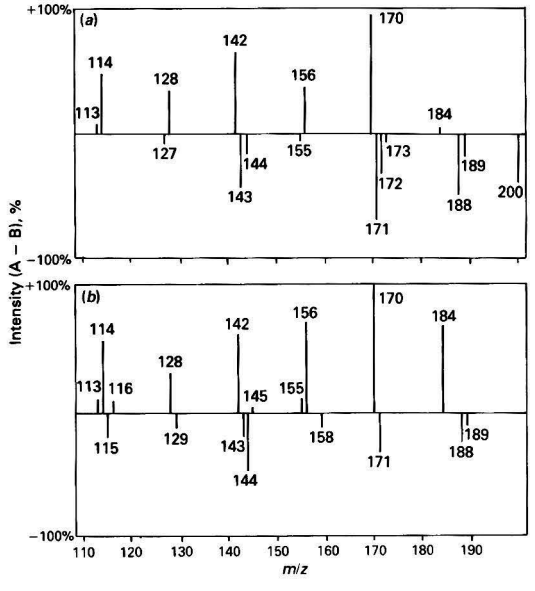

Fig. 1. (*a*) EI and (*b*) CI difference spectra; intensity for isomer A minus intensity for isomer B. Peaks are reported for intensity A − intensity B > 5%

The positive and negative FAB spectra (Table 3) of these disodium salts show peaks for $(M + H)^+$ and $(M - H)^-$, respectively. A number of strong peaks from the relative molecular mass region of these FAB spectra are listed in Table 4. In the positive spectra the most intense peak in this region is $(M + H)^+$, but in the negative spectra $(M - Na)^-$ dominates, presumably owing to the inherent stability of the carboxylate anion.

Differences between the isomers were less significant in the FAB spectra than in the EI or CI spectra. Further, information below *m/z* 200 was obscured in the FAB spectra by the background. One difference between the positive spectra of the isomers was the greater abundance at *m/z* 223 in A than in B. We cannot explain this, but it was reproducible.

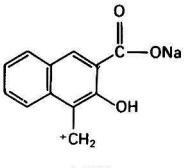

m/z 223

In conclusion, the FAB spectra showed molecular ion information and a number of strong peaks in the relative molecular mass region for the disodium salts, but any

Table 1. EI spectra of A and B. Peaks are reported whose relative intensities were above the following thresholds: *m/z* 700–280, threshold 0.1%; *m/z* 279–170, threshold 0.3%; *m/z* 169–140, threshold 0.5%; *m/z* 139–44, threshold 5%

Mass to charge ratio	Relative intensity		Mass to charge ratio	Relative intensity	
	A	B		A	B
388	0.3	0.1	155	23.2	28.0
370		0.2	154		0.6
369		0.3	145		0.9
327		0.1	144	2.5	10.2
326	0.6	0.9	143	10.0	53.8
325	0.7	1.4	142	74.9	
282		0.1	141	0.7	0.8
281	0.5	0.5	140		1.0
252	0.4	0.3	128	45.2	11.2
204		0.3	127	28.4	35.7
203	0.5	2.9	126	13.1	10.1
202	5.0	19.5	115	24.4	26.0
201	1.8	10.3	114	59.1	9.7
200	10.2	49.2	113	14.0	5.4
199		3.4	102	5.4	
191		0.3	101	6.5	5.8
190	0.8	2.0	89	6.5	7.7
189	5.8	17.7	88	9.9	
188	50.3	100.0	87	8.7	6.2
187	0.3	1.1	86	5.3	
186		0.5	85	8.1	
185	1.1	3.6	80		11.3
184	8.3	0.7	77	13.6	12.4
183	2.0	1.0	75	11.6	10.4
181		0.3	74	11.1	8.9
174		0.4	72		5.3
173	0.4	4.7	71	28.7	8.8
172	2.4	34.7	65		5.2
171	13.5	81.3	64	6.0	6.8
170	100.0	0.5	63	25.1	21.8
169	0.6		62	11.2	7.9
160		2.9	57	11.2	5.4
159	0.6	4.7	51	17.8	13.9
158	0.8	1.1	50	11.1	8.5
157	7.9	4.7	44		12.5
156	60.9	22.6			

Table 2. Methane CI spectra of A and B. Peaks are reported between *m/z* 700 and 44 whose relative intensities were greater than 1%

Mass to charge ratio	Relative intensity		Mass to charge ratio	Relative intensity	
	A	B		A	B
326	1.7	6.8	115	29.0	48.9
325	10.8	13.1	114	65.1	9.1
282		14.1	113	11.1	
281	6.5	7.9	102	10.6	
203	3.8		101	5.4	
202	40.9	57.4	92	1.6	
201		5.7	89	4.7	
189	4.2	13.5	88	8.6	
188	77.2	100.0	87	7.0	
185	15.0	19.1	86	9.4	
184	69.9		78	5.4	
171	24.3	57.6	77	4.8	
170	100.0		75	10.0	
158	6.0	17.7	74	6.9	
157	13.7	9.7	71	11.5	
156	72.2		64	5.0	
155	12.3		63	19.1	9.8
145	5.2		62	9.4	
144	41.7	89.1	61	3.6	49.9
143	12.7	32.3	60	8.1	
142	61.2		53	2.2	
141	2.7		51	22.0	
129	13.8	27.7	50	9.0	7.9
128	49.5	19.2	49	2.8	
127	20.0	17.2	45	15.2	17.4
126	8.7	12.0	44	24.3	49.4
116	9.3				

Table 3. Positive and negative FAB spectra of A and B. Peaks are reported whose intensities were above the following thresholds: positive FAB, isomers A and B, and negative FAB, isomers A and B; *m/z* 477–300, threshold 5% and *m/z* 299–200, threshold 7.5%

Mass to charge ratio	Positive FAB relative intensity		Mass to charge ratio	Negative FAB relative intensity	
	A	B		A	B
457	5.0		441	8.8	
456	13.3	6.4	433*	7.8	5.6
455	30.0	15.4	432	15.1	15.4
454		7.1	431	27.2	37.1
445	6.7		430		8.4
435*	12.8	11.5	419	5.6	
434	30.6	26.9	411*	14.2	17.5
433	63.9	66.7	410	38.6	39.9
432	23.9	20.5	409	100.0	78.3
415	8.3		408	15.9	30.8
413*	10.0	7.7	407	5.3	9.8
412	16.7	20.5	393	5.7	6.3
411	47.2	51.3	389*	6.0	11.2
410	19.4	11.5	388	13.9	12.6
395	5.6		387	47.2	36.4
393	7.2		386	17.9	9.8
391*	8.9	5.8	385	5.6	
390	7.2		367*		7.0
389	21.7	7.7	365	9.4	10.5
388	9.4		364	5.6	8.4
387	5.6		346	7.5	
371	5.0		343	10.6	5.6
369*	8.3		342		7.0
367	9.4	9.0	341	5.6	5.6
366		8.3	321	6.9	
365	5.0		320		7.0
347	8.9		319*	19.3	9.1
303	5.0		313	20.6	
299*	12.8	11.5	298		8.4
279	8.3		297*	16.1	38.5
277*	10.6	9.2	295		8.4
251		9.0	275*		55.2
247	13.9		267	12.1	
246	13.3		255		11.9
237	8.9		241	13.2	8.4
235	7.8		229		8.4
234	7.8		227*		21.7
233	50.0	50.0	213		9.8
229*	20.6	57.7	211		9.1
225	34.4	12.2	209	37.6	32.9
224	75.6	23.1	207		9.8
223	100.0	31.4	206		25.2
222	8.3		205	13.0	100.0
219		10.3	203		29.7
212	11.1	9.0	202		14.7
211	51.7	54.5	201	11.6	28.0
210	73.3	22.4	200	39.2	59.4
209		16.0			
208		15.4			
207*	38.9	100.0			
205	7.8	15.4			
202	8.9				
201	40.6				

* Peaks are probably due to glycerol or glycerol - sodium clusters.

differences between the isomers were small and the spectra below *m/z* 200 were uninterpretable. Molecular ion information for the salts could not be obtained from the EI or the CI spectra; however, these spectra showed clear differences between the isomers. The ionisation methods thus provide complementary information; together they allow rapid identification of these isomeric sodium salts.

Table 4. Fast atom bombardment spectra. Assignment of peaks in the relative molecular mass region

Positive FAB spectrum—

Mass to charge ratio	Assignment	Intensity relative to m/z 433 = 100 A	B
455	$(M + Na)^+$	47.0	23.1
433	$(M + H)^+$	100.0	100.0
411	$(M - Na + 2H)^+$	73.9	76.9
389	$(M - 2Na + 3H)^+$	33.9	11.5
367	$(M - Na - CO_2 + 2H)^+$	14.8	13.5

Negative FAB spectrum—

Mass to charge ratio	Assignment	Intensity relative to m/z 409 = 100 A	B
453	$(M + Na - 2H)^-$		4.5
431	$(M - H)^-$	27.2	47.3
409	$(M - Na)^-$	100.0	100.0
387	$(M - 2Na + H)^-$	47.2	46.4
365	$(M - Na - CO_2)^-$	9.4	13.4

The authors are grateful to M-Scan Ltd. for some of the FAB data and to Mrs. G. Banning for preparation of the manuscript and drawings.

References

1. Puetzer, B., *US Pat.*, 2 397 903, 1946; *Chem. Abstr.*, 1946, **40**, 3858(4).
2. Huber, W., and Boehme, W. R., *US Pat.*, 2 460 009, 1949; *Chem. Abstr.*, 1949, **43**, 4433e.
3. Barber, H. J., and Gaimster, K., *J. Appl. Chem.*, 1952, **2**, 565.
4. Monaghan, J. J., Barber, M., Bordoli, R. S., Sedgwick, R. D., and Tyler, A. N., *Org. Mass. Spectrom.*, 1982, **17**, 529.
5. Barber, M., Bordoli, R. S., Sedgwick, R. D., and Tyler, A. N., *J. Chem. Soc., Chem. Commun.*, 1982, 325.
6. Barber, M., Bordoli, R. S., Sedgwick, R. D., and Tyler, A. N., *Nature (London)*, 1981, **293**, 270.
7. Barber, M., Bordoli, R. S., Elliott, G. J., Sedgwick, R. D., and Tyler, A. N., *Anal. Chem.*, 1982, **54**, 645A.

Paper A3/335
Received September 28th, 1983
Accepted November 3rd, 1983

Simultaneous *In Vivo* Measurement of Total Body Nitrogen by Neutron-activation Analysis and of Protein Turnover in Humans and Animals

Thomas Preston, Ian Robertson and Brian W. East
Scottish Universities Research and Reactor Centre, East Kilbride, Glasgow, G75 0QU, UK

A knowledge of body protein content and turnover obtained by non-destructive analysis is of great value in many areas of clinical science and agriculture, concerned for example, with nutrition, growth and development. Measurement of nitrogen can be used as an indicator of protein and we describe what we believe to be some of the first simultaneous *in vivo* measurements of total body nitrogen and protein turnover in individuals and demonstrate that our techniques are suitable for sequential studies both in humans and animals as small as juvenile rats. *In vivo* neutron-activation analysis is used for total body nitrogen while mass-spectrometric measurement with a ^{15}N-labelled amino acid tracer is used for protein turnover. Neutron activation is compared with a chemical method in animal carcasses.

Keywords: *Body nitrogen; protein turnover; neutron-activation analysis; ^{15}N-labelled amino acid tracer; in vivo measurement*

Total body protein content and protein turnover are two important parameters that can be assessed by nitrogen measurements. Body protein can be obtained by *in vivo* neutron-activation analysis of nitrogen, which has found increasing application in a range of clinical and nutritional problems in humans.[1] Protein turnover can be measured by following the proportion of an oral dose of a ^{15}N-labelled amino acid tracer, which is excreted in the urine, by isotope-ratio mass spectrometry.[2] Independently, each of these non-destructive methods provides much valuable information about protein in living subjects. However, serial total body nitrogen (TBN) measurements can potentially overcome errors associated with nitrogen balance methods, which constitute a necessary part of protein turnover interpretation. A simultaneous measurement of TBN can provide a reference for nitrogen turnover in preference to normalisation against body mass and enable fractional turnover rates to be calculated. Conversely, a parallel ^{15}N turnover study can demonstrate that a changed TBN content is the result of a change in protein synthesis rate, protein breakdown rate or a combination of the two.

Body composition is studied at East Kilbride using total body neutron-activation analysis[3] and of the elements determined, nitrogen can be measured with good reproducibility (2%). The method has also been adapted to rats and the results are of similar precision.[4] Protein turnover measurements using ^{15}N-labelled glycine have been recently commenced, enabling what we believe to be some of the first simultaneous measurements of these two quantities to be made in individuals. As these analyses are non-destructive, they can be used sequentially to monitor changes *in vivo*. Our aim is to examine the interrelations between protein content and turnover and explore the usefulness of such parallel measurements in man and animals. In this report details of the analytical procedures are described, together with initial results of an experiment to measure both protein turnover and total body protein simultaneously in humans.

Experimental

Total Body Nitrogen (TBN)

Total body nitrogen was measured by *in vivo* neutron-activation analysis. Neutrons were obtained from two sealed-tube (deuterium - tritium) 14-MeV generators mounted above and below the subject. The nuclear reaction $^{14}N(n, 2n)^{13}N$ was induced and the radioactive product isotope ^{13}N ($t_{\frac{1}{2}}$ = 9.97 min) was subsequently measured in a two 29 × 10 cm NaI(Tl) detector shadow-shield whole-body counter[5] by means of its 0.51-MeV gamma-ray positron annihilation radiation. Nitrogen content (g of TBN) was calculated by calibration with man- and animal-like phantoms containing known masses of the element. Corrections were applied for interference from oxygen, which also gave rise to ^{13}N via the $^{16}O(p, \alpha)^{13}N$ recoil proton reaction, and other minor interfering activities.[3]

For human TBN measurement, the subject lay supine on a motorised couch and was scanned lengthwise between the two 14-MeV neutron generators to give a simultaneous anterior - posterior irradiation. The radiation dose equivalent was 1 mSv* (0.1 rem). At the end of the irradiation the subject was transferred to the whole body counter, where counting was carried out by a similar scanning procedure.

The live rat or rat carcass was contained in a ventilated polythene tube surrounded by a 12 cm thick annular neutron premoderator, and irradiated bilaterally in two static steps each of 300 s. Total neutron dose equivalent at the surface of the animal was 116 mSv (11.6 rem). After irradiation, the total body radioactivity was determined by counting the animal static (still in the polythene tube but removed from the premoderator assembly) between the two detectors of the whole-body counter, with the lower detector raised to increase sensitivity. TBN was calculated from the corrected 0.51-MeV gamma-ray photopeak activity compared with rat phantom calibrations.

After determination of TBN the rat carcasses were freeze dried to constant mass and their total body water (TBW) was recorded. The dried residues were powdered and the nitrogen contents of replicate sub-samples were determined by Kjeldahl digestion, followed by distillation and filtration of the ammonium formed.

Whole Body Protein Turnover

Human studies

A urinary plateau labelling technique was used to measure the body protein turnover in the subjects studied.[6] The proportion of a continuously supplied amino acid tracer (frequently ^{15}N glycine) that is excreted and therefore not used for protein synthesis, is measured by isotope analysis of urinary urea after a steady state has been reached.

Two healthy adult males of approximately 80 kg body mass and receiving normal diets (about 1.2 g of protein kg^{-1} body mass d^{-1} and about 200 kJ kg^{-1} d^{-1}) volunteered for protein turnover measurement. Dietary intake was calculated from standard tables, and total nitrogen in the excreta measured by

* Sv = sievert.

Kjeldahl digestion, over a 3-d measurement period. Multiple oral doses of ^{15}N-labelled glycine (about 10 μg of ^{15}N kg^{-1} body mass h^{-1}) were administered in drinks every 3 h in one instance and every 4 h in the other, for 60 h. Urine samples were analysed over the same period.

The tracer "bolus" method[7] provides a second approach to protein turnover measurements, which is perhaps simpler to use clinically. The cumulative excretion of a single dose of isotope is followed. The isotope enrichment (or specific activity) is measured in urinary ammonia or urea and compared with that of the source material, as in the method described.

The same two male subjects were studied using the tracer "bolus" method, some months after the previous study. Dietary intake and excreted nitrogen were measured as above. A single oral dose of ^{15}N-labelled glycine (about 100 μg of ^{15}N kg^{-1} body mass) was administered during the main meal of the day. The excreted isotope was traced in urea, ammonium and total urinary nitrogen in pooled 8-h urine samples.

Small animal studies

The same methods for protein turnover measurement as used in human studies can be applied to metabolic studies with small animals. It is necessary to confine the animals in metabolism cages to allow accurate control of dietary nitrogen and collection of excreta for isotope analysis and nitrogen balance measurement if TBN facilities are not available. For animals undergoing continuous infusion, the two experimental approaches are equally convenient. For those animals on a solid diet it is more convenient to adopt the "bolus" approach, especially when using an amino acid tracer. Problems of food spillage into the excreta collection system of metabolism cages can cause contamination. A labelled protein source can minimise this danger and allow continuous administration if homogeneity is ensured. "Bolus" methods allow parenteral injection of the tracer, avoiding the problems of contamination. Metabolism cages allow careful control of protein intake and therefore assessment of the effects of different feeding regimes.

Whole-body protein turnover was measured in four rats [about one week post-weaning (60 g)] which were fed a caesin-based diet *ad libitum*. Two rats received a 23% protein diet, the other two received a 7% protein diet. The cumulative excretion of ^{15}N in urinary ammonium, urea and total nitrogen from a single parenteral injection of labelled glycine was analysed. Rates of protein turnover were calculated and compared for each of these end-products and the two diet regimes. After 36 h equilibration and familiarisation time in individual metabolism cages, a single parenteral injection of about 1 mg of ^{15}N glycine was given. Urinary ammonium, urea, total nitrogen and total faecal nitrogen and their ^{15}N enrichment were measured in pooled 24-h urine samples for 2 d. Base line ^{15}N enrichment was measured during the 24 h before isotope addition. Dietary intake was measured by loss of mass from a pre-weighed food beaker. Protein turnover was calculated as in the human studies.[7]

^{15}N Analysis

Urinary ammonium was determined by distillation and urea by enzymatic hydrolysis and distillation after removal of ammonium. Total nitrogen was determined by distillation of a Kjeldahl digest. After titration of the ammonium formed to quantify the sample nitrogen concentration, samples were acidified and concentrated in reaction vessels at 95 °C for isotope analysis. ^{15}N was determined on a VG Micromass 602B isotope-ratio mass spectrometer after liberation of sample nitrogen by lithium hypobromite.[8] This latter step was carried out using the apparatus in Fig. 1. In order to obtain maximum sensitivity and minimise leakages from the atmosphere, the small reaction vessel in Fig. 1(*a*), consisting of a

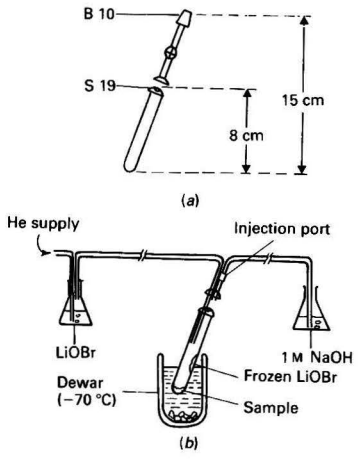

Fig. 1. (*a*) Nitrogen gas reaction vessel and (*b*) handling arrangements for mass-spectrometric analysis

Pyrex ball-joint, sealed to form a 5-ml tube approximately 8 cm long, was used. This could be attached to a remote vacuum line or mass spectrometer inlet via a conical connector and isolated by the stopcock. Volumes were kept as small as was practicable. A sample of approximately 3.5 mg of nitrogen was dried in this reaction vessel and cooled in dry ice - acetone, as shown in Fig. 1(*b*), with the helium sparging system attached. Helium de-gassed lithium hypobromite solution was injected through the port and frozen above the sample, care being taken to avoid reagent contact until the reaction vessel had been evacuated and isolated. This was then warmed in order to mix the reagents and frozen again after reaction. The sample nitrogen was admitted to the mass spectrometer for isotope-ratio analysis via a liquid nitrogen cold-trap.

Results and Discussion

Rat TBN

The accuracy of body protein determination in rats was investigated by measuring a series of rat carcasses ranging from juveniles to adults. Results using neutron-activation analysis were compared with results using total nitrogen analysis obtained by Kjeldahl digestion with excellent agreement. A linear relationship (0.985:1) was obtained (correlation coefficient = 0.999 6) with nitrogen contents ranging from 27.8 to 33.2 g kg^{-1}. This range reflected differences in the body composition of the animals, which varied from juveniles to obese adults and lean adults, respectively. The excellent agreement obtained emphasised the effectiveness of neutron-activation analysis for the accurate measurement of nitrogen, despite variations in body fat. The reproducibility was determined by the analysis of replicates and the coefficient of variation varied from 0.9% for large adults to 2.7% for juveniles. This was superior to the chemical method, which gave a mean coefficient of variation of 2.8%.

The effect of repeated irradiations on the growth of young rats was examined by comparing three groups of four animals. The first was irradiated sequentially on four occasions within 2 weeks; the second was handled as if for irradiation but was not actually irradiated and the third remained in the animal quarters. Over a subsequent period of 150 d, no significant differences in the growth rates of the 3 groups of animals, as indicated by body mass, were observed. The precision of the analysis was found to be such that daily TBN increases in young growing animals were measurable.

Table 1. Human protein turnover

Subject	Mass/kg	Intake/mg of N kg^{-1} h^{-1}	Protein synthesis (s.d.)*/mg of N kg^{-1} h^{-1}	Protein turnover (s.d.)*/mg of N kg^{-1} h^{-1}
1	75.1	9.20	14.65 (1.07)	23.80 (1.70)
2	82.2	7.13	14.99 (0.45)	22.10 (0.70)

* S.d. = standard deviation.

Table 2. Human fraction protein turnover rate

Subject	Total body nitrogen/kg	Fractional turnover rate (s.d.)/g of N per 100 g of TBN d^{-1}
1	2.056	2.09 (0.15)
2	2.114	2.06 (0.07)

Protein Turnover Studies

Tables 1 and 2 show the results of protein turnover measurements on two adult males. Similar protein turnover rates, with a mean of 22.95 mg of N kg^{-1} h^{-1}, were found for both subjects (Table 1) by the analysis of the plateau formed in urinary ^{15}N. Table 2 shows that the two subjects had similar TBN and that the fractional protein turnover rate was approximately 2% d^{-1} in both instances. The ability to measure TBN with a reduced neutron radiation dose (1.0 mSv) over that normally necessary (10 mSv) when determining the additional elements Na, P, Cl and Ca was also demonstrated.

The results of the protein turnover studies comparing different end-products and the comparison with the "bolus" approach will be presented elsewhere, as will the results from the rat protein intake and protein turnover study.

Conclusions

Procedures for the simultaneous measurement of protein and protein turnover in humans and rats have been devised. If a measurement of TBN only is desired in humans, then the neutron radiation dose can be reduced (to 1.0 mSv giving a ±4.0% counting error) from that normally used for a more complete elemental analysis. Serial *in vivo* TBN measurements could be of great value to many areas of clinical science and allow assessment of the efficacy of treatment. An accurate *in vivo* measurement of the lean body mass consisting of mineral and protein components could facilitate determination of body fat reserves in energy balance and nutritional studies. Serial TBN measurements could, in some instances, overcome the difficulties of the classical nitrogen balance experiment enabling protein turnover data to be better interpreted. These latter data are readily obtained by a urinary ^{15}N plateau technique in combination with the total body measurements.

The sequential activation analysis of growing rats, which require a radiation dose of 12 mSv in our system to obtain adequate accuracy, is possible without observable effects on growth and development. Daily changes in TBN could be monitored, which, in combination with protein turnover studies carried out in metabolism cages, would provide comprehensive data of good precision. The sensitivity of the mass-spectrometric procedure is adequate to make the analysis of urine from typical metabolic cage collections entirely feasible. Finally, the ability to study growing animals effectively would, in so far as these results suggest, avoid difficulties in studying TBN in human growth where ethical considerations preclude the use of activation analysis in children.

We acknowledge the financial support of the Medical and Agricultural Research Councils, the help of Dr. P. J. Reeds of the Rowett Research Institute and the support of the Director of the Reactor Centre, Professor H. W. Wilson, all of whom enabled this work to be carried out.

References

1. Cohn, S. H., *At. Energy Rev.* 1980, **18**, 599.
2. Halliday, D., and Lockhart, I. M., *Prog. Med. Chem.*, 1978, **15**, 1.
3. Williams, E. D., Boddy, K., Harvey, I., and Haywood, J. K., *Phys. Med. Biol.*, 1978, **23**, 405.
4. Brown, W. B., East, B. W., McAreavey, D., Robertson, J. I. S., and Shackleton, D. R., *Proc. Physiol. Soc.*, 1982, 85.
5. Boddy, K., Elliott, A., Robertson, I., Mahaffy, M. E., and Holloway, I., *Phys. Med. Biol.*, 1975, **20**, 296.
6. Picon, D., and Taylor-Roberts, T., *Clin. Sci.*, 1969, **36**, 283.
7. Waterlow, J. C., Golden, M. H. N., and Garlick, P. J., *Am. J. Physiol.*, 1978, **235**, E165.
8. Ross, P. J., and Martin, A. E., *Analyst*, 1970, **95**, 817.

Paper A3/336
Received September 26th, 1983
Accepted October 3rd, 1983

Rapid Determination of Halogens in Blood Serum by Instrumental Neutron-activation Analysis

Nathan Lavi
Soreq Nuclear Research Centre, Yavne, Israel
Zeev B. Alfassi
Department of Nuclear Engineering, Ben Gurion University of the Negev, Beer-Sheva, Israel

The absolute concentrations of bromine and iodine in blood serum have been determined by epithermal neutron activation followed by high-resolution gamma and X-ray spectrometry. The concentrations of bromine and iodine were found to be 6.66 ± 0.21 μg ml^{-1} and 88.8 ± 4.0 ng ml^{-1}, respectively, and the detection limits were 37 and 15 ng ml^{-1}, respectively. These methods were compared with thermal neutron activation of bromine, a long delay being required for gamma-ray spectrometry and the use of a magnet for X-ray measurements. For iodine a preliminary chemical separation is imperative.

Keywords: *Halogen determination; blood serum; instrumental neutron activation analysis*

Much research has been undertaken on the concentrations of halogens in biological tissues and organs. The halogens play important roles in metabolism and ion transport and the accurate and precise determination of the halogens in tissues is essential for the description of mineral metabolism. Such determinations could eventually be used for diagnostic purposes. The aim of this investigation was to develop a method for the determination of halogens by instrumental neutron-activation analysis and to determine the detection limits. It is very simple to determine chlorine by measuring ^{38}Cl because of the high concentration of chlorine in biological tissues and because of the high-energy gamma rays of ^{38}Cl, which are only slightly obscured by the Compton radiation of other radionuclides.

The neutron activation of bromine, which has two natural isotopes, ^{79}Br and ^{81}Br, at about the same abundance, produces the four radionuclides given in Table 1. Of these isotopes, ^{80}Br^{m} and ^{82}Br^{m} cannot be detected by gamma spectroscopy owing to the low energy or low yields of the photons. Most previous workers measured the long-lived ^{82}Br after long decay,[1-5] as the short-lived ^{80}Br could not be detected after a short irradiation followed by a short decay[6,7] owing to the interference of the Compton radiation from the more abundant ^{38}Cl and ^{24}Na. The sodium ions can be removed by chemical separation, for example, by extraction with hydrated antimony(V) oxide. Alternatively, bromine can be oxidised and extracted with organic solvents. However, these are destructive methods. The measurement of bromine via ^{82}Br after long decay has the drawback of requiring long irradiation and counting times for each sample, so that results can be obtained only after 1–2 weeks. The situation is worse with iodine, where only the short-lived ^{128}I (25 min) is produced, which is completely masked by the Compton radiation from the more abundant radionuclides. Various determinations of iodine in biological tissues by neutron activation analysis followed by different separation schemes have been described.[8-14]

One way of overcoming the problem of interferences from other emitted gamma rays is to measure the emission of X-rays due to electron capture or internal conversion processes. The main advantage of X-ray spectrometry is that many elements do not emit X-rays, thereby reducing the background; this is in addition to the small number of lines in the characteristic X-ray spectrum of each element and the direct correlation between the element and the energies of its X-rays. Shenberg *et al.*[15] were the first to recommend X-ray spectrometry for the non-destructive determination of bromine. Rapaport *et al.*[16] determined the bromine content of blood serum by neutron activation analysis followed by X-ray spectrometry, reducing the background due to β-electrons by a magnetic field.[17,18] Mantel and Amiel[19] measured the sensitivities of various elements to neutron activation followed by X-ray spectrometry and found that the sensitivity of bromine was 100 times greater than that of iodine.

The more abundant elements in biological tissues, Cl and Na, interfere in the measurement of Br and I by both gamma and X-ray spectrometry. An effective way of eliminating these interferences is the use of epithermal neutron activation, which is advantageous when the desired element has a nuclide with a high I/σ_0 ratio (resonance activation integral/thermal neutron cross-section) while the major interfering activities in the sample have lower ratios. This applies to Br and I in a biological matrix, as Br and I have ratios of 16.6 and 24.2, respectively, whereas the ratios for Cl and Na are 0.39 and 0.58, respectively.[20] If a sample is irradiated within a suitable cadmium cover, the thermal neutrons are excluded and only neutrons with energies higher than about 0.4 eV will contribute to the activation process. Chultem *et al.*[21] used a special fast reactor developed for neutron spectroscopy purposes to determine the iodine content in various biological samples. Brune and Wester[22] used epithermal activation for the thyroid gland, where the iodine content is much higher than in other biological samples.

Table 1. Radionuclides produced by neutron activation of natural bromine

Radionuclide	Half-life	Cross-section for formation/b	Main γ lines/keV
^{80}Br	17.6 min	8.4	618 (7%), 666 (1%)
^{80}Br^{m}	4.4 h	2.6	37 (36%)
^{82}Br^{m}	6.2 min	2.7	46 (0.3%), 777 (0.15%)
^{82}Br	35.5 h	3.0	554 (66%), 619 (41%)

Experimental

Blood serum was prepared by centrifugation of blood samples of healthy donors. A 0.2-ml volume of the serum was transferred by a micropipette on to a very thin Mylar sheet (0.006 mm) and left to dry in a vacuum desiccator containing P_2O_5 until completely dry. The samples were then covered with another piece of Mylar sheet and introduced into a polyethylene bag, which was heat-sealed. Standards of bromine and iodine were prepared in the same way using dilute solutions of NH_4Br and KI, respectively.

The samples were irradiated in the pneumatic tube of the IRR-1 reactor for 20 s–20 min. For irradiation with epithermal neutrons, the polyethylene bag was inserted into a 0.5 mm

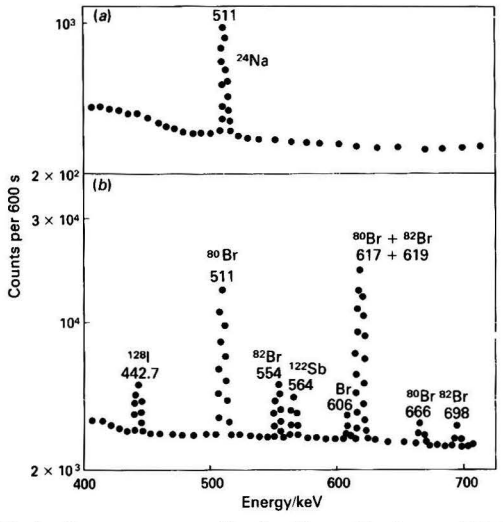

Fig. 1. Gamma-ray spectra of irradiated human blood serum. (*a*) 0.2 ml irradiated without Cd for 20 s and counted for 200 s after a cooling time of 15 min; and (*b*) 5 ml irradiated under Cd for 10 min and counted for 5 min after a cooling time of 30 min

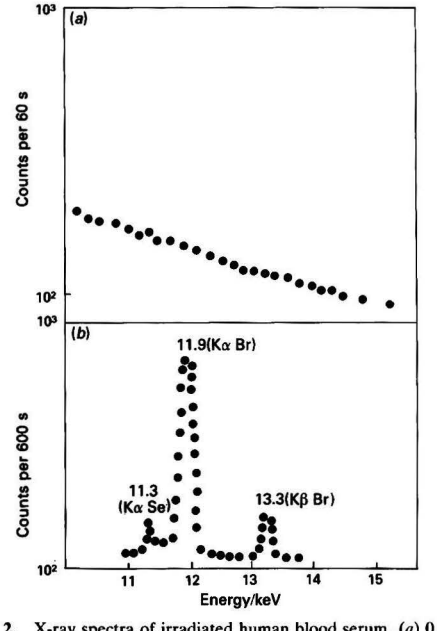

Fig. 2. X-ray spectra of irradiated human blood serum. (*a*) 0.2 ml irradiated for 1 min without Cd and counted for 100 s after a cooling time of 10 min; and (*b*) 5 ml irradiated under Cd for 10 min and counted for 5 min after a cooling time of 10 min

thick cadmium box. After irradiation the samples were removed from the plastic bag and measured directly.

The gamma rays of the activated samples were measured with a calibrated 100-cm³ Ge(Li) detector connected to a Canberra 30 multi-channel analyser. The energy resolution (FWHM) of the system was 2.5 keV for 1332-keV ^{60}Co. The samples were counted for 60–900 s after the 5–10 min necessary for the transfer of the irradiated sample to the counting room. The X-ray spectra of the activated samples

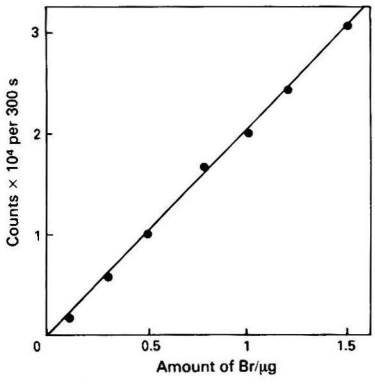

Fig. 3. Intensity of ^{80}Br gamma-ray peak (617 keV) as a function of the amount of Br in the 0.1–1.5 μg range

Table 2. Determination of iodine in human blood serum by epithermal neutron activation followed by measurement of 442.7 keV γ-rays

Sample No.	[I]/ng ml⁻¹
1	89.28
2	83.32
3	91.79
4	86.43
5	93.21
Average	88.8 ± 4.0

Table 3. Determination of bromine in human blood serum by epithermal neutron activation followed by gamma-ray (618 keV ^{80}Br) and X-ray spectrometry (Kα + Kβ of Br)

Gamma-ray spectrometry		X-ray spectrometry	
Sample No.	[Br]/μg ml⁻¹	Sample No.	[Br]/μg ml⁻¹
1	6.45	1	6.40
2	6.40	2	6.51
3	6.85	3	6.86
4	6.96	4	6.80
5	6.70	5	6.90
6	6.60	6	6.80
7	6.80	Average	6.71 ± 0.20
8	6.40		
9	6.83		
Average	6.66 ± 0.21		

were measured with an Si(Li) detector of 100 mm² area, 4 mm depth and resolution (FWHM) of 320 eV for 6.4-keV Fe K X-rays. A 1.5-mm plastic absorber was used to reduce interference from β-decay electrons for both gamma and X-ray measurements.

Results and Discussion

Fig. 1 shows the spectra obtained from the blood serum, irradiated with a Cd cover (epithermal neutrons) and without a Cd cover (reactor neutrons), in the range 400–700 keV. As can be seen in Fig. 1(*a*), the Compton radiation of ^{24}Na covers all the peaks of iodine and bromine when using reactor neutrons. Fig. 1(*b*) shows that when using only epithermal neutrons, both iodine and bromine are seen very clearly. Fig. 2 shows the X-ray spectrum measured after irradiation with reactor neutrons (*a*) and with epithermal neutrons (*b*). For reactor neutrons, the peaks of Br are masked by the activities of ^{24}Na and ^{38}Cl electrons. It is possible to remove this interference by magnets.[13] However, Fig. 2(*b*) shows that using epithermal neutrons, bromine (Kα and Kβ of Br) can be determined easily.

Fig. 3 shows a calibration graph for 0.1–1.5 μg of bromine, irradiated with epithermal neutrons, showing that the 617-keV activity varies linearly with the amount of bromine. The sensitivity obtained from this graph is 19931 ± 150 counts μg^{-1} Br (20-min irradiation, 5-min cooling and 15-min counting). An almost identical line is obtained for the Kα + Kβ X-rays, where the sensitivity is 20432 ± 180 counts μg^{-1} Br. When counting without the 1.5-mm absorber the sensitivity increases to 39940 ± 350 counts μg^{-1} Br. However, the net peak to background ratio is worse.

The sensitivity obtained for iodine was[23] 30834 ± 181 counts μg^{-1} I (10-min irradiation, 10-min cooling and 15-min counting). Table 2 gives the amounts of iodine detected in five different samples of blood serum using a calibration graph, which is linear in the range 0–1.0 μg of iodine. The average value found, 88.8 ± 4.0 ng ml^{-1}, is in good agreement with published data.[24] Table 3 gives the amount of bromine measured by gamma and X-ray spectrometry. The average value, 6.66 ± 0.21 μg ml^{-1}, is in good agreement with the published data.[16,24–26]

Detection Limits of Bromine and Iodine

The detection limit of a radionuclide is usually defined as the smallest photopeak that can be detected with certain confidence above the background continuum. Currie[27] showed that the detection limit (L_D) for the radioactivity is given by the equation

$$L_D \text{ (counts)} = 2.71 + 4.65\sqrt{\mu_B}$$

where μ_B is the true mean of the blank. The minimum detected mass, M_D, is given by $M_D = L_D/K$, where K is the sensitivity factor (counts mg^{-1}).

For a 0.2-ml sample irradiated for 20 min and counted for 5 min after a decay time of 5 min, the detection limits for the determination of Br by gamma and X-ray spectrometry are 37 and 46 ng ml^{-1}, respectively. For iodine, the detection limit was found to be 15 ng ml^{-1} using 10-min radiation, 10-min cooling and 15-min counting.

As gamma measurement has a lower detection limit and X-ray measurement has the drawback of self-absorption, it is clear that for epithermal neutron activation it is preferable to use gamma-ray spectrometry.

Another means of obtaining a simple X-ray spectrum is by irradiation with thermal neutrons, using a magnet to remove the β-ray interferences.[16–18,28] This method has the advantage of using the higher flux thermal neutrons, but it suffers from the disadvantage of counting far from the detector surface because of the magnet. When using epithermal neutrons, we were able to count on the detector surface (with a plastic absorber of thickness 1.5 mm) for both X-rays and gamma rays, reducing the detection limit considerably, whereas Rapaport *et al.*[16] had to measure the X-ray spectra 2.7 cm from the detector in order to allow the magnetic field to remove the β^- particles.

Rapaport *et al.*[16] reported an average value of 2600 counts per sample. Their figure shows that the background of the blood sample was about the same as the net counts, leading to a ratio of about 12 between the measured amount and the limit of detection. As their concentration was 7.4 μg ml^{-1}, this leads to a detection limit of 600 ng ml^{-1}, much worse than in our method. This detection limit can be lowered by increasing the volume of sample. However, increasing the volume by a factor of 10, to 0.5 ml, will lower the detection limit by a factor of only $\sqrt{10}$. This, combined with the disadvantage in X-ray spectrometry of self-attenuation of X-rays, shows clearly that it is preferable to measure bromine and iodine concentrations by epithermal neutron activation followed by gamma-ray spectrometry.

When the concentration of bromine is too low to be detected by this method, the use of longer irradiation with thermal neutrons followed by a long decay and a long counting time can permit the measurement of the bromine content, using ^{82}Br. However, long irradiation and counting times are inconvenient for routine measurement.

To summarise, the use of epithermal neutron activation facilitates the determination of iodine and bromine in biological samples without any preliminary chemical separation.

References

1. Stella, R., Genova, N., and Di Casa, M., *Radiochem. Radioanal. Lett.*, 1977, **30**, 65.
2. Behne, D., and Diel, F., "Nuclear Activation Techniques in the Life Sciences," IAEA-SM-157, International Atomic Energy Agency, Vienna, 1972, p. 41.
3. Behne, D., and Jurgensen, H., *J. Radioanal. Chem.*, 1978, **42**, 447.
4. Leonhardt, W., *Kernenergie*, 1961, **4**, 395.
5. Sklavenitis, M., and Comar, D., "Nuclear Activation Techniques in the Life Sciences," International Atomic Energy Agency, Vienna, 1963, p. 445.
6. Guzzi, G., Pietra, R., and Sabioni, E., EUR 5282e, 1974.
7. Spyrou, N. M., Fricker, M. E., Robertson, R., and Gilboy, W. B., "Symposium on Nuclear Techniques in Comparative Studies of Food and Environmental Contamination," IAEA-SM-175, International Atomic Energy Agency, Vienna, 1973, p. 20.
8. Comar, D., and Le Poec, C., "Modern Trends in Activation Analysis," Texas A and M University, College Station, 1965, p. 351.
9. Malvono, R., Buzzigoli, G., and Scarlattini, M., *Anal. Chim. Acta*, 1972, **61**, 201.
10. Rook, H. L., *J. Radioanal. Chem.*, 1977, **39**, 351.
11. Gvardjancic, L., Kosta L., and Dermely, M., *J. Radioanal. Chem.*, 1980, **58**, 359.
12. Comar, D., "L'Analyse par Radioactivation et les Applications aux Sciences Biologiques," Presses Univ. France, Paris, 1964, p. 307.
13. Malvano, R., and Grosso, P., *J. Nucl. Biol. Med.*, 1968, **12**, 86.
14. Sato, T., and Kato, M., *J. Radioanal. Chem.*, 1982, **68**, 175.
15. Shenberg, C., Gilat, J., and Finston, L. H., *Anal. Chem.*, 1967, **39**, 780.
16. Rapaport, M. S., Mantel, M., and Nothmann, R., *Anal. Chem.*, 1979, **51**, 1356.
17. Amiel, S., Mantel, M., and Alfassi, Z. B., *J. Radioanal. Chem.*, 1977, **37**, 189.
18. Mantel, M., Alfassi, Z. B., and Amiel, S., *Anal. Chem.*, 1978, **50**, 441.
19. Mantel, M., and Amiel, S., *Anal. Chem.*, 1972, **44**, 548.
20. "Handbook on Nuclear Activation Cross-Sections," Technical Report No. 156, International Atomic Energy Agency, Vienna, 1974.
21. Chultem, D., Ganzorig, Dz., and Gun-Aujav, T., *J. Radioanal. Chem.*, 1979, **50**, 195.
22. Brune, D., and Wester, P. O., *Anal. Chim. Acta*, 1970, **52**, 372.
23. Alfassi, Z. B., and Lavi N., *Radiochem. Radioanal. Lett.*, 1982, **53**, 173.
24. Altman, P. L., and Dittmer, D. S., *Editors*, "Biology Data Book," Volume 3, Federation of American Societies for Experimental Biology, Bethesda, MD, 1974, p. 1752.

Paper A3/152
Received May 25th, 1983
Accepted July 12th, 1983

Minor and Trace Element Analysis of Gallstones

Athab T. Al-Kinani and David E. Watt
Department of Medical Biophysics, The University, Dundee, DD1 4HN, UK
Brian W. East and Ian A. Harris
Scottish Universities Research and Reactor Centre, East Kilbride, Glasgow, G75 0QU, UK

Gallstone disease occurs in over 10% of the adult population. In an attempt to explore their possible role, minor and trace elements in gallstones and bile from five patients have been analysed by neutron activation, proton-induced X-ray emission and X-ray fluorescence. Calcium, phosphorus, sulphur, aluminium, manganese, copper and iodine were found at concentrations much higher than normal physiological levels. The distribution and form of calcium were examined qualitatively by scanning-electron microprobe and infrared spectroscopy. A brief discussion of the significance of the findings in relation to gallstone formation and treatment is included.

Keywords: *Minor and trace elements; gallstones; neutron-activation analysis; proton-induced X-ray emission; X-ray fluorescence*

Over 10% of the adult population suffers from gallstone disease[1] and present treatment is either by surgical removal, with accompanying risks and expense, or by oral therapy with drugs designed to dissolve stones *in situ*. Two types of gallstone can be characterised with the following approximate compositions: cholesterol, 90–99 and 1.4%; calcium bilirubinate, 0.7 and 90%; and calcium and trace minerals, 1–9 and 9%, for cholesterol stones and pigment stones, respectively.

Cholesterol stones are prevalent in Western countries whereas pigment stones are found in greatest preponderance in Asia, Japan and Third World countries. Dissolution therapy is used for cholesterol stones but can be ineffective for the pigment type. In some instances patients with cholesterol stones are also found to be resistant to this form of therapy.[2]

The formation of stones and similar deposits in man frequently involves calcium and this also occurs with gallstones. Many diseases in man have been associated with an excess of specific trace elements[3,4] and it is logical to think, therefore, that in gallstone disease the concentration of various elements might point to the fact that they have a significant role in, or provide an indication of, possible mechanisms of stone formation. In view of the prevalence of the disease and the problems associated with its treatment, we have made a preliminary investigation of some stone and bile specimens with the aim of obtaining accurate measurements of minor and trace element concentrations. The analytical methods of neutron activation analysis (NAA), proton-induced X-ray emission (PIXE) and X-ray fluorescence (XRF) spectroscopy were employed and provided results for 20 elements in all. In addition to quantitative analysis, the structure of the stones was examined qualitatively by scanning-electron microprobe and infrared (IR) spectroscopy. Elements determined by the various methods were as follows: NAA, Na, Mg, Al, P, Cl, K, Ca, Cr, Mn, Fe, Co, Zn, Se, Rb, Ag, Sb, Cs and I; PIXE, Cl, Mn, Cu, Zn and Fe; XRF, Mg, S, P, Ca and K; and IR, Ca compounds.

Experimental

Sample Preparation

Four cholesterol-type gallstones and associated bile samples were obtained by surgery together with a fifth pigment stone without associated bile. The stone specimens were handled with polythene instruments to avoid contamination[5] and were initially washed with de-mineralised water and dried under vacuum for 24 h. On division, they had a layered appearance and showed a definite nuclear structure. Sections were taken for light microscopy and scanning electron microprobe examination and the remaining material was ground to a fine homogeneous powder in an agate pestle and mortar. No separation of the "nuclei" or individual layers was attempted. The powder was divided for subsequent analysis by NAA, PIXE, XRF and IR. Bile samples were placed on a thin polythene sheet and evaporated to dryness with an infrared lamp for neutron activation or filtered using Whatman membrane filters for X-ray fluorescence analysis.

Neutron-activation Analysis

Samples were irradiated in the Argonaut UTR 300 reactor at East Kilbride at a nominal flux of 3×10^{12} neutrons s^{-1} cm^{-2}. A 20–50 mg mass of gallstone powder was transferred into cleaned polythene ampoules and subjected to the irradiation procedure shown in Fig. 1.

The 2- and 20-min irradiations were carried out in the pneumatic transfer facility of the reactor while the 54-h irradiation was loaded into a graphite stringer of the reactor thermal column. Owing to the reactor operation regime, the 54-h irradiation consisted of nine 6-h irradiations over a period of three weeks. Variations in neutron flux were monitored using either 20 mg of nichrome alloy wire attached to each ampoule for the 2- and 20-min irradiations or similar monitors of pure iron wire for the long irradiation. ^{65}Ni (2.56 h, 1.481

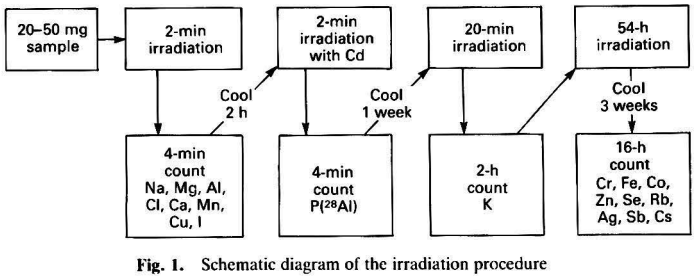

Fig. 1. Schematic diagram of the irradiation procedure

MeV) or ^{51}Cr (27.8 d, 0.320 MeV) activities were used to correct neutron flux for the short and intermediate irradiations, respectively and ^{59}Fe (45 d, 1.099 MeV) for the long irradiation. Except for phosphorus and potassium, which were in the form of solid compounds, standards for each element were made up from spectral-purity (99.95%) or AnalaR-grade (99.9%) reagents dissolved in de-ionised water or analytical-reagent grade (99.9%) hydrochloric or nitric acid. Measured volumes of solution were used to prepare multiple or single element standards for short irradiations. These were irradiated sequentially with the gallstone and bile samples. For the 54-h irradiation procedure, aliquots of the standard solutions were micropipetted on to thin polythene sheet and evaporated to dryness under a lamp before loading into polythene ampoules. In this instance standards were irradiated simultaneously with the samples.

Phosphorus and aluminium were determined by the double irradiation technique described by Gatschke and Gawlik[6] with and without a cadmium filter to enable the $^{27}Al(n,\gamma)^{28}Al$ and $^{31}P(n,\alpha)^{28}Al$ reactions to be distinguished. Magnesium and manganese were determined from the complex decay of the 0.84-MeV gamma peak after 2-min irradiation. It was found that the ratios of 0.84 : 1.014 MeV gamma peaks for ^{27}Mg and 0.84 : 1.810 MeV for ^{56}Mn agreed between standards and unknown samples and it was therefore assumed that only these two elements were contributing to the 0.84-MeV peak.

To resolve the two activities, samples and standards were therefore recounted after 1 h and the activities calculated by the solution of simultaneous equations embodying the observed gamma peak counts and the assumed radioactive half-lives of 9.45 min for ^{27}Mg and 2.58 h for ^{56}Mn. For iodine no chemical separation was performed as the concentrations found were sufficiently high for the direct observation of ^{128}I by instrumental analysis. Copper was also at sufficient concentration for direct determination instrumentally by means of 5.1-min ^{66}Cu (1.039 MeV). After irradiation, short/intermediate and long lived activities were measured using shielded 80 and 130 cm^3 Ge - Li detectors, respectively. Gamma-ray spectra were recorded in 4096 channels and gamma peak count rates calculated using standard peak identification and analysis software. The reliability of the procedures was assessed by analysing the National Bureau of Standards (NBS) standard reference materials oyster tissue (SRM 1566) and bovine liver (SRM 1577).

Proton-induced X-ray Emission Analysis

Gallstone powder was formed into 10 mm diameter × 2 mm thick pellets in a stainless-steel press and coated with a thin film of carbon by evaporation. Six such discs could be conveniently mounted on a stainless-steel holder and bombarded individually in the 3-MeV Dynamitron at the Birmingham Radiation Centre. A collimated beam of 2.5-MeV protons, approximately 1 mm^2 in area, was directed on to each pellet at 45° and the induced X-rays were detected at 90° to the beam by a 10 mm diameter Si - Li detector. A measure of integrated beam current was obtained with a Keithly electrometer coupled to a voltage to frequency converter. Spectra from the sample pellets were compared with oyster tissue standards prepared and analysed in the same manner.

X-ray Fluorescence Analysis

A Philips 1540 X-ray wavelength-dispersive system was used for X-ray fluorescence analysis. Gallstone powder was formed into 3 cm diameter × 3 mm thick pellets by hydraulic pressure (1.5×10^4 kg cm^{-2}) in a stainless-steel die. During illumination of the samples with X-radiation, the fluorescent X-rays, after selection by the Bragg crystal, were detected by means of a gas-flow proportional counter (90% argon - 10% methane). Standards were prepared by adding appropriate amounts of spectral-purity or AnalaR-grade reagents to a known amount of cholesterol.

This mixture was divided equally and one portion used as the primary standard and the other diluted successively with further cholesterol to produce a series of standards with different elemental concentrations. The use of these standards, with the same matrix as the gallstone material (at least for four of the stones), enabled errors resulting from effects such as partial absorption of incident and fluorescent radiation and enhancement of fluorescence due to X-rays produced within the sample to be kept to a minimum.

The homogeneity of the standards was also checked by measuring two pellets with the same concentration. Bile samples were prepared by vacuum filtration on to Whatman membrane filters and analysed for calcium using a rhodium target. Fixed-time counting was used for all measurements and the background beneath each peak was determined by linear interpolation of flanking background levels. Corrected

Table 1. Analysis of NBS standard reference materials.*

	Concentration, p.p.m.					
	Bovine liver SRM 1577			Oyster tissue SRM 1566		
Element	NBS value	NAA value	XRF value	NBS value	NAA value	XRF value
Na	2430 ± 100	2454 ± 135	—	5100 ± 300	5082 ± 258	—
Mg	604 ± 9	558 ± 11	638 ± 34	1280 ± 90	1451 ± 213	1430 ± 38
P	(13700)	12350 ± 2410	12056 ± 650	(8100)	7266 ± 1144	7057 ± 231
S	(8400)	—	8800 ± 273	(7600)	—	7977 ± 248
Cl	(2700)	2715 ± 151	—	(10000)	10110 ± 500	—
K	9700 ± 600	9640 ± 244	9790 ± 280	9690 ± 50	9618 ± 302	9763 ± 301
Ca	124 ± 6	130 ± 12	131 ± 5	1500 ± 200	1738 ± 153	1426 ± 44
Mn	10.3 ± 1	12 ± 2.6	—	17.5 ± 1.2	15 ± 2.4	—
Cr	0.088 ± 0.012	N.d.	—	0.69 ± 0.27	0.55 ± 0.06	—
Cu	193 ± 10	190 ± 14	—	63 ± 3.5	60 ± 6.7	—
Fe	268 ± 8	263 ± 12	—	195 ± 34	190.5 ± 9	—
Co	(0.18)	0.24 ± 0.01	—	(0.4)	0.31 ± 0.01	—
Zn	130 ± 13	129.2 ± 6	—	852 ± 13	805 ± 36	—
Se	1.1 ± 0.1	1.01 ± 0.06	—	2.1 ± 0.5	2.02 ± 0.9	—
Rb	18.3 ± 1	18.8 ± 0.85	—	4.45 ± 0.09	4.49 ± 0.05	—
Ag	(0.06)	0.1 ± 0.01	—	0.89 ± 0.09	0.88 ± 0.05	—
Cs	No value	0.03 ± 0.006	—	No value	0.05 ± 0.004	—

* Uncertified NBS values in parentheses.
† N.d. = none detected.

peak to background ratios were plotted against concentration and calibration graphs derived for each element. Unknown concentrations were found by comparing corrected peak to background ratios. The procedure was also tested with the oyster tissue and bovine liver standard reference materials.

Results and Discussion

The reliability of the NAA and XRF analysis procedures was checked for 16 of the elements by analysis of the NBS oyster tissue and bovine liver standard reference materials. The results, compared in Table 1, appeared to be satisfactory for all the elements including Mg, P, Mn and Cu. A similar check for Al, Sb, Cs and I was not possible in the absence of reference values for these elements. Over-all errors for NAA, including an estimate of the *a priori* error, varied between ±5 and ±10% except for Mg and Mn, where the range was ±8 to ±25%. For XRF analysis errors were around 3%. Errors for PIXE analysis were largely ±10% but ranged up to ±32% in one instance. This last method was not cross-checked with standard reference material as oyster tissue was itself used as the sole comparative standard for the determination of gallstone concentrations.

Table 2. Concentration of elements in gallstones by NAA

	Concentration, p.p.m.		
	Collected values for four cholesterol gallstones		
Element	Mean	Range	Pigment gallstone
Na	1 170	977–1 405	10 720 ± 532
Mg	175 (3)*	136–372	1 267 ± 280
Al	55.8	0.3–93	39 ± 5
P	814	557–1 075	1 380 ± 201
Cl	587	360–713	2 394 ± 129
K	724	100–1 629	2 128 ± 155
Ca	5 180	379–10 880	19 730 ± 1 038
Cr	0.08 (3)	0.019–0.13	N.d.†
Mn	27.2	5–83	377 ± 31
Fe	15.7	8.7–24.1	1 518 ± 67
Co	0.02	0.004–0.04	0.3 ± 0.01
Cu	28.6	3.6–68	5 487 ± 268
Zn	1.19 (3)	0.7–3.12	473 ± 21
Se	0.123 (3)	0.05–0.2	5.6 ± 0.25
Rb	0.15 (2)	0.13–0.16	3.6 ± 0.25
Ag	0.08 (2)	0.04–0.12	2.26 ± 0.1
Sb	0.034 (2)	0.018–0.05	1.24 ± 0.06
Cs	0.13	0.018–0.33	0.46 ± 0.02
I	3.36	2.95–3.9	56.3 + 6.4

* Parentheses denote number of stones; none detected in others.
† N.d., none detected.

For the seven elements Mg, P, Cl, K, Ca, Mn and Fe, NAA could be compared with either XRF or PIXE and taking into account experimental errors it was found that agreement was satisfactory.

Results for the gallstones are given in Tables 2 and 3. Mean values for the four cholesterol stones have been calculated and the observed ranges tabulated. They are compared with results for the only pigment (Ca bilirubinate) stone for which the over-all errors are given. From the clinical and physiological standpoint, comparative assessment of the findings is difficult as "normal" values for gallstones clearly do not exist to the extent that the stones themselves represent an abnormal situation. A comparison can therefore be made with concentration levels of the elements encountered in normal fluids and tissues. On this basis it is apparent that the concentrations of Ca, P, S, Al, Mn, Cu and I are very high compared with those generally accepted as normal. These elements might thus have a significant role in gallstone formation either associated with the structure of the conglomerate crystals or in combination with organic molecules. Under normal conditions calcium in the bile is bound to bile salts and remains in solution. If the calcium concentrations were increased or if there were competition by excess Na^+ and K^+ ions for the binding sites,[7] calcium would tend to be precipitated. Comparison of the calcium concentrations found in the bile associated with the cholesterol stones (Table 4) with normal bile, for which Tera[8] gives a range of 197–396 p.p.m., shows that they are very much higher, which is in line with this suggestion. Also, insofar as the stones themselves reflect levels in the bile, the high calcium concentrations observed would agree with this. (The lower levels in relation to bile are probably due to the method of sampling where the whole stone was homogenised thus giving an average concentration, whereas it was clear from scanning-electron probe microscopy that the calcium distribution was not uniform, there being a distinct concentration at the centre of all the stones).

It has also been suggested that trace elements can tend to enhance the growth rate of deposits of crystalline calcium compounds[9] and the high concentrations of those measured could be significant in this respect. Our results also suggest the possibility that other elements not analysed here might occur with high concentrations. Taken together this evidence would point to altered concentrations of minor and trace elements in the enterohepatic circulation resulting in abnormally high levels in bile.

A comparison of the cholesterol and pigment stones indicates generally higher concentrations for most elements in the latter type. The elements Fe, Cu, Zn and I particularly appear to be higher. Cu can act as a chelating agent for calcium bilirubinate[10] and Fe could be derived from small haemorrhages caused by irritation of the gall bladder walls when

Table 3. Concentration of elements in gallstones by XRF and PIXE analysis

	Concentration, p.p.m.				
	Collected values for four cholesterol gallstones				
	XRF		PIXE		
Element	Mean	Range	Mean	Range	Pigment gallstone: XRF
Mg	242 (3)*	145–380			1 368 ± 55
P	882	577–1 163			1 496 ± 67
Cl	N.a.†	N.a.	656	365–817	N.a.
S	436	110–766			1 680 ± 67
K	692	97–1 591			2 018 ± 62
Ca	4 877	366–10 180			18 530 ± 560
Mn	N.a.	N.a.	26.3	4–81.4	N.a.
Fe	N.a.	N.a.	14.6	8–20.4	N.a.

* Parentheses denote number of stones; none detected in others.
† N.a., no analysis.

Table 4. Concentration of elements in bile

Element	Collected concentration values for bile associated with four cholesterol gallstones, p.p.m.	
	Mean	Range
Na	505	100–928
Cl	387	106–648
Cu	3.1 (0.9)	
I	2.37	0.52–1.8
Ca	15 150	11 100–19 400

stones form. The finding of high iodine concentrations in this and the other stones is particularly striking but we offer no explanation. These over-all higher levels are commensurate with the higher mineralisation of this type of stone.

Qualitative examination of the stone material by IR spectroscopy showed calcium to be present as the carbonate, phosphate and bilurubinate. Interestingly, in a cholesterol stone from one patient resistant to dissolution therapy, scanning-electron probe microscopy showed an outer layer of calcium deposit that could well be a clue to the failure of the treatment as such a layer would tend to act as an insoluble barrier.

The authors gratefully acknowledge the assistance and cooperation of the following in this work: Professor I. A. Bouchier and Dr. P. E. Ross, Department of Medicine, Ninewells Hospital, Dundee, for providing the gallstone and bile samples; Dr. N. A. Dyson, Department of Physics, Birmingham University, for PIXE analysis facilities; Dr. P. M. Zarembski, Dundee University, for IR spectroscopy facilities; and Dr. F. H. Hubbard and R. J. Gill, Dundee University, for XRF facilities.

References

1. Newman, H. F., and Northup, J. D., *Int. Abstr. Surg.*, 1959, **169**, 1.
2. Bouchier, I. A. D., *Annu. Rev. Med.*, 1980, **31**, 59.
3. Gooden, D. S., *Phys. Med. Biol.*, 1972, **17**, 26.
4. Dyson, N. A., and Simpson, A. E., *Proc. Anal. Div. Chem. Soc.*, 1976, **13**, 198.
5. Versieck, J. M. J., and Speecke, A. B. H., "Nuclear Activation Techniques in the Life Sciences," International Atomic Energy Agency, Vienna, 1972, p. 39.
6. Gatschke, W., and Gawlik, D., *J. Radiat. Anal. Chem.*, 1980, **56**, 203.
7. Rajagapalan, N., and Lindenbaum, S., *Biochim. Biophys. Acta*, 1982, **711**, 66.
8. Tera, H., *Acta Chir. Scand., Suppl.*, 1960, **256**, 1.
9. Been, J. M., Mills, P. M., and Lewis, D., *Gastroenterology*, 1979, **76**, 548.
10. Suzuki, N., *J. Exp. Med., Tokyo*, 1966, **90**, 195.

Paper A3/288
Received August 25th, 1983
Accepted September 9th, 1983

Measurement of Aluminium in Dialysis Fluid and Water by a Spectrophotometric Procedure

Barry Sampson and Adam Fleck
Department of Chemical Pathology, Charing Cross Hospital, Fulham Palace Road, London, W6 8RF, UK

A method is described for the spectrophotometric assay of aluminium in dialysis fluid and water using the ternary complex formed between aluminium, Chrome Azurol S and cetylpyridinium chloride. Absorbance is measured at 640 nm. The molar absorptivity of the complex is estimated to be $1.25 \pm 0.03 \times 10^5$ l mol^{-1} cm^{-1}. The method is linear over the range 25–250 μg l^{-1} and the detection limit is approximately 5 μg l^{-1}. Interference from copper and iron is masked by the addition of ascorbic acid and 2,2′-bipyridyl. Phosphate does not interfere; fluoride shows a tolerable interference and oxalate and citrate show major interference.

Keywords: *Aluminium determination; spectrophotometry; ternary complexes; water analysis; dialysis fluids*

Aluminium is frequently added to water as a flocculating agent to remove organic impurities. It has been found that high concentrations of aluminium in the water supplies of patients with chronic renal failure being treated by haemodialysis can have severe toxic effects.[1,2] It is essential to monitor routinely the water supplies of such patients to ensure that they are not at risk, and that the water purification equipment they use is functioning correctly.

Several sensitive spectrophotometric assays for aluminium have been described,[3–5] the most sensitive involving the use of the ternary complex formed between aluminium, Chrome Azurol S and quaternary ammonium salts.[6,7] This assay, together with some similar assays, has been studied for application to the routine measurement of aluminium in water and dialysis fluid samples.

Experimental

Apparatus

Spectrophotometric measurements were made with a Pye Unicam SP1800 spectrophotometer. Disposable polystyrene cuvettes with path length 1 cm and polystyrene test-tubes were used. All glassware was prepared by immersion for 24 h in 20% *V/V* nitric acid, rinsing in de-ionised water and drying in a dust-free cabinet.

Reagents

All reagents were of AnalaR or Aristar grade (BDH Chemicals) where appropriate. All water used had a specific conductance of at least 15 Mohm^{-1} cm^{-1}. Sodium acetate buffer was prepared from AnalaR-grade reagents and purified by passage through a column of Chelex-100 chelating resin in the sodium form (Bio-Rad). Hexamine buffer prepared from AnalaR-grade hexamine and Aristar-grade ammonia was used without further purification. The hexamine buffer used in the final method contained 3 mol l^{-1} of hexamine and 1 mol l^{-1} of ammonia.

Dyes and quaternary ammonium salts were dissolved in de-ionised water to concentrations of 2–10 mmol l^{-1}. For the final method a combined solution was used containing 2 mmol l^{-1} of Chrome Azurol S and 5 mmol l^{-1} of cetylpyridinium chloride in 0.1 mol l^{-1} hydrochloric acid. The addition of acid reduces precipitation of the reagents. This is stable for about 4 weeks.

Ascorbic acid and dipyridyl were used as aqueous solutions. For the final method a combined reagent of 0.5 mol l^{-1} ascorbic acid and 0.1 mol l^{-1} 2,2′-bipyridyl was used. This is stable for 1–2 weeks if stored at 4 °C in the dark.

Standards

Standards were prepared from commercially available aluminium nitrate solution (1.000 g l^{-1} aluminium). A stock dilution of 10 mg l^{-1} in 0.1 mol $^{-1}$ hydrochloric acid was used to prepare working standards in the range 10–500 μg l^{-1}. All working standards were prepared with 0.1 mol l^{-1} hydrochloric acid. The prepared standards were stored in polythene bottles. Fresh standards were prepared every 6–8 weeks.

Procedures

Initial studies

To 5 ml of aluminium standard were added 0.1 ml of dye, 0.1 ml of quaternary ammonium salt (if used) and hexamine or acetate buffer to give the required pH. Absorbance measurements were made after approximately 1 h at room temperature. A final pH of 6–6.5 was given by the addition of 0.6 ml of the hexamine - ammonia buffer. In experiments where the pH was varied by alterations in buffer volume, water was added to maintain a constant volume.

Optimum pH

Stock buffer solutions were prepared at known pH intervals from the stock hexamine - ammonia buffer by the addition of hydrochloric acid and water and from purified 3 M sodium acetate by the addition of sodium hydroxide to give final concentrations of 0.3 M hexamine or acetate. To 5-ml aliquots of buffer were added 0.1 ml of aluminium standard solution, 0.1 ml of 2 mM Chrome Azurol S solution and 0.1 ml of 5 mM cetylpyridinium chloride solution.

Final conditions and interferences

The effects of variation in the Chrome Azurol S and cetylpyridinium chloride concentration were studied using the same volumes as under *Initial studies* with different concentrations of the reagents. The effect of interfering substances was studied similarly. A volume of up to 0.2 ml of the interfering ion solution used, or water, was added to the aluminium solution before the addition of the reagents. In some instances a standard solution of other metals was used in place of the aluminium solution. The effects of the addition of ascorbic acid and 2,2′-bipyridyl were studied by the addition of these before addition of the reagents.

Method Development

Selection of reagents

To establish the optimum reagent conditions, the use of several complexing agents and quaternary ammonium salts was studied. Aluminon did not show any improvement in

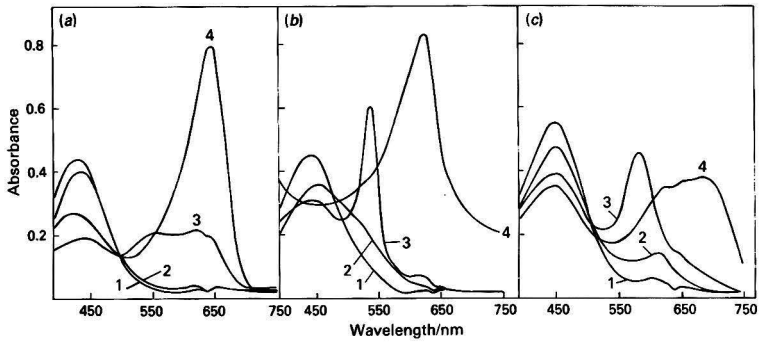

Fig. 1. Absorption spectra of aluminium - dye and aluminium - dye - cetylpyridinium chloride (CPC) complexes in hexamine buffer. Final concentrations: Al, 6.33; dye, 35; CPC, 90 μmol l^{-1}. (*a*) Chrome Azurol S; (*b*) Eriochrome Cyanine R; (*c*) Pyrocatechol Violet. (1) Blank - dye; (2) blank - dye - CPC; (3) Al - dye; and (4) Al - dye - CPC

Table 1. Spectral characteristics of aluminium complexes in the absence and presence of cetylpyridinium chloride (CP). Final concentrations: Al, 6.2 μmol l^{-1}; dye, 30–35 μmol l^{-1}; CP, 90 μmol l^{-1}. pH, 6–6.5 in hexamine buffer. Absorbances measured against water

	No CP		With CP		
Reagent	λ/nm	Absorbance	λ/nm	Absorbance	Δλ/nm
Chrome Azurol S . .	620	0.16	642	0.70	22
Eriochrome Cyanine R . .	536	0.46	622	0.72	88
Pyrocatechol Violet	580	0.37	680	0.33	100

sensitivity on the addition of quaternary ammonium salts; the complex formed with Eriochrome Black T was substantially destroyed by the addition of quaternary ammonium salts.

The effects of several quaternary ammonium salts were examined. Benzyltrimethylammonium hydroxide had no effect in any of the systems studied. The more complex long-chain quaternary ammonium salts Hyamine 1622 and Hyamine 2389 showed at best no advantage over the simpler salts. Of these, zephiramine (tetradecylbenzyldimethylammonium chloride) tended to give turbid solutions more readily than did cetylpyridinium chloride or cetyltrimethylammonium bromide, an observation confirmed by Marczenko and Jarosz.[7] The Hyamines and zephiramine gave higher bathochromic shifts than did the cetyl salts, but did not give such a high absorbance. There was no apparent advantage in using either of the cetyl salts, and cetylpyridinium chloride was selected for further development.

The spectra of the complexes formed by Chrome Azurol S, Eriochrome Cyanine R and Pyrocatechol Violet in the presence and absence of cetylpyridinium chloride are shown in Fig. 1. More details of the spectra are given in Table 1. From an appraisal of the data, the combination Chrome Azurol S - cetylpyridinium chloride was selected for development.

Reaction conditions

The effect of pH was studied using acetate and hexamine buffers. No effect of buffer was found, the optimum pH for both being 5.8–6.5. At a lower pH there is a tendency for turbidity to develop with the cetylpyridinium chloride. Hexamine buffer was chosen for routine use because it is suitable for use without pre-treatment. The acetate buffer without Chelex treatment gave a high blank. To use sodium acetate of higher purity would considerably increase the cost of the assay. A further advantage is the higher buffering capacity of hexamine at the pH selected for the assay (6.0).

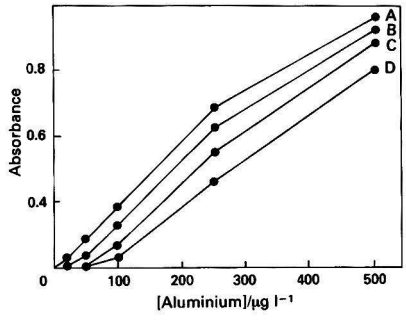

Fig. 2. Effect of cetylpyridinium chloride (CPC) concentration on the linearity of the calibration graph. Sample (5 ml): 0.1 ml of 2 mmol l^{-1} Chrome Azurol S, 0.1 ml of CPC and 0.65 ml of hexamine - acetate buffer solution. Final CPC concentration: A, 70; B, 140; C 350; and D, 690 μmol l^{-1}

The concentration of Chrome Azurol S does not significantly alter the absorbance of the complex, provided that it is present in excess. A stoicheiometry of 2:1 or 3:1 for dye to aluminium is probable,[6,7] so that a minimum excess of 4:1 at the highest concentration of aluminium was selected, *i.e.*, 35 μmol l^{-1} for aluminium at concentrations up to 250 μg l^{-1} (*ca.* 9 μmol l^{-1}).

The concentration of the cetylpyridinium chloride was found to have a marked effect on the linearity of the calibration graph obtained. At a low concentration of cetylpyridinium chloride turbidity results, although the concentration at which this occurs is pH dependent. At high concentrations the absorbance of the complexes with lowest aluminium concentrations is greatly reduced (Fig. 2). At a cetylpyridinium chloride concentration of 80–100 μM there is no turbidity in the blank and the calibration graph is linear over the range 25–250 μg l^{-1} (1–10 μmol l^{-1}).

Interferences

A number of metal ions were examined for interference in the assay. Of those tested, only copper(II) and iron(III) were found to give a significant effect. Spectra of these complexes are shown in Fig. 3. It has been found possible virtually to eliminate both of these interferences by the addition of an excess of ascorbic acid and 2,2′-bipyridyl to the reaction mixture prior to the addition of the Chrome Azurol S (Figs. 4 and 5). This addition has no effect on the absorbance of the aluminium complex. A final concentration of 10 mmol l^{-1} of ascorbate and 2 mmol l^{-1} of 2,2′-bipyridyl has been found to correct adequately for up to 25 μmol l^{-1} of copper or iron.

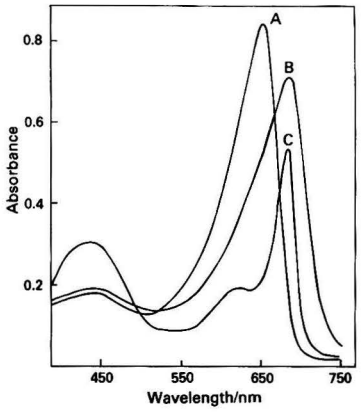

Fig. 3. Absorption spectra of ternary complexes of aluminium, iron and copper. A, Aluminium (7.4 μmol l^{-1}); B, iron (8 μmol l^{-1}); and C, copper (8 μmol l^{-1})

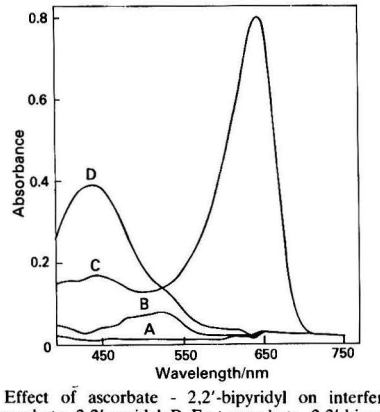

Fig. 4. Effect of ascorbate - 2,2′-bipyridyl on interferences.[1] A, Al + ascorbate - 2,2′-pyridyl; B, Fe + ascorbate - 2,2′-bipyridyl; C, Al + ascorbate - 2,2′-bipyridyl + Chrome Azurol S - cetylpyridinium chloride (CPC); and D, Fe + ascorbate - 2,2′-bipyridyl + Chrome Azurol S - CPC

Several anions are known to form stable complexes with aluminium. Nitrate and sulphate had no effect, although a blank prepared in 0.1 mmol l^{-1} nitric acid was slightly turbid; the corresponding blank in hydrochloric acid was clear. The effects of several other anions were studied in more detail (Fig. 6). Phosphate had no effect, even at high concentrations. Fluoride, oxalate and citrate all inhibited the assay. The effect of fluoride at a concentration of 1 p.p.m. (20 μmol l^{-1}), the concentration normally found in fluoridated water, is to reduce the sensitivity by about 10% at aluminium concentrations of 3–5 μmol l^{-1}. Citrate has a strong inhibitory effect at concentrations greater than 100 μmol l^{-1}, the concentration range normally found in physiological fluids. The assay will therefore be inapplicable to biological samples such as urine or protein-free filtrates of plasma or to dialysis fluids after passage through the artificial kidney. A method has been suggested for the extraction of aluminium for biological matrices by solvent extraction of the 8-hydroxyquinolinate complex.[8] Such an extraction could be used to increase the sensitivity of the assay, although it could entail an increase in the reagent blank.

Selected Method

The method given here has been in routine use in this laboratory for over 6 months and has proved simple and

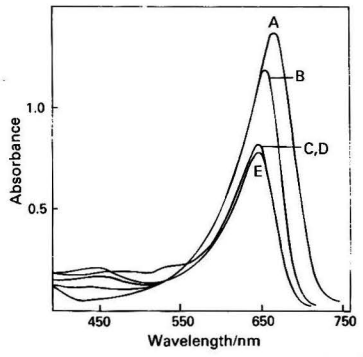

Fig. 5. Effect of ascorbate - 2,2′-bipyridyl on interferences.[2] Al, 7.4 μmol l^{-1} with Fe or Cu, 8 μmol l^{-1}. A, Al/Fe - CAS/CPC; B, Al/Cu - CAS/CPC; C, Al alone - BP + CAS/CPC; D, Al/Fe - DP + CAS/CPC; and E, Al/Cu - DP + CAS/CPC (CAS = Chrome Azurol S; CPC = cetylpyridinium chloride; BP = 2,2′-bipyridyl)

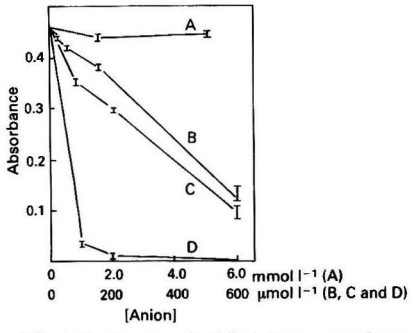

Fig. 6. Effect of anions on aluminium ternary complexes. Final concentration of Al, 6.2 μmol l^{-1}; CAS - CP concentrations as in selected method. A, Phosphate; B, fluoride; C, oxalate; and D, citrate

precise. The sample (of tap water, treated water or dialysis fluid) is collected into 50-ml polypropylene tubes. On receipt in the laboratory, sufficient 5 mol l^{-1} hydrochloric acid is added to give a final concentration of 0.1 mol l^{-1}. Samples are stored at 4 °C until analysed.

Method

Unknown samples and controls are analysed in duplicate and standards in triplicate. A 5-ml volume of sample is pipetted into a 10-ml polystyrene test-tube, 100 μl of ascorbate - 2,2′-bipyridyl reagent are added and the contents are mixed well. After at least 10 min, 100 μl of the colour reagent and 650 μl of the hexamine - ammonia buffer are added and the contents mixed well. The solution is decanted into 1-cm polystyrene cuvettes and after 60–90 min the absorbance is measured at 640 nm against a distilled water blank.

Results and Discussion

Linearity

A typical calibration graph is shown in Fig. 7. Although it is linear over the range 25–250 μg l^{-1} (correlation coefficient 0.99), by fitting a curve by hand the useful range can be extended to 5–500 μg l^{-1}. A concentration of 5 μg l^{-1} is taken as the detection limit; this is normally at least three standard deviations greater than the blank absorbances. Owing to the reduced precision due to the non-linearity of the calibration graph, a practical limit of 20 μg l^{-1} has been chosen. From the

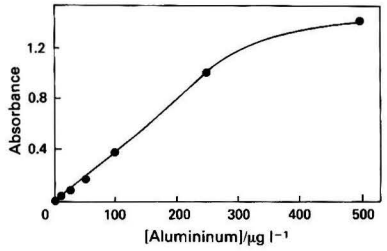

Fig. 7. Typical calibration graph using the selected method

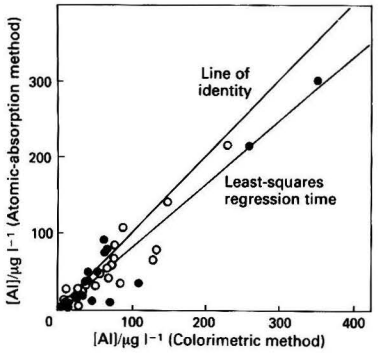

Fig. 8. Comparison of results by AAS and the selected method for (○) water samples and (●) dialysis fluid samples. Correlation coefficient, $r = 0.949$; least-squares regression line, $y = 0.834x - 1.68$ ($n = 47$)

absorbance at the upper limit of the linear range, the molar absorptivity of the complex is estimated to be $1.251 \pm 0.034 \times 10^5$ l mol^{-1} cm^{-1}.

Precision

The within-batch and between-batch variance of the method has been tested by replicate analyses of several samples at different concentration levels. For a mean concentration of 54 μg l^{-1}, the within-batch coefficient of variation (C.V.) was 3.2% (n = 10; mean 54.25 ± 1.75 μg l^{-1}) and the between-batch C.V. was 7.9% (n = 10; mean 54.2 ± 4.3 μg l^{-1}); for a concentration of 83 μg l^{-1}, the within-batch C.V. was 1.2% (n = 10; mean 84.1 ± 0.99 μg l^{-1}) and the between-batch C.V. 3.0% (n = 10; mean 81.5 ± 2.5 μg l^{-1}); for a concentration of 230 μg l^{-1} the within-batch C.V. was 1.9% (n = 10; mean 232 ± 4.4 μg l^{-1}) and the between batch C.V. was 1.8% (n = 10; mean 226 ± 4.1 μg l^{-1}).

Recovery

Known amounts of aluminium were added to samples of dialysis fluid or tap water. The recovery was 92.5–104% over the added concentration range 50–400 μg l^{-1} (Table 2). Calibration graphs prepared using dialysis fluid as a diluent for the standards instead of de-ionised water were parallel to calibration graphs prepared using standards made with de-ionised water.

Accuracy

Samples were analysed by the described methods, and also by an independent laboratory using electrothermal atomic-absorption spectroscopy (AAS). The results are shown in Fig. 8. The results obtained by the spectrophotometric assay are higher than those obtained by AAS. This may be due to a non-specific bias of either assay, but may also be caused by a number of chemical effects. It is possible that there may be species present that are volatile at low temperatures and may be lost during the ashing stage of the AAS assay, or there may be some unidentified ions present causing an interference in the spectrophotometric assay.

Table 2. Recovery of aluminium from tap water and dialysis fluid

Sample	Al added/ μg l^{-1}	Al found/μg l^{-1}*	Recovery, %
Tap water	0	25.0 ± 2.2	
	50	74.5 ± 1.6	99
	400	440 ± 30	104
Dialysis fluid	0	49.3 ± 2.5	
	200	234 ± 14	92.5

* Mean ± standard deviation (n = 15).

Table 3. Results of aluminium assays in samples from home dialysis patients

Sample	Al not detected	Al > 20 μg l^{-1}
Tap water	80 patients	28 patients (range 20–140 μg l^{-1})
Soft water	93 patients	15 patients (range 20–102 μg l^{-1})
Dialysis fluid	94 patients	14 patients (range 20–89 μg l^{-1})

Clinical Application

The assay described here has been in routine use in the screening of samples of water and dialysis fluid provided by home dialysis patients for several months. Several patients have been identified as being at risk. The findings in 108 patients, over a 6-month period, are summarised in Table 3. By observing a pink colour in the assay tubes after the addition of the ascorbate - 2,2′-bipyridyl reagent, but before the addition of the colour reagent, a few samples with a high iron content have been identified. This was confirmed and quantitated by a spectrophotometric assay with 2,4,6-tripyridyl-1,3,5-triazine (TPTZ) or by AAS.

Preliminary studies have been made on aluminium release from a Redy cartridge, which recirculates a small volume of dialysate through a purifier containing alumina as a binder. Aluminium toxicity from this system has been described previously.[9,10] Typical results found were an initial aluminium concentration of less than 10 μg l^{-1}, increasing to 50–60 μg l^{-1} after a 6-h dialysis period.

We are grateful to Dr. D. Hall and Dr. G. S. Fell of Glasgow Royal Infirmary for the AAS measurements.

References

1. Alfrey, A. C., Le Gendre, G. R., and Kaehn, W. D. *N. Engl. J. Med.*, 1976, **294**, 184.
2. Parkinson, I. S., Ward, M. K., and Kerr, D. N. S., *J. Clin. Pathol.*, 1981, **34**, 1285.
3. Dougan, W. K., and Wilson, A. L., *Analyst*, 1974, **99**, 413.
4. Chester, J. E., Dagnall, R. M., and West, T. S., *Talanta*, 1970, **17**, 13.
5. Marczenko, Z., *Crit. Rev. Anal. Chem.*, 1981, **10**, 195.
6. Tikhonov, V. N., and Ekaterina, L. A., *Zh. Anal. Khim.*, 1975, **30**, 1507.
7. Marczenko, Z., and Jarosz, M., *Analyst*, 1982, **107**, 1431.
8. Que Hee, S. S., Boyle, J., and Finelli, V. N., *Bull. Environ. Contam. Toxicol.*, 1979, **23**, 509.
9. Pierides, A. M., and Frohnert, P. P., *Trans. Am. Soc. Artif. Intern. Organs*, 1981, **17**, 629.
10. Odell, R. A., Yang, J., George, C. R., and Farrell, P. L., *Contemp. Dialysis*, 1982, **3**, 57.

Paper A3/261
Received August 12th, 1983
Accepted September 15th, 1983

Solvent Extraction and Spectrophotometric Determination of Palladium(II) with 2,2'-Bipyridyl 2-Pyridylhydrazone (DPPH)

John A. Stratis, Aristides N. Anthemidis and George S. Vasilikiotis
Laboratory of Analytical Chemistry, Aristotelian University of Thessaloniki, Thessaloniki, Greece

The described spectrophotometric determination of palladium involves the extraction of the DPPH - Pd(II) complex from an acidic aqueous solution (0.5–1.5 N HCl) into a chloroform layer. The asorbance of the extracted solution is measured at 585 nm. The molar absorptivity of the complex is 1.9×10^4 l mol^{-1} cm^{-1} at 585 nm. The effects of pH (2–12), HCl concentration, DPPH concentration and shaking time were studied. The ratio of ligand molecules to metal ions in the coloured complex was found to be 1 : 1. Tolerance amounts for many metals have been determined. Finally, a procedure for the determination of palladium in dental alloys is recommended. The determination is selective, sensitive and accurate.

Keywords: *Palladium determination; spectrophotometry; 2,2'-bipyridyl 2-pyridylhydrazone; dental alloys*

In previous work by Alexaki-Tzivanidou,[1] it was observed that palladium(II) forms a coloured complex with 2,2'-bipyridyl 2-pyridylhydrazone (DPPH) in aqueous solution, and this reaction was studied mainly at higher pH values. DPPH has been used as an organic reagent for the micro-determination of cobalt,[2–4] zinc,[5,6] iron,[7] cadmium[8] and copper.[9] DPPH is a sensitive organic reagent for the determination of these metals and is sensitive and selective for cobalt[2]; it was observed also that DPPH can be used for the extraction of some cations and anions.[4,10]

In this work we decided to study the possibility of extracting the DPPH - Pd complex in order to develop a procedure for the determination of palladium that could be applied to the analysis of dental alloys. A number of studies on the extraction of metals as their complexes with tridentate heterocyclic hydrazone ligands containing the group –N=C–N=N–NH–C=N– have been reported.[11–14] Some analytical procedures using organic reagents have also been devised for the determination of palladium(II)[15–17] and the wide range of reagents available has been the subject of some reviews.[18,19]

Because of the continuously rising price of gold and platinum, palladium is used as an effective substitute in dental alloys and jewellery. Dental alloys fall mainly into four groups: (a) noble dental alloys (Au 68–78%, Pd 1–4%), (b) precious dental alloys (Au 33–50%, Pd 6–10%), semi-precious dental alloys (Au 0–1.5%, Pd 20–30%) and (d) dental alloys for sets of artificial teeth (Cr and Ni without Pd).

Experimental

Reagents

All reagents and solvents were of analytical-reagent grade (E. Merck or BDH Chemicals).

2,2'-Bipyridyl 2-pyridylhydrazone (DPPH). The synthesis of DPPH has been reported previously.[2] An ethanolic solution (2×10^{-2} M) was prepared by dissolving 0.5506 g of DPPH in 100 ml of ethanol. The ethanolic solutions are stable for several months if they are kept in amber-glass bottles.

Stock palladium(II) solution, 1000 p.p.m. (9.4×10^{-3} M). This was prepared by dissolving 0.1000 g of palladium powder in the minimum volume of aqua regia. This solution was evaporated to dryness and 5 ml of hydrochloric acid and 25 ml of water were added to the residue. The mixture was warmed until complete dissolution and then diluted to 100 ml with distilled water. More dilute solutions were obtained by accurate dilution of the stock solution.

Chloroform. Chloroform was used without further purification after being saturated with distilled water.

Distilled water. All distilled water used in the extraction procedures was saturated with chloroform.

Apparatus

Spectrophotometric measurements were made with a Zeiss Model PMQ3 spectrophotometer and a Unicam SP700A instrument with 10-mm quartz cells. The pH values were determined with an Orion Research Model 701A digital pH meter (using a combined electrode). For the comparative determination of palladium in alloys a Perkin-Elmer Model 403 atomic-absorption spectophotometer was used with a palladium hollow-cathode lamp.

Procedure

The following procedure was used for the spectrophotometric study of the extraction of the palladium (II) - DPPH complex. Into a 50-ml calibrated flask were pipetted 1–4 ml of palladium(II) solution (1000 or 10 p.p.m.), 0.5–2.0 ml of DPPH solution (2.0×10^{-3} or 2.0×10^{-2} M) and the appropriate amount of hydrochloric acid (4.00 or 6.00 N) or sodium hydroxide solution or a buffer solution, depending on the requirements, followed by dilution to the mark with distilled water. A volume of 10 ml of the above solution was transferred into a separating funnel, 10 ml of chloroform were added and the mixture was shaken for 10 min. After the separation of the two layers, the clear extract was run off into a 10-mm quartz cell and the absorbance was measured at 560 and 585 nm using a reagent blank as a reference.

Especially for the determination of palladium in alloys, the dissolution was carried out according to the standard procedure[20] as follows. A sample of 0.2000–0.5000 g was taken (*ca.* 8×10^{-3} cm thick in a small squares of *ca.* 0.25 cm side) and dissolved at a low temperature (35–40 °C) in about 25 ml of dilute aqua regia (1 + 1) in a 250-ml beaker. Silver chloride remained as an insoluble residue, which was broken up from time to time with a glass rod until the alloy was completely decomposed. Water (100–150 ml) was added and the mixture was digested for about 1 h; after cooling, the supernatant liquid was perfectly clear. The silver chloride was filtered off and washed well with water. The final solution was evaporated to a small volume.

If there is no interest in the simultaneous determination of gold, the solution is evaporated to dryness (part of the gold ions is reduced by this procedure). After successive additions of hydrochloric acid and evaporation (twice), nitrate ions have to be removed. The remaining liquid was dissolved in 10–25 ml of 6 N hydrochloric acid and the solution was transferred into a 100-ml calibrated flask and diluted to volume with distilled water. More dilute solutions were obtained by accurate dilution to give final concentrations of palladium in the range 0.1–1.2 p.p.m., of DPPH 3.5×10^{-4} M and of HCl 0.6–1.5 N, then the extraction procedure was followed ($V_o : V_w = 5 : 20$,

where V_o is the volume of organic phase and V_w is the volume of aqueous phase in millilitres).

If gold was present in large amounts, after the removal of nitrate ions the residue was dissolved in 10–25 ml of 1 N HCl, heated until boiling and a solution of 0.1 N sodium sulphite added dropwise until the gold had stopped precipitating. The solution was then heated for a few minutes and, after filtration, was treated as above.

Results and Discussion

Absorptiometric Characteristics

Palladium(II) forms a red complex with DPPH in a wide pH range. The spectra of this complex in aqueous and chloroform solutions are shown in Fig. 1. Comparison of the two spectra shows that the spectrum in chloroform solution has a maximum at 585 nm and a shoulder at 560 nm whereas the corresponding spectrum in aqueous solution has an absorbance maximum at about 550 nm. The spectra of the DPPH - Pd(II) complex in aqueous solutions at different pH values and the spectra of the corresponding extracts are shown in Fig. 2(*a*) and (*b*).

Effect of pH

Reproducible extraction results were obtained over a wide range of pH values, *e.g.*, from pH 12 down to at least 2 N HCl, as is shown in Fig. 3. Extraction at higher pH values was ineffective because of turbidity. Because some cations can be extracted from aqueous solutions[4,10] at pH ≥ 3, we worked with acidified solutions (0.5–1.5 N HCl).

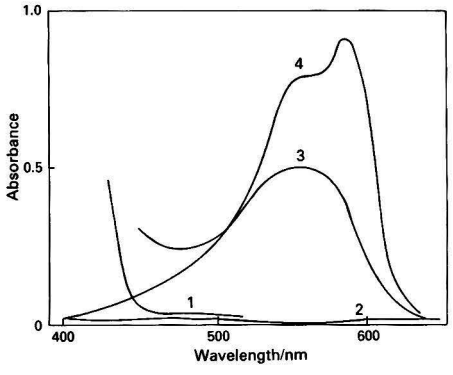

Fig. 1. Absorption spectra of 1, 3.5×10^{-4} M DPPH in 1.0 M HCl; 2, DPPH in chloroform after extraction of previous solution; 3, Pd - DPPH (Pd, 5.64×10^{-5} M; and DPPH, 3.5×10^{-4} M) in 1.0 M HCl; and 4, Pd - DPPH in chloroform after extraction of previous solution ($V_o : V_w = 1 : 1$, *i.e.*, $V_o = V_w = 10$ ml)

Effect of Shaking Time

The extraction of palladium(II) with DPPH into the chloroform layer was found to be independent of the shaking time after a period of 4 min. The recommended time is 10 min.

Effect of DPPH Concentration

Fig. 4 shows the dependence of the extraction of palladium(II) on DPPH concentration. The concentration of DPPH must be five times greater than that of the palladium(II) concentration.

Composition of the Coloured Complex

The composition of the coloured complex in aqueous solution (0.7 N HCl) and in chloroform was determined by Job's method of continuous variation. Fig. 5 illustrates the Job plots obtained from measurements at 560 and 585 nm for extracts and at 550 nm for aqueous solutions; the ratio of ligand molecules to metal ions is 1:1. The same results were obtained with 0.5 and 1 N HCl solutions.

Conformance with Beer's Law

The extraction of palladium(II) from aqueous solution (in 0.5–1.5 N HCl) is nearly complete (Fig. 3). To increase the accuracy and sensitivity of the palladium(II) determination a

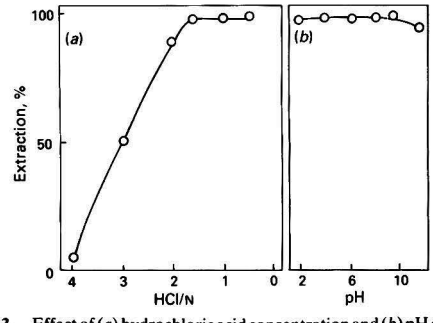

Fig. 3. Effect of (*a*) hydrochloric acid concentration and (*b*) pH on the extraction of Pd in chloroform (Pd, 5.64×10^{-5} M and DPPH, 3.5×10^{-4} M)

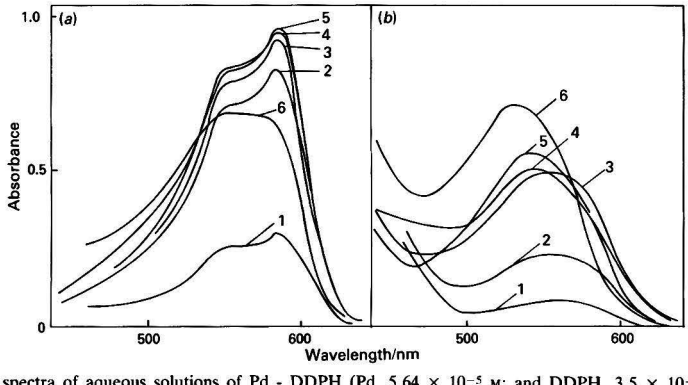

Fig. 2. (*a*) Absorption spectra of aqueous solutions of Pd - DDPH (Pd, 5.64×10^{-5} M; and DDPH, 3.5×10^{-4} M): 1, 3.0 M HCl; 2, 2.0 M HCl; 3, 0.5 M HCl; 4, pH 6.08; 5, pH 9.35; and 6, 0.5 M NaOH. (*b*) Absorption spectra of corresponding extracts ($V_o : V_w = 1:1$, *i.e.*, $V_o = V_w = 10$ ml)

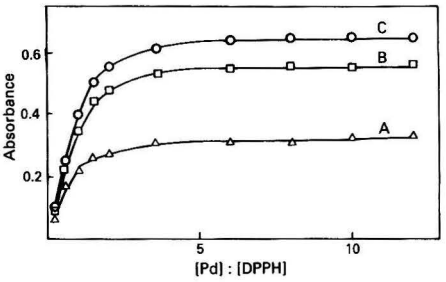

Fig. 4. Effect of DPPH concentration on the extraction of Pd. A, Aqueous solutions (λ = 550 nm); B, extracts (λ = 560 nm); and C, extracts (λ = 585 nm) (Pd, 3.76 × 10^{-5} M and HCl, 0.8 M)

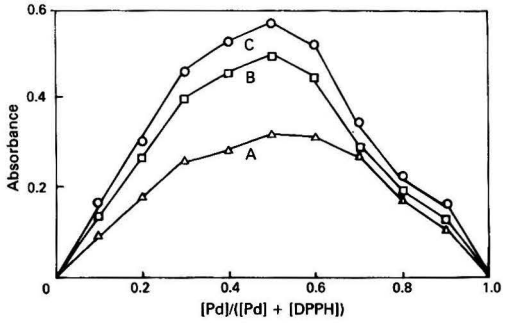

Fig. 5. Determination of the composition of the complex between palladium and DPPH by the continuous variation method. C_{Pd} + C_{DPPH} = 1.0 × 10^{-4} M. A, Aqueous solutions (λ = 550 nm); B, extracts (λ = 560 nm); and C, extracts (λ = 585 nm) (HCl, 0.7 M)

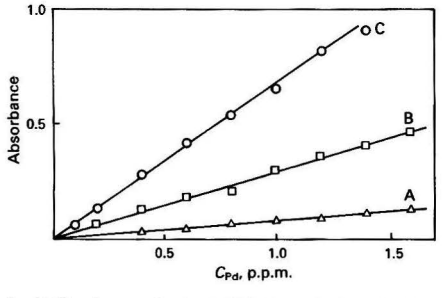

Fig. 6. Calibration graphs for Pd(II) determination. A, Aqueous solutions; B, extracts after two extractions (V_o : V_w = 5 : 20, *i.e.*, V_o = 5 ml, V_w = 20 ml); and C, extracts after one extraction (V_o : V_w = 5 : 20) (DPPH, 3.5 × 10^{-4} M; and HCl, 0.8 M)

Table 1. Precision and accuracy of determination (seven samples taken at each concentration)

Pd present/ µg	Pd found/µg	Largest error, %	Mean Pd found/ µg	Maximum deviation from the mean µg	Maximum deviation from the mean %	Average deviation from the mean µg	Average deviation from the mean %
2	1.97–2.04	2.0	2.01	0.04	2.0	0.03	1.3
8	8.03–8.09	1.1	8.06	0.04	0.5	0.02	0.2
12	11.86–12.00	−1.2	11.93	0.07	0.6	0.04	0.3
20	19.80–20.01	−0.2	19.93	0.13	0.7	0.07	0.3

Table 2. Effect of diverse ions on the determination of palladium(II)

Ion	Added as	Molar ratio
Na^+	NaCl	500
K^+	KCl	500
Ca^{2+}	$CaCl_2$	100
Mg^{2+}	$MgSO_4$	100
Ba^{2+}	$BaCl_2$	100
Al^{3+}	Al_2SO_4	100
Cu^{2+}	$CuSO_4$	100
Co^{2+}	$CoSO_4$	100
Ni^{2+}	$NiSO_4$	100
Zn^{2+}	$ZnSO_4$	100
Cd^{2+}	$CdSO_4$	100
Mn^{2+}	$MnSO_4$	100
Ag^+	$AgNO_3$	100*
Au^{3+}	$AuCl_4^-$	5
Pt	H_2PtCl_6	5
Hg^{2+}	$Hg(NO_3)_2$	50
NH_4^+	$(NH_4)_2SO_4$	100
F^-	NaF	100
Cl^-	NaCl	500
Br^-	NaBr	50
I^-	NaI	50
NO_3^-	$NaNO_3$	100
SO_4^{2-}	Na_2SO_4	500
PO_4^{3-}	$Na_2HPO_4.2H_2O$	100
CH_3COO^-	CH_3COONH_4	100

* After filtration.

single extraction was carried out. The lowest effective volume ratio of aqueous solution to organic solvent for a single extraction was determined. This ratio was found to be 1 : 4. In Fig. 6 results are shown for single and double extraction.

Precision and Accuracy

Results of determinations carried out over the range 2–20 µg of palladium are shown in Table 1.

Effect of Diverse Ions

In order to study the effect of various ions on the determination of palladium(II) with DPPH, a fixed amount (0.8 p.p.m.) of palladium(II) was taken with different amounts of foreign ions and the recommended procedure was followed. An error of ±2% in the absorbance was considered tolerable. Tolerances for various foreign ions are shown in the Table 2.

Comparison with Other Organic Reagents

Several organic reagents have been used for the spectrophotometric determination of palladium. Table 3 presents a comparison of the spectral properties of the palladium(II) complexes with several organic reagents. The present ligand, DPPH, is one of the most sensitive reagents for palladium. The triphenylphosphine - Pd complex[23] does not give a clear peak when the ligand is in excess, and only the 2,2′-bipyridyl 2″-quinolylhydrazone - Pd complex[16] gives a higher molar absorptivity.

As the studied reaction is sensitive (the molar absorptivity of the complex is 1.9 × 10^4 l mol^{-1} cm^{-1}) and the extraction of the formed complex from acidified solutions (0.5–1.5 N HCl) is almost selective, this procedure can be applied successfully to the determination of palladium.

Application

The procedure was applied to the determination of palladium in dental alloys. Samples of dental alloys (noble, precious and semi-precious) were analysed according to the recommended procedure. Table 4 gives the results of the determination of palladium by atomic-absorption spectroscopy and by the DPPH method (average values of three analyses). The full composition of the dental and jewel alloys is given in Table 5.

Table 3. Comparison of some reagents for palladium determination

Organic reagent	Solvent	$\lambda_{max.}$/nm	$\varepsilon_{max.} \times 10^4$/l mol^{-1} cm^{-1}	Ref.
Pyridine-2-aldehyde 2-pyridylhydrazone	*o*-Dichlorobenzene	562	1.65	21
Ethyl 3-phenyl-5-isoxazolone-4-carboxylate	4-Methylpentan-2-ol	370	0.39	22
Triphenylphosphine	Benzene	346(s)*	2.26	23
2-Pyridyl-1-phthalazine hydrazone (PAPhH)	Chloroform	537	1.24	17
2-Quinolyl-1-phthalazine hydrazone (QAPhH)	Chloroform	600	1.37	17
2-Benzothiazolyl-1-phthalazine hydrazone (BAPhH)	Chloroform	587	1.68	17
4-(2-Pyridylazo)resorcinol (PAR)	Mesityl oxide	610	0.39	24
2,2′-Biquinolyl ketone 2″-pyridylhydrazone	Chloroform	624	1.95	25
2,2′-Bipyridyl 2-quinolylhydrazone	Benzene	604	2.21	16
	Chloroform	603	2.01	16
DPPH	Chloroform	585	1.9	—

* s = Shoulder.

Table 4. Results of the determination of palladium in dental and jewel alloys. For full composition of alloys, see Table 5

No. of alloy	Pd found by AAS*	Pd found using DPPH†	Recovery, %
1	24.98	25.22	101
2	31.76	32.09	104
3	81.18	82.50	102
4	21.98	22.10	101
5	11.88	12.60	106
6	18.27	19.47	107
7 (s.a.)‡	2.00	1.90	95
8 (s.a.)	2.85	2.73	96
9 (s.a.)	7.96	7.82	98
10 (s.a.)	8.37	8.16	97

* AAS = atomic-absorption spectroscopy; palladium hollow-cathode lamp; λ = 244.8 nm.

† λ = 585 nm.

‡ s.a. = Standard addition, $100 > [Au]/[Pd] \geqslant 10$.

Table 5. Composition of dental and jewel alloys found by AAS

No. of alloy	Pd, %	Au, %	Pt, %	Ag, %	Cu, %	Zn, %
1	24.98	1.42	0.85	58.71	11.52	1.75
2	31.76	1.54	1.05	56.02	7.03	1.80
3	81.18	6.04	—	5.14	4.37	1.82
4	21.98	1.85	0.83	59.63	13.08	1.73
5	11.88	40.77	—	36.68	8.73	0.95
6	18.27	2.34	1.13	61.97	12.36	1.92
7	2.00	73.05	1.56	14.35	8.36	0.78
8	2.85	69.34	1.28	16.32	8.47	0.75
9	7.96	41.32	—	39.21	9.00	0.75
10	8.37	41.76	—	38.46	9.12	0.71

For noble and precious alloys, where gold is present in large amounts, the standard additions technique was applied after precipitation of the gold by reducing it with sodium sulphite solution.

It was difficult to obtain a standard palladium alloy, so several standard palladium solutions containing gold, platinum, zinc and copper were prepared. The results of the analyses are given in Table 6.

Table 6. Results of analysis of standard palladium solutions. Every sample contained 18 μg of Pd, 10 μg of Zn and 20 μg of Cu (the last two are essential elements in dental alloys)

Sample	Au added/μg	Pt added/μg	Pd found/μg A*	Pd found/μg B†
1	—	9	17.7	
2	—	18	17.8	
3	—	90	17.7	
4	—	200	17.1	17.8
5	—	1000	16.5	17.6
6	9	—	18.2	
7	18	—	17.7	
8	90	—	18.4	
9	200	—	21.2	17.6
10	1000	—	39.3	17.7
11	9	9	17.8	
12	18	18	17.7	
13	200	200	20.6	17.8
14	400	400	21.8	17.6

* A, Found by the recommended procedure; the accepted relative error is ±2%.

† B, Found by the same procedure after precipitation of Au and Pt with Na_2SO_3.

References

1. Alexaki-Tzivanidou, H., *Doctoral Thesis*, University of Thessaloniki, 1972.
2. Vasilikiotis, G. S., Kouimtzis, Th., Apostolopoulou, C., and Voulgaropoulos, A., *Anal. Chim. Acta*, 1974, **70**, 319.
3. Vasilikiotis, G. S., Kouimtzis, Th. A., and Voulgaropoulos, A., *Microchem. J.*, 1977, **22**, 479.
4. Kouimtzis, Th., Apostolopoulou, C., and Staphilakis, I., *Anal. Chim. Acta*, 1980, **113**, 185.
5. Vasilikiotis, G. S., and Alexaki-Tzivanidou, H., *Microchem. J.*, 1981, **26**, 519.
6. Alexaki-Tzivanidou, H., *Microchem. J.*, 1977, **22**, 388.
7. Alexaki-Tzivanidou, H., *Anal. Chim. Acta*, 1975, **75**, 231.
8. Alexaki-Tzivanidou, H., Kounenis, G., and Elezoglou, B., *Microchem. J.*, 1978, **23**, 329.
9. Alexaki-Tzivanidou, H., and Vasilikiotis, G. S., *Microchem. J.*, 1981, **26**, 1.
10. Stratis, J. A., *Doctoral Thesis*, University of Thessaloniki, 1979.
11. Lions, F., and Martin, K. V., *J. Am. Chem. Soc.*, 1958, **80**, 3858.
12. Geldard, J. F., and Lions, F., *J. Am. Chem. Soc.*, 1962, **84**, 2262.
13. Geldard, J. F., and Lions, F., *Inorg. Chem.*, 1963, **2**, 270.
14. Quddus, M. A., and Bell, C. F., *Anal. Chim. Acta*, 1968, **42**, 503.
15. Bell, C. F., and Rose, D. R., *Talanta*, 1965, **12**, 696.
16. Otomo, M., *Anal. Chim. Acta*, 1980, **116**, 161.
17. Otomo, M., and Nakayama, I., *Microchem. J.*, 1980, **25**, 75.
18. Beamish, F. E., and McBryde, W. A. E., *Anal. Chim. Acta*, 1953, **9**, 349.
19. Beamish, F. E., and McBryde, W. A. E., *Anal. Chim. Acta*, 1958, **18**, 551.
20. Furman, N. H., "Standard Methods of Chemical Analysis," Sixth Edition, Volume I, Van Nostrand, New York, 1962, p. 876.
21. Cameron, A. J., and Gibson, N. A., *Anal. Chim. Acta*, 1968, **40**, 413.
22. Corigliano, F., Di Pasquale, S., and Ranieri, A., *Analyst*, 1977, **102**, 25.
23. Mojski, M., and Plesnska, M., *Microchem. J.*, 1979, **24**, 117.
24. Langade, A. D., and Shinde, V. M., *Analyst*, 1982, **107**, 708.
25. Beaupré, P. W., Holland, W. J., and Sieler, R. A., *Microchim. Acta*, 1979, **II**, 479.

Paper A3/162
Received June 3rd, 1983
Accepted September 21st, 1983

Spectrophotometric and Spectrofluorimetric Study of Rose Bengal B and Its Reaction with Platinum(IV)

M. E. Martínez-Izquierdo, J. S. Durand-Alegría, A. Cabrera-Martín and R. Gallego-Andreu
Departamento de Química Analítica de la Facultad de Química and CSIC, Centro Coordinado con la Universidad Complutense de Madrid, Madrid-3, Spain

Aqueous solutions of Rose Bengal B contain four ionic species: H_3R^+ at $H_0 < -4.75$ (where H_0 is the Hammet acidity function for strongly acidic solutions); H_2R at $H_0 > -4.75$, pH < 3.6; HR^- at 3.51 < pH <4.05; and R^{2-} at pH >4.05. The pK for these equilibria in the pH zone are $pK_1 = 3.51$ and $pK_2 = 4.05$ and in the acid function (Hammet function) pK_{a_1}. Polymeric species and excimers have been found in the ground and in first excited state, respectively, at concentrations higher than 10^{-4} M. Pt(IV) reacts with Rose Bengal B giving a colourless solution that does not show any fluorescence. Platinum(IV) has been determined fluorimetrically at concentrations higher than 0.2 p.p.m. The other noble metals do not interfere.

Keywords: *Platinum(IV) determination; spectrophotometry; spectrofluorimetry; photoredox reaction; Rose Bengal B*

Rose Bengal B (2,4,5,7-tetraiodo-3′,4′,5′,6′-tetrachlorofluorescein) (RBB) (CI 45440) is a halogen derivative of fluorescein and shows four species in solution: three within the pH zone (H_2R, HR^- and R^{2-}) and another in the Hammet acidity function (H_0) zone (H_3R^+). The equilibrium constants reported for the aqueous solution are $pK_2 = 3.72$[1] and $pK_1 = 4.4$.[2] Data for the acidity function equilibrium have not been reported.

The absorption spectrum of RBB shows a maximum at 540 nm, which can be assigned to the π - π^* transition within the three-ring system, influenced by a charge transfer from the OH group to the deficient centres of triphenylmethane carbon atoms.[1] The introduction of halogen atoms into the phenyl rings leads to the delocalisation of the π-electrons of the aromatic system, which increases charge transfer from the OH groups. Halogen atoms can also act as electron donors; these effects lead to a red shift in the position of the band relative to that of fluorescein. This red shift is antagonised by the acceptor character of the halogen atom, which increases as the size of the halogen atom decreases, *i.e.*, Cl < Br < I. This can explain the decrease in pK values when the number of halogen atoms in a triphenylmethane derivative is increased.

Rohatgi and Mukhopdhyay[3] suggest that the changes in the absorption spectra of halogen derivatives of florescein are due to the polarisability of the halogen atoms; the greatest bathochromic shift occurs when the resultant of the atomic polarisabilities is the greatest and the dielectric constant of the solvent is the lowest. The associations occur at high concentrations of fluorescein derivatives in high dielectric constant solvents. Owing to the increase in the bathochromic shift as the dielectric constant of the solvent decreases, it has been suggested that the excited state of fluorescein, and its derivatives, is less polar than the ground state, which could account for the occurrence of aggregated species. Nevertheless, an occurrence of associated species has been found in the excited state for RBB.[4]

RBB is used mainly in analysis as a second anionic ligand for cationic chelates,[5–12] as a metallochromic reagent it has only been applied to the determination of Tl(I).[13]

Table 1. Parameters of Rose Bengal B

Species	$\varepsilon \times 10^{-3}$/ l mol^{-1} cm^{-1}	Acidity range† (s_0)	pK	Acidity range† (s^*)	pK^*
H_3R^+	18.25	$H_0 < -4.75$	−4.75	$H_0 < -4.75$	−4.75
H_2R	0.50	$H_0 > -4.75$ to pH < 3.51	3.51	$H_0 > -4.75$ to pH < 3.23	3.23
HR^-	5.50	3.51 < pH<4.05	4.05	3.23 < pH<3.86	3.86
R^{2-}	38.00	pH > 4.05		pH > 3.86	

† s_0 is the ground state; s^* is the first excited electronic state.

Pt(IV) reacts with RBB by a photoredox reaction, giving a colourless solution that does not exhibit fluorescence. This is in agreement with the photooxidant equilibria of $PtCl_6^{2-}$[14] and the non-fluorescent character of the reduced RBB. The mentioned reaction allows the determination of trace amounts of platinum by the quenching of the fluorescence of RBB.

Experimental

Apparatus

The following apparatus was used: a Pye Unicam SP8-200 UV - visible spectrophotometer; a Perkin-Elmer MPF 44A spectrofluorimeter, fitted with an Osram XBO, 150-W xenon lamp; and a low-voltage Halo-Stars 150-W lamp of 20 lm W^{-1}.

Reagents

All reagents were of analytical-reagent grade.

Potassium hexachloroplatinate(IV), K_2PtCl_6. Puriss grade, obtained from Fluka. All noble metals used were of this form.

Rose Bengal B, 82%. Purum grade, obtained from Serva.

Procedure

To solutions of $PtCl_6^{2-}$ add 0.5 ml of a 0.01 M ammonia - ammonium chloride buffer solution of pH 9.0 and 2.5 ml of a 10^{-4} M Rose Bengal B solution; dilute with distilled water to 10.0 ml. Measure the absorbance of the solutions, after irradiating each solution for 15 min with a halogen lamp, against a blank prepared under the same conditions. The measurements of the relative intensity of fluorescence are carried out at 568 nm by exciting the solution as well as the blank, at 550 nm, after irradiating each solution for 15 min with a halogen lamp.

Results

Acid - Base Characteristics of RBB

Absorption (or excitation) and emission spectra and the absorbance and relative intensity *versus* [H$^+$] graphs (Fig. 1) show that RBB has three coloured and fluorescent species and another coloured and non-fluorescent one, which corresponds to the uncharged species. The four species correspond to a protonated quinone group (H_3R^+), a molecular group (H_2R), an ionised carboxylic group (HR^-) and to one that has both carboxylic and phenolic ionised groups (R^{2-}) (whose optical characteristics are shown in Table 1), respectively.

The related dissociation constants can be calculated independently for sufficiently separated steps. For the equilibria

$$H_nR \overset{K_{a_n}}{\rightleftharpoons} H_{n-1}R + H^+$$

the following equations hold[15]:

$$C_R/A = 1/\varepsilon_{H_nR} + K_{a_n}(A - C_R\varepsilon_{H_{(n-1)}R})/A\,[H^+]\varepsilon_{H_nR}$$

$$C_R/A = 1/\varepsilon_{H_{(n-1)}R} + (A - C_R\varepsilon_{H_nR})[H^+]/K_{a_n}A\varepsilon_{H_{(n-1)}R}$$

$$\mathrm{Log}(C_R\varepsilon_{H_nR} - A)/(A - C_R\varepsilon_{H_{(n-1)}R}) = \log K_{a_n} + \mathrm{pH}$$

where 10^{-H_0} replaces $[H^+]$ when in high concentration in a sulphuric acid medium[16]; H_0 is the Hammet acidity function for strongly acidic solutions; C_R, the concentration of RBB; A, the absorbance; and ε, the molar absorptivity.

The pK_{a_η} in the excited state has been calculated with the same criteria, but using the Förster cycle[17] (Fig. 1, Table 1).

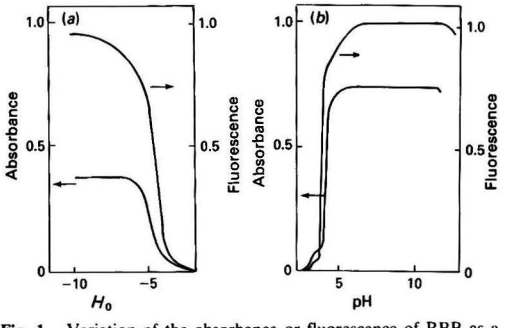

Fig. 1. Variation of the absorbance or fluorescence of RBB as a function of $[H^+]$. (*a*) [RBB] = 2×10^{-5} M; (*b*) [RBB] = 1×10^{-5} M

Influence of Concentration on the Absorbance and Fluorescence Emission of RBB

A high concentration of RBB decreases the absorbance because of the tendency of RBB molecules to dimerise. The dimer shows two absorption bands in the spectra, one at 567 nm and the other at 522 nm. The monomer shows only one band at 548 nm, which is hypochromic relative to that of the dimer bands. These results are in agreement with those of Rohatgi and Mukhopadhyay.[18]

Dimers occur at concentrations higher than 10^{-4} M; at this optimum level of concentration excimers have also been observed (Fig. 2).

By graphical analysis of the plot of fluorescence (%) *versus* [RBB] (inset in Fig. 2) it can be seen that the decreasing fluorescence is due to excimer formation and inner filter action, which agrees with the results of Kishore *et al.*[4]

Reaction of Pt(IV) and RBB

Pt(IV) reacts with RBB, after being irradiated for 15 min with a halogen lamp, in the pH range 8–10.[19] The discolouration reaction, accompanied by a loss of fluorescence, may be due to a photoredox reaction.

Detailed studies have been carried out on the photochemical exchange of Cl^- with $PtCl_6^{2-}$,[20] which, including the effect of oxidising and reducing agents on the energetic exchange, showed that a chain mechanism occurs. The catalytic effect was attributed to the Pt(III) species (assumed to be $PtCl_5^{2-}$) produced by a photoredox reaction:

$$PtCl_6^{2-} \xrightarrow{h\nu} PtCl_5^{2-} + Cl$$
$$PtCl_5^{2-} + Cl^{-*} \rightleftharpoons PtCl_5^{2-*} + Cl^-$$
$$PtCl_5^{2-*} + PtCl_6^{2-} \rightleftharpoons PtCl_5^{2-} + PtCl_6^{2-*}$$

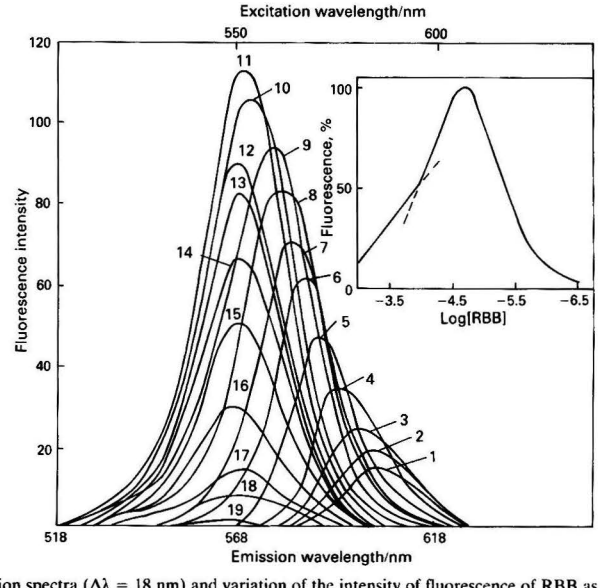

Fig. 2. Synchronous excitation spectra ($\Delta\lambda$ = 18 nm) and variation of the intensity of fluorescence of RBB as a function of its concentration ($\times 10^{-5}$ M), which were as follows:

Graph	[RBB]	Graph	[RBB]	Graph	[RBB]	Graph	[RBB]
1	100	6	10	11	2	16	0.2
2	80	7	8	12	1	17	0.1
3	60	8	6	13	0.8	18	0.05
4	40	9	5	14	0.6	19	0.01
5	20	10	3	15	0.4		

The quantum yield was found to increase with increasing temperature, and it also depended, in a complicated way, on the light intensity, wavelength of excitation and Cl^- concentration. These effects were attributed to the oxidation of a chain-carrier Pt(II) complex (considered to be present as an impurity in K_2PtCl_6) by chlorine atoms, which were thought to be formed in the first step of the above reaction sequence. However, the evidence of formation of $PtCl_5^{2-}$ has been obtained from the reaction between $e^-_{aq.}$ and $PtCl_6^{2-}$.[21]

On the other hand, studies carried out on the tetraiodofluorescein[22] showed that three polarographic waves at −0.55, −0.80 and −1.2 V *versus* S.C.E. with relative intensities of 1:2:2, respectively, were obtained. Because it is known that the first wave is associated with the reduction of the quinone group, by exchanging two electrons, the other two waves may correspond to two processes in which a four-electron exchange takes place in each one. The only reducible functions are the C–I bonds. It is also known that the electrochemical reduction of aryliodine needs two electrons for each molecule and the two well separated reduction steps imply that two positions of iodine in the molecule show a greater facility to be reduced than the other two. Those positions are 4 and 5.

As the observed stoicheiometry of the reaction gave the molar ratio of Pt(IV) : RBB as 3 : 1, it can be assumed that only two iodine atoms are reduced [those at C(4)and C(5)].

From these observations the following reaction mechanism can be deduced:

$$PtCl_6^{2-} \xrightarrow{h\nu} PtCl_5^{2-} + Cl$$

$$PtCl_5^{2-} + Cl^- \rightleftharpoons PtCl_5^{2-*} + Cl^-$$

and/or

$$3PtCl_5^{2-*} + RBB_{ox.} \longrightarrow 3PtCl_6^{2-} + RBB_{red.}$$

$$3Pt(II) + RBB_{ox.} \xrightarrow{Cl^-} 3PtCl_6^{2-} + RBB_{red.}$$

The reduced species of RBB shows no fluorescence because of the lack of conjugated double bonds.

Influence of the Time of Irradiation and pH

When Pt(IV) is present in a solution of pH 8–10, which contains RBB, no reaction is observed if sunlight or any lamp providing light of the same wavelength is absent. The reaction is complete after 15 min if the solution is irradiated by sunlight or a halogen lamp and in a medium that provides Cl^- ions, because the reaction mechanism requires Cl^- ions.

The optimum conditions for carrying out fluorescence emission (or absorbance) measurements are at a pH of 9.0 in an ammonia - ammonium chloride buffer solution, because in this way not only are Cl^- ions supplied but enough NH_3 molecules also, to complex any noble metals cations such as silver(I) that could interfere in the reaction.

Calibration Graph

As the fluorescence measurements are more sensitive than the absorbance measurements, the determination of platinum(IV) was carried out by a fluorimetric method. A linear relationship was obtained for 0.20–9.75 p.p.m. of platinum, when 2.0×10^{-5} M RBB was present, at a $\lambda_{ex.}$ of 550 nm and a $\lambda_{em.}$ of 568 nm. The limit of detection of platinum by this method is 0.20 p.p.m. for a signal to noise ratio of 3.

Statistical Analysis of Results

Precision was determined by taking the standard deviation (s) of the fluorescence of ten replicate solutions to give $s = 0.7$ in units of relative intensity of fluorescence, which corresponds to $s = 0.05$ p.p.m. of Pt(IV). The arithmetic mean ($\bar{X}$) for these measurements = 1.89 p.p.m.; the relative standard deviation (s%), = 2.6%; the confidence limit ($\bar{X} \pm s_{\bar{X}} t$) = 1.89 ± 0.03 p.p.m.; the number of degrees of freedom = 9; and t = 2.26 (95% probability level).

Interferences

The interference of noble metal cations was studied by mixing 1 ml of 10^{-4} M platinum(IV) solution, noble metal cation, ammonia - ammonium chloride buffer solution and 2 ml of 10^{-4} M RBB solution and then diluting according to the procedure. The results of these studies are shown in Table 2. According to the literature[5-12] and the results of experiments carried out in our laboratories[19] no cation reacts with RBB at this pH to form binary or ternary complexes or in a photoredox reaction. Therefore, we can conclude that this method does not present interferences if the Kirkbright criterion ($I_r = I_{r_0} \pm 2s$) (where I_r is the relative intensity of fluorescence)[23] is considered.

Table 2. Influence of noble metals ions

Interference	Metal ion: Pt(IV) molar ratio	I_r
Pt(IV)	—	23.0
Au(III)	1:1	22.5
Ru(III)	1:1	23.2
Rh(III)	1:1	23.2
Pd(II)	1:1	22.0
Os(VIII)	1:1	22.0
Ir(IV	1:1	22.0
Ag(I)	1:1	23.0

References

1. Issa, I. M., Issa, R. M., and Ghoneim, M. M., *Z. Phys. Chem.*, 1972, **3/4**, 161.
2. Stolyarov, K. P., and Firyulina, V. U., *Zh. Anal. Khim.*, 1971, **26**, 1731.
3. Rohatgi, K. K., and Mukhopadhyay, A. K., *J. Indian Chem. Soc.*, 1972, **49**, 1311.
4. Kishore, J., Machwe, M. K., Krishnan, K. G., and Chanhuri, K. D., *Indian J. Phys.*, 1962, **36**, 415.
5. Bailey, B. W., Dagnall, R. M., and West, T. S., *Talanta*, 1966, **13**, 753.
6. Bailey, B. W., Dagnall, R. M., and West, T. S., *Talanta*, 1966, **13**, 1661.
7. Dagnall, R. M., El-Ghamry, M. T., and West, T. S., *Talanta*, 1968, **15**, 1353.
8. Bailey, B. W., Chester, J. E., Dagnall, R. M., and West, T. S., *Talanta*, 1968, **15**, 1359.
9. Stolyarov, K. P., and Firyulina, V. V., *Zh. Anal. Khim.*, 1971, **26**, 1731.
10. Tananaiko, M. M., and Bilenko, N. S., *Zavod. Lab.*, 1974, **40**, 1049.
11. Tananaiko, M. M., *Khim. Teknol.*, 1975, **18**, 893.
12. Tananaiko, M. M., and Bilenko, N. S., *Zh. Anal. Khim.*, 1975, **30**, 689.
13. Dragulescu, C., and Mitranescu, M., *Bul. Stiint. Teh. Inst. Politeh. Timisoara, Ser. Chim.*, 1973, **18**, 51.
14. Balzani, V., and Carrassiti, V., "Photochemistry of Coordination Compounds," Academic Press, New York, 1970, p. 257.
15. González, V., and Sánchez-Pedreño, C., *Ion*, 1975, **35**, 254.
16. Liler, M., "Reaction Mechanisms in Sulfuric Acid and other Strong Acid Solutions," Academic Press, New York, 1971, p.37.
17. Förster, T., *Z. Elektrochem.*, 1950, **54**, 42.
18. Rohatgi, K. K., and Mukhopadhyay, A. K., *Photochem. Photobiol.*, 1971, **14**, 551.
19. Cabrera, A., Durand, J. S., and Martínez, M. E., unpublished work.
20. Rich, R. L., and Taube, H., *J. Am. Chem. Soc.*, 1954, **76**, 2608.
21. Adams, G. E., Brosakiewicz, R. B., and Michael, B. D., *Trans. Faraday Soc.*, 1968, **64**, 1256.
22. Board, P. W., Britz, D., and Holland, R. V., *Electrochim. Acta*, 1968, **13**, 1575.
23. Kirkbright, G. F., *Talanta*, 1966, **13**, 7.

Paper A3/232
Received June 21st, 1983
Accepted October 25th, 1983

Spectrophotometric Method for the Determination of Vanadium and its Application to Vanadium Steels Containing Chromium, Molybdenum, Manganese, Copper and Nickel

H. Sanke Gowda and A. Thimme Gowda
Department of Postgraduate Studies and Research in Chemistry, University of Mysore, Manasagangotri, Mysore-570 006, India

Prochlorperazine bismethanesulphonate is proposed as a selective and sensitive reagent for the spectrophotometric determination of vanadium. The reagent forms a red species with vanadium(V) instantaneously in 3.5–6 M orthophosphoric acid medium. A 15-fold molar excess of the reagent is necessary for the full development of the colour intensity. The red species exhibits an absorption maximum at 529 nm with a molar absorptivity of 1.24×10^4 l mol^{-1} cm^{-1}. Beer's law is obeyed over the range 0.1–6.2 p.p.m. of vanadium(V) with an optimum concentration range of 0.3–5.8 p.p.m. The effects of acidity, time, temperature, order of addition of reactants, reagent concentration and interferences from various ions are reported. The method has been used successfully for the determination of vanadium in vanadium steels containing chromium, molybdenum, manganese, copper and nickel.

Keywords: *Vanadium determination; vanadium steels; spectrophotometry; prochlorperazine bismethanesulphonate reagent*

Most of the reagents proposed for the spectrophotometric determination of vanadium are either extractive-photometric reagents[1–9] or require heating for maximum colour development.[10–12] The deficiencies of many of these reagents are narrow ranges of determination, lengthy procedures and interference by common ions. For example, 4-(2-pyridylazo)resorcinol[13] was proposed as the most sensitive reagent in the narrow range 0.04–1.00 p.p.m. The reagent absorbs strongly at the wavelength of maximum absorption of the complex. In addition, it does not tolerate the presence of uranium(VI), niobium(V), titanium(IV) and zinc(II). 2-(3,5-Dibromo-2-pyridylazo)-5-dimethylaminophenol[14] cannot be used in the presence of iron(III), chromium(III), copper(II) and titanium(IV). 4-Methoxybenzothiohydroxamic acid,[15] 3-hydroxy-2-methyl-1-phenylpyridin-4-one,[16] 4-hydroxy-3-salicylideneaminobenzenesulphonic acid,[17] 4-benzoyl-3-methyl-1-phenylpyrazolin-5-one[18] and pyridin-4-one[19] are not satisfactory in the presence of iron(III), niobium(V), titanium(IV), molybdenum(VI) and tungsten(VI).

In this paper, we report an investigation into the reaction of prochlorperazine bismethanesulphonate {PCPMS; 3-chloro-10-[3-(4-methyl-1-piperazinyl)propyl]phenothiazine bismethanesulphonate} with vanadium(V), and propose PCPMS as a sensitive reagent for the spectrophotometric determination of vanadium(V). The proposed method offers the advantages of simplicity, selectivity, high sensitivity and a wide range of determination without the need for extraction or heating.

Experimental

Reagents

Vanadium(V) solution. Prepare a stock solution of vanadium(V) from AnalaR-grade sodium metavanadate in doubly distilled water and standardise it with standardised iron(II) solution. Dilute this stock solution suitably to give a standard solution containing 25 μg ml^{-1} of vanadium(V).

Prochlorperazine bismethanesulphonate. Prepare a 0.1% *m/V* solution of PCPMS in doubly distilled water and store in an amber-coloured bottle in a refrigerator.

Solutions of foreign ions. Prepare solutions of various ions of suitable concentrations by using analytical-reagent grade reagents.

Instrument

A Beckman Model DB spectrophotometer with matched 1-cm silica cells was used for absorbance measurements.

Procedure and Preparation of Calibration Graph

Transfer aliquots of the stock solution containing 2.5–155 μg of vanadium(V) into a series of 25-ml calibrated flasks. Add 12.5 ml of 10 M phosphoric acid and 2 ml of 0.1% PCPMS solution to each flask and dilute to the mark with doubly distilled water. Mix well and measure the absorbance at 529 nm against the corresponding reagent blank. The graph of absorbance *versus* concentration of vanadium is a straight line passing through the origin. Determine the absorbance of the sample containing vanadium by the method described for the preparation of the calibration graph. Deduce the vanadium concentration of the sample solution from the calibration graph.

Procedure for the Determination of Vanadium in Vanadium Steels

Transfer an accurately weighed amount of vanadium steel (about 0.5 g) into a covered 250-ml beaker and treat with 15 ml of 5 M sulphuric acid, 2 ml of orthophosphoric acid (sp. gr. 1.75) and 1 ml of concentrated nitric acid. Boil the solution gently to dissolve the sample, expel the oxides of nitrogen, cool and dilute to 50 ml with doubly distilled water. Add 0.01 M potassium permanganate solution dropwise until the solution just appears pale pink in order to oxidise any vanadium(IV) to vanadium(V). Allow the solution to stand for 5 min, then warm and add 0.005 M oxalic acid solution slowly, with stirring, until the pale pink colour of the solution disappears. Transfer the solution into a 100-ml calibrated flask and dilute to the mark with doubly distilled water. A suitable aliquot of this solution and 40 mg of sodium citrate are used for the reaction with PCPMS as described under Procedure and Preparation of Calibration Graph. Measure the absorbance at 529 nm and read the vanadium concentration from the calibration graph.

Results on four samples of vanadium steel are given in Table 1.

Results and Discussion

Vanadium(V) reacts with PCPMS instantaneously at room temperature (27 °C) in orthophosphoric, sulphuric or hydrochloric acid medium to form a red species that is believed to be a radical cation.[20,21] The sensitivity and stability of the red species depend on the nature and concentration of

Table 1. Determination of vanadium in vanadium steels

Sample	Certified composition, %*	Vanadium content of solution, %†	
		Supplier's value	Found value
AISIH-11	C, 0.41; Si, 0.99; Mn, 0.27; P, 0.019; S, 0.011; Ni, 0.14; Cr, 5.06; Mo, 1.20; Cu, 0.14; V, 0.49	0.49	0.50
Heat No. 6 4828, 58 CrV4	C, 0.61; Si, 0.29; Mn, 0.86; P, 0.033; S, 0.011; Ni, 0.14; Cr, 1.12; Mo, 0.12; Al, 0.017; V, 0.09	0.09	0.09
20 CrI Mo95 V 85 Ti B ..	C, 0.21; Si, 0.35; Mn, 0.41; P, 0.017; S, 0.011; Ni, 0.16; Cr, 1.25; Mo, 0.94; Ti, 0.06; B, 0.0046; Cu, 0.11; V, 0.96	0.96	0.97
T 100 V 25	C, 1.04; Si, 0.17; Mn, 0.36; P, 0.015; S, 0.008, Ni, 0.1; Cr, 0.2; Mo, 0.03; Cu, 0.1; V, 0.245	0.245	0.25

* These values were given by the suppliers of the samples.

† A known mass of sample was dissolved and aliquots of the solution were diluted to give solutions containing three different levels of vanadium. These values, calculated from the vanadium content certified by the supplier, are expressed as the supplier's value. The results quoted as found are the means of five determinations on each solution.

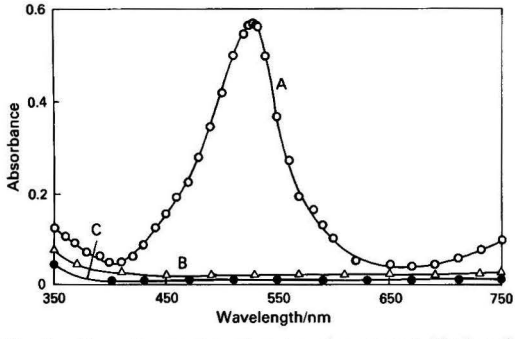

Fig. 1. Absorption spectra of red species, reagent blank and vanadium(V) in 5 M orthophosphoric acid. (A) red species of PCPMS; concentration of vanadium(V), 2 p.p.m. (B) Reagent blank; concentration of PCPMS, 0.08%. (C) Vanadium(V); concentration of vanadium(V), 2 p.p.m.

the acid medium. The red colour is not stable in either sulphuric or hydrochloric acid. Orthophosphoric acid medium is recommended because the red colour is stable for 40 min, and the reaction is more sensitive and also subject to less interference from foreign ions.

Spectral Characteristics

The absorption spectra of the red species, the reagent blank and vanadium(V) in 5 M phosphoric acid are shown in Fig. 1. The red species exhibits maximum absorption at 528–530 nm. The reagent blank and the metal ion under similar conditions do not absorb appreciably around this wavelength, thus promoting excellent analytical conditions. Therefore, subsequent studies were carried out at 529 nm.

Effect of Acid Concentration

The effect of orthophosphoric acid concentration on the absorption of the red species was studied at 529 nm with solutions containing 2 p.p.m. of vanadium(V). The absorbance increases gradually with increasing acid concentration from 0.5 to 3.5 M and then reaches a maximum over the acid range 3.5–6.0 M. At acidities higher than 6 M, the reagent slowly gives a red colour which increases the absorbance. An acid strength of 5 M was therefore chosen for all further work.

Effect of Reagent Concentration

The effect of reagent concentration was examined by measuring the absorbance of solutions containing 2 p.p.m. of vanadium(V) and various amounts of reagent. A 15-fold molar excess of the reagent is necessary for maximum colour development. The optimum amount of 2 ml of 0.1% reagent solution was used in a final volume of 25 ml of solution.

Table 2. Precision and accuracy of the determination of vanadium(V)

Amount of vanadium(V), p.p.m.		Relative error, %	Standard deviation, p.p.m.
Taken	Found*		
1.0	1.01	+1.00	0.0055
2.0	2.01	+0.55	0.0257
3.0	2.98	−0.66	0.0358
4.0	4.05	+1.25	0.0124
5.0	4.98	−0.4	0.0185

*Average of ten determinations.

There is no appreciable change in the absorbance if the order of addition of reactants is varied. The absorbance is not affected in the range 5–60 °C. Above 60 °C the absorbance gradually decreases with increase in temperature. The precision and accuracy of the method have been studied by analysing solutions containing known amounts of vanadium. The results are summarised in Table 2.

Validity of Beer's Law and Sensitivity

Beer's law is obeyed in the range 0.1–6.2 p.p.m. of vanadium(V) at 529 nm. The optimum concentration range for the effective spectrophotometric determination of vanadium(V) by Ringbom's method is 0.3–5.8 p.p.m. For log (I_o/I), the photometric sensitivity of the reaction calculated from Beer's law data is 5.14 ng cm^{-2} and the molar absorptivity is 1.24×10^4 l mol^{-1}cm^{-1}.

Effect of Diverse Ions

The effects of some ions that often accompany vanadium were studied by adding different amounts to 2 p.p.m. of vanadium(V) in solution. The colour was developed as outlined in the procedure. An error of 2% in the absorbance reading was considered tolerable. The tolerance limits of various ions are shown in Table 3. The major advantage of the proposed method is that the iron(III) which is associated with vanadium steel is tolerated up to 6000 p.p.m. in the presence of orthophosphoric acid and citrate.

Coloured species such as chromium(III) and nickel(II) do not absorb appreciably at the $\lambda_{max.}$ of the red species of PCPMS and therefore there is little interference in the determination of vanadium(V).

Table 3. Effect of diverse ions on the determination of vanadium(V). Amount of vanadium(V) taken = 2 p.p.m.

Ion added	Tolerance limit,* p.p.m	Ion added	Tolerance limit,* p.p.m.
Fe(III)	3 200	Ti(IV)	1 720
Fe(III)†	6000	Zr(IV)	650
Cu(II)	450	Cr(III)	480
Ni(II)	420	Mn(III)	2800
Co(II)	340	As(III)	650
Pt(IV)	20	Fluoride	3600
Rh(III)	45	Chloride	9000
Ir(III)	60	Bromide	9000
Zn(II)	9000	Iodide	0.1
Mg(II)	3 600	Nitrate	10 000
Pb(II)	800	Sulphate	18 000
Al(III)	930	Acetate	10 000
Mo(VI)	1 350	Citrate	1 600
Cd(II)	9 000	Oxalate	9 000
Hg(II)	750	Tartrate	640
W(VI)	240	EDTA	120
U(VI)	1 300		

* Amount of diverse ions causing an error of less than 2%.
† In the presence of 40 mg of sodium citrate.

Analysis of Vanadium Steels

The results given in Table 1 show that vanadium can be selectively determined in the presence of large amounts of iron(III), chromium(III), aluminium(III), tungsten(VI), molybdenum(VI), copper(II), nickel(II) and titanium(IV). The values obtained with PCPMS compare favourably with the certified values for vanadium.

The sensitivity of the proposed method is higher than that with tropolone,[22] 7-(2-anilinobenzyl)-8-hydroxyquinoline,[23] 8-hydroxyquinoline,[24] 3-hydroxy-2-methyl-1-(*p*-tolyl)-4-pyridine,[25] haematoxylin,[26] *N*-*p*-methylbenzyl-*N*-*p*-methylphenylhydroxylamine,[27] bis(2-aminophenyl) disulphide[28] and *N*-allyl-*N*^{1}-(*p*-benzoylglycine)thiourea,[29] which have been proposed as sensitive spectrophotometric reagents for vanadium(V).

The authors thank May and Baker Limited, India, for supplying pure PCPMS and Hindustan Steel Limited and Mahindra Ugina Steel Co. Limited, India for supplying vanadium steels. One of the authors (A.T.G.) is grateful to the University Grants Commission, New Delhi, University of Mysore, and D.V.S. College of Arts and Science, Shimoga, for the award of a Teacher Fellowship under the Faculty Improvement Programme.

References

1. Abbasi, S. A., *Anal. Lett.*, 1976, **9**, 113.
2. Anjaneyulu, Y., Sarma, B., Siva, R., and Panduranga Rao, V., *Anal. Chim. Acta*, 1976, **86**, 313.
3. Gusakova, N. N., Eremenko, S. N., Mushtakova, S. P., and Frumina, N. S., *Zh. Anal. Khim.*, 1975, **30**, 721.
4. Nripendra, N. G., and Gautam, S., *Fresenius Z. Anal. Chem.*, 1971, **253**, 207.
5. Pogranichnaya, R. M., Riznik, B. E., Nerubashchenko, V. V., Zezyanova, A. G., and Tsevina, A. V., *Zh. Anal. Khim.*, 1975, **30**, 180.
6. Caramlau, M., Duca, A., and Moroi, G., *Rev. Chim. (Bucharest)*, 1978, **29**, 983.
7. Gallego, M., Garcia-Vargas, M., and Valcarcel, M., *Microchem. J.*, 1979, **24**, 143.
8. Beaupre, P. W., and Holland, W. J., *Mikrochim. Acta*, 1980, **I**, 271.
9. Patel, K. S., Deb, K. K., and Mishra, R. K., *J. Chin. Chem. Soc. (Taipei)*, 1982, **29**, 107.
10. Barkovskii, V. F., and Novoselova, I. M., *Zh. Anal. Khim.*, 1974, **29**, 1654.
11. Doadrio, A., Garcia Carro, A., and de Frutos, M. I., *Quim. Anal.*, 1975, **29**, 331.
12. Sharma, Y., *Mikrochim. Acta*, 1982, **II**, 305.
13. Budevsky, O., and Johnova, L., *Talanta*, 1965, **12**, 291.
14. Gusev, S. I., Poplevina, L. V., and Shalamova, G. G., *Uch. Zap. Permsk. Gos. Univ.*, 1968, **178**, 214.
15. Skorko-Trylula, Z., *Chem. Anal. (Warsaw)*, 1965, **10**, 831.
16. Vojkovic, V., Tamhina, B., and Herak, M. J., *Fresenius Z. Anal. Chem.*, 1975, **276**, 377.
17. Zenki, M., and Iwaki, K., *Bunseki Kagaku*, 1979, **29**, 710.
18. Akama, Y., Nakai, T., and Kawamura, F., *Analyst*, 1981, **106**, 250.
19. Tamhina, B., Vojkovic, V., and Herak, M. J., *Microchem. J.*, 1980, **25**, 8.
20. Dwivedi, P. C., Gurudath Rao, S. N., Bhat, S. N., and Rao, C. N. R., *Spectrochim. Acta, Part A*, 1975, **31**, 129.
21. Stan., M., Dorneanu, V., and Ghimicescu, G. H., *Talanta*, 1977, **24**, 140.
22. Rizvi, G. H., and Singh, R. P., *Talanta*, 1972, **19**, 1198.
23. Bhatt, Y. N., Patel, K. K., Shah, K. J., and Patel, R. S., *Indian J. Chem.*, 1975, **13**, 847.
24. Bermejo-Barrera, P., Bermejo-Berrera, A., and Bermejo-Martinez, F., *Microchem., J.*, 1980, **25**, 458.
25. Tamhina, B., Vojkovic, V., and Herak, M. J., *Croat. Chem. Acta*, 1976, **48**, 183.
26. Valero, J., *Afinidad*, 1979, **36**, 421.
27. Bag, S. P., and Saha, S., *Indian J. Chem.*, 1980, **19A**, 358.
28. Raje, R. B., and Sane, R. T., *J. Indian Chem. Soc.*, 1977, **54**, 416.
29. Mathur, S. P., Mehta, V. P., Bhandari, C. S., and Sogani, N. C., *An. Quim.*, 1978, **74**, 1568.

Paper A3/254
Received August 8th, 1983
Accepted September 29th, 1983

Spectrophotometric Study of Binary and Ternary Systems Involving Metal Ions and Benzylidenepyruvates: Equilibria in Aqueous Solutions

Cristo B. Melios,* Vera R. Torres, Márcia H. A. Mota, João O. Tognolli and Manuel Molina
Instituto de Química, UNESP, Caixa Postal 174, Araraquara (SP), 14.800, Brazil

The protonation of 4-dimethylaminobenzylidenepyruvate (DMBP) and 2-chloro-4-dimethylaminobenzylidenepyruvate (2-Cl-DMBP) and their complex formation with Mn(II), Co(II), Ni(II), Cu(II), Zn(II), Pb(II), Cd(II) and Al(III) have been studied by potentiometric and spectrophotometric methods at 25 °C and ionic strength 0.500 M, held with sodium perchlorate. The stability order found for 1:1 complexes of both ligands is Al(III) > Cu(II) > Pb(II) > Ni(II) > Zn(II) > Co(II) > Cd(II) > Mn(II). The stability changes move in the same direction as the pK_a of the ligands. The results are compared with literature values reported for metal ion - pyruvate systems. Thermodynamic stabilities of ternary complexes formed in Cu(II) - B - L^- systems, where B = 2,2′-bipyridyl (bipy), ethylenediamine or glycinate and L^- = DMBP or 2-Cl-DMBP, were also determined. The Cu(bipy)L^+ species are more stable than would be expected on purely statistical grounds. The importance of the π system associated with bipy on the enhanced stability of its mixed ligand complexes is stressed. Analytical applications of the investigated ligands are outlined.

Keywords: *Spectrophotometry; benzylidenepyruvates; binary and ternary metal ion complexes; equilibria*

In view of the increased significance of keto acids in analytical, biological, pharmaceutical and industrial fields,[1-9] there has been considerable interest in their complexing tendency with several metals.[10-14] The benzylidenepyruvic acids and some of their salts are a group of α-keto acids at present under investigation in this laboratory as gravimetric and spectrophotometric analytical reagents; some of their reactions with metal ions give intensely coloured complexes. A knowledge of the thermodynamic stability of metal ion - benzylidenepyruvate systems is highly desirable for their proper use in analytical work.

This paper deals mainly with complex formation equilibria in M - L systems, where M = Mn(II), Co(II), Ni(II), Cu(II), Zn(II), Pb(II), Cd(II) and Al(III) and L = 4-dimethylaminobenzylidenepyruvate (DMBP) and 2-chloro-4-dimethylaminobenzylidenepyruvate (2-Cl-DMBP), at 25 °C and ionic strength (*I*) 0.500 M, adjusted by adding sodium perchlorate.

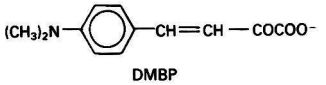

DMBP

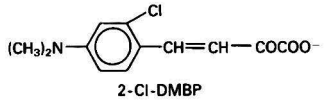

2-Cl-DMBP

As spectrophotometric methods for determining metal ions and anions based on ternary systems are generally far more sensitive than methods based on binary systems,[15] the equilibrium studies were extended to include mixed ligand complexes formed in Cu(II) - B - L systems, where B = 2,2′-bipyridyl, ethylenediamine and glycinate. The results reported are discussed mainly in connection with published stability constants for metal ion - pyruvate complexes.

Experimental

Reagents

Distilled, de-ionised water was used throughout and chemicals were of analytical-reagent grade unless indicated otherwise.

Copper(II), nickel(II), cobalt(II), manganese(II), zinc(II), lead(II) and cadmium(II) perchlorates were prepared from 30% perchloric acid and the corresponding carbonates, a slight excess of the carbonates being employed. Aluminium(III) perchlorate was prepared from aluminium chloride and silver perchlorate, as recommended by Acerete and Lacal.[16] Stock solutions of metal ions were standardised by complexometric titration with EDTA. Sodium perchlorate was prepared by reaction of perchloric acid with sodium hydroxide. Stock solutions of this salt were analysed by evaporating an aliquot and drying to constant mass at 130 °C. All sodium hydroxide solutions were freshly prepared to be as free from carbonate as possible and standardised potentiometrically against potassium hydrogen phthalate.

Sodium 4-dimethylaminobenzylidenepyruvate and the corresponding acid were synthesised by the following procedure. An aqueous solution of sodium pyruvate (24 g per 200 ml) is added dropwise, with continuous stirring, to a methanolic solution of 4-dimethylaminobenzaldehyde (28 g per 400 ml). The system is diluted with 250 ml of water and 250 ml of 10% sodium hydroxide solution are slowly added while the solution is stirred and cooled in an ice-bath. The rate of addition of the alkali is so regulated that the temperature remains between 12 and 16 °C. The system is left to stand for 24 h at room temperature (23–28 °C). The pale yellow precipitate formed is filtered off and discarded. The orange - red filtrate is diluted by adding 300 ml of water and carefully acidified with 3 M hydrochloric acid to pH 5.2–5.4, with ice - water cooling and stirring. The resulting system is vigorously shaken with five successive 200-ml portions of chloroform, to remove unreacted aldehyde and by-products. The aqueous layer is further acidified to pH 2.0–2.5 with 3 M hydrochloric acid and then quickly extracted with three 200-ml portions of chloroform. The combined chloroform extract is filtered and dried over 50 g of anhydrous sodium sulphate and then evaporated to dryness under reduced pressure from a water-bath maintained at 45–50 °C. The crude product (4-dimethylaminobenzylidenepyruvic acid, 5.8 g) is suspended in 200 ml of water and treated dropwise with 0.5 M sodium hydrogen carbonate solution to pH 5.8–6.0. The remaining precipitate is filtered off and the filtrate is evaporated at 60 °C under reduced pressure. The yellow residue (sodium 4-dimethylaminobenzylidenepyruvate) is recrystallised from boiling 1,4-dioxane - water (50% *V/V*) and dried at 110 °C (4.5 g). Pure 4-dimethylaminobenzylidenepyruvic acid could not be obtained according to the procedure recommended by Kageura *et al.*[17] The

* To whom correspondence should be addressed.

compound was finally obtained by dissolving the purified sodium salt in water, acidifying with hydrochloric acid and extracting with chloroform, as described above (yield: 0.62 g, starting with 1.0 g of the sodium salt). The acid is a reddish brown solid, m.p. 143.1–144.0 °C. Analysis: calculated for $C_{12}H_{13}O_3N$, C 65.74, H 5.98, N 6.39; found, C 65.51, H 6.00, N 6.32%.

Sodium 2-chloro-4-dimethylaminobenzylidenepyruvate was prepared by a closely related procedure in which 4-dimethylaminobenzaldehyde is replaced with an equivalent amount (32.5 g) of 2-chloro-4-dimethylaminobenzaldehyde. The yields of the crude and recrystallised salt were 5.5 and 4.7 g, respectively, and the yield of 2-chloro-4-dimethylaminobenzylidenepyruvic acid was 0.54 g from 1.0 g of recrystallised sodium salt. The keto acid is a dark-red solid, m.p. 105.4–106.0 °C. Analysis: calculated for $C_{12}H_{12}O_3NCl$, C 56.82, H 4.77, N 5.52; found, C 56.46, H 4.87, N 5.34%.

Solutions of the benzylidenepyruvic acids were analysed by conductometric titrations with standard sodium hydroxide solution; stock solutions of their sodium salts were standardised spectrophotometrically, the calibration graphs being prepared with standard solutions of the corresponding acids, previously neutralised with 10^{-3} M sodium hydroxide solution. Ethylenediamine, 2,2′-bipyridyl and glycine (AnalaR, BDH Chemicals) were purified by the usual methods[18]; their stock solutions were analysed by potentiometric acid - base titrations. End-points were located from Gran plots.[19]

Instruments

Absorption spectra and absorbance measurements at fixed wavelengths were performed on a Varian-Cary Model 219 recording spectrophotometer. Absorbance values are given to four decimal places in a digital display. The water-jacketed cell holder was thermostated to ±0.05 °C using a Forma Model 295 external circulating bath. Matched 1-cm quartz cells were used. Potentiometric measurements were made on a Metrohm E-512 pH - mV meter. All measurements were carried out in aqueous medium at 25.00 °C and ionic strength (I) 0.500 M (adjusted with sodium perchlorate), in a room thermostated at 25 ± 1 °C. Experimental data were processed by a Hewlett-Packard Model 9810A programmable electronic calculator, with graphical output plotted by a Hewlett-Packard Model 9125B incremental plotter.

Methods

Determination of hydrogen-ion concentrations

Acidities of solutions were measured by using cell (I) shown below.

The electrodes were Metrohm EA 109 glass and Corning 476002 calomel electrodes, modified as indicated in the cell. The measuring assembly was first standardised by using an acetate buffer (0.100 M acetic acid - 0.100 M sodium acetate - 0.400 M sodium perchlorate) whose ph = 4.61 (h = hydrogen-ion concentration) was assigned by taking into account the thermodynamic dissociation constant of acetic acid determined by Harned and Ehlers[20] at 25 °C and the ionic activity coefficients given by Meites.[21] The pH meter readings (pH') for the test solutions were converted into ph by means of the calibration factor H'/h experimentally determined as recommended by McBryde.[22]

Determination of dissociation constants (K_a)

The dissociation constants of the benzylidenepyruvic acids (carboxylate group) were determined by titrating 2.5–3.3 mM solutions of the keto acids (made up to I = 0.500 M, by adding sodium perchlorate) with 0.025 M sodium hydroxide solution, I = 0.500 M, adjusted with sodium perchlorate. Regular titration curves, characteristic of monoprotic acids, were obtained for both keto acids considered in this work. The K_a values were derived[19] from C_L, C_H, K_w, h data, where C_L and C_H are the total concentrations of keto acids and dissociable hydrogen ions, respectively. The pK_w value (13.57 at 25 °C and I = 0.500 M) was previously determined.[23]

Calculation of formation constants from spectrophotometric data

Binary complexes. For a series of solutions in which $C_M \gg C_L$ (where C_M and C_L are total metal and ligand concentrations, respectively) and if only the first mononuclear complex ML is formed, the following relationship holds[24–26]:

$$\frac{bC_MC_LK_a}{[A-(\varepsilon_0C_M+\varepsilon_LC_L)](K_a+h)}+\frac{[A-(\varepsilon_0C_M+\varepsilon_LC_L)]K_a}{(\Delta\varepsilon_1)^2[K_a+h]}=\frac{1}{\Delta\varepsilon_1\beta_1}+\frac{1}{\Delta\varepsilon_1}\left[\frac{(C_M+C_L)K_a}{K_a+h}\right] \quad \ldots \quad (1)$$

where b = optical path length (cm), A = measured absorbance, ε_0, ε_L and ε_1 = molar absorptivities of metal salt, ligand and complex, respectively, $\Delta\varepsilon_1 = \varepsilon_1 - (\varepsilon_0 + \varepsilon_L)$ and β_1 = stability constant of the ML species.

As a rule, the second term on the left-hand side of equation (1) will be smaller than the others and may be temporarily dropped. This gives

$$\frac{bC_MC_LK_a}{[A-(\varepsilon_0C_M+\varepsilon_LC_L)](K_a+h)}=\frac{1}{\Delta\varepsilon_1\beta_1}+\frac{1}{\Delta\varepsilon_1}\left[\frac{(C_M+C_L)K_a}{K_a+h}\right] \quad \ldots \quad (2)$$

If the term on the left-hand side of equation (2) is plotted against $(C_M + C_L)K_a/K_a + h$, it is possible to find ε_1 and β_1 from the slope and intercept of a straight line (ε_0 and ε_L are easily determined from independent experiments). Once preliminary values of ε_1 and β_1 have been determined [equation (2)], the final (refined) constants are obtained by successive approximations through application of equation (1).

Ternary complexes. The following equilibria have been investigated (charges omitted for clarity):

$$CuB + L \rightleftharpoons CuBL$$
$$K_{11} = [CuBL]/[CuB][L]$$

where B = 2,2′-bipyridyl (bipy), ethylenediamine (en) and glycinate (gly$^-$). The K_{11} values were determined as recommended by Neves and Peters.[27,28]

Results

The absorption spectra of copper(II) perchlorate and mixtures of this salt with 2-Cl-DMBP (C_M/C_L ratios from 0 to 600), at constant C_L, covering the range 220–700 nm are given in Fig. 1. The ligand displays two absorption maxima located at 264–266 nm and 412–414 nm. Addition of copper(II) gives rise to an absorption band with a maximum at 535 nm, which intensifies as C_M/C_L increases; a simultaneous decrease in intensity of the 412–414-nm band (assigned mostly to the uncomplexed ligand) is observed. These features clearly indicate the occurrence of complex formation, pointing to the feasibility of a spectrophotometric study of the system.

$$\oplus\ Hg(l)\,|\,Hg_2Cl_2(s)\ \Big|\ \begin{matrix}0.100\text{ M NaCl (aq.)}\\0.400\text{ M }NaClO_4\text{ (aq.)}\end{matrix}\ \Big\vdots\ \begin{matrix}\text{Test solution}\\(0.500\text{ M }ClO_4^-)\text{ (aq.)}\end{matrix}\ \Big|\ \begin{matrix}\text{Glass}\\\text{electrode}\end{matrix}\ \ominus$$

(I)

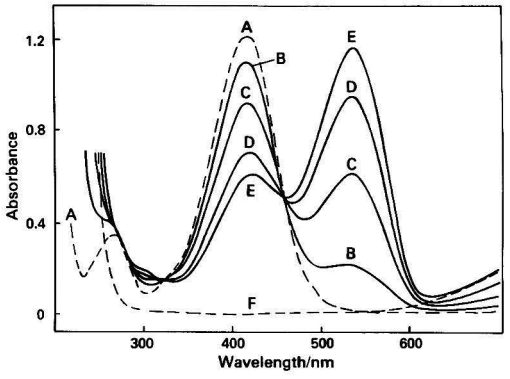

Fig. 1. Absorption spectra of $Cu(ClO_4)_2$ - 2-Cl-DMBP with various concentrations of added Cu(II). C_M: 0, 1.05, 3.78, 8.40 and 12.6 mM for A–E, respectively; and F, 12.6 mM $Cu(ClO_4)_2$. Conditions: C_L, 0.021 mM; *ph*, 5.53 ± 0.32; *I*, 0.500 M; temperature, 25 °C; path length, 1 cm; and measurements against 0.500 M $NaClO_4$

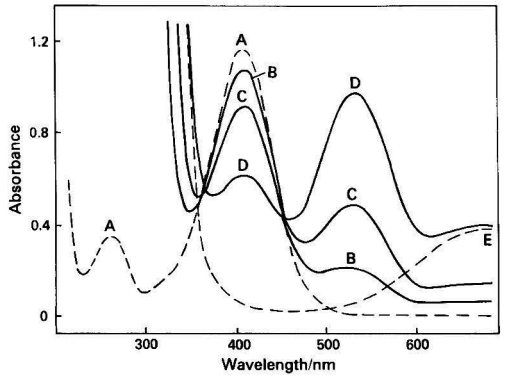

Fig. 2. Absorption spectra of $Cu(bipy)^{2+}$ - 2-Cl-DMBP with various concentrations of added $Cu(bipy)^{2+}$. C_L: 0, 0.60, 1.60 and 5.00 mM for A–D, respectively; and E, 5.00 mM $Cu(bipy)^{2+}$ (equimolar amounts of Cu^{2+} and bipy). Conditions: C_L, 0.020 mM; *ph*, 5.91 ± 0.19; *I*, 0.500 M; temperature, 25 °C; path length, 1 cm; and measurements against 0.500 M $NaClO_4$

Table 1. Stability constants and molar absorptivities determined at various wavelengths for copper(II) - 2-Cl-DMBP. Conditions: C_L = 0.025 mM; C_M = 1.15–15.0 mM; p*h* = 5.10–6.05; *I* = 0.500 M ($NaClO_4$); and *T* = 25.00 ± 0.05 °C

λ/nm	520	530	535	540	545	550	560	565	570
$\varepsilon_l \times 10^{-4}$/l mol^{-1} cm^{-1}	4.56	4.86	4.91	4.86	4.71	4.47	3.75	3.37	2.97
β_1*/l mol^{-1}	91.2	91.4	91.3	91.4	91.3	90.9	92.3	92.6	92.0

* $\beta_1 = 91.6 \pm 0.5$; $\log\beta_1 = 1.962 \pm 0.003$.

Table 2. Stability constants and molar absorptivities of binary complexes of metal ions with DMBP, 2-Cl-DMBP and pyruvate. Conditions: *I* = 0.500 M ($NaClO_4$) and *T* = 25.00 ± 0.05 °C (for benzylidenepyruvates)

	DMBP			2-Cl-DMBP			Pyruvate†			
Ion	Logβ_1 (or pK_a) ± σ*	λ_{max}/nm	$\varepsilon_{l\,max.}$ ×10^{-4}/ l mol^{-1} cm^{-1}	Logβ_1 (or pK_a) ± σ*	λ_{max}/nm	$\varepsilon_{l\,max.}$ ×10^{-4}/ l mol^{-1} cm^{-1}	Logβ_1 (or pK_a)	*I*/M (*T*/°C)	Ref.	C_A‡
H^+	3.79 ± 0.02	414	2.90	3.08 ± 0.02	414	2.89	2.45, 2.35, 2.39	0(25), 0.50(25), 0.65(25)	11	1.009
Mn^{2+}	0.489 ± 0.004	495	2.04	0.441 ± 0.009	≤480§	≥1.92	1.26	0.65(25)	11	0.223
Co^{2+}	1.082 ± 0.004	508	3.68	0.977 ± 0.007	505	3.24	—	—	—	0.276
Ni^{2+}	1.350 ± 0.002	512	4.33	1.223 ± 0.006	510	3.75	1.12, 1.15, 0.883	0.50(25), 0.65(25), 1.0(25)	11	0.300
Cu^{2+}	2.207 ± 0.002	538	5.89	1.962 ± 0.003	535	4.91	2.3, 2.11, 2.78	0(25), 0.10(30), 1.0(30)	11, 31, 32	0.466
Zn^{2+}	1.254 ± 0.008	505	3.72	1.136 ± 0.005	500	3.35	1.26, 1.28, 1.16	0.50(25), 0.65(25), 1.0(25)	11	0.312
Pb^{2+}	1.796 ± 0.004	510	3.71	1.782 ± 0.014	500	2.85	2.96, 2.04	1.0(30), 3.0(25)	32, 33	0.413
Cd^{2+}	0.783 ± 0.006	≤480§	≥1.93	0.715 ± 0.005	≤480§	≥1.84	0.98	3.0(25)	11	0.300
Al^{3+}	2.563 ± 0.003	535	7.20	1.979 ± 0.003	535	6.62	—	—	—	0.657
Fe^{2+}	0.79¶	—	—	0.72¶	—	—	0.69	3.0(25)	11	0.256
Cr^{2+}	0.94‖	—	—	0.83‖	—	—	—	—	—	—

* σ, Standard deviation.

† Literature values. Experimental conditions concerning ionic strength and temperature, along with references are given in the 9th and 10th columns, respectively.

‡ Hancock's parameter,[30] defined as $K_1(OH^-)/14.00$, where $K_1(OH^-)$ is the stability constant for metal ion - monohydroxo complex (aqueous medium, $I = 0$, $T = 25$ °C).

§ No absorption maximum could be detected up to $C_M/C_L = 3\,000$. Analytical spectral range: 480–520 nm.

¶ Calculated by interpolation of the Irving - Williams stability order.[34]

‖ Calculated by applying the empirical equation derived by Cannon[35] and Cannon and Gholami.[36]

Further, the presence of isosbestic points at 322 and 458 nm indicates the presence of at least two independent absorbing species[29]; the determination of the number of light-absorbing species in solution[29] led to the conclusion that the 1:1 complex is the only one formed for the fixed experimental conditions (Fig. 1, Table 1). The absorption band whose maximum is located at 535 nm is obviously the most sensitive to complex formation; the spectral range between 520 and 570 nm was therefore selected for absorbance measurements and evaluation of the stability constant of the corresponding 1:1 complex. The results are given in Table 1.

Addition of copper(II) to DMBP and of other metal ions considered in this work to DMBP or 2-Cl-DMBP solutions showed spectral changes similar to those displayed in Fig. 1. The exclusive formation of the first mononuclear species was also confirmed for all investigated binary systems, provided that $C_M > C_L$. The main results concerning equilibrium studies on the aforementioned systems as well as pK_a values are summarised in Table 2.

Fig. 2 shows the absorption spectra associated with the Cu(II) - bipy - 2Cl-DMBP system. The spectra closely resemble those given in Fig. 1; formation of $Cu(bipy)L^+$ species is indicated by the absorption band with a maximum at 540 nm. The absorption spectra for the Cu(II) - en - L^- and Cu(II) - gly^- - L^- systems are very closely related to those shown in Fig. 2; formation of $Cu(en)L^+$ and Cu(gly)L species is clearly indicated. The presence of CuBL as a single complex species in the investigated ternary systems is further supported by the conclusions from determinations of the number of absorbing species in solution.[29] The determined stability constants for mixed ligand complexes are listed in Table 3.

Discussion and Conclusions

There was no major difficulty in obtaining steady and reproducible absorbance and p*H′* values. The constancy of absorbances as a function of time, for the metal ion and ligand concentrations encompassed in this work, indicates that the

Table 3. Formation constants of mixed ligand complexes involving copper(II) and benzylidenepyruvates. Conditions: I = 0.500 M ($NaClO_4$) and T = 25.00 ± 0.05 °C

Central group	DMBP			2-Cl-DMBP		
	Log K_{11} (or log β_1) ± σ	$\lambda_{max.}$/nm	ΔLog K*	Log K_{11} (or log β_1) ± σ	$\lambda_{max.}$/nm	ΔLog K*
Cu^{2+}	2.207 ± 0.002	538	—	1.962 ± 0.003	535	—
$Cu(bipy)^{2+}$	2.47 ± 0.07	545	0.26	2.13 ± 0.01	540	0.17
$Cu(en)^{2+}$	1.61 ± 0.03	545	−0.60	1.24 ± 0.06	540	−0.72
$Cu(gly)^{+}$	1.40 ± 0.03	545	−0.81	0.92 ± 0.06	540	−1.04

* $\Delta\text{Log } K = \log K_{11} - \log \beta_1$.

attainment of equilibria is rapid relative to the time necessary to prepare a sample for examination. These favourable properties are reflected in the very good precision achieved in determining the stability constants of binary and ternary complexes (Tables 1–3). The ligands are stable within the range p*h* 3–9; outside this range, a progressive decomposition of these substances as a function of time takes place and they are quickly destroyed at p$h \leqslant 2$.

The stability sequence for binary complexes, *i.e.*, Al(III) > Cu(II) > Pb(II) > Ni(II) > Zn(II) > Co(II) > Cd(II) > Mn(II) is observed for both ligands. The Irving - Williams stability series[34] is obeyed. For all metal ions, log β_1 (DMBP) > log β_1 (2-Cl-DMBP), indicating that the stability is governed, at least in part, by ligand basicity. This last order is also observed for ε_l values. An irregular stability pattern is displayed by the pyruvate complexes (Table 2), especially for the Irving - Williams stability order; this can mostly be assigned to different pyruvate species present in solutions of metal ions (keto, diol and dimer forms); as a result, three distinct 1 : 1 complexes are formed with a same metal ion.[12,37] The stability constants for pyruvate complexes listed in Table 2 are thus useful only to describe the net complexation. The relative proportions of the three types of complexes in solution as well as the thermodynamic parameters associated with the individual complexation reactions were determined only for the La(III) and Ce(III) systems.[12] It is worth noting that the stabilities reported for metal ion - pyruvate complexes (Table 2) are higher than expected as judged by the low basicity of the ligand and by comparison with the pK_a and β_1 values for the benzylidenepyruvate systems.

The β_1 values found for complexes involving benzylidenepyruvates are reasonably well correlated with Hancock's parameter[30] (Table 2), suggesting the –COCOO– moiety as the metal binding site of the ligands. The investigation of possible higher binary complexes (ML_n, $n > 1$) was prevented by solubility limitations; for most of the considered metal ions, working with C_M = 0.010–0.19 mM, precipitation takes place as soon as C_L/C_M is equal to or higher than 1.3.

The complexes of $Cu(bipy)^{2+}$ with DMBP and 2-Cl-DMBP are more stable than those formed by the corresponding reactions with the free (hydrated) Cu(II) ion, *i.e.*, $\Delta\log K > 0$ (Table 3). Replacement of 2,2'-bipyridyl by ethylenediamine or glycinate leads to a complete loss of the enhancement, *i.e.*, the $\Delta\log K$ values for the $Cu(en)^{2+}$ and $Cu(gly)^{+}$ systems with benzylidenepyruvates (Table 3) are of the order expected on statistical considerations for the coordination of two different bidentate ligands to the distorted octahedral coordination sphere of copper(II).[38] Further, the negative $\Delta\log K$ values indicate that en and gly^- do not form Schiff bases with the named keto acids within the coordination sphere of copper(II).[39]

These results are in line with the findings of several other workers[4, 28, 38–40] concerning the highly enhanced stability of ternary complexes in solution through the participation of heteroaromatic nitrogen bases or intramolecular covalent bond formation between two ligands bound to the same metal ion (*e.g.*, formation of Schiff bases). It is known that the formation of π back-bonds, as is possible between Cu(II) and bipy, enhances the stability of mixed ligand complexes, provided the second ligand has oxygen donor sites, such as those present in phenolates, phosphates and carboxylates.[38]

Copper(II) reacts with DMBP to give a sparingly soluble and stable reddish brown precipitate, $Cu(C_{12}H_{12}O_3N)_2$, which is suitable for gravimetric determination. A 0.015 M solution of the sodium salt of DMBP is added to the test solution containing 1.5–6.0 mg of copper (p*h* 4.5–4.7). Stoicheiometrically, 1 mg of copper(II) requires 2.1 ml of 0.015 M DMBP solution; for complete precipitation a 4–6-fold excess of DMBP is necessary. The system is allowed to stand for 1 h at room temperature. The precipitate is then filtered through a fine porosity sintered-glass crucible, washed with cold water and dried to constant mass at 110–120 °C.

The gravimetric factor for copper is 0.1271. No interference from Li(I), K(I), Rb(I), Cs(I), Ag(I), Hg(I), Hg(II), Mg(II), Ca(II), Sr(II), Ba(II), Fe(II), Pd(II), B(III) and As(III) was found. Interference from Be(II), Al(III), Fe(III), Ce(III), Ge(III), Sn(IV), Ti(IV), Zr(IV), Hf(IV) and U(IV) was prevented by adding sodium fluoride as a masking agent. Co(II), Ni(II), Cd(II), Zn(II), Pb(II), Ti(III) and Th(IV) interfere markedly and should be removed. The other ligand considered, *i.e.*, 2-Cl-DMBP, behaves like DMBP towards Cu(II) and interfering metal ions. The precipitate is weighed as $Cu(C_{12}H_{11}O_3NCl)_2$ (gravimetric factor 0.1117). It was found that Cu(II) is also quantitatively precipitated at p*h* 4.5–5.0 in the presence of 2,2'-bipyridyl, DMBP and sodium perchlorate; the sparingly soluble compound formed is a mixed ligand complex, $Cu(C_{10}H_8N_2)(C_{12}H_{12}O_3N)ClO_4$.

The high molar absorptivity and favourable stability constant of the Th(IV) - DMBP 1 : 1 complex ($\lambda_{max.}$ = 542 nm, $\varepsilon_{1max.} = 7.38 \times 10^4$ l mol^{-1} cm^{-1}, log β_1 = 4.10, at 25 °C and I = 0.500 M) offer attractive applications in titrimetric analyses involving Th(IV). Thus, direct titration of milligram amounts of Th(IV) with 0.01 M EDTA solution at p*h* 3.1 is successfully performed by using the sodium salt of DMBP (two drops of a 0.3% *m*/*V* aqueous solution, for an initial volume of 100 ml) as a metallochromic indicator; a sharp colour change from red to yellow is observed at the end-point. Accurate and reproducible values are obtained; DMBP is a good alternative indicator to Xylenol Orange or Pyrocatechol Violet, which are commonly used for this titration.[41] Al(III) in 5–15 mg amounts was determined by adding an excess of 0.05 M EDTA solution; the resulting solution (adjusted to p*h* 4.3–4.5) was boiled for 2 min, cooled and back-titrated with standard Th(IV) nitrate solution using DMBP as indicator. The colour change at the end-point (yellow to red) is much sharper than the one observed by using Alizarin S.[41]

Samples containing 3–35 mg of fluoride were titrated at p*h* 3.2 with 0.01 M Th(IV) nitrate solution by using DMBP or 2-Cl-DMBP as indicators; the end-point is given by the appearance of a permanent red colour. This procedure was adapted for micro-titration of samples containing not more than 70 μg of fluoride; the end-point was located from the graph of absorbance (at 542 nm) against volume of titrant added. The devised procedure compares well with those in

which sodium alizarin sulphonate or the sodium salt of 2-(*p*-sulphophenylazo)-1,8-dihydroxynaphthalene-3,6-disulphonic acid are used as indicators,[42] in so far as sensitivity, precision and accuracy are concerned.

Further work on complexes of benzylidenepyruvates with trivalent lanthanides and on analytical applications of ternary complexes containing transition metal ions and the named keto acids is currently in progress.

This work was carried out in part under the sponsorship of CNPq (Proc. 305632/78) and FAPESP (Procs. 78/1492 and 81/0108), Brazil.

References

1. Semonsky, M., Beran, M., Neumannova, J., Skovorova, H., and Jelinek, V., *Collect. Czech. Chem. Commun.*, 1967, **32**, 4439.
2. Rouschdi, I. M., El Sebai, A., Ibrahim, Y. A., Shafik, R. M., and Soliman, F. S. G., *Pharmazie*, 1972, **27**, 731.
3. Toshimitsu, U., *Chem. Pharm. Bull. (Tokyo)*, 1975, **23**, 62.
4. Hay, R. W., *in* Sigel, H., *Editor*, "Metal Ions in Biological Systems," Volume 5, Marcel Dekker, New York, 1976, pp. 127–172.
5. Abbasi, S. A., *Proc. 18th. Internat. Conf. Coord. Chem.*, 1977, São Paulo, Brazil, p. 170.
6. Ibrahim, Y. A., *Chem. Ind. (London)*, 1980, 536.
7. Kidwai, M. M., and Khan, N. H., *Indian J. Chem. Part B*, 1980, **19**, 802.
8. Schulz, G., Andries, T., and Steglich, W., *Synth. Commun.*, 1980, **10**, 405.
9. Mayer, W., Rudolph, H., and De Cleur, E., *Angew. Makromol. Chem.*, 1981, **93**, 83.
10. Smith, J. T., and Doctor, V. M., *J. Inorg. Nucl. Chem.*, 1975, **37**, 775.
11. Forsberg, O., Gelland, B., Ulmgren, P., and Wahlberg, O., *Acta Chem. Scand., Ser. A*, 1978, **32**, 345, and references cited therein.
12. Choppin, G. R., and Cannon, R. E., *Inorg. Chem.*, 1980, **19**, 1889.
13. Jawaid, M., and Ingman, F., *Talanta*, 1981, **28**, 137.
14. Kubala, G., and Martell, A. E., *Inorg. Chem.*, 1982, **21**, 3007.
15. Marczenko, Z., *Crit. Rev. Anal. Chem.*, 1981, **11**, 195.
16. Acerete, J. G., and Lacal, R. U., *Rev. Acad. Cienc. Exactas. Fis. Quim. Nat. Zaragoza*, 1954, **9**, 117.
17. Kageura, M., Ohkura, Y., and Momose, T., *Chem. Pharm. Bull.*, 1971, **19**, 2294.
18. Perrin, D. D., Armarego, W. L. F., and Perrin, D. R., "Purification of Laboratory Chemicals," Pergamon Press, Oxford, 1966.
19. Rossotti, H. S., *Talanta*, 1974, **21**, 809.
20. Harned, H. S., and Ehlers, R. W., *J. Am. Chem. Soc.*, 1933, **55**, 65.
21. Meites, L., "Handbook of Analytical Chemistry," McGraw-Hill, New York, 1963, pp. 1–8.
22. McBryde, W. A. E., *Analyst*, 1969, **94**, 337.
23. Faraglia, G., Rossotti, F. J. C., and Rossotti, H. S., *Inorg. Chim. Acta*, 1970, **4**, 488.
24. Rossotti, F. J. C., and Rossotti, H., "The Determination of Stability Constants," McGraw-Hill, New York, 1961, pp. 276–277.
25. Neves, E. F. A., and Senise, P., *J. Inorg. Nucl. Chem.*, 1972, **34**, 1915.
26. McBryde, W. A. E., *Talanta*, 1974, **21**, 979.
27. Neves, E. F. A., and Peters, M. P., *Proc. 124th Annu. Meet. Am. Chem. Soc., Kansas City, USA*, 1982, paper CHAS No. 60.
28. Peters, M. P., *PhD Thesis*, Universidade de São Paulo, Brazil, 1980, pp. 155–158.
29. Hartley, F. R., Burgess, C., and Alcock, R., "Solution Equilibria," Halsted Press, Chichester, 1980, pp. 33–40.
30. Hancock, R. D., and Marsicano, F., *Inorg. Chem.*, 1978, **17**, 560; 1980, **19**, 2709.
31. Palrecha, M. M., and Gaur, J. N., *Indian J. Chem.*, 1969, **7**, 1035.
32. Ramamoorthy, S., Raghavan, A., Vijayaraghavan, V. R., and Santappa, M., *J. Inorg. Nucl. Chem.*, 1969, **31**, 1851.
33. Lenarcik, B., and Warnke, Z., *Rocz. Chem.*, 1969, **43**, 1329.
34. Irving, H., and Williams, R. J. P., *J. Chem. Soc.*, 1953, 3192.
35. Cannon, R. D., *J. Inorg. Nucl. Chem.*, 1976, **38**, 1222.
36. Cannon, R. D., and Gholami, M. J., *Bull. Chem. Soc. Jpn.*, 1982, **55**, 594.
37. Leussing, D. L., and Stanfield, C. K., *J. Am. Chem. Soc.*, 1964, **86**, 2805.
38. Sigel, H., *Angew. Chem., Int. Ed. Engl.*, 1975, **14**, 394.
39. Sigel, H., *in* Barnerjea, D., *Editor* "Coordination Chemistry-20," Pergamon Press, Oxford, 1980, pp. 27–45.
40. John, E. *Microchem. J.*, 1981, **26**, 174.
41. Schwarzenbach, G., and Flaschka, H., "Complexometric Titrations," Methuen, London, 1969, pp. 185 and 209–213.
42. Headridge, J. B., "Photometric Titrations," Pergamon Press, Oxford, 1961, pp. 102–104.

Paper A3/303
Received September 5th, 1983
Accepted November 11th, 1983

Toxicity and Spectrophotometric Determination of Sulphur Dioxide in Air Using a New Absorbing Agent

Abha Chaube, Anil K. Baveja and V. K. Gupta
Department of Chemistry, Ravishankar University, Raipur, 492 010, India

An aqueous solution of succinyldihydroxamic acid (SDHA) is proposed as an efficient absorbing agent for ambient sulphur dioxide. The agent (SDHA) is easy to prepare, has an absorption efficiency of approximately 100% and its resulting sulphite solution is stable for more than 30 d. The absorbed sulphur dioxide has been subsequently determined spectrophotometrically by condition optimised *p*-aminoazobenzene - formaldehyde in hydrochloric acid. The pink dye formed has an absorption maximum at 505 nm. The proposed method is superior to the widely used tetrachloromercurate method in terms of manipulation, speedy results and use of stable, pure and non-toxic reagents. The interference from nitrogen dioxide has been removed by the use of sodium azide - malonyl dihydrazide. The procedure has been applied to the determination of sulphur dioxide both in the vicinity of a superphosphate fertiliser plant and in work-room air.

Keywords: *Atmospheric sulphur dioxide determination; succinyldihydroxamic acid; spectrophotometry; p-aminoazobenzene - formaldehyde*

Sulphur dioxide, a well know toxic air pollutant, enters the atmosphere in large amounts from car exhausts and chemical industries, namely as a by-product in ore smelting and combustion of various sulphur-bearing products such as in petroleum refining, production of coke, steel plants, blast furnaces and thermal power plants.[1–3] It is also used as a food stabiliser. The US Environmental Protection Agency has recommended a maximum allowable limit of 0.03 p.p.m. (daily exposure for 1 h averaged over a year) and 0.14 p.p.m. daily exposure for 8 h, whereas the US Occupational Safety and Health Administration (OSHA) has recommended a value of 5 p.p.m. over an 8-h exposure.[4]

Sulphur dioxide is almost an irrespirable gas and causes irritation to the nose, throat and eyes.[5] It readily affects the respiratory tract causing a sore throat, chest pains, constriction, burning and tearing of eyes, vomiting, nausea, excessive nasal discharge as well as breathlessness.[3] Its presence in the atmosphere is also undesirable as it plays a vital role in the formation of photochemical smog along with particulate matter, moisture and other flue gases. Such smogs adversely affect persons suffering from bronchitis, causing acute bronchitis, bronchopneumonia and heart diseases (chiefly affecting coronary daudicative intermettens.[3] Epidemiological studies showed a significantly higher rate of acute respiratory illness in smokers compared with non-smokers at increasing levels of sulphur dioxide.[3]

Sulphur dioxide is suspected to cause mutagenic effects as well as lung tumours and several types of cancer.[3] Damage to vegetation is also reported in the form of localised destruction of leaf tissue at concentrations as low as 2–3 p.p.m. of sulphur dioxide. In sensitive plants chronic damage may occur even at a concentration of 0.3 p.p.m.[1] Sulphur dioxide causes inhibition of carbon dioxide fixation, blockage of starch hydrolysis, silvering or bronzing of leaves and breakdown of chlorophyll-containing cells along with early dropping of foliage.[6] Apart from these hazards it is also corrosive to metals and acid-sensitive materials such as concrete, limestone etc. Because it represents a serious health hazard many methods have been reported for its detection and determination in air.[1,2] Almost all of the methods employed for the determination of atmospheric sulphur dioxide have two stages, *i.e.*, fixation and storage of sulphur dioxide from air in a suitable medium and its subsequent determination in the sample solution using a suitable reagent.

Several reagents have been reported for absorption of sulphur dioxide.[7] The method of West and Gaeke[8] in which atmospheric sulphur dioxide is stabilised in tetrachloromercurate (TCM) as dichlorodisulphitomercurate(II) and determined colorimetrically by *p*-rosaniline - formaldehyde is the most widely used method.The major drawbacks of this method are air oxidation of dichlorodisulphitomercurate(II) (1% decay per day at room temperature),[9] the use of a relatively high concentration of expensive and toxic mercury-(II) chloride and variation in the purity of the commercially available *p*-rosaniline dye. To overcome these, modified West and Gaeke methods using formaldehyde[10] and triethanolamine[11] as absorbing media have been recommended but these methods are tedious or pH dependent, respectively.

Recently, monoethanolamine has been reported as an absorbing medium for sulphur dioxide.[7] In searching for a better absorbing medium for the fixation and storage of atmospheric sulphur dioxide it was found that an aqueous solution of succinyldihydroxamic acid (SDHA) can profitably be employed. The system is independent of pH and the absorbed sulphur dioxide is stable for a period of more than 30 d. The absorbing agent (SDHA) can easily be prepared, is pure, stable and non-toxic. The resulting sulphite ion was subsequently determined spectrophotometrically using *p*-aminoazobenzene - formaldehyde, following the procedure of Kniseley and Throop.[12] The absorbing agent gives reproducible results and is available in a pure form. The pink dye formed has an absorption maximum at 505 nm. The system has been optimised for sulphur dioxide determination with respect to various reaction conditions. The absorption efficiency of the agent is comparable to methods using TCM, formaldehyde and monoethanolamine. The method has been successfully applied to the determination of sulphur dioxide in the vicinity of a superphosphate fertiliser plant and in work-room air.

Experimental

Apparatus

An ECIL Model GS 865 spectrophotometer and Carl Zeiss Spekol with 1-cm matched glass cells was used for spectral measurements. Fritted midget impingers (frit diameter, *ca.* 10 mm) of 35-ml capacity were used for air sampling. A flow-rate adjustable, calibrated rotameter was used for air sampling.

Reagents

All chemicals used were of AnalaR grade and de-ionised, de-aerated water was used for preparing solutions.

Sodium sulphite solution, 0.32–40 mg ml^{-1}. A stock solution was prepared by dissolving 0.2 g of pre-dried sodium sulphite in 250 ml of distilled water. The sulphite solution was standardised iodimetrically.[13] Working standards were prepared by the appropriate dilution of the stock solution in SDHA (0.01 M).

p-*Aminoazobenzene* (0.02%) - *formaldehyde* (0.2%). Prepared as reported earlier.[7]

Sodium azide - malonyl dihydrazide solution, 0.6%. Prepared in de-aerated, doubly distilled water.

Succinyldihydroxamic acid. Prepared by the dropwise addition of 17.2 g of diethyl succinate to an ammonia solution containing 13 g of hydroxylammonium chloride with vigorous stirring at 0 °C. The white precipitate of succinyldihydroxamic acid obtained was filtered and recrystallised twice from distilled water (melting-point, 164–166 °C).

Procedure

Collection of samples

Two midget impingers (35-ml capacity) each containing 10 ml of 0.01 M SDHA solution were connected in series to an air sampling train fitted with a rotameter. Air containing various concentrations of sulphur dioxide was passed through the impingers at a flow-rate of 0.75 l min^{-1}. A 38.2-l volume of air sample was collected and later analysed for sulphur dioxide content. No antifoaming reagent was used for the collection of the sample.

Analysis of samples

After sampling, an aliquot (depending upon the concentration of sulphur dioxide) was transferred into a 25-ml calibrated flask and to it 1 ml of *p*-aminoazobenzene was added and the acidity was adjusted to between 0.02 and 0.2 M hydrochloric acid. A 1-ml volume of 0.2% formaldehyde solution and a 1-ml volume of concentrated hydrochloric acid were added and the volume was made up to the mark with distilled water. After 20 min the absorption of the pink solution was measured against a reagent blank, at 505 nm. The absorbance of the sample solution was calculated by subtracting the absorbance value of the reagent blank from the value of the sample.

The calibration graph was prepared by taking aliquots of sodium sulphite solution in 0.01 M SDHA containing 0.1–1 p.p.m. of sulphur dioxide in a final volume of 25 ml and developing the colour as described above. The concentration of sulphur dioxide was then calculated from the calibration graph.

Results and Discussion

The absorption efficiency of SDHA, stability of sulphur dioxide in SDHA, effect of time, temperature and aeration were taken into account in order to optimise the reaction conditions. Generation of synthetic sulphur dioxide was carried out as reported earlier,[7] but in this instance the generation was performed by taking a 2.5 mg ml^{-1} sulphur dioxide solution prepared in 0.01% SDHA. It was found that generation of sulphur dioxide is quantitative. The data given in Table 1 show that synthetic generation is reproducible and accurate.

Absorption Efficiency

The absorption efficiency of SDHA was evaluated by passing through it air containing 2.5–500 μg of sulphur dioxide for various lengths of time and at different flow-rates. Samples containing higher concentrations of sulphur dioxide were diluted appropriately with distilled water prior to analysis. In such instances the reagent blank was diluted accordingly. Almost 100% absorption was achieved in the first impinger. The second impinger gave a negative test for sulphur dioxide. Different concentrations of SDHA solutions, *i.e.*, 0.005–0.25 M SDHA had no effect on the absorption efficiency. Flow-rate variation from 0.25 to 2 l min^{-1} and temperature variation from 15 to 40 °C did not affect the absorption efficiency (Tables 2 and 3).

Stability of Sulphur Dioxide Containing Samples

Sulphur dioxide was absorbed to the extent of 100 μg ml^{-1} in 10 ml of 0.01 M SDHA. A 25-ml volume of 0.005 M solution of SDHA was found to stabilise 500 μg of sulphur dioxide. The sulphite solution prepared in SDHA was found to be stable for

Table 1. Reproducibility of the method for the generation of sulphur dioxide and its determination. Flow-rate, 0.75 l min^{-1}; and volume of air sampled for each analysis, 38.2 l

Set No.	Amount of sulphur dioxide added/μg	Concentration of sulphur dioxide added,* p.p.m.	Amount of sulphur dioxide found †/μg
1	2.50	0.025	2.48 ± 0.014
2	5.00	0.050	4.96 ± 0.041
3	10.00	0.100	9.97 ± 0.026
4	15.00	0.150	14.98 ± 0.019
5	20.00	0.200	19.98 ± 0.031
6	30.00	0.300	29.96 ± 0.062
7	40.00	0.400	39.95 ± 0.056
8	50.00	0.500	49.98 ± 0.021
9	100.00	1.000	99.98 ± 0.017

* p.p.m. of sulphur dioxide are calculated by multiplying amount in μg by a factor of 0.01, as 38.2 l of air are sampled in each instance.[8]
† Mean of six replicate analyses.

Table 2. Effect of concentration of SDHA on absorption efficiency. Flow-rate, 0.75 l min^{-1}; volume of air sampled in each analysis, 38.2 l

Set No.	Concentration of SDHA/ M	SO_2 passed/ μg	SO_2 found in 1st impinger*/ μg	Absorption, %
1	0.005	2.50	2.48 ± 0.015	99.26
		5.00	5.02 ± 0.190	100.04
		10.00	9.98 ± 0.02	99.80
		100.00	99.94 ± 0.07	99.94
2	0.01	2.50	2.46 ± 0.03	98.40
		5.00	4.96 ± 0.02	99.20
		10.00	9.94 ± 0.05	99.40
		100.00	99.98 ± 0.015	99.98
3	0.025	2.50	2.49 ± 0.01	99.80
		5.00	4.97 ± 0.04	99.94
		10.00	9.95 ± 0.04	99.50
		100.00	99.92 ± 0.07	99.92
4	0.10	2.50	2.48 ± 0.02	99.20
		5.00	4.98 ± 0.01	99.60
		10.00	9.92 ± 0.050	99.20
		100.00	99.62 ± 0.04	99.62
5	0.20	2.50	2.47 ± 0.030	98.80
		5.00	4.92 ± 0.060	98.40
		10.00	9.97 ± 0.06	99.10
		100.00	99.26 ± 0.08	99.26

* Mean of three replicate analyses; in each instance the SO_2 found in the 2nd impinger was nil.

Table 3. Effect of flow-rate on absorption efficiency. Concentration of SDHA, 0.01 M; volume of air sampled in each analysis, 38.2 l

Set No.	Flow-rate/ ml min^{-1}	Amount of SO_2 taken/ μg	SO_2 found in 1st impinger*/ μg	Absorption, %
1	250	2.5	2.47 ± 0.02	98.80
		5.0	4.97 ± 0.04	99.40
		15.0	14.90 ± 0.065	99.33
2	500	2.5	2.49 ± 0.02	99.60
		5.0	4.98 ± 0.025	99.60
		15.0	14.93 ± 0.05	99.53
3	750	2.5	2.49 ± 0.02	99.60
		5.0	5.01 ± 0.03	100.00
		15.0	14.96 ± 0.01	99.70
4	1000	2.5	2.46 ± 0.04	98.40
		5.0	4.98 ± 0.02	99.60
		15.0	14.98 ± 0.01	99.93
5	2000	2.5	2.45 ± 0.05	98.00
		5.0	4.96 ± 0.04	99.20
		15.0	14.96 ± 0.03	99.78

* Mean of three replicate analyses.

more than 30 d at room temperature. The loss of absorbance after 30 d was 1–2%. No effect of aeration in absorbed samples was observed. The probable reaction involved in the fixation of sulphur dioxide as aminosulphonic acid in SDHA can be represented as follows:

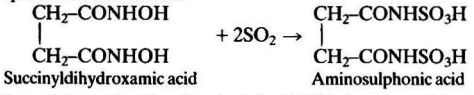

Succinyldihydroxamic acid — Aminosulphonic acid

The sulphur dioxide absorbed in SDHA is released by the addition of 2 drops of 0.2% HCl. The released sulphur dioxide combines *in situ* with *p*-aminoazobenzene in the presence of formaldehyde to give a pink dye having an absorption maximum at 505 nm. The mechanism is similar to that proposed earlier,[10,15] *i.e.*, formation of aminomethanesulphonic acid. The *p*-aminoazobenzene containing only one amino group is preferred over *p*-rosaniline because it is more sensitive and gives a dye of known structure.

Effect of Variables on Colour Development

The order of addition of reagents to the absorbed sulphur dioxide solution in SDHA was investigated. The order of addition for maximum colour development was *p*-aminoazobenzene, formaldehyde and hydrochloric acid. After addition of *p*-aminoazobenzene an acidity between 0.02 and 0.2 M in hydrochloric acid was found to be most suitable. After the addition of formaldehyde solution, maximum colour development was found to take place between 0.2 and 2.0 M hydrochloric acid. This is in agreement with the earlier reported method. Thus in the present method the acidity was maintained at 0.1 and 1.2 M hydrochloric acid after the addition of *p*-aminoazobenzene and formaldehyde, respectively, to the SDHA solution containing absorbed sulphur dioxide. In the earlier method 10 min were required for full colour development and the product was stable for 1 h.[12] In this method the full colour development takes 15 min but the product is stable for 12 h, which is an added advantage of the method.

Beer's Law and Reproducibility

Beer's law is obeyed over the concentration range 2.5–25 μg per 25 ml of sulphur dioxide in 0.01 M SDHA. The method was found to be reproducible. The standard deviation and relative standard deviation for 25 μg of sulphur dioxide per 25 ml of solution were found to be 0.048 and 0.19%, respectively.

Effect of Foreign Species

To assess the applicability of the method, the effect of foreign ions on the determination of sulphur dioxide was studied. The effect of Fe(III), Cu(II), V(V), Mn(II) and Cr(III), which are known to catalyse the aerobic oxidation of sulphite ions, was studied by adding 500 μg of each to 15 μg per 25 ml of sulphur dioxide solution. The change in absorbance was within ±2%, except for V(V). An amount of 200 μg of V(V) was found to interfere with the method, as V(V) forms a violet complex with SDHA.

The effect of nitrogen dioxide, a common interferent in the determination of atmospheric sulphur dioxide was also studied. The nitrite ion when added directly to the absorbing medium caused interference. It was observed that the addition of 2 ml of 0.6% malonyl dihydrazide solution directly to the absorbing solution gave 2–3% lower results. This may be due to the fact that there is no stoicheiometric conversion of nitrogen dioxide to the nitrite ion when nitrogen dioxide is passed through malonyl dihydrazide-containing absorbing solution. Similar studies carried out using sodium azide solution gave 5–6% lower results whereas the use of sulphamic acid gave 10–15% lower results[7,8] (Table 4). Hydrogen sulphide can be eliminated by lead acetate as reported earlier.[7] Other gases such as ammonia, chlorine and halogen acids do not interfere.

Table 4. Interference of nitrogen dioxide. Flow-rate, 0.75 l min^{-1}; and volume of air passed in each analysis, 38.2 l

Amount of sulphur dioxide taken/μg	Amount of nitrogen dioxide taken/μg	Method of determination*	Absorbance at 505 nm
5	—	—	0.125
	2.5	—	—
	25	a	0.110
	25	b	0.125
	50	a	0.100
	50	b	0.125
	100	b	0.125
	500	b	0.120
10	—	—	0.280
	25	—	—
	25	a	0.220
	25	b	0.225
	50	a	0.205
	50	b	0.250
	100	b	0.250
	500	b	0.245
20	—	—	0.505
	25	—	—
	25	a	0.495
	25	b	0.505
	50	a	0.480
	50	b	0.510
	100	b	0.505
	500	b	0.500

* a, Sulphur dioxide and nitrogen dioxide bubbled through a tube containing 0.6% sulphamic acid; b, sulphur dioxide and nitrogen dioxide bubbled through a tube containing 0.6% malonyl dihydrazide.

Comparison of Absorption Efficiencies of Tetrachloromercurate[8] and SDHA

In order to check the analytical applicability of the proposed reagent, a comparative study of absorption efficiencies of tetrachloromercurate and SDHA was carried out. Two sets of fritted midget impingers were connected in series; one set contained 0.1 M SDHA and the other 10 ml of 0.04 M TCM solutions as absorbing media (as recommended by West and Gaeke).[8] The sampled air containing different concentrations of sulphur dioxide was divided into two parts, each having a flow-rate of 0.75 l min^{-1} (38.2 l of air were passed in each). After sampling, the TCM solution and SDHA solution were analysed for sulphur dioxide by the recommended procedure. The results given in Table 5 show that the analytical values obtained by both the reagents are almost identical. Thus it can be concluded that SDHA can be satisfactorily used for the absorption of atmospheric sulphur dioxide.

Application of the Method to the Determination of Atmospheric Sulphur Dioxide

Analyses of atmospheric sulphur dioxide in the vicinity of a superphosphate fertiliser plant near Raipur as well as in the laboratory (artificial sulphur dioxide) were carried out by both the conventional West and Gaeke method and the proposed method. Air sampling at different locations around the plant was done as recommended above but the sulphur dioxide content in TCM solution was determined using the West and Gaeke method (using *p*-rosaniline) and in SDHA by the recommended procedure. In both samples the results obtained by the conventional method were compared with those of the proposed method (Table 6). The values obtained are

Table 5. Comparison of absorption efficiences for tetrachloromercurate and SDHA methods. Flow-rate, 0.75 l min^{-1}; and volume of air sampled in each analysis, 38.2 l. In both the methods absorbed sulphur dioxide was analysed by the Kniseley and Throop method. The correlation coefficient of the two methods was found to be 0.998

Set No.	SO_2 passed/ μg	SO_2 found in 0.04 M TCM*/ μg	Absorption, %	SO_2 found in 0.01 M SDHA*/ μg	Absorption, %
1	2.5	2.48 ± 0.02	99.20	2.49 ± 0.01	99.60
2	7.5	7.47 ± 0.04	99.60	7.48 ± 0.02	99.73
3	10.0	9.94 ± 0.05	99.40	9.96 ± 0.03	99.60
4	15.0	14.97 ± 0.04	99.80	14.98 ± 0.02	99.93
5	20.0	19.95 ± 0.06	99.75	19.97 ± 0.04	99.85
6	25.0	25.00 ± 0.03	100.00	24.88 ± 0.03	99.52
7	50.0	49.98 ± 0.02	99.96	50.01 ± 0.04	100.02
8	100.0	99.97 ± 0.06	99.97	99.98 ± 0.03	99.98

* Mean of three repetitive analyses.

Table 6. Analysis of sulphur dioxide in the vicinity of a superphosphate fertiliser plant and in work-room air. Flow-rate, 0.75 l min^{-1}; and volume of air sampled, 38.2 l. The concentration of sulphur dioxide was calculated by applying the equation SO_2 (p.p.m.) = $(A-A_0)0.328B/V$, where A is the simple absorbance; A_0 is the blank absorbance; 0.328 is the volume (μl) of 1 μg of SO_2 at 25 °C, 760 mm Hg; B is the calibration factor × 25 ml (μg/A); and V is the sample volume in litres corrected at 25 °C and 760 mmHg

Sample	Sulphur dioxide obtained by West and Gaeke method*/μg	Suphur dioxide obtained by West and Gaeke method, p.p.m	Sulphur dioxide obtained by present method*/μg	Sulphur dioxide obtained by present method, p.p.m.
From vicinity of superphosphate plant—				
FP_1	9.94	0.099	10.00	0.100
FP_2	6.07	0.060	6.03	0.060
FP_3	1.94	0.019	1.96	0.019
FP_4	0.60†	0.006	0.61†	0.006
FP_5	0.20†	0.002	0.22†	0.002
FP_6	21.97	0.219	21.92	0.219
FP_7	5.60	0.056	5.54	0.055
FP_8	3.28	0.032	3.22	0.032
FP_9	25.52	0.255	25.50	0.255
From work-room air—				
1	117.03	1.170	117.09	1.170
2	78.79	0.787	79.83	0.798
3	29.94	0.299	29.32	0.293

* Absorption and sampling of sulphur dioxide from eight different locations around the superphosphate plant near Raipur.
† Standard additions method applied.

almost identical. To check the results more precisely in some examples, a standard addition of sulphur dioxide was performed. The results show that the method can be satisfactorily applied to the determination of sulphur dioxide.

Conclusion

The stability of the sulphite solution in the present method is far greater than in the method of West and Gaeke; the system is independent of pH; and oxidising agents such as Fe(III), Cr(III), Mn(II) and Cu(II) do not interfere with the method. *p*-Aminoazobenzene, used for colour development, has added advantages in terms of simplicity, allowable acidity range, reproducibility and stability of the reaction product.

The authors are grateful to the Head of the Department of Chemistry, Ravishankar University, Raipur, for providing laboratory facilities, and to the University Grants Commission and Council of Scientific and Industrial Research, New Delhi, for awards of research fellowships to A.C. and A.K.B., respectively.

References

1. Leithe, W., "The Analysis of Air Pollutants," Ann Arbor Science Publishers, Ann Arbor, MI, 1971, pp. 154–166.
2. Patty, F. A., "Industrial Hygiene and Toxicology," Volume II, Interscience, New York, 1962, pp. 892–895.
3. Calabrese, E. J., "Pollutants and High Risk Groups," Interscience, New York, 1976.
4. Den, P., Gobbe, R., Kasperson, R. E., and Kates, R. W., *Sci. Today*, 1982, **16**, 36.
5. Jacobs, M. B., "The Analytical Toxicology of Industrial Inorganic Pollutants," Interscience, New York, 1967.
6. Websten, B. D., *US Dept. Agric. Agric. Res. Serv.*, 1971, No. 24.
7. Bhatt, A. and Gupta, V. K., *Analyst*, 1983, **108**, 374.
8. West, P. W. and Gaeke, G. C., *Anal. Chem.*, 1956, **28**, 1816.
9. Scaringelli, F. P., Saltzman, B. E., and Fray, S. A., *Anal. Chem.*, 1967, **39**, 1709.
10. Dasgupta, P. K., Kymron, D., and James, U. V., *Anal. Chem.*, 1980, **52**, 1912.
11. Tokudo, M., Kumio, H., Shozo, F., and Subora, K., *Eisei Kagaku*, 1978, **24**, 213; *Chem. Abstr.*, 1979, **91**, 11174v.
12. Kniseley, S. J., and Throop, L., *Anal. Chem.*, 1966, **38**, 1246.
13. Warner, P. O., "Analysis of Air Pollutants," Wiley-Interscience, New York, 1976.
14. Coffey, S., "Rodd's Chemistry of Carbon Compounds," Second Edition, Volume IC, Elsevier, Amsterdam, 1965, p. 189.
15. Nauman, R. U., West, P. W., Francis, T., *Anal. Chem.*, 1960, **32**, 1307.

Paper A3/168
Received June 7th, 1983
Accepted September 19th, 1983

Photometric Titration of Fluoride with Zirconyl Chloride Using the Brinkmann Probe Absorptiometer

Philip E. A. Asea and Michael A. Leonard
Department of Analytical Chemistry, The Queen's University of Belfast, Belfast, BT9 5AG, UK

Fluoride masses in the range 0.15–25 mg in a total volume of 30 cm³ were titrated photometrically at 520 nm using zirconyl chloride as titrant and sodium alizarin-3-sulphonate as indicator. The instrument used was the highly suitable Brinkmann fibre-optic probe absorptiometer. The influence of pH and other variables was assessed. The coefficient of variation for medium and high fluoride concentrations in the range covered was 0.18%. Phosphate, aluminium and iron(III) interfere badly. Comparison was made with the lanthanum nitrate potentiometric titration.

Keywords: *Photometric titration; fluoride determination; zirconium(IV) titrant; alizarin sulphonate indicator*

In 1967, Harzdorf of Bayer showed that good quality photometric titrations of fluoride were possible with thorium, aluminium, zirconyl,[1] lanthanum and yttrium salts.[2] Zirconyl chloride was a particularly appropriate titrant because at moderate fluoride concentrations no precipitate was produced. The aim of our investigation was to apply the excellent and available Brinkmann fibre-optic probe absorptiometer to this titration. Harzdorf's indicator was the commercially unobtainable purpurin-3-sulphonate; we have used the readily obtainable alizarin-3-sulphonate (sodium 1,2-dihydroxyanthraquinone-3-sulphonate; Alizarin Red S).

Experimental and Results

Reagents

All reagents were of analytical-reagent grade unless indicated otherwise.

Zirconyl chloride titrant, 0.01 M. Warm 3.22 g of $ZrOCl_2.8H_2O$ (BDH Chemicals, "For fluoride determinations" grade) with 6.0 cm³ of glacial acetic acid and a small volume of water. When solution is complete, dilute to about 800 cm³ and filter into a 1-litre calibrated flask through a fine filter-paper. Wash the filter with water and dilute the filtrate and washings to 1 l. Standardise by titration against standard EDTA in hot acid (*ca.* 0.05 M nitric acid) solution using Xylenol Orange as indicator.

Sodium fluoride solution, 0.060 M. Dry sodium fluoride at 110 °C for 2 h, dissolve 2.519 4 g in water and dilute to 1 l.

Chloroacetate buffer, 1 M, *pH* 3.2. Dissolve 94.5 g of monochloroacetic acid in about 850 cm³ of water then add fresh concentrated sodium hydroxide solution until pH 3.2 is achieved. Beware of the heat produced. Dilute to 1 l and filter through a fine filter-paper.

Alizarin Red S indicator, 5×10^{-4} M. Dissolve 0.171 2 g of Alizarin Red S (BDH Chemicals, "For fluoride determinations" grade) in about 200 cm³ of water and raise the pH to 4.0 with a small volume of sodium hydroxide solution. Dilute to 1 l and filter through a fine filter-paper into a brown glass bottle. This grade of Alizarin Red S is markedly superior to many indicator-grade samples.

Apparatus

A Sybron - Brinkmann Model PC 801 Digital Probe Colorimeter fitted with a 520-nm interference filter and a 2-cm polycarbonate probe tip was used. A Pye Unicam PW 9415 ion-selective meter was used for pH measurements.

Basic Method

Pipette x cm³ of 0.060 M sodium fluoride solution into a 50-cm³ tall-form beaker held on a magnetic stirrer. Add $15 - x$ cm³ of water and 10.0 cm³ of 1 M chloroacetate buffer (pH 3.2), then immerse the probe, introduce and activate an appropriate stirring bar and set the instrument to read zero absorbance. Check carefully for air bubbles in the light path. Add 5.0 cm³ of indicator solution then titrate photometrically at 520 nm with 0.01 M zirconyl chloride solution added from a 10-cm³ microburette. A magnifying burette reader is a great help. When the absorbance begins to increase add the titrant in, for example, 0.1-cm³ steps with a constant waiting time of *ca.* 20 s. Plot a graph of absorbance against volume of titrant added using the usual $(V + v)/V$ correction of absorbance for dilution, where V is the starting volume (30 cm³) and v is the volume of titrant added. Note the intersection of the tangent to the point of inflection with the extension of the initial horizontal line. The volume indicated is, as will be demonstrated, accurately proportional to the mass of fluoride taken.

Effect of Variables

The most critical experimental factor is the titration solution pH. Fig. 1 shows the change in shape of the titration curve with this variable; it is apparent that the method is feasible at any pH between 1 and 4. The main reactions occurring in solution can be represented approximately as follows:

$$6F^- + ZrO^{2+} + 2H^+ \rightleftharpoons ZrF_6^{2-} + H_2O \quad (1)$$

$$F^- + H^+ \rightleftharpoons HF \quad (2)$$

$$\underset{\text{(yellow)}}{H_2In^-} + ZrO^{2+} \rightleftharpoons \underset{\text{(red)}}{\text{"ZrOIn"}} + 2H^+ \quad (3)$$

$$\underset{\text{(red)}}{H_2In^-} \rightleftharpoons \underset{\text{(red)}}{HIn^{2-}} + H^+ \quad (4)$$

At low pH reaction (3) dominates by inhibiting the formation of the zirconium - indicator complex and end-points are high. At high pH the starting absorbance is high because an indicator phenolic group is partially ionised [reaction (4)]. The end-point is low because the metal - indicator complex forms readily [reaction (3)] and this is not compensated for by the increased proportion of F^- with respect to HF [reaction (2)].

Fig. 2 shows the changes in point of inflection, point of intersection and gradient at inflection with pH. A pH of 3.2 was chosen as a compromise between high gradient and low Δ(titre)/Δ(pH). Harzdorf[1] also came to this conclusion. The buffer concentration in the titration solution is very high in order to minimise pH change as the titration proceeds. Also, the titrant is made up in 0.1 M acetic acid instead of nitric or hydrochloric acid to minimise change of pH. From the ease with which zirconyl chloride dissolves in about 2 M acetic acid acetato complexes must be formed; these seem to stabilise the solution and are in no way deleterious.

Because of the complex interrelation of reactions, the over-all titration reaction is slow and Fig. 3 shows the change of absorbance with time when the required volume of titrant to reach inflection is added as a slug. A pause is thus recommended following each titrant addition, but Fig. 4

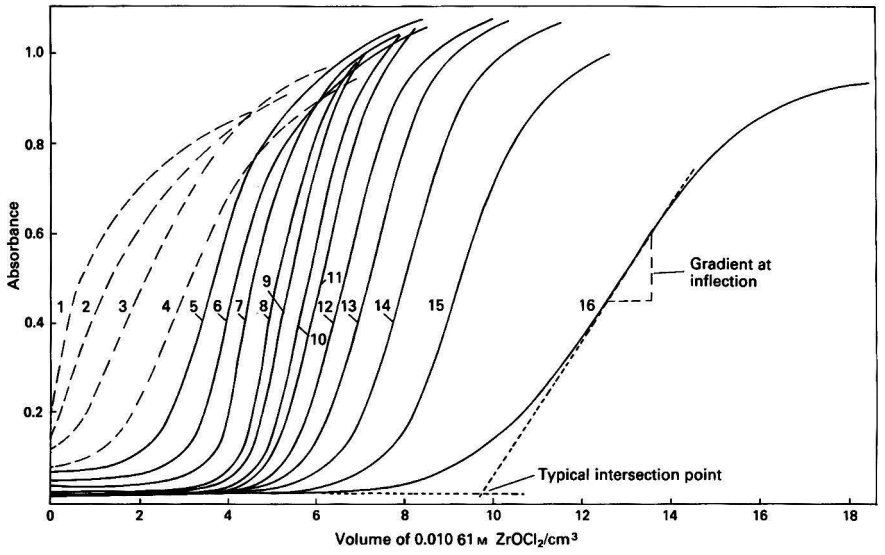

Fig. 1. Change of titration curve with pH. Basic method applied to 5.0 cm³ of 0.060 M sodium fluoride solution. pH varied by the appropriate addition of sodium hydroxide solution or hydrochloric acid. Full lines, chloroacetate buffer solution; and broken lines, acetate buffer at the same concentration. Mean pH over titration: 1, 4.77; 2, 4.64; 3, 4.44; 4, 4.23; 5, 4.01; 6, 3.83; 7, 3.63; 8, 3.35; 9, 3.25; 10, 3.07; 11, 2.81; 12, 2.48; 13, 2.19; 14, 1.81; 15, 1.24; and 16, 0.68

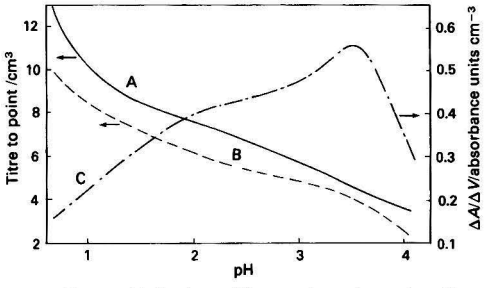

Fig. 2. Change of inflection and intersection points and gradient at inflection with pH. Conditions as for Fig. 1. A, Inflection points; B, intersection points; and C, gradient at inflection

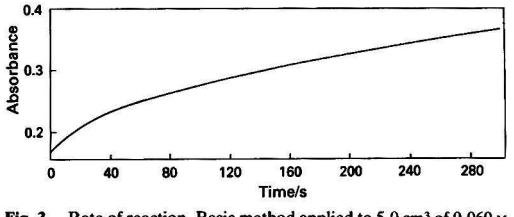

Fig. 3. Rate of reaction. Basic method applied to 5.0 cm³ of 0.060 M sodium fluoride solution. 5.3 cm³ of 0.010 61 M zirconyl chloride solution added all at once

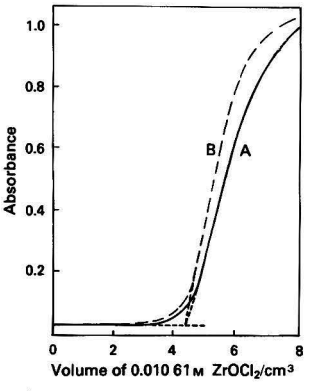

Fig. 4. Effect of different pause times. Basic method applied to 5.0 cm³ of 0.060 M sodium fluoride solution. A, Pause time of 5 s; B, pause time of 30 s. The titre is 4.40 cm³ in both instances

illustrates that the duration of this pause is not critical. The temperature of the titration is unimportant—by linear regression $\Delta(\text{titre})/\Delta T = -0.004\,2$ cm³ K⁻¹; so too is the amount of indicator added (Table 1). Addition of ethanol causes problems with bubble formation and does not improve location of the intersection point.

Titration of different amounts of fluoride

A volume of 0–15 cm³ of 0.060 M sodium fluoride was titrated as in the basic method. Table 2 shows the titres obtained and their *y*-axis distances from the regression line. The mean deviation was 0.036 cm³. Probably owing to kinetic factors, the deviation of points from 5 to 15 cm³ of fluoride solution is lower at 0.016 cm³ (Table 3). This is a relative mean deviation of 0.18% at 10.0 cm³ of fluoride taken.

For lower amounts of fluoride volumes of 0.015 M sodium fluoride solution were titrated with 0.002 7 M zirconyl chloride solution using smaller amounts of buffer and indicator. Here the mean deviation from the line was 0.057 cm³ (Table 4). Chloroacetate complex formation with zirconium(IV) is

Table 1. Variation of intersection end-point with amount of indicator added. Basic method applied to 5.0 cm³ of 0.060 M sodium fluoride

Volume of 5×10^{-4} M Alizarin Red S taken/cm³	0.2	0.5	1.0	1.5	2.0	3.0	5.0
Titre/cm³	4.54	4.54	4.54	4.54	4.50	4.55	4.45

Table 2. Linearity and precision of titration of different amounts of fluoride

0.060 M NaF taken/cm³ (x)	0.010 61 M $ZrOCl_2$ titre/cm³ (y)	y value from linear regression line/cm³	y-axis deviation of point from line/cm³
0	0	−0.026	0.026
0.10	0.100	0.064	0.036
0.20	0.180	0.154	0.026
0.50	0.445	0.424	0.021
1.00	0.842	0.874	−0.032
2.00	1.695	1.774	−0.079
3.00	2.595	2.673	−0.078
4.00	3.652	3.573	0.079
5.00	4.482	4.473	0.009
7.00	6.265	6.272	−0.007
10.00	8.935	8.971	−0.036
12.00	10.800	10.770	0.030
15.00	13.475	13.469	0.006

Slope = 0.900.
Correlation coefficient = 0.999 9.
Mean y-axis deviation = 0.036.
Relative mean deviation at 5.0 cm³ of fluoride taken = 0.80%.
Relative mean deviation at 10.0 cm³ of fluoride taken = 0.40%.

Table 3. Linearity and precision for the titration of larger volumes of fluoride solution from Table 2

0.060 M NaF taken/cm³ (x)	0.010 61 M $ZrOCl_2$ titre/cm³ (y)	y value from linear regression line/cm³	y-axis deviation of point from line/cm³
5.00	4.482	4.468	0.014
7.00	6.265	6.270	−0.005
10.00	8.935	8.972	−0.037
12.00	10.800	10.773	0.027
15.00	13.475	13.475	0.000

y intercept = −0.035 cm³.
Slope = 0.901.
Correlation coefficient = 1.000 0.
Mean y-axis deviation = 0.016 cm³.
Relative mean deviation at 10.0 cm³ of fluoride taken (11.4 mg F) = 0.18%.

Table 4. Linearity and precison for the titration of fluoride at the lower limit of the method. x cm³ of 0.015 M sodium fluoride + 18 − x cm³ of water + 2.0 cm³ of chloroacetate buffer + 2.0 cm³ of indicator. Titrant, 0.002 70 M zirconyl chloride solution

0.015 M NaF taken/cm³ (x)	Titre/cm³ (y)	y value from linear regression line/cm³	y-axis deviation of point from line/cm³
0	0	0.090	−0.090
0.5	0.49	0.538	−0.048
1.0	1.10	0.987	0.113
2.0	1.94	1.884	0.057
3.0	2.81	2.780	0.030
4.0	3.66	3.677	−0.017
5.0	4.53	4.574	−0.044

Slope = 0.897.
Correlation coefficient = 0.999 1.
Mean y-axis deviation = 0.057 cm³.
Relative mean deviation at 2.0 cm³ of fluoride taken (0.57 mg F) = 3.03%.

strong, and therefore at low titrant concentrations the chloroacetate concentration must be correspondingly reduced. If sample solutions have a low buffer capacity, reduced chloroacetate concentrations will sharpen titration curves in any situation.

For large amounts of fluoride, volumes of 0.24 M sodium fluoride solution were titrated with 0.04 M zirconyl chloride solution under basic method conditions. If more than 6 cm³ of the fluoride solution were taken, precipitation occurred. Table 5 shows the mean deviation to be 0.008 cm³ and the relative mean deviation at 5.0 cm³ of fluoride taken to be 0.18%.

Table 5. Linearity and precision for the titration of large amounts of fluoride. Basic method. Titrant, 0.042 4 M zirconyl chloride solution

0.24 M NaF taken/cm³ (x)	Titre/cm³ (y)	y value from linear regression line/cm³	y-axis deviation of point from line/cm³
0	0	−0.014	0.014
1.00	0.880	0.883	−0.003
2.00	1.785	1.781	0.004
2.00	1.780	1.781	−0.001
2.00	1.769	1.781	−0.012
3.00	2.672	2.678	−0.006
3.00	2.660	2.678	−0.018
4.00	3.587	3.576	0.011
4.00	3.588	3.576	0.012
4.00	3.573	3.576	−0.003
5.00	4.481	4.473	0.008
5.00	4.480	4.473	0.007
5.00	4.461	4.473	−0.012
6.00	5.378	5.371	0.007
6.00	5.364	5.371	−0.007

Slope = 0.898.
Correlation coefficient = 1.000 0.
Mean y-axis deviation = 0.008 cm³.
Relative mean deviation at 5.0 cm³ of fluoride taken (22.8 mg F) = 0.19%.

Table 6. Linearity and precision of fluoride - lanthanum potentiometric titration (details in text)

0.060 M NaF taken/cm³ (x)	0.020 M $La(NO_3)_3$ titre/cm³ (y)	y value from linear regression line/cm³	y-axis deviation of point from line/cm³
1.00	0.968	0.982	−0.014
2.00	2.017	1.999	0.018
3.00	3.021	3.016	0.005
4.00	4.038	4.034	0.004
5.00	5.050	5.051	−0.001
5.00	5.040	5.051	−0.011
6.00	6.057	6.068	−0.011
7.00	7.095	7.085	0.010
8.00	8.102	8.102	0.000
9.00	9.120	9.119	0.001

y axis intercept = −0.035 cm³.
Slope = 1.017.
Correlation coefficient = 1.000 0.
Mean deviation of points from the line = 0.008 cm³.
Relative mean deviation at 5.0 cm³ of fluoride taken (5.7 mg F) = 0.15%.

Titration of a fixed amount of fluoride

Nine 9.0-cm³ volumes of 0.060 M sodium fluoride were titrated under basic conditions. The mean titre was 8.089 cm³ with a standard deviation of 0.015 cm³ and a corresponding coefficient of variation of 0.18%.

Interferences

Anionic

These compete with fluoride and the indicator for zirconium(IV) and important ones were deemed to be sulphate, phosphate and tartrate. Their influence is shown in Figs. 5, 6 and 7, respectively. Phosphate and tartrate interfere as expected but the effect of sulphate is odd. Even though for $Zr(SO_4)_3^{2-}$ log β_3 = 7.6,[3] absorbance is enhanced; ternary complex formation may be responsible.

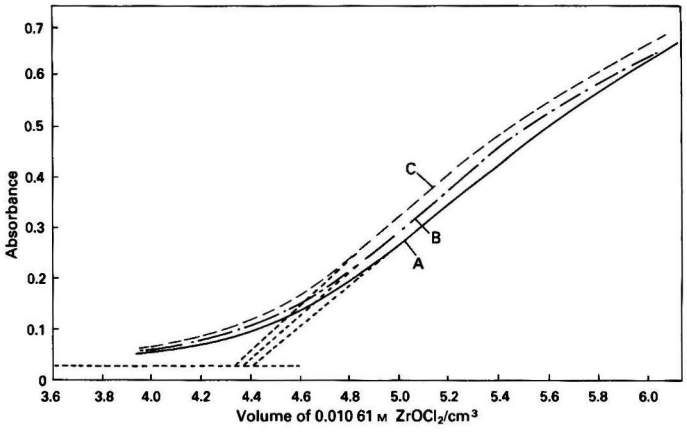

Fig. 5. Interference of sulphate. A, Basic method applied to 5.0 cm³ of 0.060 M sodium fluoride solution with B, 5.0 cm³ and C, 10.0 cm³ of 0.02 M potassium sulphate solution

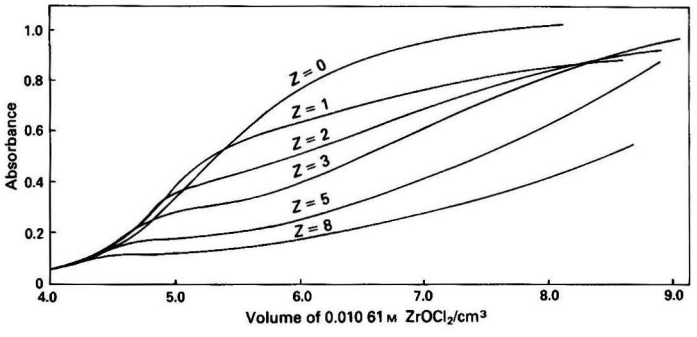

Fig. 6. Interference of phosphate. Basic method applied to 5.0 cm³ of 0.060 M sodium fluoride solution. Z = cm³ of 0.01 M sodium dihydrogen phosphate solution added. End-points: for Z = 0, 4.37 cm³; Z = 1.0, 4.37 cm³; Z = 2.0, 4.29 cm³; Z = 3.0, 4.25 cm³; Z = 5.0, 3.96 cm³; and Z = 8.0, 3.82 cm³

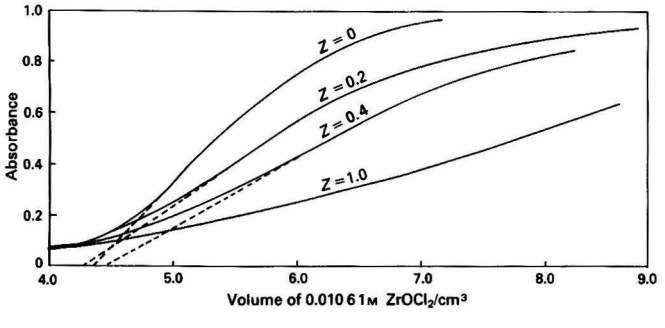

Fig. 7. Interference of tartrate. Basic method applied to 5.0 cm³ of 0.060 M sodium fluoride solution. Z = cm³ of 0.05 M tartaric acid solution added

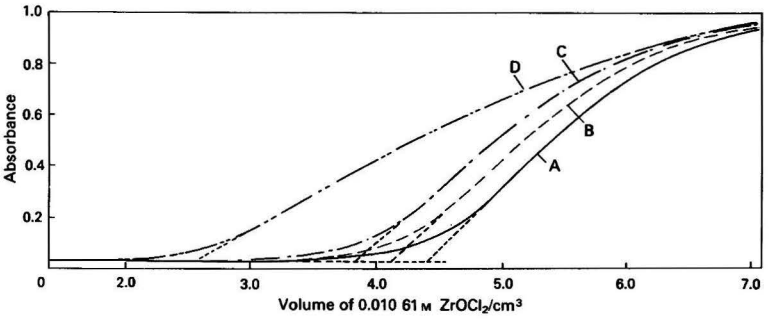

Fig. 8. Interference of aluminium. A, Basic method applied to 5.0 cm³ of 0.060 M sodium fluoride solution with B, 0.5 cm³, C, 1.0 cm³ and D, 2.0 cm³ of 0.01 M aluminium nitrate solution

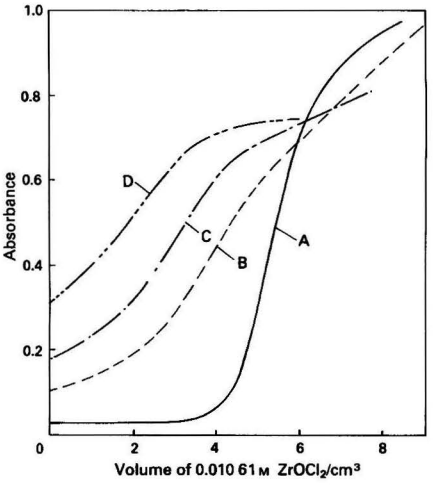

Fig. 9. Interference of iron(III). A, Basic method applied to 5.0 cm³ of 0.060 M sodium fluoride solution with B, 0.5 cm³, C, 1.0 cm³ and D, 2.0 cm³ of 0.01 M iron(III) ammonium sulphate solution

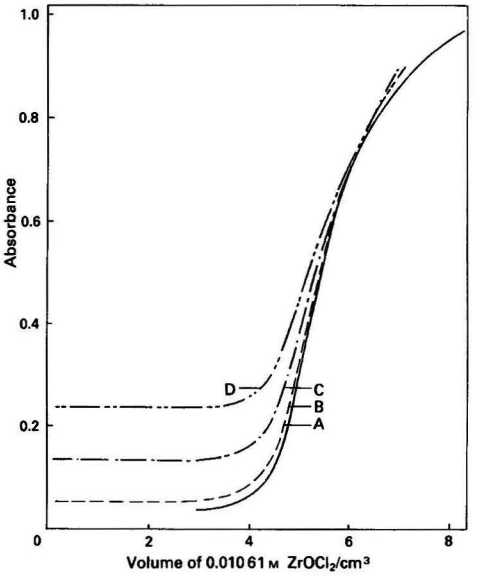

Fig. 10. Interference of copper(II). A, Basic method applied to 5.0 cm³ of 0.060 M sodium fluoride with B, 1.0 cm³, C, 5.0 cm³ and D, 10.0 cm³ of 0.01 M copper(II) sulphate solution

Cationic

These complex with fluoride and/or Alizarin Red S. Aluminium (Fig. 8) interferes principally by competing with zirconyl for fluoride, effectively weakening the Zr - F complexes. Iron(III) (Fig. 9) is interesting in that it complexes with both the indicator (note the high starting absorbance) and fluoride. The colour changes as the titration proceeds because zirconium replaces iron in the indicator complex. Copper(II) (Fig. 10) is an example of a metal that complexes with the indicator (high starting absorbance) but not fluoride (the titre is largely unchanged). A useful study concerning interference removal appears in reference 6.

Sulphonated Alizarin Fluorine Blue as indicator[4]

Purely out of interest this compound, 3-*N*,*N*-di(carboxymethyl)aminomethyl-1,2-dihydroxyanthraquinone-5-sulphonic acid, was tried. The curious result (Fig. 11) can, we think, be explained only on the basis of ternary complex formation.

Comparison of photometric and potentiometric titration

Volumes of 1–9 cm³ of 0.060 M sodium fluoride solution were diluted to 40 cm³ with water and titrated with 0.02 M lanthanum nitrate solution using a 14-year-old Orion fluoride electrode as indicator with a calomel reference electrode. An EIL 46A pH meter on the expanded scale setting followed the potential difference. Table 6 shows the results that were obtained with no great attention to experimental detail. The mean deviation from the line was only 0.008 cm³ and the relative mean deviation at 5.0 cm³ of fluoride taken was 0.15%.

Conclusion

This photometric fluoride titration is, we feel, as good a method as one is likely to achieve with this type of system. Even so, it is slightly inferior in terms of precision to the excellent potentiometric titration method of Frant and Ross.[5]

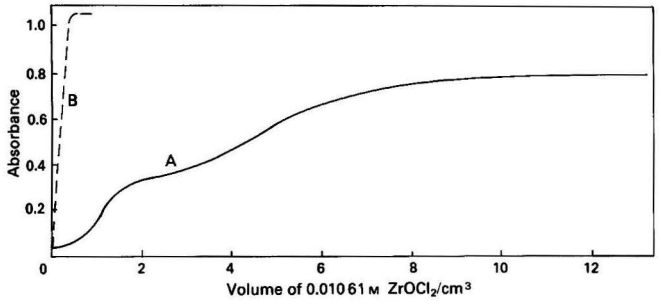

Fig. 11. Use of sulphonated Alizarin Fluorine Blue as indicator. A, With the following: 2.0 cm³ of 0.060 M sodium fluoride solution; 2.0 cm³ of 1 M chloroacetate buffer solution (pH 3.2); 21 cm³ of water; and 5.0 cm³ of 5×10^{-4} M "indicator." B, As above, with no fluoride

References

1. Harzdorf, C., *Z. Anal. Chem.*, 1967, **232**, 172.
2. Leonard, M. A., *in* Svehla, G., *Editor*, "Wilson and Wilson's Comprehensive Analytical Chemistry," Volume VIII, Elsevier, Amsterdam, Oxford and New York, 1977, p. 322.
3. Inczedy, J., "Analytical Applications of Complex Equilibria," Ellis Horwood, Chichester, 1976, p. 327.
4. Leonard, M. A., and Murray, G. T., *Analyst*, 1974, **99**, 645.
5. Frant, M. S., and Ross, J. W., *Science*, 1966, **154**, 1553.
6. Deane, S. F., Leonard, M. A., McKee, V., and Svehla, G., *Analyst*, 1978, **103**, 1134.

Paper A3/269
Received August 17th, 1983
Accepted September 27th, 1983

SHORT PAPERS

Novel Sampling and Support Media for the Infrared Analysis of Water-immiscible Oil-based Environmental Pollutants

Peter Jackson
Severn–Trent Water Authority, Coalport Laboratory, Coalport, Telford, Shropshire, TF8 7JF, UK

Keywords: *Organic pollutants; separation/support media; PTFE film; infrared spectroscopy*

In any environmental pollution investigation, rapid identification of the components is essential in order that effective preventative and protective action can be taken. Many such problems in the water industry involve the discharge of water-immiscible organic compounds into the aqueous environment, necessitating their recovery from this matrix. Often laboratory facilities are remote from the pollution incident and consequently the analysis is dependent on the effectiveness of the sampling process. Conventionally separation is achieved by solvent extraction, which can be difficult, tedious and time consuming and can often alter the chemical integrity of mixtures.

In developing an alternative technique, the solid - liquid interface is preferred to the liquid - liquid interface, particularly for an on-site application. As infrared spectroscopy is routinely used in the Coalport Laboratory for preliminary identification, the solid had to possess good infrared transparency in the range 4 000–625 cm^{-1}. It was essential that the solid should afford a clean separation from the water matrix or contaminated materials from the scene of a pollution. The material had to remain chemically inert with a sufficient absorption capacity to permit sample pre-concentration and storage. In the examination of mixtures it was necessary that the separation should maintain chemical integrity.

Experimental

The materials most suited to this task are polyfluorinated hydrocarbons, which are readily available, chemically inert and hydrophobic. From the spectra published in Moynihan's paper,[1] their prospects as supports for infrared spectroscopy did not appear promising, but technological improvements in materials such as the ICI Fluon range of polytetrafluoroethylene (PTFE) has provided more acceptable materials. A suitable product is a low-density engineering thread-sealing tape (12.5 mm wide, 0.1 mm thick), manufactured from a coagulated dispersion polymer. During the course of manufacture, extrusion and calendering processes promote fibre formation, which in turn endow the finished tape with ductility and tacticity. Although hydrocarbon lubricants are used in the extrusion process thermal treatment after calendering appears to remove any hydrocarbon residues.

Pre-stretched PTFE film suitable for analysis (0.05 mm thick) is prepared by self-adhesion to an inert former or by pressure adhesion to the surface of the standard cell holder bracket of the instrument. This type of film has good infrared transmission (Fig. 1) with strong absorption bands at 1 225 and 1 160 cm^{-1} from the C–F stretching modes and moderate bands at 620 and 505 cm^{-1} for the C–F bending modes. The ductile nature of the tape permits a variation in film thickness down to 0.01 mm, while the tacticity permits adhesion to a variety of surfaces.

The use of the cell holder bracket for support is suitable for direct sample application via a micropipette tip, whereas some type of former is required for *in situ* work such as sample recovery from polluted surfaces either aqueous or solid. With solid substrates slight pressure contact with the PTFE film is normally sufficient to permit transfer to take place. Any excess pollutant or water droplets are removed with the aid of a paper tissue. As the absorption takes place within the PTFE film the absorbate is stabilised under ambient conditions and if spectral resolution is required this can be achieved by further stretching of the film, removing any excess sample that may be exuded with a paper tissue.

Results

Under normal conditions a film area of about 2 cm^2 is exposed in the spectrometer sample beam and contains approximately 3 mg of sample. The sample is held in the fibrous matrix of the tape, which enhances its stability against evaporation under ambient conditions. Table 1 gives data on this stabilisation for a variety of oil products.

Table 1. Retention of various oils on PTFE film after 18 h at 20 °C

Oil type	Retention, %
20/50 engine oil	100
Vegetable oil	100
Light mineral oil	75
Gas oil	55
Kerosene (28 s)	0
Gasoline	0

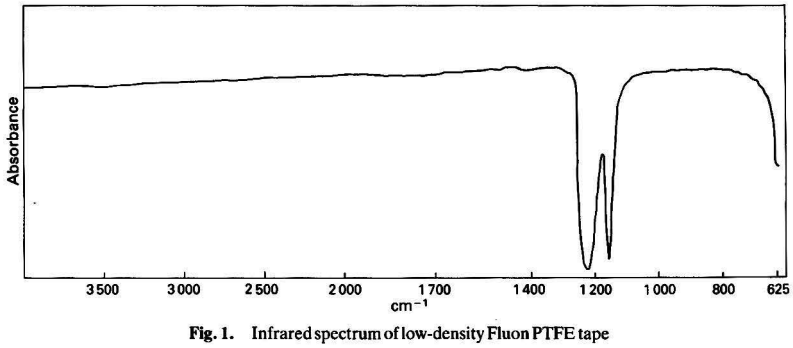

Fig. 1. Infrared spectrum of low-density Fluon PTFE tape

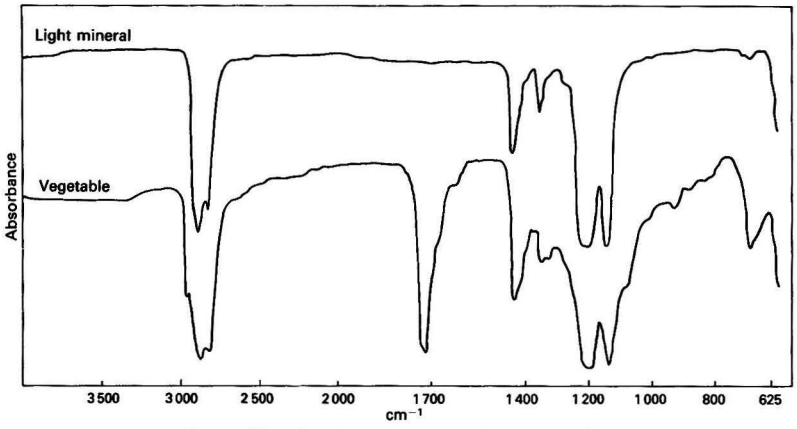

Fig. 2. Oil typing using PTFE tape as the support medium

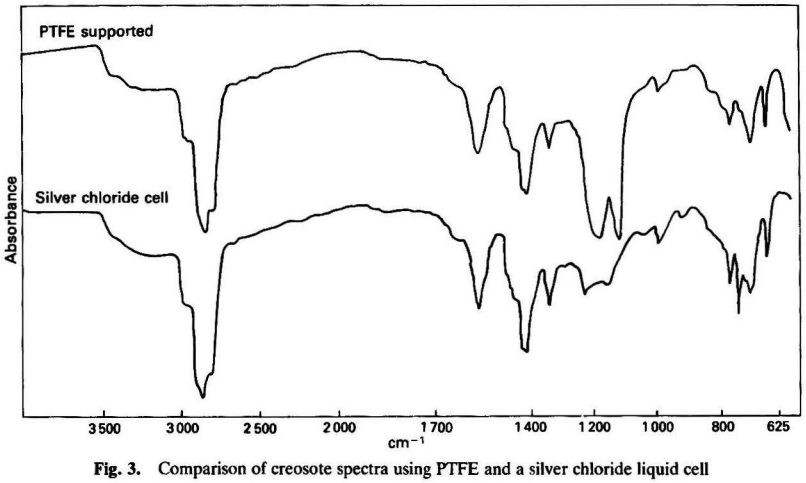

Fig. 3. Comparison of creosote spectra using PTFE and a silver chloride liquid cell

With kerosene there was a 50% retention after 0.5 h at 20 °C, whereas gasoline was retained for a sufficient time to permit a spectrum to be recorded. The technique permits an *in situ* study of thermal stability, which can aid identification, particularly when dealing with mixtures.

A high proportion of organic pollutant identification work in the water industry involves oil typing, for example the need to differentiate mineral and vegetable oils as shown in Fig. 2. In this situation the technique is valuable, as it effects a rapid separation and can cope with emulsions or provide pre-concentration of dilute dispersions.

When faced with a mixed pollutant the use of solvent extraction can complicate the identification process because of incomplete transfer of all the components into a particular solvent. The use of the PTFE tape procedure for water-immiscible deposits appears to overcome this problem, as shown in Fig. 3, which compares the spectra of creosote in PTFE with that of the free liquid in a silver chloride cell. Similar results were obtained with Cuprinol.

Discussion

Low-density PTFE tape has been found to be a suitable material for the recovery of water-immiscible organic pollutants and to provide a good support medium for infrared spectroscopy. The procedure provides a simple physical method for sample recovery with possible application to chromatographic analysis (both GLC and HPLC). The absorbed materials can be released by stretching the film, thus making them available for further analysis.

The effectiveness of the separation coupled with the stability of the absorbed pollutant within the PTFE matrix offers a useful on-site technique for sample collection and monitoring. The availability of the material in the form of a filter membrane could enhance the technique for applications involving the pre-concentration of dilute dispersions and possibly aerosols. The advent of micoprocessor-controlled infrared spectrometers has extended the infrared transmission of the PTFE tape as the stretching and bending modes are amenable to spectral subtraction. The use of such an instrument may also permit quantifiable investigations of *in situ* thermal desorption studies.

I thank the Severn–Trent Water Authority for the opportunity to publish this paper.

References

1. Moynihan, R. E., *J. Am. Chem. Soc.*, 1959, **81**, 1045.

Paper A3/233
Received July 18th, 1983
Accepted October 11th, 1983

Use of Infrared Spectroscopy in the Identification of Lubricating Greases

Dhoaib Al-Sammerrai and Elham Said
Petroleum Research Centre, P.O. Box 10039, Jadiriyah, Baghdad, Iraq

Keywords: *Lubricating greases; infrared spectroscopy; thickening agent*

Infrared spectroscopy has proved to be a very useful technique in the identification of lubricating greases, as it is fast and accurate and needs only small amounts of sample.[1]

Lubricating greases are the products of the dispersion of a thickening agent in a liquid lubricant. Most thickening agents are metal soaps of long-chain fatty acids (R–CO–O–M, $R \approx C_{17}H_{35}$) and constitute 10–15% of the composition.[2] The conventional infrared region which extends from 650 to 4 000 cm^{-1} has proved very useful for the identification of these compounds where the prominent group present is carbonyl (C=O).[3] The carbonyl group of these long-chain fatty acids absorbs round 1 700 cm^{-1}. When metals such as lithium, calcium, sodium, barium and aluminium replace the hydrogen of the acid, a shift of the carbonyl towards lower frequencies is observed, each metal contributing to a specific shift.[4]

In the work described in this paper, it was noticed that each metal soap absorbs infrared energy at characteristic wavelengths in the region of the spectrum from 200 to 600 cm^{-1}, and we propose the use of this region for additional qualitative identification of lubricating greases.

Experimental

Apparatus

The infrared spectra were recorded using a Pye Unicam Model SP3-300 infrared spectrophotometer. Samples were applied as a thin layer between two polystyrene films, each 0.5 mm thick. Similar films were placed in the reference beam of the spectrophotometer. The scanning time was 3 min.

Materials

Lubricating greases were prepared at elevated temperature by dissolving the individual metal soap of the fatty acid in a suitable mineral oil. The thickening agent input ranging from 8 to 12% by mass. Organic aluminium silicate grease, referred to as bentonite grease, was prepared by adding 6% of the thickening agent to a suitable oil followed by processing in a colloidal mill.

The greases were thoroughly homogenised prior to examination in the spectrophotometer.

Results and Discussion

From the analysis of the spectra for the different lubricating greases, and as shown in Fig. 1, different metal soaps were distinguishable as they absorb infrared energy at characteristic wavelengths in the low-frequency region of the spectra. The differences in the absorbances depend on the molecular environments, which are largely due to two effects: the extent to which different metal cations perturb the internal vibration of the carboxylate anions and the type of the fibrillar metal soap crystallites, which interlock in a three-dimensional network structure.

Greases based on lithium stearate and lithium 12-hydroxystearate showed strong absorbances at 355, 390 and 560 cm^{-1} and weak absorbances at 450 and 480 cm^{-1}. Sodium base grease showed two weak absorbances at 425 and 575 cm^{-1} and a strong absorbance at 535 cm^{-1}. Both lithium and sodium base greases possess long fibrillar crystallites, which are thicker in the sodium structure.

Calcium stearate base grease showed two strong absorbances at 430 and 570 cm^{-1}, while the normal and complex calcium base greases, which are derived from calcium salts of fatty acids, had strong absorbances at 480 and 470 cm^{-1}, respectively. Calcium base greases usually possess short, twisted fibrillar crystallites.

The barium base grease showed weak absorbances at 390, 490 and 515 cm^{-1} and very strong absorbances at 435 and 560 cm^{-1}.

Aluminium stearate base grease showed strong absorbances at 360, 390 and 455 cm^{-1}, while the bentonite grease showed a weak absorbance at 330 cm^{-1} and very strong absorbances at 460 and 510 cm^{-1}. The thickeners in aluminium and bentonite

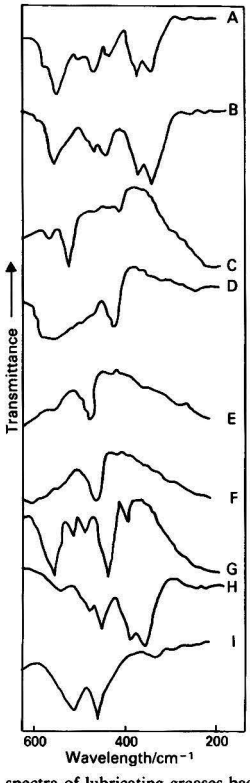

Fig. 1. Infrared spectra of lubricating greases based on A, lithium stearate; B, lithium 12-hydroxystearate; C, normal sodium; D, calcium stearate; E, normal calcium; F, complex calcium; G, normal barium; H, aluminium stearate; and I, bentonite

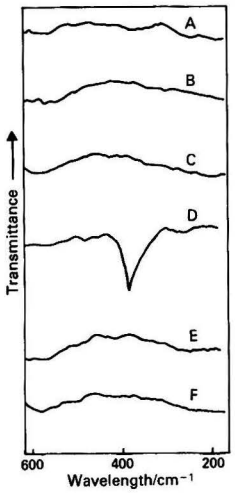

Fig. 2. Infrared spectra of A, mineral oil; B, stearic acid; C, animal tallow; D, silicone oil; E, hydrocarbon grease and; F, polyethylene grease

base greases are usually particulate rather than fibrous in nature, and in this instance the structure is maintained by three-dimensional linkages owing to very short-range inter-particle forces.

The infrared spectra of the mineral oil constituents of lubricating greases and the acids from which the metal soaps are derived exhibited no absorbances in the region 200–600 cm^{-1} and, as shown in Fig. 2, a very strong absorbance at 380 cm^{-1} was observed in the spectrum of silicone oil. Fig. 2 also shows two infrared spectra recorded for non-soap base greases, a hydrocarbon and a polyethylene base grease. Again, no absorbances were observed in the low-frequency region.

It is obvious that the infrared spectra of the soap base lubricating greases examined could be used in characterising these types of products and subsequently in a standard fingerprint.

References

1. Wiberley, S. E., Bauer, W. H., and Cox, D. B., *NLGI (Natl. Lubr. Grease Inst.) Spokesman*, 1960, **24**, 328.
2. Boner, C. J., "Modern Lubricating Greases," Scientific Publications (G.B.) Limited, Broseley, 1976, p. 1.3.
3. Stanton, G. M., *NLGI (Natl. Lubr. Grease Inst.) Spokesman*, 1974, **38**, 153.
4. Putinier, R. A., *NLGI (Natl. Lubr. Grease Inst.) Spokesman*, 1970, **34**, 204.

Paper A3/236
Received July 27th, 1983
Accepted September 21st, 1983

New Analytical Assays Using Hydrogen Peroxide and Peroxidase

K. V. S. S. Murty, K. Ekambareswara Rao and Ch. Suryaprakasa Sastry
Department of Chemistry, Andhra University, Waltair-530 003, India

Keywords: *Phenols determination; benzidine determination; peroxidase activity; spectrophotometry; hydrogen peroxide*

Peroxidases from various sources contain the ferriproto porphyrin prosthetic group, which catalyses the oxidations of electron donors with hydrogen peroxide to produce coloured species. Donors such as *p*-phenylenediamine,[1] *o*-phenylenediamine,[2] *p*-amino-*N*,*N*-dimethylaniline[3] and 4-methoxy-1-naphthol[4] were employed to determine peroxidase activity in foodstuffs using hydrogen peroxide. Earlier literature on peroxidase activity was summarised by Bergmeyer.[5]

Oxidative coupling reactions between 4-aminoantipyrine[6] or *N*,*N*-dimethyl-*p*-phenylenediamine[7] and phenols with hydrogen peroxide and peroxidase were utilised for the spectrophotometric determination of phenols. This paper describes the spectrophotometric determination of peroxidase activities of foodstuffs using *o*-aminophenol and hydrogen peroxide and the peroxidase activities of phenols and benzidine using an oxidative coupling reaction with hydrogen peroxide and peroxidase.

Experimental

Apparatus

A Systronics spectrophotometer (Model 105 MK 1) with 1-cm glass cells was used for measuring absorbance and an Elico (Model LI 120) digital pH meter was used for the pH measurements.

Reagents

All phenols used were of commercially available G.R. or C. P. grade. Stock solutions were prepared in distilled water; compounds that were insoluble in water were initially dissolved in the minimum volume of ethanol. Working solutions were prepared by the appropriate dilution of the stock solutions.

Hydrogen peroxide standard solution, 0.01 M. Prepared from 30% *m*/*V* hydrogen peroxide by titration against standard potassium permanganate solution.

Benzidine solution, 0.1%. Prepared by dissolving G.R. grade material (Loba Chemie) in ethanol.

o-Aminophenol solution, 0.2%. Prepared freshly by dissolving the solid (Reachim, USSR) in methanol.

Foodstuffs. Horseradish root (1 g) or beans were ground in a mortar and the enzyme was extracted two or three times with buffer solution. This was centrifuged and the centrifugate was suitably diluted. Milk (1 ml) was diluted to 200 ml with distilled water.

Horseradish peroxidase. Obtained from Sigma, USA. Prepared in 3.2 M ammonium sulphate solution containing phosphate buffer (pH 6.0) and standardised by using the donor pyrogallol adopting the procedure suggested by Sigma.

Potassium dihydrogen orthophosphate and disodium hydrogen orthophosphate buffer solutions, pH 7.0 and 6.0. Prepared according to the procedure of Lurie.[8]

Resorcinol solution, 1%. Obtained from Purex.

Phloroglucinol solution, 1%. Obtained from BDH Chemicals, laboratory-reagent grade.

m-*Aminophenol solution*, 1%. Obtained from BDH Chemicals, laboratory-reagent grade.

Phenol solution, 1%. Obtained from Sarabhai M, G.R. grade.

1-*Naphthol solution*, 1%. Obtained from BDH Chemicals, laboratory-reagent grade.

Hydroquinone solution, 1%. Obtained from Sarabhai M, laboratory-reagent grade.

Procedure

Phenols

Buffer solution (pH 7.0) (15 ml), benzidine solution (0.1%) (1 ml), hydrogen peroxide solution (0.01 M) (1 ml), horseradish root solution (1.0%) (2 ml) and phenolic solution (1.0–4.0 ml) were successively added to a 25-ml calibrated flask and the solution was made up to 25 ml with distilled water. After maximum colour development the absorbance at the $\lambda_{max.}$ was measured against a reagent blank prepared under similar conditions. The concentration of the phenolic compound was deduced from a calibration graph. The optical characteristics are shown in Table 1.

Benzidine

Buffer solution (pH 7.0) (15 ml), thymol solution (0.1%) (1 ml), hydrogen peroxide solution (0.01 M) (1 ml), horseradish root solution (1.0%) (2 ml) and benzidine solution (1.0–4.0 ml) were successively added to a 25-ml calibrated flask and the solution was made up to 25 ml with distillled water. The absorbance was measured at 530 nm after 8 min (8–16 min stability period) against a reagent blank prepared under similar conditions. The benzidine concentration was deduced from a calibration graph.

Peroxidase activity

Buffer solution (pH 6.0) (6 ml), *o*-aminophenol solution (0.2%) (1 ml), hydrogen peroxide solution (0.01 M) (1 ml) and

Table 1. Optical characteristics

Compound	Wavelength range/nm	Wavelength chosen for determination/nm	Time taken for maximum colour development/min	Stability of colour/min	Beer's law limits/μg per 25 ml	Sandell's sensitivity/μg cm^{-2} per 0.001 absorbance unit	Molar absorptivity/l mol^{-1} cm^{-1}
BHA	530–550	530	8	10	40–300	0.033	5.41×10^3
Thymol	550–570	550	8	7	40–200	0.032	4.69×10^3
Catechol	530–550	530	4	5	40–100	0.032	3.44×10^3
Benzidine	520–540	530	8	8	40–300	0.032	5.83×10^3

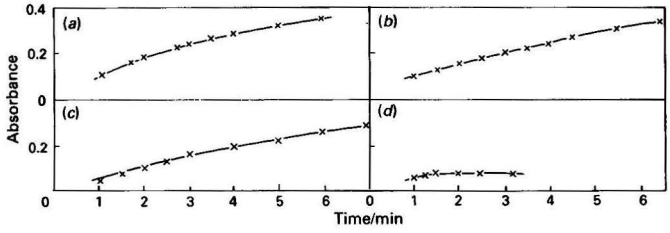

Fig. 1. Peroxidase activity of foodstuffs using *o*-aminophenol as donor. (*a*) 1 ml of 0.1% horseradish root in 10 ml; (*b*) 1 ml of 0.5% Bangalore beans in 10 ml; (*c*) 1 ml of 0.2% round beans in 10 ml; and (*d*) 1 ml of milk (1 : 200) in 10 ml. *o*-Aminophenol concentration, 1.833×10^{-3} M; hydrogen peroxide concentration, 1.0×10^{-3} M; and pH, 6.0. Absorbance increases at zero time: (*a*) 0.025; (*b*) 0.03; (*c*) 0.005; and (*d*) 0.005

Table 2 Peroxidase activity of foodstuffs

Foodstuff	ΔE (increase in absorbance per 120 or 90 s)*	Peroxidase activity†
Horseradish root (A)	0.165–0.025 = 0.14/120	1.166
Bangalore beans (B)	0.15–0.03 = 0.12/120	0.2
Round beans (C)	0.09–0.005 =0.085/120	0.345
Buffalo milk (D)	0.07–0.005 =0.065/90	0.144

* ΔE: A, for 1 ml of 0.1% solution; B, 1 ml of 0.5% solution; C, 1 ml of 0.2% solution; and D 1 ml of 1 : 200 solution.

† Measured per 1 g of A, B and C; and per 1 ml of 1 : 10 solution of D.

enzyme solution (prepared separately from horseradish root, beans and milk) (0.5–2.0 ml) were added to a 10-ml calibrated flask and diluted to the mark with distilled water. The rate of change in absorbance of the solution with time was recorded at 410 nm against a reagent blank. The absorbances were plotted against time and from this the absorbance increase at zero time was calculated. The peroxidase activity (K'') of the foodstuff was calculated using the relationship $K'' = \Delta E/\Delta T$, where ΔE and ΔT are the increases in absorbance and time, respectively. The results are shown in Fig. 1 and Table 2.

Determination of butylated hydroxyanisole (2-tert-*butyl*-4-*methoxyphenol* - 3-tert-*butyl*-4-*methoxyphenol*) (*BHA*) *in edible oils*

Oil (10 g) was dissolved in 100 ml of light petroleum and successively extracted with 5 × 15 ml aliquots of acetonitrile. The combined acetonitrile phase was diluted with water and re-extracted with light petroleum. The light petroleum was evaporated just to dryness and the residue was dissolved in 50% ethanol in order to obtain the desired concentration of BHA and the proposed procedure was subsequently followed. Studies of the recovery of added BHA from edible oils (groundnut and sunflower oil) using the proposed method gave a 96–98% recovery.

Results and Discussion

The optimum conditions for phenols (BHA, thymol and catechol) and benzidine determinations, based on the development of maximum colour and its stability through a varying parameter such as pH, peroxidase concentration, hydrogen peroxide concentration, phenol or benzidine concentration and sequence of addition, were established. The colorations may be due to the formation of quinoneimine derivatives formed from benzidine and phenolic compounds with hydrogen peroxide in the presence of peroxidase.

For the peroxidase activity determination, the optimum conditions were established by varying parameters such as pH, *o*-aminophenol concentration and hydrogen peroxide concentration. In the determination of peroxidase activity, the oxidation product of *o*-aminophenol appears to be 2-aminophenoxazin-3-one.[9]

For expressing the peroxidase activity of a horseradish root sample (obtained using this method) in terms of well known purpurogallin units, the crystalline principle of horseradish peroxidase (Sigma) was taken and its activity was determined separately using two donors, *o*-aminophenol (or pyrogallol) and hydrogen peroxide. The relationship between peroxidase activity values for each of the two methods was obtained. Samples of horseradish peroxidase ranging from 0.0023 to 0.0186 purpurogallin units per 10 ml can be determined within a 2% error. The peroxidase activity of the horseradish root sample (1 ml of 0.1 % solution) was found to be 0.0072 purpurogallin units per 10 ml.

Interference Studies

The interferences of other phenolic compounds in the determination of each mentioned phenolic compound (100 μg) were studied. It was noticed that resorcinol (less than four-fold excess), phloroglucinol (less than two-fold excess) and *m*-aminophenol (less than three-fold excess) do not interfere. However phenol, 1-naphthol and hydroquinone interfere seriously.

The new procedures developed for the determination of peroxidase activity of foodstuffs, phenols and benzidine are rapid, sensitive and accurate and can be applied even with turbid enzymic solutions. The procedure can be extended to the determination of BHA in oils.

We are grateful to the authorities of Andhra University, Waltair, and UGC and CSIR, New Delhi, for the awards of Teacher Research Fellowships under FIP and JRF to K.V.S.S.M. and K.E.R., respectively.

References

1. Aurand, L. W., Roberts, W. M., and Cardwell, J.T., *J. Dairy Sci.*, 1956, **39**, 568.
2. Vetter, J. L., Steinberg, M. P., and Nelson, A. I., *J Agric. Food Chem.*, 1958, **6**, 39.
3. Cervigni, T., and Giacomelli, M., *Ital. J. Biol. Chem.*, 1961, **10**, 65.
4. Guilbault, G. G., and Kramer, D. N., *Anal. Chem*, 1964, **36**, 2494.
5. Bergmeyer, H. U., *Editor*, "Methods of Enzymic Analysis," Academic Press, New York and London, 1965, pp. 895–897.
6. Miyamot, K., Santo, H., and Yokoyamma, T., *Eisei Kagaku*, 1978, **24**, 175; *Chem. Abstr.*, 1979, **90**, 174416p.
7. Kramer, D. N., and Hackley, B. E., *Anal. Lett.*, 1971, **4**, 223.
8. Lurie, Yu., "Handbook of Analytical Chemistry," Mir, Moscow, 1975, p. 257.
9. Gerber, N. N., *Can. J. Chem.*, 1968, **46**, 790.

Paper A3/58
Received February 23rd, 1983
Accepted June 20th, 1983

BOOK REVIEWS

The Interpretation of Analytical Chemical Data by the Use of Cluster Analysis

D. Luc Massart and Leonard Kaufman. *Chemical Analysis. A Series of Monographs on Analytical Chemistry and its Application, Volume 65.* 1983. Price £42.75. ISBN 0 471 07861 1

The need to interpret analytical data in fresh ways is becoming increasingly obvious. Modern analytical techniques produce, for a given sample, much more data than in the past, more rapidly and as output from a digital computer. One of the methods of data analysis that is attracting attention is pattern recognition analysis, which seeks multivariate associations in, or patterns within, the data. There are several divisions, each containing a variety of methods, so that the newcomer to the field is overwhelmed either by the mathematical aspects or by the bewildering number of options that are before him.

This book brings a very welcome clarification. It deals with cluster analysis, which is that part of pattern recognition analysis that seeks to classify raw data, without a prior assumption of the number of classes (it is also known as unsupervised learning techniques). By restricting it to these limits, the authors have been able to explain the principles of the method in depth and have included a very helpful section on the practical aspects of the matter. Their plan is to discuss the principles in qualitative terms and then with mathematical rigour, but it can be read by those whose maths education stopped some while ago.

The book can be unreservedly recommended to all of those chemists who want to know what cluster analysis is all about and how to do it. It is to be regretted that the structure does not permit consideration of supervised learning methods of classification, but it is to be hoped that a follow up book is in preparation.

The only irritation detected by this reviewer was one of editing; SIMCA, mention in many places in the text, described for one and a half pages and credited with being a major method of pattern recognition analysis, does not appear in the index.

D. Betteridge

GC/LC, Instruments, Derivatives in Identifying Pollutants and Unknowns

Raymond C. Crippen. Pp. xxx + 421. Pergamon Press. 1983. Price $75. ISBN 0 08 027185 5

The slightly unusual title covers a slightly unusual book. It comprises fourteen chapters and commences with a general discussion on the isolation of unknowns or pollutants. This is followed by a chapter on the preparation of derivatives of unknowns and pollutants; the succeeding nine chapters deal with the preparation of derivatives of particular groups of compounds. There is then a chapter about auxiliary identification techniques, which includes the various spectrophotometric instrumentation and thermometric and electrometric methods. Information is provided on procedures for collection and purification, and mention is made of automation of gas and liquid chromatographs with computers. A penultimate chapter is concerned with the utilisation of GC/LC data in physico-chemical measurements, and the text is completed with a chapter about recent developments in the identification of unknowns and pollutants.

The text proper is preceded by a list of illustrations, which the reviewer considered to be helpful. The chapter notes (references) are also extensive, and are grouped at the end of the volume. An author index is provided, and a fairly good subject index, which commences with a list of the abbreviations used.

The book contains a great deal of information that many users of chromatographic techniques will find familiar: in the present volume the intention is to relate this body of knowledge particularly to the indentification of "pollutants and unknowns." Unfortunately, the approach falls somewhere between that of the elementary textbook and the general *vade mecum* and, although many useful data are presented in convenient form, the banal and repetitive nature of the connecting text sometimes impairs appreciation. As an example, Chapter 2 opens with the observation, "Derivatives should not be prepared until some idea of the functional groups present is determined." Disregarding the doubtful sequence of tenses, there must surely be better ways in which this subject could be introduced for the more experienced reader. If subsequent editions should be required, a rather more rigorous editorial approach to the connecting text would be beneficial.

The book has been printed from typescripts which are clear, although corrections of errors can sometimes be seen.

It is a volume of many facts and should be helpful to the student and also for reference for the experienced worker in the fields mentioned.

D. Simpson

Chromatography in Organic Microanalysis. A Laboratory Guide

Raphael Ikan. Pp. 108. Academic Press. 1983. Price $22.50. ISBN 0 12 370580 0

This book contains only five chapters in slightly over 100 pages, but what there is of it is good. The text is in clear English and arranged in a convenient form. The first chapter covers various microsyntheses on thin layers of silica gel, followed by separation of isomers and other complexes. The remaining chapters cover reaction chromatography, the determination of food constituents by chromatographic techniques and forensic analysis. There are references at the end of each chapter (36 in all), together with a short bibliography of recommended reading.

The microsynthesis reactions included are those involving elimination of water, acylations, oxidations, reductions, nitration and azo coupling. The isomer separations include polyunsaturated fatty acids, *cis,trans*-azobenzene, polycyclic aromatic hydrocarbons, carbohydrates and optical enantiomers of amino acids.

The food constituents dealt with include sugars, synthetic sweeteners, an adulterant in honey, theobromine and caffeine, pepper, tocopherols, food preservatives, vitamins, antioxidants, dyes, carotenes, cholesterol and aflatoxins. The examples of forensic analysis are examination of ink for ball-point pens, some alkaloids, identification of residues after explosion and uses of ninhydrin as a spray reagent for the detection of some basic drugs.

In the work described, thin-layer, gas - liquid and high-performance liquid chromatographic techniques are all used, and experimental details are given.

The resulting volume is a handy manual that can be recommended to libraries, students and experienced chromatographers.

D. Simpson

Ions and Molecules in Solution
Edited by N. Tanaka, H. Ohtaki and R. Tamamushi. *Studies in Physical and Theoretical Chemistry, Volume 27.* Pp. viii + 470. Elsevier. 1983. ISBN 0 444 42208 0 (Volume 27); 0 444 41699 4 (Series).

This volume contains most of the session lectures and lectures delivered at microsymposia of the "VI International Symposium on Solute - Solute - Solvent Interactions" held at Minoo, Osaka Prefecture, Japan, in July 1982. The plenary lectures are excluded, having been published in *Pure and Applied Chemistry,* 1982, **54**, No. 8.

The material is divided into four sections: (i) Theoretical Treatments of Solute - Solvent Interactions; (ii) Thermodynamic and Structural Properties of Solutions; (iii) Equilibria and Kinetics in Solution; and (iv) Interactions between Water and Biological Molecules. The only material of direct interest to analytical chemists is papers in Section (iii) on "Analytical Chemical Aspects of Solution Chemistry," one of the conference's seven themes: "The Activity Concept in Analytical Chemistry" (R. G. Bates); "Some Applications of Macrocyclic Polyethers in Analytical Chemistry; Extraction Photometry of Alkali Metal Ions (K. Ueno and M. Takagi); and "Ionic Interaction and Phase Stability, Enthalpy - Entropy Linear Compensation and the Application of Solvophobic Theory" (S. S. Davis and E. Tomlinson). The paper "Effects of Nonaqueous Solvents on the Electronic Structure of Mixed Copper(II) Chelates" (K. Sone and Y. Fukuda) is of interest and potential importance as the compounds studied may be useful alternatives to the difficult to prepare Dimroth - Reichardt compounds, for the measurement of solvent polarity via solvatachromic spectral shifts.

Overall this is a scholarly volume. Amazingly, it has no index, which makes it difficult to locate quickly all mention of themes, such as concepts and measures of solvent polarity.

D. Thorburn Burns

Treatise on Analytical Chemistry. Second Edition. Part I. Theory and Practice. Volume 3. Section D. Solution Equilibria and Chemistry (Continued).
Edited by I. M. Kolthoff and P. J. Elving. Pp. xxiv + 592. Wiley-Interscience. 1983. Price £66.50. ISBN 0 471 49969 2

This volume must be viewed in the context of the broad aim and plan of the series. The Treatise was not designed as an extensive textbook nor was it intended to take the place of monographs on specific subjects but to serve as a thorough introduction to the methods of analytical chemistry, and also to provide the background for the detailed evaluation of topics and the efficient use of the literature, including specialised monographs. Section D of Volume 3 deals with six topics to complete the revised account of Solution Equilibria and Chemistry.

"Oxidation - Reduction Equilibria and Titration Curves" (88 pp., 368 references) by J. A. Goldman is a well balanced overview of experimental and theoretical aspects of titration curves, including non-ideal conditions, titration errors and end-point detection. A. M. Schwartz and P. J. Elving discuss selected, fundamental, aspects of "Surface Chemistry: Utilization in Analysis" (67 pp., 83 references); these include surface thermodynamics, capillarity, adsorption, electrical effects at interfaces, lyophilic and lyophobic colloids and foams. The physical, chemical and molecular aspects of the solubility of gases, liquids, amorphous polymers, biological compounds, solids and salts are interestingly detailed by E. S. Amis (117 pp., 287 references). The coherent scholarly review of "Precipitates: Formation, Coprecipitation and Ageing" by A. E. Nielsen (79 pp., 45 references) fills a gap in the modern literature of what is falsely regarded by many as an old fashioned, classical topic. The related topic "Precipitation Equilibria and Titrations in Aqueous and Nonaqueous Media" by J. F. Coetzee (45 pp., 65 references) includes a discussion of deviations between theoretical and experimental titration curves, detection of equivalence point and the role of the solvent.

The final chapters deal with selected aspects of reagent and reaction chemistry. H. Freiser, on "Reactive Groups as Reagents: Introduction and Inorganic Applications" (111 pp., 336 references), gives a good introduction to the principal uses of analytical reagents and classes of chelating ligands via the functional group approach. The "Organic Applications" of the same topic, reactive groups as reagents, are considered by J. G. Hanna (62 pp., 255 references). A useful survey is presented of redox, addition, condensation and substitution reagents.

The high standards of production and scholarship of the First Edition are maintained. This volume, as the others in the series, is an important source book for postgraduate course material both for students and academic staff. It is a pity the price inhibits personal purchases of such long-term, useful volumes. The Treatise is essential for every third-level institution library, and indeed every respectable departmental library.

D. Thorburn Burns

The Analysis of Gases by Chromatography
C. J. Cowper and A. J. DeRose. *Pergamon Series in Analytical Chemistry, Volume 7.* Pp. xii + 147. Pergamon Press. 1983. Price £14; $25. ISBN 0 08 024027 5.

Gas analysis is an ever important subject for which the technique of gas chromatography has obvious attractions. Such applications were described several years ago by Jeffery and Kipping in their valuable book "Gas Analysis by Gas Chromatography."

In the present volume, the authors aim to bring practitioners of gas analysis up to date with modern techniques, which include multi-column and valve-switching systems. These topics are described in Chapter 5, which follows the "usual" chapters on equipment, columns and carrier gases.

Applications are described in Chapter 6 and, not surprisingly as the authors are from the British Gas Corporation, are concerned primarily with fuel gases and related mixtures and components. A few chromatograms are shown to illustrate separations achieved by various techniques, but unfortunately are not accompanied by enough details on instrumental conditions. Such information would surely be valuable to fulfil the aim of the book in enabling workers to select equipment and analyse complex mixtures.

The remaining chapters concern gases in liquids, quantification, standards preparation and sampling. Certainly the last two chapters seem inadequate in view of the importance of calibration and sampling to analysis. For example, no mention is made of adsorptive trapping and desorption techniques which, despite their problems, are widely used.

Overall, this is a book likely to appeal to those seeking to obtain an introduction to gas analysis by chromatography rather than the specialist seeking further information.

R. S. Barratt

Calculations in Advanced Physical Chemistry. Third Edition.
P. J. F. Griffiths and J. D. R. Thomas. Pp. viii + 303. Edward Arnold. 1983. Price £8.95. ISBN 0 7131 3483 6.

Previous editions of this book of physical chemistry problems have proved invaluable to both staff and students involved in physical chemistry courses at university or equivalent level. This Third Edition contains a larger number and wider range of questions, including for the first time a number on statistical thermodynamics. At the beginning of each chapter is a set of worked examples. These are followed by additional problems drawn from examination papers to which answers are given at the end of the book.

In this revised edition the nomenclature has been modernised and the units are largely but not exclusively SI. Occasionally this revision has not been as thorough as it might have been. Thus, in Example 9.5 pressures still have non-pressure units of kg cm^{-2}. Such errors, however, are few.

The book is open to one other criticism. Although the authors in the Preface mention that pocket calculators are now generally available, in modernising the book they have not really taken this into account. Calculators permit values of natural logarithms to be obtained directly, yet the authors throughout still assume natural logarithms can best be obtained from logarithms to base 10 by introduction of the factor 2.303. This factor and its introduction are unnecessary complications in many of the worked examples. Only in a few special areas, such as calculations involving pH, is there any longer a need to use logarithms to base 10, which, if required, can be obtained from a pocket calculator. So the tables of logarithms to base 10 and antilogarithms that appear at the back of the book are superfluous.

These criticisms, however, do not affect the merit and value of this book. Physical chemical principles underpin most analytical methods. Hence, it is desirable that analysts have a working knowledge of basic physical chemistry. Anyone who makes use of this book and works through the problems it contains will be greatly helped to acquire such knowledge.

A. N. Strachan

Analytical Aspects of Environmental Chemistry.
Edited by David F. S. Natusch and Philip K. Hopke. *Chemical Analysis, Volume 64.* Pp. xii + 267. Wiley-Interscience. 1983. Price £35.50. ISBN 0 471 04324 9.

The aspects referred to in the title are Chemical Speciation (60 pp.), Capillary Gas Chromatography (52 pp.), Gas Chromatography/Mass Spectrometry (24 pp.), Surface Analysis Techniques (54 pp.), ESCA (28 pp.) and Multivariate Analysis (44 pp.). Each of these chapters is written by an author or authors at a number of North American Universities and thus all examples of applications to real environmental samples reflect their geographical origins. The book is written for environmental specialists and most chapters are state-of-the-art reviews rather than introductions to the various techniques. This, together with the rather fragmented set of topics themselves, makes the book unsuitable for student use, except at the postgraduate level. Students on an MSc course in environmental analysis (if such a thing exists) would find the book useful. On the whole the chapters are free from errors (apart from a number of easily recognised printer's errors) and omissions and are well referenced, providing a useful starting point for someone wishing to find out more about a particular topic. The book is not really aimed at analytical chemists, as very early in the book it is made apparent that spending time devising analytical methods for new environmental problems is "not very pleasant" and "particularly upsetting" and the terminology used assumes at least some knowledge of environmental science. On the whole, the style is as lively as one comes to expect from a text of this sort and occasionally the jargon becomes intrusive; for example, "The accelerated exposure to toxic trace elements is the direct consequence of their increased mobilization in the biosphere resulting from raw materials acquisition and the energy consumption to sustain advanced technologies. The sudden nature of the mobilization is of ecological significance in that organisms do not have the benefit of evolutionary mechanisms to provide effective homeostatic defences against these xenobiotic materials."

The final chapter provides a useful starting point for anyone, not just environmental scientists, contemplating the use of multivariate analysis and, although the necessary statistical background is taken at a brisk pace, a "worked example" based on literature data is given in some detail.

On the whole, not the sort of book every analytical chemist should have on his or her desk, but your library should have a copy.

J. F. Tyson

Tables of Spectral Data for Structure Determination of Organic Compounds. Chemical Laboratory Practice
E. Pretsch, T. Clerc, J. Seibl and W. Simon (translated from German by K. Biemann). Pp. ix + 316. Springer-Verlag. 1983. Price DM32; $12.70. ISBN 3 540 12406 3; 0 387 12406 3.

A proper understanding of the interpretation and of the relative merits of carbon-13 nuclear magnetic resonance (NMR), proton NMR, mass, infrared absorption and ultraviolet absorption spectra is an essential requisite for structural studies on new organic compounds. The five spectroscopic techniques provide different but complementary analytical information, which must be assessed impartially and considered jointly before a verdict can be reached on the composition of an organic compound.

Such assessments are helped by this English translation of the Second Edition (1981) of a successful German compendium of tables and charts, correlating carbon-13 and proton NMR, infrared, ultraviolet - visible and mass spectral data with molecular structures. The compendium is based on compilations made by the Swiss authors, when presenting spectroscopic courses to students at the Federal Institute of Technology (ETH) in Zurich. The authors assume that the reader is familiar with the basic principles of, and the experimental procedures for, each technique, and the tables, which supplement standard spectroscopic texts and reference works, are set out with minimal editorial comment.

An unusual feature of the book is that the pages are numbered in increments of five to "facilitate later additions," and are letter coded "to aid rapid access to relevant data." However, there is no suggestion as to when or how "later additions" will be supplied; the letter-coded pagination is the same as that in the first German edition (1976).

In the introductory section (coded KOMB), which was planned to assist tyros and to provide preliminary information on new compounds, summaries of the characteristic NMR, mass, infrared and ultraviolet spectral values for each structural feature are grouped together on double pages. The remaining tables, which are arranged conventionally, permit

detailed checks for a wide range of chemical features, and can be used to predict spectral data for new structures. The mass spectrometry section contains mass correlation and isotope abundance tables and has suggestions for interpreting simple electron-impact spectra. Charts showing spectra of common solvents appear at the end of each section. Detailed literature references are not given, but there is a short bibliography of books for further reading.

Chemical shift values for NMR spectra are quoted for solutions in deuteriochloroform or carbon tetrachloride, whereas the infrared measurements refer to solutions in chloroform or carbon disulphide. Solvent effects, which are often of major importance in NMR and infrared studies, are not discussed. The volume contains a remarkable amount of tabulated information, but it is of limited value to chemists concerned with steroids, sugars, β-lactam antibiotics and other compounds, where small spectral differences may be associated with large structural changes; for these compounds, reference must be made to specialised monographs.

The compendium, which has a soft cover and was printed by photographic reproduction of typescript, is reasonably up to date; thus, tables containing carbon-13 NMR data, the latest technique to be accepted for routine structural studies and now becoming the most important, are given priority. The volume should find a place as a first reference work alongside spectrometers, on open access, in analytical laboratories.

J. E. Page

Drogenanalyse. Dünnschichtchromatographische Analyse von Arzneidrogen

H. Wagner, S. Bladt and E. M. Zgainski. Pp. xiv + 321. Springer-Verlag. 1983. Price DM148; $63.80. ISBN 3 540 11867 5.

The essential feature of this book is the presentation of an atlas of 165 colour photographs showing the thin-layer chromatography (TLC) of around 100 vegetable drugs, spices and dyestuffs. The book is divided into 13 major sections, each dealing with a class of natural product, *e.g.*, volatile oils and resins, alkaloids, phenolic and anthracene glycosides, coumarins, cardiac glycosides. Except for the narcotics section, which deals solely with cannabis, each part contains a set of monographs showing the solvent system, fluorescence characteristics, colour reaction with a variety of spray reagents and R_F values of the individual components and reference compounds. Each monograph has a facing colour plate. In addition, each section is prefaced by a table of chemical structures of representative members together with experimental details for the extraction of the plant material and the preparation of reference solutions. Further tables show the proportion of major constituents in each drug. Later sections deal with the TLC of an unknown drug and with the analysis of mixtures. Using two solvent systems and a range of detection reagents, a test extract can be allocated to one of the major groups; subsequent identification can then be achieved by reference to the respective monograph.

Documentation in TLC so often involves either simple descriptions or idealised diagrams. The authors' objective was to produce a true record of the chromatograms using visible and UV fluorescence photography. In this respect, the colour plates are excellent. A particular problem with the chromatography of complex mixtures is the inherent variability in their composition. On the basis of their long experience in photographic documentation, the authors claim to have chosen representative chromatograms.

To a certain extent, this book is designed as a supplement to those continental Pharmacopoeias in which TLC is used as a standard method of drug assay. Nevertheless, this publication should prove useful to any analyst engaged in the extraction and quality control of herbal substances, and provides a valuable work of reference for those already familiar with, for example, Egon Stahl's handbook "Drug Analysis by Chromatography and Microscopy" (1973).

Although many poisonous and hallucinogenic plants and fungi are beyond the scope of a publication devoted to natural products of medicinal value, their inclusion in an appendix would have made this book of much greater interest to clinical and forensic toxicologists. In view of the number of colour plates and the general high quality of this publication, its high cost (12 pence per page) is probably not excessive.

L. A. King

Chemical Methods in Gas Chromatography

V. G. Berezkin. *Journal of Chromatography Library, Volume 24.* Pp. x + 313. Elsevier. 1983. Price $73.25 (USA and Canada); Dfl190 (Rest of World). ISBN 0 444 41951 9.

In an introductory chapter, the author explains something of the scope and intention of the present work, quoting among other things the results of polling carried out to determine the frequency of use of various analytical techniques, giving a comparison of analytical reaction gas chromatography with "classical" chromatography, and examples of chromatograms derived.

The text proper contains nine chapters and commences with the application of chemical methods to the pre-treatment of samples prior to chromatographic separation. The ensuing chapters are on kinetic methods; pyrolysis - gas chromatography; determination of the carbon skeleton in organic compounds; subtraction method; chemically selective stationary phases; reaction gas-chromatographic methods of elemental analysis; reaction methods of trace analysis; and functional group analysis.

Methods of derivatisation, for the most part fairly well established, are given in some detail, pyrolysis - gas chromatography is introduced and discussed, and among other topics the structure of polymers is investigated. The chapter on the subtraction method is of particular interest, covering the removal from a mixture under analysis of one or more components, and methods of elemental analysis involving reaction gas chromatography could also be of general interest.

The text is lucid and somewhat wider in scope than the earlier volumes in this series on the subject of chemical derivatisation. It is an unusual book, into which a great deal of work has gone. It provides a review of the techniques mentioned and contains a total of almost two thousand references (including some in the Introduction). The purchase of the volume by libraries as a book of reference could be recommended.

D. Simpson

A Guide to the Analysis of Hydrocarbons by Gas Chromatography. Third Edition.

Seaton T. Preston, Jr., and Ronald E. Pankratz. Pp. vi + 344. PolyScience Corporation. 1983. ISBN 0 913106 21 6.

There is not a lot to say about this publication. It is produced by PolyScience Corporation and is a soft-backed volume containing data, probably exhaustive, on the gas - liquid chromatography of hydrocarbons.

There are general instructions covering nomenclature, liquid phase and solid support selection, detector selection, some details of qualitative and quantitative determinations

and physical properties. These are followed by retention data, which represent a significant proportion of the book, a liquid phase index to retention data and a bibliography said to include all references pertinent to the subject published prior to 1 March 1968 with selected papers up to and including 1981.

To anyone involved much in the analysis of hydrocarbons using gas - liquid chromatography this would be a very useful reference volume.

D. Simpson

A Handbook of Inductively Coupled Plasma Spectrometry
M. Thompson and J. N. Walsh. Pp. xx + 273. Blackie. 1983. Price £35. ISBN 0 412 00371 6.

In choosing the title of handbook rather than textbook, the authors immediately indicate the intended scope of their book and to a great extent they succeed in their objective. An early impression is that they are "bending over backwards" to be fair and they exhibit some neat footwork in side-stepping the more controversial areas. However, they do not always succeed in being fair, as, for instance, their comments on high power where they make no mention of torch size and do not indicate that this is crucial to the argument. Neither are they always accurate. It was not "suggested that differences in ICP discharges do not vary significantly at high or low frequencies, but depend more on the injector gas flow-rate," it was said that "the size of the hole in the plasma did not depend on frequency but depended on the injector gas flow-rate," a small but essential difference.

Another statement with which statisticians might argue is that internal standards improve the precision of an analysis. They cannot improve precision although they may correct for drift and as a result improve accuracy.

Many successful "retrofitters" would not agree that "retrofitting is only for instrumental experts." This is not a task for a technician but should not be beyond the capabilities of a graduate chemist.

Some definitions are "woolly." Spectral interference, chemical matrix effects, ionisation effects and transport problems are well known and well used terms that most spectroscopists use, and have used, for a very long time. The lumping together of these terms into three categories is confusing.

This reviewer also finds it amazing that in 1983, 21 years after work first started on ICP - OES, that the authors state that they "believe that ICP - OES will become a dominant force in elemental analysis comparable to AA." How long does it take for a technique to be accepted?

These, and many other generalities in what might be described as the theoretical sections of the book, detract from what might otherwise be said to be a sound, authoritative account of ICP - OES.

Where the authors become more sure-footed is in the practical analysis sections, which are obviously written by practising analytical chemists—a skill which is not always a prerogative of academics.

The remainder of the book, "ICPs–Now and in the Future," might be considered padding, as might the chapter on safety (practically mandatory these days), but a tyro might be interested in reading it.

All in all, a book that can be recommended to those new to the field seeking to obtain an overview of the subject and who are not likely to notice the many over-simplifications which in themselves do not reduce the usefulness of the practical information contained in this reasonably priced handbook.

S. Greenfield

Introduction to Photoelectron Spectroscopy
Pradip K. Ghosh. *Chemical Analysis. A Series of Monographs on Analytical Chemistry and Its Applications, Volume 67.* Pp. xii + 377. Wiley–Interscience. 1983. Price £52.25. ISBN 0 471 06427 0.

Photoelectron spectroscopy has witnessed a meteoric rise in importance during the past decade, from a rather esoteric academic pursuit to having widespread, if specific, uses in industry and research. It is the technique *par excellence* for the analysis of surfaces, and not simply elemental analysis as shifts of characteristic peaks can be related to valency and a study of anisotropic photoelectron emission can be used to reveal the structure and composition of surface layers. An understanding of these and other chemical effects in photoelectron spectroscopy has been facilitated by rapid advances in the theory of photoelectron emission itself and by the development of new theoretical models to rationalise the energies and relative intensities of photoelectrons emitted from molecules, complexes, alloys and other solids.

Because of the wealth of original research material that has been produced, there is a great need for a concise but thorough review of all aspects of photoelectron spectroscopy, X-ray and UV induced, experimental and theoretical, as well as of practical applications. This is what Dr. Ghosh has succeeded in doing in this book. Whilst there is little that is new or original, it provides an excellent review of previous work. Indeed, it would be ideal for someone new to the field who seeks a clear exposition of the state of the art, the achievements and limitations of the technique and its potential for the future. Dr. Ghosh's style is clear and the development of his narrative is helped by his careful choice of significant examples. It should be stressed, however, that this book is not specifically oriented to the needs or interests of analysts. There are sub-sections in some chapters such as "Applications to Analytical Chemistry" (2 pages) and "Analysis of Organic Polymers" (1 page), but these would appear to have been introduced as a sop to explain the book's presence in a "Chemical Analysis" series rather than seriously to alter the main aim, which is to be "an introduction to the principles and scope of applications of PES." The book achieves its aim and can be warmly recommended as an introduction to all aspects of photoelectron spectroscopy.

D. S. Urch

Electrophoretic Techniques
Edited by Colin F. Simpson and Mary Whittaker. Pp. x + 280. Academic Press. 1983. Price £26; $44. ISBN 0 12 644480 3.

In recent years there has been increasing interest in electrophoretic techniques and in their application to the separation of biological substances, particularly proteins. Papers on the subject, and textbooks too, seem to be multiplying in an exponential manner. This publication is a welcome addition to this list as it presents the reader with up-to-date reviews of the major developments that have taken place within the past 5 years and also includes some new techniques that have hardly been more than demonstrated.

The book contains 11 chapters, the first being an historical review of electrophoresis by Rilbe. The chapter is largely theoretical but it includes practical details of the early electrophoretic equipment, the most notable being that of Tiselius, and it leads on from there to developments in zone electrophoresis. My only regret is that the review appears to stop short at the end of the 1960s, a small point maybe, as the

later developments are amply covered in the chapters that follow.

Chapter 2, on electrophoretic methods for characterisation of proteins, by the Editors themselves, gives detailed attention to two-dimensional separations with respect to both technique and application. It includes some very new work by Righetti on the determination of titration curves by IEF.

Chapter 3 by Fawcett, on recent developments in isoelectric focusing, gives useful practical tips for optimising both the separation and the subsequent staining of proteins, although there is some overlap with the previous chapter. Alternative supports to polyacrylamide are discussed in Chapter 4 (cellulose acetate and agarose) and in Chapter 5 the practical aspects of ultra-thin-layer isoelectric focusing on agarose and polyacrylamide are described in detail. Chapter 6, on gel immunoelectrophoresis, is presented as a practical guideline to the latest procedures and is supplemented by suitable references for further reading. Isotachophoresis is given perhaps a surprising amount of space (81 pages) considering that it is still a relatively slightly used technique and not particularly new. Chapter 7 covers the analytical aspects, both theoretical and practical, and applications of isotachophoresis to preparative separations are described in Chapter 8. Preparative displacement electrophoresis (Chapter 9) is presented by Hampson as one solution to the problem of heat removal in scaled up systems. These and the subsequent chapters on preparative isoelectric focusing (Chapter 10) and free-flow electrophoresis (Chapter 11) offer potential solutions to this major problem.

Overall, the book is a well balanced blend of theory and practice and, although there is some overlap between some chapters, this is no bad thing as each one is essentially self-contained and covers one particular aspect of electrophoresis. It is a useful practical guide to IEF and gel immunoelectrophoresis as well as being an up-to-date review of the state of the art across the diverse field of electrophoretic techniques currently being investigated.

I. M. Mackie

Evaluation of Analytical Methods in Biological Systems—Part A. Analysis of Biogenic Amines

Edited by Glen B. Baker and Ronald T. Coutts. *Techniques and Instrumentation in Analytical Chemistry, Volume 4.* Pp. xvi + 308. Elsevier. 1982. Price $76.75; Dfl165; £35. ISBN 0 444 42110 6 (Volume 4); 0 444 417443 3 (Series).

This book represents Volume 4 of a series on techniques and instrumentation in analytical chemistry and is the first concerned with the evaluation of analytical methods in biological systems. The intention of the series is to provide a problem-orientated forum for critical and comprehensive discussion of the approaches available for solving the problem in question. In this book on biogenic amines the Editors and authors have, I believe, succeeded admirably.

The 13 chapters range in subject matter from biological assays, fluorescence techniques, histochemical assays and electrochemical approaches through chromatographic (TLC, HPLC, GC) and mass spectrometric (GC - MS, SIM, quantitative high-resolution MS) methods to radioenzymatic, radioreceptor and radioimmuno assays. As with any multi-author volume there is some overlap between specific chapters, but this has been kept to a minimum and critical comparisons with other approaches are made in most chapters. The references are generally comprehensive and current (up to 1981 in some chapters) and the book is a highly readable and practical text with a useful subject index.

There are inevitably some areas for criticism but these are relatively minor and overall the presentation is good, including figures and tables, although the typescript used in some chapters is very small and not easy to read. This book is recommended and should find a place not only in the libraries of institutions concerned with this subject but also as a bench book in the laboratories involved in analysis and research on biogenic amines, although regretfully the price may take it out of reach of most individual workers' personal resources.

R. A. Chalmers

KONTRON TRACER MCS 670: METHOD DEVELOPMENT

Method development in HPLC involves changing many chromatographic parameters such as
(i) solvent selection
(ii) column selection
(iii) selection of isocratic or gradient conditions
(iv) selection of detection method (detector, λ etc.)
(v) combinations of columns and solvents

This procedure is very time-consuming and cannot be carried out unattended. Consequently, most users do not optimise their separations.
Using the KONTRON gradient system, autosampler, TRACER and detectors controlled by the programmer model 205, you are able to automatically change all the parameters previously mentioned. In addition, the automation of column equilibration and system purging is possible. The same approach can be used in routine method selection.

BUFFER SELECTION — PHENOLS

The logical approach to reversed phase separation is to progress from
(i) aqueous solvents to
(ii) ion suppression solvent systems (M1–M5) to
(iii) ion-pairing solvent systems (M6)
Phenols are weakly acidic and consequently pH is known to affect not only retention but the sharpness of the peaks. Usually separation is carried out at low pH where ionisation is suppressed.
This application demonstrates how the effect of pH can be studied automatically and finally ion-pairing can be investigated. The Kontron Tracer MCS 670 allows not only selection of the aqueous phase but also of columns. This is important because it enables columns to be dedicated to certain solvents, thus diminishing the equilibration time necessary when going from one extreme to the other.
The unusual result of this experiment is the major retention change of pentachlorophenol at pH = 6.1. Fine tuning of pH dependence could be carried out if the separation demands, otherwise mobile phases M1 or M3 are recommended. There appears to be little advantage in going to ion-pairing conditions for phenols.

Valve switching configuration

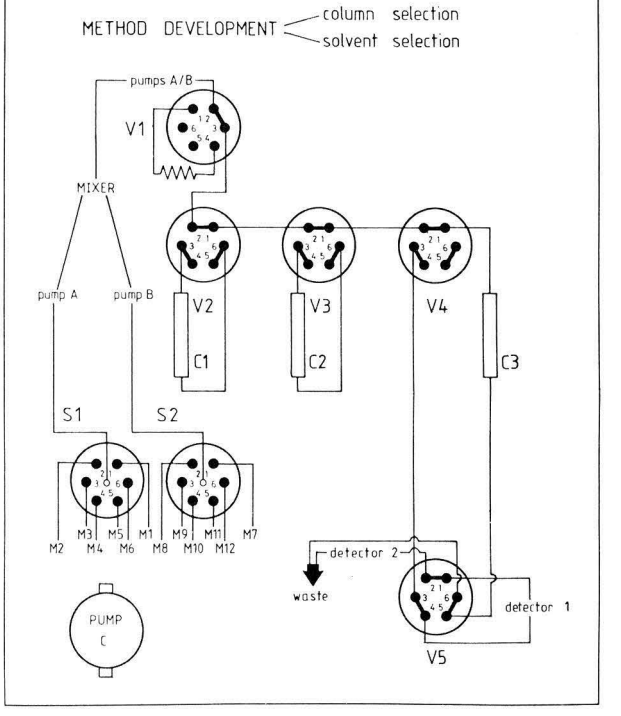

To obtain further details of this Company's series of Application Notes, please use our Reader Enquiry Service quoting No. 204.

Advertisement Feature

KONTRON MCS 670	**Valve switching schematic – Phenols, aqueous solvent selection**					
FUNCTION ACTIVATED	0 30 60	0 30 60	0 30 60	0 30 60	0 30 60	0 30 60 90
Equilibration (E) and Inject	E ↑	E ↑	E ↑	E ↑	E ↑	E ↑
C1	0% B → 100% B	0% B → 100% B	0% B → 100% B			
C2				0% B → 100% B	0% B → 100% B	
C3						0% B → 100% B
Pump A (PA)	1.0 ml/min	1.0 ml/min	1.0 ml/min	1.0 ml/min	1.0 ml/min	1.0 ml/min
Pump B (PB)	Total flow 1 ml/min	Total flow 1 ml/min	Total flow 1 ml/min	Total flow 1 ml/min	Total flow 1 ml/min	Total flow 1 ml/min
Valve V 2 position	b			a		
Valve V 3 position	a			b		a
Valve V 4 position	b					a
Valve V 5 position	a					b
Selector Valve S 1 position	1 = M1	2 = M2	3 = M3	4 = M4	5 = M5	6 = M6
Selector Valve S 2 position	1 = M7					
Detector	Uvikon 720 LC, 254 nm, 0.5 AUFS					
Recorder	0.5 cm/min					
	0 30 60	0 30 60	0 30 60	0 30 60	0 30 60	0 30 60 90

COLUMNS		MOBILE PHASES			
C1	25 cm Kontron Spherisorb S5-ODS	M1	0.01 M NaH_2PO_4 (pH = 2.4)	M 7	Methanol
C2	25 cm Kontron Spherisorb S5-ODS	M2	0.01 M NaH_2PO_4 (pH = 4.7)	M 8	Methanol : Acetonitrile (9:1)
C3	25 cm Kontron Spherisorb S5-ODS	M3	0.01 M NaH_2PO_4 (pH = 6.1)	M 9	Methanol : Acetonitrile (8:2)
C4		M4	0.1 M perchloric acid	M 10	Methanol : THF (9:1)
		M5	0.1 M L-serine in M1	M 11	Methanol : Acetonitrile : THF (8:1:1)
		M6	0.1% heptane-sulphonic acid in M1	M 12	Methanol : DMSO (9:1)

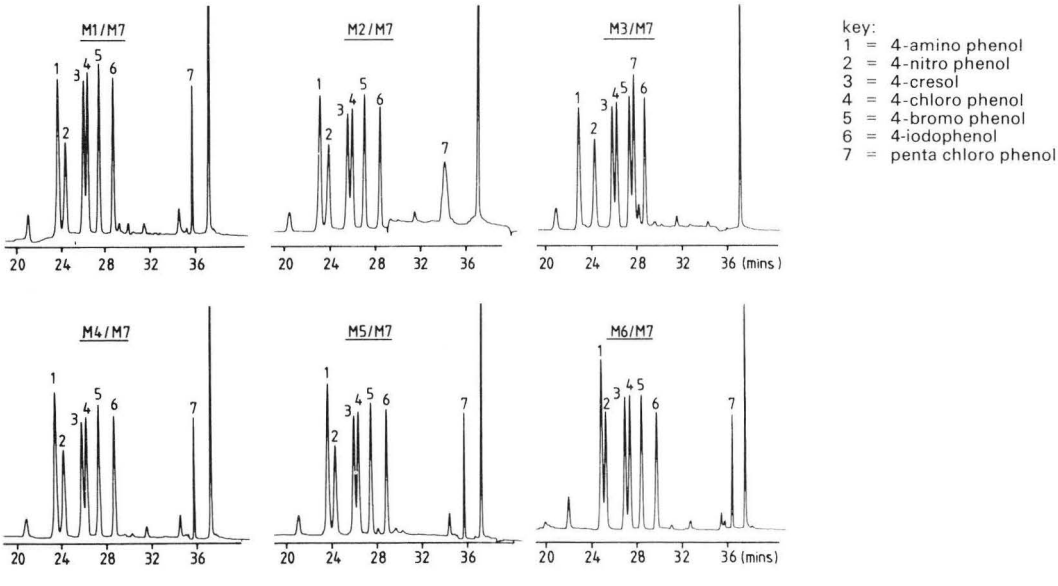

key:
1 = 4-amino phenol
2 = 4-nitro phenol
3 = 4-cresol
4 = 4-chloro phenol
5 = 4-bromo phenol
6 = 4-iodophenol
7 = penta chloro phenol

KONTRON ANALYTICAL

To obtain further details of this Company's series of Application Notes, please use our Reader Enquiry Service quoting No. 204.

The company appearing below is able to offer scientific support to users of laboratory instrumentation. THE ANALYST will regularly publish specific Application Notes provided by their applications chemists.

A201 for further information. See page xii.

FEDERATION OF EUROPEAN CHEMICAL SOCIETIES

EUROANALYSIS V

Cracow, Poland,

August 26–31, 1984

The Scientific Programme of this conference will consist of plenary lectures, keynote lectures and contributed papers and posters as well as special sessions on Computer Based Analytical Chemistry (COBAC III) and Speciation in Trace and Environmental Analysis. The plenary lecturers will be Yu. J. Belyaev, R. E. Dessy, D. Jagner and H. W. Nurnberg, while the keynote lecturers will be J. Buffle, P. Camus, K. Doerfel, Z. Hippe, J. F. K. Huber, T. K. Kantor, R. Kellner, W. E. van der Linden, G. Mouvier and G. Nickless.

The closing date for abstracts from potential authors has now passed, so any late submissions should be made immediately.

A comprehensive social programme will be organised, including a gala dinner, sightseeing tour of Cracow, excursions to Wieliczka salt mine, Ojców National Park, Pieskowa Skała castle and the former Auschwitz concentration camp. There are post-symposium tours to Zakopane in the Tatra Mountains (3 days) and to Częstochowa (1 day).

For full details, second circular and registration forms, contact Euroanalysis V, Professor Zygmunt Kowalski, Academy of Mining and Metallurgy, Al. Mickiewicza 30, 30–059 Cracow, Poland.

CUT HERE

FIRST FOLD HERE

THE ANALYST READER ENQUIRY SERVICE
For further information about any of the products featured in the advertisements in this issue, write the appropriate number on the postcard, detach and post.

FOLD HERE

THE ANALYST READER ENQUIRY SERVICE

MAR'84

For further information about any of the products featured in the advertisements in this issue, please write the appropriate number in one of the boxes below.
Postage paid if posted in the British Isles but overseas readers must affix a stamp.

PLEASE USE BLOCK CAPITALS LEAVING A SPACE BETWEEN WORDS *Valid 12 months*

1 NAME

2 COMPANY

PLEASE GIVE YOUR BUSINESS ADDRESS IF POSSIBLE. IF NOT, PLEASE TICK HERE ☐

3 STREET

4 TOWN

5 COUNTY, POST CODE

6 COUNTRY

7 DEPARTMENT/ DIVISION

8 YOUR JOB TITLE/ POSITION

9 TELEPHONE NO.

OFFICE USE ONLY REC'D PROC'D

FOLD HERE

Postage will be paid by Licensee

Do not affix Postage Stamps if posted in Gt. Britain, Channel Islands, N. Ireland or the Isle of Man

BUSINESS REPLY SERVICE
Licence No. WD 106

2

Reader Enquiry Service
The Analyst
The Royal Society of Chemistry
Burlington House, Piccadilly
London W1E 6WF
England

ANALAO 109(3) 189–412 (1984) March, 1984

The Analyst

The Analytical Journal of The Royal Society of Chemistry

CONTENTS

6TH SAC INTERNATIONAL CONFERENCE ON ANALYTICAL CHEMISTRY, EDINBURGH, UK, 17–23 JULY 1983

continued inside back cover

Electronically typeset and printed by Heffers Printers Ltd, Cambridge, England

CONTENTS—*continued*